SYNTHESIS AND EVALUATION OF NOVEL HIV-1 ENZYME INHIBITORS

A thesis submitted in fulfilment of the requirements for the degree of

DOCTOR OF PHILOSOPHY

of

RHODES UNIVERSITY

by

TEMITOPE OLORUNTOBA OLOMOLA
B.Sc (Hons), M.Sc (Ibadan), M.Phil (Ile-Ife)

December 2011

ABSTRACT

This study has involved the design, synthesis and evaluation of novel HIV-1 enzyme inhibitors accessed by synthetic elaboration of Baylis-Hillman adducts. Several series of complex coumarin-AZT and cinnamate ester-AZT conjugates have been prepared, in high yields, by exploiting the click reaction between appropriate Baylis-Hillman derived precursors and azidothymidine (AZT), all of which have been fully characterised using spectroscopic techniques. These conjugates, designed as potential dual-action HIV-1 inhibitors, were tested against the appropriate HIV-1 enzymes, *i.e*. HIV-1 reverse transcriptase and protease or HIV-1 reverse transcriptase and integrase. A number of the ligands have exhibited % inhibition levels and IC_{50} values comparable to drugs in clinical use, permitting their identification as lead compounds for the development of novel dual-action inhibitors. *In silico* docking of selected ligands into the active sites of the respective enzymes has provided useful insight into binding conformations and potential hydrogen-bonding interactions with active-site amino acid residues. A series of furocoumarin carboxamide derivatives have been synthesised in four steps starting from resorcinol and these compounds have also been tested for HIV-1 integrase inhibition activity.

The structures of unexpected products isolated from Aza-Baylis-Hillman reactions of *N*-tosyl-aldimines have been elucidated by spectroscopic analysis, and confirmed by single crystal X-ray analysis. A mechanism for what appears to be an unprecedented transformation has been proposed. Microwave-assisted SeO_2 oxidation of Baylis-Hillman-derived 3-methylcoumarins has provided convenient and efficient access to coumarin-3-carbaldehydes, and a pilot study has revealed the potential of these coumarin-3-carbaldehydes as scaffolds for the construction of tricyclic compounds.

The HCl-catalysed reaction of *tert*-butyl acrylate derived Baylis-Hillman adducts has been shown to afford 3-(chloromethyl)coumarins and α-(chloromethyl)cinnamic acids, the *Z*-stereochemistry of the latter being established by X-ray crystallography. ^{1}H NMR-based experimental kinetic and DFT-level theoretical studies have been undertaken to establish the reaction sequence and other mechanistic details. Base-catalysed cyclisation on the other hand, has been shown to afford 2*H*-chromene rather than coumarin derivatives.

ACKNOWLEDGEMENTS

I will like to thank my supervisor, Prof. Perry Kaye, for his guidance and support throughout the duration of this work. I deeply appreciate your calm and insightful mentorship style; it made the training experience a lot better. It has been a honour to be a part of your research group.

I also wish to thank Dr. Rosalyn Klein for being such a wonderful co-supervisor. Your constant encouragement and willingness to help has really been invaluable.

My appreciation goes to the entire Chemistry department staff and students for being such a unique department and providing such a good support for me. I will like to particularly thank Dr. K. Lobb, for his help with computation-related problems, Dr. P. Kempgens for his assistance with the NMR instruments and Mr. F. Chindeka for helping with the elemental analysis.

I wish to acknowledge the following: Dr. Nicodemus Mautsa, Centre for Chemico- and Biomedicinal Research, Rhodes University, and Dr. Salerwe Mosebi, MINTEK, for helping conduct the bioassays; Prof. M. Caira, Univerisity of Cape Town, for helping with X-ray crystallography; Dr. Y. Sayed, University of Witwatersrand, for providing some of the enzymes used during this research.

To my friends, Samson, Mosiuoa, Mamello, Anthonia and Tungai, you guys helped make my Grahamstown experience more exciting. I also appreciate my colleagues in the F22 laboratory over these three years for making me smile even when things got tough on the bench.

I deeply appreciate the support I have received from my family during the period of this research. Thank you so much for always being there.

Finally, thanks to the Medical Research Council and Rhodes University for generous financial support.

LIST OF ABBREVIATIONS

Ac	-	acetyl
AIDS	-	acquired immunodeficiency syndrome
AZT	-	azidothymidine
Bn	-	benzyl
t-Bu	-	tertiary butyl
DABCO	-	1,4-diazabicyclo[2.2.2]octane
DBU	-	1,8-diazabicyclo[5.4.0]undec-7-ene
DCM	-	dichloromethane
DMAP	-	4-dimethyl aminopyridine
DMSO	-	dimethylsulphoxide
EWG	-	electron-withdrawing group
3HQ	-	3-quinuclidinol
HIV	-	human immunodeficiency virus
IN	-	integrase
μW	-	microwave
MVK	-	methyl vinyl ketone
NMR	-	nuclear magnetic resonance
NRTI	-	nucleoside reverse transcriptase inhibitor
NtRTI	-	nucleotide reverse transcriptase inhibitor
PR	-	protease
RT	-	reverse transcriptase
STD	-	saturation transfer difference
TsOH	-	*p*-toluenesulphonic acid
TMEDA	-	tetramethylethylenediamine

CONTENTS

1. INTRODUCTION

1.1. THE HUMAN IMMUNODEFICIENCY VIRUS

1.1.1. A Brief Overview

Arguably the "most intelligent" virus known to man, the Human Immunodeficiency Virus (HIV) remains a very serious challenge for chemotherapy in the 21st century.[1] HIV is a member of the genus *Lentivirus* (a class of viruses noted for immune system attack) and the family *Retroviridae*.[2] The name *Lentivirus* literally means 'slow virus', indicative of the length of time it takes to produce any adverse effects in the body. There are two species of HIV known to exist: HIV-1 and HIV-2, with HIV-1 as the more virulent, pandemic strain. HIV is zoonotic and believed to be of African primate origin; HIV-1 is closely related to *lentiviruses* found in chimpanzees, while HIV-2 has been found in sooty mangabeys, also harbouring the Simian Immunodeficiency Virus (SIV).[3-6]

Acquired Immunodeficiency Syndrome (AIDS) is the name given to the condition where HIV has severely compromised the immune system, thus allowing opportunistic infections to affect the host.[7,8] Estimates point to more than twenty-five million human deaths arising from AIDS-related diseases since 1981, with over 33.3 million people around the world living with HIV in 2009. Approximately 2.6 million people were newly infected with HIV in 2009, and 1.8 million men, women and children lost their lives from the disease in the same year. Sub-Saharan Africa remains the continent worst hit by the impact of this deadly virus.[9,10]

There are three sub-groups of HIV-1: M (main or major), N (new) and O (outlier). Within the M-group there are at least nine subtypes or clades: A, B, C, D, F, G, H, J, and K. A 2006 survey[10] revealed that the B-clade is dominant in North America, Latin America (together with clade F) and the Caribbean, Western Europe, South, East and South-East Asia and Australia. Most sub-types are found in sub-Saharan Africa with clades A and D recording the highest rates in Central and Eastern Africa, with Central Africa also having the highest prevalence rate of clades F, H, J and K. Clade A is also dominant in Eastern Europe and Central Asia. Subtypes A and G are the dominant strains in West Africa with Nigeria accounting for the largest infection rate in the region. In Southern Africa, with *ca* 30% of the world's infection level, subtype C is found almost exclusively; subtype C is also the predominant form in India and Nepal. Subtype I was a name given to an apparent subtype found in Cyprus but the name is no longer used. There have been

reports of mosaics (recombinants) between different subtypes in some countries. These arise when two different subtypes infect a person at the same time and recombination occurs. The former subtype I has been found to be a circulating recombinant form (or CRF) of subtypes A, G, H and K.[10-15]

1.1.2. Structure of HIV-1

An HIV particle (virion) is spherical in shape with a diameter of approximately 0.1 micron and, like other viruses, requires a living host to be able to grow and reproduce. The outer coat of the virus, made up of fatty material, is referred to as the viral envelope and protruding from this envelope are spikes of protein called Env. Env exists as a trimer (or tetramer) on the surface of HIV-infected cells and comprises a cap called glycoprotein 120 (gp120) and a stem called glycoprotein 41 (gp41).[16,17] Just below the viral envelope is a layer called the matrix, which is made from the protein p17 (Figure 1). Classical vaccination approaches to develop a vaccine for the prevention of HIV infection have focused on these envelope proteins, but, thus far, to no avail.[18]

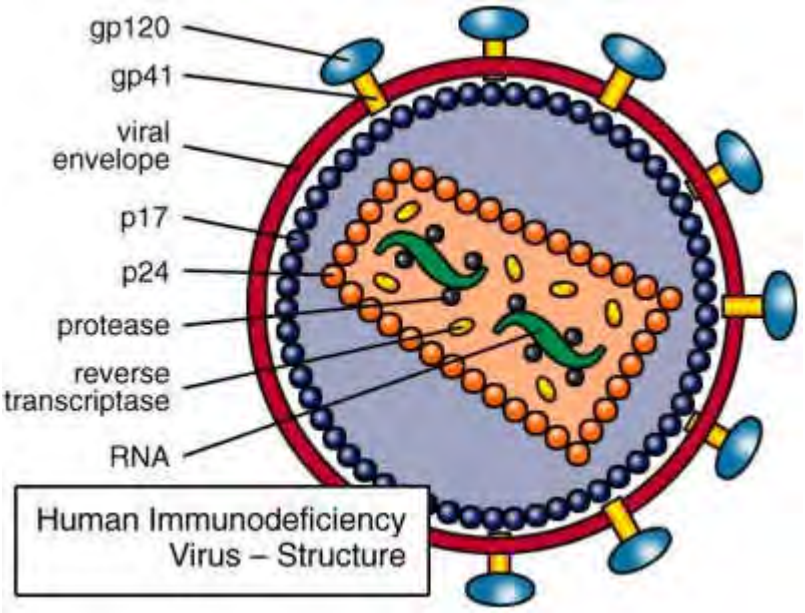

Figure 1. Mature HIV-1 virion (reproduced by permission).[19]

Within the viral envelope is the viral core (or capsid), which is usually bullet-shaped and made from the protein p24. The capsid surrounds two single strands of viral RNA, each containing the genetic material of the virus.[17] HIV has a total of nine genes: gag, pol, env, tat, rev, nef, vif, vpr and vpu.[20] The first three (gag, pol and env) contain information needed to make structural proteins for new virions;[21] the remaining six genes code for proteins that control the ability of

HIV to reproduce and infect a new host cell.[17] Also situated within the core are three enzymes required for HIV replication, *viz*., reverse transcriptase (RT), integrase (IN) and protease (PR).[22]

1.1.3. Replicative Cycle of HIV-1

Infection typically begins when an HIV particle containing two copies of RNA encounters a host cell. The surface cluster designation 4 (CD4) molecules interact with glycoproteins on the viral surface.[23,24] This is followed in succession by: (i) fusion of the viral envelope with the cell membrane; (ii) release of the HIV capsid contents into the cell; (iii) transcription of viral RNA into proviral DNA; (iv) integration of proviral DNA into the cellular genome in the nucleus and DNA replication; (v) transcription of the viral DNA to RNA; (vi) translation of the viral precursor mRNA to mature mRNA; and (vi) maturation, budding and release of new mature virions[25-27] (Figure 2).

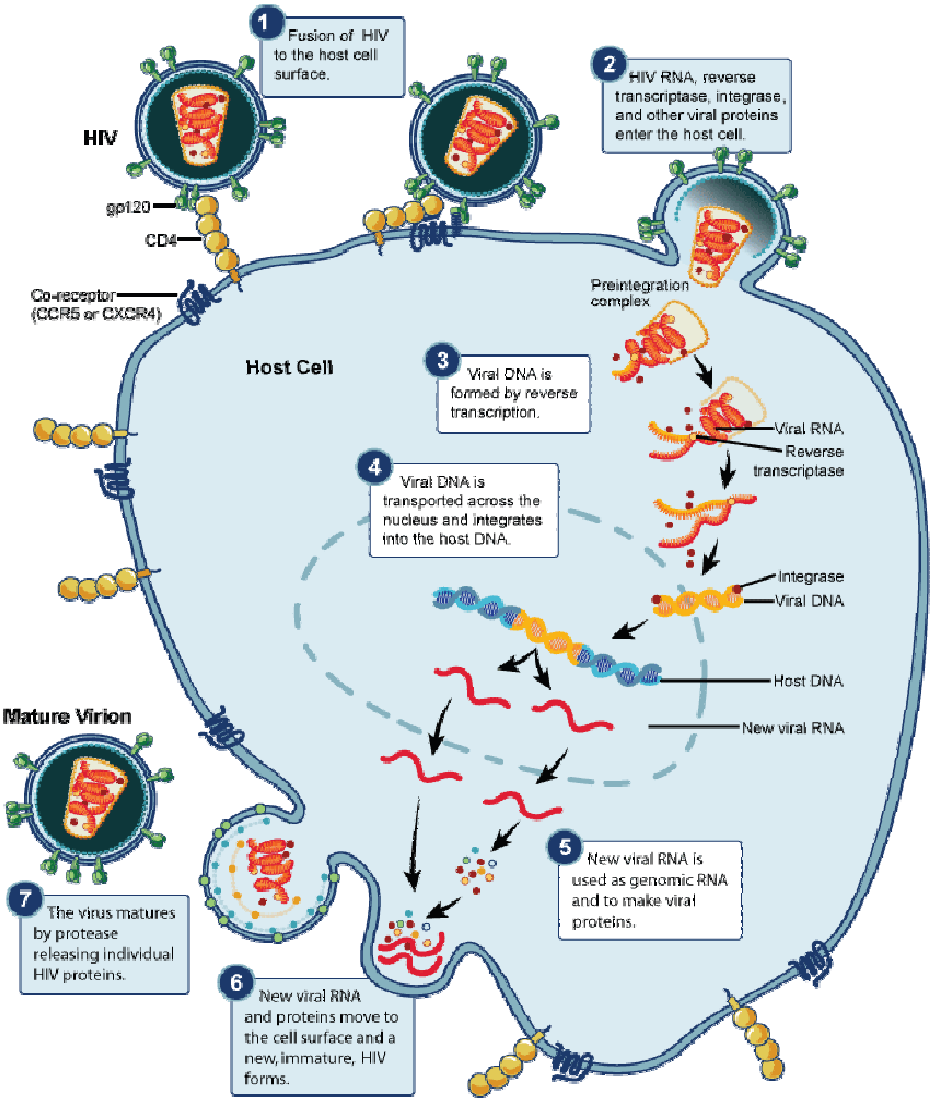

Figure 2. The HIV Replicative Cycle (reproduced by permission).[27]

1.1.4. HIV-1 Reverse Transcriptase: Structure and Function

HIV-1 reverse transcriptase (RT) plays a key role in the retroviral life-cycle and it does this mainly in the cytoplasm of the infected cell. HIV-1 reverse transcriptase is a DNA polymerase enzyme responsible for transcribing a single-stranded viral RNA genome into double-stranded DNA.[28,29] The HIV-1 reverse transcriptase enzyme contains two main domains: a DNA polymerase domain, capable of copying either an RNA or a DNA template, and a ribonuclease H (RNase H) domain which cleaves and degrades the template RNA after DNA synthesis so that the newly made DNA can generate a second DNA strand.[30]

HIV-1 reverse transcriptase is an asymmetric heterodimer composed of two distinct, but related chains (Figure 3). The first of these two chains is a 66-kD subunit (p66), which is 560 amino acid residues in length and contains the active sites for both of the enzymatic activities of RT (polymerase and RNase H). The other chain, a 51kD subunit (p51), is 440 amino acid residues long and has a structural role.[29-31] The polymerase domain of p66 and p51 each contain four sub-domains: fingers, palm, thumb and connection; however, the positions of the sub-domains relative to each other are different in the two subunits.[31-32]

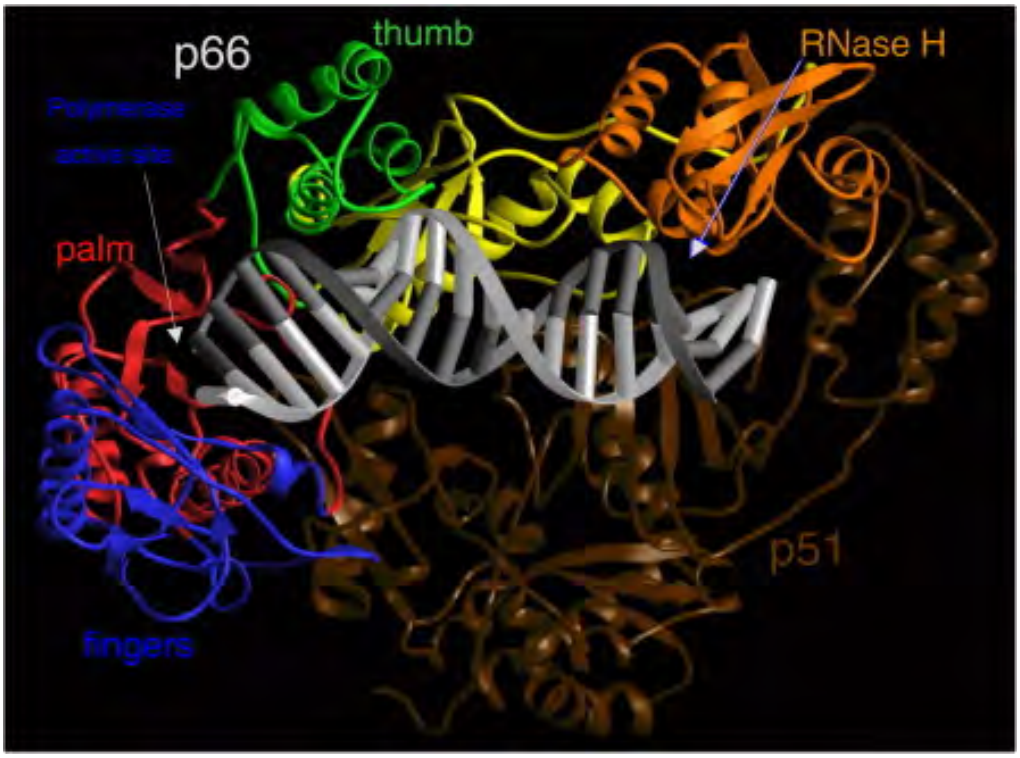

Figure 3. Ribbon representation of HIV-1 RT in a complex with nucleic acid. The fingers, palm, thumb, connection, and RNase H subdomains of the p66 subunit are shown in blue, red, green, yellow, and orange, respectively. The p51 subunit is shown in dark brown. The template and primer DNA strands are shown in light gray and dark gray, respectively (reproduced by permission).[30]

HIV-1 RT contains a (*ca* 60 Å long) groove between the polymerase and RNase active sites and the connection subdomains of p66 and p51 form the floor of this groove. The binding groove is configured so that the nucleic acid contacts both the polymerase and the RNase H active sites, the contact points being 17 or 18 base pairs apart on the nucleic acid substrate. Like many other DNA polymerases, RT requires both a primer and a template. The DNA primer grip in HIV-1 RT, a highly conserved structural motif that consists of the p66 β12-β13 hairpin, helps position the 3′-OH end of the primer strand at the polymerase active site.[32,33] The polymerase active site comprises three catalytic carboxylate groups in the palm subdomain of p66 that bind the two divalent metal ions that are required for catalysis (Mg^{2+} appears to be used *in vivo*, while Mn^{2+} can support polymerization *in vitro*).

1.1.5. HIV-1 Integrase: Structure and Function

HIV-1 integrase (IN) mediates the insertion of proviral DNA into host chromosomes thereby causing the host cell machinery to produce viral proteins – a step that has been found to be critical for all retroviral infections.[34,35]

HIV-1 IN, a 288-amino acid protein (32 kDa) encoded by the end of the *pol* gene, consists of three domains: the N-terminal (which binds zinc), catalytic core (which binds magnesium) and C-terminal (which binds DNA) domains (Figure 4). The structures of each domain and of two-domain fragments have been determined; however the complete structure of the enzyme as found *in vivo* is, as yet, unavailable.[36-38] The catalytic core domain contains the active site responsible for catalysis of all the integration/disintegration reactions. *In vitro* studies have indicated that functional HIV-1 integrase is a multimeric protein, existing in solution as a mixture in dynamic equilibrium of monomers, dimers, tetramers, and higher-order oligomers.[39-41]

The pre-integration complex (newly synthesized viral DNA from the reverse transcription process as well as Gag, Pol, Vpr, Vpx and at least one cellular protein) migrates to the nucleus where proviral integration takes place.[42] The integration of proviral DNA involves two-steps (3' processing and 5' strand transfer), which have been well characterized through *in vitro* studies.[43,44] During the first reaction catalysed by IN, two nucleotides are cleaved from the 3' end of the viral DNA, thus generating 3'-hydroxyl nucleophilic ends.[45] Strand transfer then occurs in the nucleus through a transesterification reaction, in which the viral DNA with the recessive 3' end becomes covalently linked to the 5' protrusion of the host DNA.[46] The integration process is

completed by degradation of the two unpaired nucleotides at the 5' end of the viral DNA, gap filling and ligation by cellular repair enzymes.[47,48]

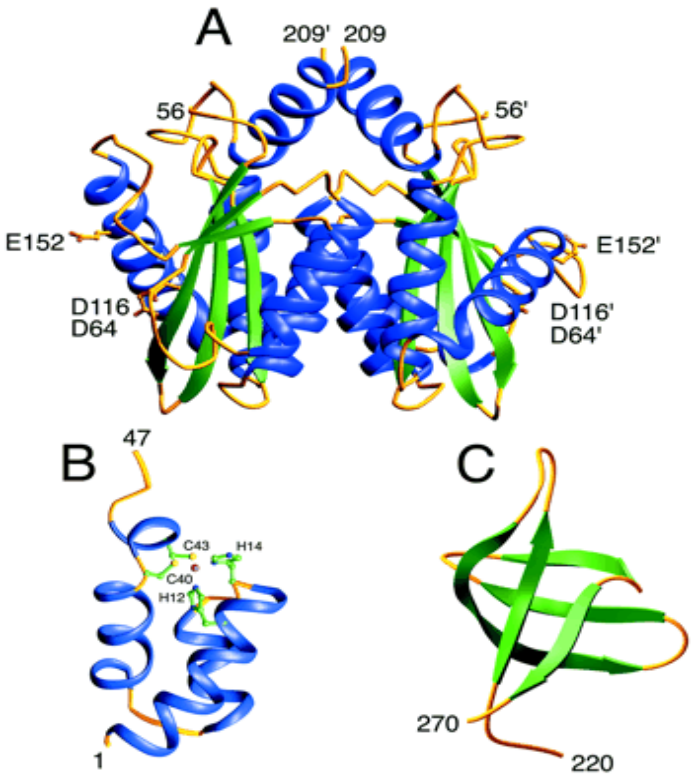

Figure 4. Ribbon representation of the 3 domains of HIV-1 integrase: A, the catalytic core domain; B, the N-terminal domain; and C, the C-terminal domain. The Protein Data Bank codes for the domains are 1BIS, 1WJC, and 1IHV, respectively (reproduced by permission).[49]

1.1.6. HIV-1 Protease: Structure and Function

HIV-1 Protease (PR) is an aspartic protease essential for proper virion assembly and maturation. The HIV-1 virus generates long polypeptide chains containing many proteins; HIV-1 PR simply cuts these polyproteins into smaller functional proteins.[50] HIV-1 PR is a homodimer as shown in Figure 5, with each monomeric unit consisting of an independently inactive 99 amino acid polypeptide chain (11 KDa) containing the signature sequence Asp-Thr-Gly.[51-53] Each monomeric subunit contains two twisted beta sheets and a small alpha helix which come together in such a way as to form a cavity.[54,55] The two Asp-Thr-Gly catalytic triads, one on each chain, are situated in the cavity and make up the active site. The two Asp residues act as the main catalytic agents and, together with a water molecule, facilitate cleavage of the protein substrate bound in the cavity by acting as a "molecular pair of scissors".[56] It is believed that hydrolysis of an amide carbonyl group, by a water molecule accommodated between the side-chains of the aspartic acid residues, involves a tetrahedral intermediate.[57]

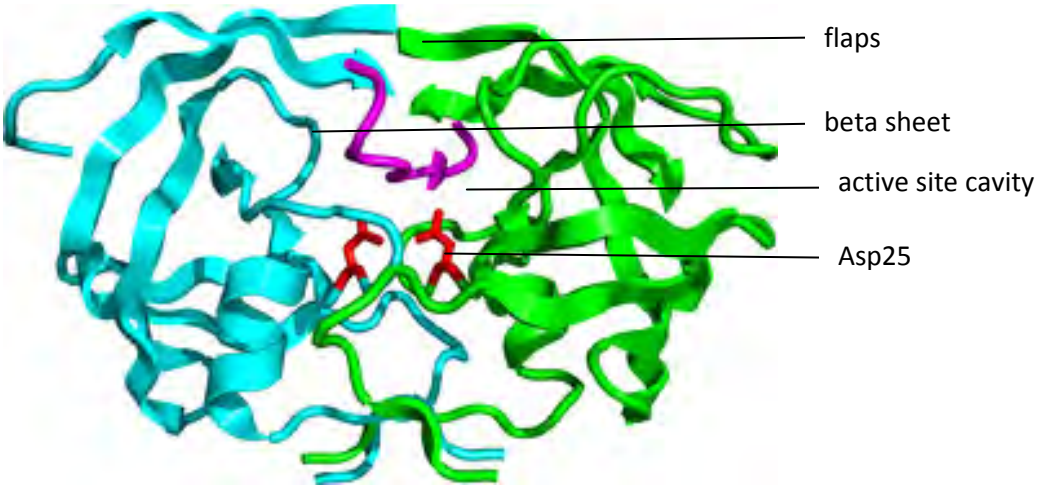

Figure 5. A schematic structure of HIV-1 protease. The monomers are shown in green and cyan, the Asp25 and Asp25´ residues are shown in red, and the Ile50 and Ile50´ residues linked to a water molecule are shown in purple (adapted from PDB 1KJF).[58]

During protein-substrate binding, the active site of the HIV-1 PR enzyme has a number of well-defined subsites in which substrate side-chains can be accommodated. According to the nomenclature developed by Schechter and Berger,[59] the amino acid residues constituting the subsites in the enzyme active site are termed S_1, S_2, …, S_n and S_1', S_2', …, S_n' (Fig. 7), while the corresponding groups in the substrate are denoted by P_1, P_2, …, P_n and P_1', P_2', …, P_n' counted from the scissile bond which is cleaved during hydrolysis, and which is situated between P_1 and P_1'.[59] The HIV-1 PR subsites S_1 and S_1' are largely hydrophobic, with the exception of the active-site aspartates. Thus, most of the current inhibitors have hydrophobic moieties at P_1 and P_1'.[60]

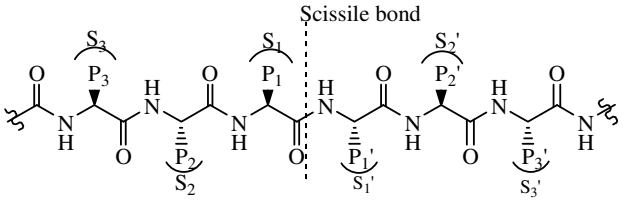

Figure 6. Standard nomenclature for HIV-1 PR complex-substrate subsites.[59]

1.1.7. Targets for Anti-HIV Chemotherapy

A close look at the replicative cycle of HIV reveals several stages that could be considered as potential targets for chemotherapeutic intervention. [61] Such targeting requires identification of stages that are unique to the virus and not common to host cells. Such stages in the replicative cycle of the virus include: binding to surface receptors; virus-cell fusion; uncoating of the nucleocapsid; reverse transcription of RNA to DNA; integration of proviral DNA into the host

genome; proviral DNA replication; proviral DNA transcription to viral messenger RNA; viral messenger RNA translation to viral precursor proteins; viral maturation (proteolysis of viral polyproteins); assembly of the virus at the host cell membrane; and budding.[62] While reverse transcription and viral maturation steps have, thus far, received most attention in HIV chemotherapy, inhibition of other stages is being explored.[62,63]

1.2. RATIONAL DRUG DESIGN

1.2.1. Molecular Modelling and Computational Chemistry

Computational chemistry is simply the application of mathematical methods in solving chemical problems.[64] With increased computing power and availability, computational chemistry has become a rapidly developing ancillary to experimental research.

1.2.2. Computer-Aided Drug Design

The discovery of new drugs has often involved identifying the active principles from plant extracts used in traditional medicine, a classic example being the isolation of quinine for the treatment for malaria.[65] Ordinarily, drug design and development is a lengthy interdisciplinary process which involves target discovery, lead development and optimization followed by series of pre-clinical and clinical trials.[66] High-throughput screening may be used to find suitable lead compounds which exhibit some degree of activity; synthetic modification may then afford analogues with improved biological properties.

Structure-based rational drug design typically involves identification of the active site of a disease-related receptor protein or enzyme from its 3-dimensional structure obtained by X-ray crystallography, NMR spectroscopy or homology modelling.[67] Ligands may then be designed that are able to interfere with or inhibit normal function at such sites.[68] In some cases, a database search may be used to identify and dock small ligands in the active site (fragment docking approach); additional molecular fragments or atoms are then added to maximize occupation of the space within the binding pocket.[68,69] Alternatively, incremental construction of novel molecular structures capable of docking within the receptor may lead to the identification of active compounds.[70] Computer-aided drug design assists in the prediction of a ligand's ability to

bind to the active site, with consensus scoring, geometric analysis and cluster analysis being some of the methods presently used for evaluating binding data.[71,72]

When the structure of the receptor is unknown, drug design may be based on key features of a known, active ligand (pharmacophore model), from which certain properties of the receptor site may be inferred; this is known as ligand-based drug design.[67] This could involve the construction of compounds which are structurally similar to an active compound (ligand similarity approach) and the application of quantitative structure-activity relationship (QSAR) data.[73-75]

1.2.3. Rational Design of HIV-1 Reverse Transcriptase Drugs

There are two classes of drugs which inhibit the normal function of the RT enzyme in viral DNA synthesis (Section 1.1.4). The first class comprises compounds referred to as nucleoside or nucleotide RT inhibitors (NRTI or NtRTI). These are compounds which resemble the nucleosides in structure but in which the 3′-hydroxyl group is modified or replaced. Once an inhibitor, lacking a free 3' hydroxyl group, is incorporated into the template primer complex, formation of the critical 3′ - 5′ phosphodiester bond with the next base required to extend the DNA chain, is no longer possible.[76,77] Nucleoside inhibitors are prodrugs that are phosphorylated by host cell kinases; the resulting nucleotide-triphosphates then compete with the endogenous deoxynucleotide-triphosphate for insertion into the DNA chain.[78] These compounds are administered as the corresponding nucleosides, which are able to cross cell membranes more easily than charged nucleotides.[79]

The discovery and development of nucleoside analogues as AIDS drugs based on an understanding of the mechanism of RT action before the full structure was unravelled.[32,41] The eight currently approved NtRTI and NRTIs used in the treatment of AIDS are shown in Table 1. Two of these compounds are analogues of thymidine **1**, *viz*., Retrovir® **2** (Zidovudine or azidothymidine, AZT), the first antiretroviral drug to be approved by the Food and Drug Administration (FDA) in the United states for the treatment of HIV (1987), and Zerit® **3** (Stavudine or d4T; approved in 1994). Three are analogues of deoxycytidine **4**, *viz*., Emtriva® **5** [Emtricitabine or (-) FTC; approved 2003], Epivir® **6** (Lamuvidine or 3TC; approved 1995) and Hivid® **7** (Zalcitabine or ddC, approved 1992). Ziagen® **9** (Abacavir; approved 1998), is an analogue of deoxyguanosine **8** while the last two approved drugs are analogues of adenosine **10**, *viz*., the NRTI Videx® **11** (Didanosine or ddI; approved 1991) and Viread® **12** (Tenofovir; approved 2001) - the only NtRTI thus far approved for HIV treatment.[80]

Table 1. Approved NRTIs and NtRTI and their corresponding endogenous deoxynucleosides

Deoxynucleoside	Drug
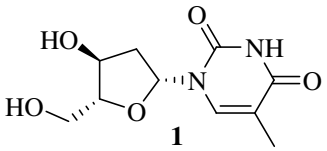 **1** Thymidine	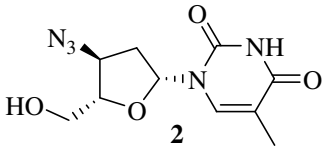 **2** Azidothymidine
	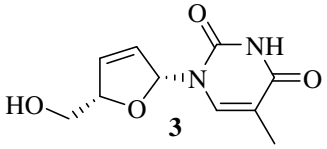 **3** Stavudine
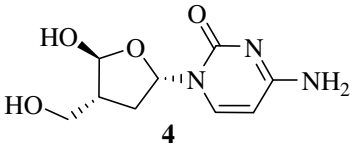 **4** Deoxycytidine	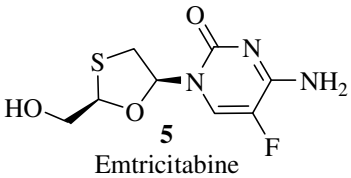 **5** Emtricitabine
	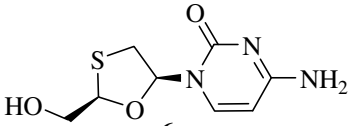 **6** Lamuvidine
	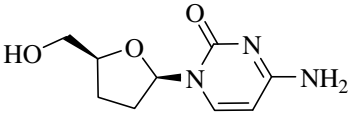 **7** Zalcitabine
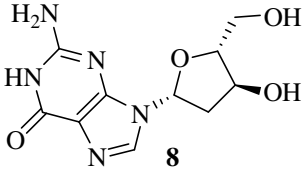 **8** Deoxyguanosine	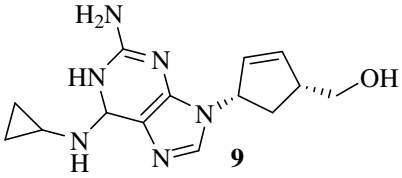 **9** Abacavir
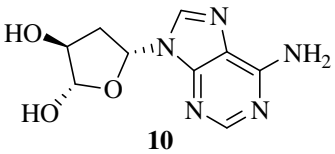 **10** Deoxyadenosine	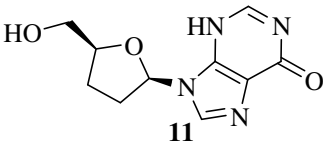 **11** Didanosine
	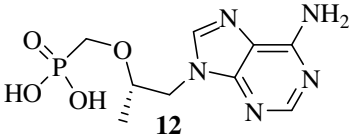 **12** Tenofovir

The other class of RT inhibitors comprises the non-nucleoside inhibitors (NNRTIs). These compounds, which do not require phosphorylation, have been designed to complement the structure of a binding pocket close to the active site of the RT enzyme.[81] NNRTIs do not actually bind to the active site of RT; instead they bind to a less conserved (allosteric) pocket, distinct from but near the substrate binding site. Binding to the allosteric pocket results in a conformational change in the enzyme, which prevents DNA chain propagation and hence inhibits HIV-1 replication.[82] While active against HIV-1, these compounds have not proved to be effective against the HIV-2 virus.[83] NNRTIs belong to a widely diverging class of compounds[82] and there are four currently approved NNRTI drugs, *viz*., Sustiva® **13** (Efavirenz; approved 1998), Viramune® **14** (Nevirapine; approved 1996), Rescriptor® **15** (Delavirdine; approved 1997) and Intelence® **16** (Etravirine approved 2008).

Broad-range screening has led to the discovery of the tetrahydroimidazobenzodiazepinethione (TIBO) derivative **17**, as an anti-HIV lead compound. Synthetic modification and structure activity relationship (SAR) studies then led to compounds **18** and **19**, with the latter exhibiting activity equivalent to that of AZT.[84,85]

High-throughput, cell-based screening led to the identification of the α-anilinophenylacetamide (α-APA) **20**, as another potential anti-HIV lead compound, optimisation of which afforded loviride **21**, a compound with better inhibition but poorer pharmacokinetic properties and, hence, offering no advantage over other NNRTIs.[83,85,86] SAR studies on loviride analogues, in which the length of the spacer between the two aryl groups was varied, led to the imidoyl thiourea (ITU) derivatives (*e.g*. compound **22**) as anti-HIV compounds; the analogue **23** exhibits activity comparable with that of nevirapine **14**.[85,87] Research on improving the metabolic stability then led to discovery of the diaryltriazine (DATA) analogue **24** and, in turn, to the diarylpyrimidine (DAPY) derivative etravirine **16** – a highly potent inhibitor effective against wild-type and drug-resistant HIV-1 strains. Other DAPY derivatives that have emerged as drug candidates include dapivirine **25** (currently being tested as a topical microbicide to prevent HIV infections) and rilpivirine **26** (presently in clinical trials).[83,88] Numerous other compounds have also been identified as NNRTIs.[63]

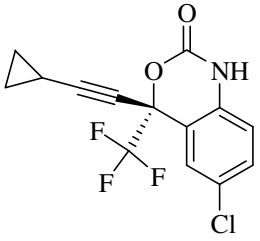

13
Efavirenz

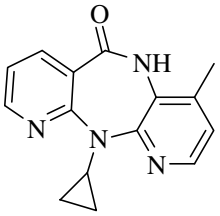

14
Nevirapine

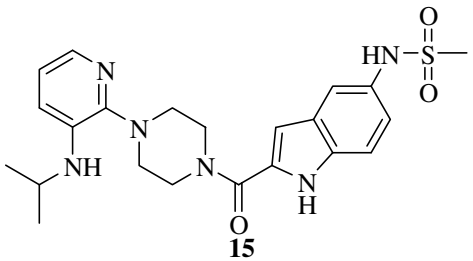

15
Delavirdine

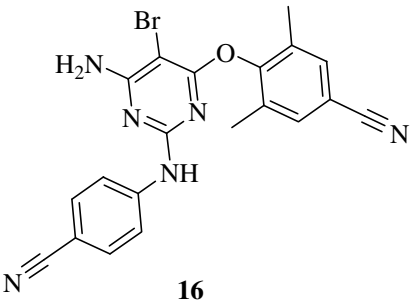

16
Etravirine

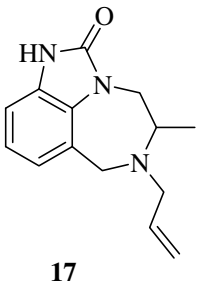

17
HIV-1 EC_{50} = 62 µM

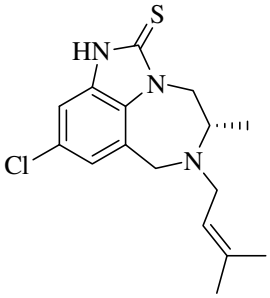

18
HIV-1 EC_{50} = 33 nM

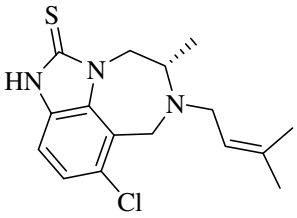

19
HIV-1 EC_{50} = 4.6 nM

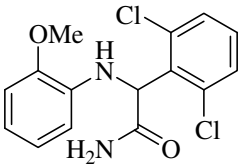

20
HIV-1 EC_{50} = 610 nM

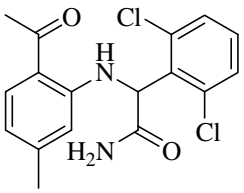

21
Loviride
HIV-1 EC_{50} = 13 nM

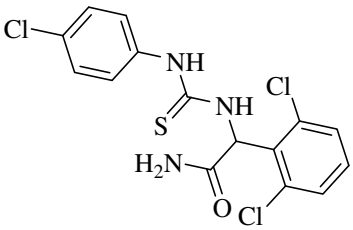

22
HIV-1 EC_{50} = 0.16 µM

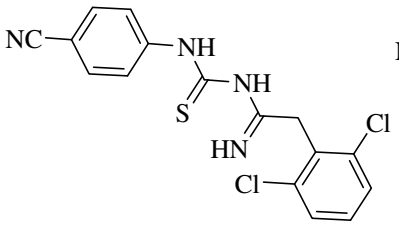

23
HIV-1 EC_{50} = 3 nM

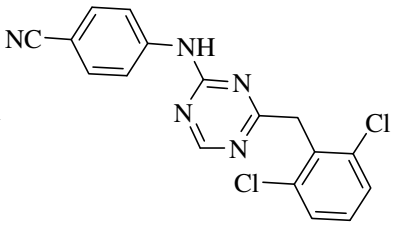

24
HIV-1 EC_{50} = 6 nM

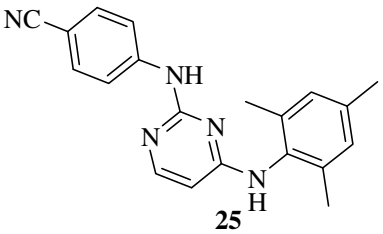

25
Dapivirine
HIV-1 EC_{50} = 1.2 nM

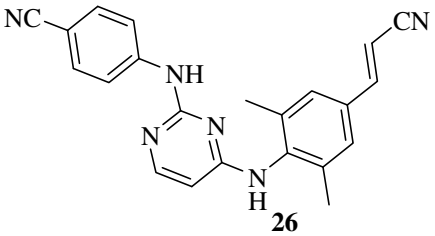

26
Rilpivirine
HIV-1 EC_{50} = 0.4 nM

1.2.4. Rational Design of HIV-1 Integrase Drugs

HIV-1 IN, one of the three encoded enzymes required for viral replication, has more recently received attention as a target for HIV therapy. Compounds found to inhibit HIV-1 IN can do so either by acting as strand transfer inhibitors, thereby blocking the strand transfer of viral DNA into the host genome, or by disrupting the 3′ processing of the viral DNA LTR units.[89] At present there is only one drug currently approved by the FDA as an HIV-1 IN inhibitor, *viz*., Isentress™ **27** (Raltegravir; approved 2007).

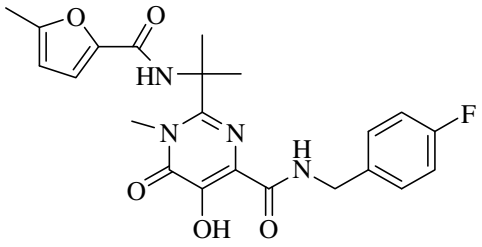

27
Raltegravir

Random screening of compounds has led to the identification of the β-diketo acid (DKA) moiety as an important structural motif capable of coordinating to metal ions in the enzyme active site.[90] This motif is highlighted in compound **28**, which proved to be particularly active. In a parallel study 5CITEP **29** was developed – a DKA analogue in which the acid moiety is replaced by a tetrazole group and the β-keto moiety is enolised.[91]

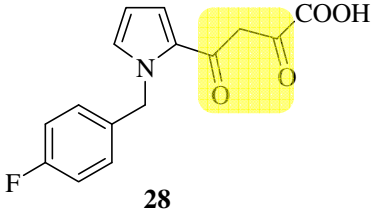

28
IC_{50} 3′ processing = 6 μM
IC_{50} strand transfer = 0.08 μM

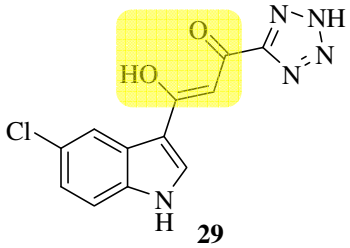

29
IC_{50} 3′ processing = 35 μM
IC_{50} strand transfer = 0.65 μM

Further modification of 5CITEP **29** by replacing the indole ring with other heterocycles led to a new series of potential IN inhibitors; one of these, compound **30**, showed significant promise but production was abandoned when it failed clinical efficacy trials.[91,92] Replacing the diketo acid moiety with a naphthyridine carboxamide system afforded compound **31**, which exhibits a similar mode of action and potent antiviral activity.[93] However, toxicity to the kidneys and liver during pre-clinical trials halted its production.[91]

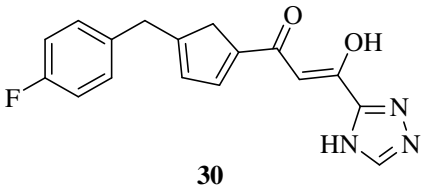

30

IC_{50} = 20 nM

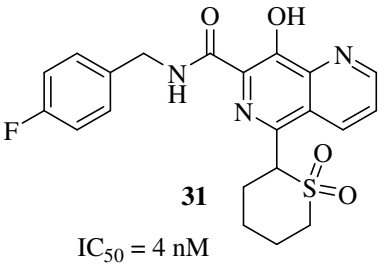

31

IC_{50} = 4 nM

Further development led to the pyrimidinone carboxamide analogues, with raltegravir **27**, emerging as a drug with good activity and pharmacokinetic profile.[94] Other compounds classified as IN inhibitors include cinnamoyl derivatives, coumarins and styrylquinolines.[95]

1.2.5. Rational Design of HIV-1 Protease Drugs

Enzymatic cleavage of polypeptide precursors, a process catalysed by HIV-1 PR, is a critical stage in the maturation of infectious viral particles.[96] The development of HIV-1 PR inhibitors has relied heavily on structure-based rational drug design. Such peptidomimetic inhibitors were designed to prevent polypeptide cleavage by acting as stable transition-state analogues which would resist proteolysis.[97] In order to address oral bioavailability, absorption and other pharmacological issues, non-peptidic inhibitors have been designed.[98] These compounds have almost no peptidic character.

Currently there are seven approved peptidomimetic HIV-1 PR inhibitors, *viz*., Invirase® **32** (Saquinavir; approved 1995), Norvir® **33** (Ritonavir; approved 1996), Crixivan® **34** (Indinavir; approved 1996), Agenerase® **36** (Amprenavir; approved 1999), Kaletra® **37** (Lopinavir, marketed with ritonavir; approved 2000), Lexiva® **38** (Fosamprenavir; approved 2003) and Reyataz® **39** (Atazanavir; approved 2003). There are also three non-peptidic HIV-1 PR inhibitors, *viz*., Viracept® **35** (Nelfinavir; approved 1997), Aptivus® **40** (Tipranavir; approved 2005) and Prezista® **41** (Darunavir; approved 2006).

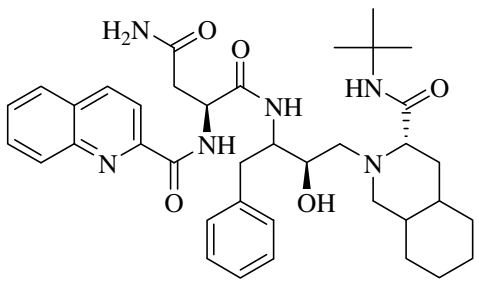

32

Saquinavir

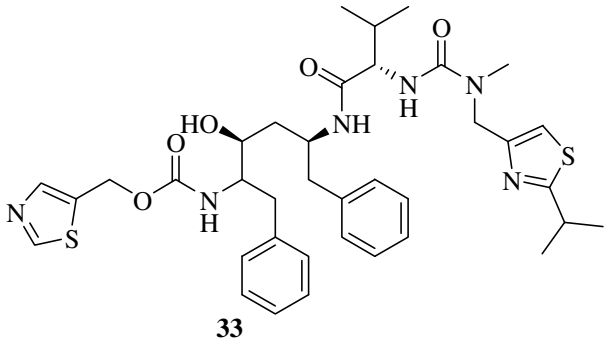

33

Ritonavir

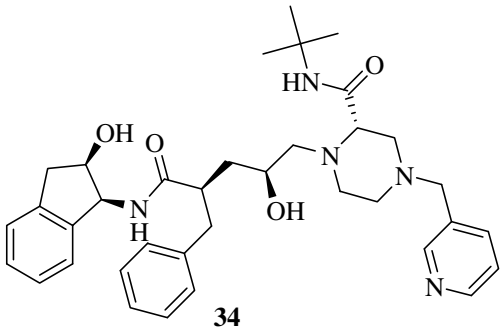

34
Indinavir

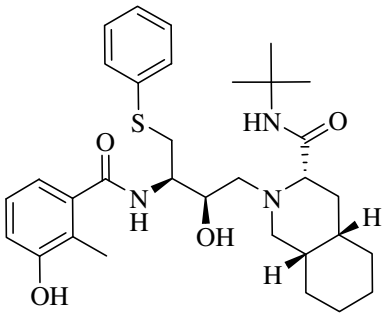

35
Nelfinavir

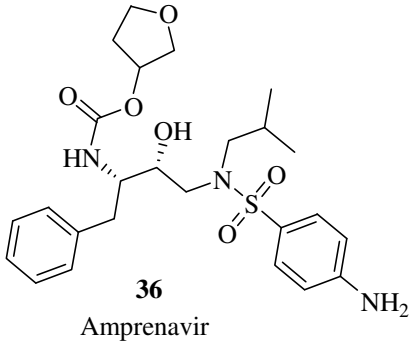

36
Amprenavir

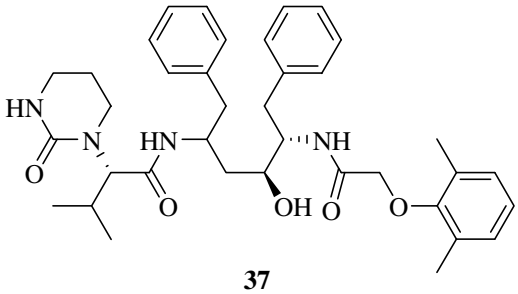

37
Lopinavir

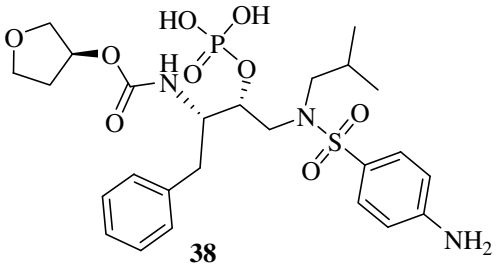

38
Fosamprenavir

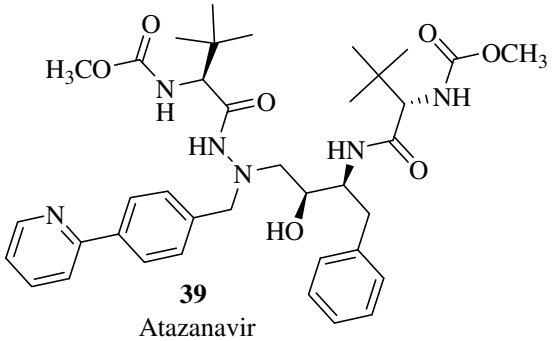

39
Atazanavir

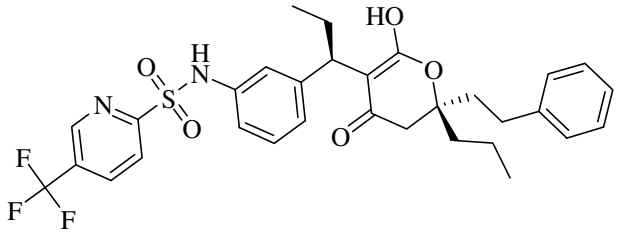

40
Tipranavir

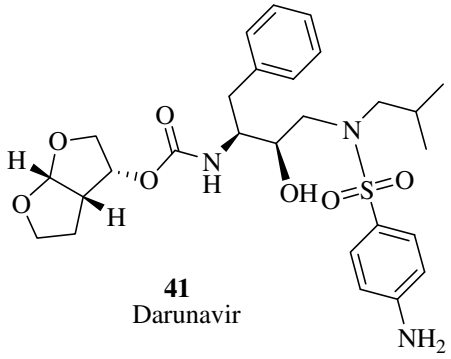

41
Darunavir

Broad-based, library screening (*i.e.* fluorescence-based bioassay) for potential non-peptidic protease inhibitors led to the identification of the 4-hydroxycoumarins warfarin **42** and then phenprocoumon **43** as suitable lead compounds with good oral bioavailabilty.[99] Modification of the coumarin nucleus eventually led to the 4-hydroxypyrone **44**, but its production was stopped

in preference to newer drugs with better activity profiles. Further modification of the coumarin moiety led to the sulphonamide dihydropyrone derivative, tipranavir **40**.[100]

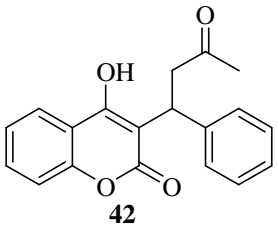

42
Warfarin

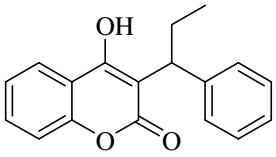

43
Phenprocoumon

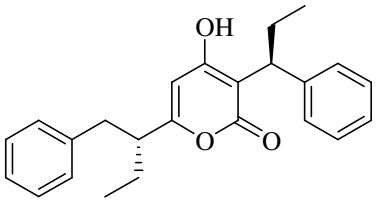

44

A 3D-database search, followed by theoretical calculations and a rational design process, led to the discovery of the cyclic ureas as another class of potential non-peptidic HIV-1 PR inhibitors, with compound **45** as an early lead compound.[101] Optimisation led to compound **46**, which entered clinical trials but had to be stopped due to poor solubility and the observation of variable blood levels following administration in humans.[101,102] Introduction of weakly basic *m*-aminobenzyl P_2/P_2' side groups led to the drug candidate, Mozenavir **47**, which reached clinical trials but its programme was stopped due to the absence of advantages over existing HIV-1 PR inhibitors.[100]

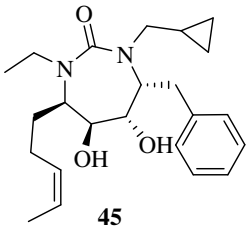

45

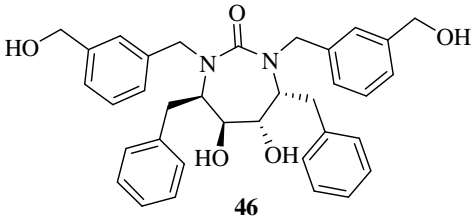

46

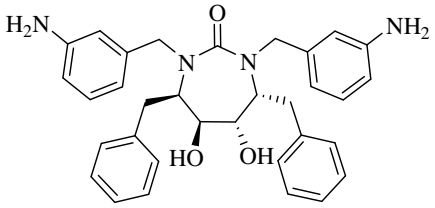

47
Mozenavir

Other scaffolds that have received attention as potential non-peptidic HIV-1 PR inhibitors include tricyclic ureas,[103] dimeric 4-aryl-1,4-dihydropyridines,[104] diaminopyranosides[105] and β-D-mannopyranosides.[106]

1.2.6. Dual-Action Compounds

Dual-action drugs are compounds which exhibit two different but desired pharmacological actions. For the treatment of AIDS, the highly active antiretroviral therapy (HAART), which is a combination treatment involving the use of several HIV drugs, has been used to address the problem of drug resistance encountered with single drug treatment. However, failure to adhere strictly to complicated dosing regimes with their associated side effects has often led to viral

rebound, and, in worse cases, multidrug resistance.[107] Consequently, there is an emerging interest in multi-target therapy where single drugs are designed to inhibit more than one viral enzyme, typically two, with the possibility of reduced toxicity and simplified dosage.[108]

Morphy and Rankovic proposed the name Designed Multiple Ligands (DMLs), to describe compounds with multiple biological profiles, rationally designed to target a specific disease.[109] Depending on the ligand structure they also proposed names for different classes of DMLs, *viz*., "*conjugates*" – compounds in which two scaffolds are joined by a linker; "*fused*" – compounds that are directly coupled with no linker; and "*merged*" – compounds with different functionalities integrated into a single scaffold. It is also possible to classify these compounds in terms of the target binding sites, *e.g*. dimeric and hybrid anti-Alzheimer drug candidates which bind to adjacent pockets of the same protein.[110,111] In 2007, Wang and co-workers proposed the term, portmanteau inhibitor, to define a drug that is a combination of two scaffolds, each of which is an inhibitor.[108]

It has been observed that the catalytic core of both HIV-1 IN and RNase H share an αβ-fold with similar topology, have analogous active site geometries, have active sites that require a divalent metal (probably Mg^{2+}) co-factor and are folded in a similar way.[112-114] Thus, IN and RT have received increased attention as dual targets in HIV chemotherapy. By chemically linking an IN pharmacophore to a known, potent RT inhibitor, Wang and co-workers were able to synthesise the first class of rationally designed RT/IN inhibitors.[108] A typical example involves the incorporation of the DKA moiety in a 6-benzyl-1-(benzyloxymethyl)-5-isopropyl-uracil derivative **50** (Figure 7).

The synthetic route to compound **50**, outlined in Scheme 1, involves chemoselective reduction of the aldehyde **51** to give the benzyl alcohol intermediate **52**, from which the chloromethyl ether **53** is prepared. Regioselective N-1 alkylation of compound **54** (prepared according to a known procedure)[115] by the chloromethyl ether **53** affords the ketone **55**, which is then condensed with diethyl oxalate and hydrolysed to produce compound **50**.

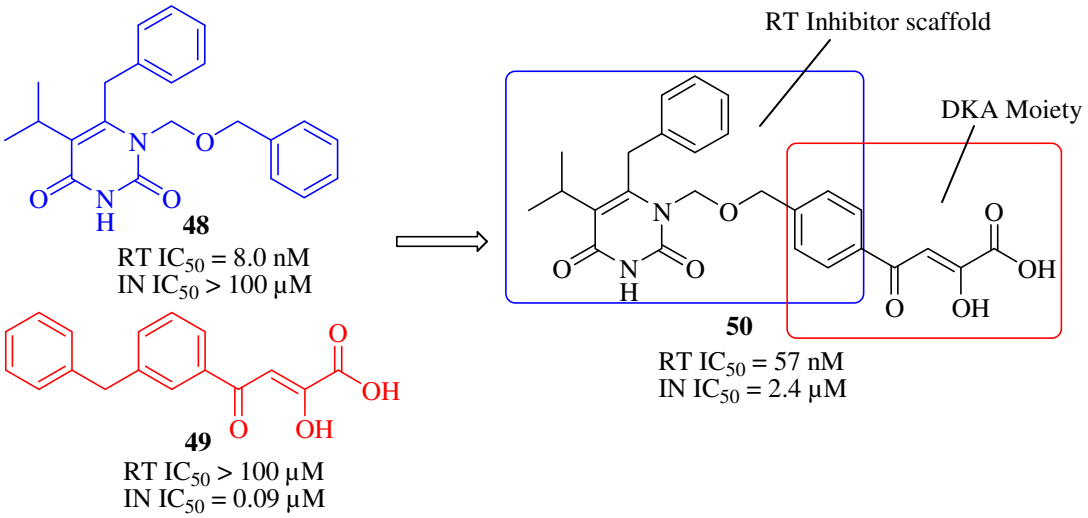

Figure 7. Design of RT-IN dual inhibitor **50** based on RT inhibitor **48** and IN inhibitor **49**.[108]

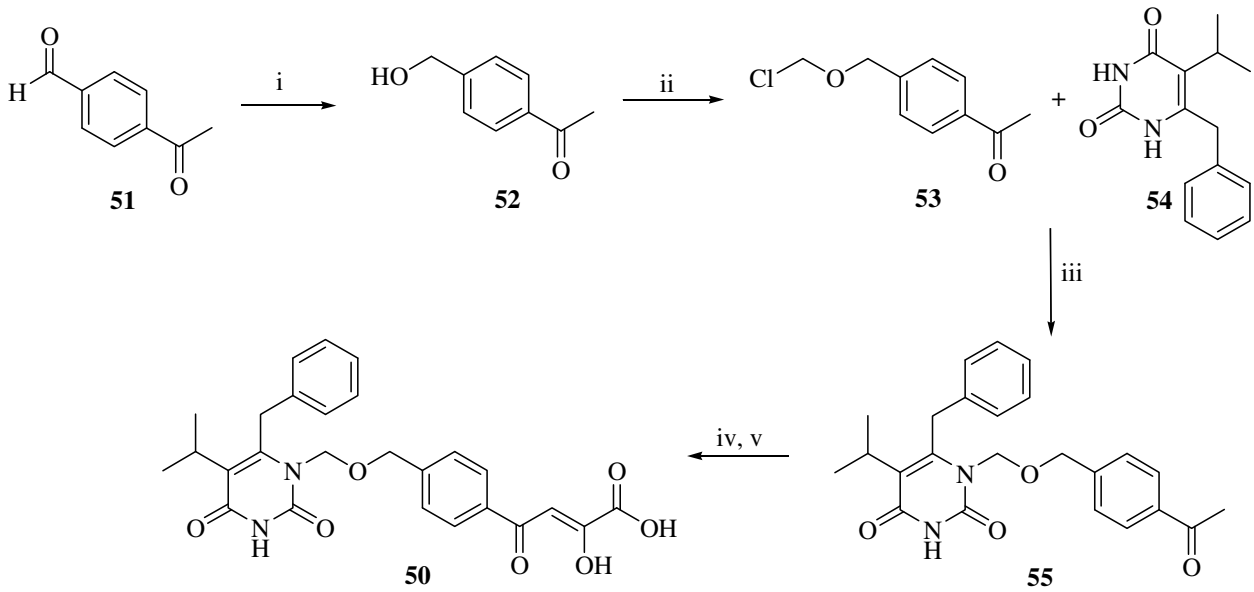

Scheme 1. Synthesis of RT-IN dual inhibitor **50**.

Reagents and conditions: (i) $NaHB(OAc)_3$, THF, 65 °C, 83%; (ii) (HCHO)*n*, TMSCl, r.t.; (iii) $CH_3(OTMS)C{=}NTMS$ (BSA), CH_2Cl_2, r.t., then **53**, tetrabutylammonium iodide (TBAI), 76%; (iv) NaOEt, EtOH, diethyl oxalate; (e) 1N-NaOH, EtOH – CH_2Cl_2, r.t., 79% over two steps.[108]

Following the successful development of compound **50**, which showed good dual RT-IN inhibition, the approach was used to synthesise compound **56** by replacing the methylsulphonamide group in compound **15** with a DKA moiety (Figure 8).[116] Compound **56** was prepared as shown in Scheme 2. Thus, the aniline derivative **57** was diazotized and then reacted with ethyl α-methylacetoacetate **58** to give the hydrazone **59**.[117] Microwave irradiation of the hydrazone in trifluoroacetic acid gave the desired indolecarboxylate ester **60**, saponification

of which gave the acid **61**. Coupling with the piperazine derivative **62** produced intermediate **63**, which, when condensed with ethyl oxalate followed by saponification, afforded the desired dual inhibitor **56**.

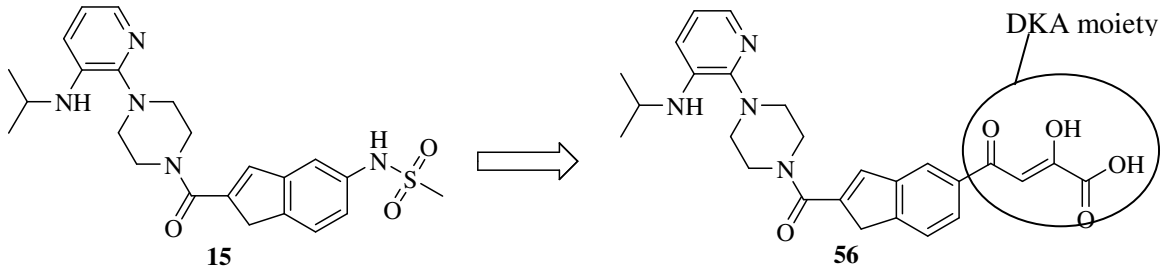

Figure 8. Design of RT-IN dual inhibitor **56** involving replacing the sulphonamide group in compound **15** with a DKA moiety.[116]

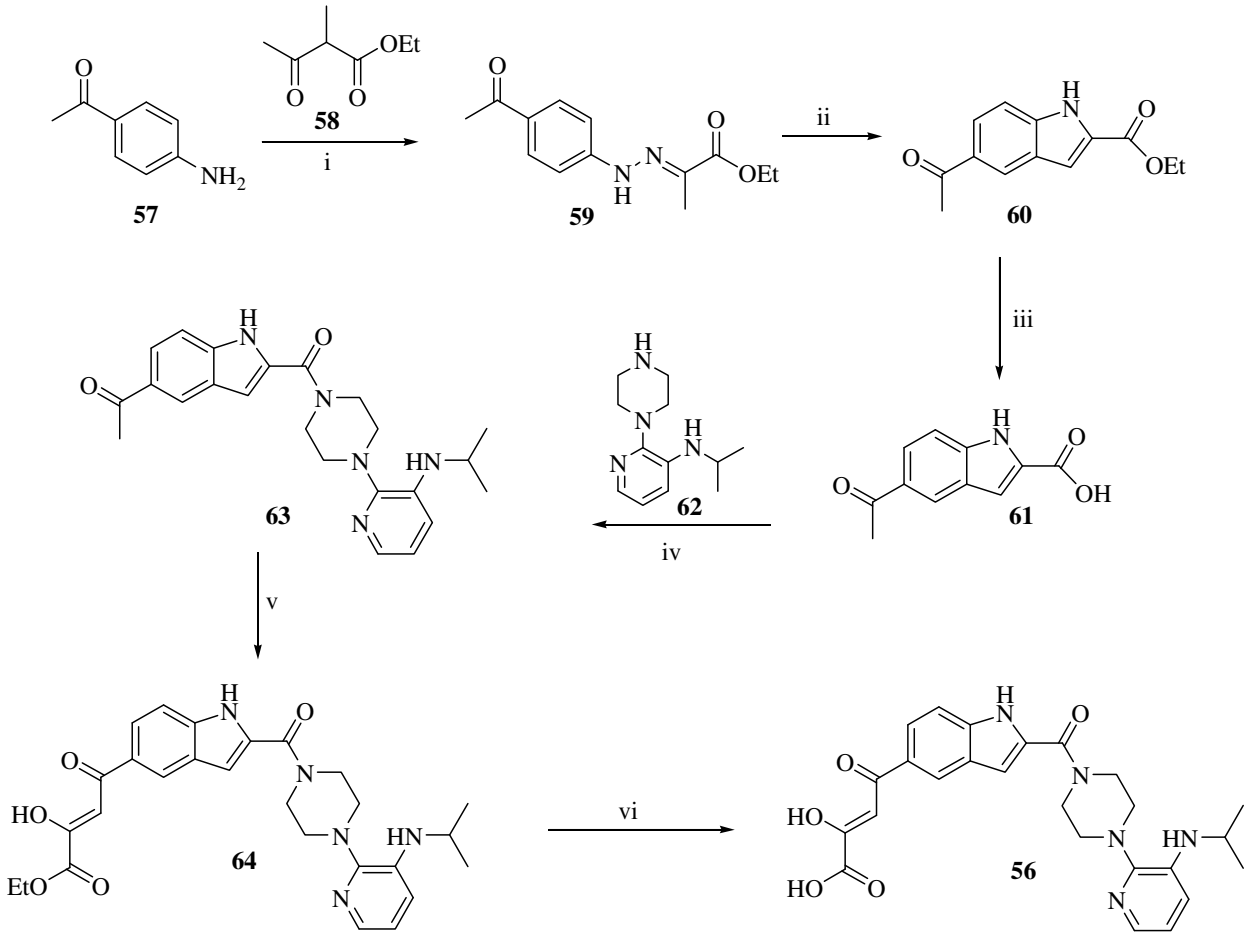

Scheme 2. Synthesis of RT-IN dual inhibitor **56**.

Reagents and conditions: (i) $NaNO_2$, HCl; **58**, KOH, 91%; (ii) microwave, 140 °C, 15 min, 45%; (iii) NaOH (aq), EtOH, reflux, 3 h, 44%; (iv) **62**, CDI, DMF, r.t., 62%; (v) Na / EtOH, diethyl oxalate, r.t., 3 h; (vi) NaOH (aq), EtOH – $CHCl_3$, r.t., 1 h, 41% over 2 steps.[116]

SAR and docking studies have been used to identify key pharmacophores and to explore the importance of the nature and length of the linkers in portmanteau inhibitors.[118,119] Other families of compounds with potential as dual RT-IN inhibitors are also being investigated.[116,118-121]

In a separate investigation, 3,7-dihydroxytropolone **65** and other tropolone derivatives were shown to chelate the metal ions in the active site and thus inhibit both HIV-1 RT and IN activity.[112,122,123] However, cellular toxicity has limited the application of these compounds as antiviral agents.[122] Madurahydroxylactone derivatives, such as compound **66**, have been reported to show good dual inhibition against both HIV-1 RT and IN enzymes. Some of these compounds showed selectivity for one of the enzymes over the other and so could be useful in generating pharmacophores for each enzyme.[124]

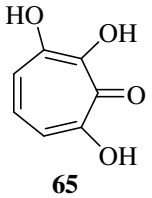

65

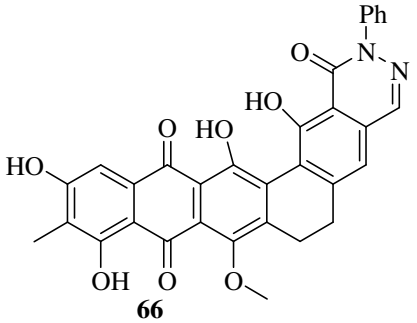

66

2-Hydroxyisoquinoline-1,3(2*H*,4*H*)-dione derivatives have been found to selectively chelate metal ion catalytic active sites, showing HIV-1 RT and IN enzyme inhibitory activity at micromolar concentrations. Compound **67**, synthesized as shown in Scheme 3, displayed a high selectivity for IN with a submicromolar IC_{50} value. However these compounds have also exhibited high cellular cytotoxicity in cell culture thereby presently limiting their application in antiviral chemotherapy.[125]

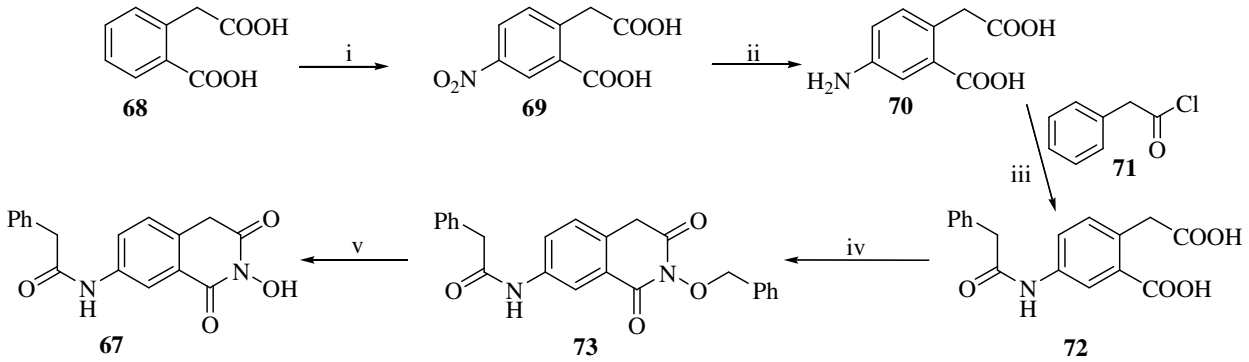

68 **69** **70** **71** **72** **73** **67**

Scheme 3. Synthesis of RT-IN dual inhibitor **67**.

Reagents and conditions: (i) fuming HNO_3, 0 °C, 2 h; (ii) H_2, 5% Pd/C, MeOH; (iii) (a) 1.0 equivalent of **71**, 2N-KOH, 2 h, r.t., (b) 2N-HCl, r.t.; (iv) 1.2 equivalent of NH_2OBn, toluene, Dean-Stark apparatus, reflux, 12 h; (v) BBr_3, 4.0 equivalent, r.t., 1 h; H_2O, r.t., 15 min.[125]

1.3. COUMARINS

Coumarin **73** (2*H*-chromen-2-one, 2*H*-1-benzopyran-2-one, *o*-hydroxycinnamic acid lactone or 2-oxo-1-benzopyran) is a benzo-α-pyrone – a heterocyclic compound in which a benzene ring is fused to a pyrone ring with an oxygen atom at the α-position.[126] Coumarins are mostly formed *via* the shikimate-chorismate biosynthetic pathway.[127] Daphnin **74** (7-β-D-glucopyranosyloxy-8-hydroxycoumarin) was the first coumarin derivative to be isolated (in 1812 from *Daphne alpine*) and shortly afterwards (1820), coumarin itself was isolated from the tonka bean (*Dipteryx odorata* L.) by Vogel.[126,128] Coumarin and its derivatives have been found to occur naturally in a wide array of plants where they are known to regulate plant growth and absorb UV-radiation.[126,128]

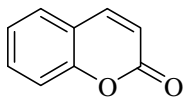

73
Coumarin

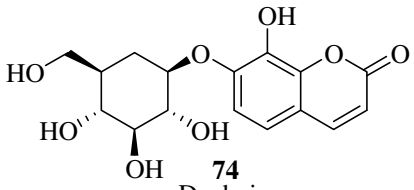

74
Daphnin

Coumarins can be classified into eight subtypes according to their structures: (i) *simple coumarins* – this includes compounds hydroxylated, alkoxylated or alkylated on the benzene ring, and their glycosides (*e.g.*, umbelliferone **75**);[128,129] (ii) *furanocoumarins* (or furocoumarins) – coumarin derivatives with a five-membered furan ring attached to the coumarin moiety, exemplified by the linear furanocoumarin psoralen **76** and the angular analogue angelicin **77**;[128,129] (iii) *pyranocoumarins* – which contain a six-membered ring attached to the coumarin moiety, as in the *linear* pyranocoumarin xanthyletin **78** and the *angular* analogue seselin **79**;[129] (iv) *pyrone-substituted coumarins* – which bear substituents at positions 3 or 4, *e.g.*, warfarin **42**;[129] (v) *benzocoumarins*, *e.g.*, ellagic acid **80**;[128] (vi) *coumestans*, *e.g.*, coumestrol **81**;[128] (vii) *isocoumarins*, *e.g.*, hydrangenol **82**;[128] and (viii) *complex structures* which include a coumarin moiety, *e.g.*, novobiocin **83**.[128]

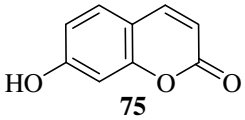

75
Umbelliferone

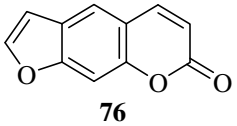

76
Psoralen

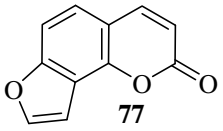

77
Angelicin

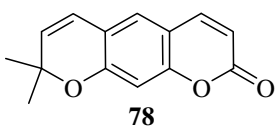

78
Xanthyletin

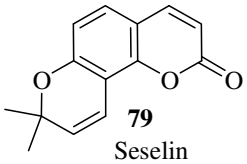

79
Seselin

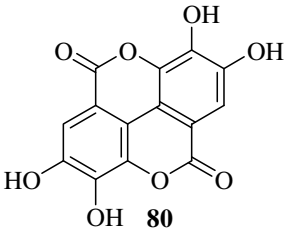

80
Ellagic acid

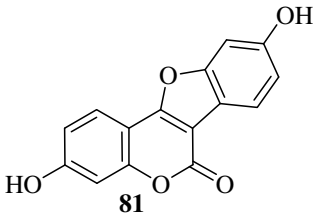

81
Coumestrol

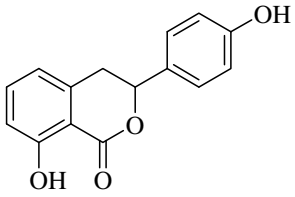

82
Hydrangenol

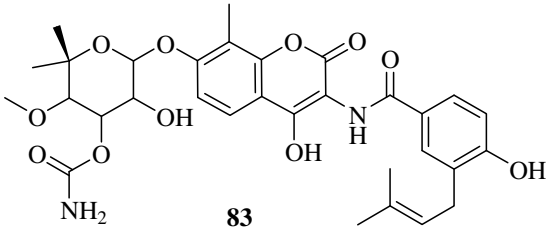

83
Novobiocin

Owing to the large number of naturally occurring coumarin derivatives, it is not surprising that many of these compounds have found application in various fields including perfumery and cosmetics, alcoholic beverages and medicine.[130] The biological activities of coumarin derivatives include anticoagulant (*e.g.*, tromexan **84**),[131] antibiotic (*e.g.*, novobiocin **83**), antipsychotic (*e.g.*, compound **85**),[132] antitumor (*e.g.*, umbelliferone **75**)[133] and anti-HIV properties (*e.g.*, compounds **86** and **87**).[134-136] Due to the importance of these compounds, there continues to be significant interest in their chemistry.

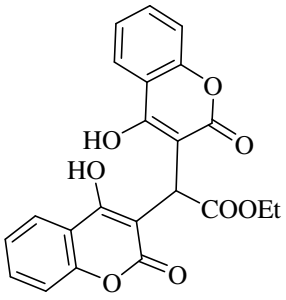

84
Tromexan

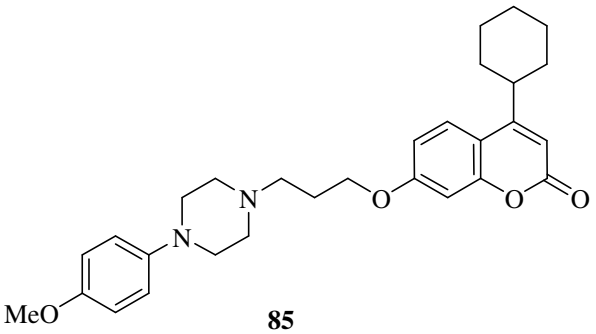

85

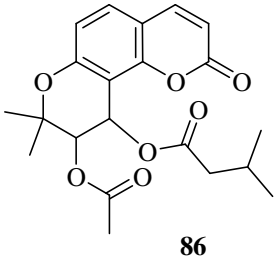

86

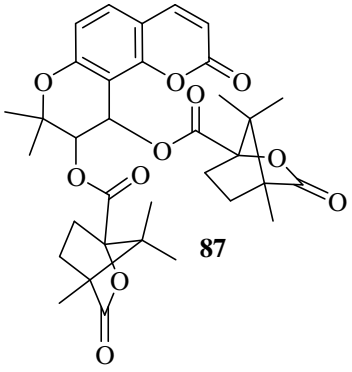

87

1.3.1. Synthesis of Coumarins

A number of classical methods have been developed for the synthesis of coumarins. These include the Perkin,[137] Pechmann,[138] Knoevenagel,[139] Michael[140] and Wittig[141] reactions; more recent methods involve palladium-catalysed addition[142] and ring-closing metathesis.[143]

1.3.1.1. Perkin Reaction

The Perkin reaction, which appears to be the first method to have been used for the synthesis of coumarins, involves the formation of α,β-unsaturated carboxylic acids by aldol condensation of aromatic aldehydes (*e.g.*, *o*-hydroxybenzaldehydes) and acid anhydrides in the presence of an alkali salt of the acid.[137,144] Several alternative catalysts have been used for this reaction; these include carbonates, acetates, sulphides and sulphites of sodium or potassium and even tertiary amines and pyridine (Scheme 4).[144,145]

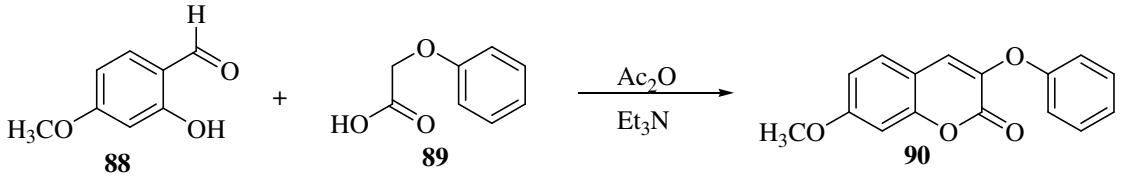

Scheme 4. Synthesis of a coumarin analogue *via* the Perkin reaction. [145]

1.3.1.2. Pechmann Reaction

This reaction involves the synthesis of coumarins by condensation of a phenol with a β-ketoester in the presence of a catalyst.[138] Traditionally, homogenous catalysts, such as H_2SO_4, HCl, H_3PO_4 and CF_3COOH, have been used,[146,147] but long reaction times, high temperature requirements and side products are accompanying challenges. Lewis acids, such as $ZnCl_2$, $SnCl_4$, $AlCl_3$, $InCl_3$, GaI_3 and $Sm(NO_3)_3$, have also proved to be good catalysts for the Pechmann reaction, although some of these also require high temperatures or long reaction times.[148-150] Heterogeneous catalysts, such as cation exchange resins, zeolites, acidic ionic liquids and solid acids have also found application as Pechmann reaction catalysts.[151-154] Recently microwave irradiation has been employed to reduce the reaction time.[152,155]

As shown in Scheme 5, the mechanism of the Pechmann reaction begins with an acid-catalysed transesterification step followed by a keto-enol tautomerism. The next step involves the formation of the coumarin skeleton *via* Michael addition, followed by re-aromatisation and dehydration.[156]

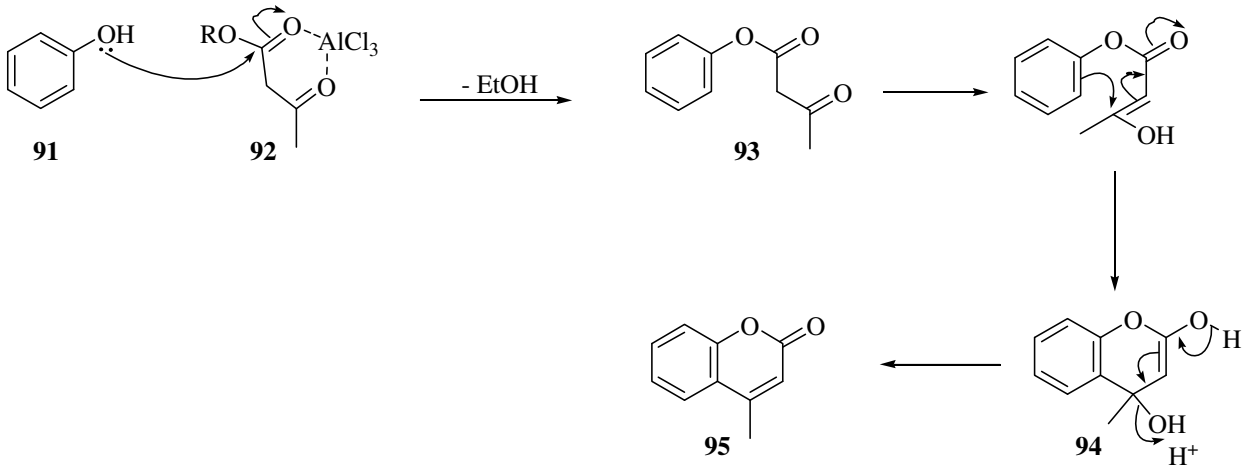

Scheme 5. Mechanism of the Pechmann condensation.[156]

1.3.1.3. Knoevenagel Reaction

The Knoevenagel reaction is a modification of the aldol reaction and involves the condensation of an aldehyde or ketone (often without an α-hydrogen) with an activated methylene compound in the presence of an organic or inorganic base, a Lewis acid or Lewis base or even an ionic liquid to give an α,β-unsaturated compound.[139,157,158] The reaction is activated by electron-withdrawing groups, such as CN, CHO, NO_2, COR, COOH, COOR, SO_2R, SO_2OR. Several coumarins have been synthesized *via* the Knoevenagel procedure by using *o*-hydroxy-arylaldehydes, such as 2-hydroxy-1-naphthaldehyde **96** and an activated methylene compound, as illustrated in Scheme 6.[159-161]

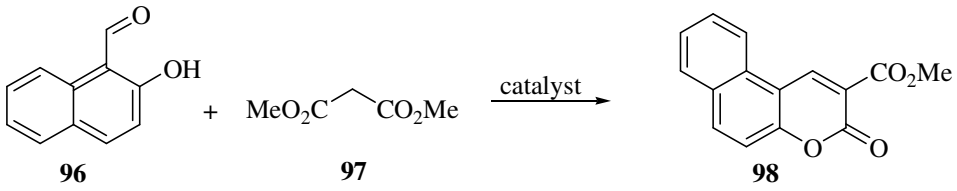

Scheme 6. A typical Knoevenagel reaction.[160]

1.3.1.4. Michael Reaction

Coumarin derivatives can also be synthesised by addition of aryllithiums (generated by reacting a protected phenol with BuLi) to ethoxymethylenemalonate or ethoxymethyleneacetoacetate esters, followed by acid-catalysed lactonisation (Scheme 7).[140] 4-Arylchroman-2-ones have also been synthesized by a Michael-type reaction, in which di- or trihydric phenols are treated with *p*-substituted *N*-cinnamoylazoles in the presence of DBU.[162]

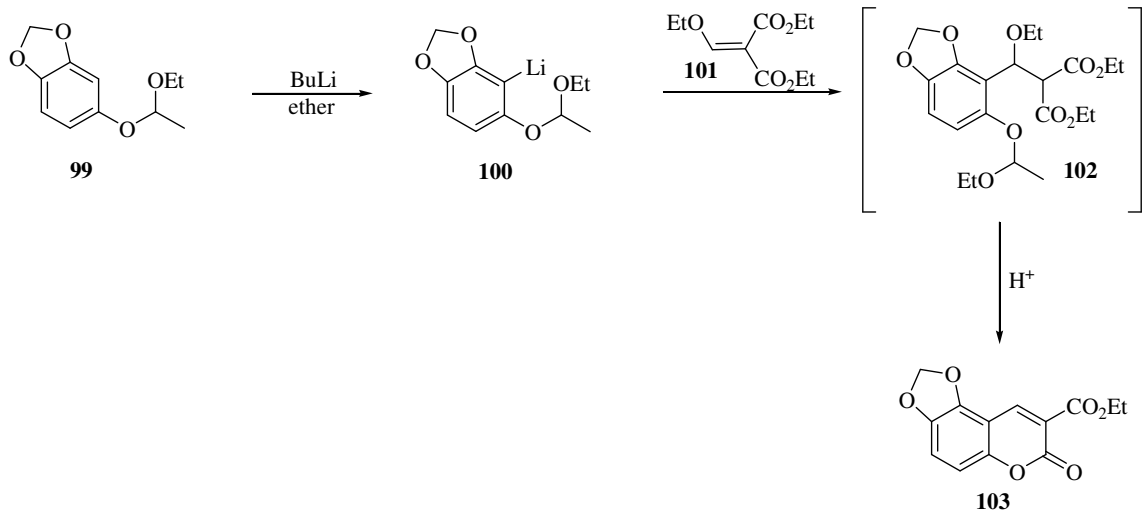

Scheme 7. Synthesis of the coumarin analogue **103** *via* a Michael reaction.[140]

1.3.1.5. Wittig Reaction

This involves reaction of an aldehyde or ketone with a phosphonium ylide to give an alkene, as shown in Scheme 8.[141,163,164] Thus, 4-methoxysalicylaldehyde **88** reacts with the carbethoxy-methylenephosphorane **104** (Wittig reagent) to give a cinnamate intermediate which is then cyclised to the coumarin.[165,166]

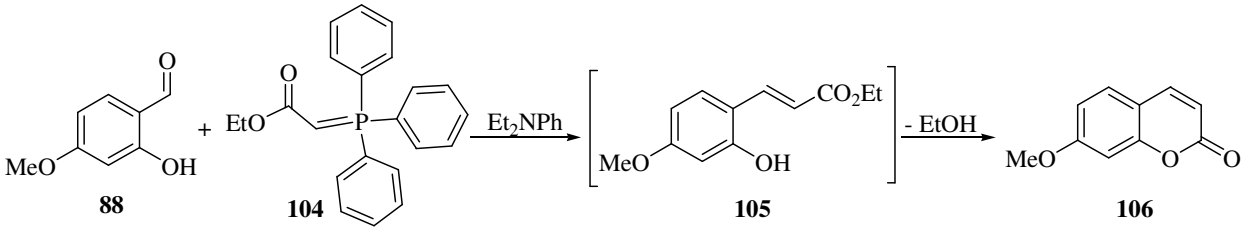

Scheme 8. Synthesis of 7-methoxycoumarin using the Wittig reaction.[166]

1.3.1.6. Palladium-Catalysed Addition

Palladium(0) has been found to catalyse the reaction of phenolic substrates with ethyl propynoate to form coumarins in good yields. Pd(0), which is formed *in situ* by formic acid reduction of Pd(II), catalyses the reaction *via* electrophilic palladation, followed by carbametallation, protonolysis and finally cyclisation to give the product **107** (Scheme 9).[142]

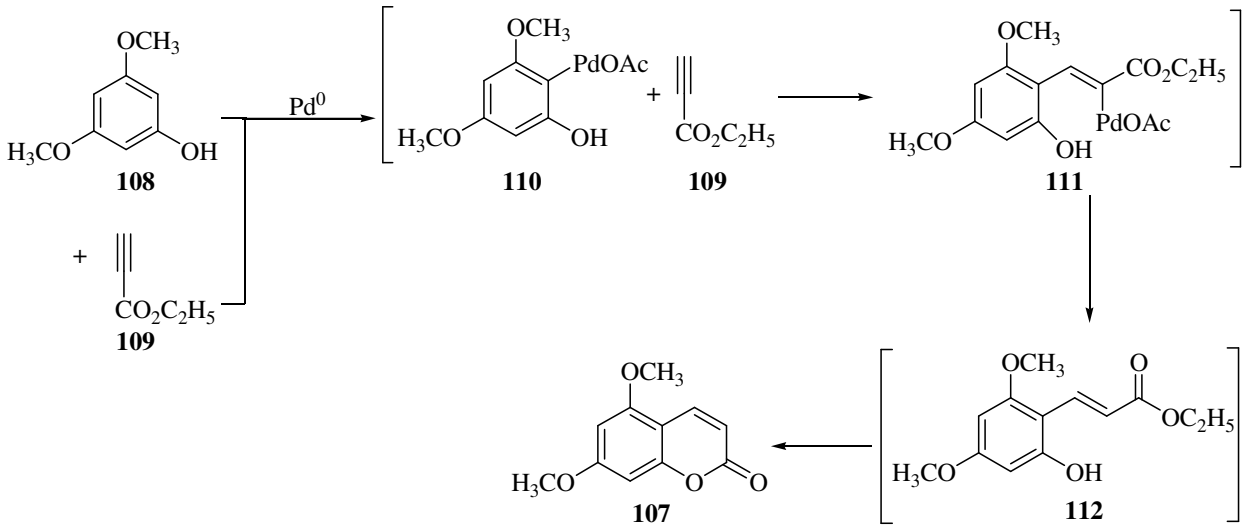

Scheme 9. Palladium-catalysed synthesis of coumarin analogue **107**.[142]

1.3.1.7. Ring-Closing Metathesis

Metathesis is a convenient method for making alkene-containing compounds by redistributing the alkene fragments in olefins.[167] The ring-closing metathesis route to coumarins has been shown to give excellent yields with the highly active ruthenium-based catalyst **116** (Grubbs' second-generation catalyst).[143] Scheme 10 shows the synthetic path to coumarin **73** using this approach.

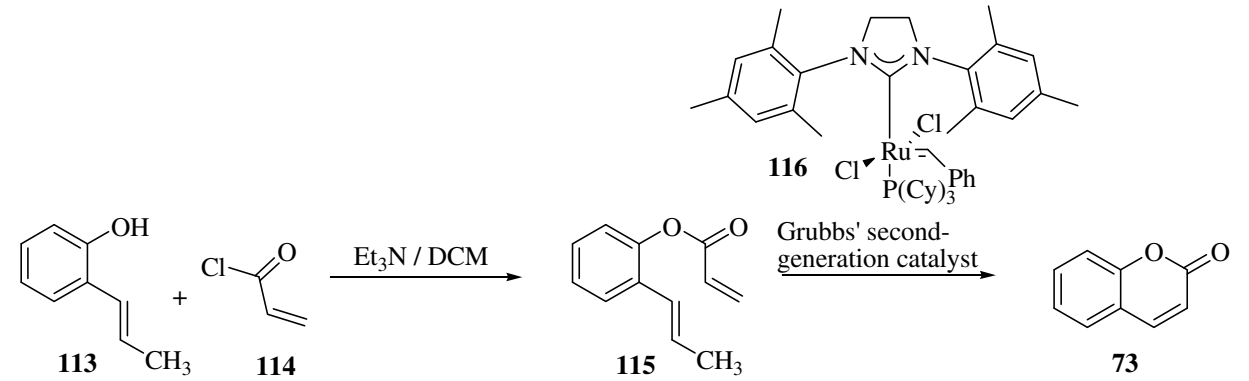

Scheme 10. Synthesis of coumarin **73** *via* ring-closing metathesis.[143]

1.4. CINNAMATE ESTERS

Cinnamic acid (3-phenylprop-2-enoic acid) **117** and its esters have found important applications as agrochemicals (*e.g.*, phenethyl cinnamate **118**), food additives (*e.g.*, methyl *p*-methoxy-

cinnamate **119**), fragrances (*e.g.*, ethyl cinnamate **120**), light-sensitive (*e.g.*, octyl *p*-methoxycinnamate **121**) and electrically conductive materials (*e.g.*, polytolane cinnamate **122**) and pharmaceuticals (*e.g.*, isoamyl cinnamate **123**).[168] Cinnamates are distributed widely in plants and their biological properties, particularly antioxidant activity exhibited, for example, by ethyl ferulate **124**, have been documented.[169-171] Cinnamate esters, such as L-chicoric acid **125** have recently enjoyed attention as potential anti-HIV compounds.[172]

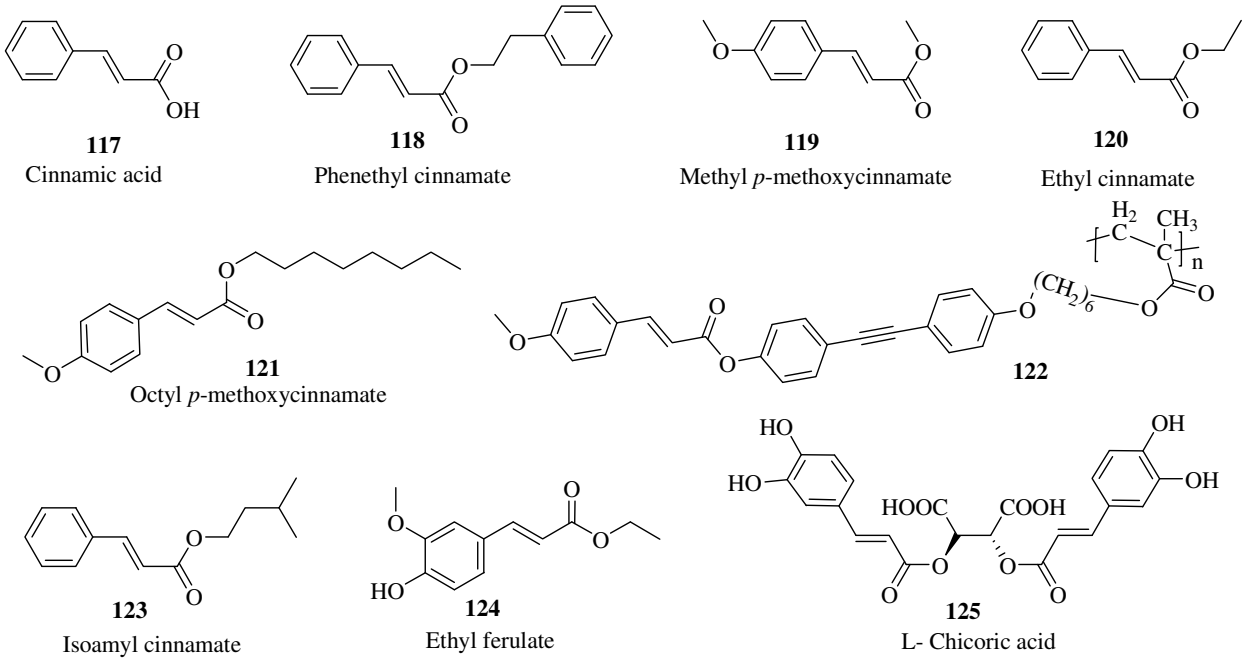

1.4.1. Synthesis of Cinnamate Esters

Conventional methods for synthesising cinnamate esters include the aldol-type reaction,[173-174] direct esterification of cinnamic acids[171,175] and organopalladium-catalysed arylation or carboalkoxylation of olefins (Heck reaction).[176] Other methods include the Wittig and Horner-Wadsworth-Emmons (HWE) reactions.[177,178]

1.4.1.1. Aldol-type Reaction

The aldol-type condensation, a well-established method of preparing cinnamate esters, involves reaction between an aromatic aldehyde and an ester in the presence of a basic catalyst (sodium metal, sodium alkoxide or lithium dialkylamides).[174,179,180] Scheme 11 illustrates the sodium ethoxide-catalysed synthesis of ethyl cinnamate **120** from benzaldehyde **126** and EtOAc **127**.

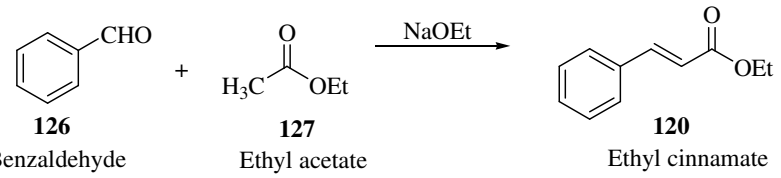

126 Benzaldehyde + **127** Ethyl acetate → **120** Ethyl cinnamate

Scheme 11. Synthesis of ethyl cinnamate **120** by an aldol-type reaction.[174]

1.4.1.2. Esterification of Cinnamic Acids

Ethyl cinnamate **120** can be readily prepared by reacting cinnamic acid with ethanol in the presence of either hydrogen chloride or sulphuric acid.[174] Interestingly the esterification of cinnamic acids can now be effected biocatalytically using lipase enzymes, such as porcine pancreatic lipase immobilised on hydrogel and Novozym 435 (*Candida antarctica* lipase immobilized on acrylic resin).[170,171] Immobilized lipases are inexpensive, commercially available, stable to heat and chemicals, require mild reaction conditions, are easy to handle and afford fewer side-reactions.[170,181] Such esterification of ferulic acid is illustrated in Scheme 12.

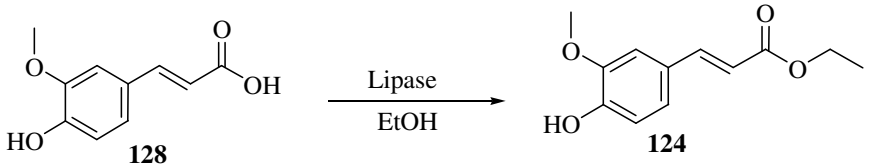

128 Ferulic acid → **124** Ethyl ferulate

Scheme 12. Synthesis of ethyl ferulate using lipase.[171]

1.4.1.3. Heck Reaction

The Heck reaction is the name given to the palladium-catalyzed carbon-carbon coupling between an aryl or vinyl halide (or triflate) and an activated alkene in the presence of a base.[176,182] Two mechanisms have been proposed for this reaction: one involving a neutral Pd pathway, which favours electron-deficient alkenes, and the other involving a cationic Pd pathway, which favours electron rich alkenes.[183-185] There have been several modifications to the Heck reaction with regard to reaction conditions and the choice of catalyst and base.

Methyl cinnamate **129** has been synthesised from the Heck reaction between iodobenzene **130** and methyl acrylate **131** in *N*-methylpyrrolidone (NMP) as solvent and Pd/C as catalyst under ultrasonic conditions (Scheme 13).[186] $PdCl_2$, $Pd(OAc)_2$, $PdCl_2(CH_3CN)_2$, $Pd(PPh_3)_4$ and $Pd(dba)_2$ are some of the catalysts used for Heck reactions, while secondary or tertiary amines and alkali

metal salts (*e.g.*, NaOAc, KOAc, K_2CO_3 and $KHCO_3$) have been used as bases.[186,187] When a Pd(II) source is used, it must be reduced to Pd(0) before entering the catalytic cycle.[187]

Recently the scope of the Heck reaction has been extended by the introduction of "ligand-free" palladium catalysis, using palladium nanoparticles immobilized on a solid support. Under these conditions, water can be used as the solvent and tetrabutylammonium bromide (TBAB) as a phase transfer catalyst.[188,189]

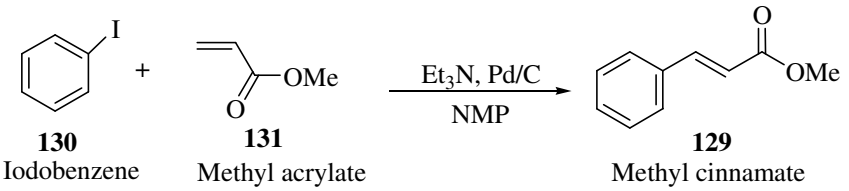

130 Iodobenzene | **131** Methyl acrylate | **129** Methyl cinnamate

Scheme 13. Heck reaction of iodobenzene with methyl acrylate.[186]

1.5. THE BAYLIS-HILLMAN REACTION

The atom economical Baylis-Hillman reaction, typically involves formation of a carbon-carbon bond between an aldehyde **132** and an activated alkene **133** bearing an electron-withdrawing group (EWG), in the presence of a tertiary base to afford a multi-functional product **134** as illustrated in Scheme 14.[190,191] It has been described as a three-step reaction combining successive Michael, aldol and elimination reactions in one pot in the presence of a catalyst.[191,192] The activated alkenes used have varied from cyclic and acyclic alkenes to alkynes and even allenes. Typical catalysts for this reaction include 1,4-diazabicyclo[2.2.2]octane **135** (DABCO), 1,8-diazabicyclo[5.4.0]undec-7-ene **136** (DBU), tetramethylethylenediamine **137** (TMEDA) and 3-quinuclidinol **138** (3HQ).[190-192] Tertiary phosphines have also been found to catalyse this reaction.[193] Prochiral electrophiles may afford products with one or more stereogenic centres, and the reaction has lent itself to asymmetric versions.[194] Functional elaboration (*e.g.* acetylation or bromination) of Baylis-Hillman adduct **134** (Scheme 15), may facilitate access to more complex scaffolds.[191]

A major challenge associated with the Baylis-Hillman reaction is the time requirement. Some of these reactions have been reported to require days or even weeks depending on the aldehyde (or electrophile), activated alkene and the catalyst in use.[194] Efforts at improving the reaction rate have involved, *inter alia*, the use of dual catalysts, high pressure conditions, microwave

irradiation, ultrasound, temperature variation, solid support, polar solvents, ionic liquids and additives.[190,195]

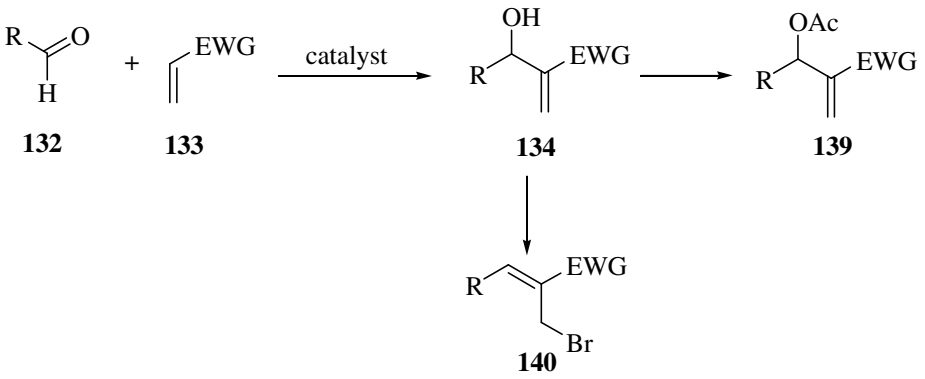

Scheme 14. General representation of the Baylis-Hillman reaction.[191]

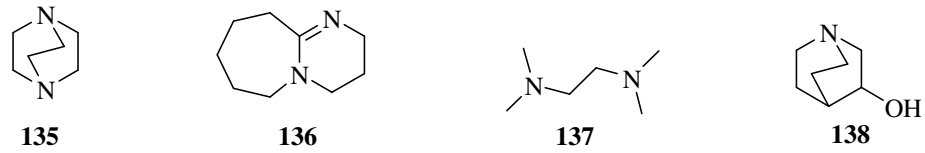

Efforts have been made to understand the mechanism and kinetic parameters of this transformation.[196] However, after about 40 years since its discovery (including some 30 years of extensive study), some mechanistic questions remain unresolved.[197]

1.6. PREVIOUS WORK IN THE GROUP

Applications of the Baylis-Hillman reaction in the construction of benzannulated heterocycles and the isolation of various unexpected products have been carried out by our research group during recent years – results which have provided the platform for the present study. Compounds obtained in earlier studies include indolizines,[198] quinolines,[199] thiochromenes,[200] chromenes, coumarins[209,210] and the complex polycyclic systems illustrated in Scheme 15.[201,202]

There has been extensive work on the reactions of salicylaldehydes with activated alkenes in the presence of DABCO and on exploring the mechanism of the Baylis-Hillman reaction.[203] Bode established the route to indolizines[198,204] and on reacting salicylaldehyde **142a** with methyl

acrylate **131**, observed that a coumarin derivative **143** had formed instead of the expected Baylis-Hillman adduct (Scheme 16).[205]

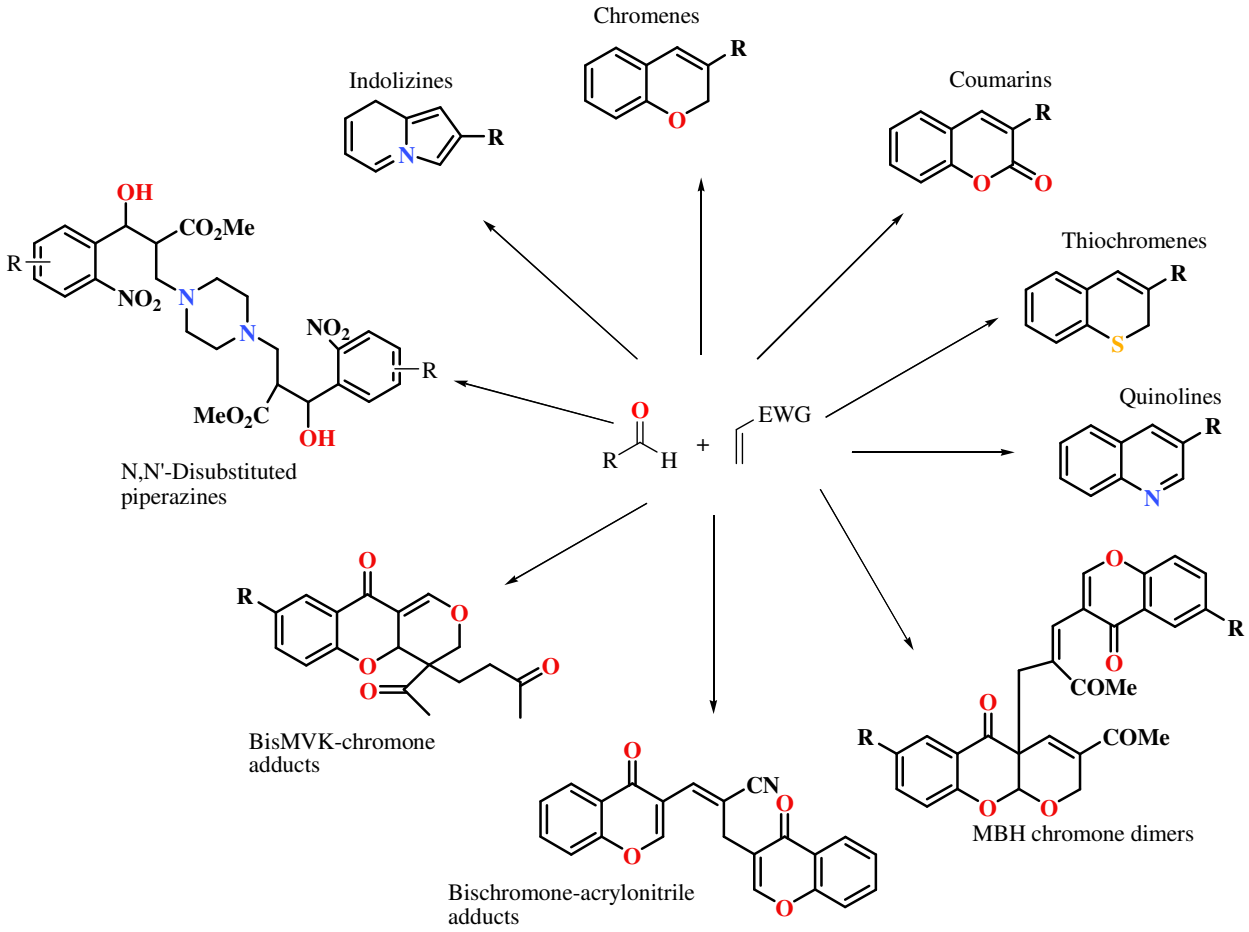

Scheme 15. Different compounds accessed *via* the Baylis-Hillman reaction in our group.

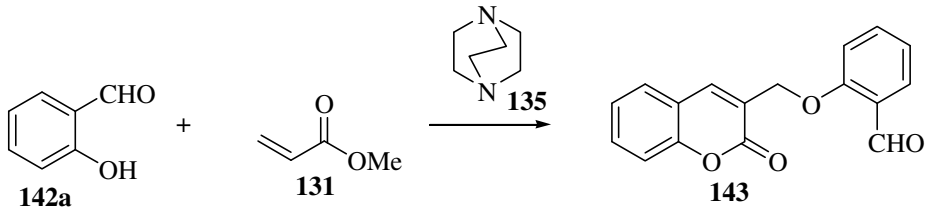

Scheme 16. Reaction of salicylaldehyde with methyl acrylate.[205]

Robinson later showed that the reaction illustrated in Scheme 18 actually leads to a cascade of chromene and coumarin derivatives (Scheme 17).[206,207] This has since been shown to proceed *via* an intermediate Baylis-Hillman adduct **144** which cyclises spontaneously following path I (conjugate addition) or II (acyl substitution).[201]

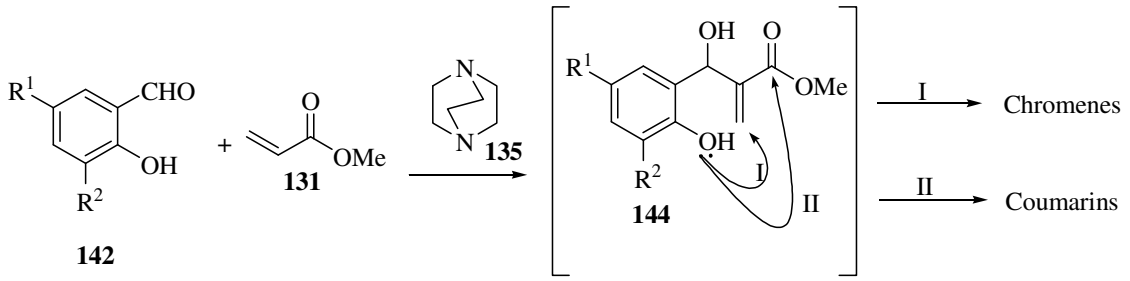

Scheme 17. Non-regioselective Baylis-Hillman cyclisation.[208]

By varying the activated alkene to preclude acyl substitution, Nocanda was able to achieve regioselective cyclisation to afford chromenes (Scheme 18).[202]

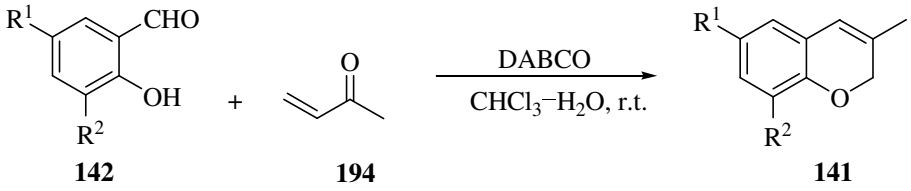

Scheme 18. Regioselective Baylis-Hillman cyclisation to chromenes.[202]

Musa, on the other hand, synthesized coumarin derivatives initially using the *O*-benzylated Baylis-Hillman adducts (Scheme 19). This method gave access to 3-substituted coumarins of different types depending on the haloacid used for the cyclisation procedure. He then showed that by using *tert*-butyl acrylate **152** as the activated alkene, it was possible to isolate the Baylis-Hillman adduct without prior protection, thereby affording a convenient and chemoselective route to 3-substitituted coumarins (Scheme 20).[208-210]

Musa explored the susceptibility of the three electrophilic centres in 3-(halomethyl) coumarins to nucleophilic attack (Figure 9), and found that various N- and C-nucleophiles attacked exclusively at the exocyclic C-1′ electrophilic centre.[211]

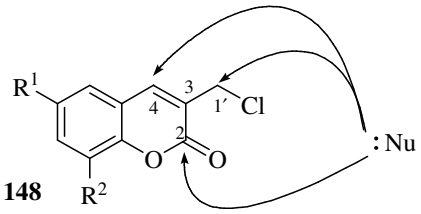

Figure 9. Possible modes of nucleophilic attack on 3-halomethyl coumarins.[211]

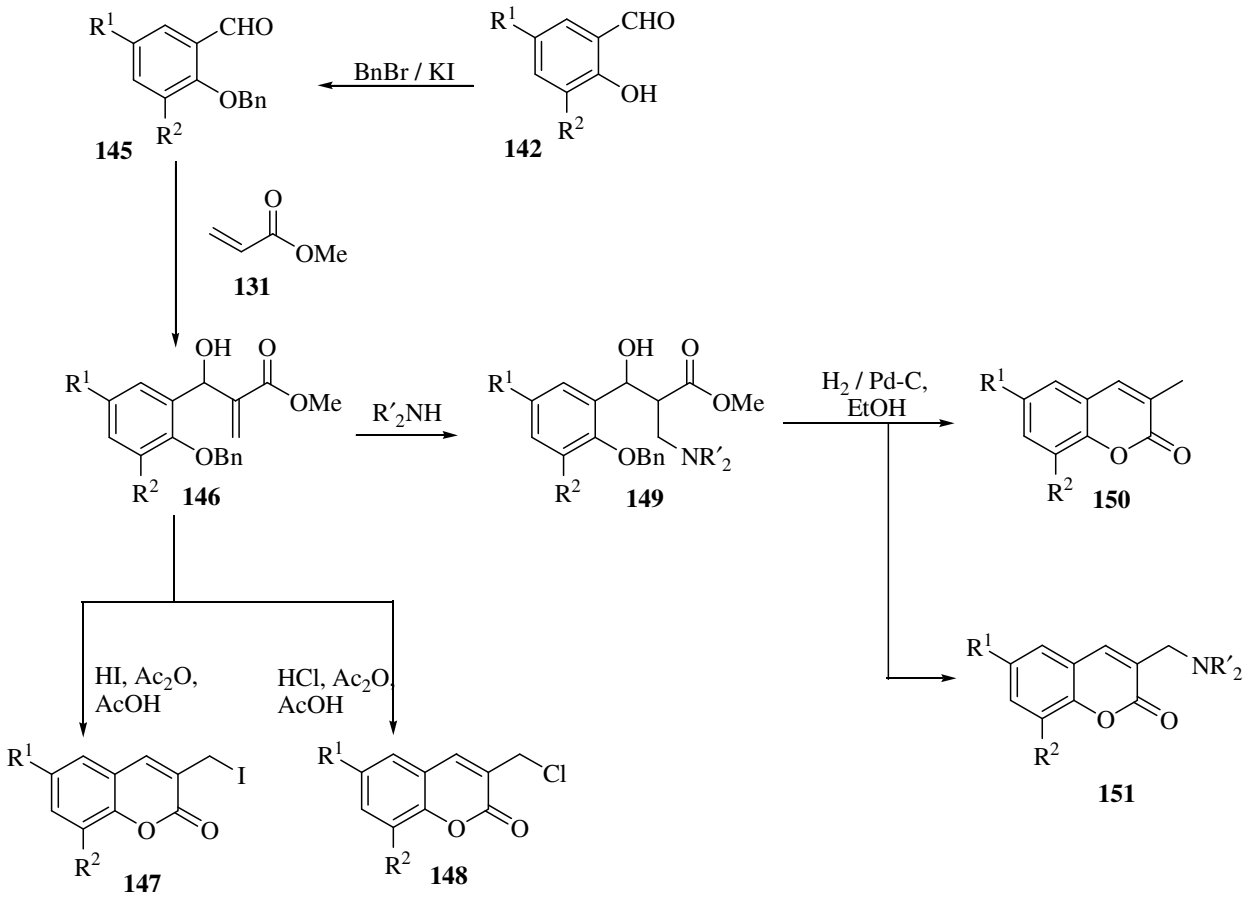

Scheme 19. Cyclisation of protected Baylis-Hillman adducts to coumarins.[210]

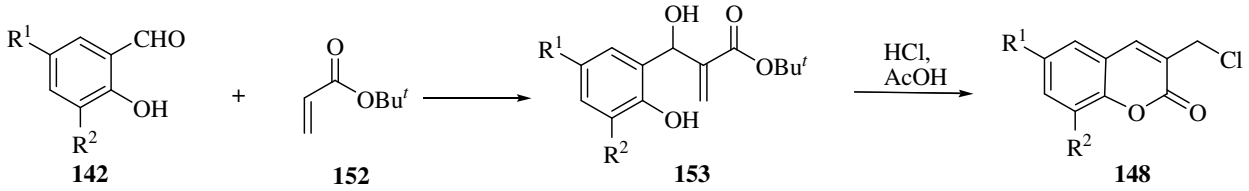

Scheme 20. Cyclisation of unprotected Baylis-Hillman adducts to coumarins.[210]

Rashamuse, however, was able to obtain substitution by the P-nucleophile, triethylphosphite, at the 4-position on the coumarin nucleus using the Michaelis-Arbuzov reaction. The study revealed the possibility of chemoselective access to either the 4-phosphonated or the 1′-phosphonated coumarin analogues, depending on the halide group (Scheme 21).[212]

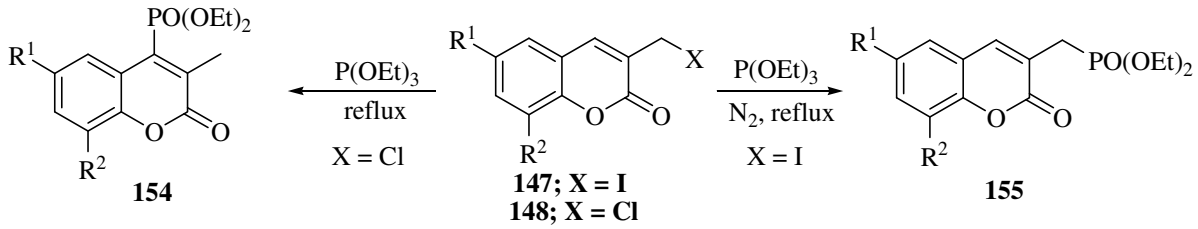

Scheme 21. Michaelis-Arbuzov reaction of 3-(halomethyl)coumarin analogues.[212]

Rashamuse also synthesized a series of phosphonated 3-(benzylaminomethyl)coumarin derivatives **158** by subjecting coumarin analogues obtained *via* Baylis-Hillman methodology to step-wise amination, chloroacetylation and Michaelis-Arbuzov phosphonation reactions (Scheme 22).[213] Preliminary *in silico* docking studies of the hydrolysed analogues of these compounds as potential HIV-1 PR inhibitors, were also undertaken.[213]

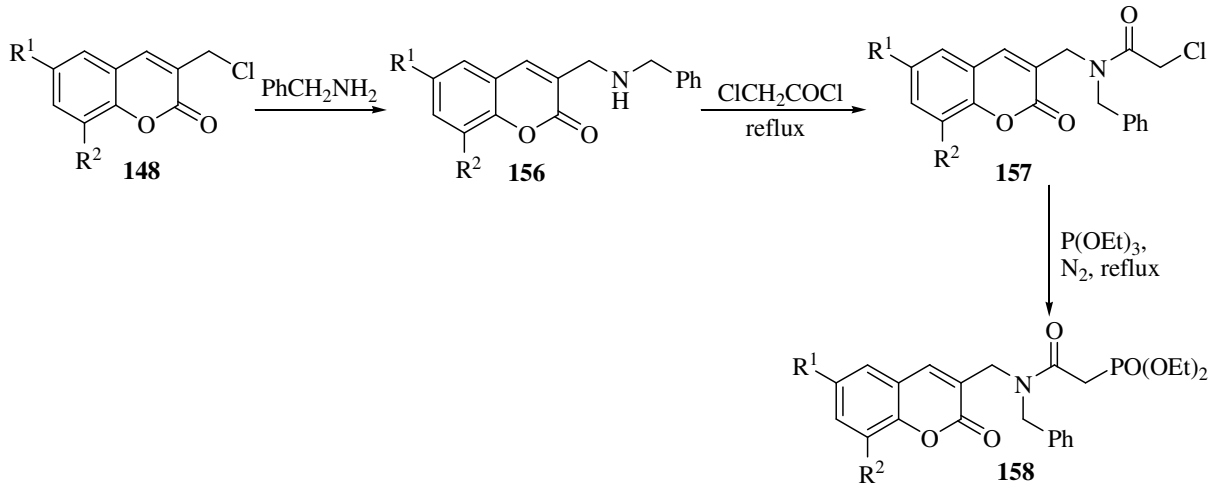

Scheme 22. Synthesis of phosphonated 3-(benzylaminomethyl)coumarin analogues.[213]

In an attempt to access potential HIV-1 IN inhibitors, Lee synthesised some cinnamate esters **162** *via* 1-ethyl-3-(3-dimethylaminopropyl)carbodiimide (EDC)-mediated dehydration of the hydro-cinnamate derivatives **161** produced, in turn, by amination of Baylis-Hillman adducts (Scheme 23); the products were obtained as diastereomeric mixtures, with the (*E*)-isomer predominating.[214]

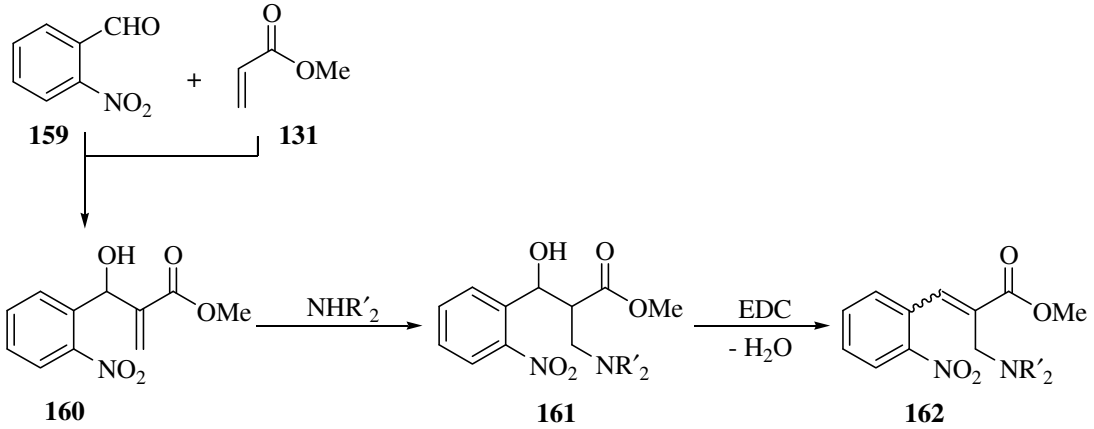

Scheme 23. Synthesis of cinnamate esters *via* Baylis-Hillman methodology.[214]

1.7. AIMS OF CURRENT INVESTIGATION

The focus of the present study has been to extend the application of Baylis-Hillman methodology to the preparation of novel coumarin derivatives, which could exhibit interesting biological activities. More specifically attention has been given to the following objectives.

1) Microwave-assisted synthesis of Baylis-Hillman adducts and their use in the synthesis of coumarins and cinnamate esters as potential HIV-1 PR and IN inhibitors, respectively.
2) Exploitation of click chemistry in connecting both coumarins and cinnamate esters to AZT to afford potential bi-functional HIV-1 RT/PR and RT/IN inhibitors, respectively.
3) Synthesis of coumarin-3-carbaldehydes and their use as substrates in unusual Baylis-Hillman reactions.
4) Preparation of 4-substituted coumarins using Baylis-Hillman methodology.
5) Synthesis of furocoumarins as potential HIV-1 IN inhibitors.
6) Evaluation of potential HIV-1 enzyme inhibitors using computer-simulated docking, saturation transfer difference (STD) NMR and bioassay data.

2. RESULTS AND DISCUSSION

This discussion will cover the following areas: synthesis of coumarin-AZT analogues (Section 2.1.); preparation of cinnamate derivatives (Section 2.2.); preparation of coumarin carbaldehydes (Section 2.3.); accessing 4-substituted coumarins (Section 2.4.); synthesis of furocoumarins (Section 2.5.); and evaluation of compounds as HIV-1 enzyme inhibitors (Section 2.6.).

2.1. SYNTHESIS OF COUMARIN-AZT ANALOGUES

Certain coumarins have been shown to exhibit HIV-1 PR inhibition activity (see Section 1.2.5.), while AZT is used clinically as an HIV-1 RT inhibitor. A major aim in this research has been to develop dual-action HIV-1 RT/PR inhibitors. Thus, using Baylis-Hillman methodology, viable routes to two different classes of coumarin-AZT conjugates (Scheme 24) were designed.

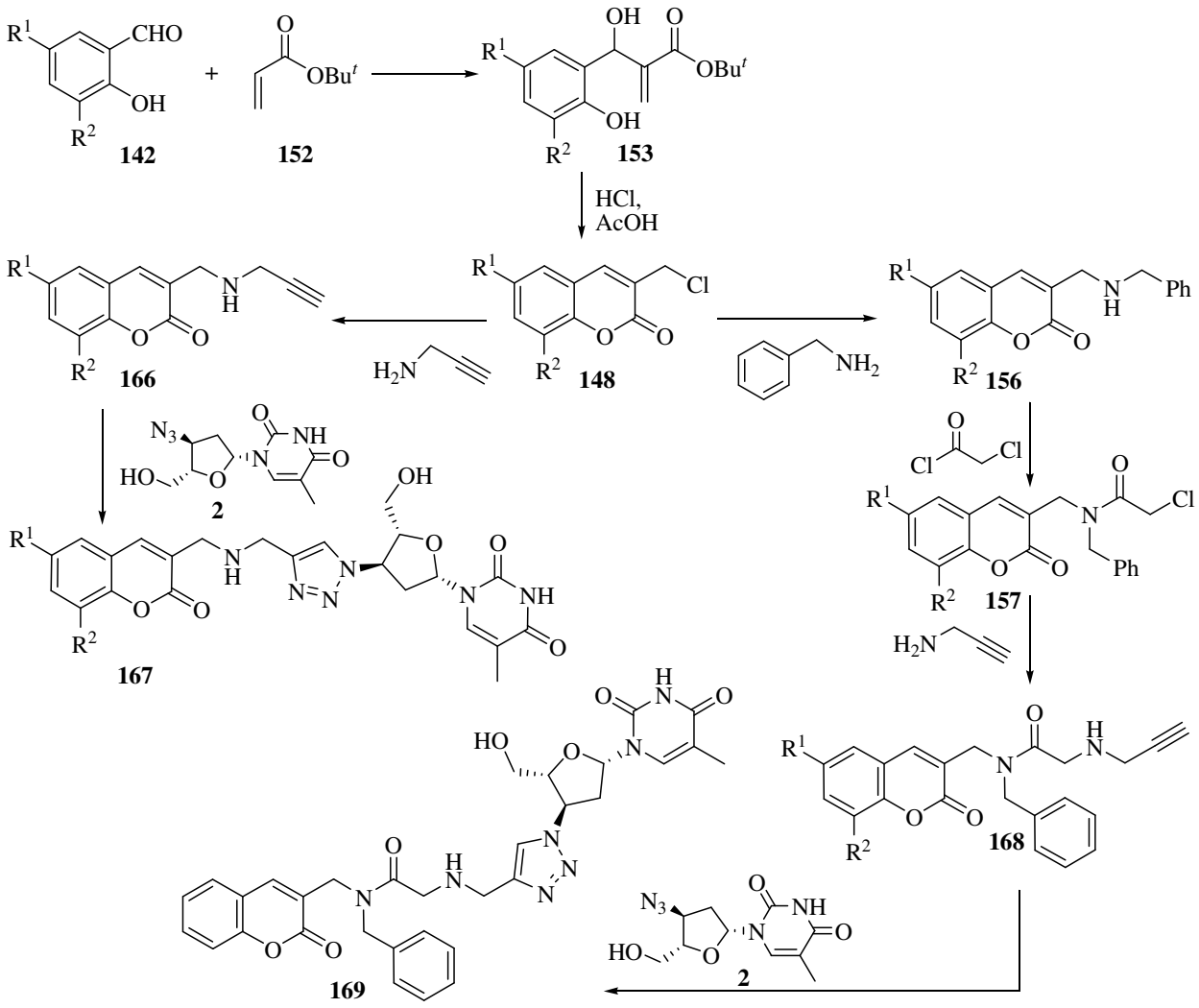

Scheme 24. Strategic reaction plans.

2.1.1. Baylis-Hillman Reaction with *tert*-Butyl Acrylate

As mentioned in Section 1.6, it has been demonstrated that the use of *tert*-butyl acrylate **152** as an activated alkene permits the isolation of salicylaldehyde-derived Baylis-Hillman adducts and their regioselective cyclisation to coumarin derivatives.[210] In an attempt to accelerate the normally sluggish Baylis-Hillman reaction, the differences between conventional stirring and microwave-assisted irradiation procedures were explored.

2.1.1.1. Conventional Method

The Baylis-Hillman adducts **153a-e** were synthesised by reacting the substituted salicylaldehydes **142a-e** with *tert*-butyl acrylate **152** in the presence of DABCO using $CHCl_3$ as solvent (Scheme 25). The mixtures were stirred at room temperature for periods ranging from 4 to 21 days, affording up to 55% yield (Table 2) of the corresponding Baylis-Hillman adducts, after purification.

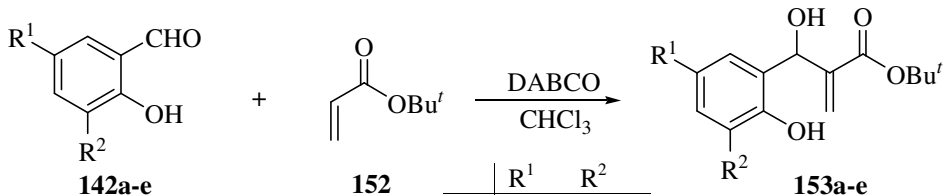

	R^1	R^2
a	H	H
b	Br	H
c	H	OMe
d	H	OEt
e	Cl	H

Scheme 25. Baylis-Hillman reaction with *tert*-butyl acrylate

2.1.1.1. Microwave Method

Direct and rapid heating by microwave irradiation has been shown, in many cases, to reduce reaction times significantly, increase product yields and give cleaner products when compared with conventional heating techniques.[215] In a preliminary study, it was shown that microwave-assisted methodology can indeed be successfully applied to the above Baylis-Hillman reactions.[216] The Baylis-Hillman adducts **153a-e** were prepared using microwave irradiation with DABCO as catalyst and $CHCl_3$ as solvent. The reaction was monitored by TLC and ^{1}H NMR spectroscopy, and Figure 10 shows the changes in the NMR data with time and reveals that after 60 minutes there was no significant increase in the intensity of the new signals at *ca* 5.65-5.70

and 6.22 ppm, which characterise the vinylic and the 1′-methine protons of the Baylis-Hillman adducts. Hence, subsequent reactions were carried out for 1 hour – a significant decrease from the 4-21 days required under conventional conditions as shown in Table 2; however, the yields (27-40%) were, at best, comparable with those obtained under conventional conditions.

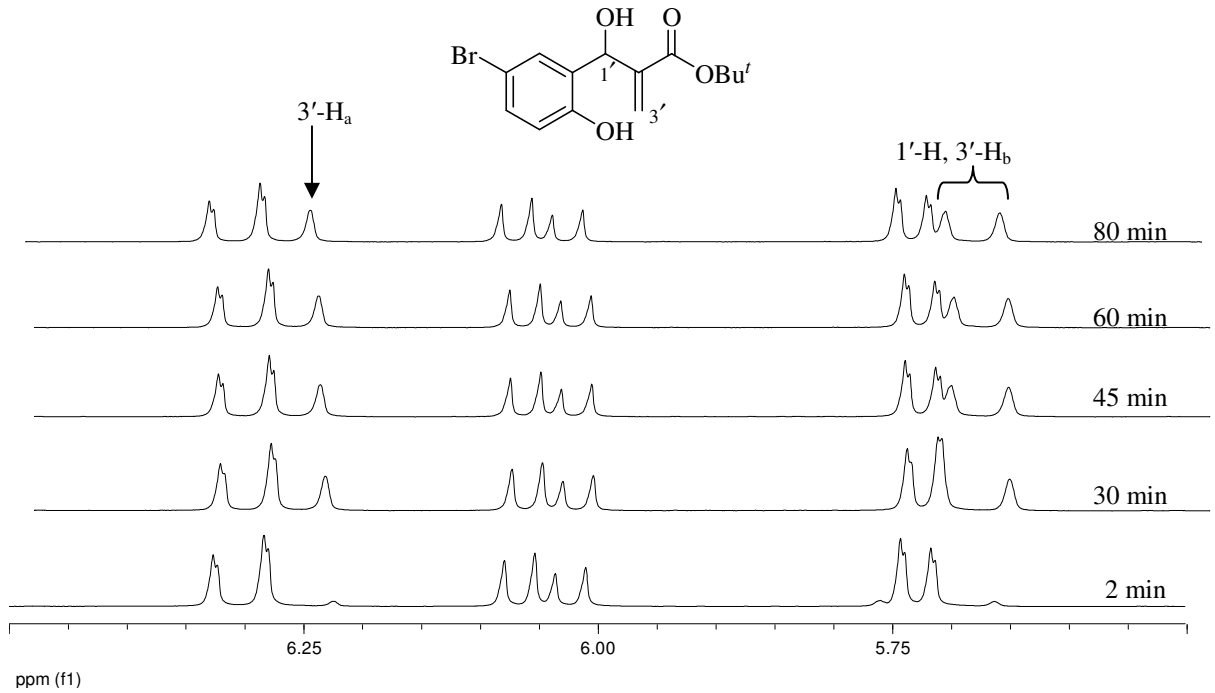

Figure 10. 400 MHz ^{1}H NMR spectra showing increase in intensity of signals diagnostic of the formation of the Baylis-Hillman adduct **153b** with time under microwave irradiation.

Table 2. Comparison of times and yields for conventional *vs* microwave-assisted Baylis-Hillman reactions.

	153a	**153b**	**153c**	**153d**	**153e**
Conventional stirring Isolated yields (time)	39% (18 d)	55% (4 d)	29% (21 d)	31% (21 d)	55% (4 d)
μ-Wave Isolated yields (time)	27% (1 h)	40% (1 h)	32% (1 h)	30% (1 h)	36% (1 h)

The ^{1}H NMR spectrum of *tert*-butyl 3-(5-bromo-2-hydroxyphenyl)-3-hydroxy-2-methylenepropanoate **153b**, which is typical of the series, shows the *tert*-butyl singlet at δ 1.32 ppm (Figure 11). One of the two vinylic methylene proton singlets overlaps with the 4-methine proton singlet at *ca* 5.65 ppm, while the other vinylic proton resonates as a singlet at 6.05 ppm; the three aromatic proton signals appear at *ca* 6.74 and 7.19 ppm. The DEPT 135 NMR spectrum (Figure 12) shows the vinylic carbon signal at 123.9 ppm and the 4-methine carbon signal at 65.5 ppm. The three methyl carbons resonate as an intense signal at 28.4 ppm.

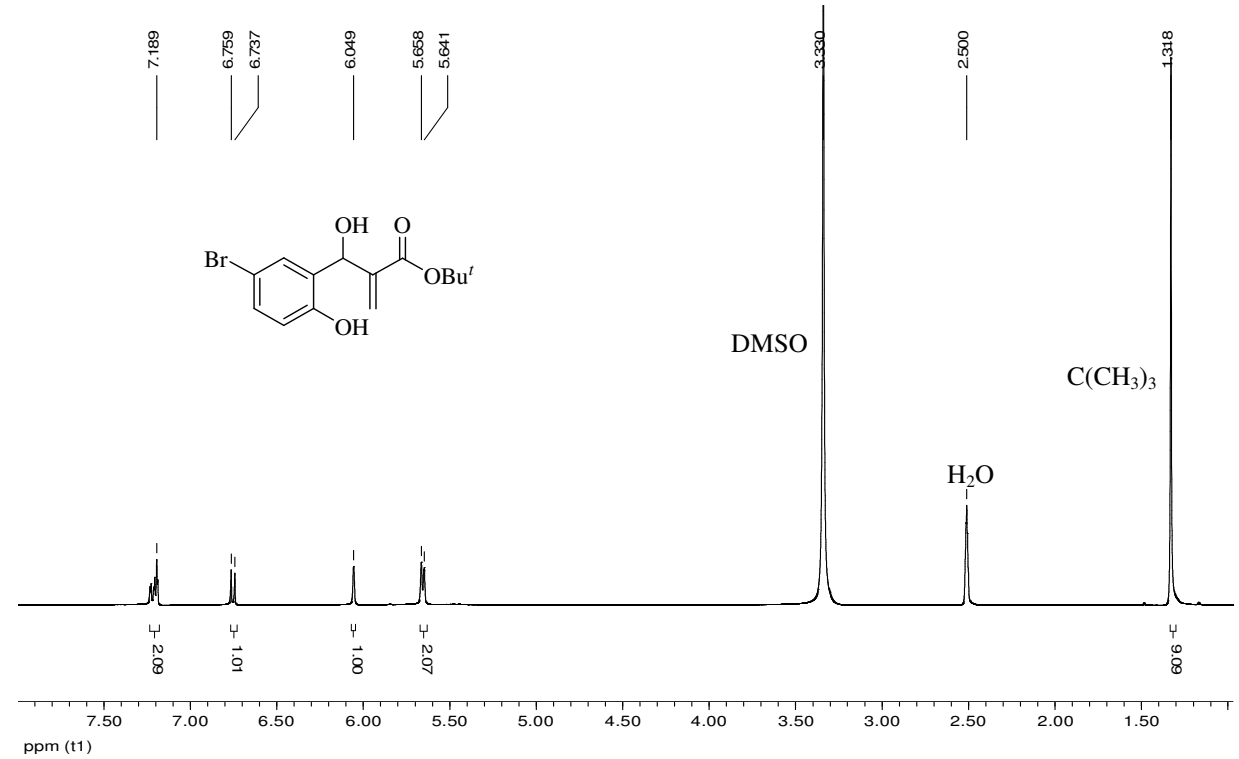

Figure 11. 400 MHz ^{1}H NMR spectrum of compound **153b** in DMSO-d_6.

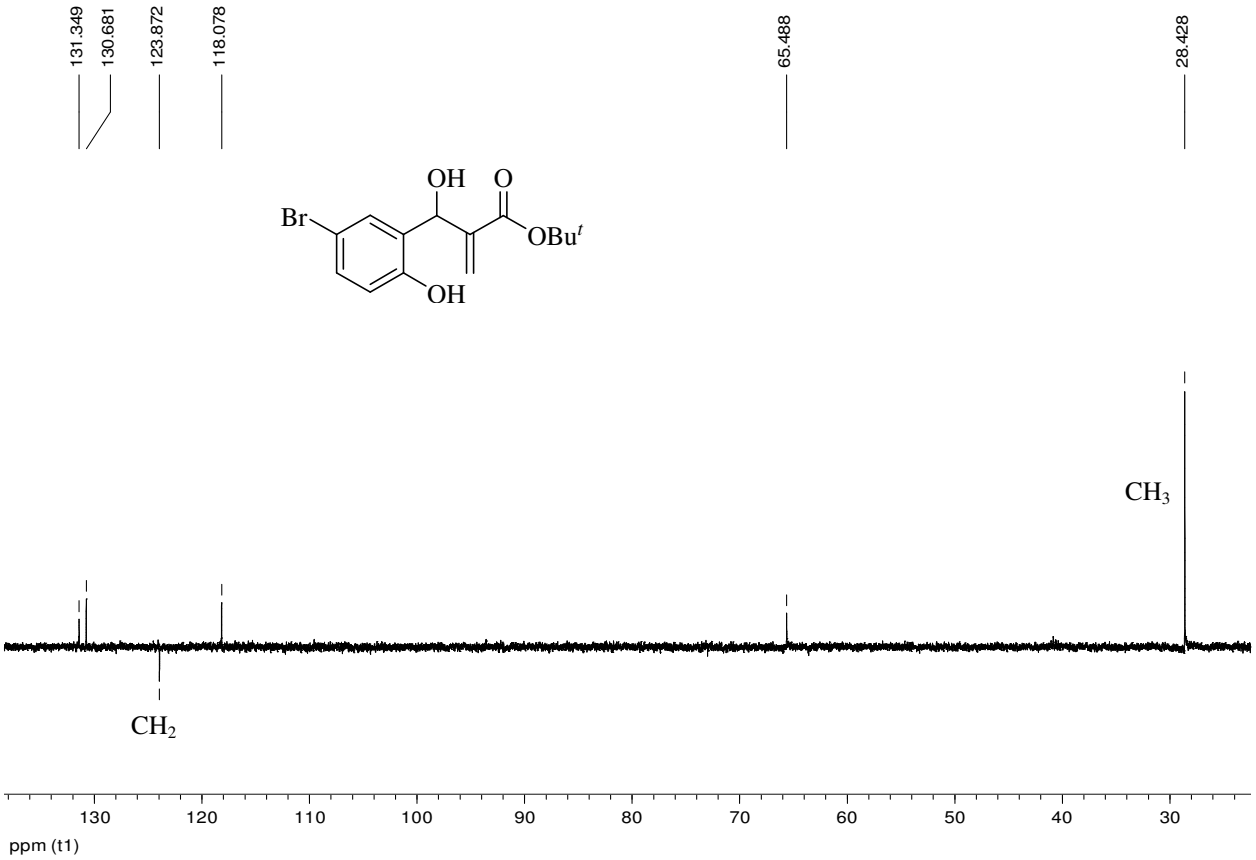

Figure 12. DEPT 135 NMR spectrum of compound **153b** in DMSO-d_6.

2.1.2. Base-Catalysed Cyclisation of Baylis-Hillman Adducts

As mentioned in Section 1.6., salicylaldehyde-derived Baylis-Hillman adducts have been cyclised previously under acid-catalysed conditions,[210] and it was decided to investigate what would happen if such Baylis-Hillman adducts were to be subjected to basic conditions. Compound **153a** was thus treated with KOH solution in acetonitrile under reflux for 5 hours. After work-up and purification using flash chromatography, the products obtained were identified as the chromene derivative **164a** and chroman-4-ol derivative **163a** (Scheme 26). The apparent absence of the isomeric coumarin (observed under acid-catalysed conditions[208,210]) suggests that while acid-catalysed cyclisation of such Baylis-Hillman adducts proceeds *via* acyl substitution, under basic conditions, conjugate addition appears to be the preferred route of attack (see Scheme 17, p. 32). However, poor yields of 32% for compound **163a** and 24% for the dehydration product **164a** leaves room for improvement in the base-catalysed protocol. In the absence of heat, no reaction was observed, even with overnight stirring.

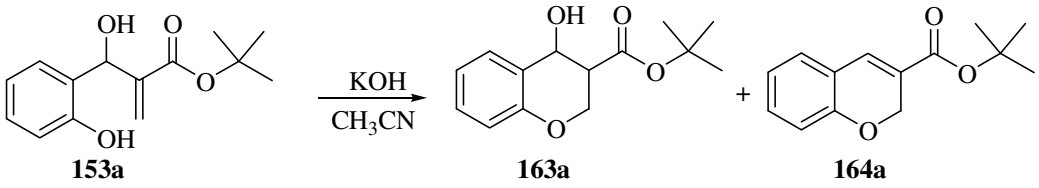

153a **163a** **164a**

Scheme 26. Base-catalysed cyclisation of Baylis-Hillman adduct **153a**.

The ^{1}H NMR spectrum of *tert*-butyl 2*H*-chromene-3-carboxylate **164a** shown in Figure 13 reveals that the methylene protons resonate as a singlet at 4.95 ppm and the 4-methine proton appears as a singlet at 7.33 ppm. In the corresponding spectrum of the chroman-4-ol **163a** (Figure 14) the methylene protons are revealed as being diastereotopic (consistent with the presence of the new stereogenic centres), with one resonating as a multiplet at 4.20 ppm and the other as a poorly resolved doublet of doublets at 4.37 ppm. The DEPT 135 NMR spectrum of the former product **164a** (Figure 15) confirms the presence of a methylene carbon signal at 65.1, the *tert*-butyl methyl carbon signals at 28.6 ppm and the expected total of five methine carbons in the vinylic-aromatic region. The ^{13}C NMR spectrum of the chroman-4-ol **163a** shows, as expected, twelve different carbon types, with the carbonyl carbon resonating at δ 170.9, appropriate for an ester carbonyl, while the DEPT 135 spectrum (Figure 16) confirms that the two diastereotopic protons are attached to the same carbon atom (C-2), which resonates at δ 64.7 ppm.

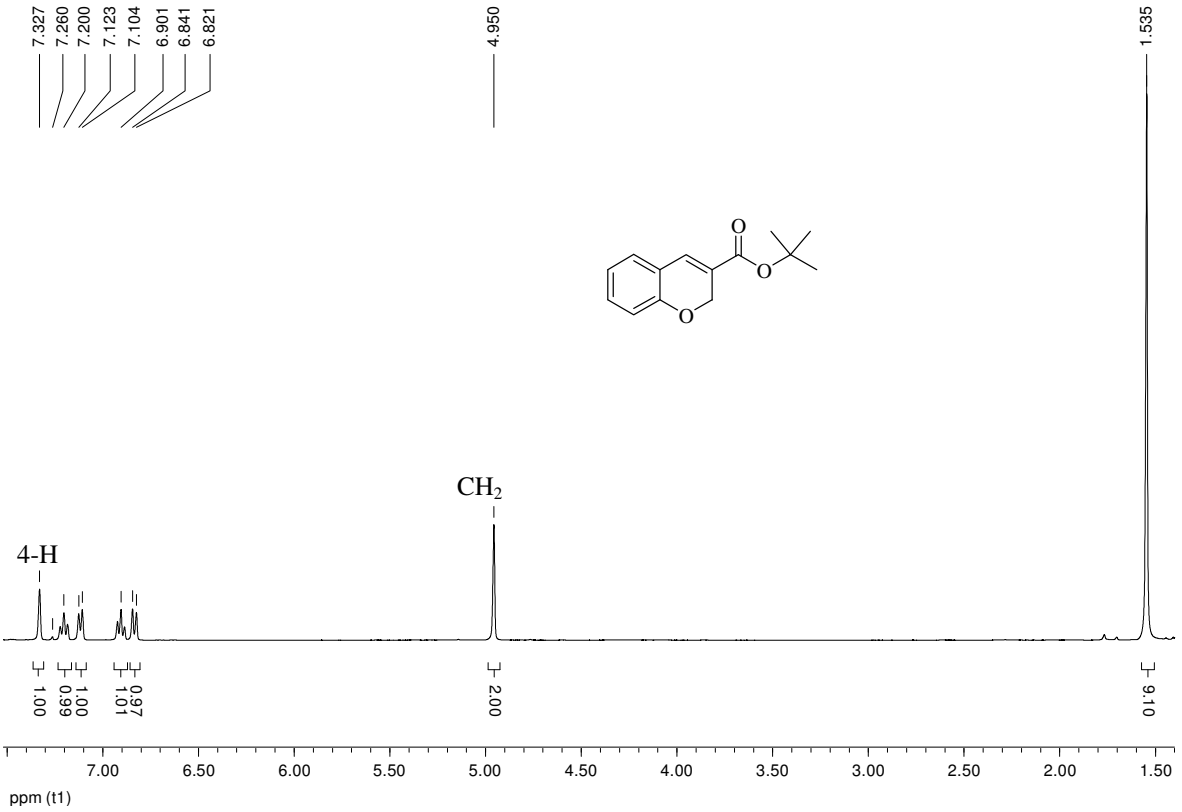

Figure 13. 400 MHz ^{1}H NMR spectrum of compound **164a** in $CDCl_3$.

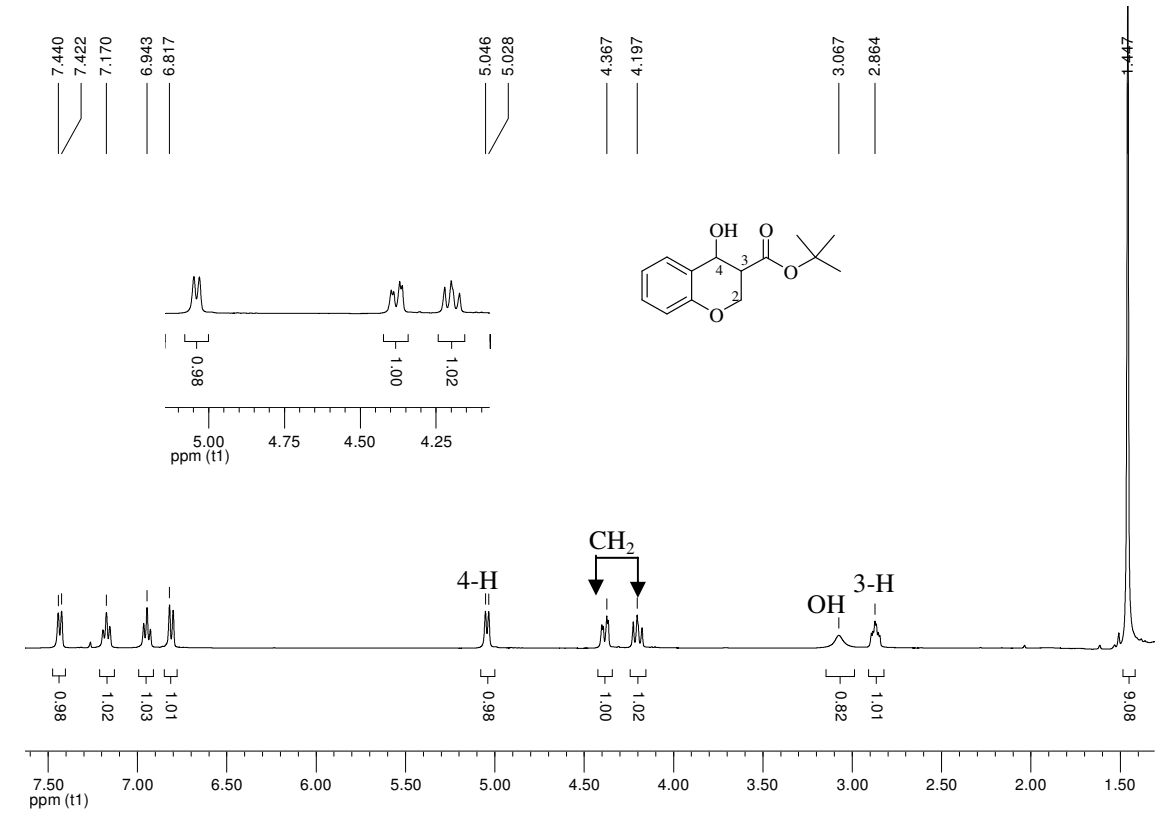

Figure 14. 400 MHz ^{1}H NMR spectrum of compound **163a** in $CDCl_3$.

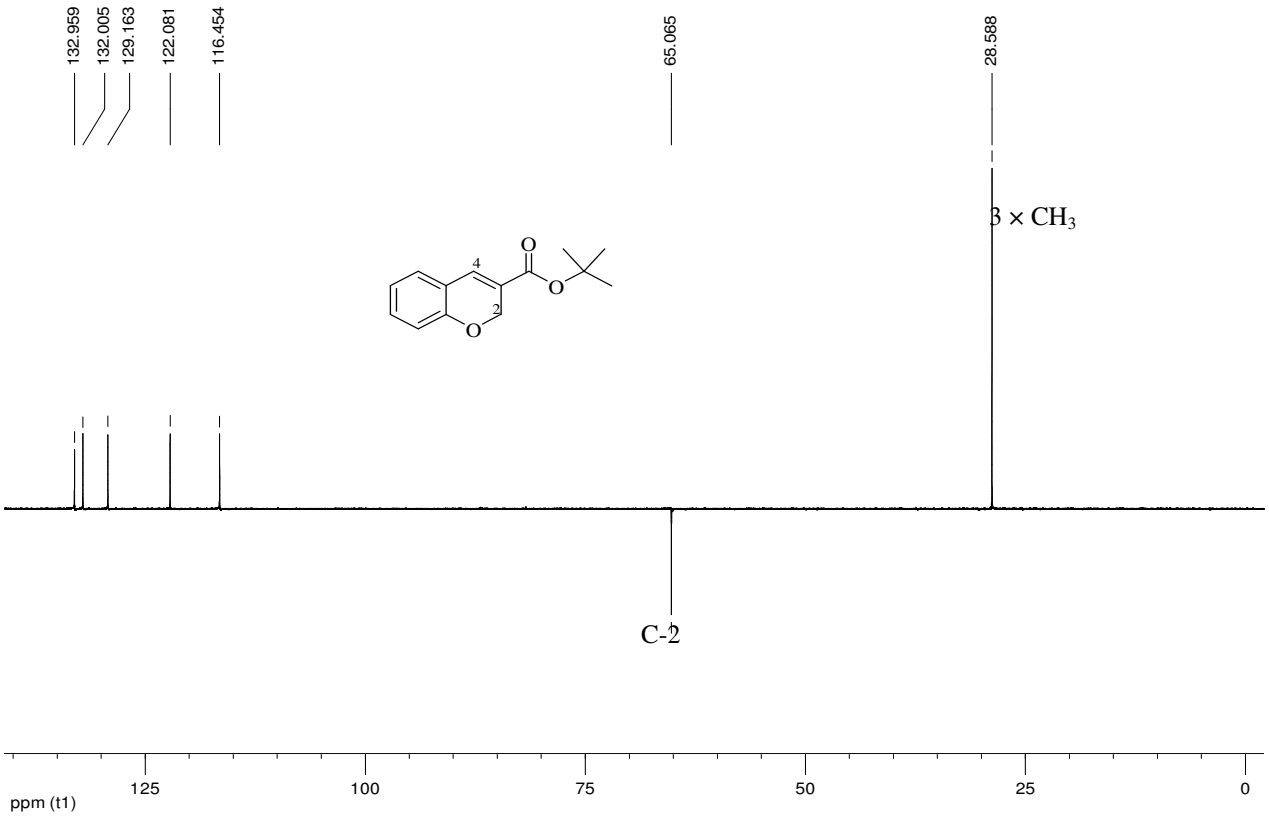

Figure 15. DEPT 135 NMR spectrum of compound **164a** in $CDCl_3$.

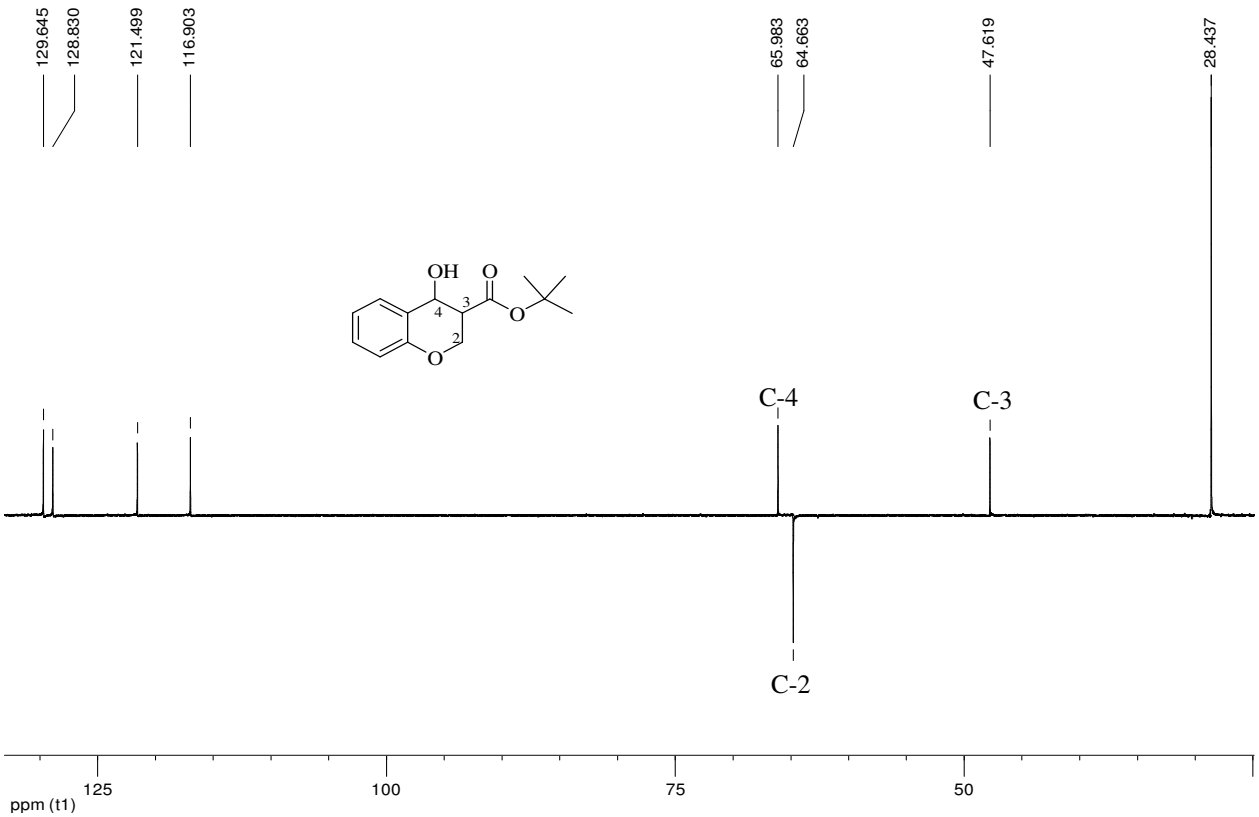

Figure 16. DEPT 135 NMR spectrum of compound **163a** in $CDCl_3$.

2.1.3. Acid Catalysed Cyclisation of Baylis-Hillman Adducts

While the base catalysed approach appears to offer regio-controlled cyclisation *via* a conjugate addition pathway, the isomeric acyl substitution products were required in this study, and attention was turned to the acid catalysed protocol, which provides access to coumarin derivatives (see Schemes 19 and 20).[210]

2.1.3.1. Synthesis of (3-Chloromethyl)coumarins

The substituted 3-(chloromethyl)coumarins **148a-e** were prepared by refluxing compounds **153a-e** in an HCl–AcOH mixture for 2h (Scheme 27). Yields of up to 92% were obtained after purification by flash chromatography and, in some cases, the 3-(acetoxymethyl)-coumarins **165** were obtained as minor competition products (Table 3). The ^{1}H NMR spectrum of 3-(chloromethyl)-8-ethoxycoumarin **148d** shows the 4-methine proton resonating as a singlet at 7.85 ppm and the 1′-methylene protons as a singlet at 4.56 ppm (Figure 17). The ^{1}H NMR spectrum of 3-(acetoxymethyl)-8-ethoxycoumarin **165d** differs from that of the chloromethyl analogue **148d**, in that the acetyl methyl singlet is present at δ 2.15 ppm and the 1′-methylene singlet moves further downfield to 5.07 ppm (4.56 ppm in compound **148d**). The ^{13}C NMR spectral data confirm the presence of fourteen carbons as expected.

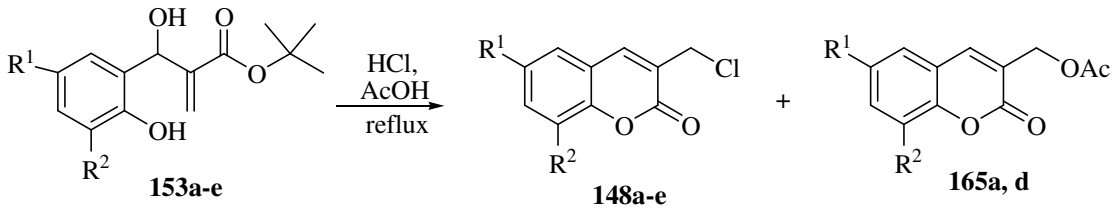

Scheme 27. Acid-catalysed cyclisation of Baylis-Hillman adducts **153a-e** using HCl.

Table 3. Yields obtained for the HCl-mediated cyclisation of Baylis-Hillman adducts **153a-e**.

Substrate	R^1	R^2	148 (%)	165 (%)
153a	H	H	70	6
153b	Br	H	88	-
153c	H	OMe	71	-
153d	H	OEt	72	10
153e	Cl	H	92	-

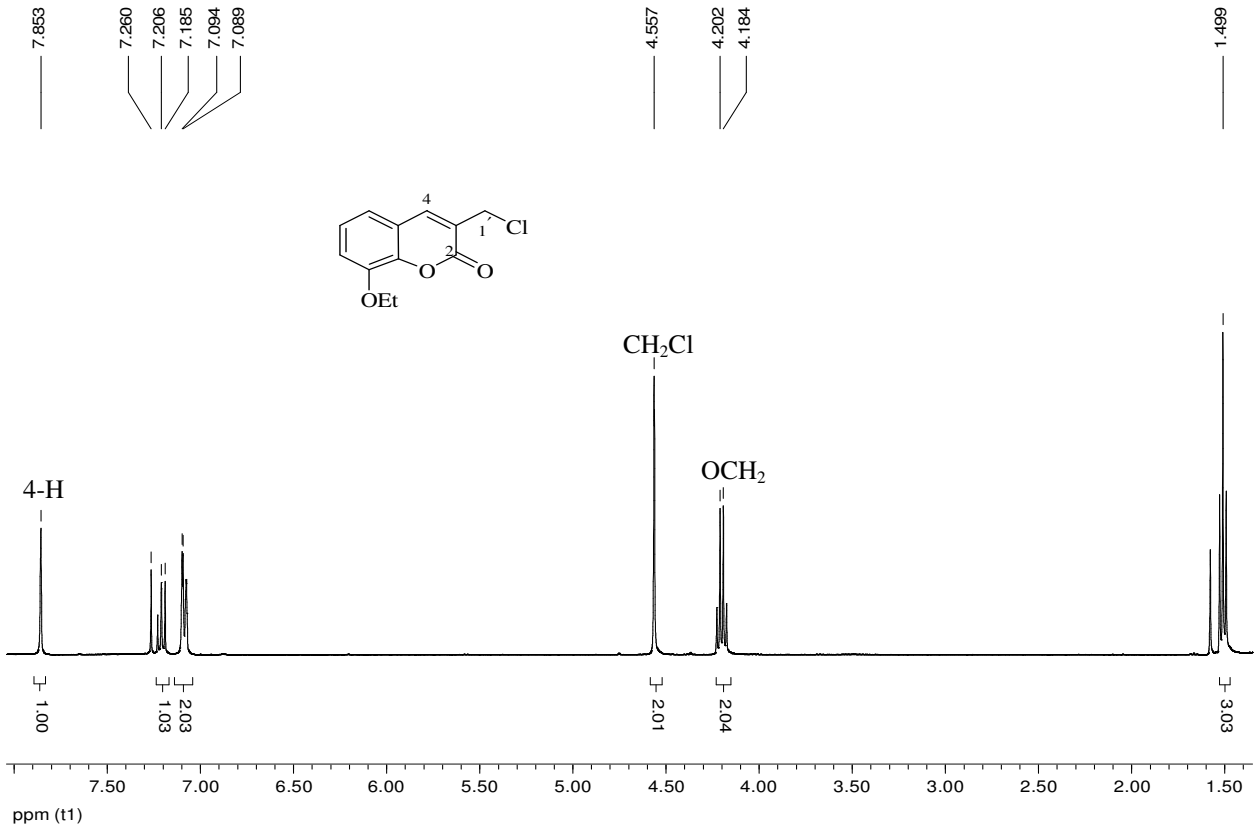

Figure 17. 400 MHz ^{1}H NMR spectrum of compound **148d** in $CDCl_3$.

2.1.3.2. Synthesis of 3-Methylcoumarins

The 3-iodomethyl analogues of the 3-(chloromethyl)coumarins **148** may be viewed as ideal substrates for the intended amination reactions illustrated in Scheme 24. However, 3-methyl-coumarins **150** had been isolated in some cases, together with 3-(iodomethyl)coumarins **147**, as unwanted competition products during the HI-catalysed cyclisation of Baylis-Hillman adducts **153**.[212] In this study (Scheme 28), acid-catalysed cyclisation of the Baylis-Hillman adducts **153a-e**, effected in a refluxing mixture of hydroiodic acid, acetic acid and acetic anhydride for 2 hours, afforded the corresponding 3-methylcoumarins **150a**,**b**,**e**,**f** in yields of up to 94% (Table 4)! Thus, it seems that the methodology can be adjusted to give either the 3-(iodomethyl)coumarins **147** or 3-methylcoumarins **150**, exclusively. The reaction is presumed to proceed *via* HI-mediated cyclisation to form the 3-(iodomethyl)coumarins **147**, followed by HI-mediated reduction to the 3-methyl analogues **150**. Interestingly, the ether groups in compounds **150c** (R^2 = OMe) and **150d** (R^2 = OEt) were also reduced under these conditions to afford the common 8-hydroxy analogue **150f**. Compounds **150a**,**b**,**e**,**f** were fully characterized. The ^{1}H NMR spectra of the 3-methylcoumarins **150** all show the methyl protons resonating as a singlet at *ca* 2.21 ppm.

While these reactions failed to afford the expected 3-(iodomethyl)coumarin **147**, the reaction provided convenient access to the 3-methylcoumarins used to prepare the 3-coumarin-carbaldehydes discussed in Section 2.3.

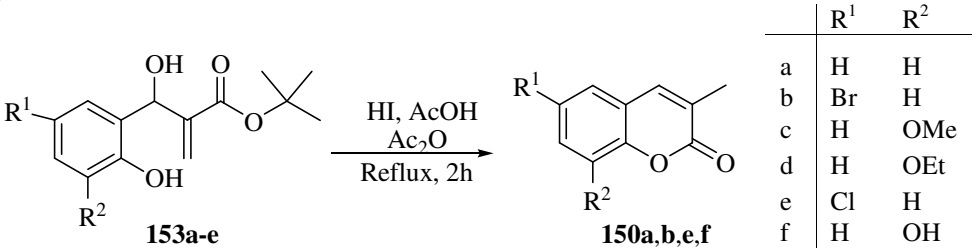

	R^1	R^2
a	H	H
b	Br	H
c	H	OMe
d	H	OEt
e	Cl	H
f	H	OH

Scheme 28. HI-catalysed cyclisation of Baylis-Hillman adducts **153a-e**.

Table 4. Yields obtained for the HI cyclisation of Baylis-Hillman adducts **153a-e**.

Substrate	Product	Isolated yields (%)
153a	**150a**	53
153b	**150b**	94
153c	**150f**	85
153d	**150f**	87
153e	**150e**	91

2.1.4. Nucleophilic Substitution Reactions of 3-(Chloromethyl)coumarins

As mentioned in Section 1.6., nitrogen nucleophiles appear to attack the 3-substituted coumarin nucleus exclusively at the exocyclic C-1′ electrophilic centre,[211] and this regioselectivity was exploited to access amine derivatives from the 3-(chloromethyl)coumarins **148** (Scheme 29).

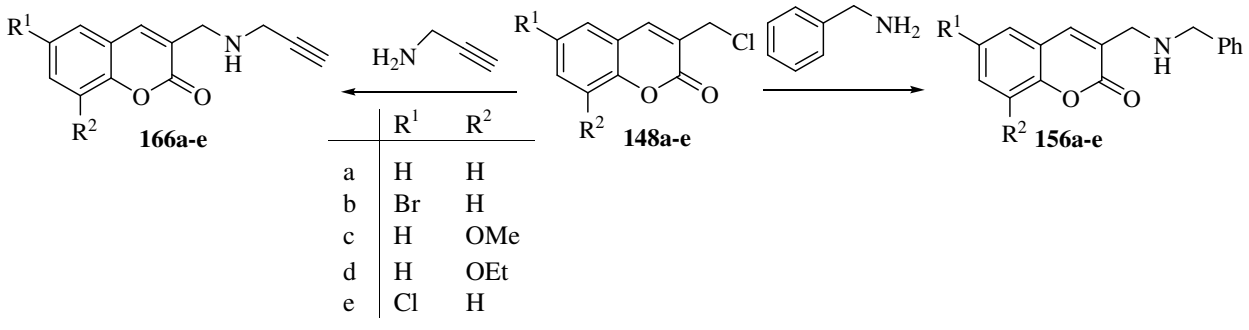

	R^1	R^2
a	H	H
b	Br	H
c	H	OMe
d	H	OEt
e	Cl	H

Scheme 29. Nucleophilic substitution reactions of 3-(chloromethyl) coumarins

2.1.4.1. Synthesis of 3-[(Benzylamino)methyl]coumarins

Secondary amines are generally prepared by reacting a primary amine with an alkyl halide in a suitable solvent with or without heating,[217] and the 3-(chloromethyl)coumarins **148a-e** were

reacted with benzylamine in dry THF by stirring at room temperature for 4 hours. Concentration *in vacuo* and purification using flash chromatography afforded the 3-[(benzylamino)methyl]-coumarins **156a-e** (Scheme 29) in good yields (73-85%; Table 5), *i.e*. better than the 35-74% obtained by Rashamuse.[213] The ^{1}H NMR spectrum of compound **156b** (Figure 18) reveals the amine proton resonating as a broad singlet at 1.75 ppm and the two methylene proton singlets at 3.76 and 3.86 ppm. The DEPT 135 NMR spectrum (Figure 19) confirms the presence of corresponding methylene carbon signals at 48.6 and 53.7 ppm.

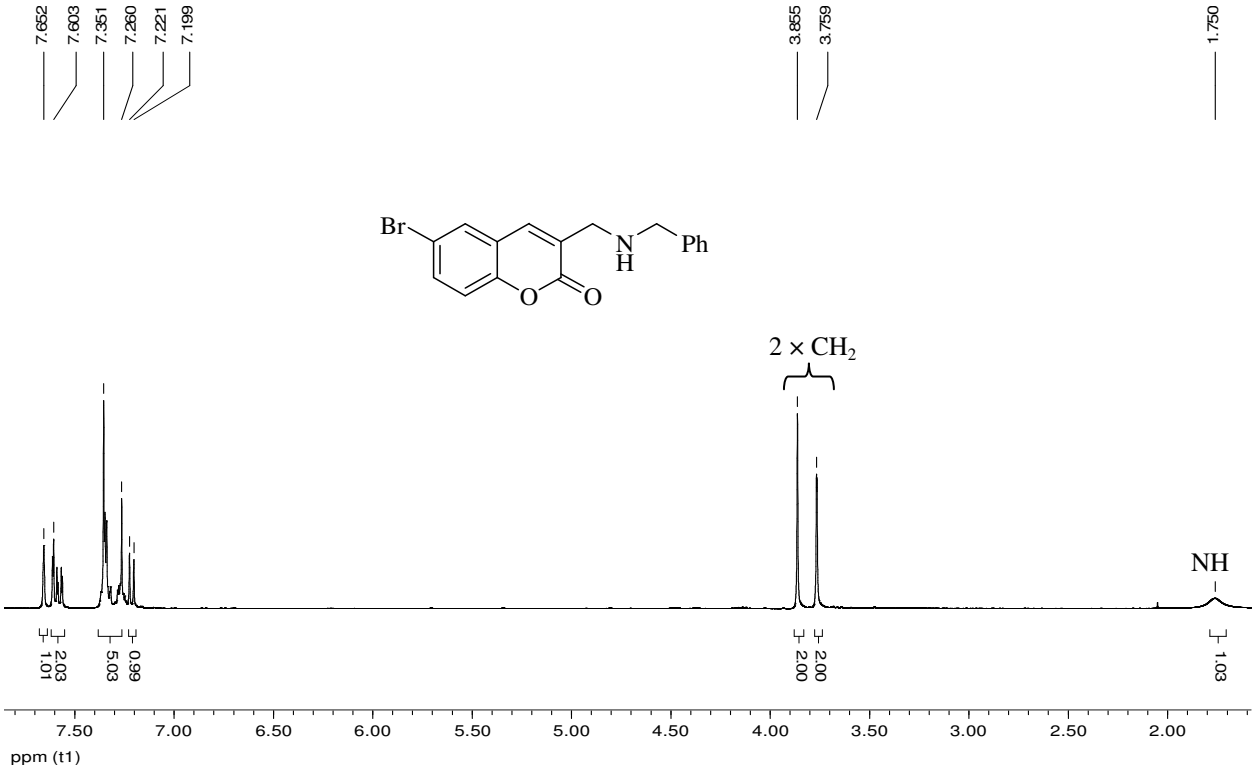

Figure 18. 400 MHz ^{1}H NMR spectrum of compound **156b** in $CDCl_3$.

Table 5. Yields of 3-[(benzylamino)methyl]coumarins **156a-e**.

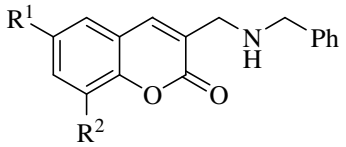

Compound	R^1	R^2	Isolated yields (%)
156a	H	H	85
156b	Br	H	73
156c	H	OMe	83
156d	H	OEt	78
156e	Cl	H	80

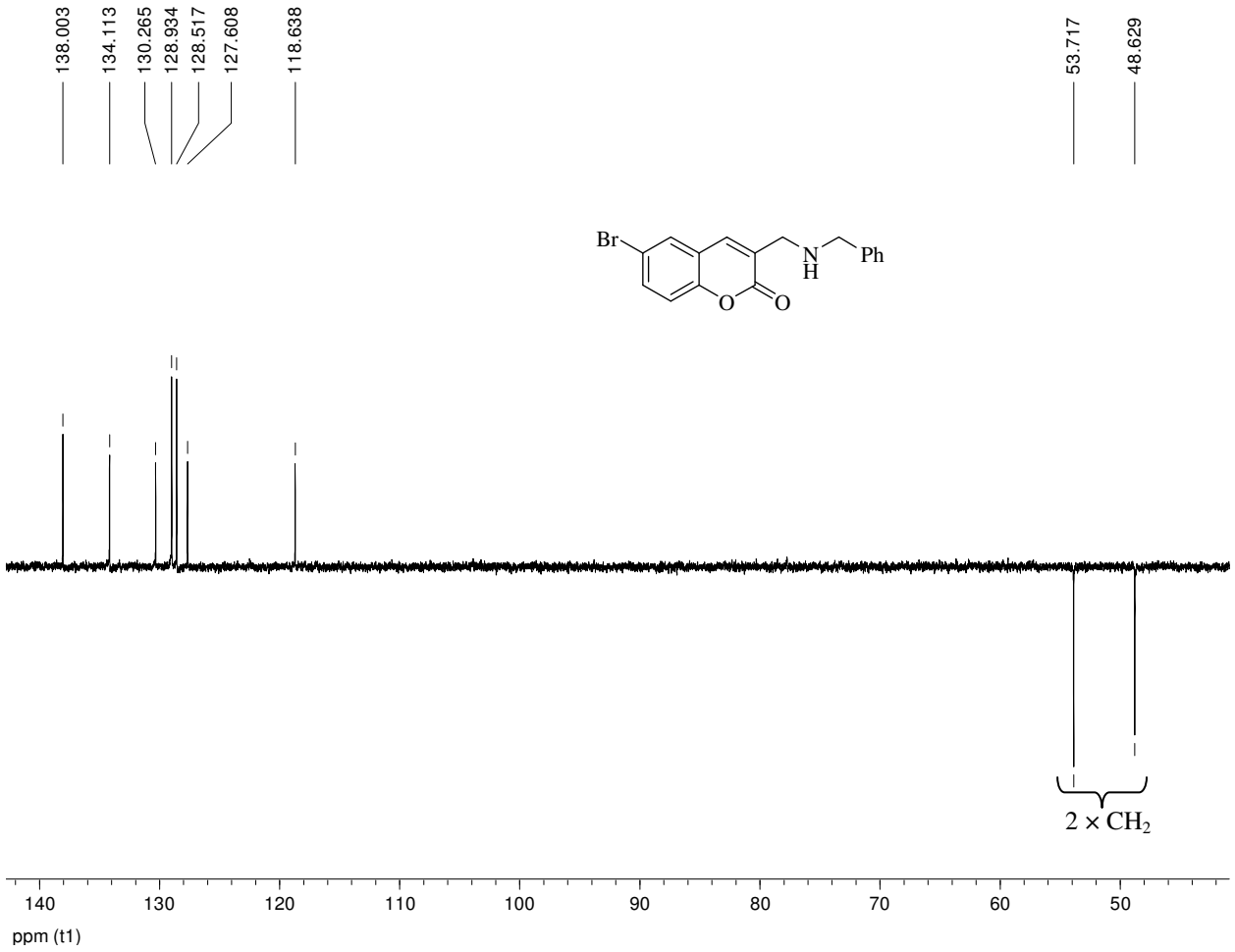

Figure 19. DEPT 135 NMR spectrum of compound **156b** in $CDCl_3$.

2.1.4.2. Synthesis of 3-[(2-Propynylamino)methyl]coumarins

With the aim of 'connecting' the coumarin and azidothymidine (AZT) moieties, it was decided to explore the introduction of a propargyl group on the coumarin to facilitate linkage of the AZT *via* a "Click" reaction. The 3-(chloromethyl)coumarins **148a-e** were reacted with propargylamine in THF by stirring the mixture for 48 hours at room temperature to afford the 3-[(2-propynylamino)methyl]coumarins **166a-e** (Scheme 29) in yields of 52-80% (Table 6). Compounds **166a-e** were fully characterised using both 1D- and 2D-NMR, IR and high resolution MS analysis. The preparation and use of these compounds to access coumarin-AZT conjugates as potential HIV-1 RT/PR inhibitors has been published.[218] The ^{1}H NMR spectrum of 6-bromo-3-[(2-propynylamino)methyl]coumarin **166b**, for example, reveals the amino proton resonating as a broad singlet at 1.77, the two amino methylene groups as singlets at 3.47 and 3.81 ppm and the acetylenic proton at 2.24 ppm. Interestingly, the DEPT 135 (Figure 20) shows the appearance of two signals in the alkyne carbon region (*ca* 75 ppm) suggesting that the

quaternary acetylenic carbon signal was also bearing a proton. This apparent anomaly was resolved by running a proton-undecoupled ^{13}C spectrum (Figure 21), which revealed both the terminal and quaternary alkyne carbon signals resonating as doublets of triplets. The triplet splittings are due to coupling with the 3′-methylene protons. The doublet splitting observed for the non-terminal alkyne (C-4′) is attributed to polarisation transfer from the 5′-alkyne proton due to the large $^{2}J_{C,H}$ value of 249 Hz.[219]

Table 6. Yields of 3-[(2-propynylamino)methyl]coumarins **166a-e**.

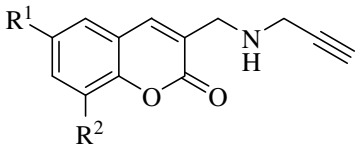

Compound	R^1	R^2	Isolated yields (%)
166a	H	H	80
166b	Br	H	52
166c	H	OMe	65
166d	H	OEt	70
166e	Cl	H	70

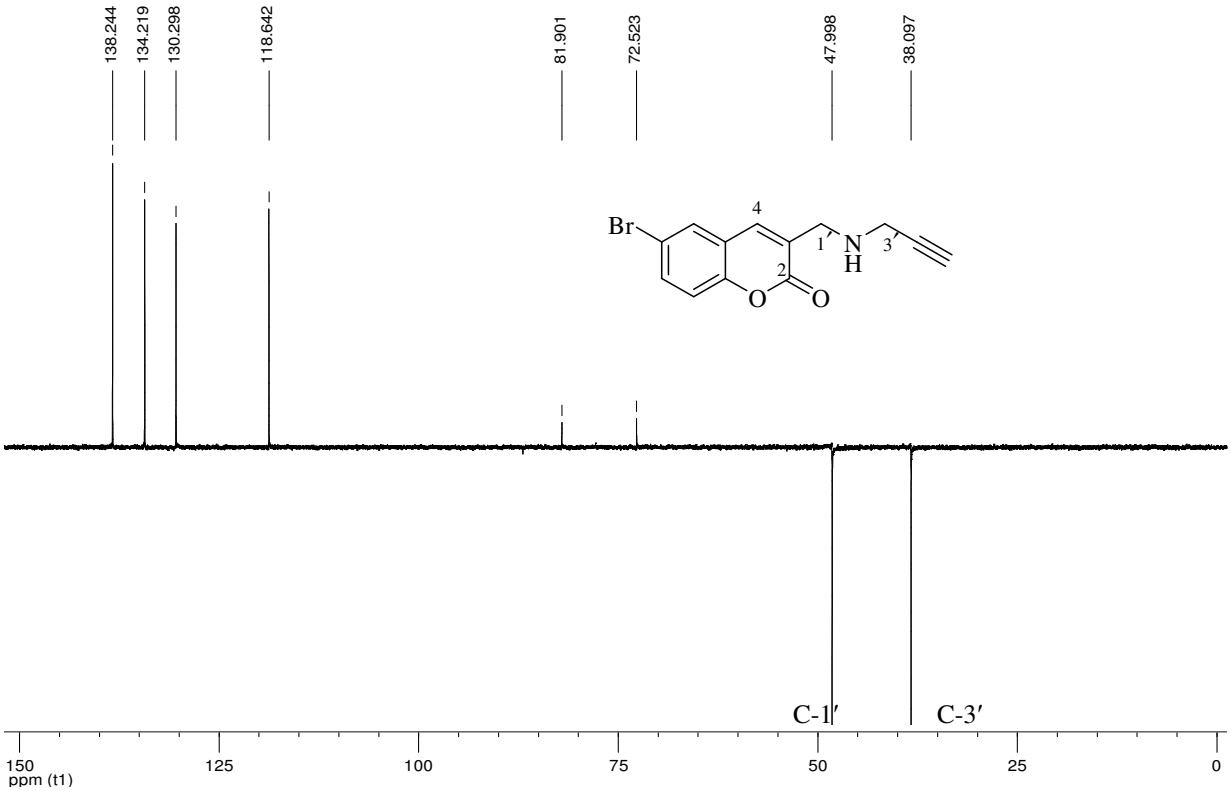

Figure 20. DEPT 135 NMR spectrum of compound **166b** in $CDCl_3$.

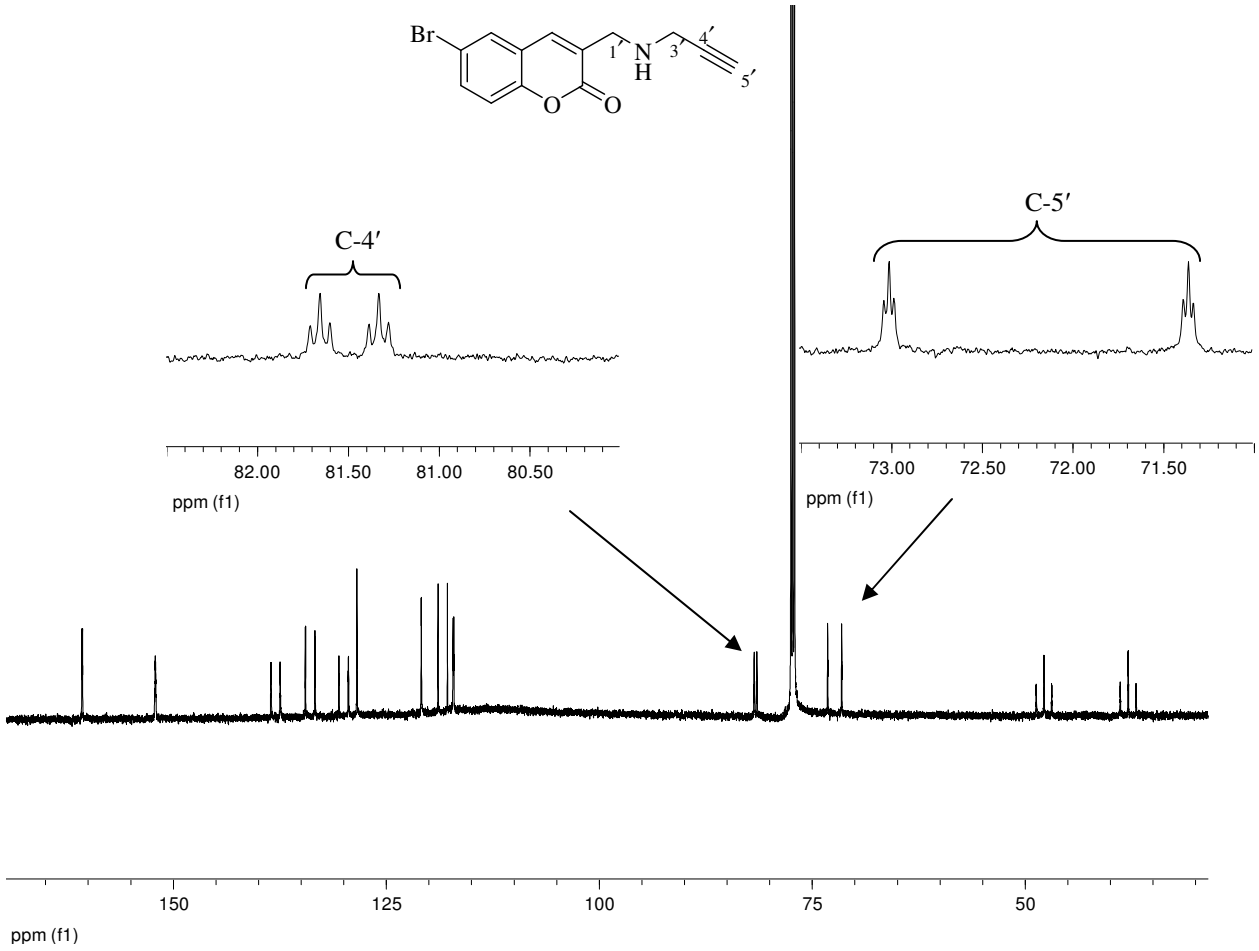

Figure 21. 150 MHz proton-undecoupled ^{13}C NMR spectrum of compound **166b** in $CDCl_3$.

2.1.5. Click Reactions of 3-[(2-Propynylamino)methyl]coumarins

The "Click" reaction is, in fact, a "chemical philosophy" that describes not just one specific reaction but encompasses the concept of using defined chemical reactions in a modular approach for the generation of new pharmacophores.[220] This principle, introduced by Sharpless in 2001 the same year in which he received a Nobel Prize in Chemistry, describes a nature-mimic in which small molecules are joined together in a quick and reliable manner.[220,221] Click conditions usually mean that a reaction is easy to perform using readily available materials, has wide application scope, gives high product yields, avoids offensive by-products, is stereospecific and is oxygen and water tolerant. A typical example of a reaction that meets the click-chemistry requirements is the cycloaddition reaction and, in particular, the Huisgen 1,3-dipolar cycloaddition reaction.[222] The 1,3-dipolar cycloaddition between a terminal alkyne and an azide is a versatile reaction with a known mechanism and, under thermal conditions, gives a mixture of roughly equimolar quantities of 1,4- and 1,5-disubstituted triazoles (Scheme 30).[223] Cu(I) catalysis of this reaction,

however, affords the 1,4-susbtituted triazole **172** exclusively. Due to the rather unstable nature of Cu(I) salts, the reduction of a more stable Cu(II) salt, such as $CuSO_4 \cdot 5H_2O$, to Cu(I) *in situ* using sodium ascorbate is the preferred protocol for this reaction.[222,224] In contrast, use of a ruthenium catalyst gives the 1,5-disubstituted triazole **173** exclusively.[225] Thus, it is possible to modulate the regioselectivity of this reaction to give a particular product by changing the metal catalyst. This makes the Huisgen 1,3-dipolar cycloaddition a classic example of a click reaction.

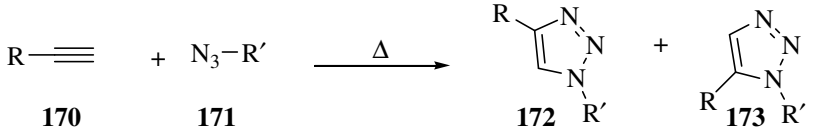

Scheme 30. Thermal Huisgen 1,3-dipolar cycloaddition reaction.[223]

In the present study, this click reaction protocol was explored to access the coumarin-AZT conjugates **167** as potential bi-functional ligands. The 3-[(2-propynylamino)methyl]coumarins **166a-e** were reacted with AZT **2** using a *tert*-BuOH / H_2O (1:1) mixture as solvent and an active Cu(I) catalytic species, generated *in situ*, at room temperature (Scheme 31). Under these conditions, the reaction did not appear to occur or was sluggish, at best, even after 48 hours. On changing the solvent system to a THF / H_2O (1:1) mixture, the desired products **167a-e** were formed after stirring for 24 hours and, following purification by flash chromatography, were obtained in yields of 64-76% (Table 7). The coumarin-AZT conjugates **167a-e** were characterized using high resolution MS, NMR and IR analysis. In the ^{1}H NMR spectrum of compound **167d** (Figure 22) the amide NH proton resonates as a broad downfield singlet at 11.37 ppm and five methylene groups are evidenced by: – multiplets at 2.58-2.73 ppm (10′-CH_2); an overlapping singlet and doublet of doublets at 3.60-3.71 ppm (1′- and 1″-CH_2); a singlet at 3.83 ppm (3′-CH_2); and a quartet (corresponding to the ethoxy methylene group) overlapping a multiplet (due to the 9′-methine proton) at 4.14-4.20 ppm. The 11′-methine proton resonates as a triplet at 6.41, while the 13′-methine and the OH proton signals overlap at 5.31-5.38 ppm. The ethoxy methyl protons appear as a triplet at 1.40 ppm and the pyrimidinone methyl protons as a singlet at 1.81 ppm. The DEPT 135 NMR spectrum (Figure 23) confirms the presence of the five methylene groups and a total of eleven methine and methyl groups. These assignments were confirmed by the COSY (Figure 24), HSQC (Figure 25) and HMBC (Figure 26) NMR spectral data.

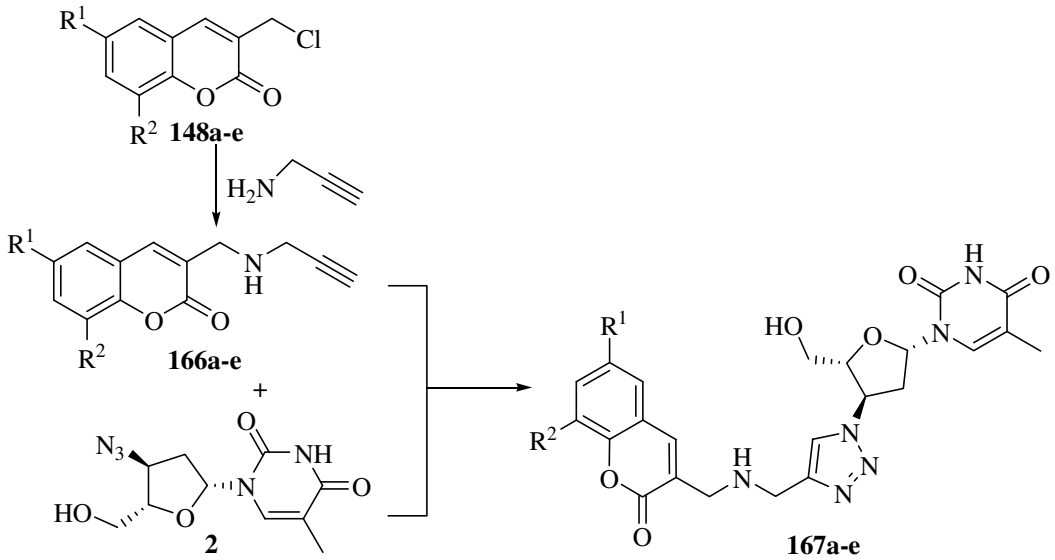

Scheme 31. Synthesis of coumarin-AZT conjugates.

Table 7. Yields of coumarin-AZT conjugates **167a-e** from the alkynes **166a-e**.

Compound	R^1	R^2	Isolated yields (%)
167a	H	H	65
167b	Br	H	76
167c	H	OMe	75
167d	H	OEt	70
167e	Cl	H	64

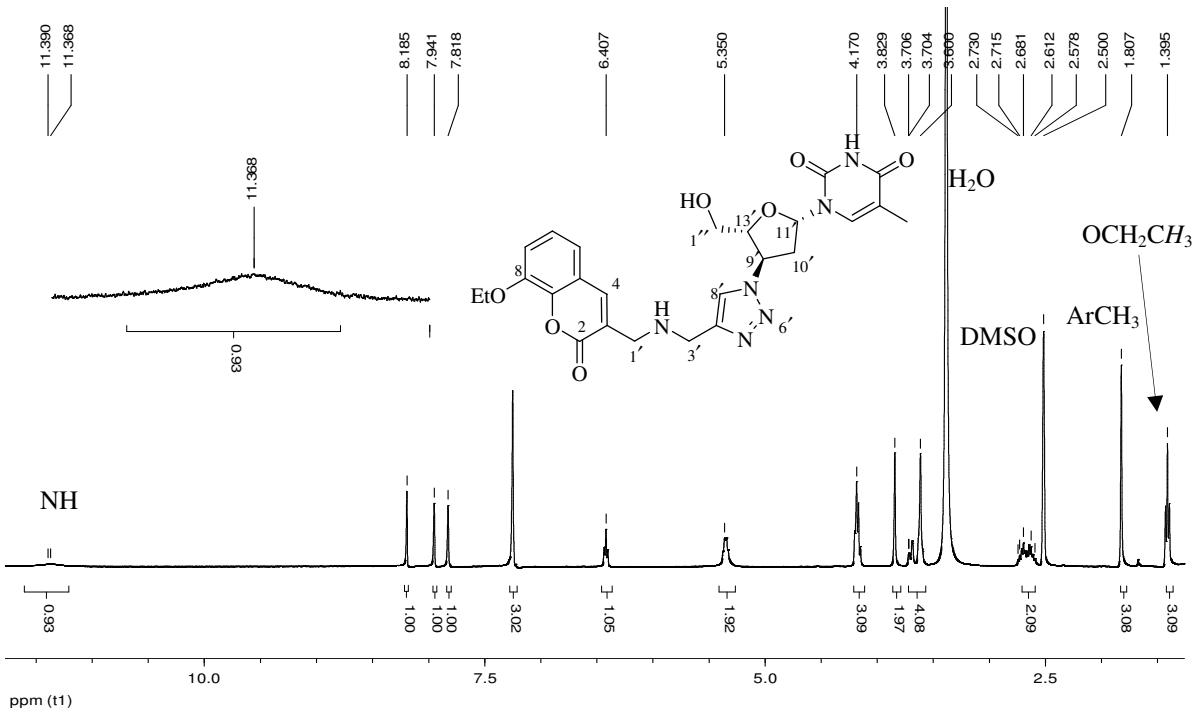

Figure 22: 400 MHz ^{1}H NMR spectrum of compound **167d** in DMSO-d_6.

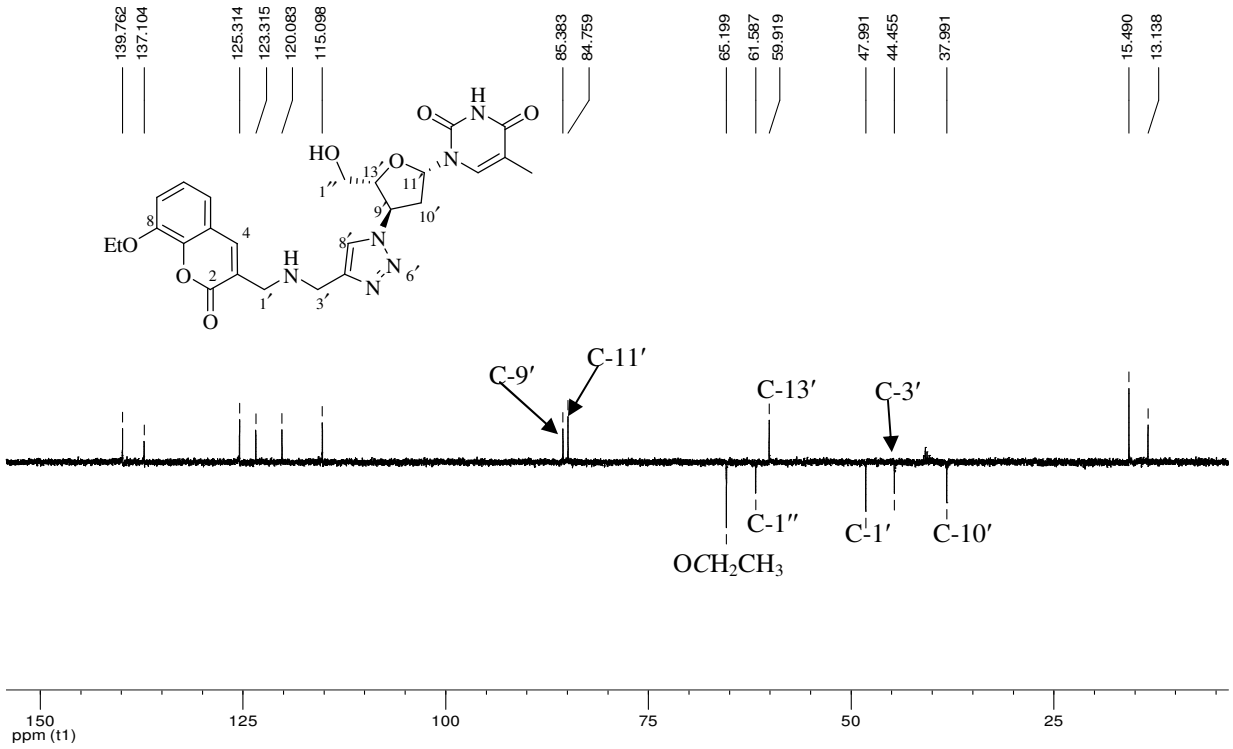

Figure 23. DEPT 135 NMR spectrum of compound **167d** in DMSO-d_6.

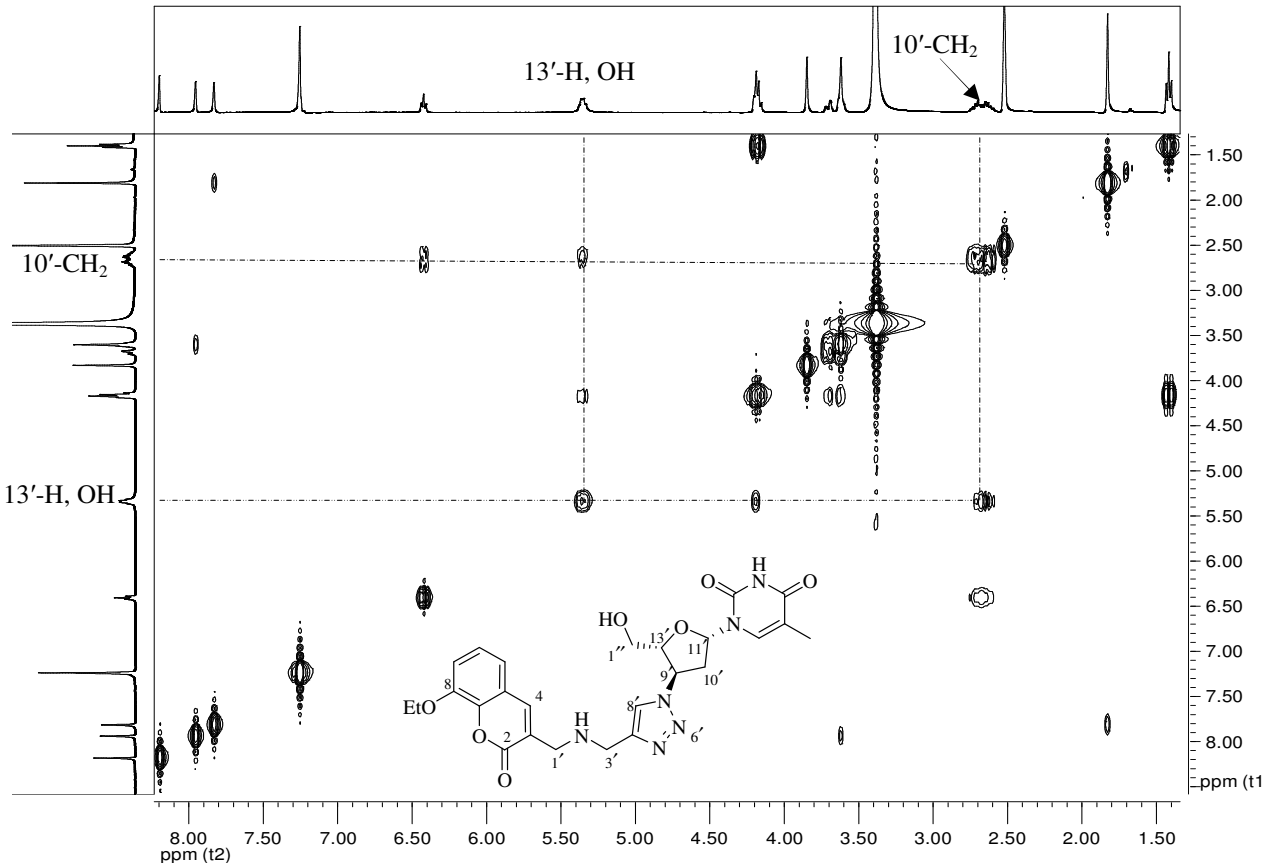

Figure 24. COSY spectrum of compound **167d** in DMSO-d_6.

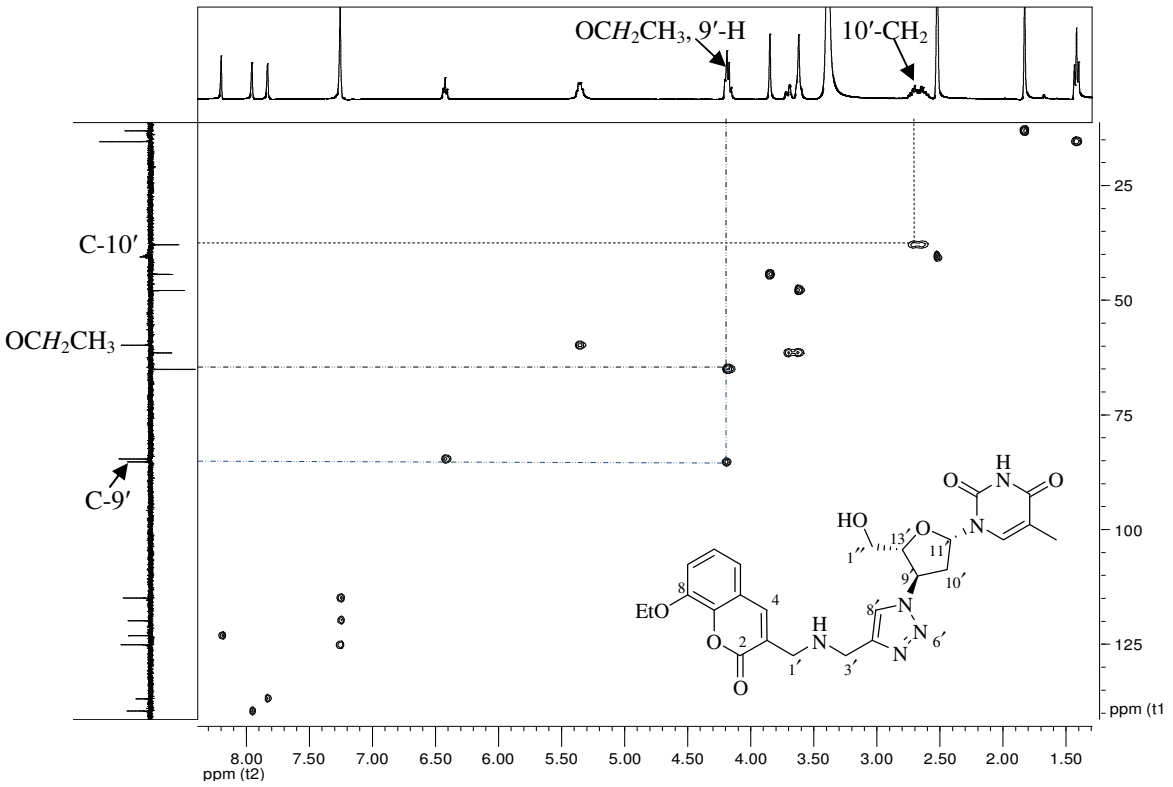

Figure 25. HSQC spectrum of compound **167d** in DMSO-d_6.

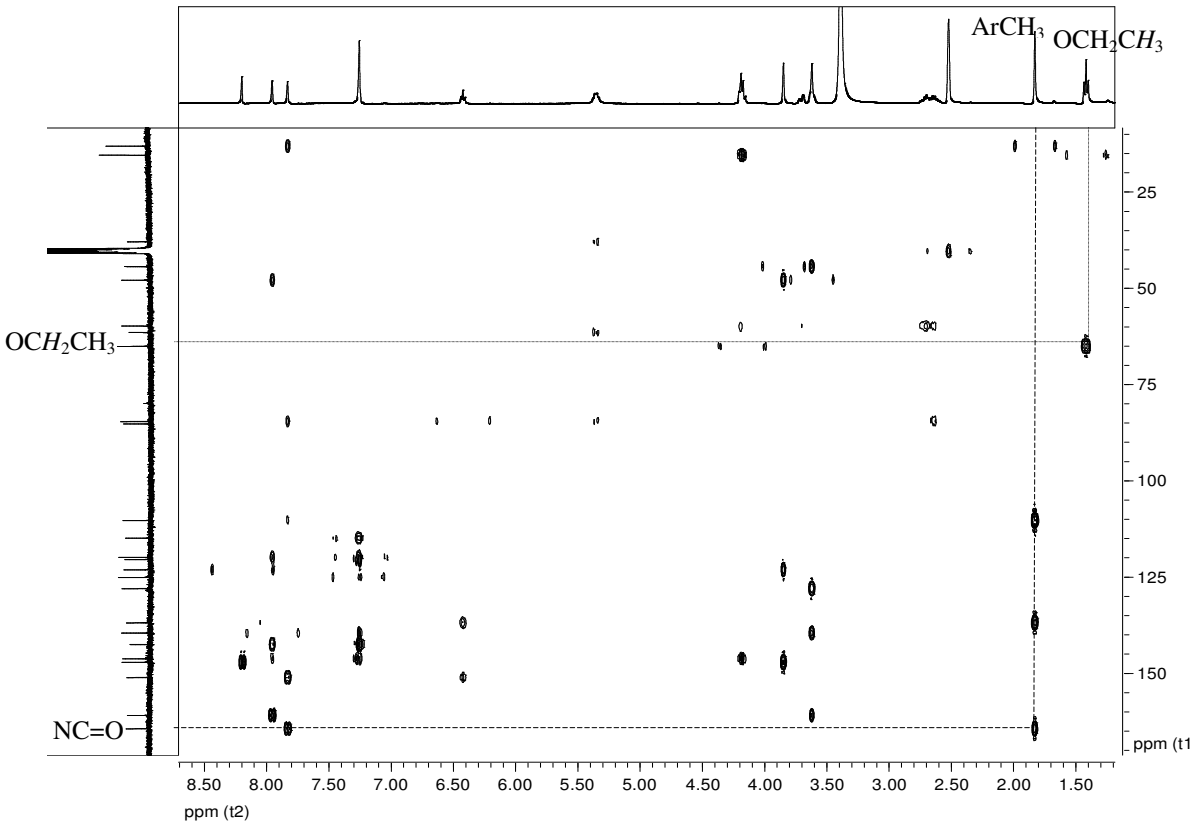

Figure 26. HMBC spectrum of compound **167d** in DMSO-d_6.

2.1.6. Synthesis of 2-[(Chloroacetamido)methyl]coumarins

As mentioned in Section 1.1.6., due to the hydrophobic character of the S_1 subsite in HIV-1 PR enzyme active site, most of the present inhibitors have hydrophobic moieties, in many cases a benzyl group, at the P_1 position.[60] It was envisaged that a benzyl group, on analogues of compounds **168a-e**, could occupy such hydrophobic pocket within the HIV-1 PR enzyme and thus enhance the binding of such ligands. The synthesis of 2-[(chloroacetamido)methyl]coumarins has been previously established in our group by reacting 3-(benzylaminomethyl)coumarins **156** with chloroacetyl chloride to give the direct S_N substitution products (Scheme 22, p. 34).[213] The NMR spectra of these compounds is complicated by the presence of rotamers arising from restricted rotation about the N-CO amide bond, and variable temperature studies on these compounds have been undertaken previously.[213] In the present study, compounds **156a-e** were reacted with chloroacetyl chloride under nitrogen in dry THF for 45 minutes to afford the corresponding chloroacetamides **157a-e** in yields of 78-98% (Scheme 32, Table 8) – a considerable improvement on the 35-74% reported by Rashamuse.[213] Due to the presence of rotamers the ^{1}H NMR spectrum of the 6-bromocoumarin derivative **157b** at 303 K (Figure 27) shows the three methylene groups resonating as a series of signals, some of which overlap, instead of three singlets in the region 4.29-4.73 ppm,. However, at 373 K, the previously split signals coalesce, due to accelerated internal rotation, and the three methylene groups resonate as singlets at *ca* 4.41, 4.50 and 4.89 ppm (Figure 28). Compound **157c**, which was not reported in the previous study by Rashamuse,[213] has been fully characterised and the molecular formula is supported by the high resolution MS data.

Table 8. Yields of the chloroacetamido derivatives **157a-e**.

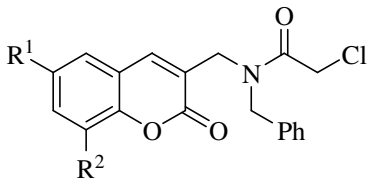

Compound	R^1	R^2	Isolated yields (%)
157a	H	H	91
157b	Br	H	78
157c	H	OMe	85
157d	H	OEt	98
157e	Cl	H	96

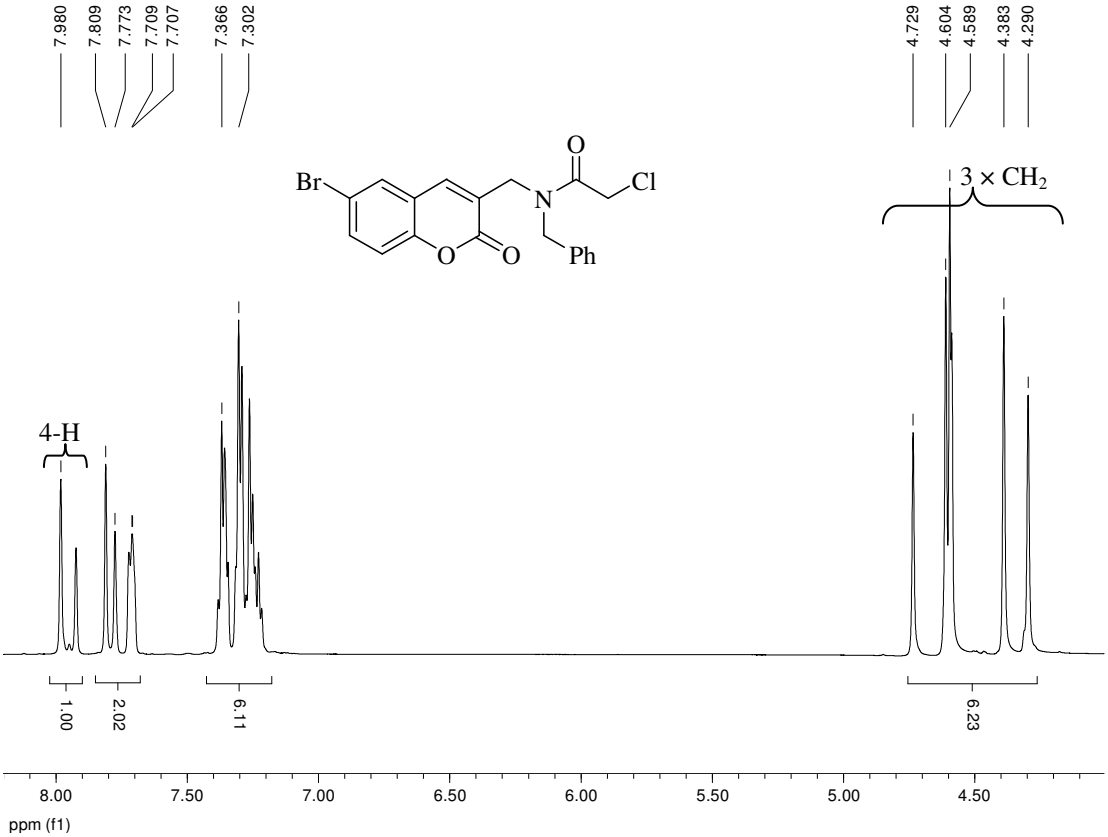

Figure 27. 600 MHz ^{1}H NMR spectrum of compound **157b** in DMSO-d_6 at 303 K.

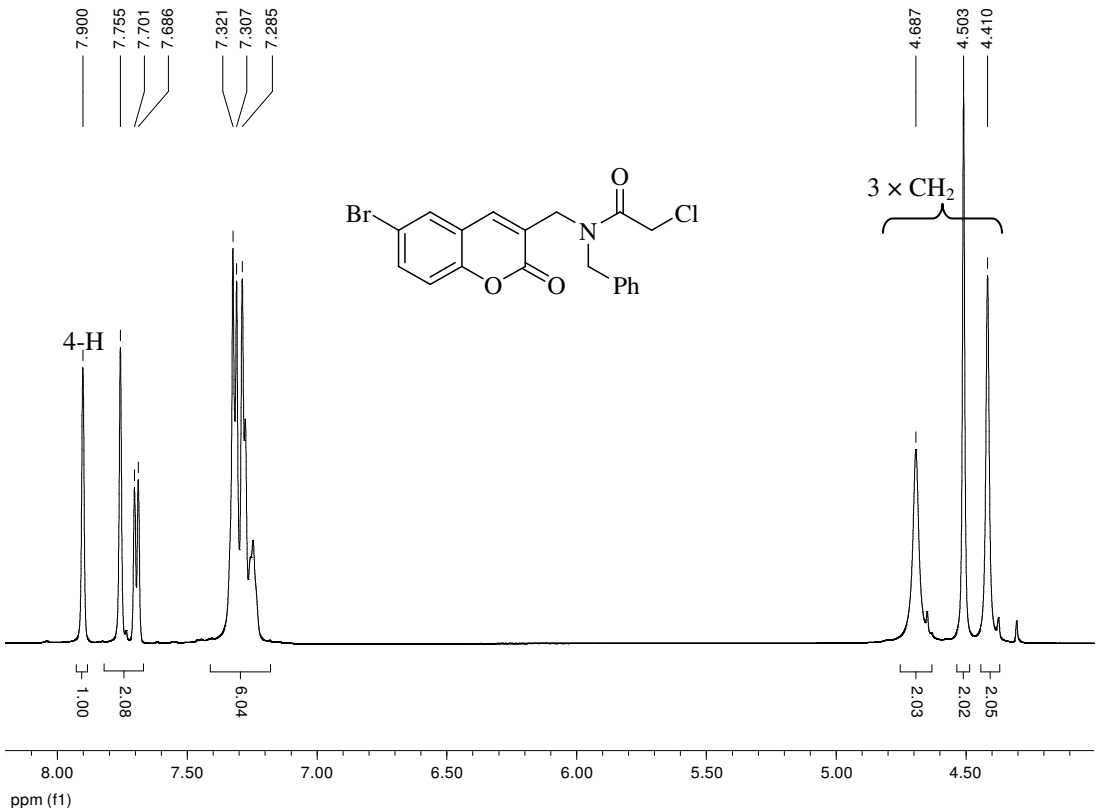

Figure 28. 600 MHz ^{1}H NMR spectrum of compound **157b** in DMSO-d_6 at 373 K.

2.1.7. Reaction of *N*-Benzylated 2-[(Chloroacetamido)methyl]coumarins with Propargylamine

With the previous success in reacting propargylamine with 3-(chloromethyl)coumarins **148** (Section 2.1.4.2.) and the aim of creating a linking group to AZT, compounds **157a-e** were reacted with propargylamine in THF for 48 hours at room temperature (Scheme 32). Purification by means of flash chromatography afforded the corresponding *N*-benzylated analogues **168a-e** in yields of 79-86% (Table 9). Compounds **168a-e,** like their simpler analogues have complicated NMR spectra due to the presence of rotamers, but were fully characterized using high resolution MS, NMR and IR analysis. The ^{1}H NMR spectrum of the 6-bromocoumarin derivative **168b** (Figure 29) reveals four sets of split singlets between 3.47 and 4.72 ppm instead of just four singlets for the four different methylene groups. The acetylenic proton resonates as two slightly overlapping singlets at *ca* 2.14 ppm, while the NH proton resonates as a broad singlet at 2.03 ppm. The ^{13}C NMR spectrum of compound **168b** shows additional signals consistent with the presence of rotamers. Despite their complicated nature, both the ^{1}H and ^{13}C NMR data still correlate properly with the assigned structures of compounds **168a-e** and the high resolution MS data correspond to the molecular formulae in all cases.

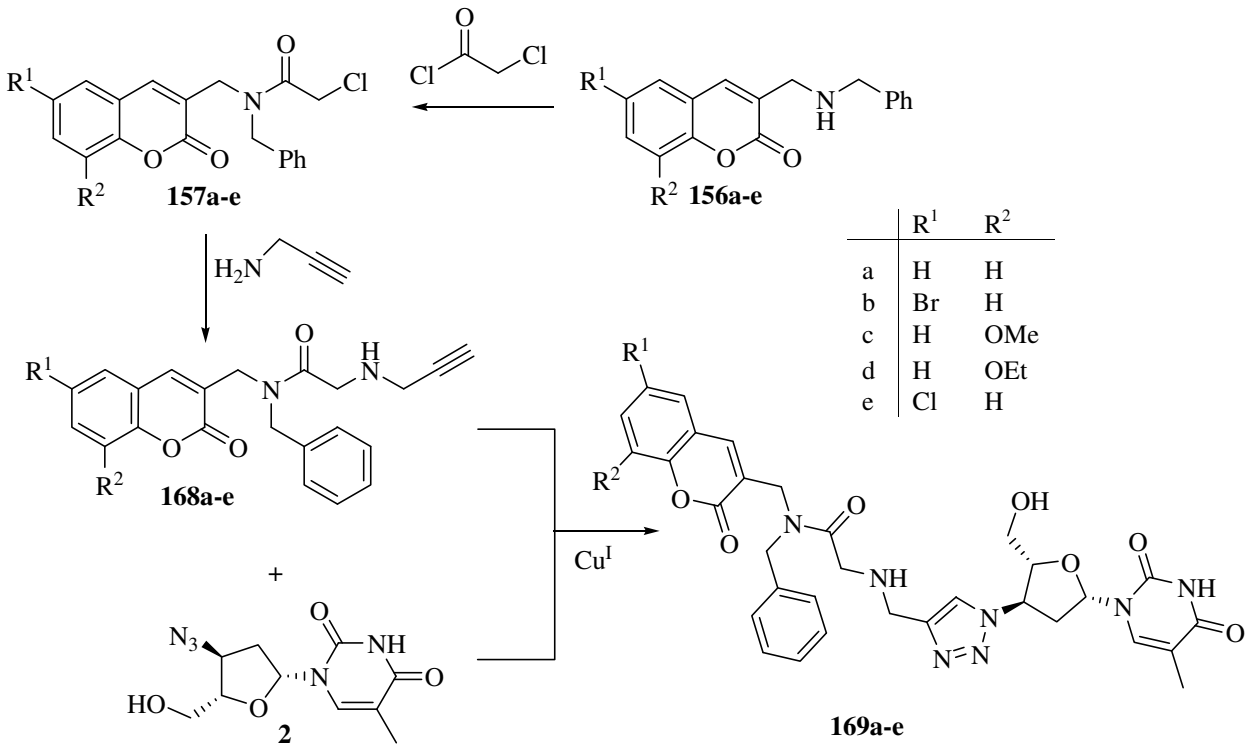

Scheme 32. Synthesis of *N*-benzylated coumarin-AZT conjugates

Table 9. Yields of *N*-benzylated 2-[(acetamido)methyl]coumarin derivatives **168a-e**.

Compound	R^1	R^2	Isolated yields (%)
168a	H	H	79
168b	Br	H	86
168c	H	OMe	86
168d	H	OEt	82
168e	Cl	H	85

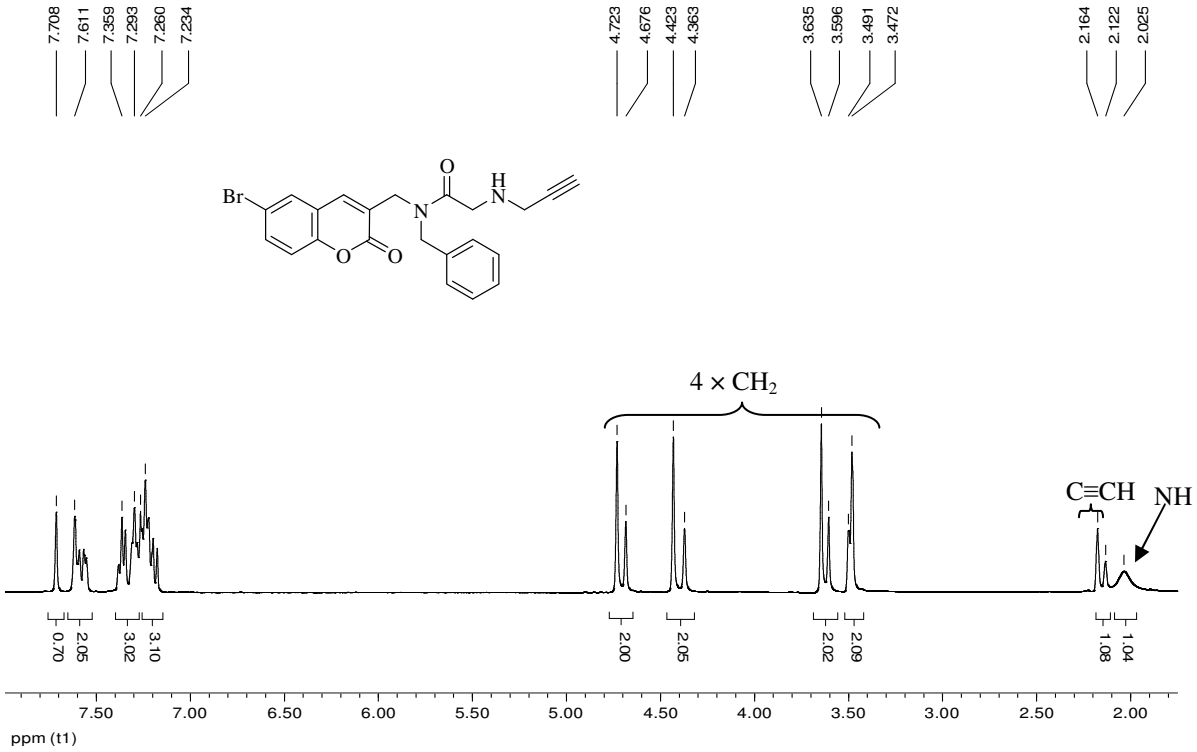

Figure 29. 400 MHz ^{1}H NMR spectrum of compound **168b** in $CDCl_3$.

2.1.8 Click Reactions of *N*-Benzylated 2-[(Acetamido)methyl]coumarin Derivatives

In continuation of our interest in bi-functional compounds as potential dual-action drugs, compounds **168a-e** were clicked to AZT **2** (Scheme 32). The *N*-benzylated 2-[(acetamido)methyl]coumarin derivatives **168a-e** were reacted with AZT **2** in THF / H_2O (1:1) with catalytic amounts of $CuSO_4 \cdot 5H_2O$ and sodium ascorbate for the *in situ* generation of Cu(I). Purification by flash chromatography gave compounds **169a-e**, as sharp-melting solids, in yields of 70-80% (Table 10). These compounds were fully characterized as usual using high resolution MS, NMR and IR analysis. The presence of rotamers again makes the NMR data for these compounds rather complicated, as illustrated in the ^{1}H NMR of the *N*-benzylated coumarin-AZT

conjugate **169a** (Figure 30) but careful analysis of the 2-D spectra permits unambiguous structural assignments and confirms the purity of the products. The high-resolution MS data are clearly consistent with the expected molecular formula of the compounds as illustrated for compound **169a** in Figure 31.

Table 10. Yields of *N*-benzylated coumarin-AZT conjugates **169a-e**.

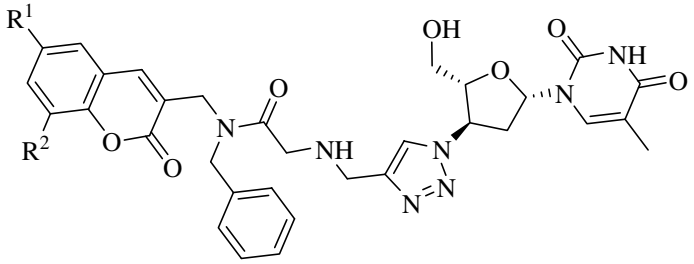

Compound	R^1	R^2	Isolated yields (%)
169a	H	H	70
169b	Br	H	80
169c	H	OMe	72
169d	H	OEt	78
169e	Cl	H	74

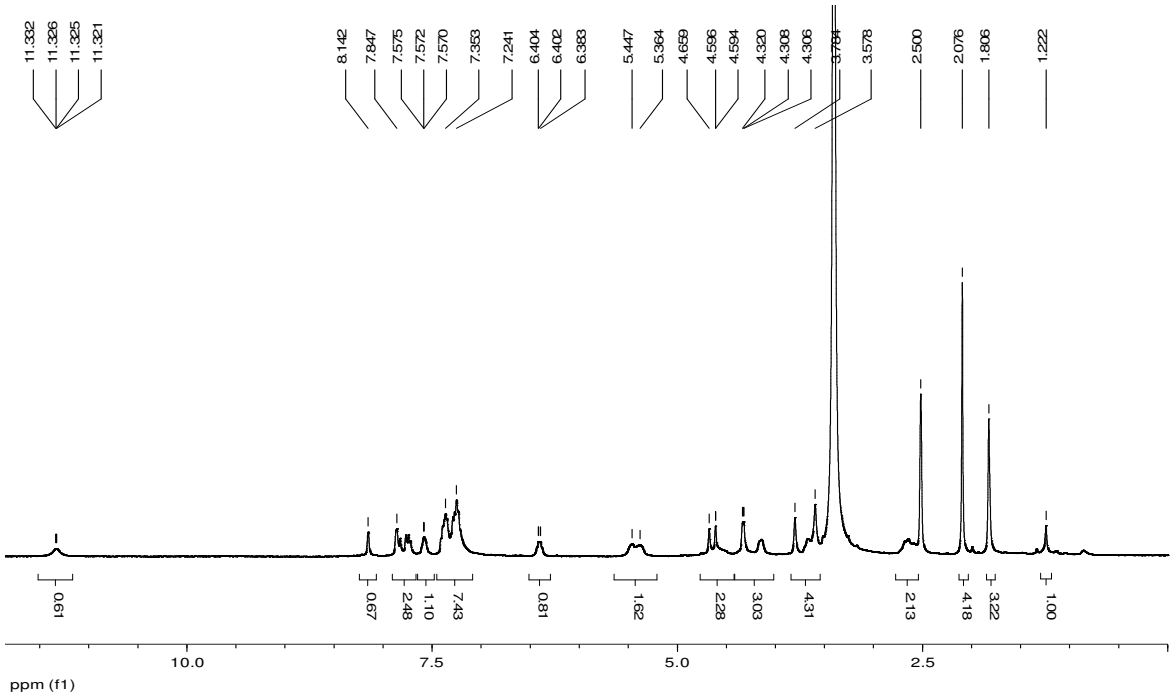

Figure 30. 400 MHz ^{1}H NMR spectrum of compound **169a** in DMSO-d_6.

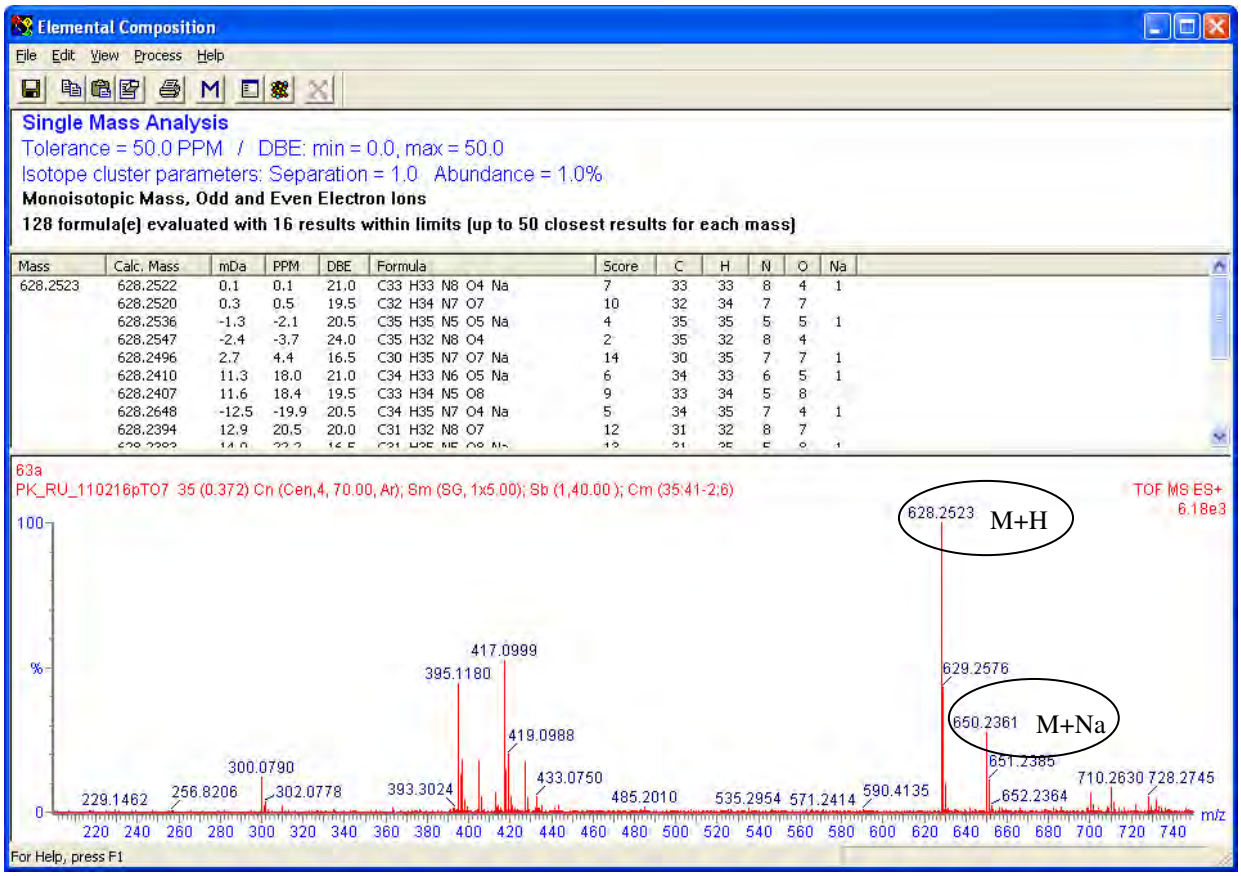

Figure 31. HRMS spectrum of compound **169a** obtained using electrospray ionization positive source conditions.

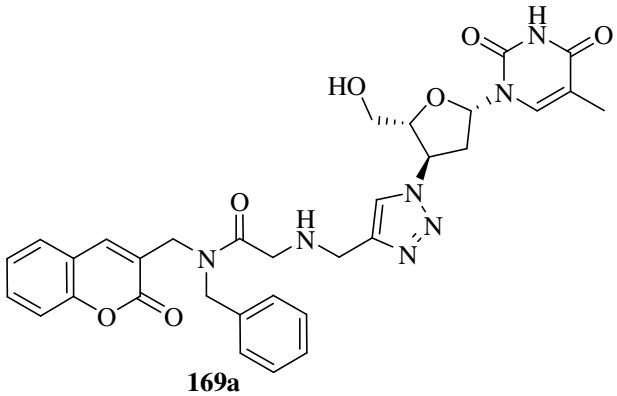

169a

Molecular formula: $C_{32}H_{33}N_7O_7$
Requires: M+H 628.2520
M+Na 650.2339

2.2. PREPARATION OF CINNAMATE DERIVATIVES

2.2.1. Conjugate Addition of Piperidine to Baylis-Hillman Adducts

Baylis-Hillman adducts are essentially α,β-unsaturated carbonyl compounds. By reacting them with primary or secondary amines in aza-Michael-type addition reactions, it is possible to access β-hydroxy hydrocinnamates, which can then be dehydrated to cinnamate esters. The Baylis-Hillman adducts **153a**,**b**,**d**,**e** were reacted with piperidine by stirring in dry THF for 48 hours at room temperature (Scheme 33). Purification by flash column chromatography gave the conjugate addition products **170a**,**b**,**d**,**e** in yields of 84-97% (Table 11). Despite the presence of two stereogenic centres, the ^{1}H NMR of the products generally suggest a single stereoisomer, however close inspection of the ^{13}C NMR indicates the formation of diastereomeric mixtures. The products were all characterized using high resolution MS, NMR and IR analysis. The ^{1}H NMR spectrum of compound **170b** (Figure 32) reveals the 1′-methine proton resonating as a doublet at 5.05 ppm and the 2′-methine proton as double doublet of doublets at 2.96, due to coupling to the diastereotopic 3′-methylene protons and to the 1′-methine proton. One of the diastereotopic 3′-methylene protons resonates as a triplet at 2.77 ppm, the other as a multiplet overlapping with a pair of piperidine methylene protons in the region 2.66-2.70 ppm. The DEPT 135 spectrum of compound **170b** reveals two non-aromatic methine carbon signals at 77.6 (C-1′) and 48.1 (C-2′) ppm (Figure 33). It also confirms the presence of four distinct methylene carbon signals representing the six methylene carbons in four different chemical environments. These assignments of the overlapping ^{1}H signals were facilitated by the HSQC data (Figure 34).

Table 11. Isolated yields of Aza-Michael addition products **170a**,**b**,**d**,**e** and **171a-e**.

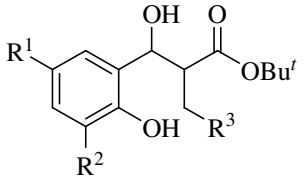

Substituent	R^1	R^2	$R^3 = N(CH_2)_5$	Yield (%)	$R^3 = NHCH_2C{\equiv}CH$	Yield (%)
a	H	H	**170a**	84	**171a**	99
b	Br	H	**170b**	97	**171b**	90
c	H	OMe	–	–	**171c**	88
d	H	OEt	**170d**	93	**171d**	95
e	Cl	H	**170e**	95	**171e**	91

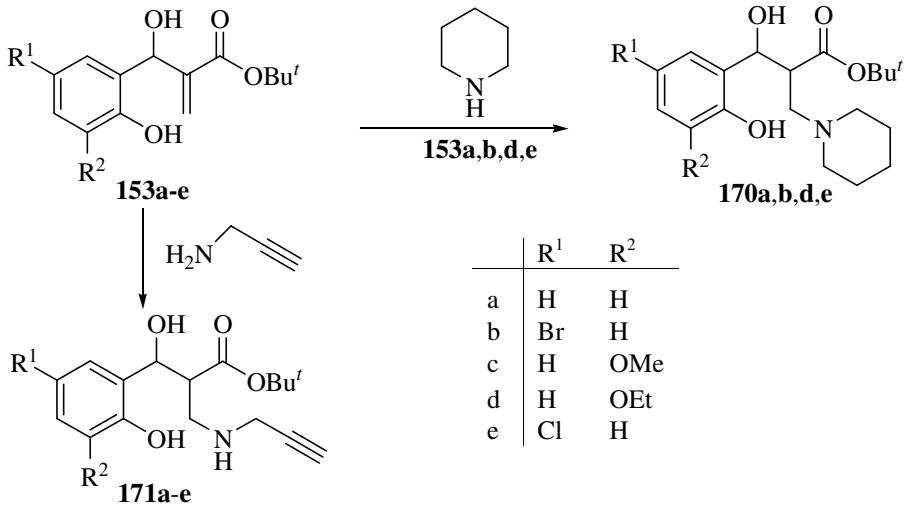

Scheme 33. Conjugate addition of nucleophiles to Baylis-Hillman adducts.

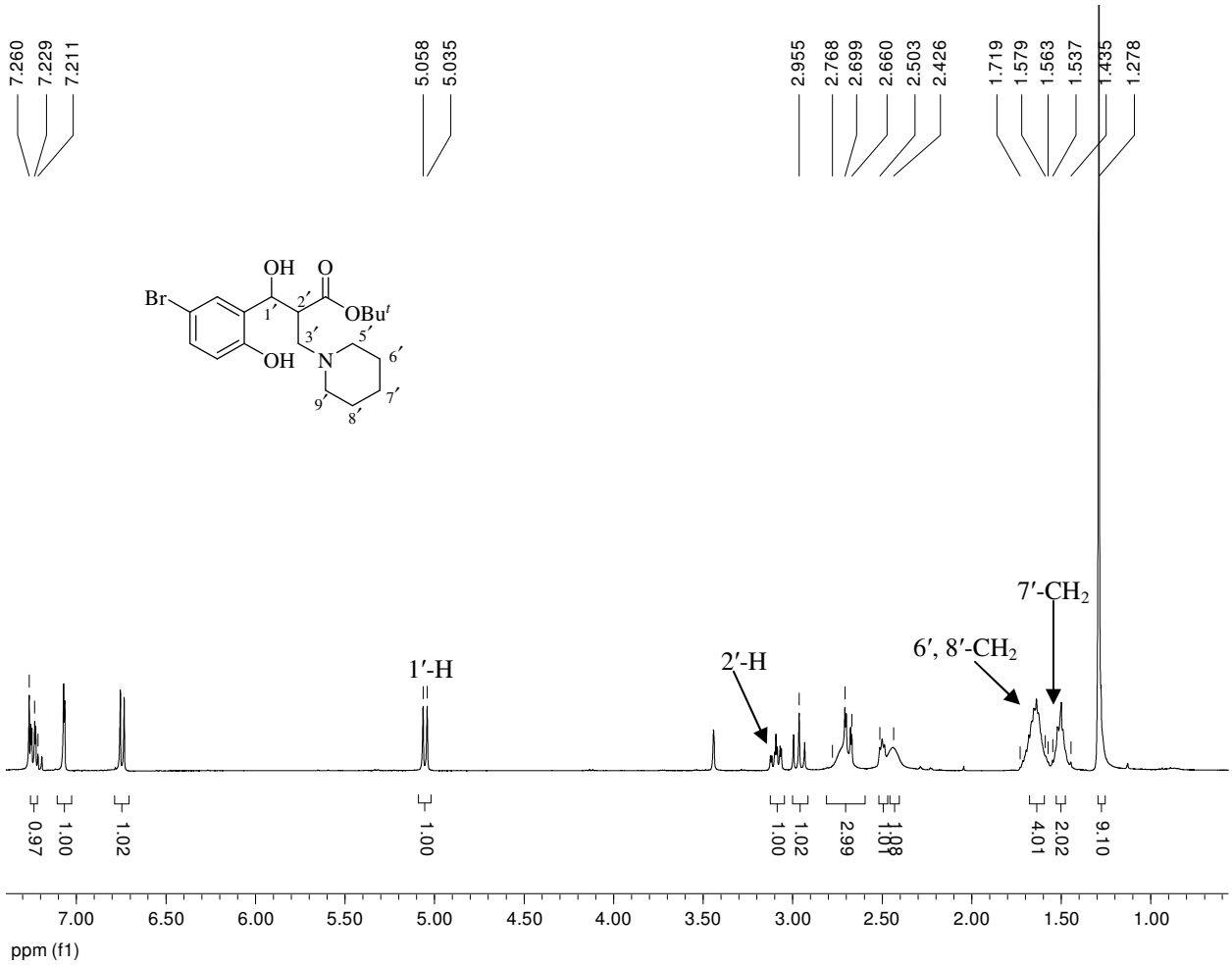

Figure 32. 400 MHz ^{1}H NMR spectrum of compound **170b** in $CDCl_3$.

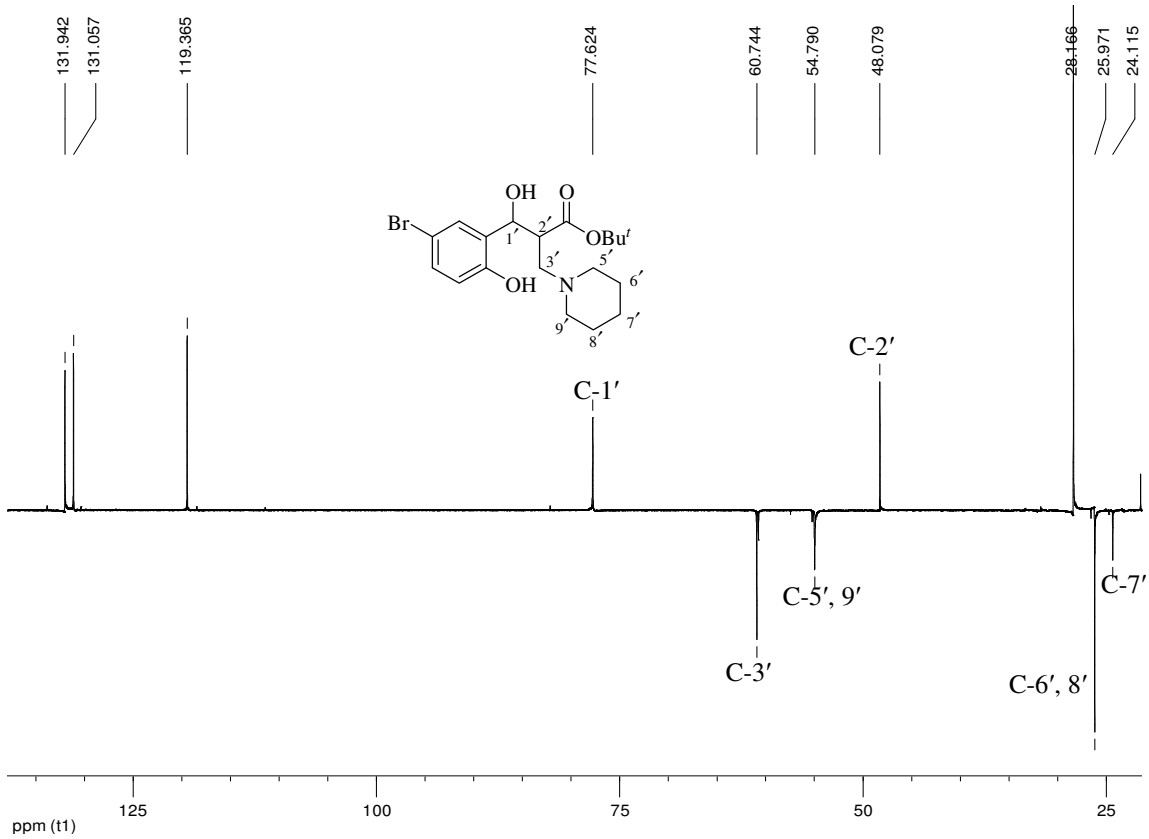

Figure 33. DEPT 135 NMR spectrum of compound **170b** in $CDCl_3$.

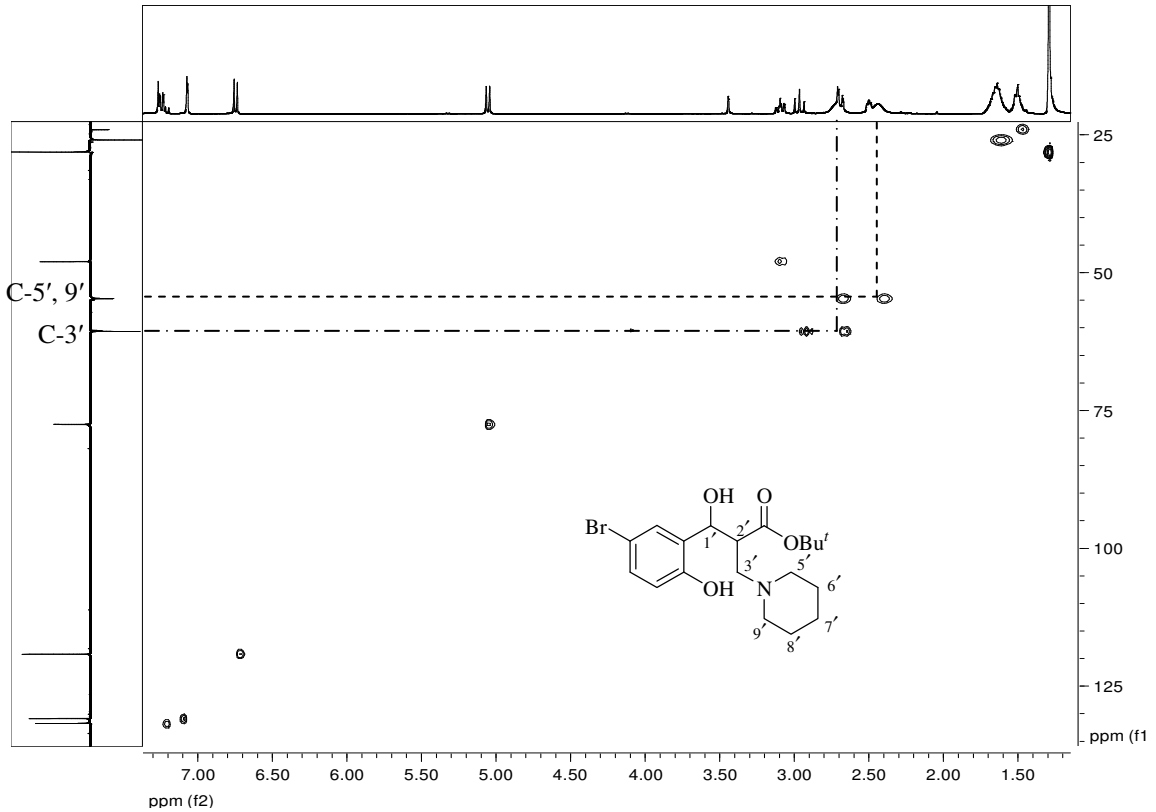

Figure 34. HSQC spectrum of compound **170b** in $CDCl_3$.

2.2.2. Conjugate Addition of Propargylamine to Baylis-Hillman Adducts

Following a procedure similar to the one described in Section 2.2.1., compounds **171a**-**e** were prepared in yields of 88-99% (Table 11) by reacting the Baylis-Hillman adducts **153a**-**e** with propargylamine in dry THF (Scheme 33). The products were fully characterized as usual. The ^{1}H NMR spectrum of compound **171e**, illustrated in Figure 35, reveals the absence of the vinylic proton signals of the Baylis-Hillman precursor, with the new diastereotopic 3′-methylene protons resonating as a double doublet at 2.70 ppm and as a multiplet overlapping the 2′-methine proton 2.78-2.84 ppm. The propargyl group is evidenced by a triplet at 3.04 (acetylenic proton) and a triplet at 3.25 ppm (methylene group). The DEPT 135 NMR spectrum of compound **171e** (Figure 36) shows a total of two methylene carbon atoms, two non-aromatic and three aromatic methine carbon atoms and an intense methyl signal.

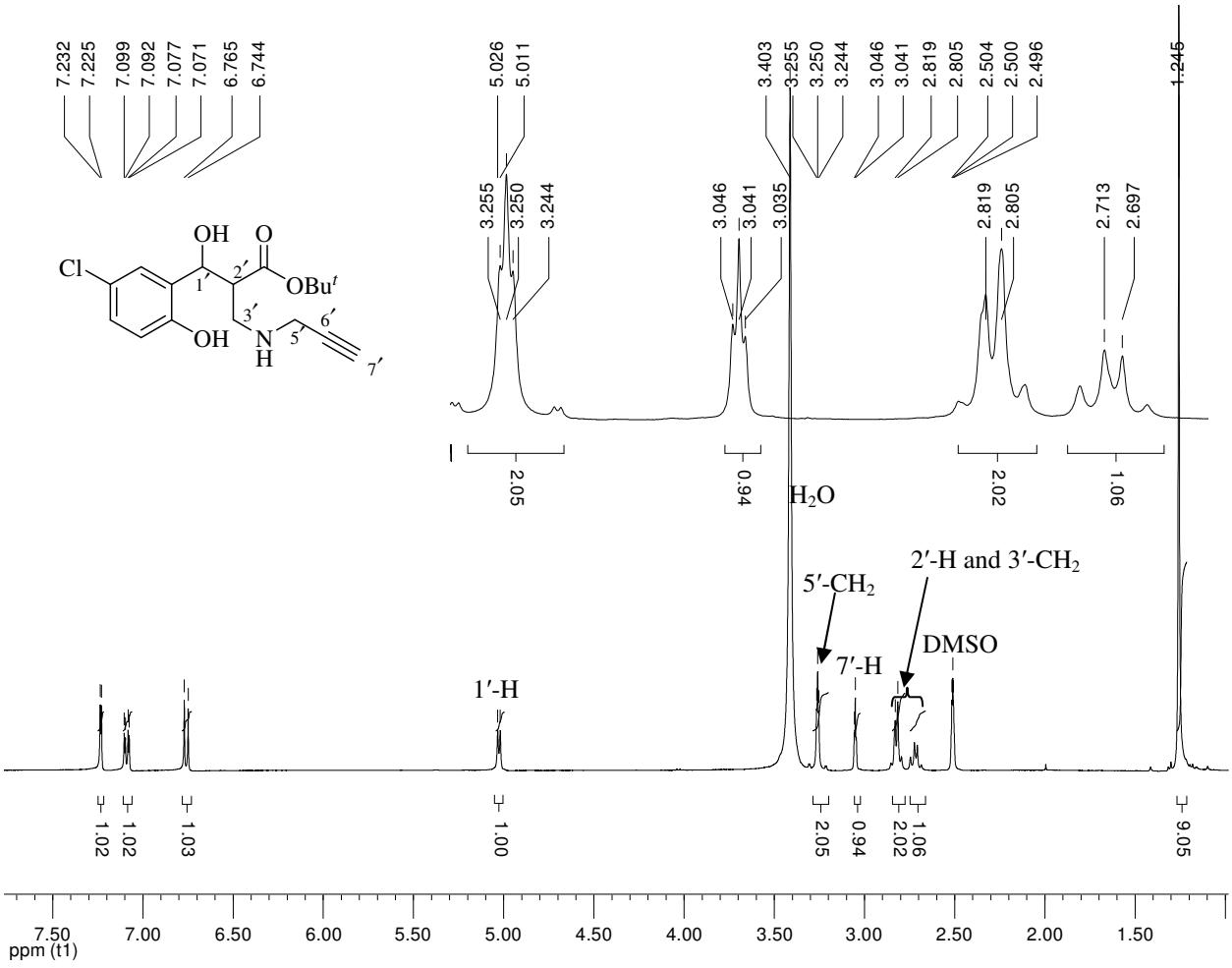

Figure 35. 400 MHz ^{1}H NMR spectrum of compound **171e** in DMSO-d_6.

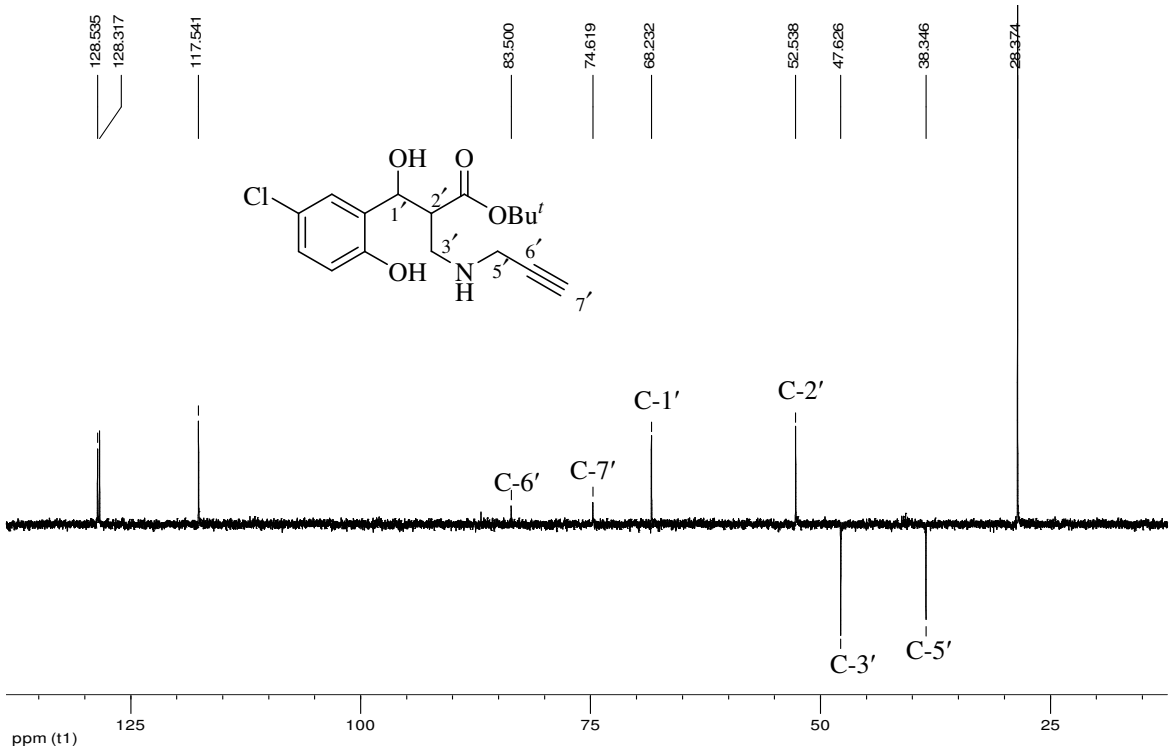

Figure 36. DEPT 135 NMR spectrum of compound **171e** in DMSO-d_6.

2.2.3. Attempted Dehydration of β-Hydroxy Esters using EDC

α-Substituted-β-hydroxyesters have been shown to undergo E2 elimination to give α-substituted (*E*)- and (*Z*)-cinnamates when a double stoichiometric ratio of 1-ethyl-3-(3-dimethyl-aminopropyl)carbodiimide **172** (EDC) is used as a dehydrating agent.[226] As described in Section 1.6., Lee had previously used this method of dehydration to afford a diastereomeric mixture of products.[214] To access its cinnamate ester derivative, compound **171e** was treated with EDC **172** in refluxing toluene for 2 hours in the presence of a small amount of $CuCl_2$. Careful investigation of the product suggested that, EDC had participated in a cycloaddition reaction to give compound **173e** with almost no evidence of dehydration (Scheme 34). Evidence for the formation of the [2+2] cycloaddition product was provided by the ^{1}H and ^{13}C NMR data. Thus, the ^{1}H NMR spectrum of compound **173e** reveals four signals in the aromatic / vinylic region, while the DEPT 135 confirms the presence of four methine signals in the corresponding region and the absence of characteristic acetylenic signals at *ca* 72 and 82 ppm.

Lee previously explored the conjugate addition of HCl to the Baylis-Hillman MVK adducts, *e.g.* compound **175**, as amination of these adducts *via* conjugate addition did not appear to be possible (Scheme 35).[214,227] The method, involving *in situ* generation of HCl from the reaction of

acetyl chloride with ethanol, had not been applied to Baylis-Hillman esters but, since it proceeded with concomitant dehydration of the MVK derivative, it seemed reasonable to explore this approach to the desired cinnamate esters.

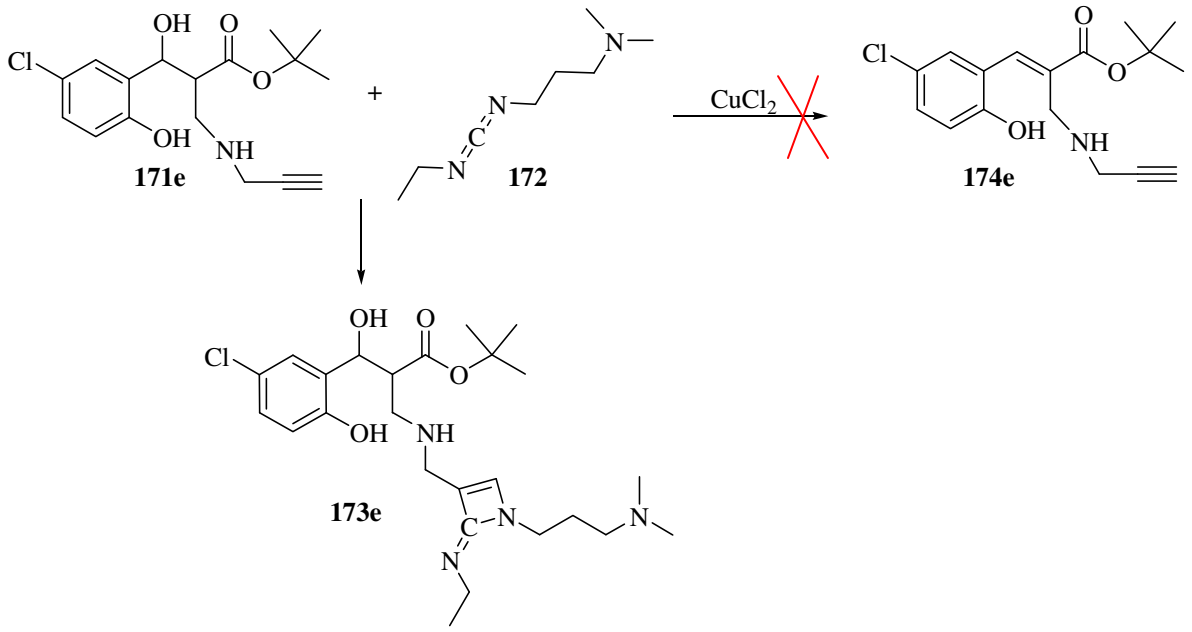

Scheme 34. Attempted dehydration of compound **171e** using EDC.

Scheme 35. Reaction of the Baylis-Hillman adduct **175** with *in situ*-generated HCl.[214]

Hydrochlorination of the *tert*-butyl 3-hydroxy-3-(2-hydroxyphenyl)-2-methylenepropanoates **153a-e** using *in situ*-generated HCl (Scheme 36) gave two products in each case, the hydrolysed cinnamic acid derivative **177** as the major product and the cyclised coumarin analogue **148** (Table 12). Fractional recrystallisation permitted separation of compounds **177a** and **148a**, and the structure of compound **177a** was confirmed unequivocally by X-ray crystallography, which also indicated the *Z*-configuration about the double bond (Figure 37). Refluxing the crude mixture of compounds **177a** and **148a** in acetic acid for 1 hour resulted in a complete conversion to compound **148a**.

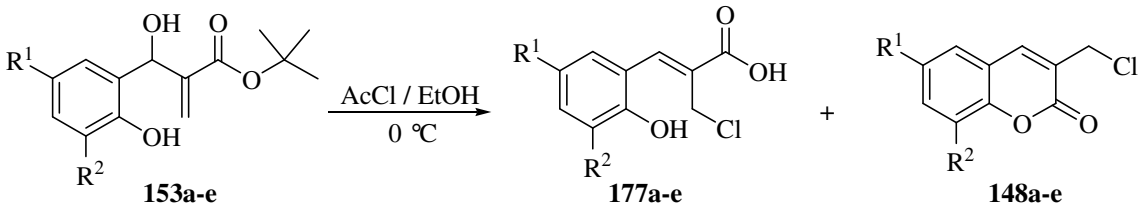

Scheme 36. Hydrochlorination of Baylis-Hillman adducts **153a-e** using *in situ*-generated HCl.

Table 13: Yields obtained for chlorination of Baylis-Hillman adducts **153a-e**.

Substrate	R^1	R^2	Yield of 177[a] (%)	Yield of 148[a] (%)
153a	H	H	83[b]	13[b]
153b	Br	H	84	14
153c	H	OMe	90[b]	10[b]
153d	H	OEt	85	10
153e	Cl	H	90	10

[a] Estimated by ^{1}H NMR analysis.
[b] Isolated yields.

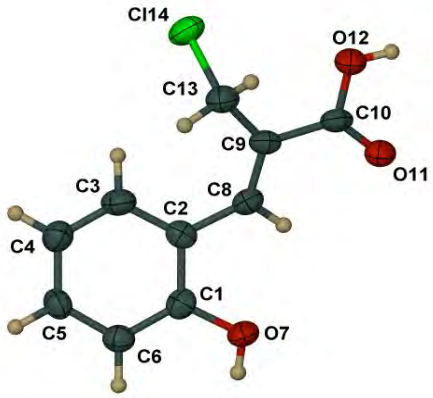

Figure 37. Crystal structure of cinnamate ester derivative **177a**, showing the crystallographic numbering.

2.2.4. Tandem "Hydrolytic", Conjugate Addition and Elimination Reactions of Baylis-Hillman Adducts – Mechanistic and Theoretical Study

With the establishment of the structure of the major and minor products resulting from the reaction of the Baylis-Hillman adducts **153a-e** with HCl, attention was given to unravelling the mechanistic sequence involved in the formation of these products. Both experimental kinetic and theoretical approaches were used to explore the reaction, which clearly involves: – ester hydrolysis; either S_N' or conjugate addition–elimination; and cyclisation steps. The reaction of the parent system **153a** was monitored by ^{1}H NMR spectroscopy. This revealed that the hydrolysis of the tertiary butyl ester proceeds early in the course of the reaction, leading to the conclusion that the formation of the acid is the first step in the reaction. Once compound **179a** is

formed (Scheme 37), there appear to be two possible subsequent pathways, *viz*., path A (leading to the formation of the acyclic, chloromethyl product **177a**) and path B (leading to the cyclised, coumarin analogue **148a**). The expectation[228] that path A is initiated by protonation of the carbonyl oxygen and conjugate addition of the chloride anion to the hydrogen-bonded chelate **179aI** (Scheme 37) – rather than protonation of the hydroxyl oxygen followed by S_N' displacement of water by chloride ion – is supported by computational data. Thus, calculation of the condensed local softness values for the carbonyl and hydroxylic carbons (Figure 38), using the electrophilic Fukui function (f^+) evaluated at a B3LYP/6-31G(d) level of theory on Gaussian 03,[229] shows that the carbonyl carbon has a greater local softness.[230] This suggests that the shift of the π-electrons would favour conjugate addition rather than an S_N' mechanism, supporting a previously suggested mechanism for a similar system.[228] Conjugate addition of Cl^- is then followed by tautomerism and dehydration to afford compound **177a**. In path B, on the other hand, acid-catalysed lactonisation might be expected to proceed *via* intermediate **180a**. Computational data suggests that the protonated intermediate **179a** is converted to **177a** spontaneously (*i.e*. negligibly small transition state is involved), the NMR kinetic data however shows the presence of a signal corresponding to compound **179aIII**, *viz*., the CHOH methine doublet, which disappears in the course of the reaction (Figure 40). A plot of the concentrations of the starting material, intermediates and products affords curves shown in Figure 41. By increasing the concentration of generated HCl significantly higher than the concentration of **153a** the pseudo-first order approximation was employed and the rate of the reaction consequently determined. Thus the rate is given by Equation 1:

$$r = k[A][B] = k_{obs}[B] \qquad (\mathbf{1})$$

and $k_{obs} = k[A]_0$

where $[A]_0$ the initial concentration of HCl = 2.35 M. Then by creating a plot of ln[B] against time, the pseudo-first order rate constant k_{obs} was determined (Figure 42).

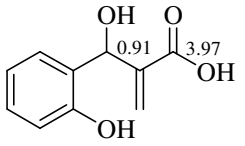

Figure 38. Structure of compound **179a**, showing condensed local softness values for possible movement of π-electrons following nucleophilic attack at the vinylic carbon centre.

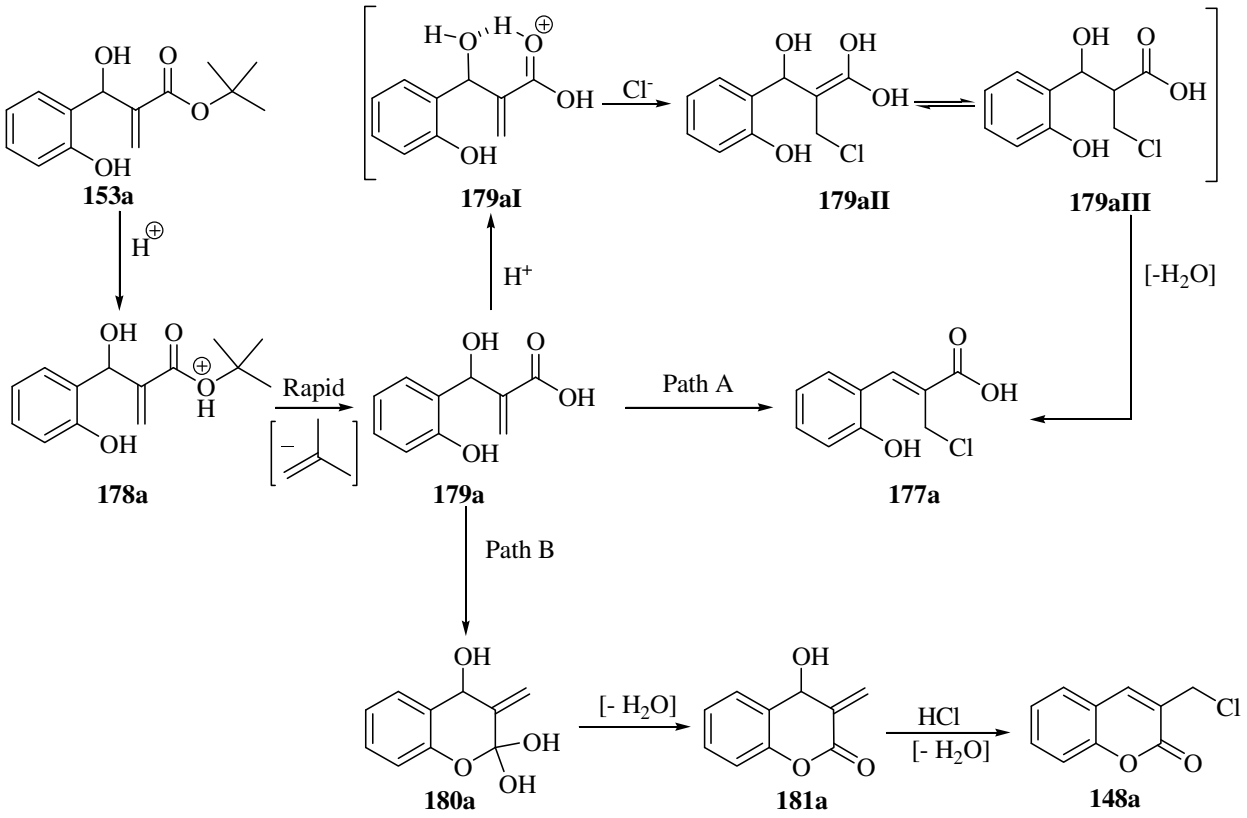

Scheme 37: Proposed pathways leading to compounds **177a** and **148a**.

Compound	Signal	ppm
153a	3′-methylene	5.797-5.866
179a	ArH	7.933-8.029
177a	3′-methylene	4.565-4.513
148a	ArH	8.286-8.357
180a	4-H	5.585-5.667

Figure 39. Tabulated values of signals and their origin used to calculate the concentrations used for the kinetic plots.

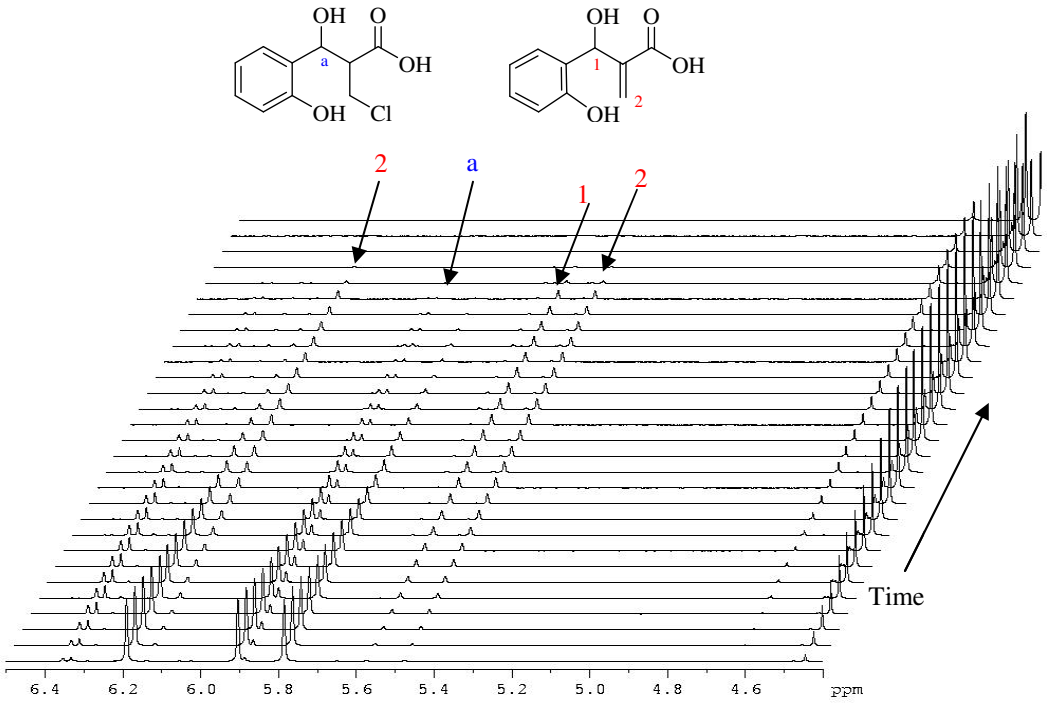

Figure 40. Time-dependent partial 600 MHz ^{1}H NMR spectra in MeOD.

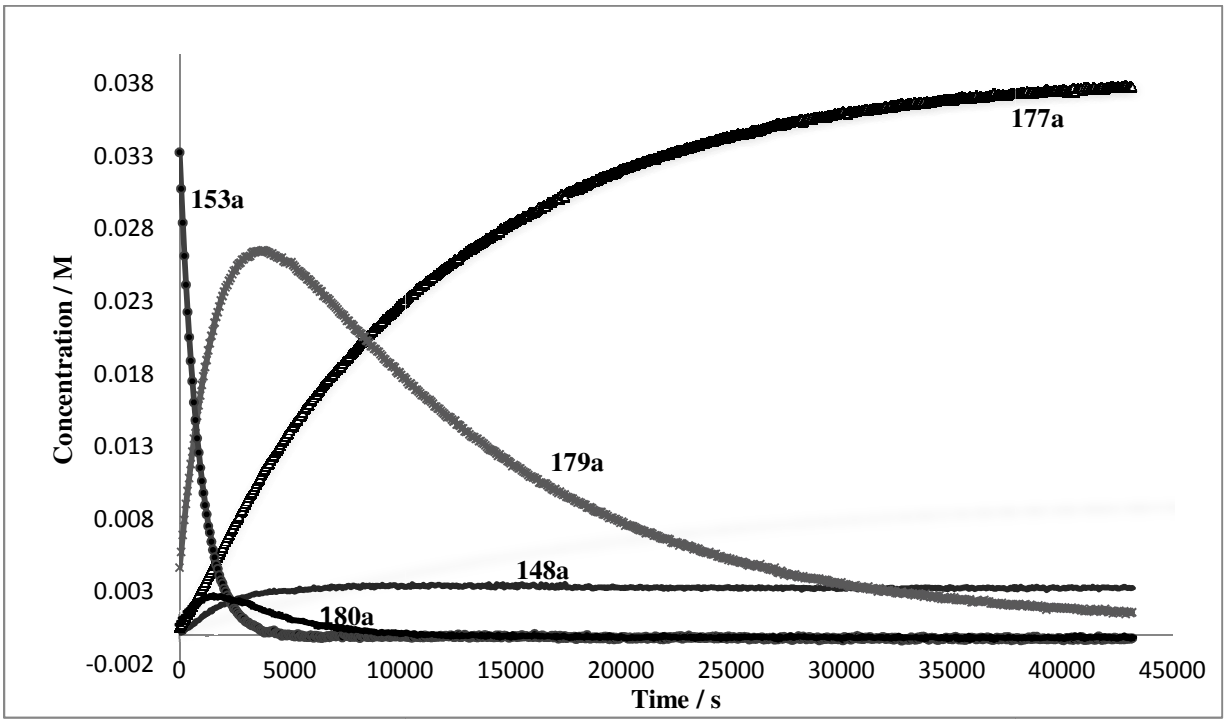

Figure 41: Graph of concentration against time for the reaction of Baylis-Hillman adduct **153a** with *in situ*-generated HCl at 276.2K, showing the starting material **153a**, intermediate **179a**, **180a**, major product **177a**, and minor product **148a**.

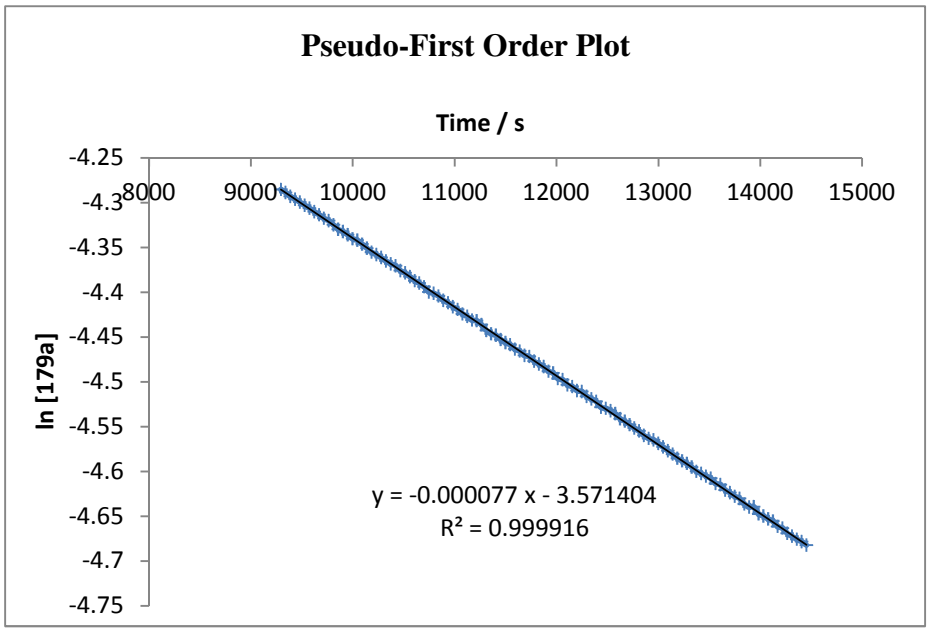

Figure 42. Logarithmic curve fit indicating a pseudo-first order kinetic path for **179a** → **177a** at 286.45 K from 9,000 s onwards; [HCl] = 2.35M.

Examination of kinetic plots in Figure 41 reveals that formation of the minor product, the coumarin derivative **148a**, effectively ceases once the *tert*-butyl ester has been consumed. This is consistent with its formation *via* intramolecular transesterification of the protonated ester prior to the rapid "hydrolysis" (in fact, the *O*-alkyl cleavage) of the latter to the intermediate carboxylic acid **179a**. The results of the theoretical study clearly indicate that the lactonisation **179a** → **148a** *via* path B is energetically disfavoured. Thus, after *ca* 5,000 s, the rate of consumption of the intermediate **179a** may be equated to the rate of formation of product **177a.**

With the aim of determining the activation energy parameters ($\Delta G^{\ddagger}$), ($\Delta H^{\ddagger}$) and ($\Delta S^{\ddagger}$) components for the rate determining step, the effect of temperature on reaction rates was studied at six different temperatures between 276.2 and 293.4 K and the Arrhenius plot (R^2 = 0.8848) permitted evaluation of the activation energies E_a (Table 14) and an Eyring plot (R^2 = 0.8783) permitted direct evaluation of the activation parameters $\Delta H^{\ddagger}$ and $\Delta S^{\ddagger}$. The Gibbs-free energy of activation $\Delta G^{\ddagger}$, at 298K, was thus calculated. The role of the common, transient intermediate **179a** in the formation of both products, **177a** and **148a**, is supported by the experimental NMR data. Its rapid conversion to compound **177a** (rather than compound **148a**) is consistent with a very low activation-energy barrier. In fact, the failure to locate a transition state for the transformation **179a** → **177a**, suggests that it may be virtually spontaneous.

Table 14. Kinetic parameters obtained from Arrhenius and Eyring plots for the formation of compound **177a**.

E_a (kCal/mol)	18.95 ± 0.30
$\Delta H^{\ddagger}$ (kCal/mol)	18.39 ± 0.30
$\Delta S^{\ddagger}$ (Cal/mol/K)	-15.09 ± 6.06
$\Delta G^{\ddagger}$ (kCal/mol)	22.89 ± 0.31

Error values were calculated from the respective standard errors for the slope and intercept for each graph.

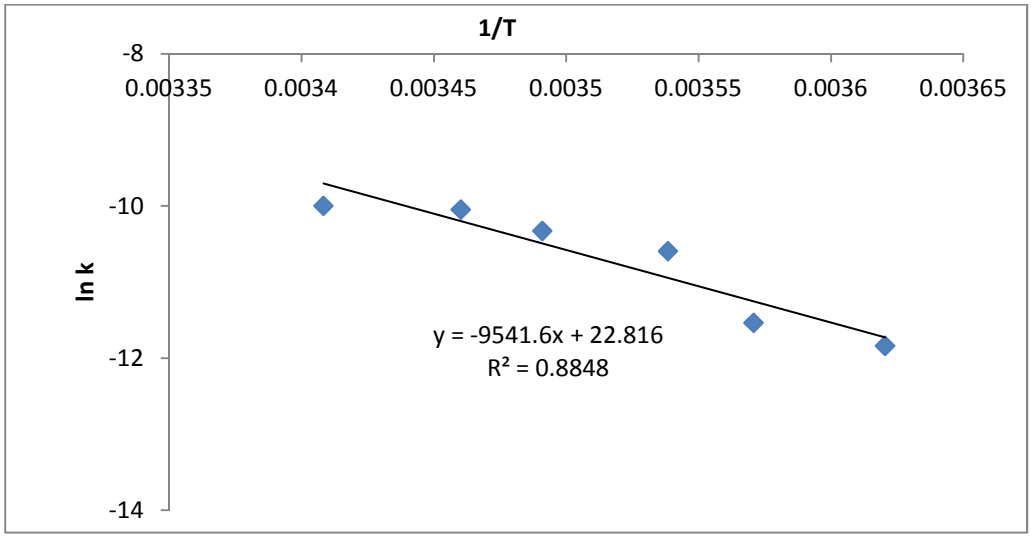

Figure 43. Arrhenius plot of ln k against 1/T for the formation of compound **177a**.

Energy minimization of compounds to determine their global minimum conformation was achieved using the Universal Force Field on Cerius 2. The resulting structures were then optimised at the B3LYP level with basis set 6-31G(d); DFT and UHF (for transition state) calculations were done using the Gaussian 03 programme[229] running on an Intel/Linux cluster and Gaussview 4.1 was used for visualization. Intermediates were set up as indicated in Scheme 37, and approximate transition structures were obtained by the quadratic synchronous transit method of Halgren and Lipscomb,[231] except in the case of the transformation of **179a** to **177a**. Transition states were characterised by a single imaginary frequency. The free-energy profile diagram shown in Figure 44 is mass-balanced and, the minor product **148a** is thermodynamically more stable. It can be inferred from the energy profile that the route to the major product **177a** is kinetically controlled.

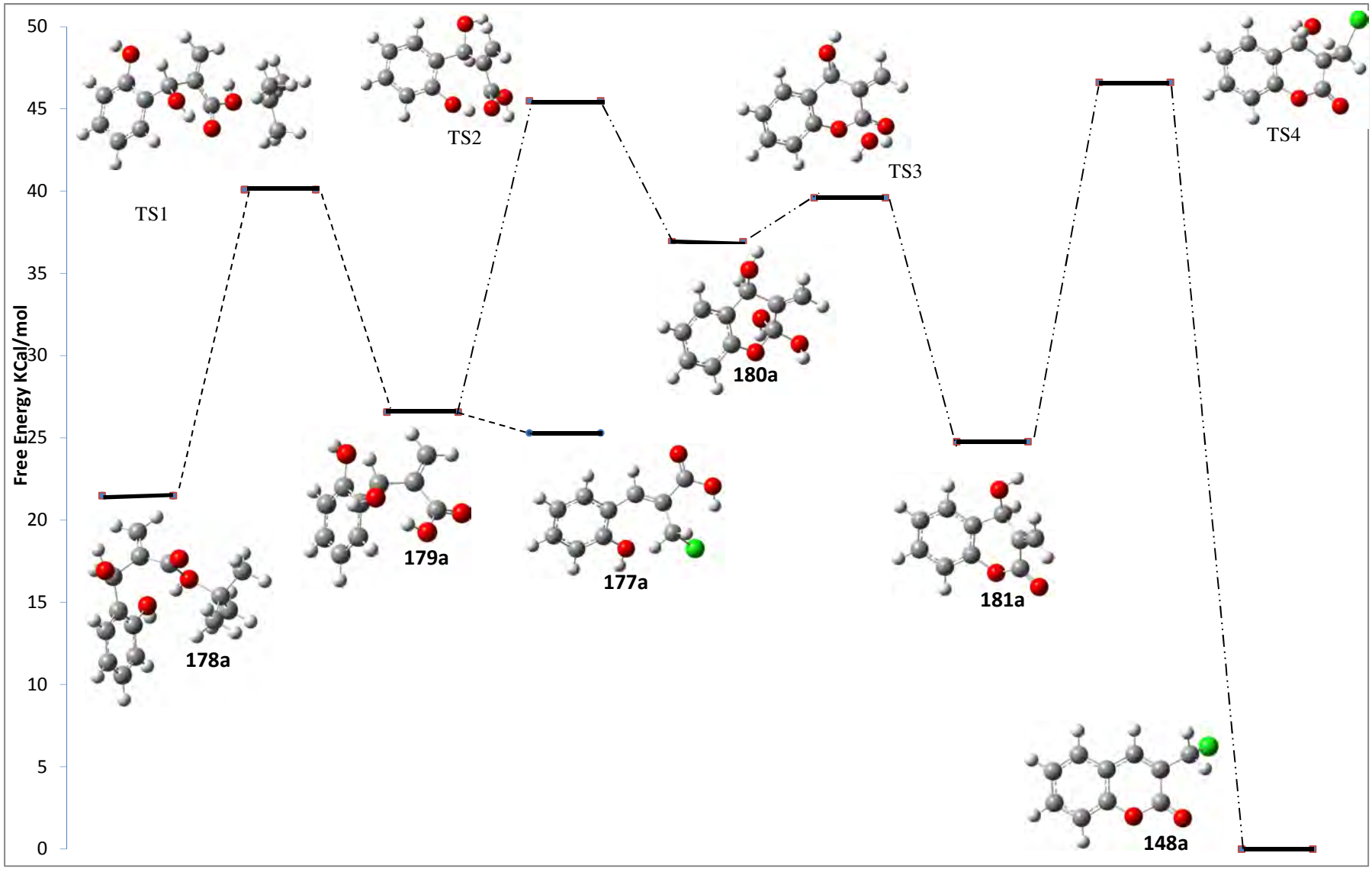

Figure 44. Mass balanced energy profile diagram for the formation of compounds **177a** and **148a**.

2.2.5. Use of Benzyl-protected Salicylaldehydes for the Preparation of Cinnamate Esters

With initial attempts to access cinnamate esters being unsuccessful, a different approach, illustrated in Scheme 38 was explored. This involved benzylation of the phenolic group to prevent lactonisation.[210] When substituted salicylaldehydes **142a**,**b** were heated with *in situ*-generated benzyl iodide in the presence of anhydrous K_2CO_3 in acetone the β-hydroxyketones **220a**,**b** were obtained instead of the desired **145a**,**b**. This transformation clearly involves a base-catalysed crossed aldol reaction between acetone enolate and the aldehyde group to give compounds **220a**,**b** in yields of 92 and 95%, respectively. The ^{1}H NMR spectrum of **220b** (Figure 45) reveals that one of the diastereotopic 2′-methylene protons resonates as a doublet at 2.94 ppm, the other as a doublet of doublets at 2.67 ppm. The methyl group resonates as a singlet at 2.13 ppm and the methine proton as a doublet at 5.44 ppm. ^{13}C NMR spectrum confirms the presence of fifteen carbon atoms in different environments, as expected, while the DEPT 135 spectrum reveals the benzylic and C-2′ methylene carbon signals at 70.2 and 49.9 ppm, respectively. In order to obtain the benzyl-protected salicylaldehydes **145a-e**, the solvent was changed to absolute ethanol and using the above reaction conditions the desired compounds were obtained in yields of 80-92% (Table 15). The ^{1}H NMR spectrum of 2-(benzyloxy)-5-bromobenzaldehyde **145b** (Figure 46) reveals the presence of the benzylic proton singlet at 5.18 ppm and the aldehydic proton singlet at 10.46 ppm, while the ^{13}C NMR spectrum (Figure 47) shows the corresponding carbon signals at 71.3 and 188.7 ppm, respectively.

Table 15. Yields of 2-(benzyloxy)benzaldehydes **145a-e**

Compound	Isolated yields (%)
145a	99
145b	90
145c	88
145d	95
145e	91

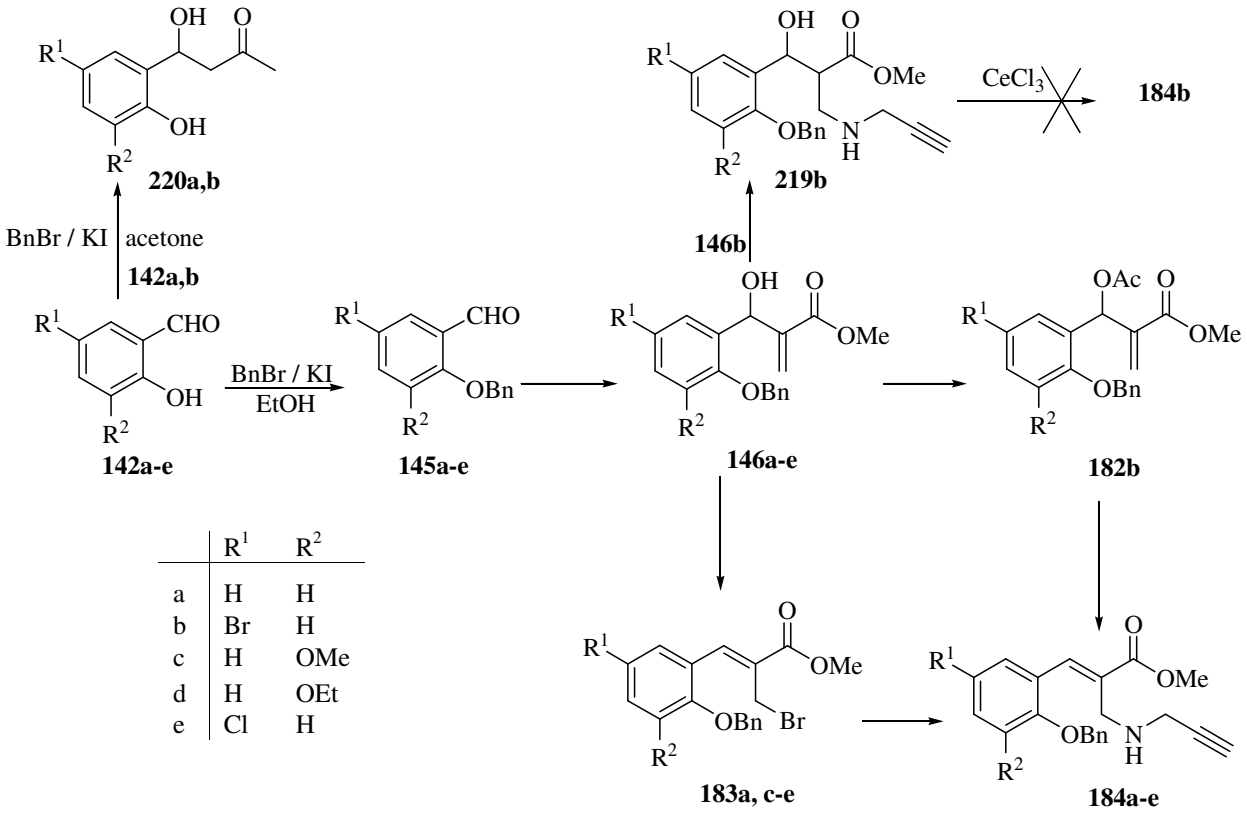

Scheme 38. Proposed route to cinnamate esters.

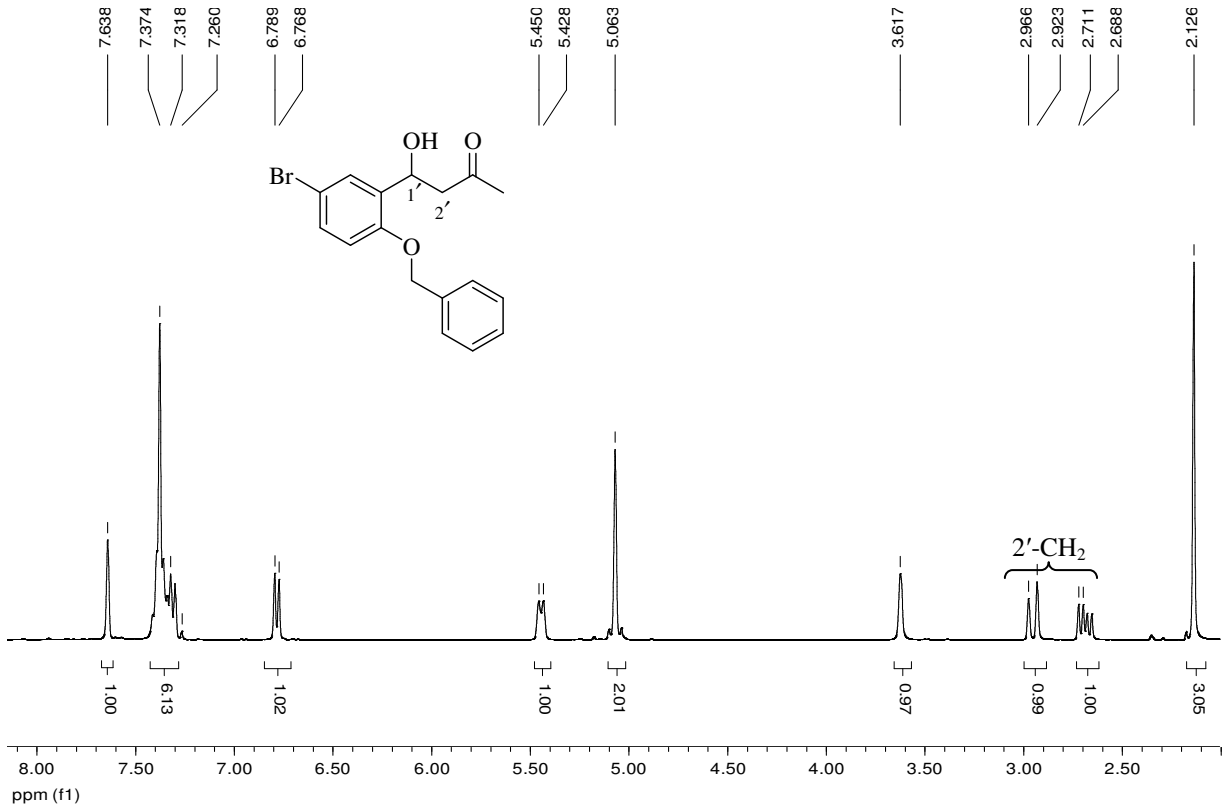

Figure 45. 400 MHz ^{1}H NMR spectrum of compound **220b** in $CDCl_3$.

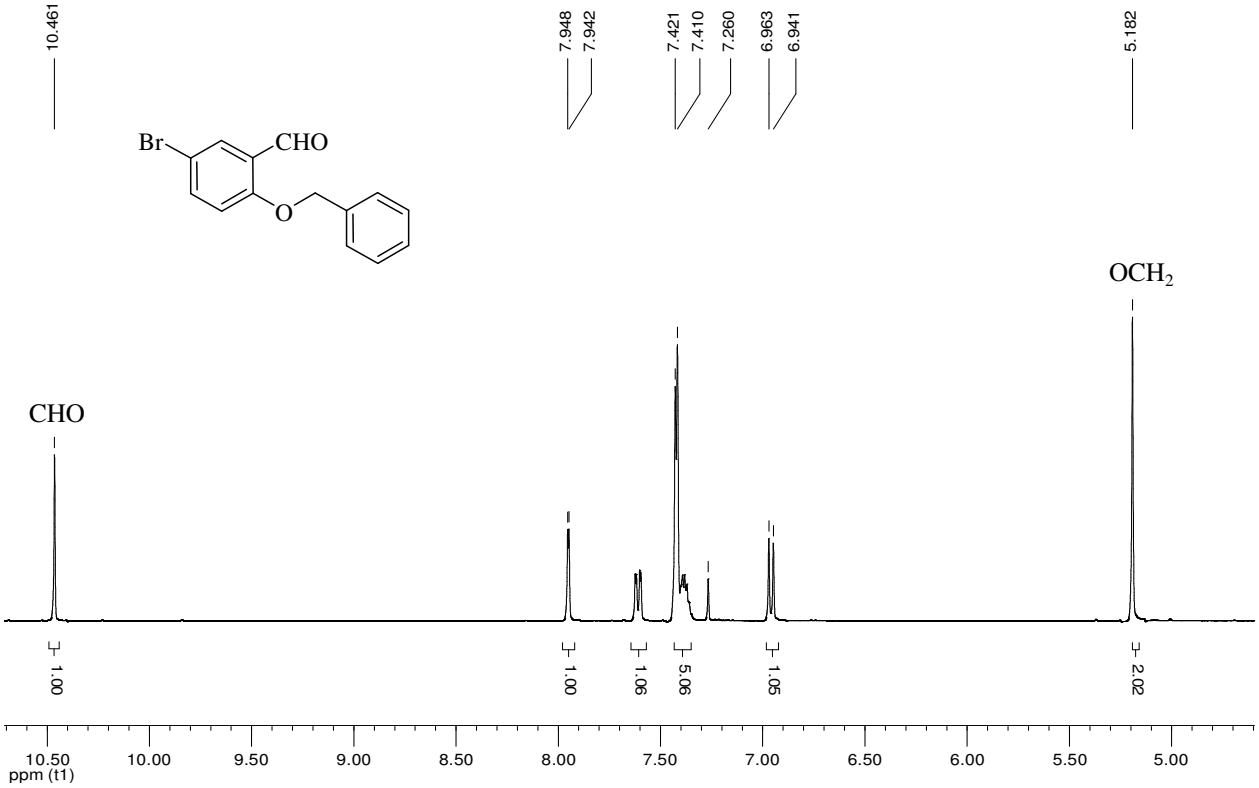

Figure 46. 400 MHz ^{1}H NMR spectrum of compound **145b** in $CDCl_3$.

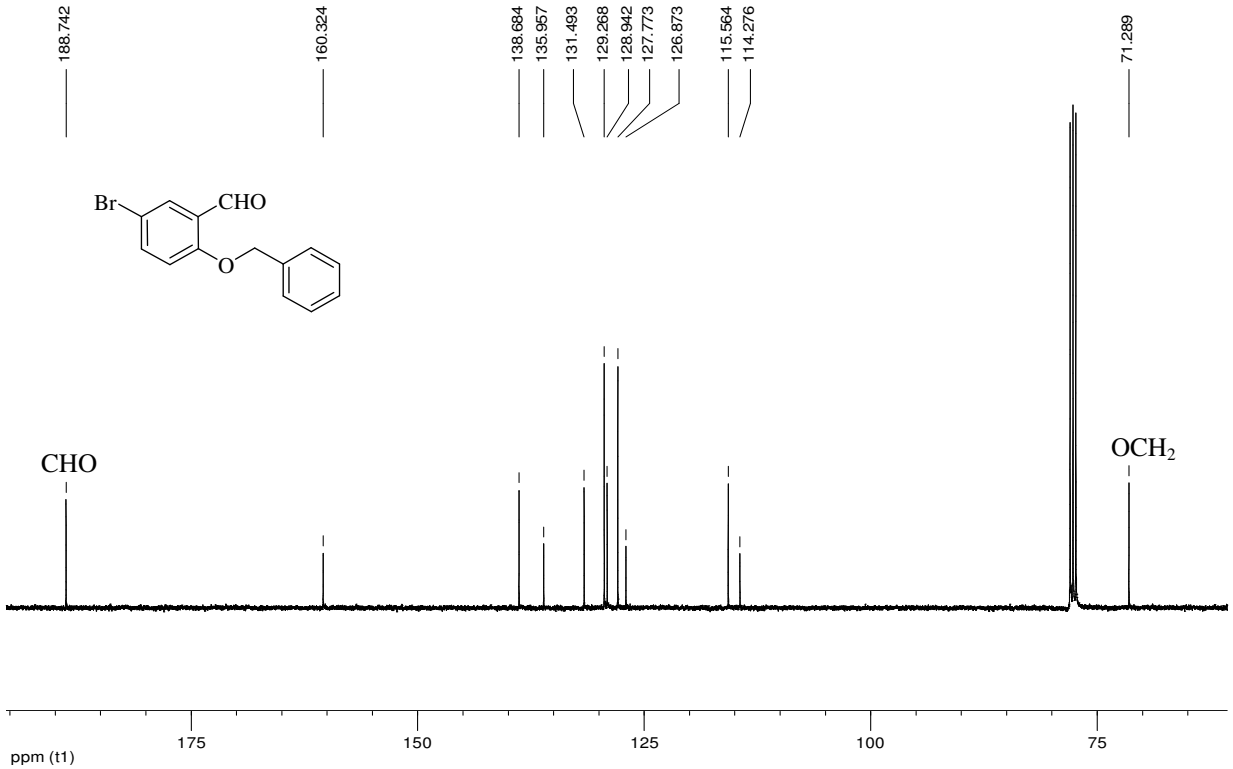

Figure 47. 100 MHz ^{13}C NMR spectrum of compound **145b** in $CDCl_3$.

2.2.6. Baylis-Hillman Reaction with Methyl Acrylate

The benzylated salicylaldehydes **145a-e** were then reacted with methyl acrylate using DABCO as catalyst. The $CHCl_3$ used as solvent was passed through basic alumina to remove contaminating HCl and thus prevent the acid-catalysed deprotection of the benzylated salicylaldehydes. After stirring at room temperature for 21 days, the crude mixture was chromatographed to afford the Baylis-Hillman adducts **146a-e** in yields up to 94% (Table 16). The ^{1}H NMR spectrum of methyl 3-(2-benzyloxy-5-bromophenyl)-3-hydroxy-2-methylene-propanoate **146b** (Figure 48) reveals the two vinylic proton singlets at 5.67 and 6.30 ppm, while the non-aromatic 1′-methine proton resonates as a doublet at 5.92 ppm due to coupling to the hydroxyl proton which also resonates as a doublet at 3.47 ppm. The benzylic protons resonate as a singlet at 5.04 ppm and the methyl protons as a singlet at 3.72 ppm. The DEPT 135 NMR spectrum (Figure 49) confirms that the two vinylic protons are attached to the same carbon (C-3′) which resonates at 126.9 ppm. The benzylic carbon resonates at 70.9 ppm and the 1′-methine and methyl carbons at 68.0 and 52.4 ppm, respectively.

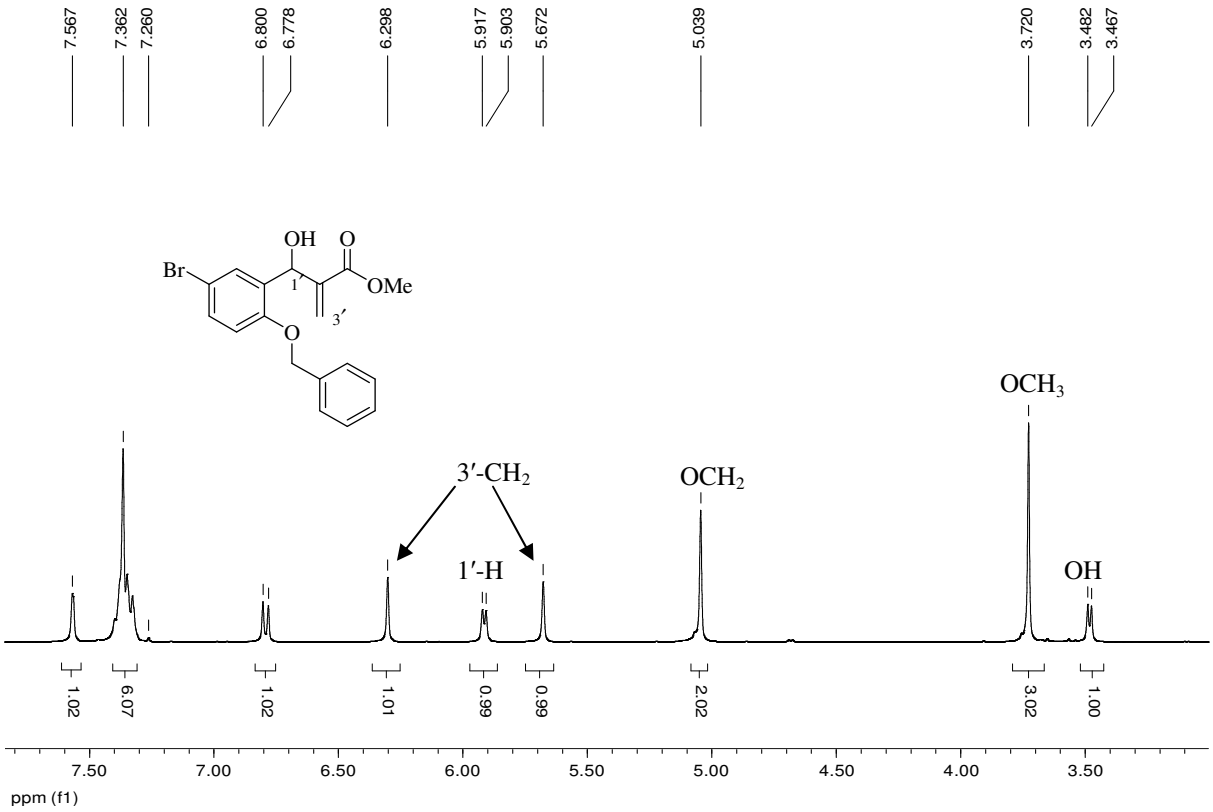

Figure 48. 400 MHz ^{1}H NMR spectrum of compound **146b** in $CDCl_3$.

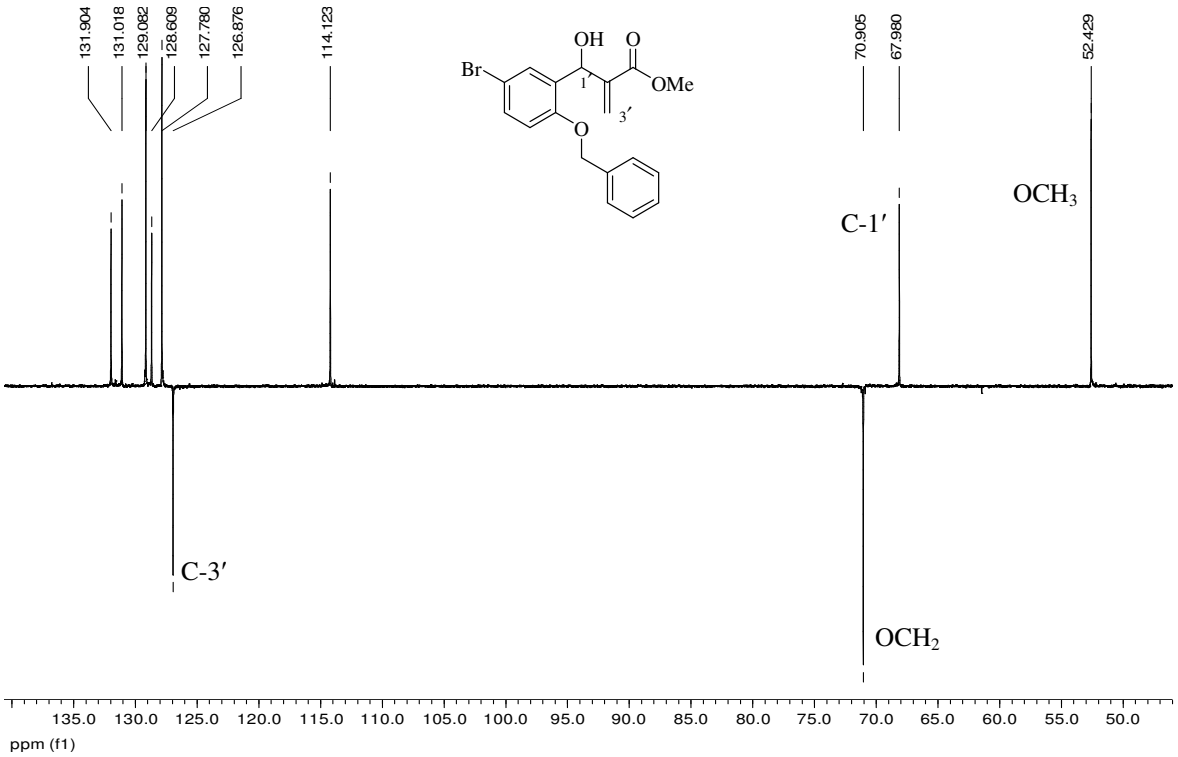

Figure 49. DEPT 135 NMR spectrum of compound **146b** in $CDCl_3$.

Table 16. Yields of methyl 3-(2-benzyloxyphenyl)-3-hydroxy-2-methylenepropanoates **146a-e**.

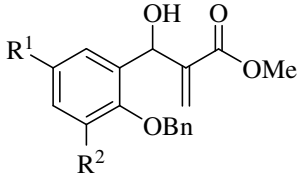

Compound	R^1	R^2	Isolated Yields (%)
146a	H	H	82
146b	Br	H	94
146c	H	OMe	88
146d	H	OEt	86
146e	Cl	H	90

Bartoli *et al*. had earlier reported a $CeCl_3.7H_2O$ / NaI-catalysed procedure for diastereoselective dehydration of β-hydroxycarbonyl compounds.[232] To explore this route to cinnamate esters, compound **146b** was first reacted with propargylamine (Scheme 39); purification by flash chromatography afforded compound **219b** in 92% yield. Attempts to dehydrate the β-hydroxycarbonyl compound **219b** using the method reported by Bartoli *et al*., however, proved unsuccessful, and attention was then given to the acetylation route described in Section 2.2.7.

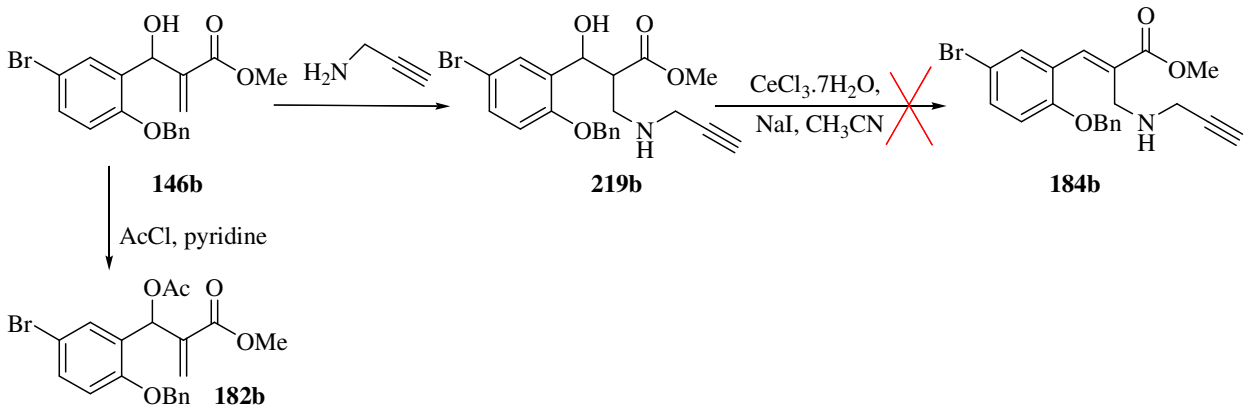

Scheme 39. Attempted $CeCl_3$-catalysed dehydration to cinnamate ester and acetylation of Baylis-Hillman adduct **146b**.

2.2.7. Acetylation of Baylis-Hillman Adducts

Acetylation of Baylis-Hillman adducts has previously been carried out using acetyl chloride in the presence of pyridine[233] or acetic anhydride in the presence of catalytic amounts of DMAP.[234] In this study, the Baylis-Hillman adduct **146b** was reacted with acetyl chloride in the presence of pyridine in dry DCM for 4 hours to afford compound **182b** in 55% yield following flash chromatography (Scheme 39). Comparison of the ^{1}H NMR spectra of the acetylated product **182b** (Figure 50) with that of precursor **146b** (Figure 48), confirms the absence of a hydroxyl proton signal, the appearance of the new acetyl methyl singlet at 2.10 ppm and the shift of the 1′-methine proton signal downfield to 7.11 ppm.

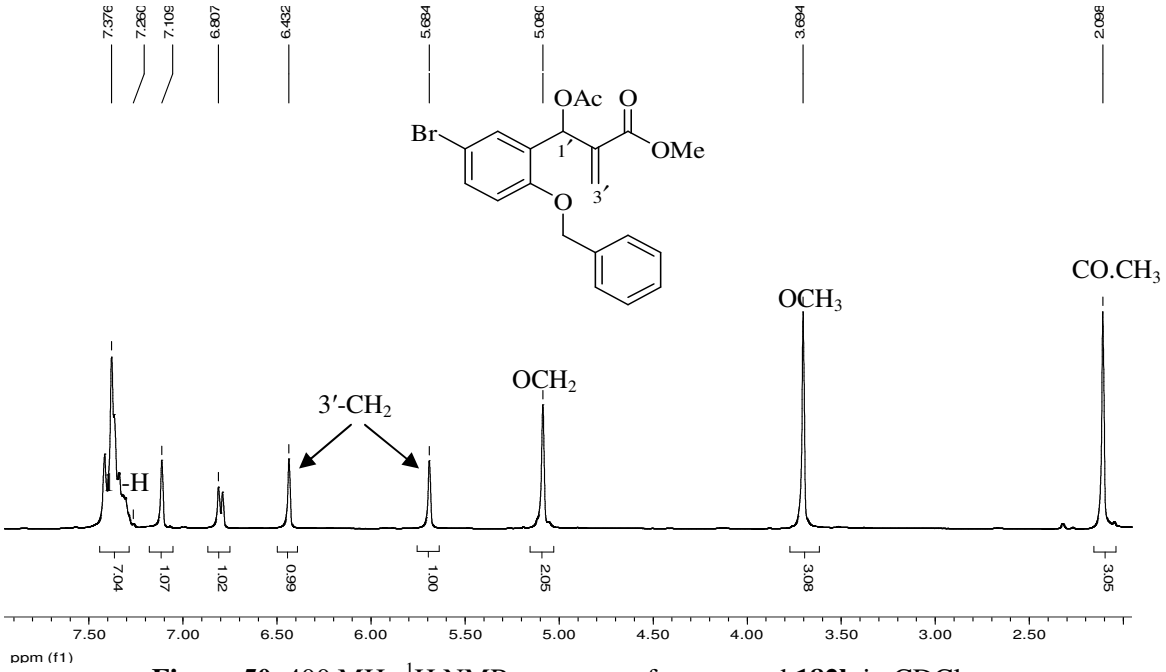

Figure 50. 400 MHz ^{1}H NMR spectrum of compound **182b** in $CDCl_3$.

In the hope of increasing the yield of the acetylated products, acetyl bromide was used in place of acetyl chloride. Thus, the cooled Baylis-Hillman adducts **146a**,**c-e** were treated with acetyl bromide in the presence of pyridine in dry DCM. However, flash chromatography of the products afforded the bromomethyl compounds **183a**,**c-e** in yields up to 95% (Table 17), instead of the expected acetylated derivatives **182a**,**c-e** (Scheme 40). The transformations were, however, fortuitous since the required dehydration had been effected to afford the cinnamate esters containing a reactive bromomethyl group susceptible to direct attack by nucleophilic propargylamine in the next step. The formation of the (*Z*)-cinnamate esters **183a**,**c-e** is attributed to the displacement of the acetyl group *via* conjugate addition – elimination or S_N' pathways. The configuration about the double bond is assumed by analogy with the X-ray crystal structure chloromethyl of cinnamate derivative **177a**. The ^{1}H NMR spectrum of compound **183a** (Figure 51) reveals the 1′-methine proton singlet at 8.12 ppm and the homotopic 3′-methylene protons resonating as a singlet at 4.39 ppm. The ^{13}C NMR spectrum (Figure 52) confirms the presence of sixteen carbon atoms in different environments, while the DEPT 135 spectrum (Figure 53) reveals the benzylic and C-3′ methylene signals at 27.9 and 70.8 ppm, respectively. These assignments were confirmed by correlations in the HSQC spectrum (Figure 54).

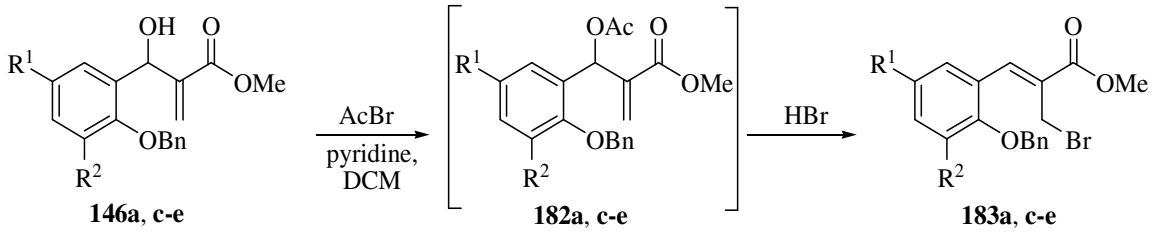

Scheme 40. Acetylation of Baylis-Hillman adducts **146a**,**c-e** using acetyl bromide

Table 17. Yields of (*Z*)-methyl 3-[2-(benzyloxy)phenyl]-2-(bromomethyl)-2-propenoates **183a**,**c-e**.

Compound	R^1	R^2	Isolated Yields (%)
183a	H	H	83
183c	H	OMe	94
183d	H	OEt	88
183e	Cl	H	91

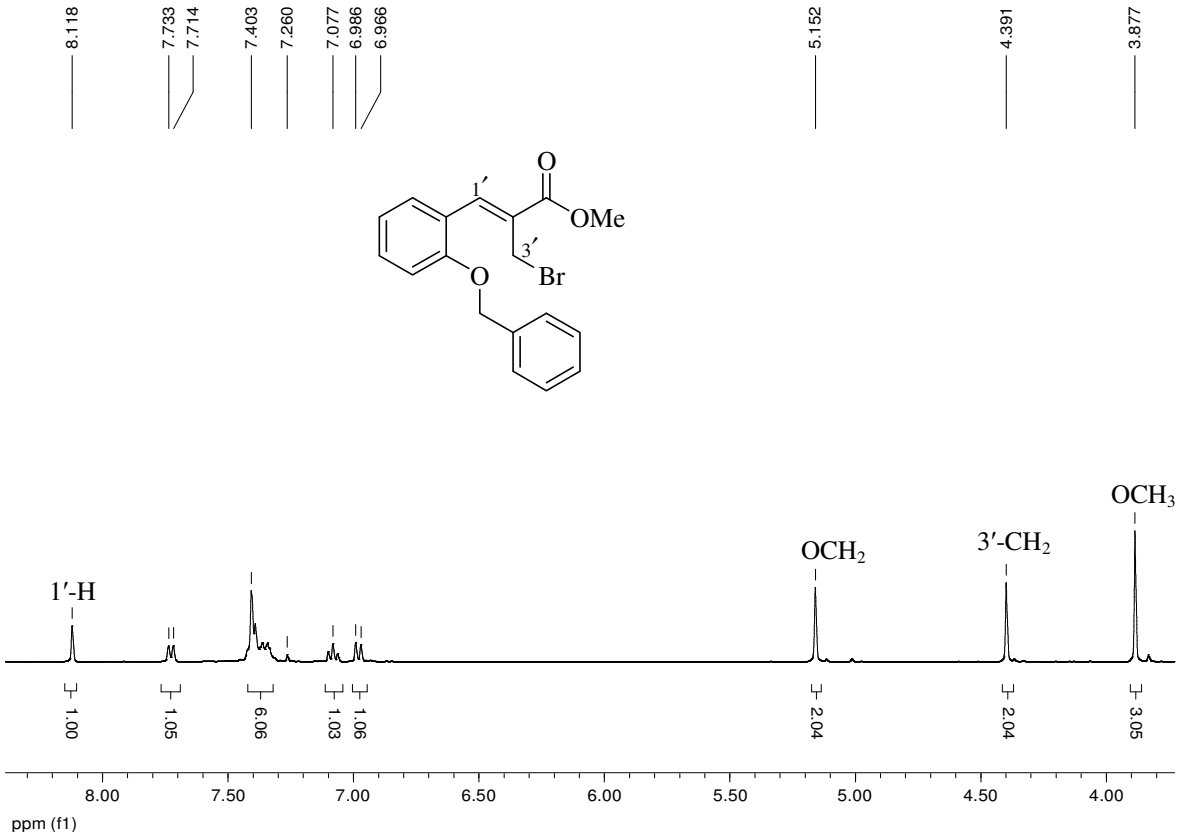

Figure 51. 400 MHz ^{1}H NMR spectrum of compound **183a** in $CDCl_3$.

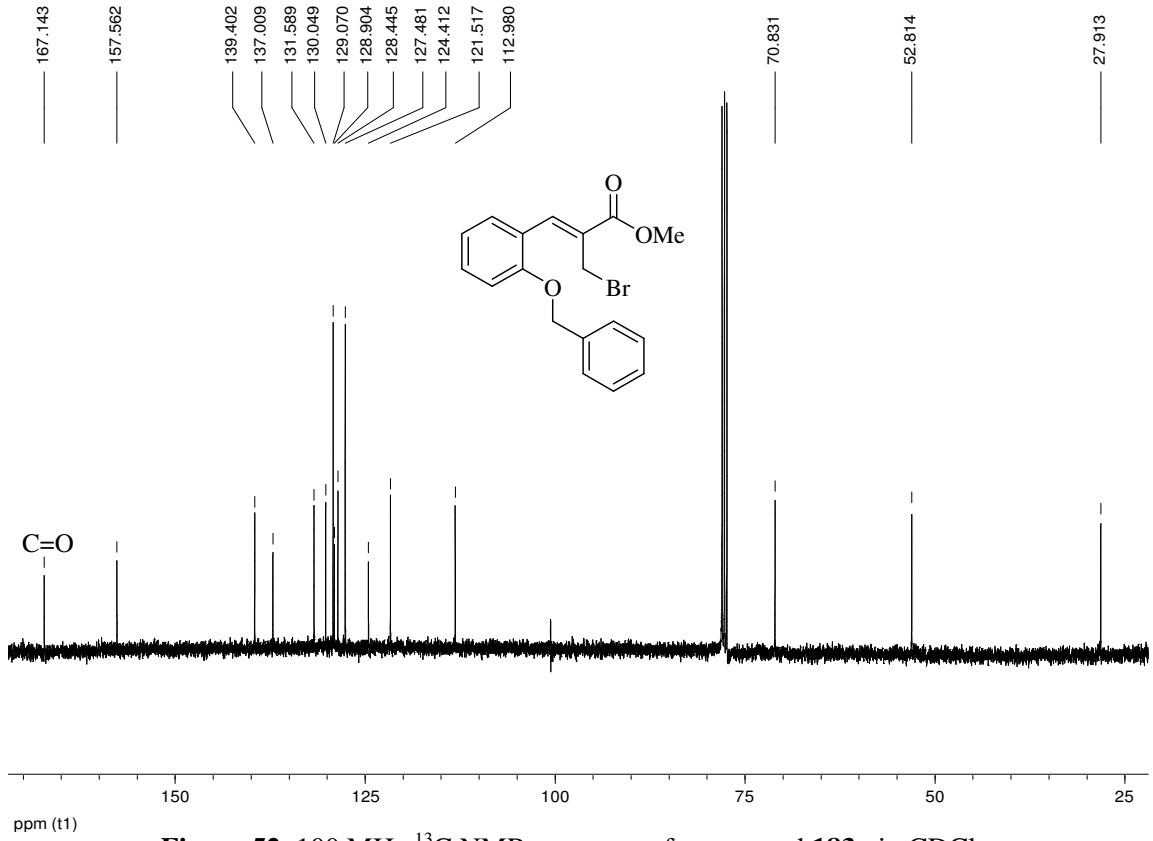

Figure 52. 100 MHz ^{13}C NMR spectrum of compound **183a** in $CDCl_3$.

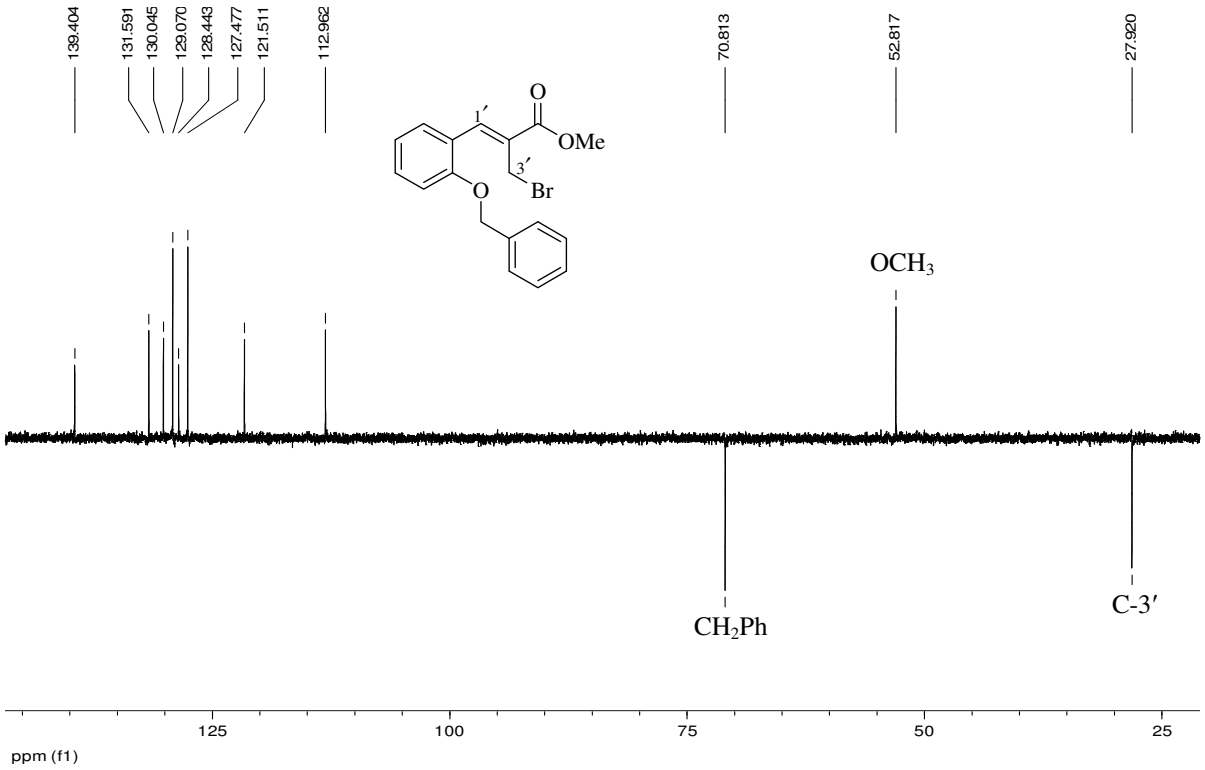

Figure 53. DEPT 135 NMR spectrum of compound **183a** in $CDCl_3$.

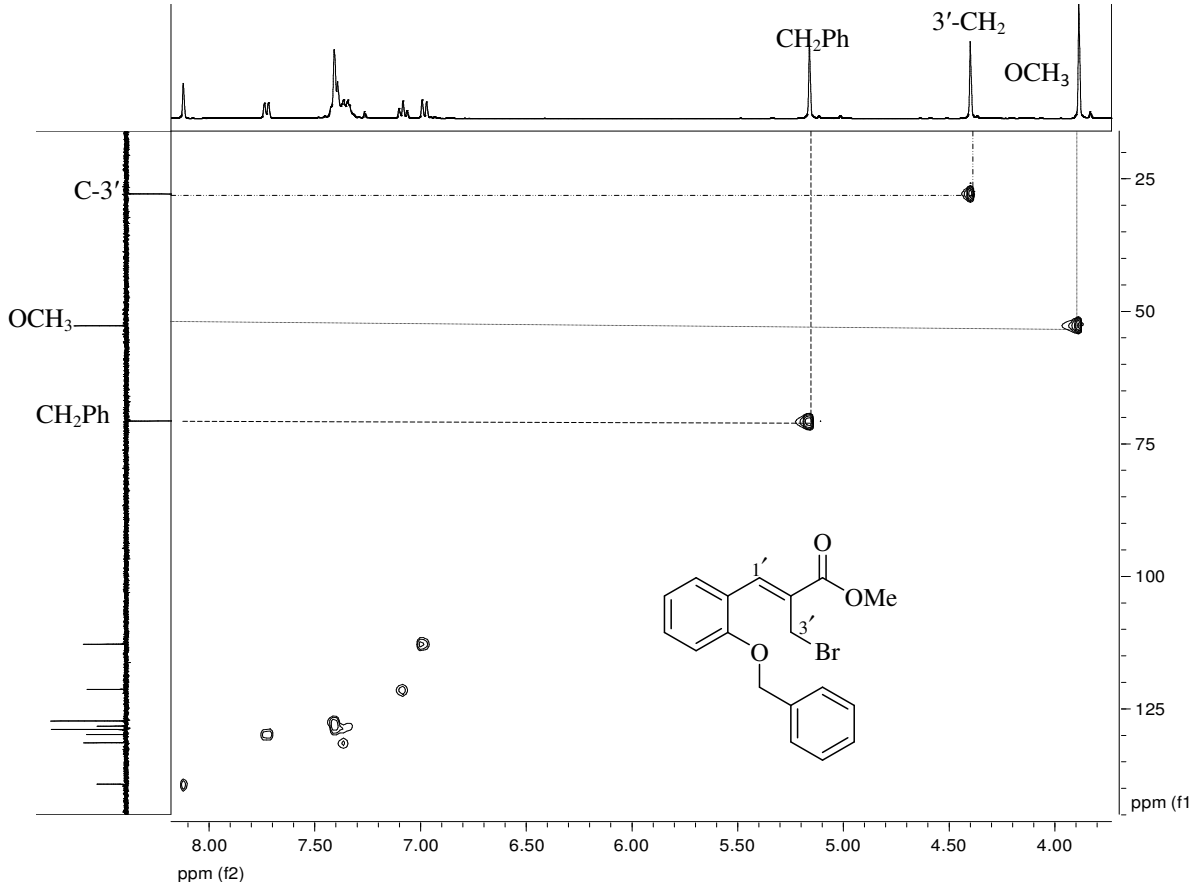

Figure 54. HSQC spectrum of compound **183a** in $CDCl_3$.

2.2.8. Synthesis of Methyl (*E*)-3-[2-(benzyloxy)phenyl]-2-[(prop-2-ynylamino)methyl]-2-propenoates

With the aim of synthesising dual-action compounds, attention was given to adding the propargyl system to the cinnamate compounds to enable a subsequent click reaction with AZT. The acetate **182b** was treated with propargylamine and potassium carbonate in acetonitrile and flash chromatography afforded the rearranged product **184b** in 82% yield (Scheme 41). Significant features in the ^{1}H NMR spectrum of compound **184b** (Figure 55) include the three methylene group singlets, corresponding to the benzylic (OCH_2) at 5.10 ppm and two sets of *N*-methylene protons at 3.61 and 3.44 ppm and acetylenic proton resonating as a singlet at 2.22. The effect of the large $^{2}J_{C,H}$ coupling, responsible for the appearance of the quaternary alkyne carbon signal in the DEPT 135 and 2D NMR spectra of compound **166b** (Section 2.1.4.2.), is also evident in the corresponding spectra of the propargyl cinnamates **184** reported in this section. The ^{13}C NMR spectrum accounts for the presence of nineteen different carbon environments as expected, while the DEPT 135 NMR confirms the presence of one methyl and three methylene carbons. In order to synthesise the rest of the series, the bromomethyl derivatives **183a**,**c-e** were stirred with propargylamine in dry THF for 24 hours to afford compounds **184a**,**c-e** in yields of up to 89% (Table 18) *via* simple nucleophilic substitution (S_N). In one case, however, the S_N' reaction product, **185e** was also formed (Scheme 41). A major distinguishing feature between the ^{1}H NMR spectra of the normal (S_N) product **184e** and the rearranged (S_N') product **185e** is the presence of the 1′-methine and 3′-vinylic methylene proton signals, which characterise compound **185e** (Figure 57) which are clearly absent in the spectrum of compound **184e** (Figure 56). The signal assignments for compound **185e** were confirmed by the DEPT 135 NMR data and all of the products **184a-e** and **185e** were fully characterized using high resolution MS, NMR and IR analysis.

Table 18. Yields of propargyl cinnamate esters **184a-e**.

Substrate	R^1	R^2	Isolated yields of 184 (%)	Isolated yield of 185 (%)
183a	H	H	77	-
182b	Br	H	82	-
183c	H	OMe	85	-
183d	H	OEt	89	-
183e	Cl	H	75	20

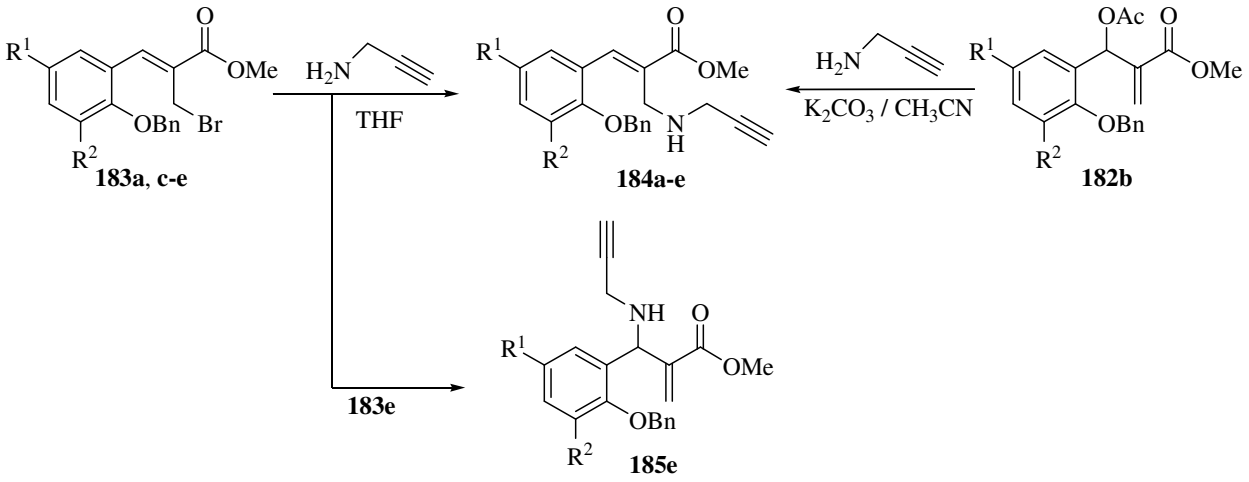

Scheme 41. Synthesis of substituted cinnamate esters **184a-e**.

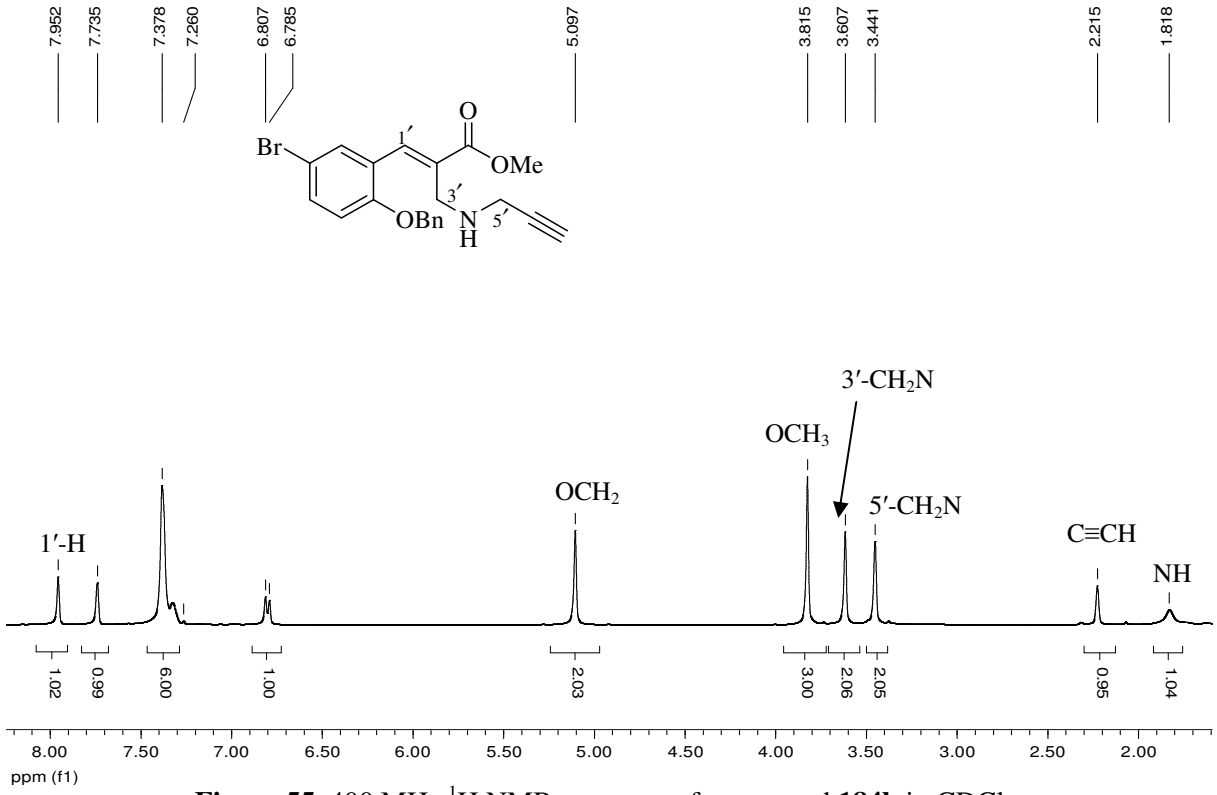

Figure 55. 400 MHz ^{1}H NMR spectrum of compound **184b** in $CDCl_3$.

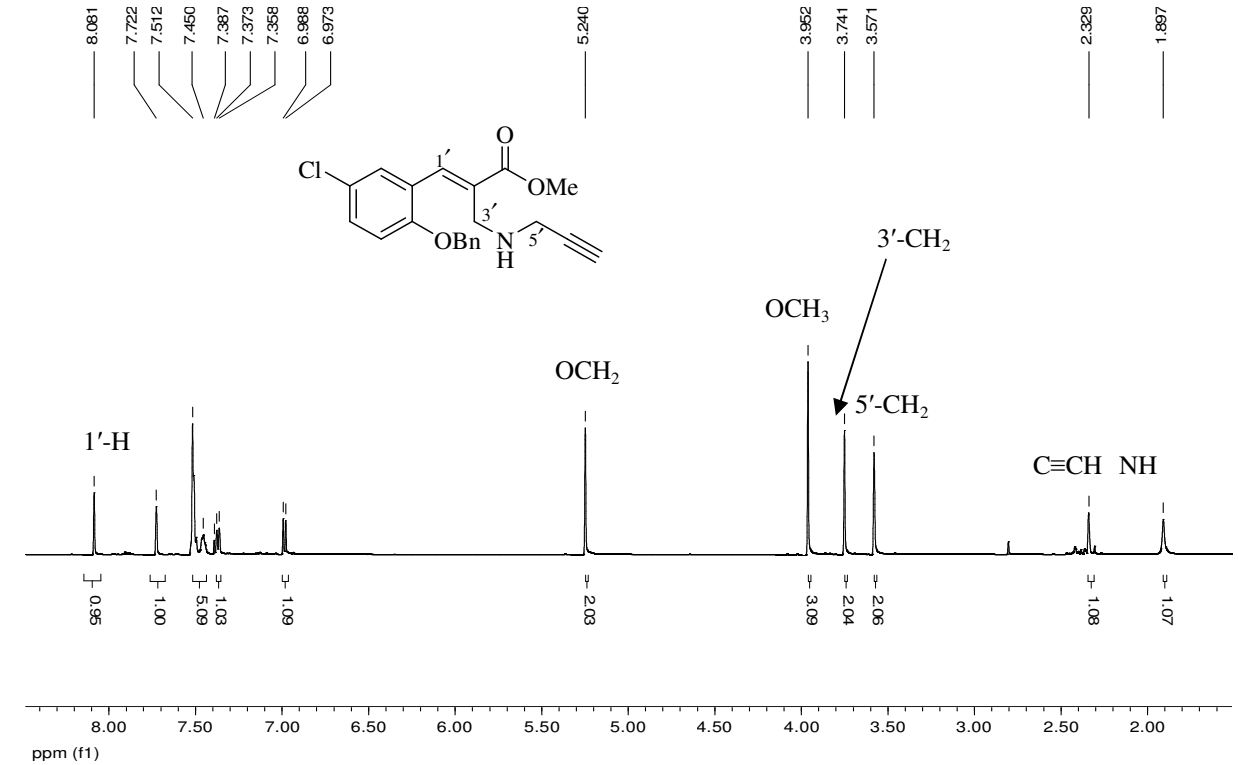

Figure 56. 600 MHz ^{1}H NMR spectrum of compound **184e** in $CDCl_3$.

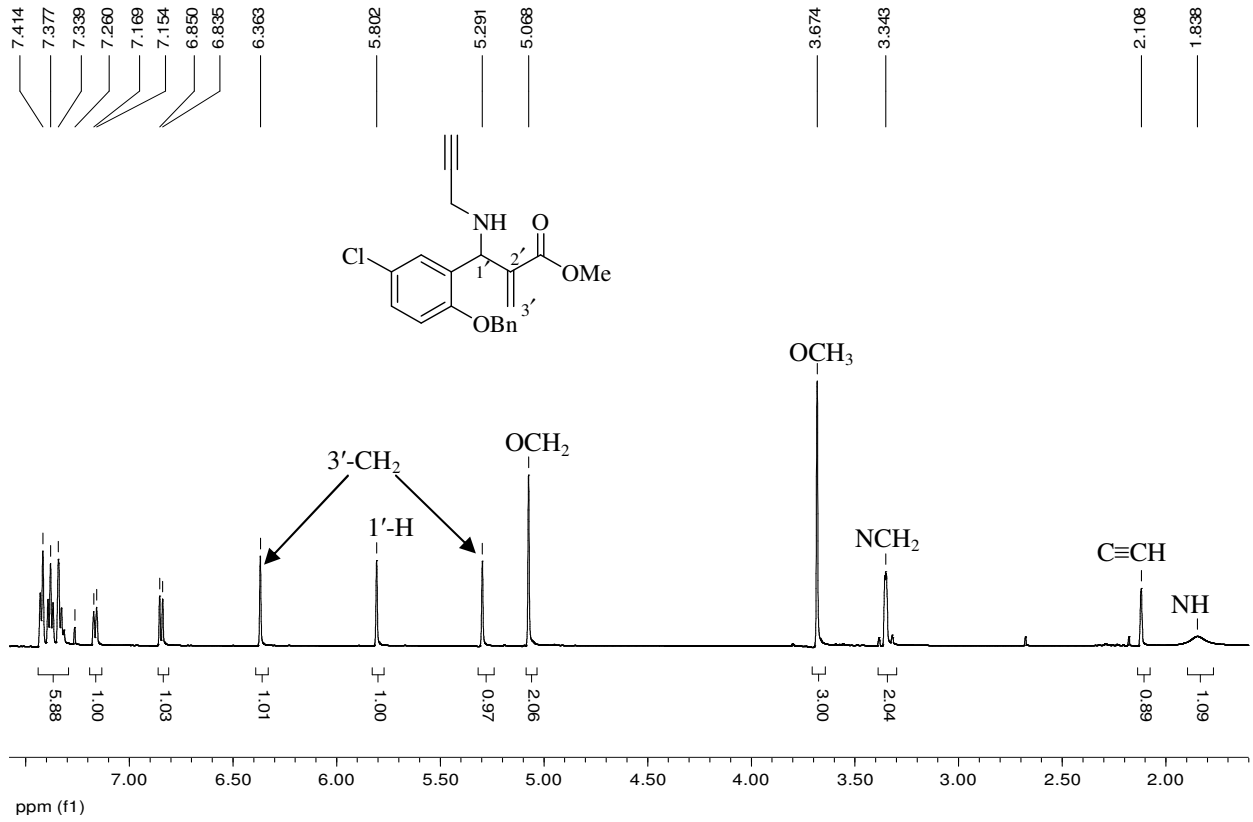

Figure 57. 600 MHz ^{1}H NMR spectrum of compound **185e** in $CDCl_3$.

2.2.9. Click Reaction of Cinnamate Esters

The propargyl derivatives **184a-e** were then reacted with AZT **2** in aqueous THF in the presence of a Cu(I) catalyst (Scheme 42). The expected products **186a-e** were obtained in yields of 87-92% (Table 19) following flash chromatography, and fully characterised. The ^{1}H NMR spectrum of compound **186c**, for example, reveals the presence of ten aromatic methine protons, four non-aromatic methine protons, five pairs of methylene protons and three methyl groups, with signal assignments as indicated in Figure 58. The expanded section in Figure 58 shows the 5′-methylene proton signals sandwiched between the two methoxy group signals. The ^{13}C NMR spectrum of compound **186c** (Figure 59) confirms the presence of the expected thirty NMR-unique carbon atoms, with the ester carbonyl carbon resonating at 168.2 ppm, and the amide and imide carbonyl carbons resonating at 163.9 and 152.9 ppm, respectively. Methyl, methylene and methine signals were assigned using the DEPT 135 NMR (Figure 60), COSY (Figure 61) and HSQC (Figure 62) spectra.

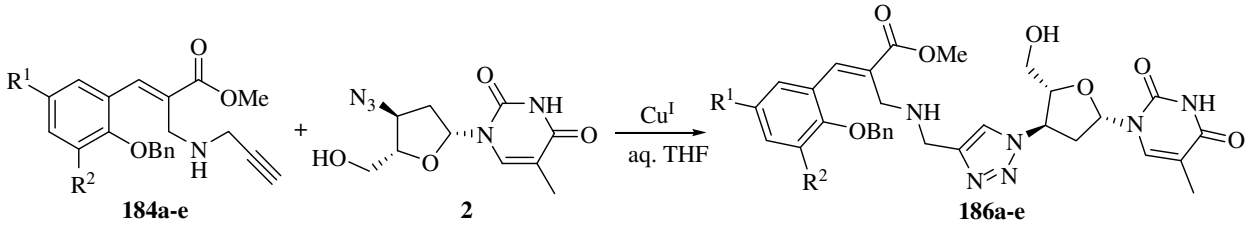

Scheme 42. Click reaction of cinnamate esters **184a-3** with AZT **2**.

Table 19. Yields of cinnamate ester-AZT conjugates **186a-e**.

Compound	R^1	R^2	Isolated Yields (%)
186a	H	H	87
186b	Br	H	92
186c	H	OMe	89
186d	H	OEt	89
186e	Cl	H	90

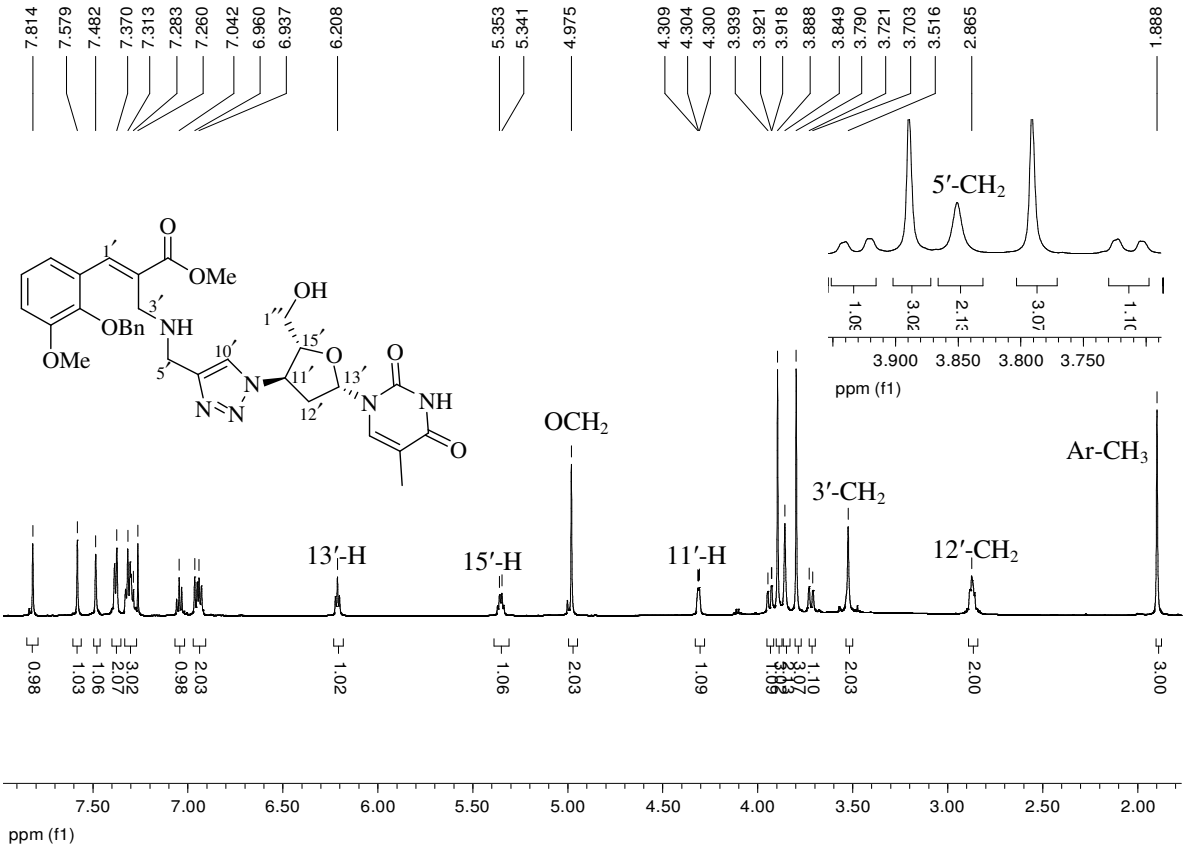

Figure 58. 600 MHz ^{1}H NMR spectrum of compound **186c** in $CDCl_3$.

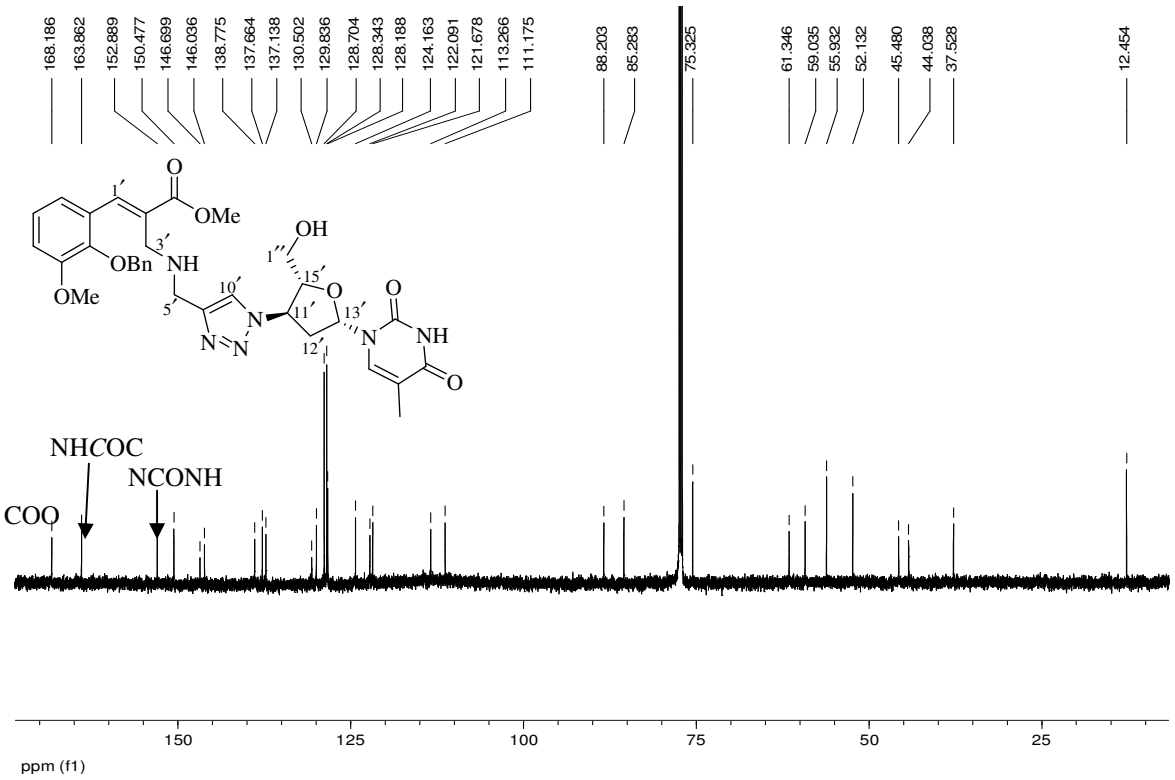

Figure 59. 150 MHz ^{13}C NMR spectrum of compound **186c** in $CDCl_3$.

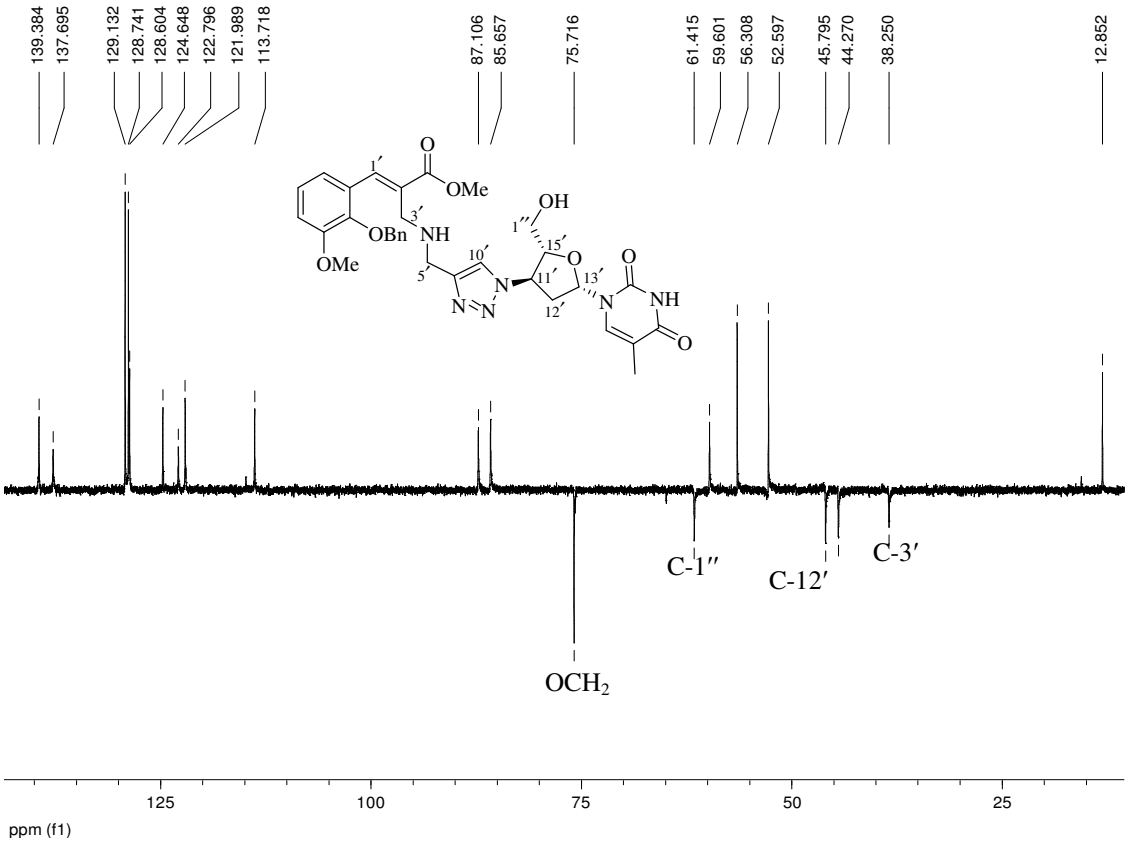

Figure 60. DEPT 135 NMR spectrum of compound **186c** in $CDCl_3$.

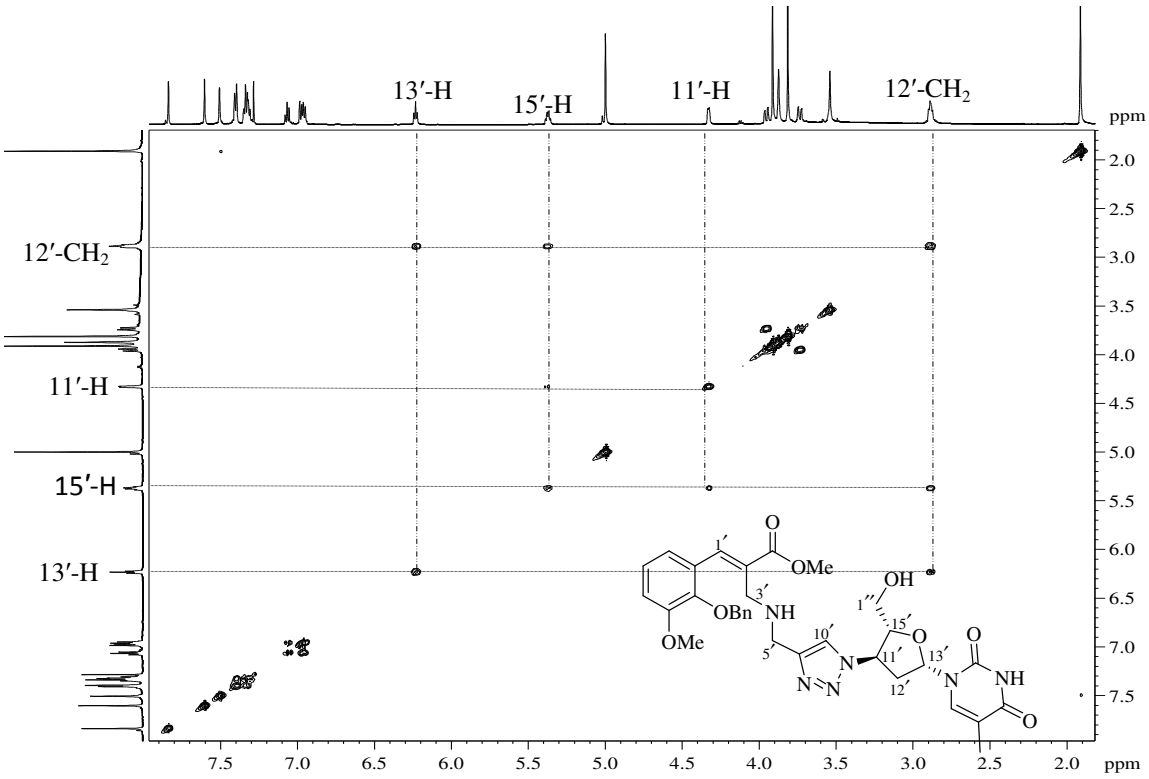

Figure 61. COSY spectrum of compound **186c** in $CDCl_3$.

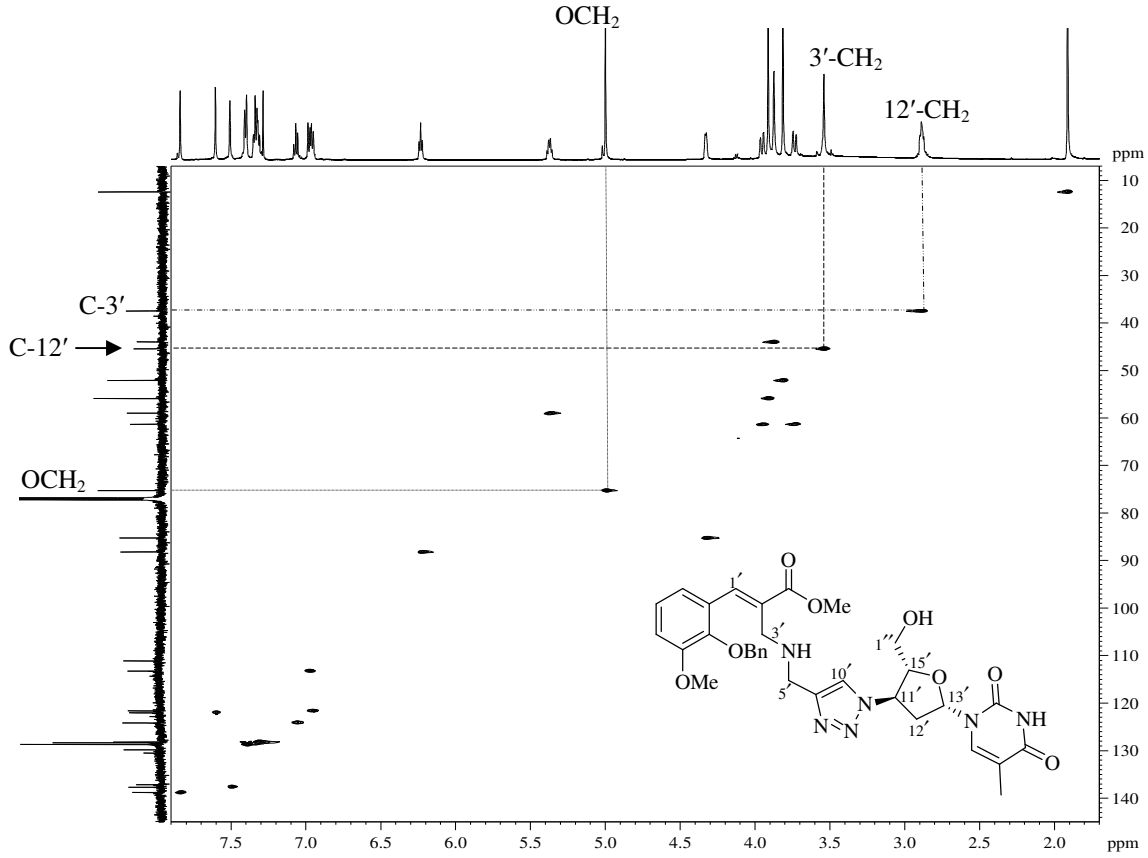

Figure 62. HSQC spectrum of compound **186c** in $CDCl_3$.

2.2.10. Phosphorylation of Azidothymidine (AZT)

As stated in section 1.2.3., AZT is a prodrug that is phosphorylated *in vivo* by host-cell kinases.[78] It was thus envisaged that monophosphorylation of the AZT derivatives **186a-e** might facilitate the enzymatic phosphorylation step to the required triphosphosphate within the host. Tenofovir **12**, the only NtRTI currently in clinical use, is a phosphonated adenosine analogue (see Section 1.2.3.). There are a number of established methods for the phosphorylation and phosphonation of AZT **2**.[235-238] In the current study, phosphonation of AZT **2** was first explored by subjecting the bromo derivative **187** to the Michaelis-Arbuzov reaction as illustrated in Scheme 43. This approach has been reported to permit the formation of compounds similar to the desired phosphonate ester **188**.[239] Bromination was carried out by adding AZT **2** to an ice-cooled mixture of bromine and PPh_3 in dry DCM, [240] work-up and purification affording compound **187** in 65% yield. Compound **187** was then refluxed in triethyl phosphite for 4 hours under N_2 at 140 °C. The ^{1}H NMR spectrum of the crude product indicated that the reaction had been successful, but compound **188** appeared to decompose during flash chromatography, and could not be isolated. Consequently, attention was turned to the phosphorylation of AZT **2** using diethyl

chlorophosphate in the presence of a base. When sodium hydride was used as the base, the reaction appeared to have been unsuccessful, and the reaction was repeated using butyllithium instead (Scheme 44). The butyllithium was added to a solution of AZT **2** in dry THF at 0 °C under argon and stirred for 30 minutes, after which diethyl chlorophosphate was added and the mixture stirred overnight. Flash chromatography afforded the phosphorylated AZT **189** in 66% yield. ^{1}H NMR analysis of the product revealed the ethoxy methylene protons resonating as a multiplet at 4.13-4.18 ppm and the ethoxy methyl protons as a doublet of triplets at 1.34 ppm – multiplicities which reflect coupling to the phosphorus (Figure 63). The ^{31}P NMR spectrum, obtained using phosphoric acid in a sealed capillary tube as the internal standard, revealed a single phosphorus signal at -0.24 ppm.

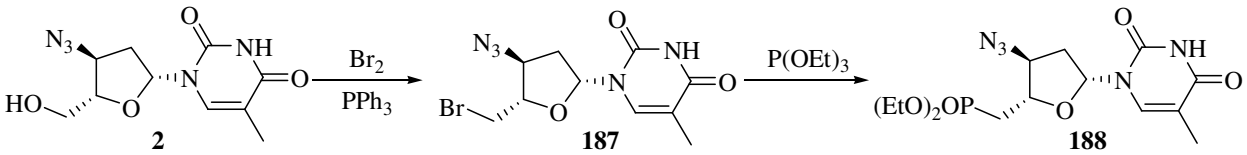

Scheme 43. Initial approach for the phosphonation of AZT **2**.

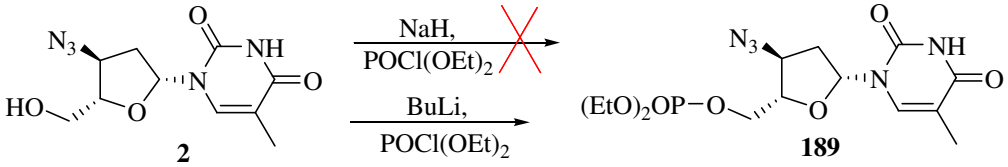

Scheme 44. Phosphorylation of AZT **2**.

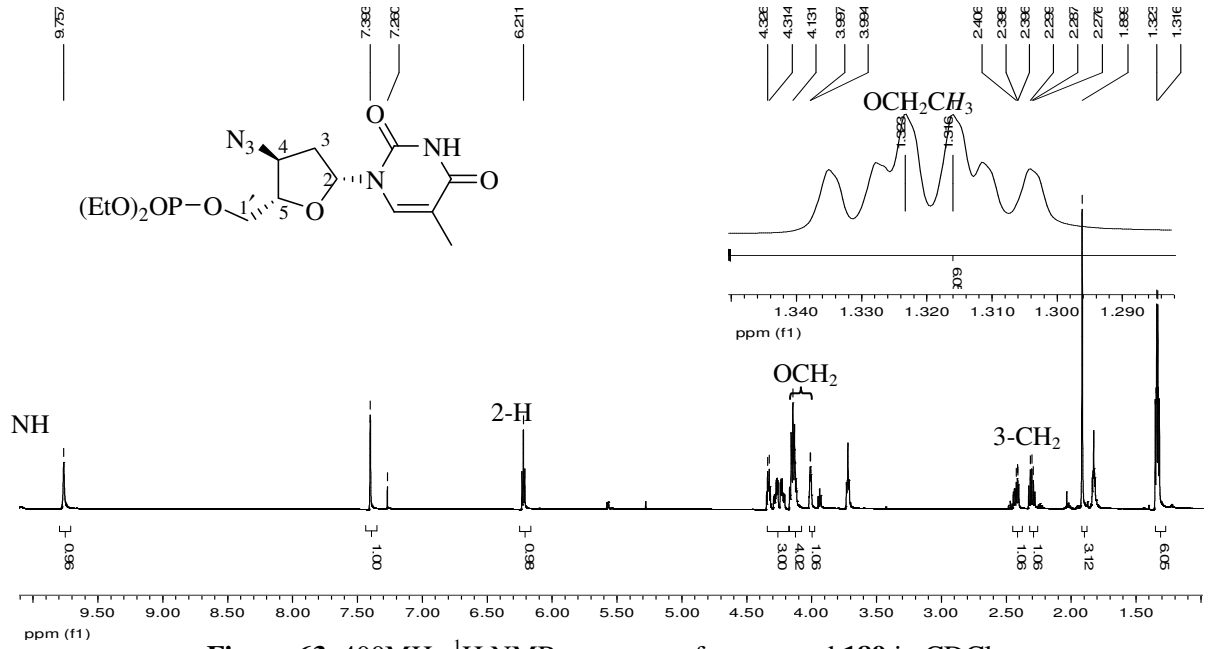

Figure 63. 400MHz ^{1}H NMR spectrum of compound **189** in $CDCl_3$.

2.2.10. Click Reaction of Phosphorylated Azidothymidine

The phosphorylated AZT **189** was then clicked with the propargylamine derivative **184a** to access the monophosphorylated derivative **190a**. Reaction of compound **184a** with phosphorylated AZT **189** in aqueous THF with a Cu(I) catalyst (Scheme 45), afforded compound **190a** in 82% yield, following flash chromatography and was fully characterised as usual. The ^{1}H NMR spectrum (Figure 64) of the phosphorylated conjugate reveals the ethoxy methylene proton resonating as a multiplet at 4.14 ppm, while the DEPT 135 NMR (Figure 65) shows the presence of all the expected proton-bearing carbons.

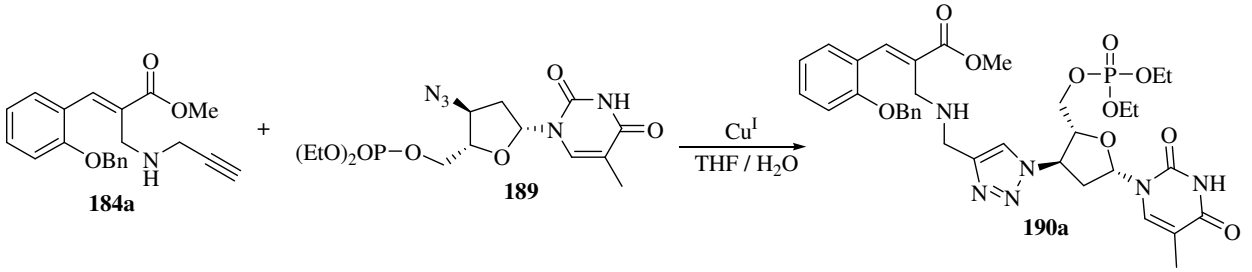

Scheme 45. Click reaction of phosphorylated AZT **189**.

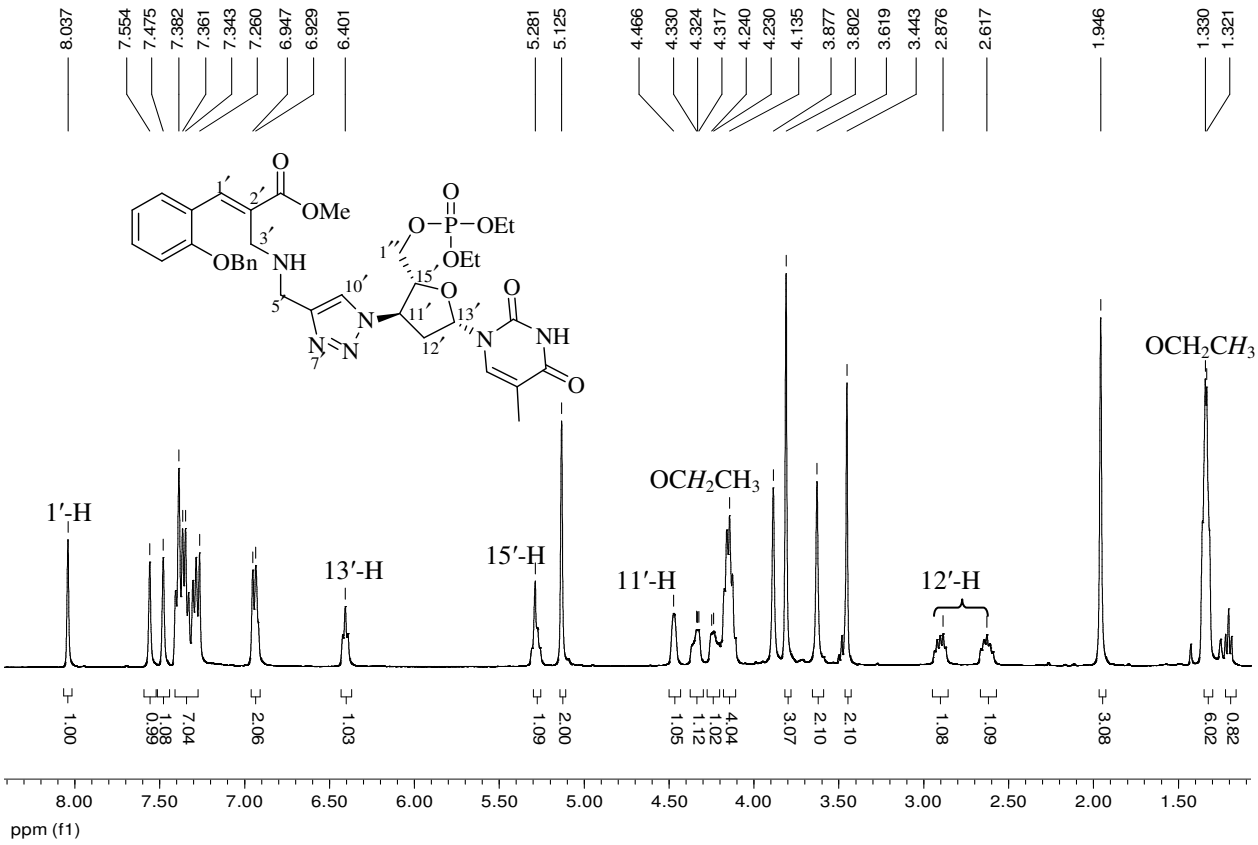

Figure 64. 400MHz ^{1}H NMR spectrum of compound **190a** in $CDCl_3$.

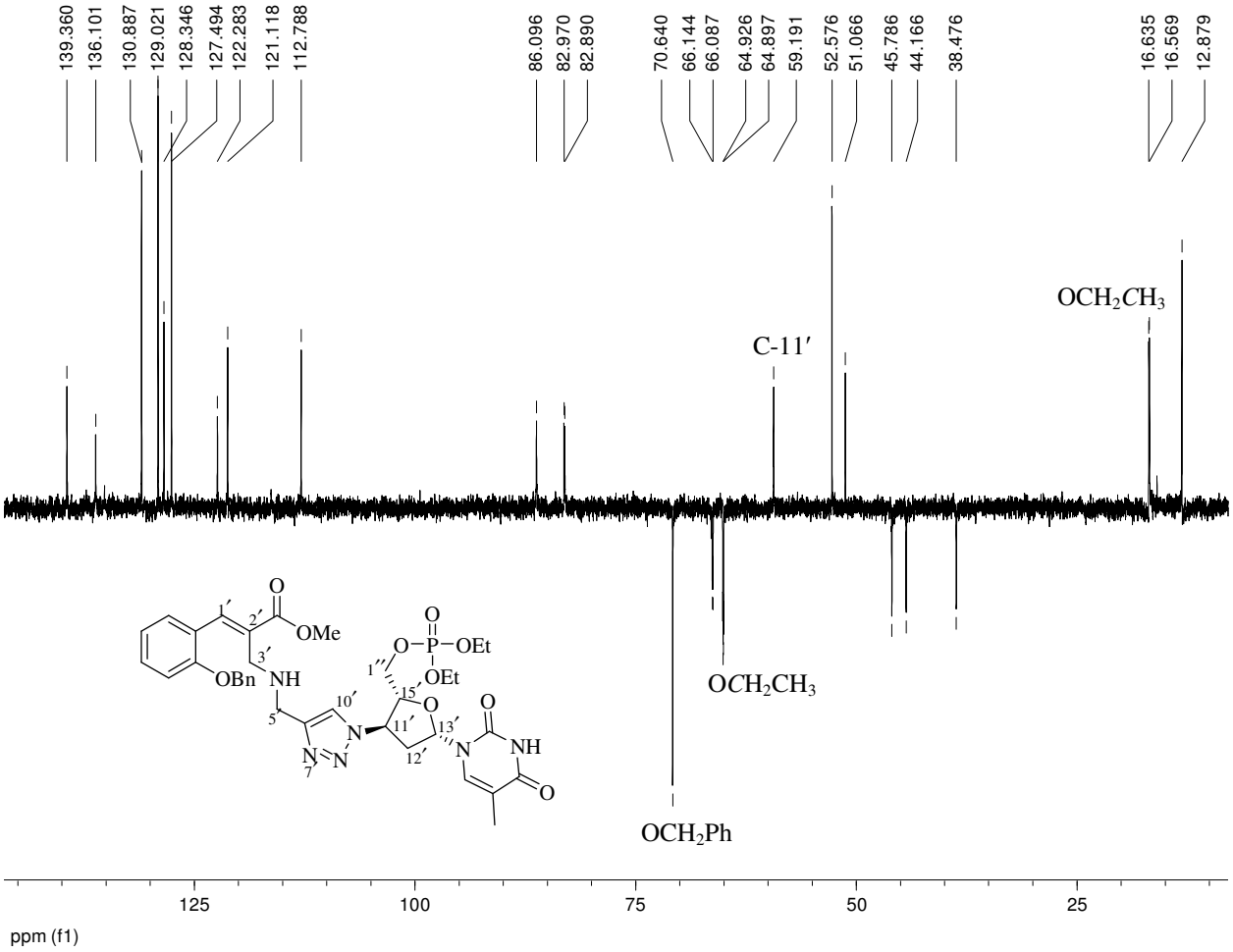

Figure 65. DEPT 135 NMR spectrum of compound **190a** in $CDCl_3$.

2.3. BAYLIS-HILLMAN REACTIONS OF COUMARIN-3-CARBALDAHYDES

As stated in Section 1.3., many coumarin derivatives exhibit medicinal properties. In particular warfarin **42** and phenprocoumon **43**, both coumarin derivatives, have been found to be suitable non-peptidic anti-HIV-1 lead compounds with good oral bioavailability.[99] Furthermore, in the light of the interesting products obtained from Baylis-Hillman reactions of chromone carbaldehydes in earlier studies in our research group,[241] it was decided to investigate the use of the Baylis-Hillman methodology in the construction of the isomeric coumarin-3-carbaldehydes, and explore their use as electrophiles in further Baylis-Hillman reactions, with the possibility of forming the novel tricyclic systems shown in Scheme 46.

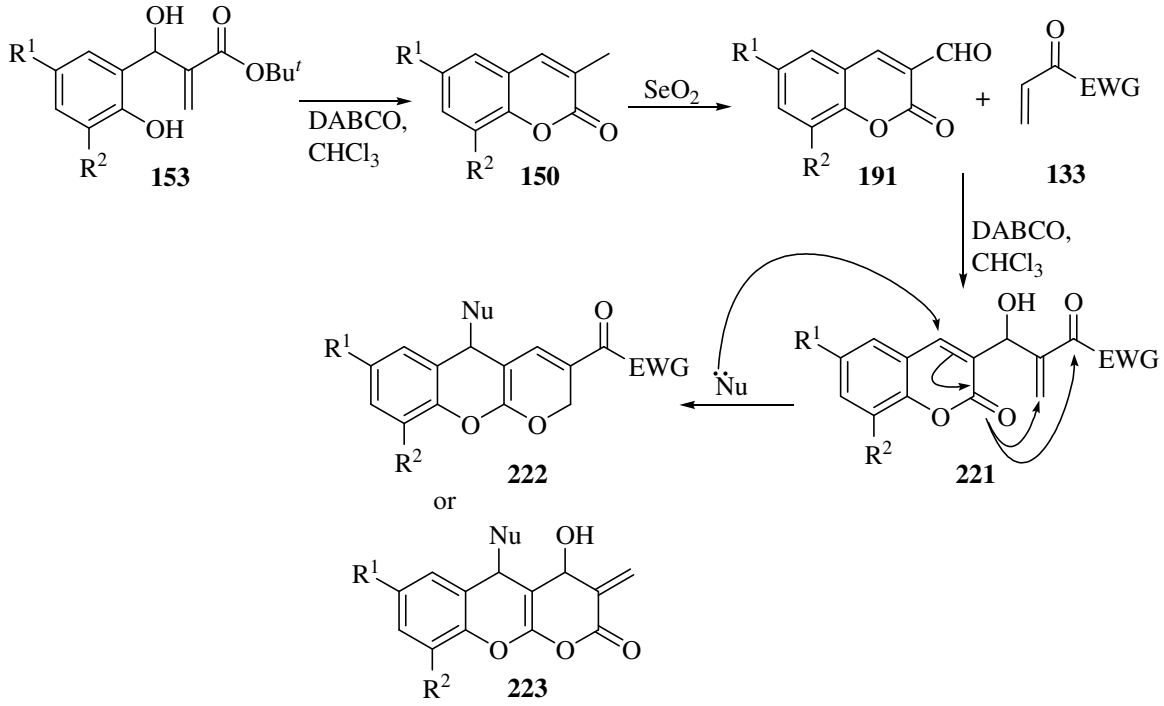

Scheme 46. Synthesis and potential application of Baylis-Hillman derived coumarin-3-carbaldehyde **191**.

2.3.1. Synthesis of Coumarin-3-carbaldehydes

Methods used in preparation of coumarin-3-carbaldehydes include acetoxymethylation of coumarins,[242] Rosenmund reduction of 3-chloroformylcoumarins[243,244] and the oxidation of 3-methylcoumarin at high temperature using selenium dioxide.[245] In the present study, it was decided to treat the 3-methyl coumarins **150a**,**b**,**e**,**f** with selenium dioxide. Thus, 3-methylcoumarin **150a** was heated together with selenium dioxide at 170 °C in the absence of solvent for a total of 9 hours. However, the coumarin-3-carbaldehyde **191a** was isolated in only

24% yield. In an attempt to improve the yield, 3-methylcoumarin **150a** was ground together with selenium dioxide and the mixture irradiated in the microwave apparatus at 170 °C for 1 h to afford the desired coumarin-3-carbaldehyde **191a** in better yield (52%) and in shorter time. The microwave-assisted approach was successfully applied to the synthesis of the other coumarin-3-carbaldehyde derivatives **191b**,**e** (Scheme 47), which were isolated in yields of 60% and 56%, respectively. This convenient efficient approach to coumarin-3-carbaldehydes, has been published.[246] Given the susceptibility of phenolic systems to ring oxidation, however, this methodology could not be used to access 8-hydroxycoumarin-3-carbaldehyde as the reaction resulted in the formation of a complex mixture of degradation products. The ^{1}H NMR spectrum of 6-bromocoumarin-3-carbaldehyde **191b** (Figure 66) reveals the presence of the aldehydic proton at 10.25 ppm.

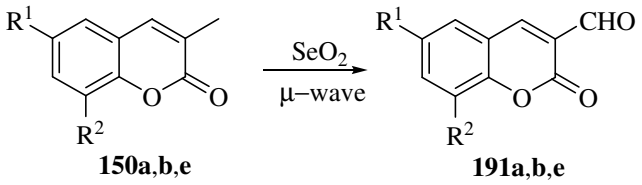

150a,**b**,**e** **191a**,**b**,**e**

Scheme 47. SeO_2 oxidation of 3-methylcoumarins **150a**,**b**,**e**.

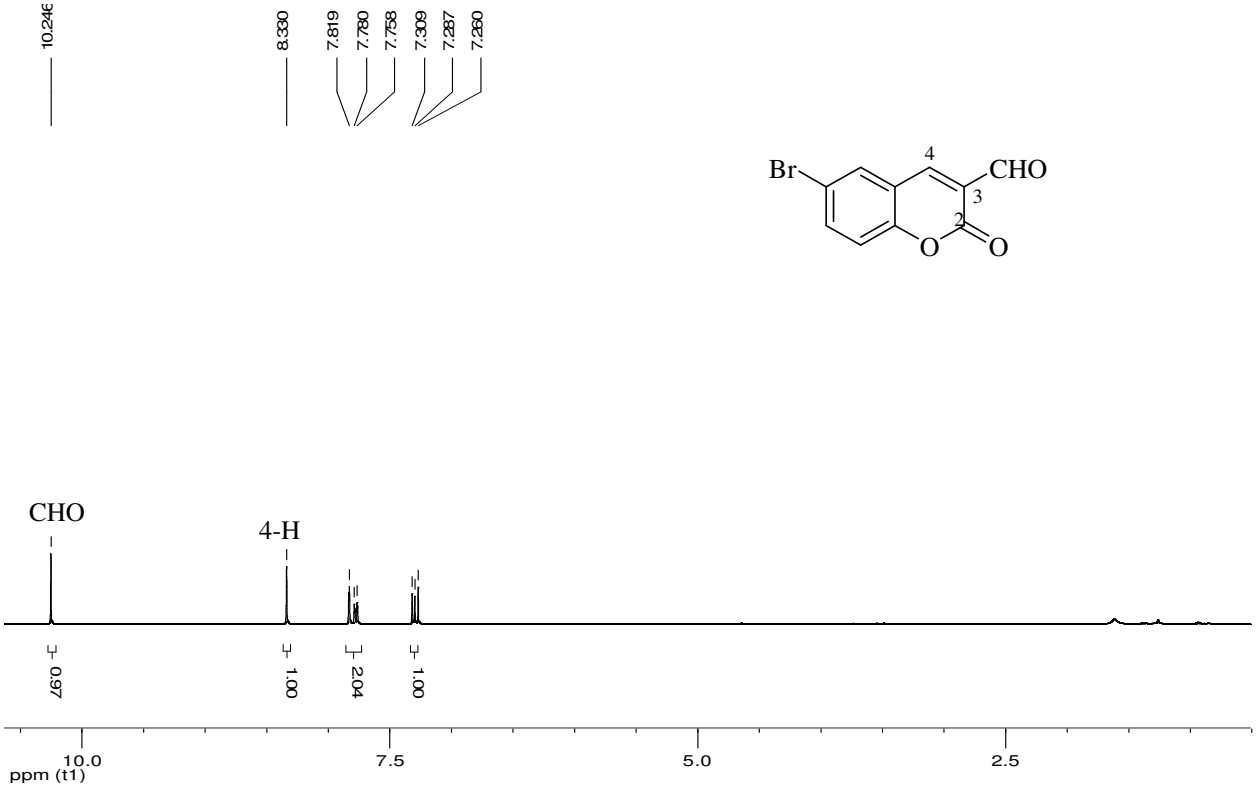

Figure 66. 400MHz ^{1}H NMR spectrum of compound **191b** in $CDCl_3$.

An alternative method of preparing coumarin-3-carbaldehydes, involving the oxidation of 3-(hydroxymethyl)coumarin **192** was then explored. Initial attempts to hydrolyse the tertiary butyl esters **153a**,**b**,**d**,**e** involved their treatment with iodine in acetonitrile and a small quantity of water following a procedure reported by Yadav *et al.*[247] This resulted in cyclisation to give the corresponding 3-(hydroxymethyl)coumarins **192a**,**b**,**d**,**e** (Scheme 48) in yields of 60-85% following flash chromatography (Table 20) and none of the earlier reported analogues **193** was isolated. The ^{1}H NMR spectrum of 6-bromo-3-(hydroxymethyl)coumarin **192b** (Figure 67) reveals the methylene protons resonating as a singlet at 4.93 ppm and the hydroxyl proton as a broad signal far downfield, at 13.00 ppm, suggests intramolecular hydrogen bonding with the carbonyl oxygen. A pilot study on the oxidation of 3-(hydroxymethyl)coumarin **192a** using Dess-Martin periodinane (DMP) on silica under microwave irradiation at 100 °C for up to 30 minutes gave only 30% yield of the coumarin-3-carbaldehyde **191a**. However, due to time constraints, this approach to the coumarin-3-carbaldehydes could not be optimised.

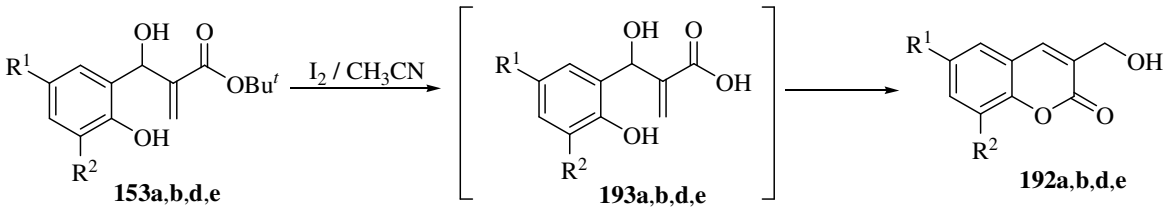

Scheme 48. Formation of 3-(hydroxymethyl)coumarins **192a**,**b**,**d**,**e**.

Table 20. Yields of 3-(hydroxymethyl)coumarins **192a**,**b**,**d**,**e**.

Compound	R^1	R^2	Isolated Yields (%)
192a	H	H	85
192b	Br	H	69
192d	H	OEt	65
192e	Cl	H	60

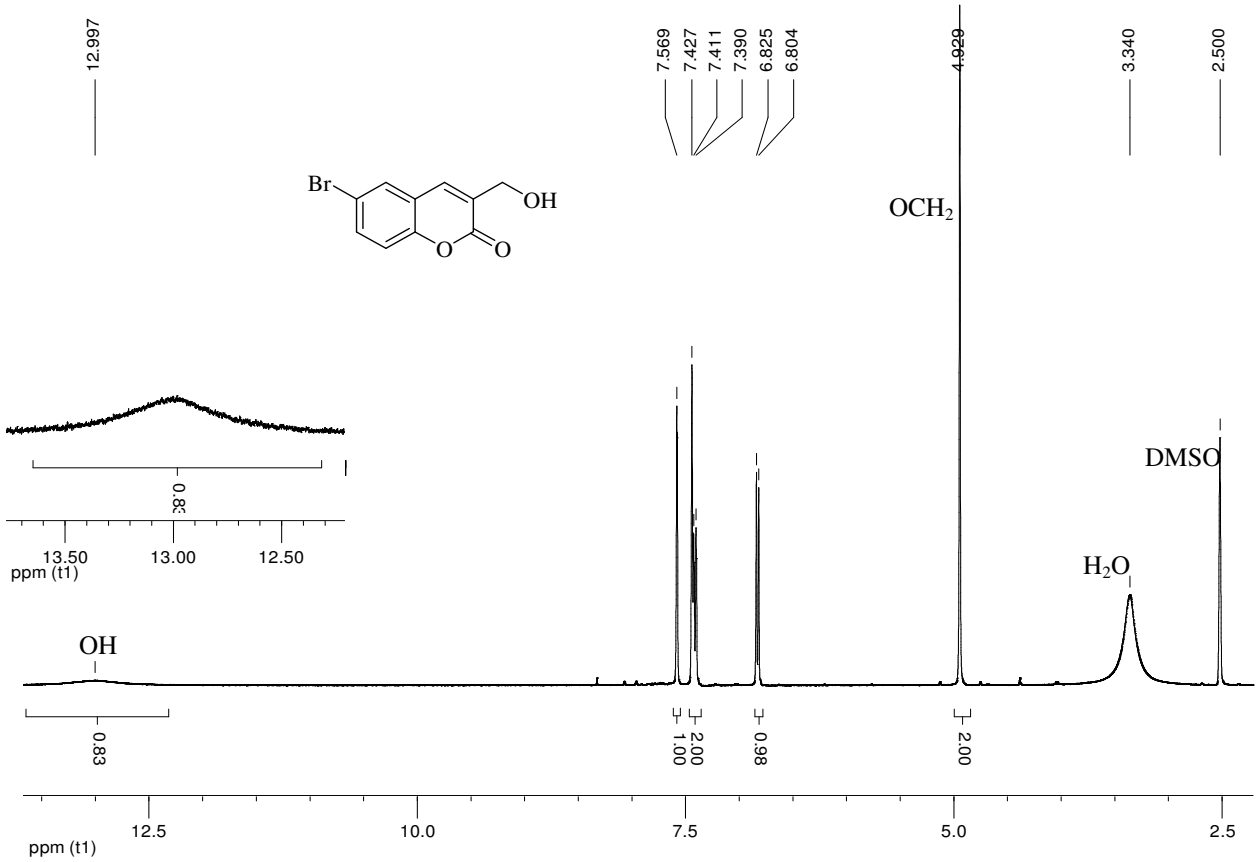

Figure 67. 400MHz ^{1}H NMR spectrum of compound **192b** in DMSO-d_6.

2.3.2. Baylis-Hillman Reactions of Coumarin-3-carbaldehydes

With the coumarin-3-carbaldehydes **191a**,**b**,**c** in hand, their use as electrophiles in the Baylis-Hillman reaction was investigated using methyl vinyl ketone (MVK) and methyl acrylate as the activated alkenes. 6-Bromocoumarin-3-carbaldehyde **191b** was reacted with MVK **194** (Scheme 49) in the presence of DABCO using chloroform as solvent by stirring at room temperature for 4 days. Chromatographic purification afforded the expected product **195b** in 42% yield. The DEPT 135 NMR (Figure 68) confirms the presence of a single vinylic methylene carbon which resonates at 128.8 ppm, while the ^{1}H NMR spectrum (Figure 69) reveals the two characteristic vinylic proton singlets at 6.25 and 6.31 ppm, and the 1′-methine and hydroxyl proton signals appear as doublets at 5.56 ppm at 4.12 ppm, respectively, due to mutual coupling. The ^{13}C NMR spectrum (Figure 70) reveals the ketonic carbonyl signal at 200.4 ppm and the lactone carbonyl signal at 160.1 ppm, and confirms the presence of the fourteen expected carbon signals expected for this compound.

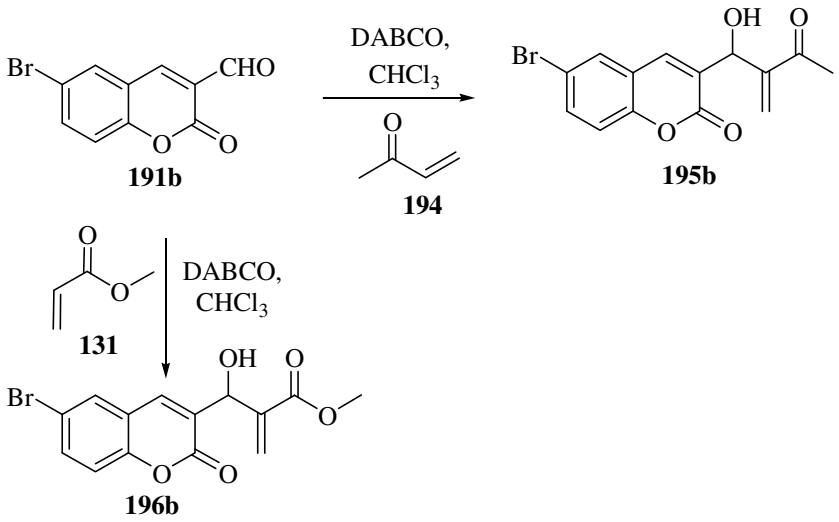

Scheme 49. Baylis-Hillman reaction of compound **191b** with MVK and methyl acrylate.

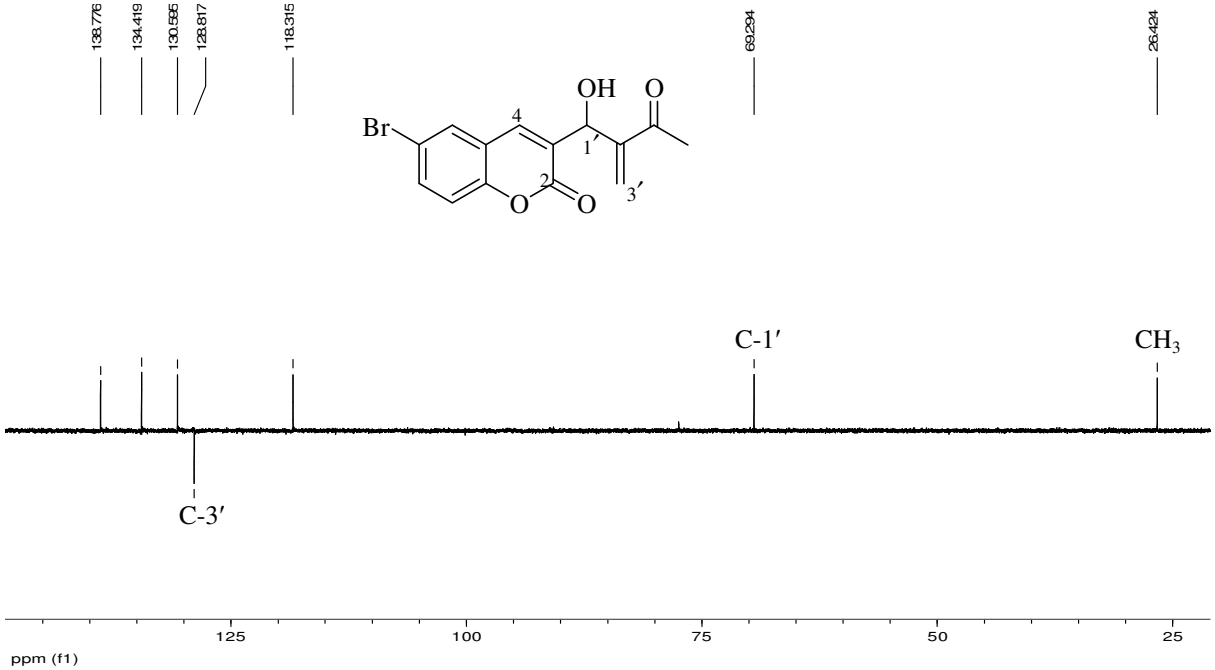

Figure 68. DEPT 135 NMR spectrum of compound **195b** in $CDCl_3$.

6-Bromocoumarin-3-carbaldehyde **191b** was also successfully reacted with methyl acrylate **131** (Scheme 49) in chloroform using DABCO as catalyst at room temperature for 4 days. Chromatographic purification afforded the expected Baylis-Hillman adduct **196b** in 45% yield. The major difference in the ^{1}H NMR spectrum of compound **196b** (Figure 71) compared to that of compound **195b** (Figure 69) is the shift in the position of the methyl signal from 2.37 ppm for the methyl ketone to 3.76 ppm for the methyl ester. Due to time constraints, cyclisation of Baylis-Hillman adducts **195b** and **196b** could not be explored during the present study.

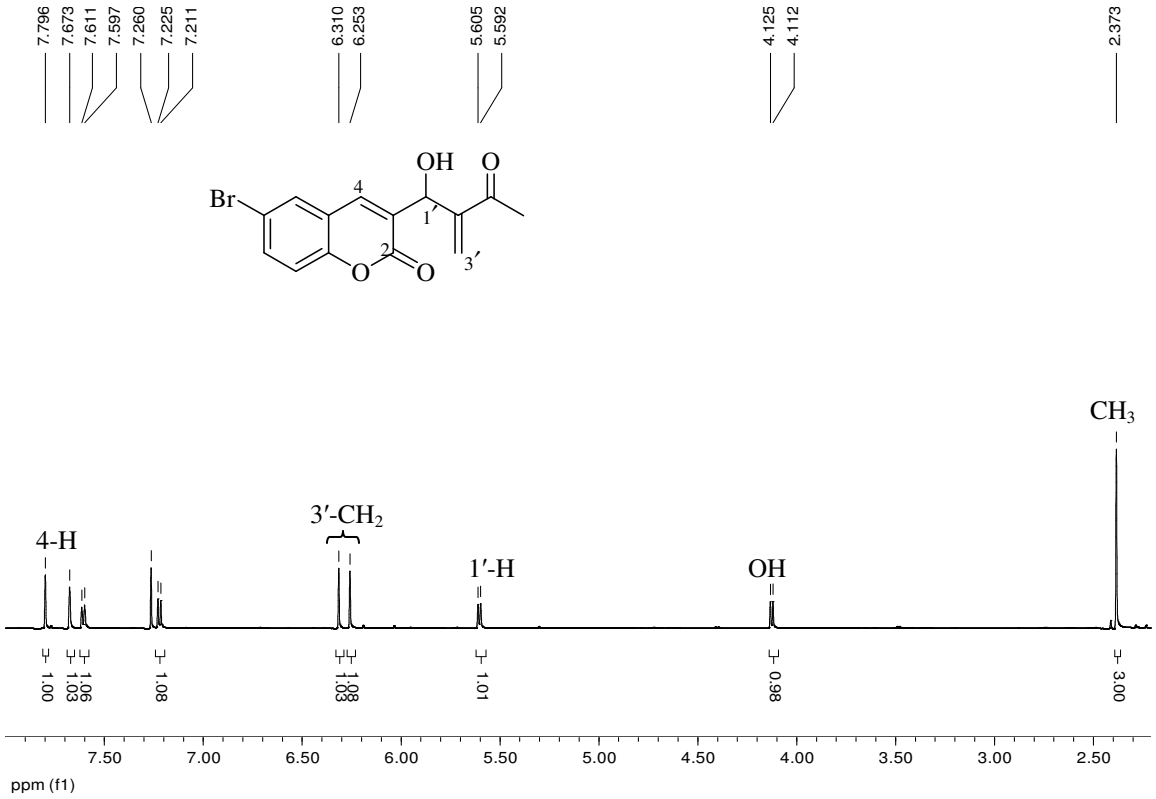

Figure 69. 600 MHz ^{1}H NMR spectrum of compound **195b** in $CDCl_3$.

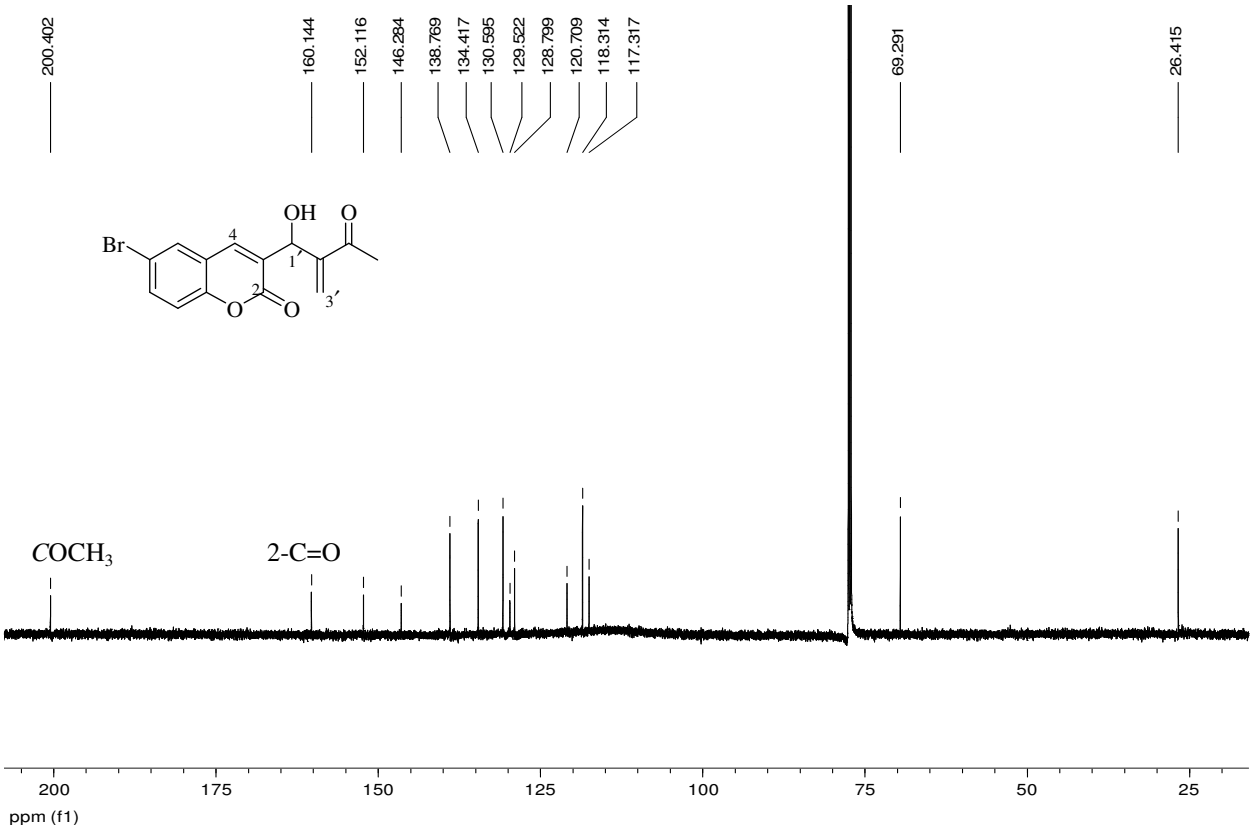

Figure 70. 150 MHz ^{1}H NMR spectrum of compound **195b** in $CDCl_3$.

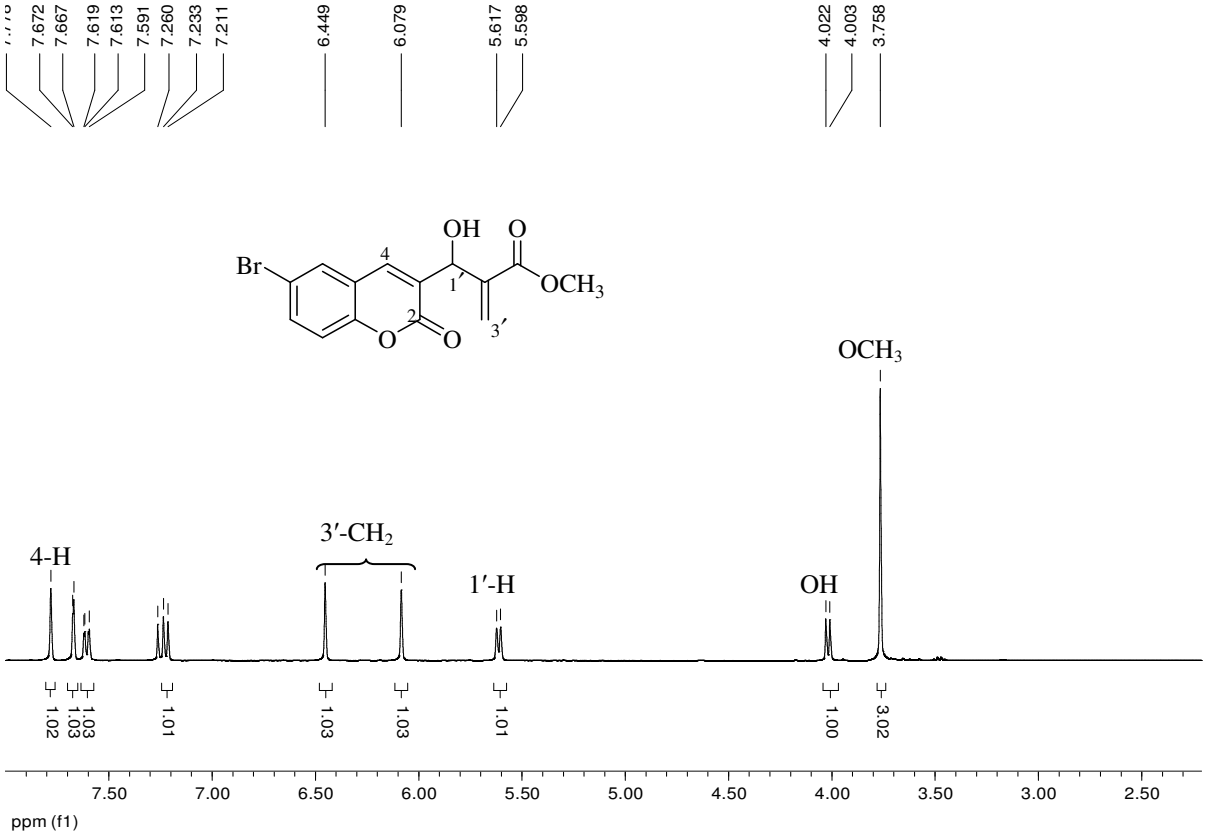

Figure 71. 400 MHz ^{1}H NMR spectrum of compound **196b** in $CDCl_3$.

2.4. ACCESSING 4-SUBSTITUTED COUMARINS

In the crystal structure of the phenprocoumon / HIV-1 PR complex, the 4-hydroxy group was found to be within hydrogen bonding distance of the essential catalytic aspartic acid residues.[99] Since various unsuccessful attempts have been made to prepare 4-hydroxycoumarins using Baylis-Hillman methodology,[248] it was hoped that the 4-amino analogues may prove more accessible and exhibit similar hydrogen bonding interactions in the HIV-1 PR active site. Consequently, a series of exploratory reactions were conducted.

2.4.1. Condensation of Salicylaldehydes with *p*-Toluenesulphonamide

The hydroxyl group in Baylis-Hillman adducts is usually lost during the cyclisation process leading to the formation of coumarins. It was envisaged that introduction of an amino group in place of the hydroxyl group might allow cyclisation of Baylis-Hillman adducts without loss of the amino group. Attention was initially focussed on the use of benzaldimines as alternative Baylis-Hillman electrophiles as illustrated in Scheme 50.

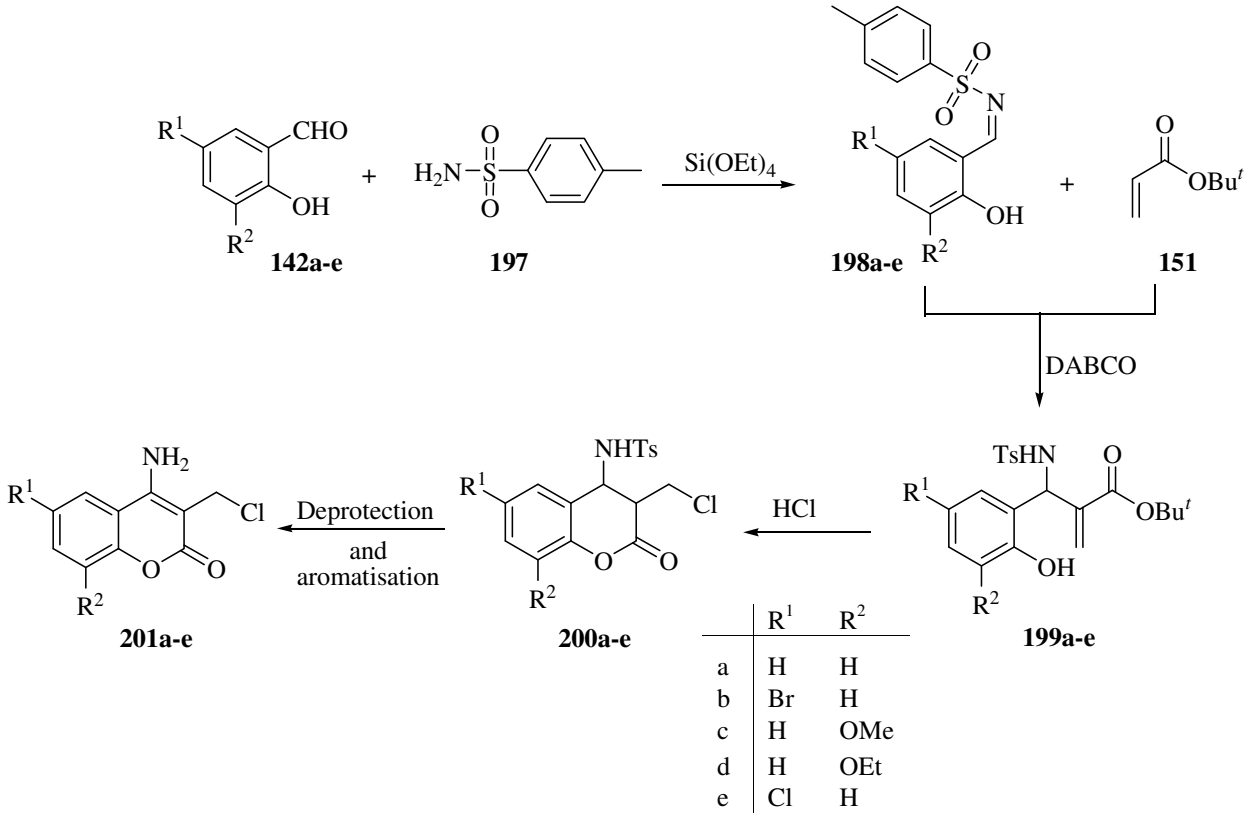

Scheme 50. Proposed route to 4-aminocoumarin analogues.

Compounds **142a-e** were reacted with *p*-toluenesulphonamide in tetraethyl orthosilicate (Scheme 50) under reflux at 150 °C for 8 hours, to afford the condensation products **198a-e** in yields of up to 93% (Table 21). The ^{1}H NMR spectrum of the 5-bromo derivative **198b** (Figure 72) reveals the imine proton resonating as a singlet at 9.00 ppm and the *p*-methyl protons as a singlet at 2.44 ppm. The ^{13}C NMR (Figure 73) confirms the presence of the imine carbon signal at 170.7 ppm and the presence of the expected twelve carbon signals.

Table 21. Yields of 2-hydroxy-*N*-tosylaldimines **198a**- **e**.

Compound	R^1	R^2	Isolated yields (%)
198a	H	H	87
198b	Br	H	93
198c	H	OMe	90
198d	H	OEt	92
198e	Cl	H	93

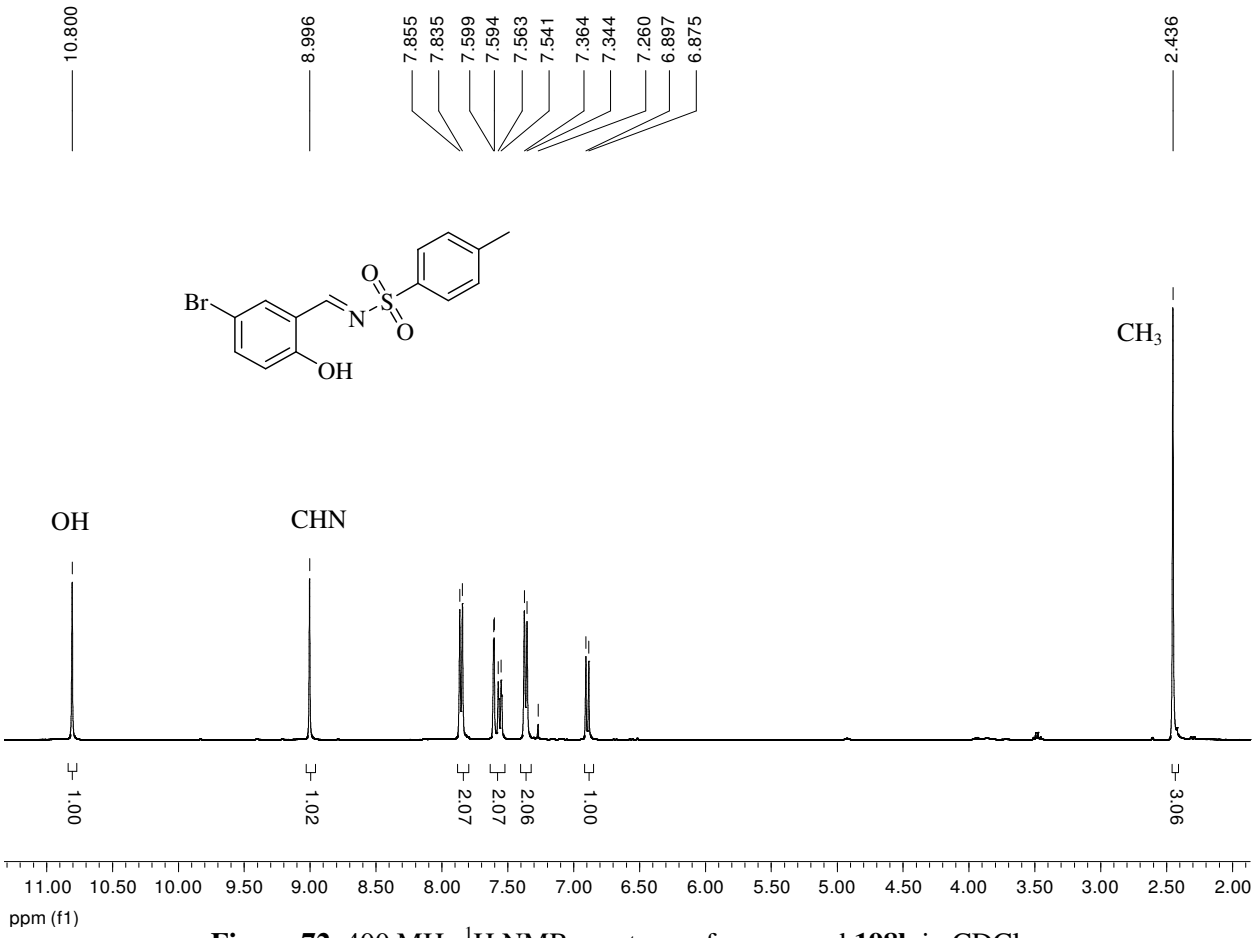

Figure 72. 400 MHz ^{1}H NMR spectrum of compound **198b** in $CDCl_3$.

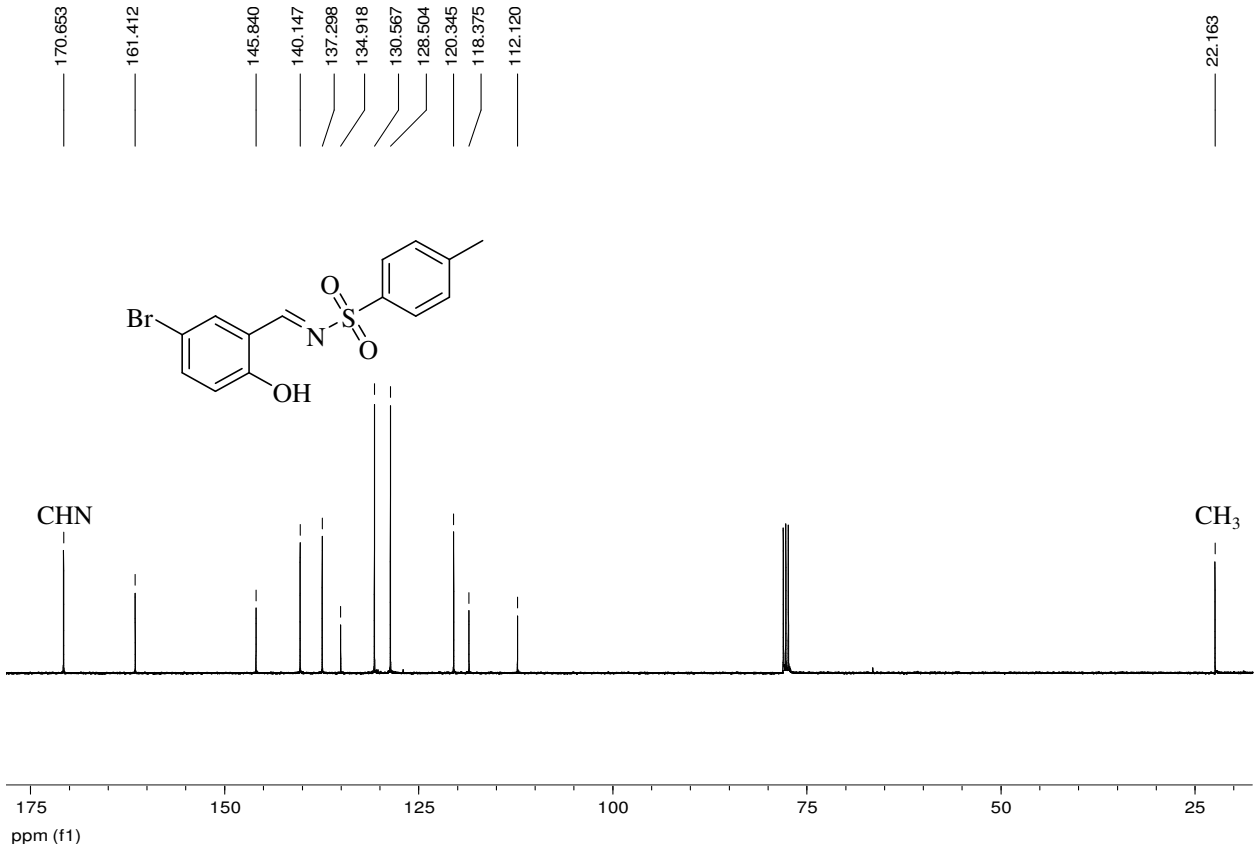

Figure 73. 100 MHz ^{13}C NMR spectrum of compound **198b** in $CDCl_3$.

2.4.2. Aza-Baylis-Hillman Reaction of 2-Hydroxy-*N*-tosylaldimines

Having successfully synthesised the *N*-tosylaldimines **198a-e**, the next step in the proposed route (Scheme 50) was to prepare the Baylis-Hillman adducts **199a-e** by reaction with *tert*-butyl acrylate. However, reaction of compound **198b** with *tert*-butyl acrylate **151** and DABCO in $CHCl_3$ / THF (as the substrate was not sufficiently soluble in $CHCl_3$ alone) led to a range of products. Flash chromatography permitted isolation of three different products (Scheme 51): the desired tosylamino derivative **199b**, in 15% yield; the normal Baylis-Hillman adduct **153b**; and compound **202b** in 28% yield, the formation of which was difficult to rationalise. Repeating the reaction in the absence of solvent simply resulted in hydrolysis of the aldimine to the aldehyde precursor and the formation of the Baylis-Hillman product **153b**. The ^1H NMR spectrum of the desired Baylis-Hillman adduct **199b** (Figure 74) reveals the presence of the two vinylic proton singlets at 5.72 and 6.11 ppm and the tosyl methyl group singlet at 2.37 ppm. Careful examination of the NMR and HRMS data permitted tentative assignment of structure **202b** to the unusual and unexpected product. The ^1H NMR spectrum (Figure 75) shows the diastereotopic 2′-methylene protons resonating as a multiplet at 3.81 ppm and coupling to the diasterotopic 1′-

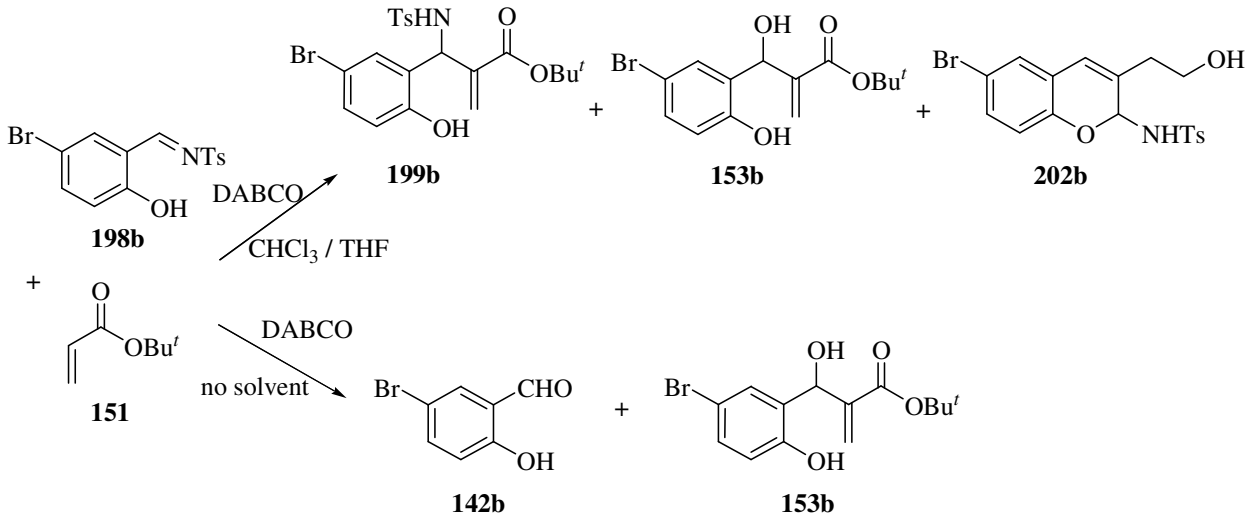

Scheme 51. Baylis-Hillman reaction of 5-bromo-2-hydroxy-*N*-tosylbezaldimine **198b**.

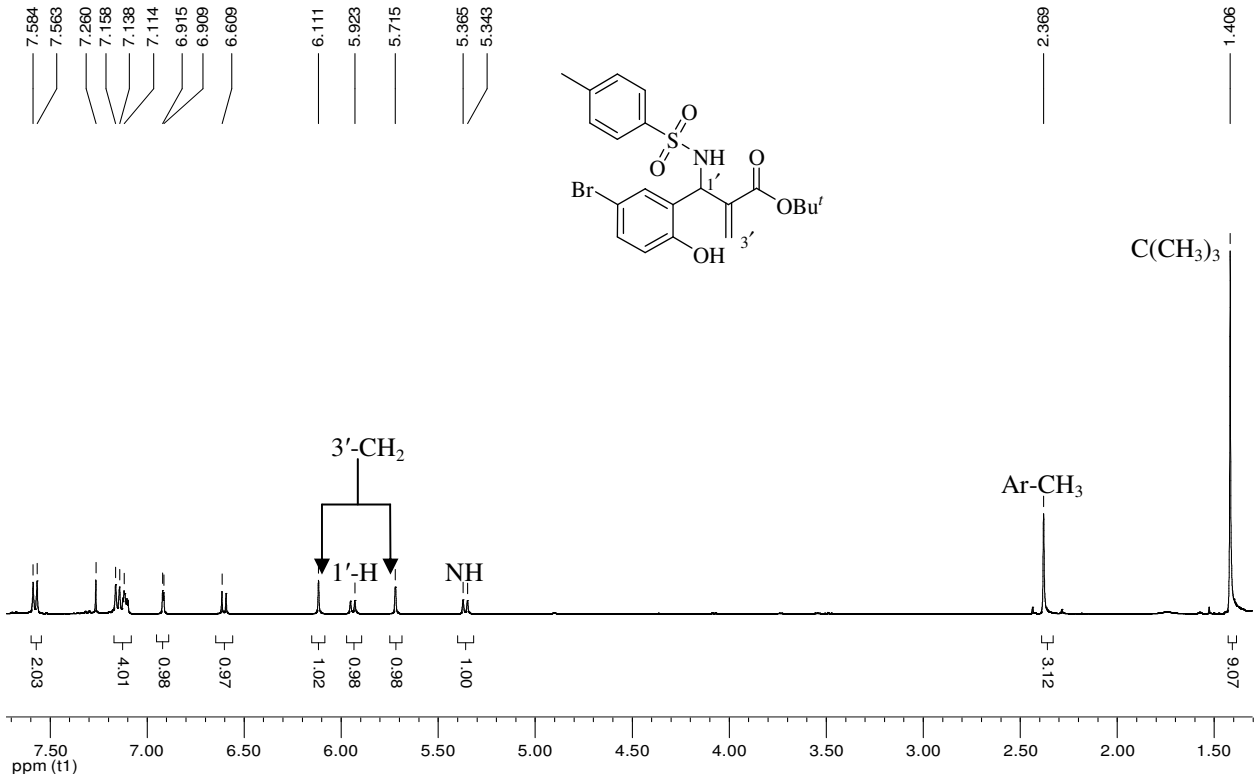

Figure 74. 400 MHz ^{1}H NMR spectrum of compound **199b** in $CDCl_3$.

methylene protons resonating as a multiplet which overlaps the tosyl methyl singlet at *ca* 2.5 ppm. The DEPT 135 NMR (Figure 76) confirms the presence of two methylene, one methyl and seven methine carbon signals, some of which are in the aromatic region. The HSQC spectrum (Figure 77) confirms the 1′-methylene and the methyl group ^{1}H NMR assignments, while the HMBC spectrum (Figure 78) shows 3-bond correlations between the 4-methine proton and the

1′-methylene and the 2-methine carbons. The proposed structure of compound **202b** was confirmed by X-ray crystallography. The X-ray crystal structure (Figure 79) clearly reveals migration of the tosyl group and the introduction of four additional carbon atoms and a hydroxyl group. While the mechanism of formation of compound **202b** is yet to be fully explored, it appears that the reaction involves ring scission of 2,3-dihydrofuran which is a known impurity and oxidation product of THF[249] – a co-solvent used in the reaction. Two possible pathways for the formation of compound **202b** are shown in Scheme 52. While the ring-opening of THF is a known process,[250-252] there has been no prior report of this happening under Baylis-Hillman reaction conditions.

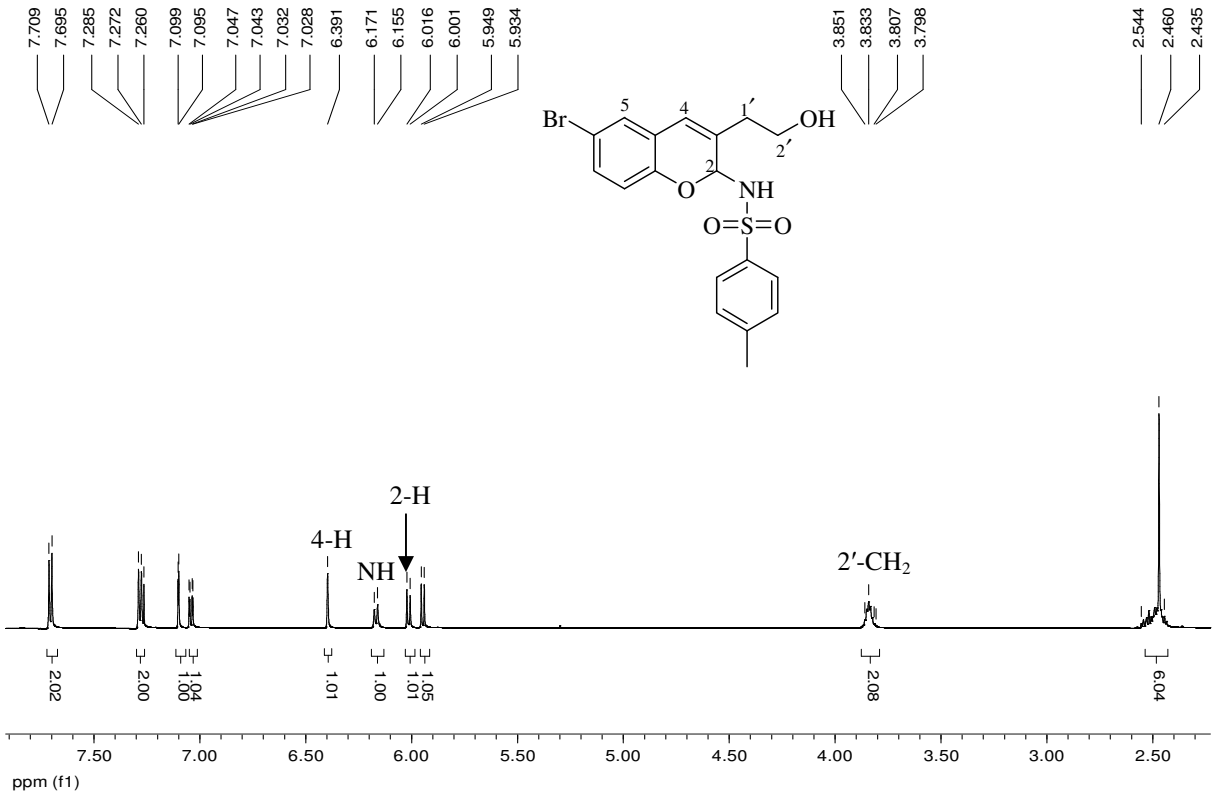

Figure 75. 600 MHz ^{1}H NMR spectrum of compound **202b** in $CDCl_3$.

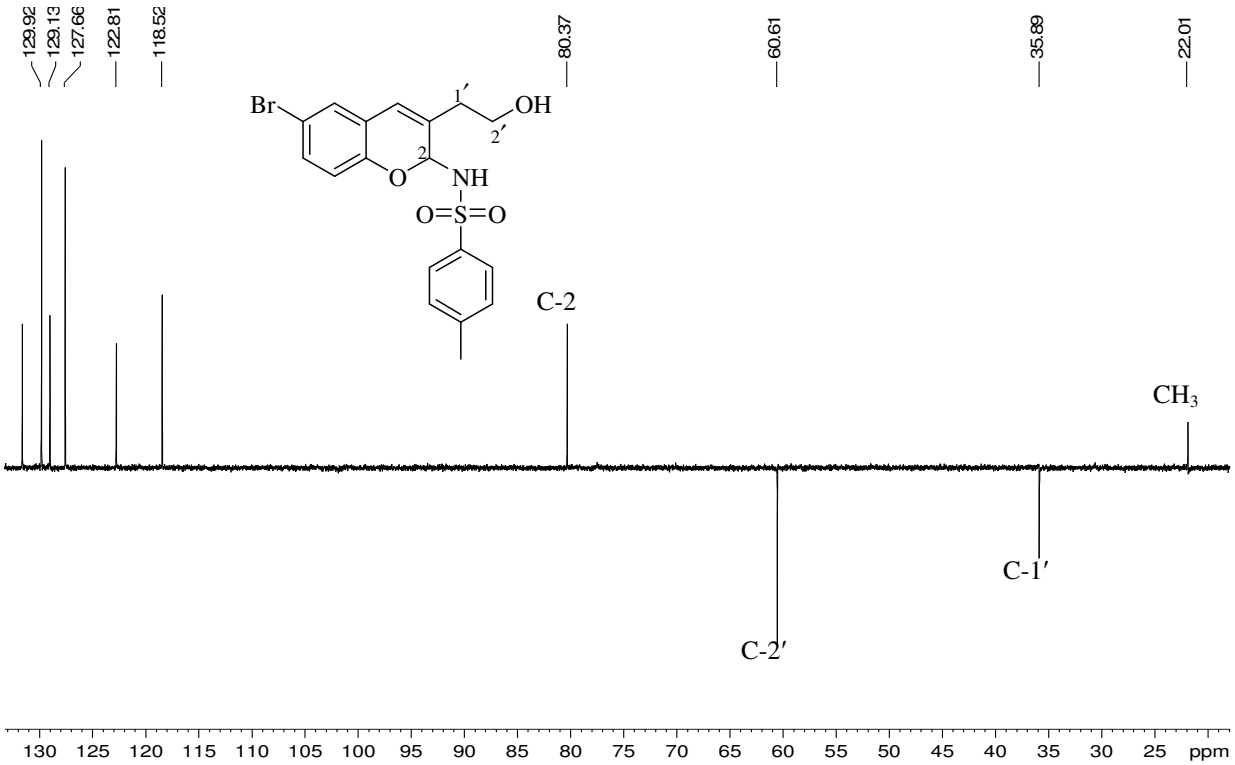

Figure 76. DEPT 135 NMR spectrum of compound **202b** in $CDCl_3$.

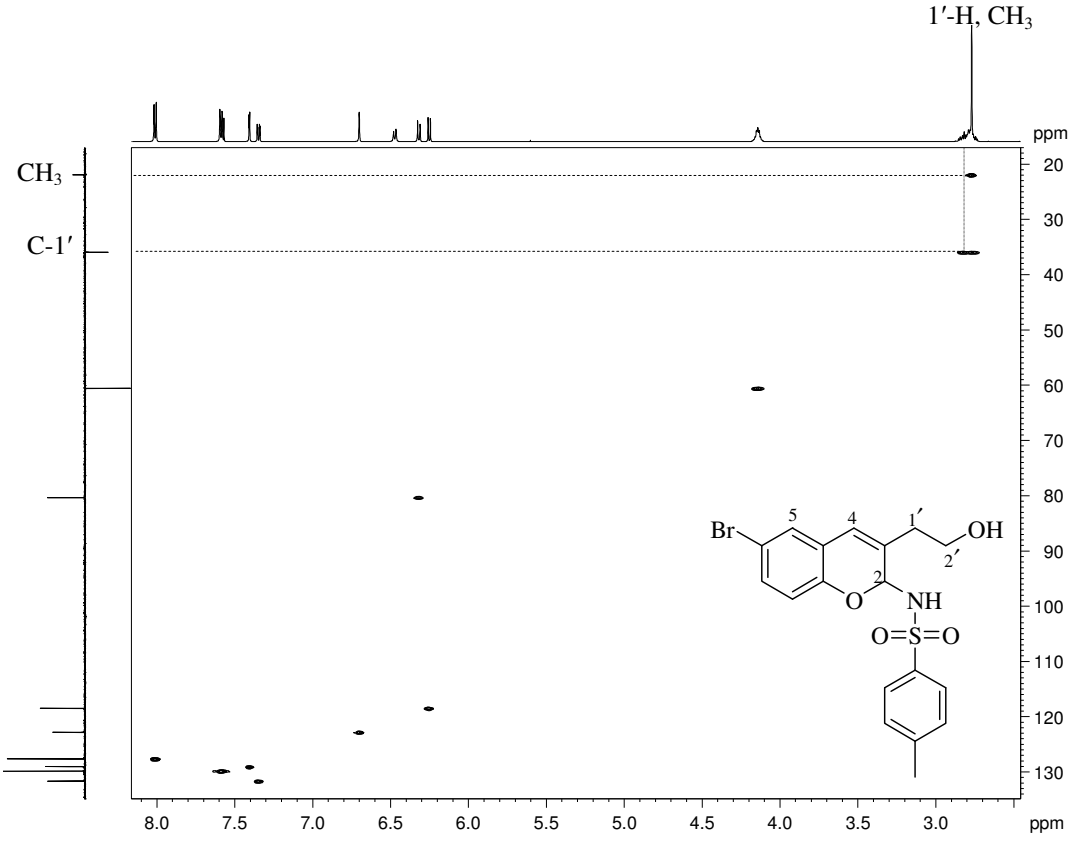

Figure 77. HSQC spectrum of compound **202b** in $CDCl_3$.

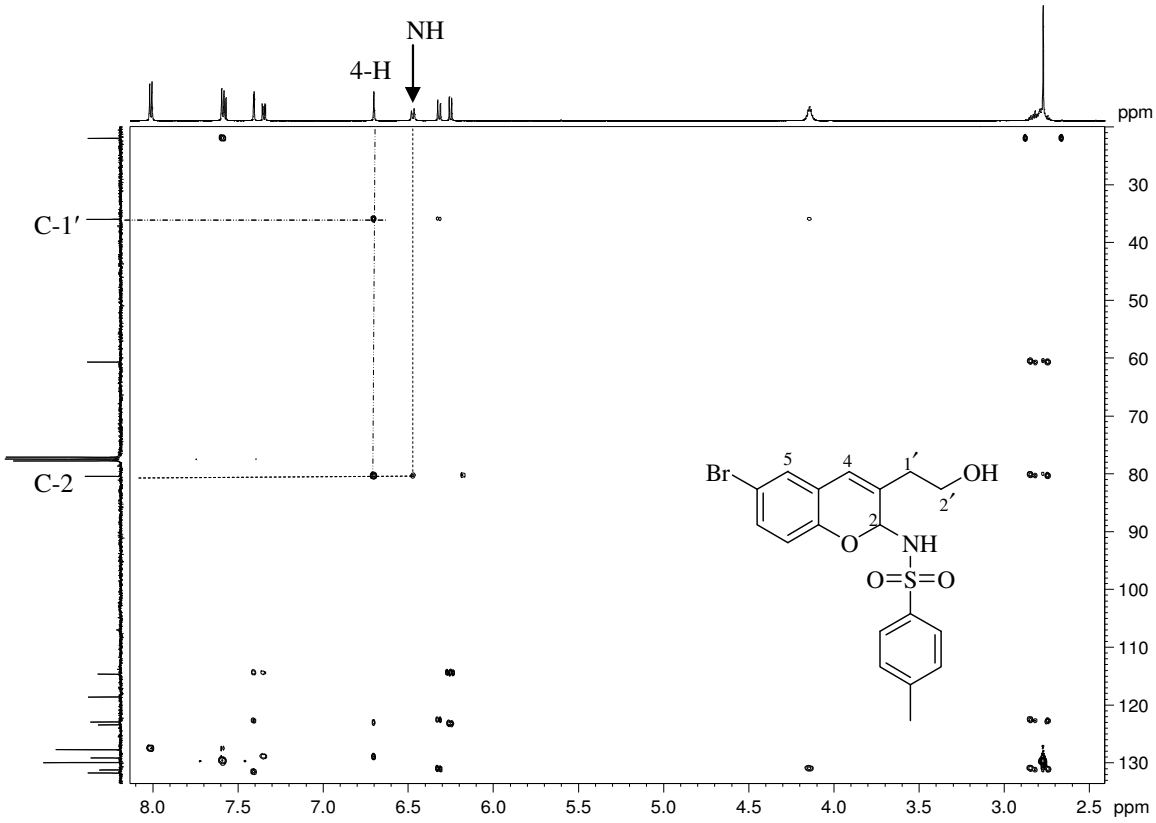

Figure 78. HMBC spectrum of compound **202b** in $CDCl_3$.

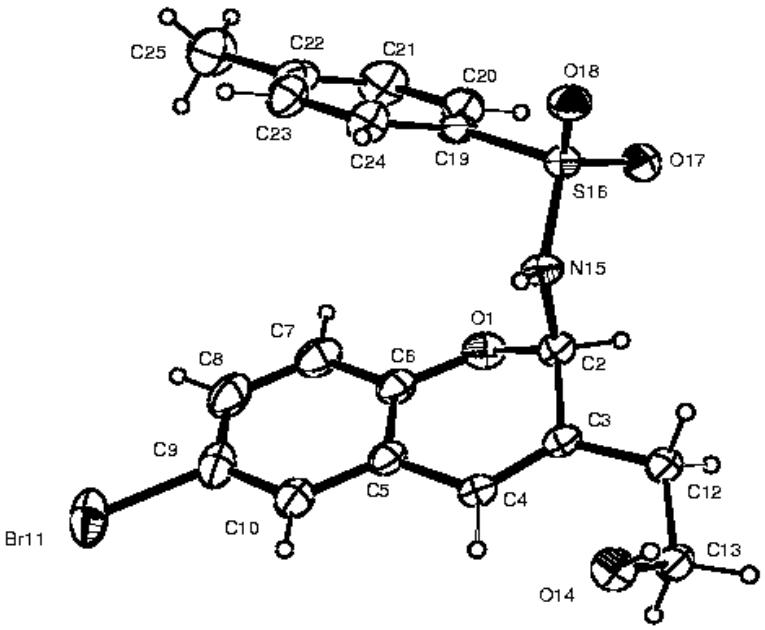

Figure 79. Crystal structure of compound **202b**, showing crystallographic numbering.

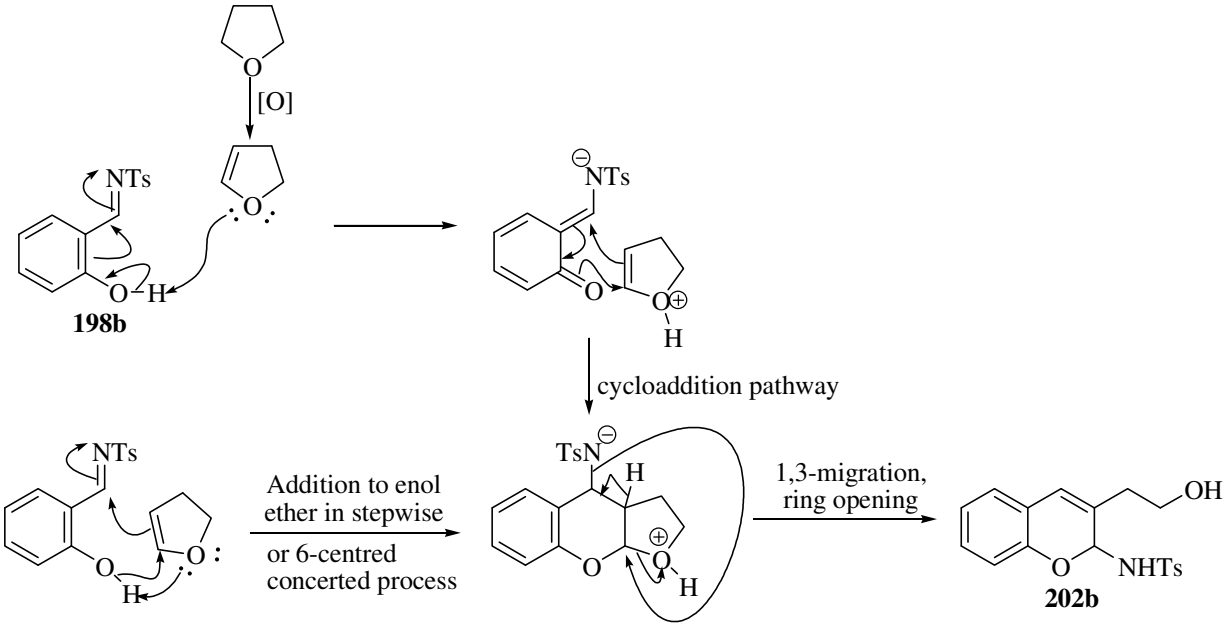

Scheme 52. Possible mechanisms for formation of compound **202b**.

When the benzaldimine **198d** was reacted similarly with $CHCl_3$ / THF as solvent, the rearranged product **202d** was isolated in 22% yield, together with compound **164d** (Scheme 53). Compound **164d**, a chromene derivative, was obtained in 12% yield and is assumed to have been formed by cyclisation of hydrolysed intermediate **153d**.

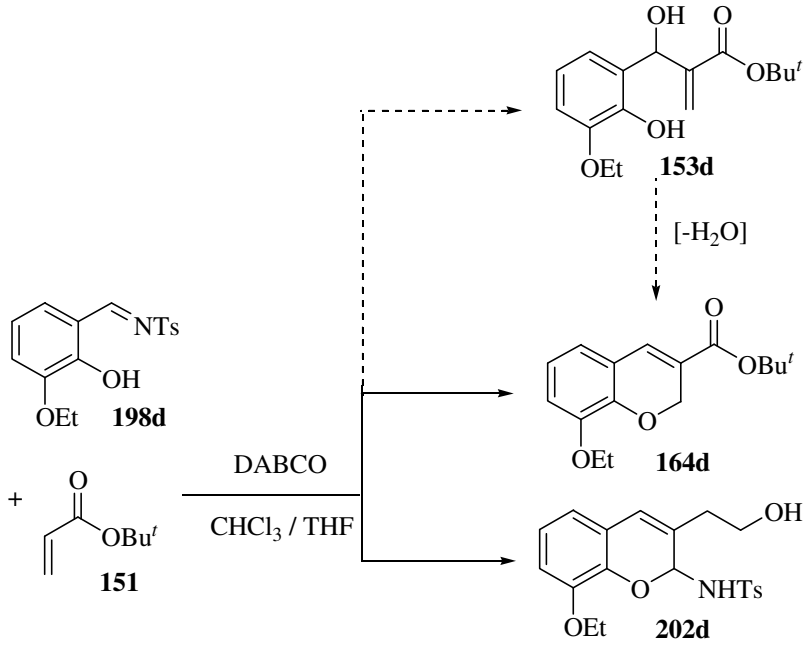

Scheme 53. Aza-Baylis-Hillman reaction of 3-ethoxy-2-hydroxy-*N*-tosylbenzaldimine **198d**.

The aza-Baylis-Hillman adduct **199b** was treated with a mixture of HCl / AcOH under reflux for 2 hours but, unfortunately, cyclisation occurred with loss of the tosylamino group to afford compound **148b** (Scheme 54). Benzyl protection of the phenolic hydroxyl group is known to prevent the formation of multiple products during the Baylis-Hillman reactions[208,253] and, consequently, compounds **204e** and **205e** (Scheme 55) were synthesised but, due to time constraints the oxidation of compound **205e** to the intermediate imine **206e** could not be pursued. In a final exploratory study, attention was given to the preparation of 4-phthalimido derivatives.

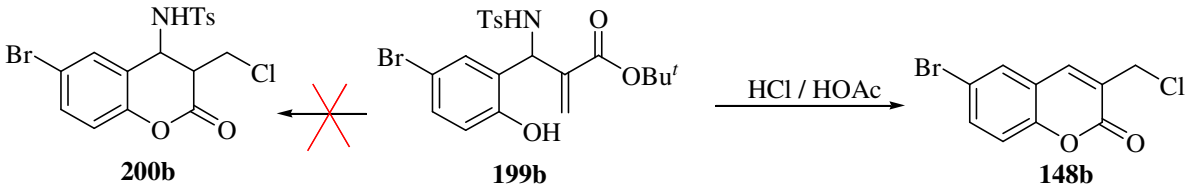

Scheme 54. Acid catalysed cyclisation of Baylis-Hillman adduct **199b**.

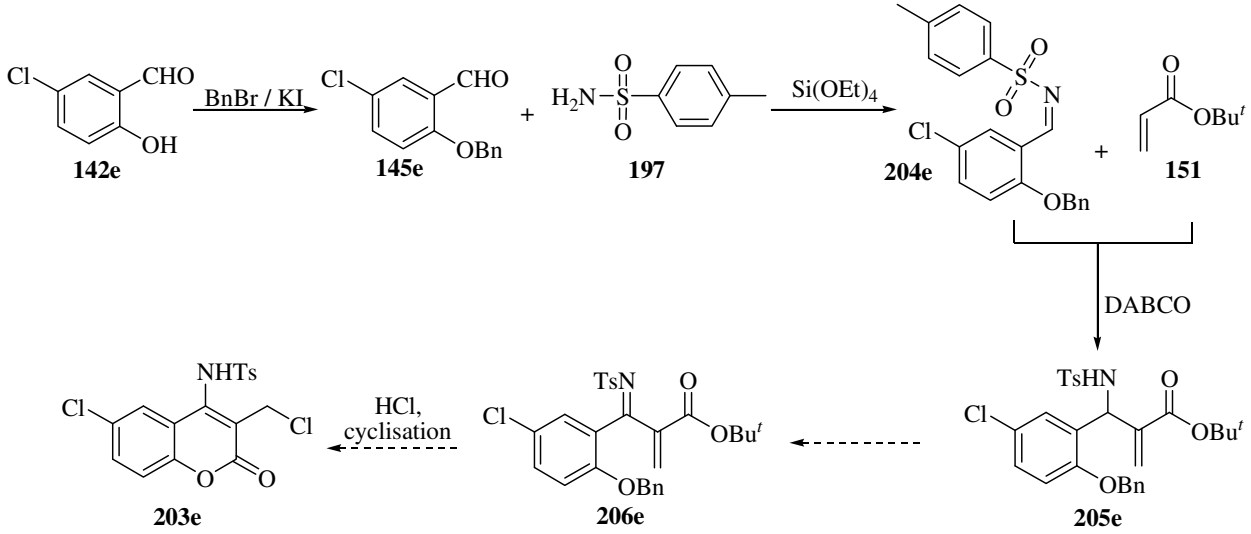

Scheme 55. Potential route to *N*-tosyl-4-aminocoumarins.

2.4.3. Use of Phthalimide in the Synthesis of 4-Substituted Coumarin Analogues

Phthalimide can be cleaved to afford primary amines, and with a view to achieving access to 4-aminocoumarins *via* S_N' displacement of chloride, compound **148e** was treated with potassium phthalimide in the presence of DABCO and TBAB,[254] and the mixture stirred at 100 °C for 10 hours. Purification by flash chromatography afforded compound **208e** – the S_N rather than the S_N' product of interest (Scheme 56). The ^{1}H NMR spectrum of the phthalimide derivative **208e** (Figure 80) reveals the methylene proton singlet at 4.82 ppm and signals accounting for all eight

aromatic protons. Another route, illustrated in Scheme 57, was then explored. In this case the dibromo compound **183b** was reacted with potassium phthalimide **207** in dry THF by stirring at room temperature overnight to afford the S_N' reaction product **209b** in 62% yield after chromatography. The ^{1}H NMR spectrum of this product (Figure 81) shows the benzylic protons resonating as a singlet at 5.05 ppm and the methoxy protons resonating as a singlet at 3.70 ppm. Reductive cyclisation was effected by stirring overnight under hydrogen using a Pd/C catalyst in EtOH and subsequent purification afforded compound **210a** in 56% yield. This procedure appears promising provided a suitable hydrogenation method can be found. The 4-phthalimido-dihydrocoumarin **210a** was fully characterised and the molecular formula is supported by the high resolution MS data. While the ^{1}H, ^{13}C and HSQC NMR spectra illustrated in Figures 82, 83 and 84, respectively, provide unambiguous support for the structural assignment, there appears to be some rotational barrier on the phthalimide moiety as reflected in the broad signals in the ^{1}H NMR and the absence of the phthalimide quaternary carbon signals in the ^{13}C NMR.

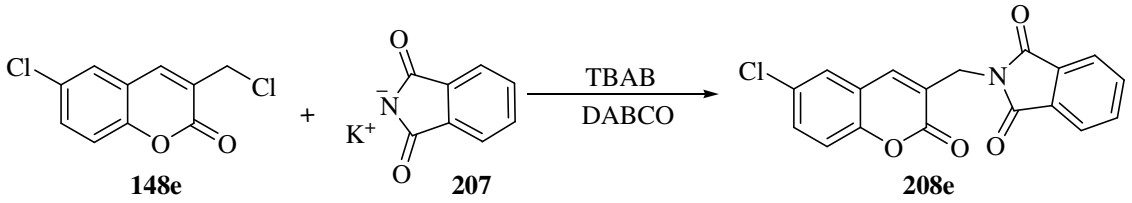

Scheme 56. Reaction of potassium phthalimide with compound **148e**.

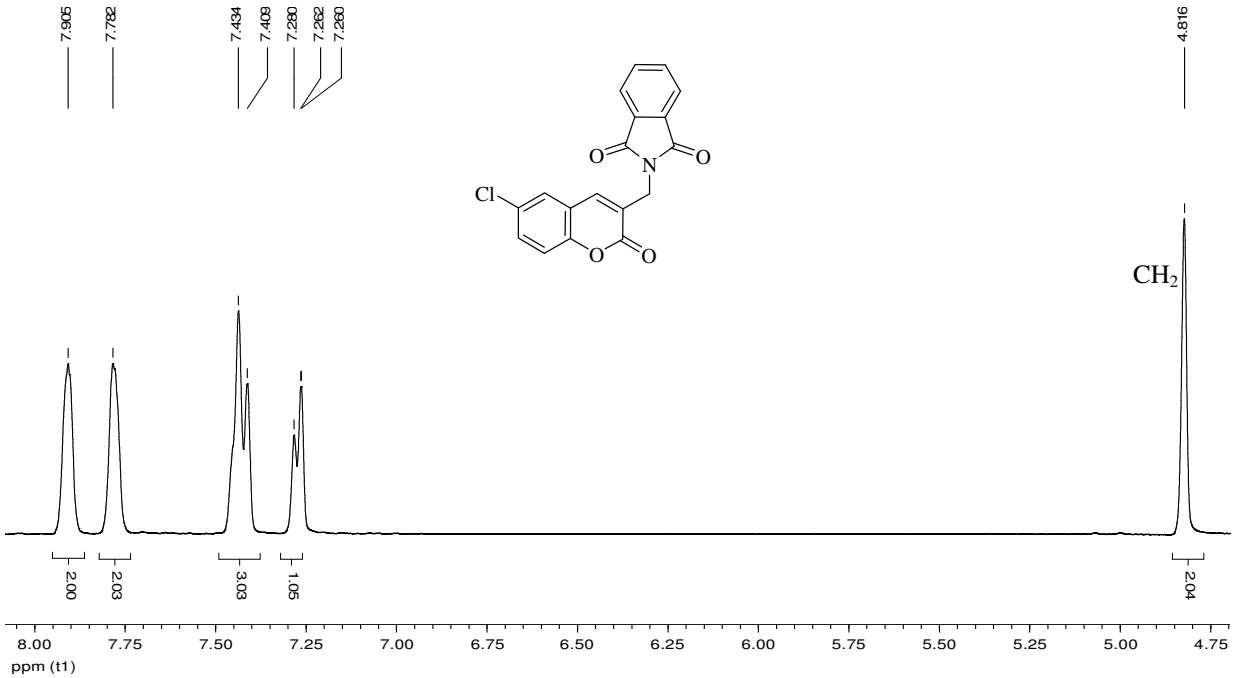

Figure 80. 400 MHz ^{1}H NMR spectrum of compound **208e** in $CDCl_3$.

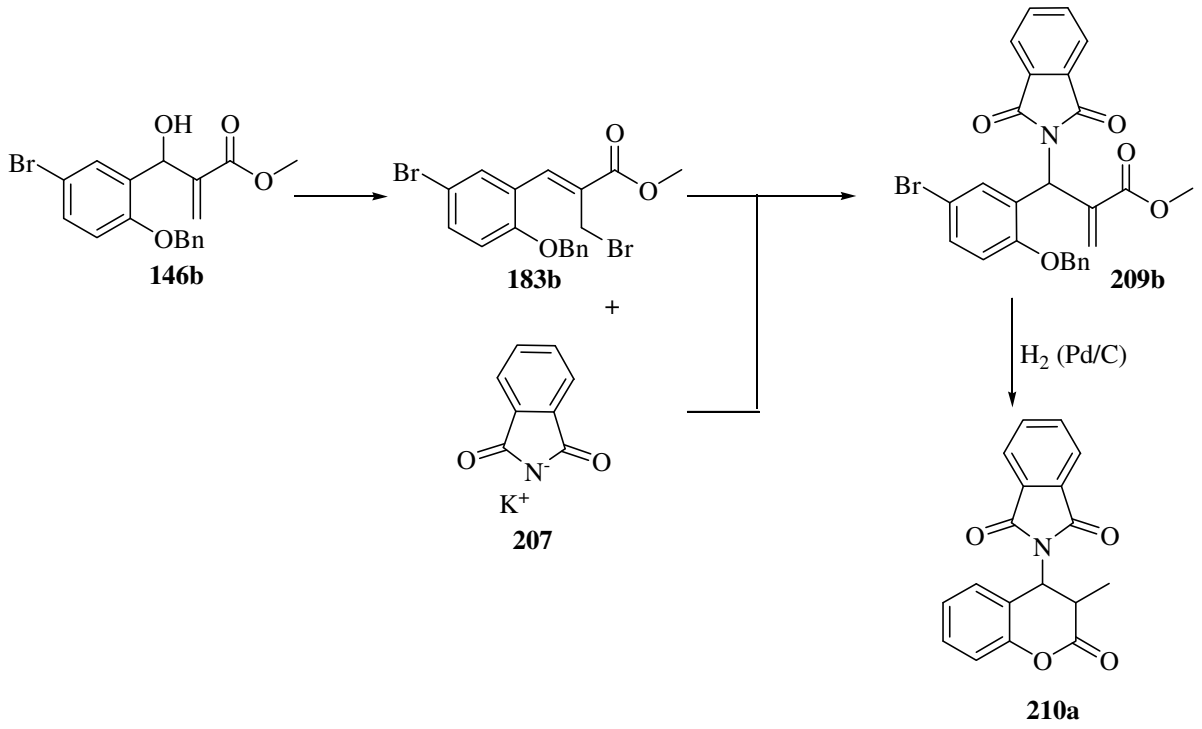

Scheme 57. Route to the 4-phthalimide derivative **210a**.

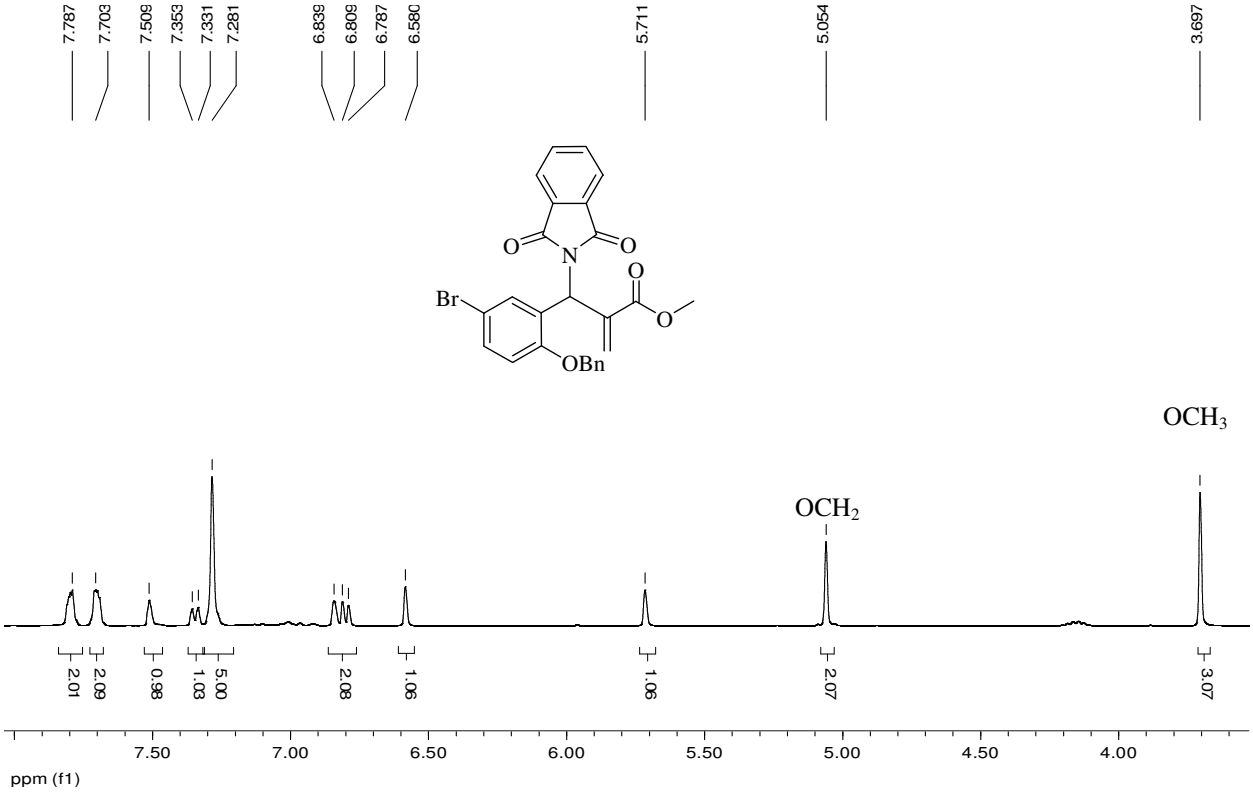

Figure 81. 400 MHz ^{1}H NMR spectrum of compound **209b** in $CDCl_3$.

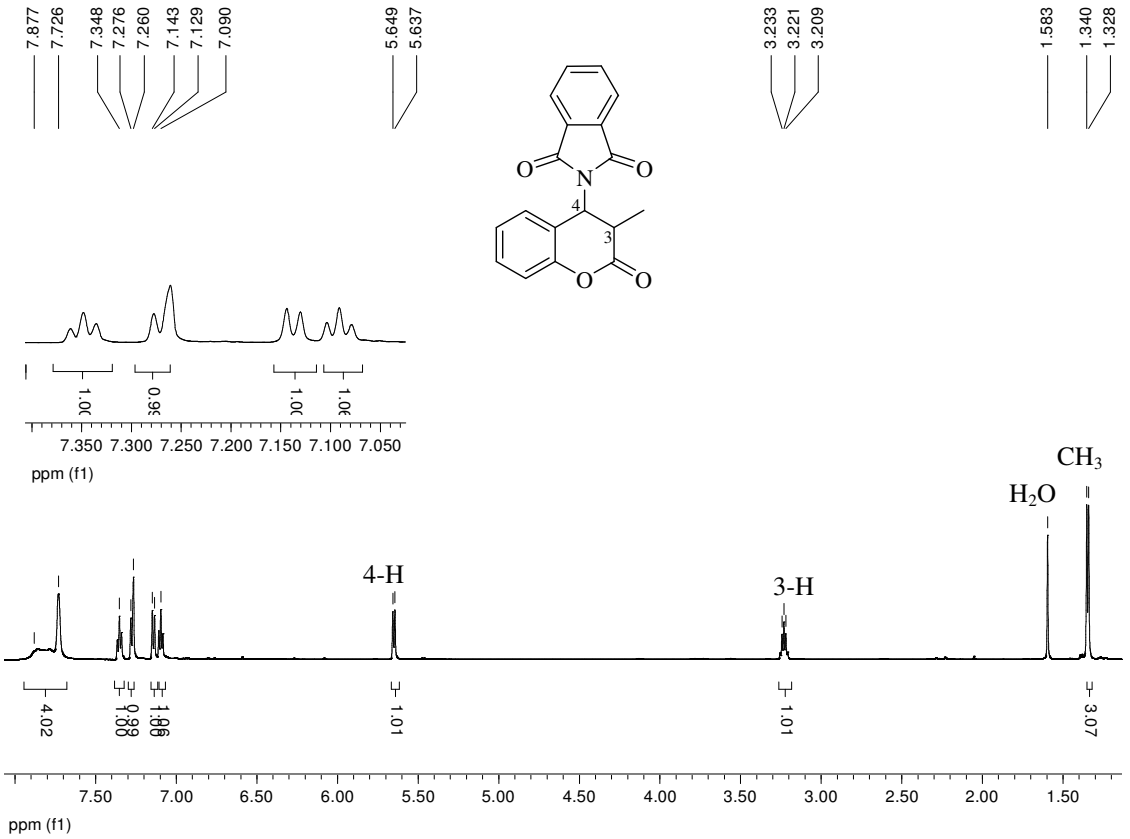

Figure 82. 600 MHz ^{1}H NMR spectrum of compound **210a** in $CDCl_3$.

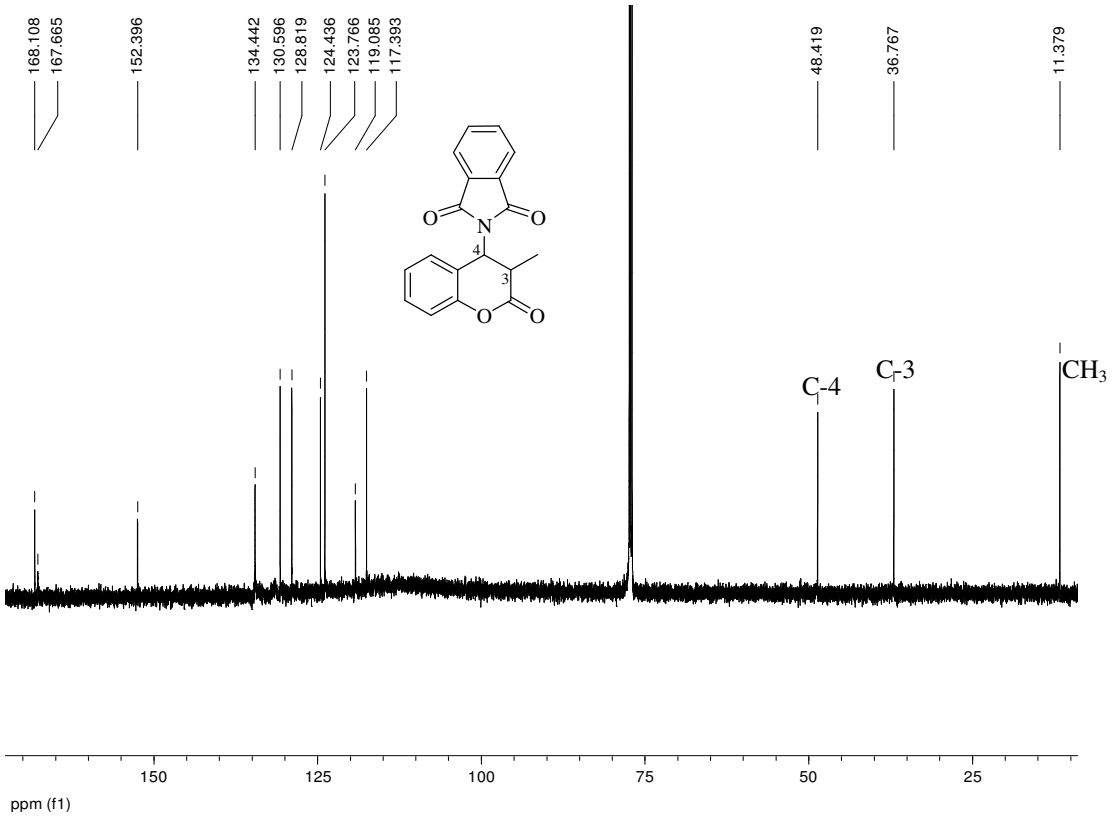

Figure 83. 150 MHz ^{13}C NMR spectrum of compound **210a** in $CDCl_3$.

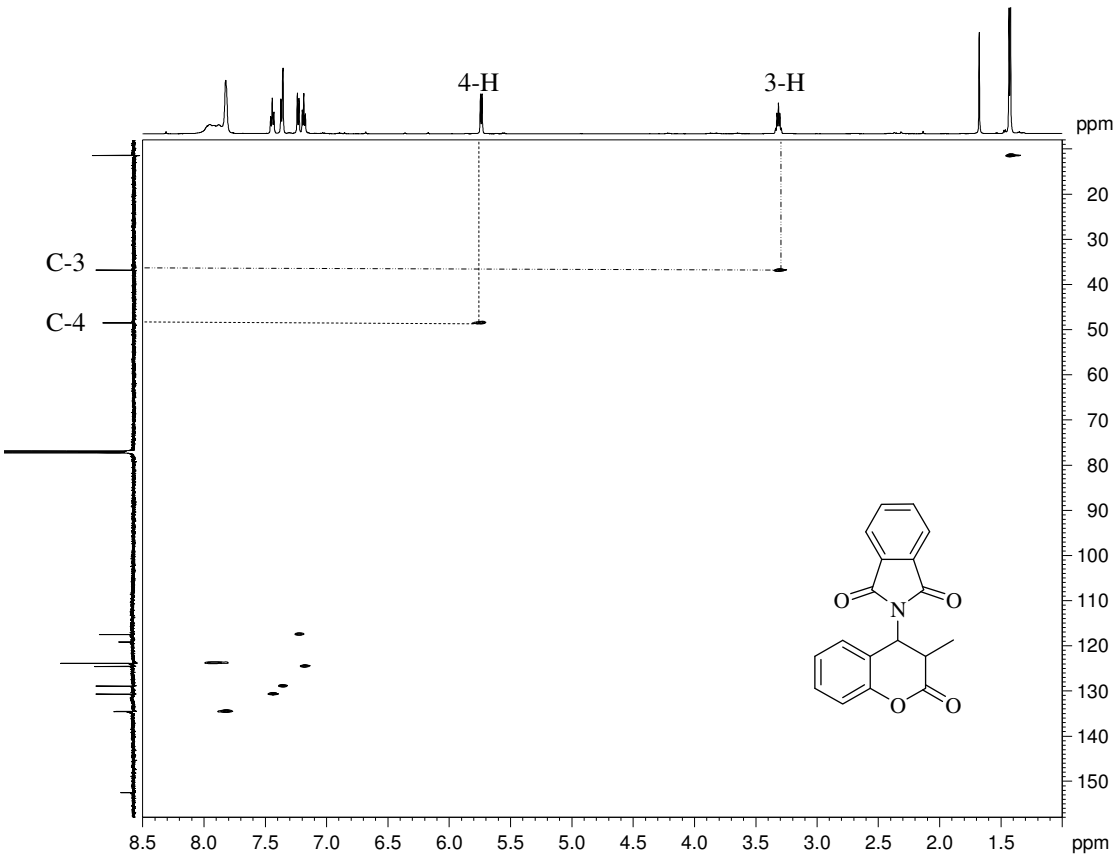

Figure 84. HSQC spectrum of compound **210a** in $CDCl_3$.

The exploratory research in this section has uncovered some interesting transformations which will receive further attention in future studies. Perhaps the most promising approach involves the synthesis of the 4-phthalimidodihydrocoumarin systems **210a**. Hydrolysis of the phthalimide moiety and aromatisation (or more selective initial reduction) could well provide access to the 4-aminocoumarin systems.

2.5. SYNTHESIS OF FUROCOUMARINS

Computer modelling studies conducted at MINTEK had suggested that furocoumarin derivatives, such as compound **212a** (Figure 85), should bind well in the HIV-1 IN active site and could thus inhibit the integration of viral DNA. Given our common interest in coumarin chemistry and the development of HIV-1 integrase inhibitors, a collaborative interaction was undertaken with MINTEK as part of this research programme. The results are included in the thesis with the permission from MINTEK. Although furocoumarins can also be accessed by the Baylis-Hillman route, an alternative method of preparation, using literature methods,[255-257] was adopted as outlined in Scheme 58.

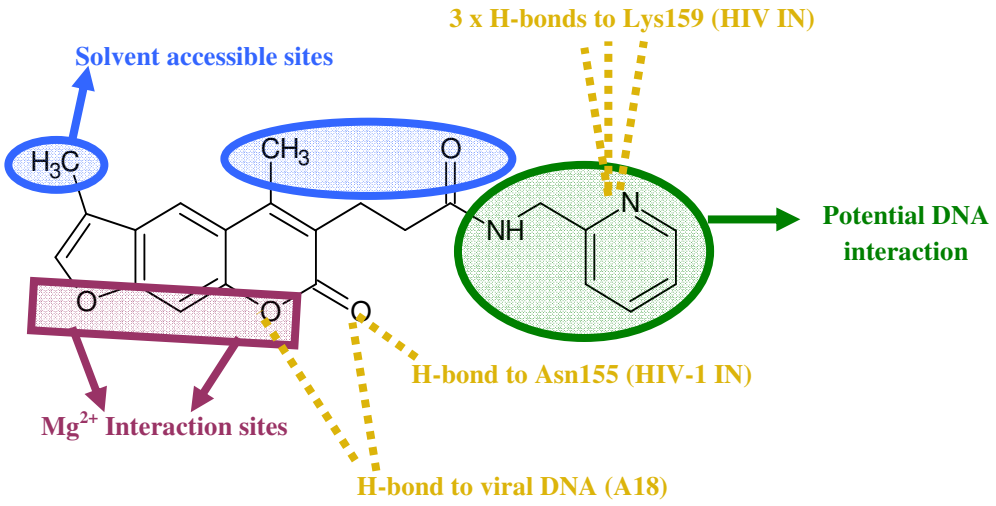

Figure 85. 2-D interactions of compound **212a** with the HIV-1 IN active site (docked by using Tripos™ Sybyl molecular modelling software; data provided by MINTEK).

Resorcinol **213** was reacted overnight with diethyl 2-acetylglutarate **214** at 0 °C in an ethanolic solution of HCl, generated *in situ* by the cautious addition of acetyl chloride to dry ethanol. The coumarin derivative **215** was isolated in 64% yield (Scheme 58). The ^{1}H NMR spectrum of this product **215** (Figure 86) reveals the ester methylene quartet at 4.08 ppm and the methyl triplet at 1.19 ppm. The other methylene protons resonate as triplets at 2.89 and 2.55 ppm. Reaction of compound **215** with chloroacetone in the presence of freshly calcined K_2CO_3 at 60 °C for 3 hours afforded compound **216** in 73% yield, following recrystallisation. The latter reaction involved an alkylation of the phenolic hydroxyl group. The ^{1}H NMR spectrum of the resulting ether (Figure 87) shows the appearance of new signals corresponding to the acetyl methyl group as a singlet at 2.24 ppm and an additional methylene group singlet at 4.59 ppm.

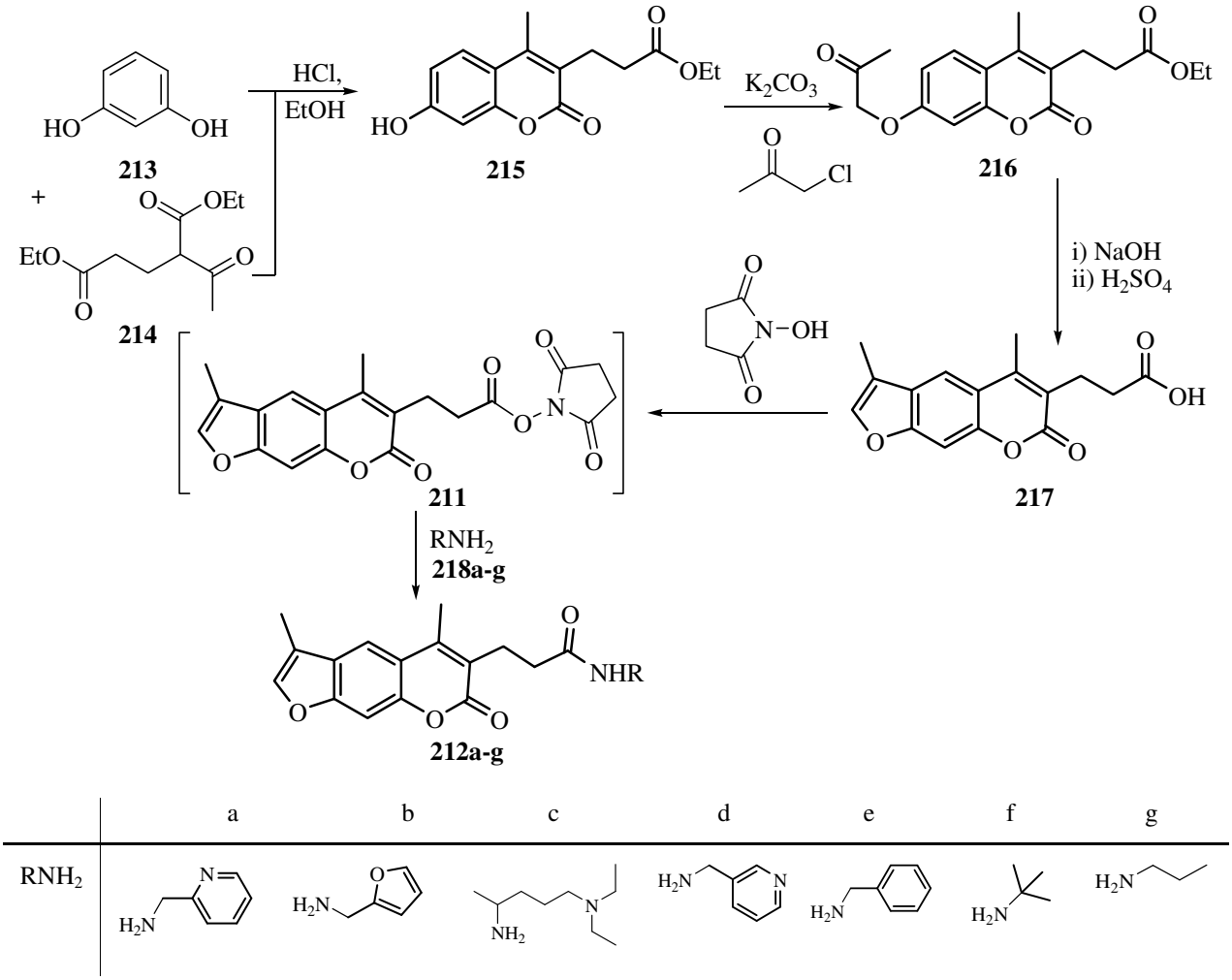

Scheme 58. Synthetic route to furocoumarin analogues **212a-g**.

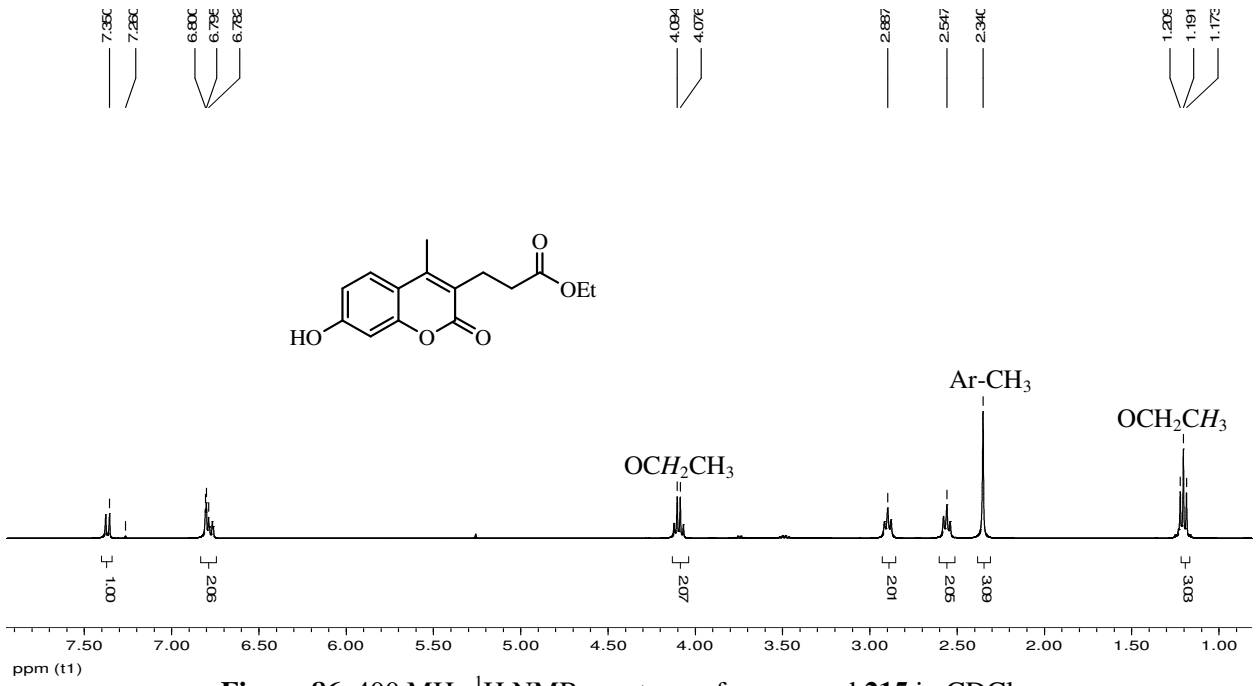

Figure 86. 400 MHz ^{1}H NMR spectrum of compound **215** in $CDCl_3$.

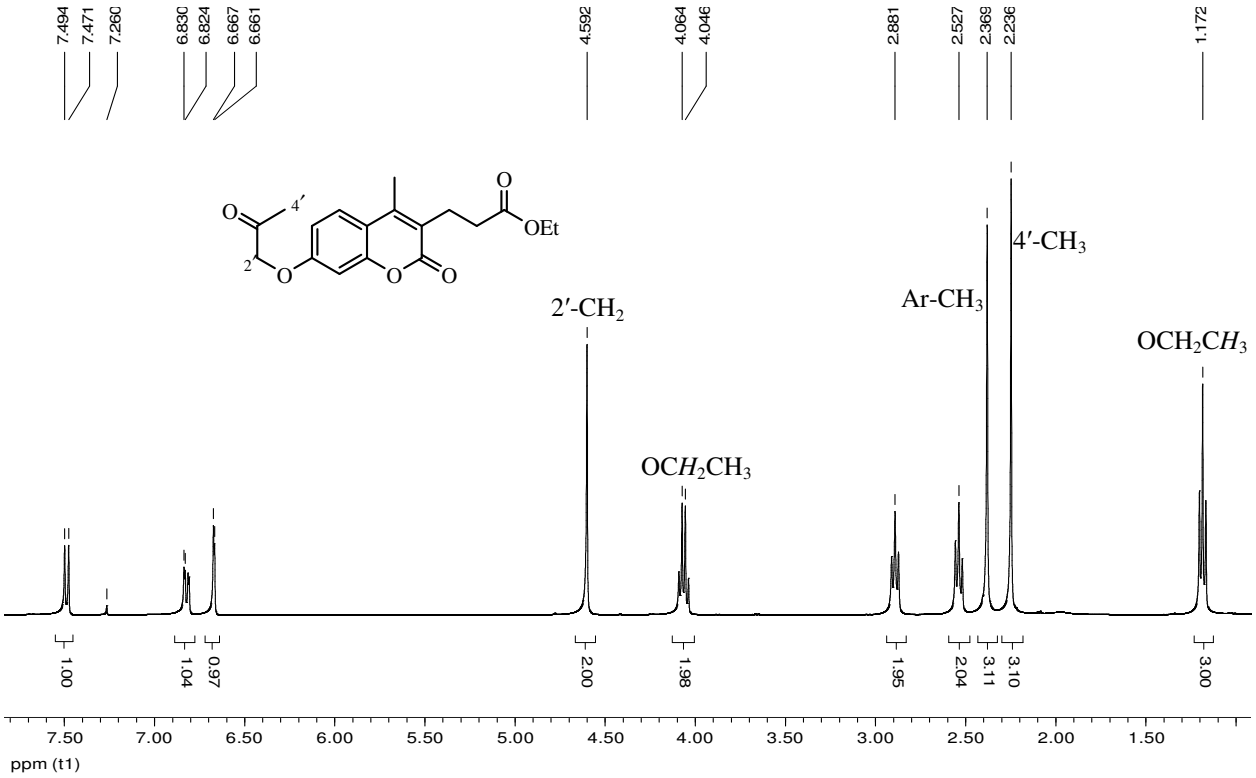

Figure 87. 400 MHz ^{1}H NMR spectrum of compound **216** in $CDCl_3$.

Cyclisation of the ether **216** was effected under basic conditions by heating for 3 hours. Following work-up and recrystallisation, the furocoumarin carboxylic acid **217** was obtained in 79% yield. The cyclisation is considered to involve opening of the coumarin ring to afford a phenoxide ion which, in turn, activates the *para*-position to intramolecular electrophilic substitution; protonation and acid-catalysed dehydration then leads to the product **217**.[255] The ^{1}H NMR spectrum of the furocoumarin carboxylic acid **217** (Figure 88) is characterised by the absence of signals corresponding to the ester moiety and the presence of a broad carboxylic acid proton signal at 12.20 ppm, confirming hydrolysis of the ester to the carboxylic acid. The final phase in accessing the target carboxamides **212a-g** was achieved in two steps, *viz.*, activation of the carboxylic acid group by treatment with *N*-hydroxysuccinimide and *N,N'*-diisopropylcarbodiimide (DIC) to generate the amide intermediate **211** (Scheme 57), followed by *in situ* reaction with each of the amines **218a-g**. These reactions afforded the series of carboxamides **212a-g**, which were recrystallised and characterised as usual, using the IR, NMR and high resolution MS data. The ^{1}H NMR spectrum of carboxamide **212b** (Figure 89) reveals the amino-methylene protons resonating as a doublet at 4.39 ppm and the NH proton as a broad signal at 6.24 ppm. The DEPT 135 (Figure 90) confirms the presence of the three methylene and two methyl carbon atoms. Chromatographed samples of each of the coumarin carboxamides

212a-g were submitted to MINTEK for bioassay, the results of which are included with our bioassay data in Section 2.6.2.4.

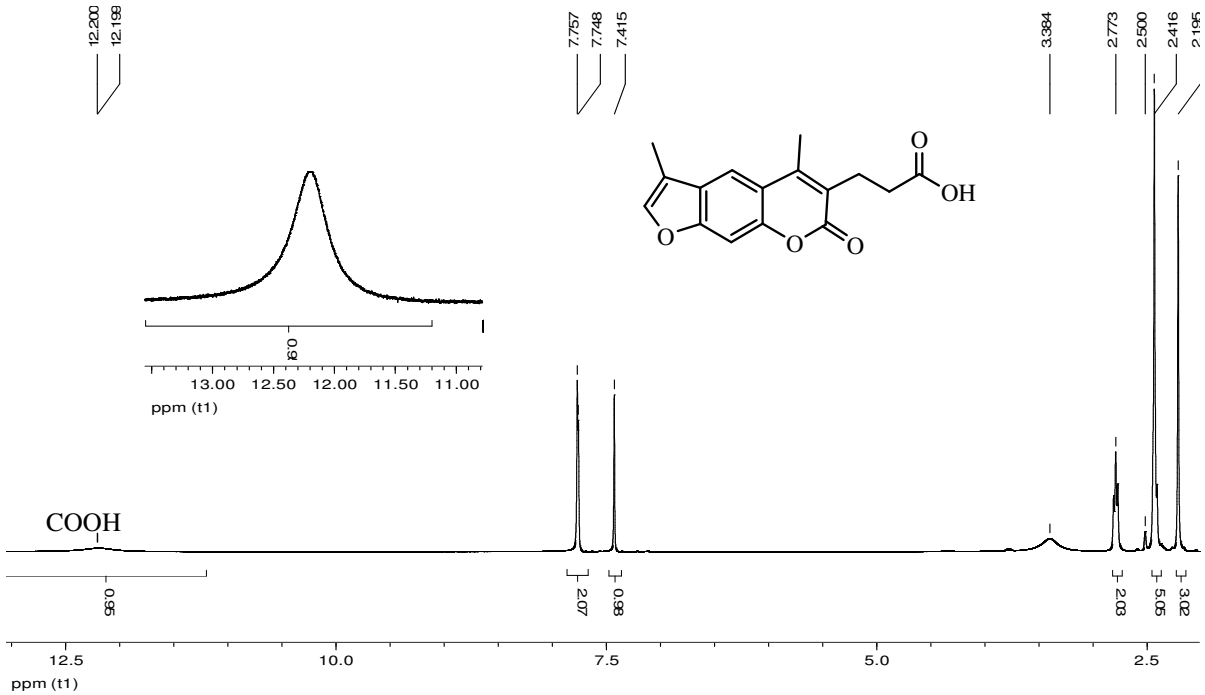

Figure 88. 400 MHz ^{1}H NMR spectrum of compound **217** in DMSO-d_6.

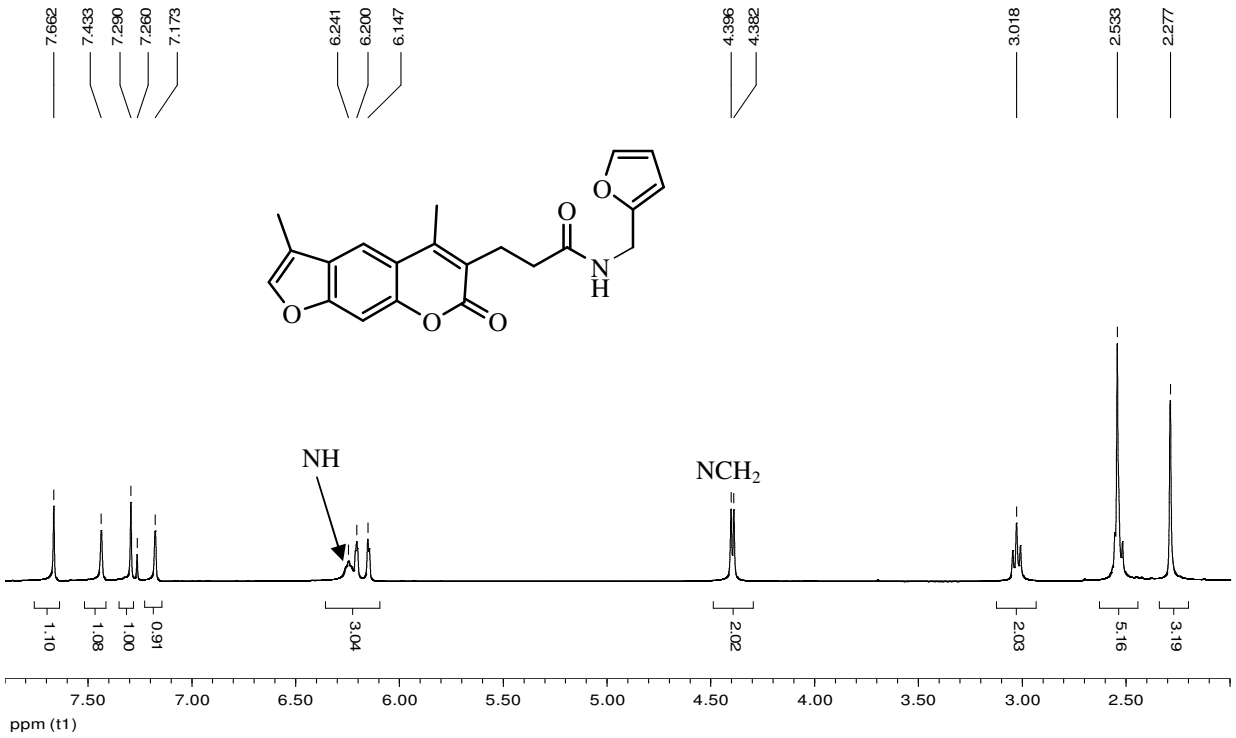

Figure 89. 400 MHz ^{1}H NMR spectrum of compound **212b** in $CDCl_3$.

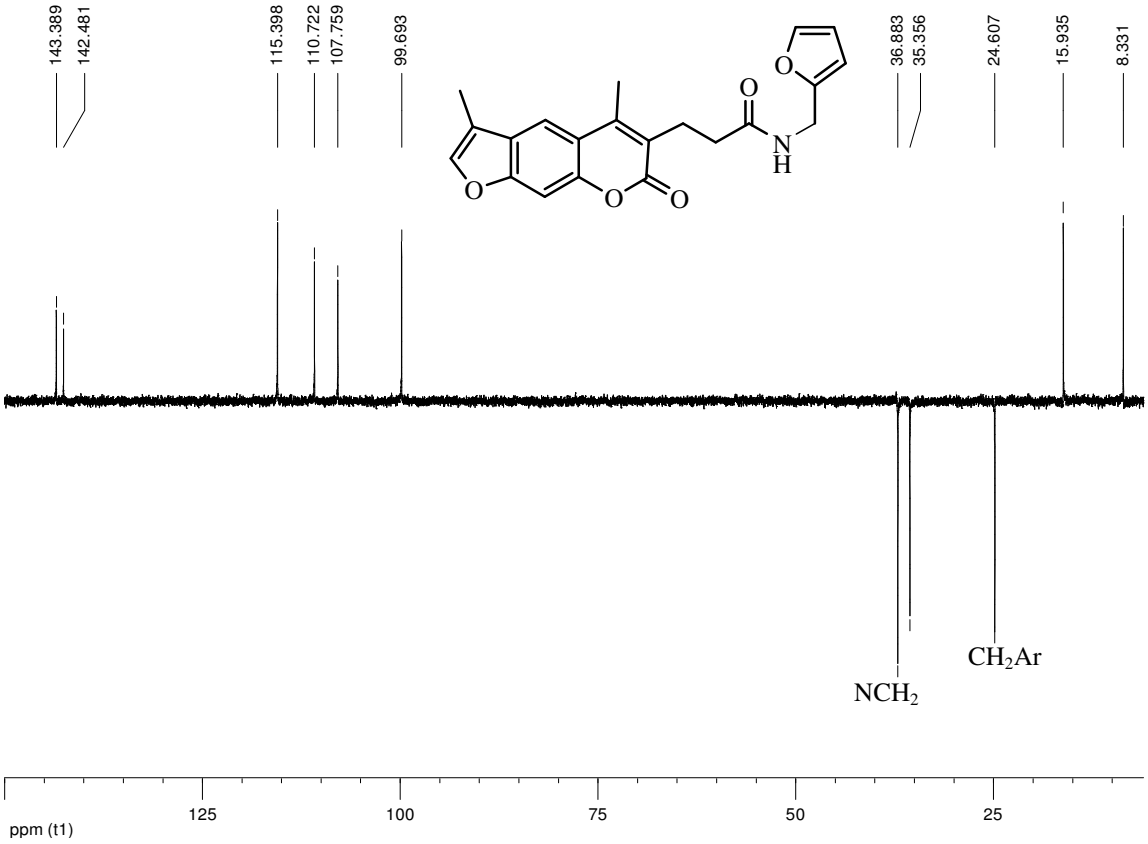

Figure 90. DEPT 135 NMR spectrum of compound **212b** in $CDCl_3$.

2.6. EVALUATION OF COMPOUNDS AS HIV-1 ENZYME INHIBITORS

Following the successful completion of the synthesis of various series of coumarin and cinnamate ester derivatives, the evaluation of selected systems was undertaken to explore their potential as HIV-1 enzyme inhibitors.

2.6.1. Saturation Transfer Difference NMR Studies

The saturation transfer difference (STD) NMR experiment is a useful method for studying ligand-protein interactions in solution and can accommodate up to seven ligands in one experiment.[258] It is a method which involves the transfer of the magnetisation to bound ligands from the protein. Low protein concentrations are required (typically μM levels), while the ligand is normally used in up to 100-fold molar excess over the protein.[258,259] The STD NMR experiment involves the selective saturation of the protein, normally at a frequency at which the ligands do not absorb. The saturation is transferred by spin diffusion to any bound ligand, which may be detected on release into the solution.[258] The difference spectrum, obtained by subtracting the saturated spectrum from one without protein saturation (*i.e*. off-resonance irradiation), shows signals corresponding only to the ligands which have bound to the protein.[260] The binding epitope of the ligand may be deduced from the STD spectrum because the degree of saturation of the individual protons of a small ligand molecule is directly related to the proximity of such protons to the protein.[258,260] STD NMR is able to serve as a preliminary guide indicating binding potential to a particular enzyme and is particularly useful for working with proteins which are high in molecular weight (but still soluble in D_2O), cannot be labelled, are membrane-bound or can only be obtained in small quantities. It is also important to mention that evidence of binding of ligand to protein, as indicated from this experiment, does not rule out the possibility of non-specific binding in regions other than the active site of the enzyme.

The coumarin-AZT conjugates **167a-e** were dissolved together in D_2O and the resulting solution was added to a solution of HIV-1 PR subtype C (freeze dried to remove H_2O and reconstituted in D_2O).[261] Comparison of individual ligand spectra with the difference spectrum (Figure 91) shows evidence of binding of some of the ligands to the HIV-1 PR. However, due to the similarity in the structures of compounds **167a-e**, it appears that some of the signals are additive in the difference spectrum, giving high intensity STD signals (*e.g*. signals at 6.2-6.4 ppm). Since this

preliminary STD experiment clearly provided some indication of ligand binding, these and other compounds were tested for enzyme inhibition activity (Section 2.6.2.).

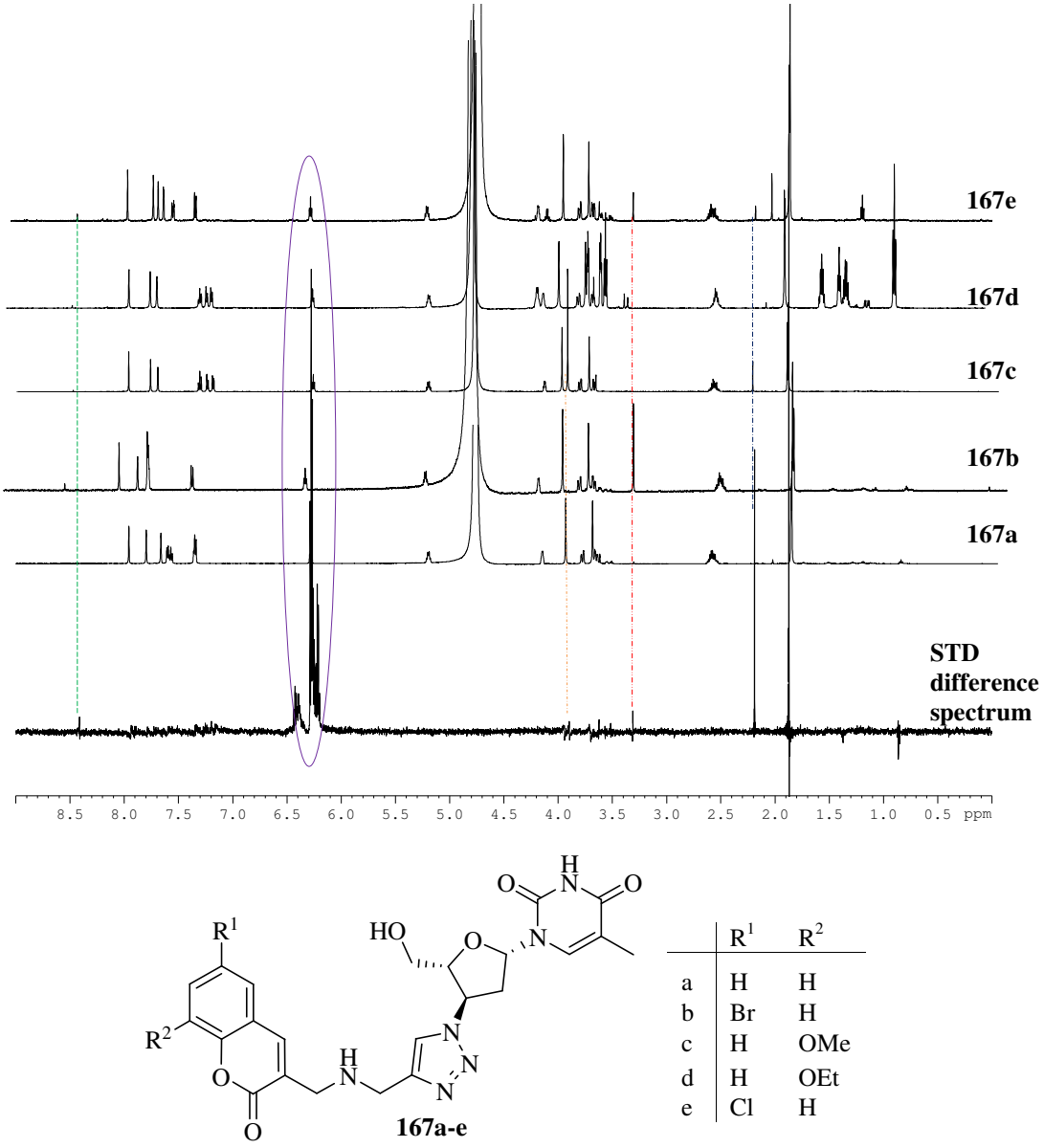

Figure 91. HIV-1 PR STD difference spectrum for compounds **167a-e** showing correlations between characteristic ligand signals and signals in the STD difference spectrum (coloured dash lines and oval shape). Individual ligand spectra are shown from bottom to top.

2.6.2. Enzyme Inhibition Assays

Inhibition assays are important *in vitro* methods of testing enzyme inhibition in the laboratory. They provide clarity beyond whether a compound is simply able to bind to an enzyme, by indicating binding which results in inhibition of enzymatic activity. These assays help in determining the medicinal potential of synthesised compounds and may guide the process of new

ligand design. Ligands designed as potential dual-action inhibitors were thus subjected to enzyme inhibition assays for both respective enzymes, HIV-1 PR and HIV RT or HIV-1 IN and HIV-1 RT. The bioassays were conducted for the author in the Bioassay Laboratory of the Rhodes Centre for Chemico- and Biomedicinal Reasearch.

2.6.2.1. Evaluation of Coumarin-AZT Conjugates 167a-e

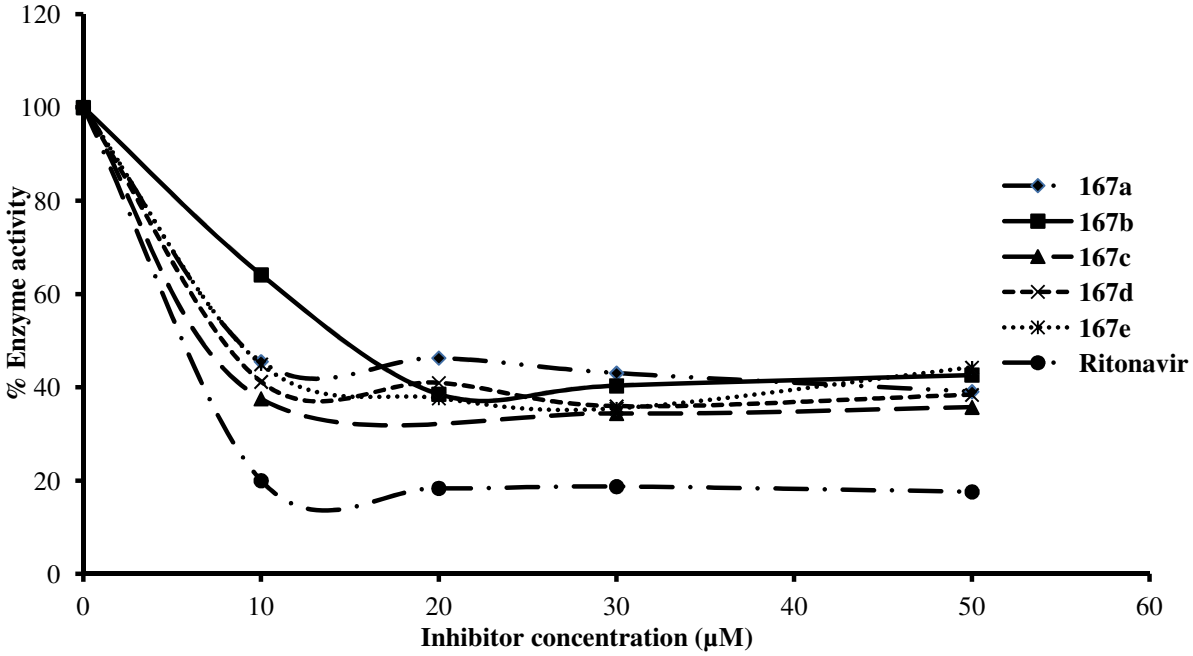

Figure 92. The inhibitory effect of compounds **167a-e** as potential HIV-1 PR inhibitors (against Ritonavir as standard), showing percentage enzymatic activity of HIV-1 PR at various concentrations.

Table 22. HIV-1 PR % enzyme inhibition and IC_{50} values, calculated at inhibitor concentrations of 50 µM.

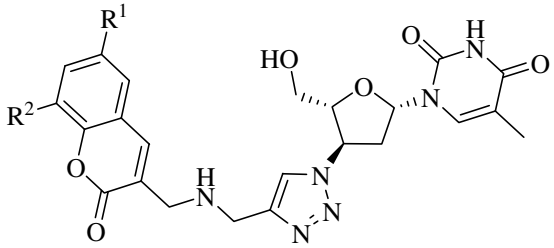

167a-e

	R^1	R^2
a	H	H
b	Br	H
c	H	OMe
d	H	OEt
e	Cl	H

Compound	% Inhibition	IC_{50} (µM)
167a	61	27.06
167b	57	28.91
167c	64	21.60
167d	62	23.35
167e	56	24.81
Ritonavir	72	9.85

Compounds **167a-e** were designed for dual-action HIV-1 RT/PR inhibition. Quantification of the inhibitory effect of compounds **167a-e** as potential HIV-PR inhibitors was performed using a commercial HIV-PR kit. For each ligand **167a-e** and Ritonavir **33** (an HIV-1 PR inhibitor in clinical use), the percentage enzyme activity was plotted against the ligand concentration (Figure 92). The IC_{50} value (ligand concentration that reduces enzyme activity by 50%) determined for each ligand **167a-e** and Ritonavir **33** are summarised in Table 22. These results show that the synthesised compounds **167a-e** have similar inhibition levels with percentage inhibition of 56-64% at 50 μM, and compound **167c** exhibits better inhibition than the other ligands. The IC_{50} values clearly show Ritonavir to be the best inhibitor. In comparison to the inhibition profile of Ritonavir, all five compounds exhibit slightly lower percentage inhibition levels. However, from the possibility of a dual-action point of view, these results are considered to be very promising with IC_{50} values in the micromolar range and not very different from Ritonavir **33**.

Quantification of the inhibitory effect of compounds **167a-e** as potential HIV-RT inhibitors was performed using a commercial HIV-RT kit. For each ligand **167a-e** and AZT **2** (a known HIV-1 RT inhibitor currently used as a clinical drug), the percentage enzyme activity was plotted against the ligand concentration (Figure 93). Table 23 shows the percentage inhibition and IC_{50} values calculated for compounds **167a-e** and AZT **2** at the final ligand concentration used (50 μM). The results reveal that compounds **167a**,**b** show high percentage inhibition values of 92 and 94% at 50 μM, respectively, comparable with that of AZT **2** with a percentage inhibition of 95% at 50 μM. A very interesting observation for compounds **167a**,**b** is that the HIV-1 RT inhibition property of AZT is not impaired despite the synthetic modification.

Table 23. HIV-1 RT % enzyme inhibition and IC_{50} values, calculated at inhibitor concentrations of 50 μM.

Compound	% Inhibition	IC_{50} (μM)
167a	92	5.59
167b	94	6.10
167c	29	106.40
167d	21	114.00
167e	24	101.60
AZT	95	4.54

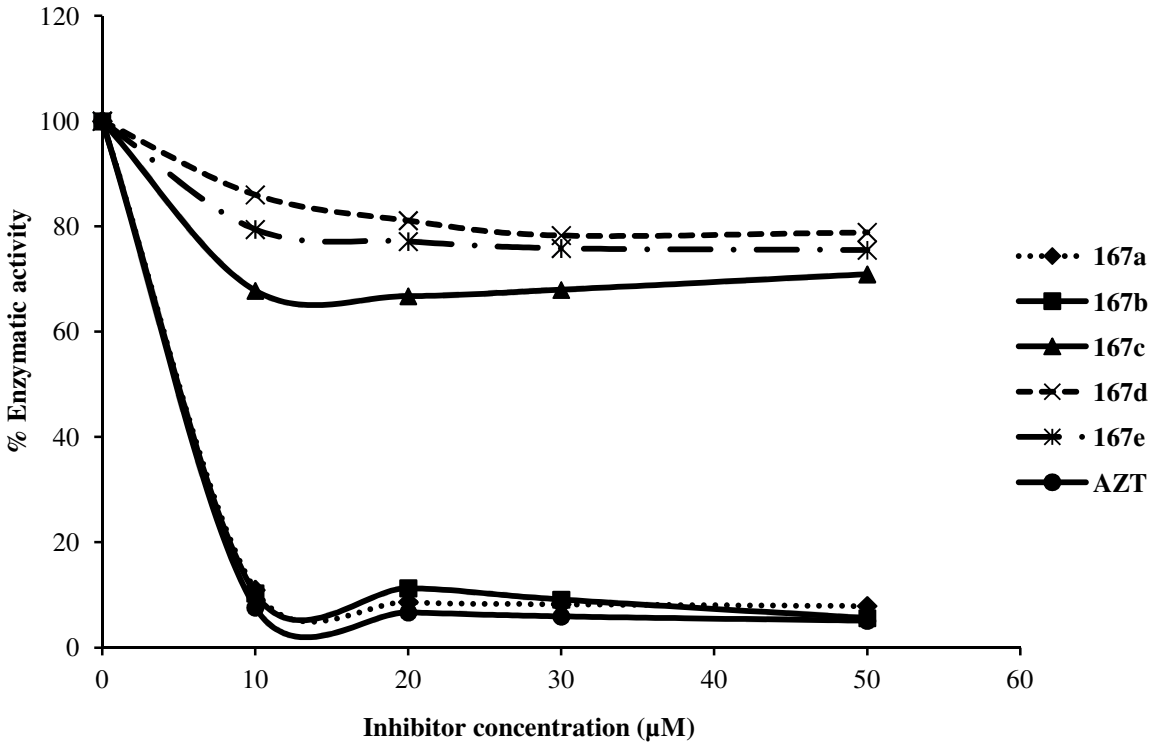

Figure 93. The inhibitory effect of compounds **167a-e** as potential HIV-1 RT inhibitors (against AZT as standard), showing percentage enzymatic activity of HIV-1 RT at various concentrations.

2.6.2.2. Evaluation of Coumarin-AZT Conjugates 169a-e

The second class of coumarin-AZT conjugates **169a-e** were also evaluated for inhibition of both HIV-1 PR and HIV-1 RT enzymes using similar standards. Figure 94 shows plots of the percentage HIV-1 PR enzyme activity against the ligand concentration for compounds **169a-e** and Ritonavir **33**, while Table 24 shows the percentage HIV-1 PR inhibition and IC_{50} values calculated for these compounds at 50 µM. Compounds **169a-e** all show similar percentage inhibition levels in the range 52-60% at 50 µM, with compound **169c** showing the best inhibition. It is somewhat surprising that compounds **169a-e** actually show slightly lower HIV-1 PR inhibition values than compounds **167a-e**, as the former were designed to better fit the active site of HIV-1 PR, and were expected to be better inhibitors.

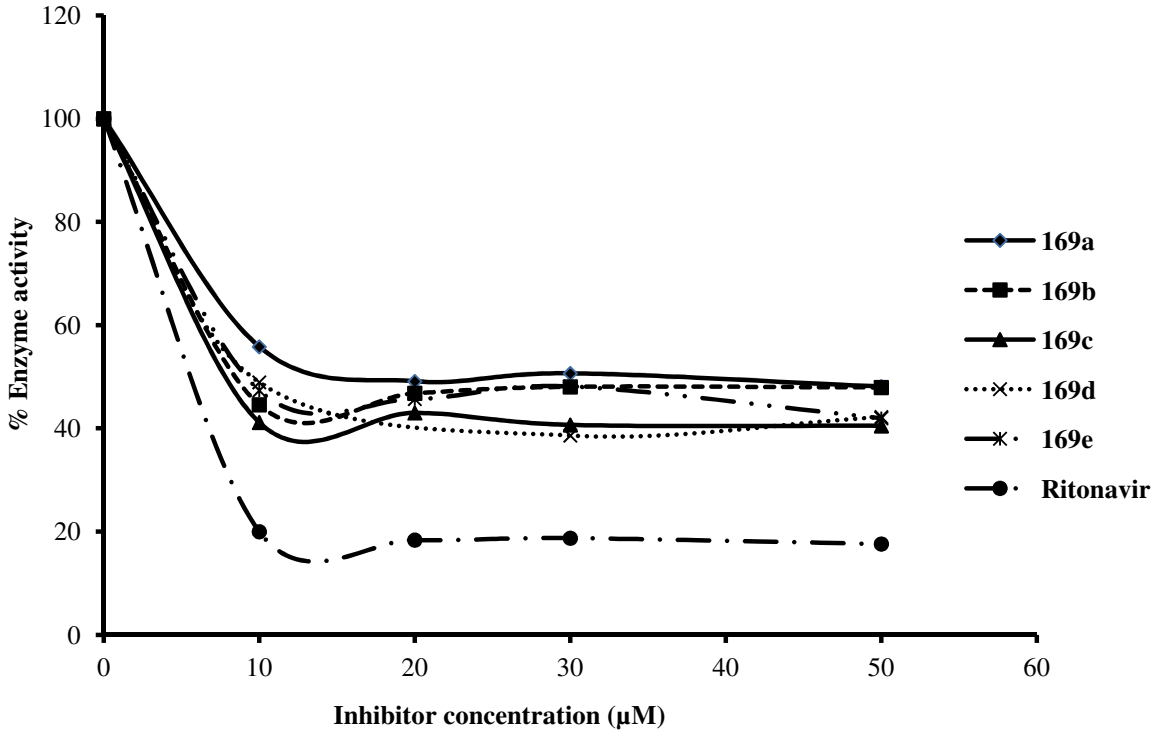

Figure 94. The inhibitory effect of compounds **169a-e** as potential HIV-1 PR inhibitors (against Ritonavir as standard), showing percentage enzymatic activity of HIV-1 PR at various concentrations.

Table 24. HIV-1 PR % enzyme inhibition and IC_{50} values calculated at inhibitor concentrations of 50 µM.

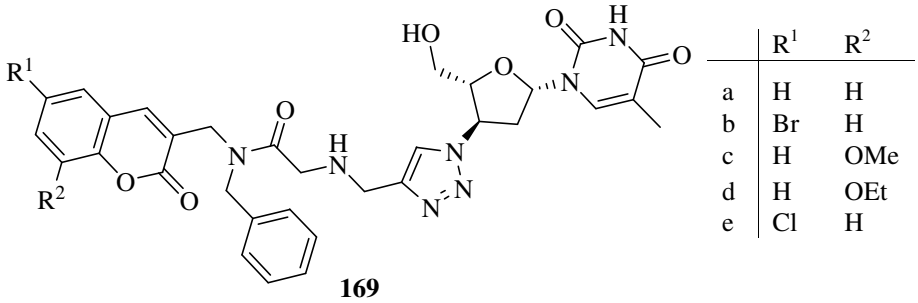

	R^1	R^2
a	H	H
b	Br	H
c	H	OMe
d	H	OEt
e	Cl	H

169

Compound	% Inhibition	IC_{50} (µM)
169a	52	35.06
169b	52	32.04
169c	60	22.70
169d	58	27.29
169e	58	29.55
Ritonavir	72	9.85

HIV-1 RT inhibition assays were also carried out on compounds **169a-e** and AZT **2** and a plot of the percentage enzyme activity against ligand concentration is shown in Figure 95. As indicated in Table 25, the percentage inhibition and IC_{50} values obtained for compounds **169a-e** and AZT **2** at 50 μM show very good activity (up to 99% inhibition), with all of the compounds, remarkably, showing better IC_{50} values than AZT. The introduction of the benzyl group which was originally aimed at making this class of compounds better HIV-1 PR inhibitors now appears to have enhanced HIV-1 RT inhibition activity (*cf* Tables 23 and 25). Thus, compounds **169a-e** all show good HIV-1 PR inhibition and excellent HIV-1 RT inhibition – the properties expected for a good dual-action compound!

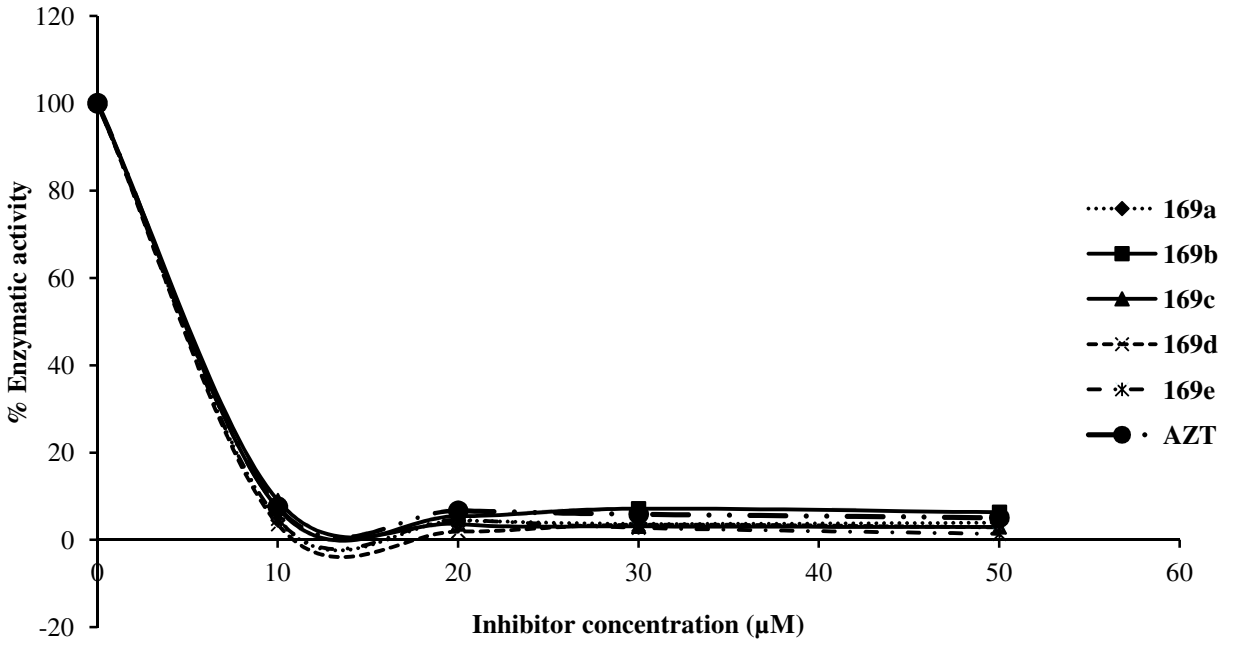

Figure 95. The inhibitory effect of compounds **169a-e** as potential HIV-1 RT inhibitors (against AZT as standard), showing percentage enzymatic activity of HIV-1 RT at various concentrations.

Table 25. HIV-1 RT % enzyme inhibition and IC_{50} values, calculated at inhibitor concentrations of 50 μM.

Compound	% Inhibition	IC_{50} (μM)
169a	96	3.40
169b	94	4.24
169c	97	2.88
169d	97	2.86
169e	99	3.69
AZT	95	4.54

2.6.2.3. Evaluation of Cinnamate Ester-AZT Conjugates 186a-e

Compounds **186a-e** were designed as potential HIV-1 RT/IN dual inhibitors and were thus evaluated for their inhibition of each enzyme. The HIV-1 IN assay was performed using a commercial kit. The results of the assays are shown as plots of HIV-1 IN enzymatic activity against inhibitor concentration (Figure 96) and tabulated as percentage enzyme inhibition and IC_{50} values (Table 26).

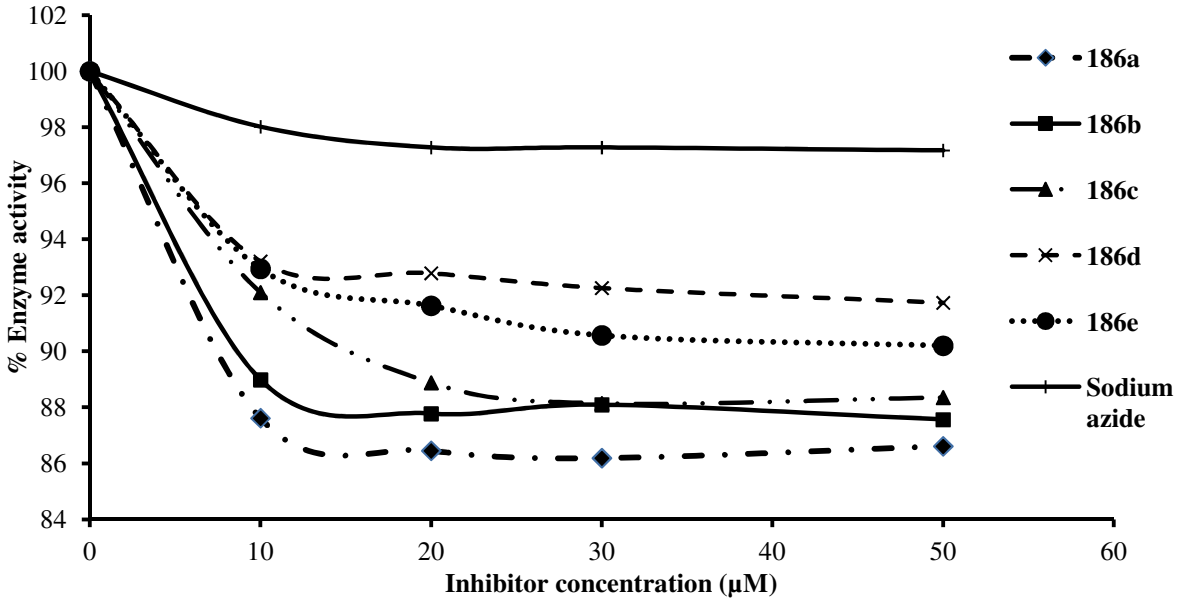

Figure 96. The inhibitory effect of compounds **186a-e** as potential HIV-1 IN inhibitors (against sodium azide as standard), showing percentage enzymatic activity of the HIV-1 IN at various concentrations.

Table 26. HIV-1 IN % enzyme inhibition and IC_{50} values calculated at inhibitor concentrations of 50 µM.

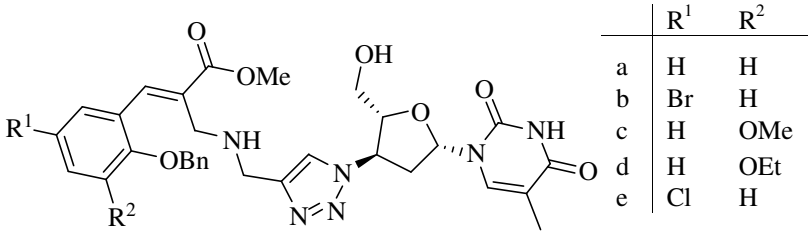

	R^1	R^2
a	H	H
b	Br	H
c	H	OMe
d	H	OEt
e	Cl	H

186a-e

Compound	% Inhibition	IC_{50} (µM)
186a	13	210.22
1869	12	230.79
186c	12	224.03
186d	8	351.84
186e	10	278.68
Sodium azide	3	1012.73

The percentage inhibition values show that these compounds exhibit low percentage inhibition of the HIV-IN enzyme (8-13%). Even more surprising is the inhibition value for the sodium azide that was used as a standard for the experiment, with percentage inhibition of only 3% and an IC_{50} value of over 1 mM. The fact that the ligands exhibit some inhibition is, perhaps, sufficient to warrant further synthetic modification in the hope of increasing the inhibition levels.

HIV-1 RT inhibition assays were also carried out following the procedure described earlier and plots of percentage enzyme activity against ligand concentration for compounds **186a-e** and AZT **2** are shown in Figure 97. Table 27 shows the percentage inhibition and IC_{50} values calculated at 50 μM.

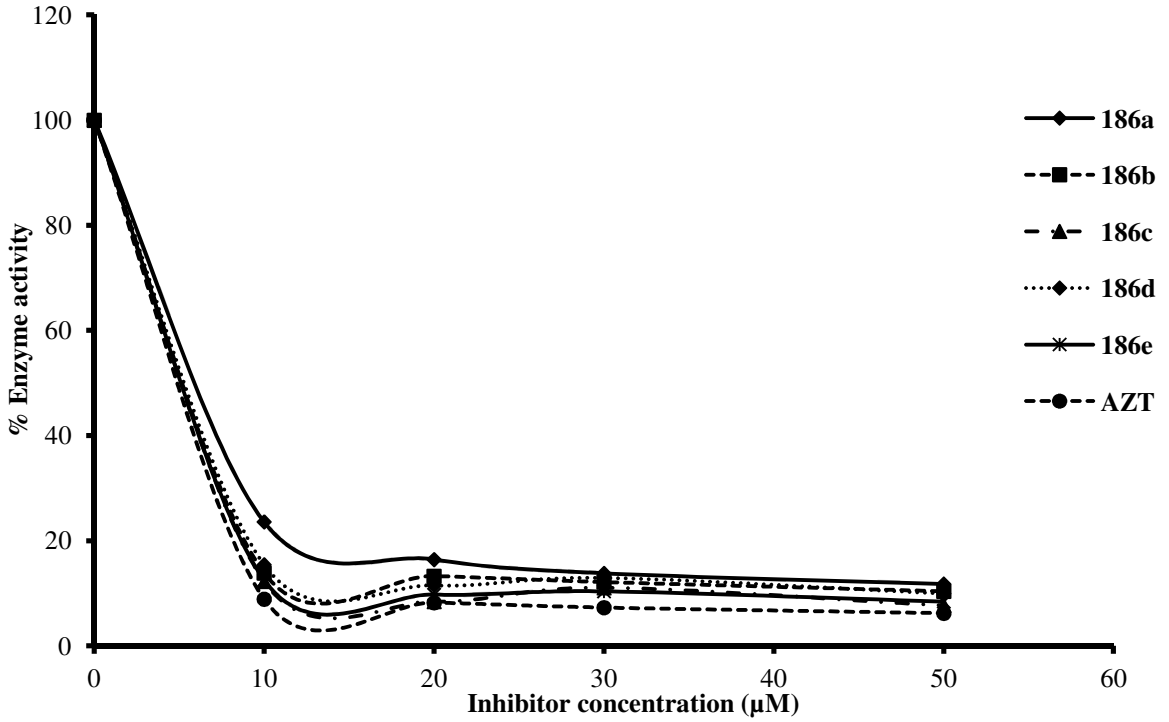

Figure 97. The inhibitory effect of compounds **186a-e** as potential HIV-1 RT inhibitors (against AZT as standard), showing percentage enzymatic activity of the HIV-1 RT at various concentrations.

Table 27. HIV-1 RT % enzyme inhibition and IC_{50} values calculated at inhibitor concentration of 50 μM.

Compound	% Inhibition	IC_{50} (μM)
186a	88	9.96
186b	90	7.19
186c	92	6.11
186d	90	7.36
186e	92	6.28
AZT	94	5.10

In contrast to the low HIV-1 IN inhibition values obtained for compounds **186a-e**, these ligands show extremely good HIV-1 RT inhibition activity (up to 92% inhibition) and IC_{50} values comparable with AZT. Clearly, the potential of these compounds as dual-action inhibitors warrants further exploration; modification of the cinnamate ester moiety may well afford compounds with better HIV-1 IN inhibition profiles.

2.6.2.4. Evaluation of Furocoumarins 212a-g

Carboxamides **212a-g**, designed as potential HIV-1 IN inhibitors, were tested at MINTEK for their inhibition of the HIV-1 IN strand transfer process using the method described by David *et al*.[262] The results of the assays for compounds **212a-g** and L-chicoric acid (a known HIV-1 IN inhibitor) are tabulated as percentage enzyme inhibition (Table 28); IC_{50} values were not determined because of the low inhibitory activities of compounds **212a-g** at 10 μM. The reason for the low inhibition levels of these compounds is not yet well understood.

Table 28. HIV-1 RT enzyme inhibition

Compound	% Inhibition
212a	17
212b	5
212c	5
212d	10
212e	11
212f	8
212g	16
L-Chicoric acid	101

2.6.3. Computer Modelling Studies

Computer simulated docking is a useful and efficient method of sampling complementary fits (often in hundreds or even thousands of orientations and conformations) between a ligand (small molecule drug candidate) and the active site of a molecular receptor (such as a protein), and of accessing ligand-receptor interaction energy data.[68,263,264] The molecular recognition process is modelled with the aim of optimising the interactions between a ligand and a receptor to afford a minimised free energy for the whole system.[263] *In silico* docking permits the potential binding orientations of ligands within molecular receptors to be explored and predictions to be made concerning the binding affinity and likely activity of such ligands. Consequently, computer

simulated docking plays an important role in the rational design of drugs as well as in drug evaluation.[69] In order to explore the nature of the interaction between the bi-functional compounds, synthesised in this study, and the active site of each enzyme, the unsubstituted analogue in each series was docked in the active site of the relevant HIV-1 enzymes. Crystal structure data for the HIV-1 PR and RT enzymes and the catalytic core of HIV-1 IN were accessed from the Research Collaboratory for Structural Bioinformatics (RCSB) protein data base (PDB). The modelling studies were executed by the author.

2.6.3.1. Modelling Studies of Coumarin-AZT Conjugate 167a

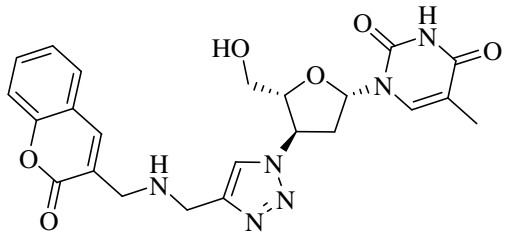

Docking of the parent coumarin-AZT conjugate **167a** into both the HIV-1 PR and the HIV-1 NNRT receptor cavity was explored. The X-ray crystal structure of the receptor cavity of the HIV-1 PR enzyme (PDB 1HXW) was used,[265] and the structures of the coumarin derivative **167a** and the protein were prepared using Discovery Studio Visualizer.[266] The ligand occupying the receptor cavity and all water molecules were removed from the original PDB file, hydrogen atoms were added and each atom assigned an Autodock Type using AutoDock Tools (ADT). The Autodock 4.2 programme[267] was used to explore the binding mode of compound **167a**, when docked in the HIV-1 PR active site using a flexible dock approach. The protein active site and surrounding residues were mapped using the AutoGrid 4.2 algorithm, and a generic algorithm was used to perform the conformation search. Atom maps were generated for all potential interactions between the ligand and the active site residues, while the Arg8 catalytic residues were kept flexible. For docking calculations, Gasteiger partial charges[268] were assigned to compound **167a** and non-polar hydrogen atoms were merged. All torsions were allowed to rotate during docking. Docked conformations were then viewed and explored using Discovery Studio Visualizer.[266]

The docking simulation revealed potential hydrogen-bonding interactions between proximate protein residues (Arg8, Asp29, Asp30 and Ile50) and both the coumarin and AZT moieties of compound **167a** (Figure 98). It is also apparent that compound **167a** fits well in the active site of

HIV-1 PR and this is supported by the relatively close correspondence between the docked conformation of compound **167a** and the X-ray crystal structure of the known inhibitor, Ritonavir **33**, in the active site (Figure 99). This perhaps explains why these compounds (**167a-e**) exhibit good HIV-1 PR inhibition when compared with Ritonavir. The proximity of C-8 of the coumarin nucleus to residues Gly49 and Ile50 (Figure 100) also explains why the presence of hydrogen-bonding donor groups, such as methoxy (in compound **167c**) and ethoxy (in compound **167d**), results in even better binding and consequently better inhibition for such assays as evidenced in the bioassay results (*cf* Table 22).

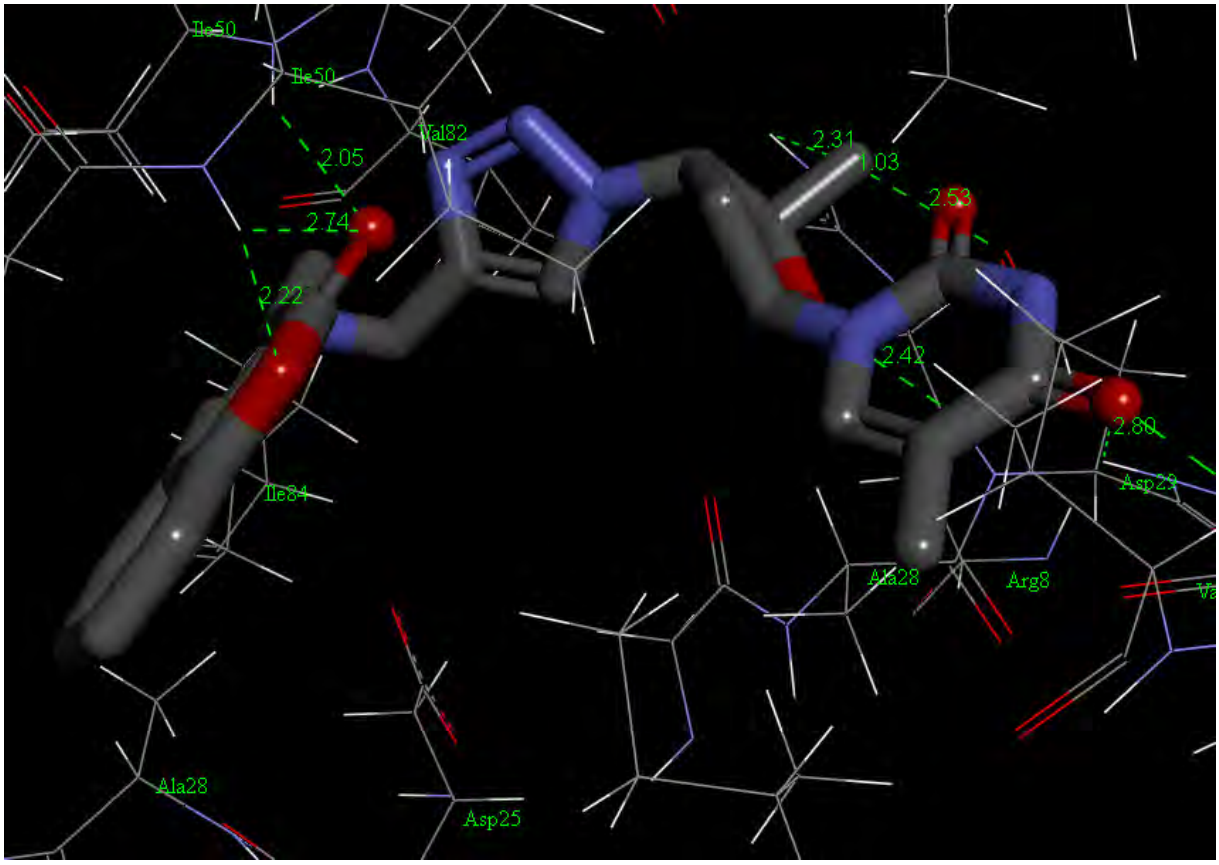

Figure 98. Docked conformation of coumarin-AZT conjugate **167a** in the HIV-1 PR active site (PDB 1HXW).[265] Protein active-site residues are shown in wire-frame and coloured by atom type, and the ligand is shown as sticks coloured by atom type. Hydrogen atoms have been omitted for clarity and H-bonding interactions are shown as green dashed lines with distances in Å.

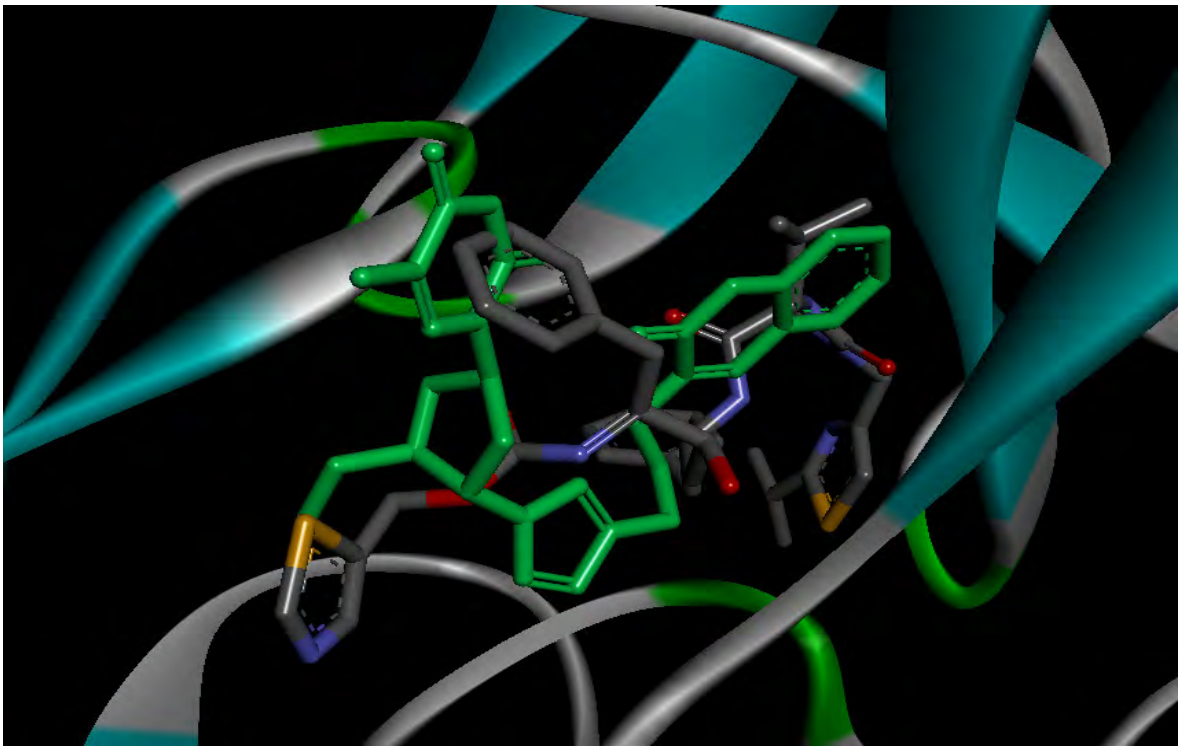

Figure 99. Overlay of the docked conformations of coumarin-AZT conjugate **167a** (in green) and Ritonavir (in atom type colours) in the HIV-1 PR active-site (in solid ribbon), the latter ligand as it is found in the crystal structure of HIV-1 (PDB 1HXW).[265]

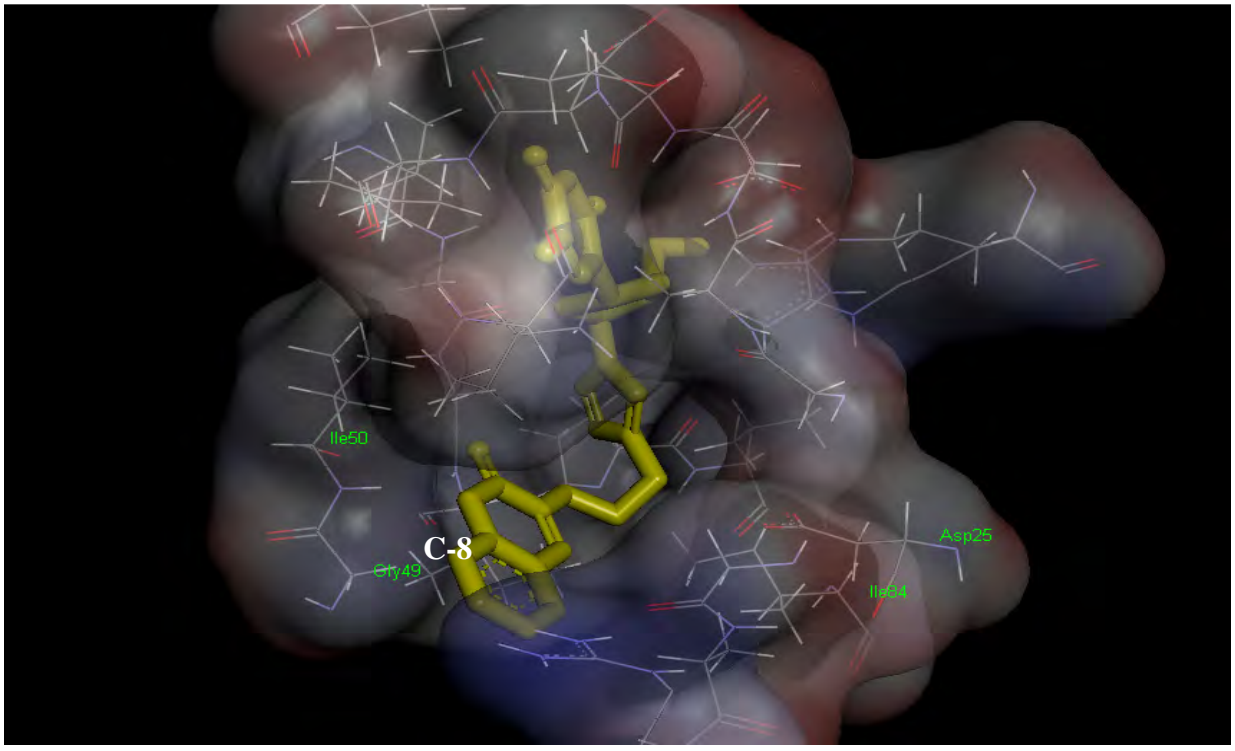

Figure 100. Docking of coumarin-AZT conjugate **167a** (in yellow) in HIV-1 PR (PDB 1HXW),[265] showing the surface around the active-site of the enzyme. The surface zone is shown with 45% transparency and coloured by atom type. Protein residues are shown in wireframe, coloured by atom type.

Compound **167a** was also docked, following a similar approach to that described above in the HIV-1 NNRT active site using the X-ray crystal structure of the HIV-1 RT enzyme (PDB 1IKW)[269], and using Tyr181 and Lys101 as flexible residues. The non-nucleoside binding pocket of HIV-1 RT appears to be quite forgiving in the variety of structural motifs it can accommodate.[270] Docking of compound **167a** into this pocket shows that the ligand exhibits hydrogen-bonding interactions with amino acid residues Lys101, Lys172, Ile178, Ile180, Ile1135, Glu1138 and Thr1139 (Figure 101). It also reveals that the coumarin moiety occupies the same cavity as the heterocyclic group of Efavirenz[269] – observations which indicate the possibility of this class of compounds acting as non-nucleoside RT inhibitors (NNRTIs).

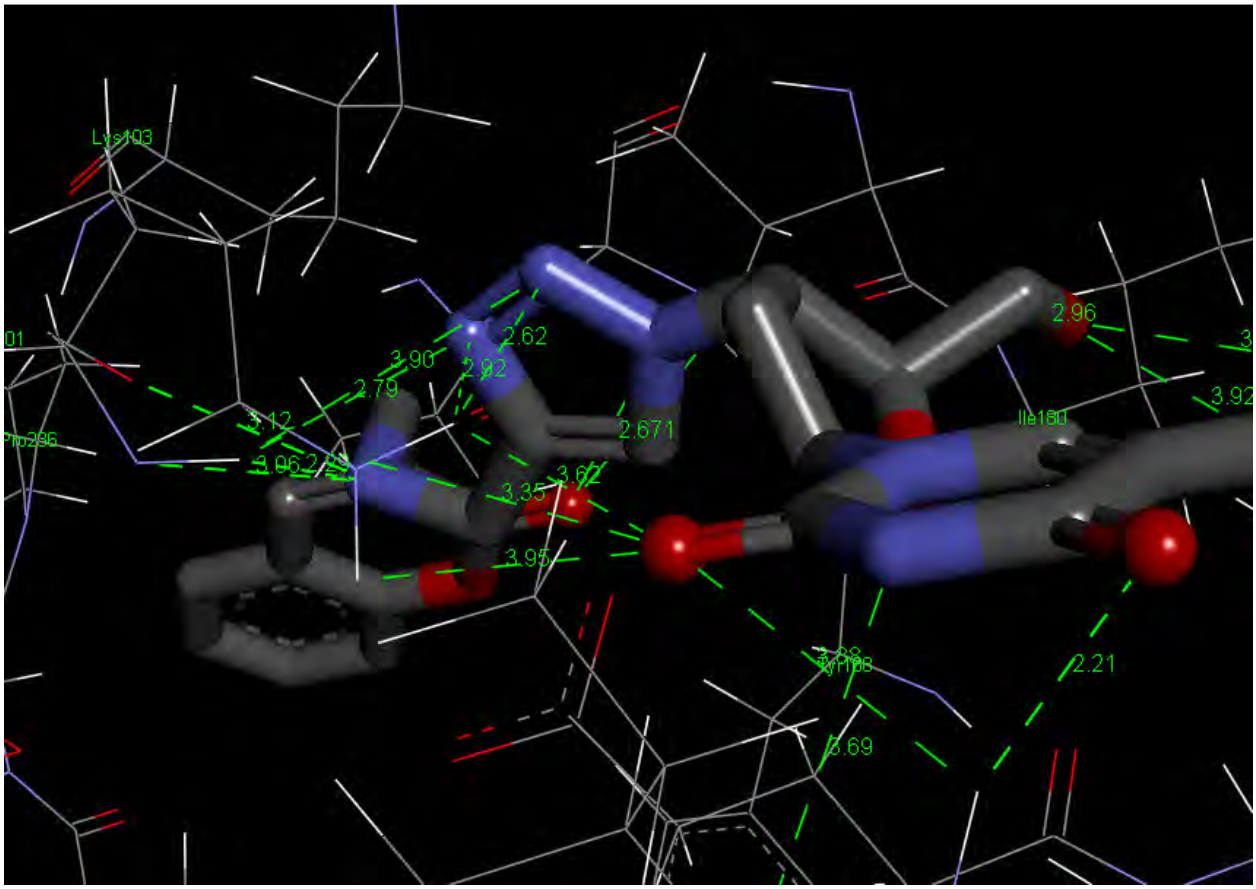

Figure 101. Docked conformation of coumarin-AZT conjugate **167a** in the HIV-1 NNRT active site (PDB 1IKW).[269] Protein active-site residues are shown in wire-frame and coloured by atom type, and the ligand is shown as sticks coloured by atom type. Hydrogen atoms have been omitted for clarity and H-bonding interactions are shown as green dashed lines with distances in Å.

2.6.3.2. Modelling Studies of the N-*Benzylated Coumarin-AZT Conjugate 169a*

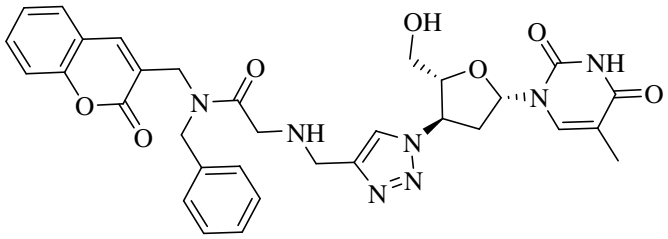

As mentioned in Section 2.1.7., the benzyl group was introduced to fit into the S_1 hydrophobic pocket of the HIV-1 PR active site. The *N*-benzylated coumarin-AZT conjugate **169a** was docked into the active site of HIV-1 PR (PDB 1HXW),[265] prepared as described in Section 2.6.3.1. using similar docking parameters and flexible residues. Docking reveals that compound **169a** fits well in the active-site of the enzyme and that several potential hydrogen-bonding interactions are possible between proximate protein residues (Arg8, Gly27, Asp29, Asp30, Gly48, Gly49 and Ile50) and both the coumarin and AZT moieties of the ligand (Figure 102). Interestingly, the benzyl group of compound **169a** does actually occupy the S_1 hydrophobic pocket of the enzyme active site as illustrated in Figure 103. It is perhaps surprising that an apparently improved fit of the compound in the HIV-PR active-site does not translate into improved HIV-1 PR enzyme inhibition (*cf*. Tables 22 and 24).

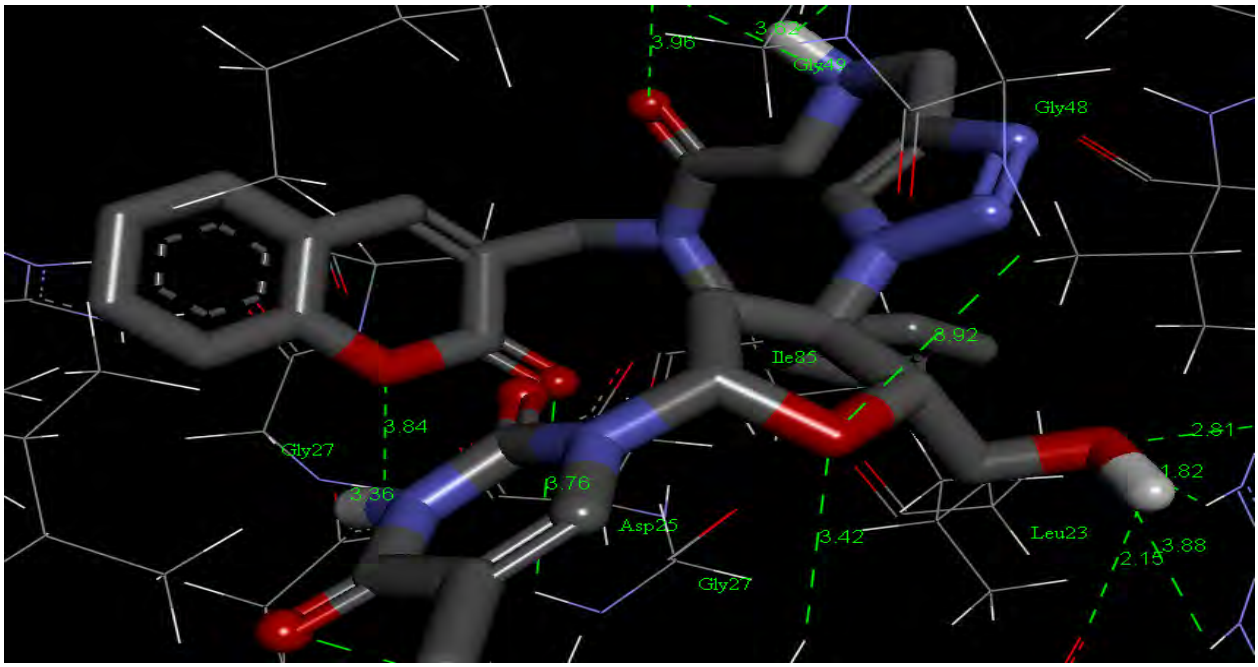

Figure 102. Docked conformation of the *N*-benzylated coumarin-AZT conjugate **169a** in the HIV-1 NNRT active site (PDB 1HXW).[265] Protein active-site residues are shown in wire-frame and coloured by atom type, and the ligand is shown as sticks coloured by atom type. Non-polar hydrogen atoms have been omitted for clarity and H-bonding interactions are shown as green dashed lines with distances in Å.

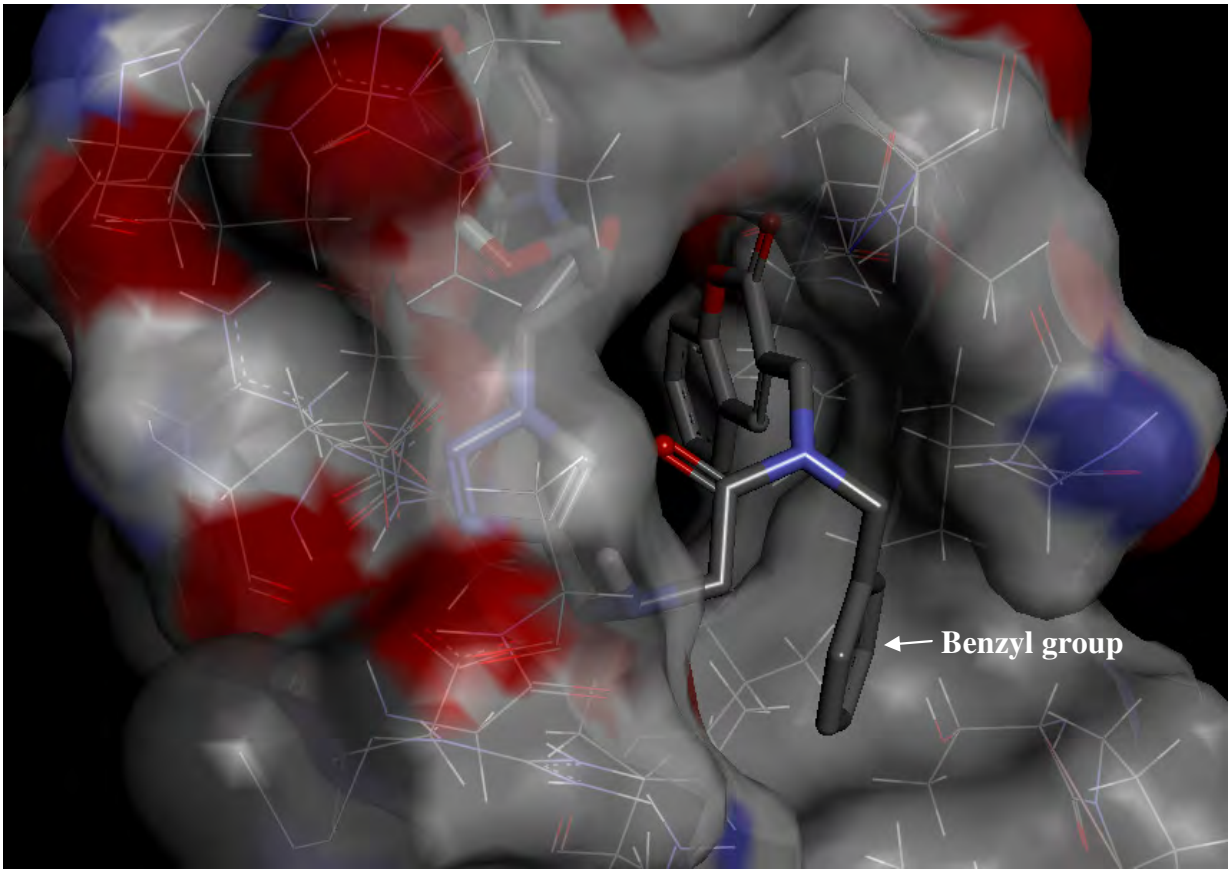

Figure 103. Active site of HIV-1 PR (PDB 1HXW),[265] showing benzyl group of compound **169a** occupying the S_1 hydrophobic pocket. The surface zone is shown at 45% transparency and coloured by atom type. The ligand is shown as sticks coloured by atom type and the protein residues are shown in wire-frame, also coloured by atom type.

Compound **169a** was also docked into the HIV-1 NNRT (PDB 1IKW)[269] active site. As shown in Figure 104, the *N*-benzylated coumarin-AZT conjugate **169a** fits well in the active site of the enzyme and shows potential hydrogen-bonding interactions with amino acid residues Trp88, Glu89, Val90, Leu92, Tyr181, Glu182, Thr1139 and Pro1140. The high number of potential hydrogen-bonding interaction might explain why this class of compounds exhibited such good enzyme-inhibition activity – in some cases, slightly better than that of AZT **2** (Table 25). A closer look (Figure 105) reveals that the benzyl group actually fits into a hydrophobic pocket within the active site of the HIV-1 RT enzyme and may account for the high inhibition values obtained for this series of ligands (**169a-e**).

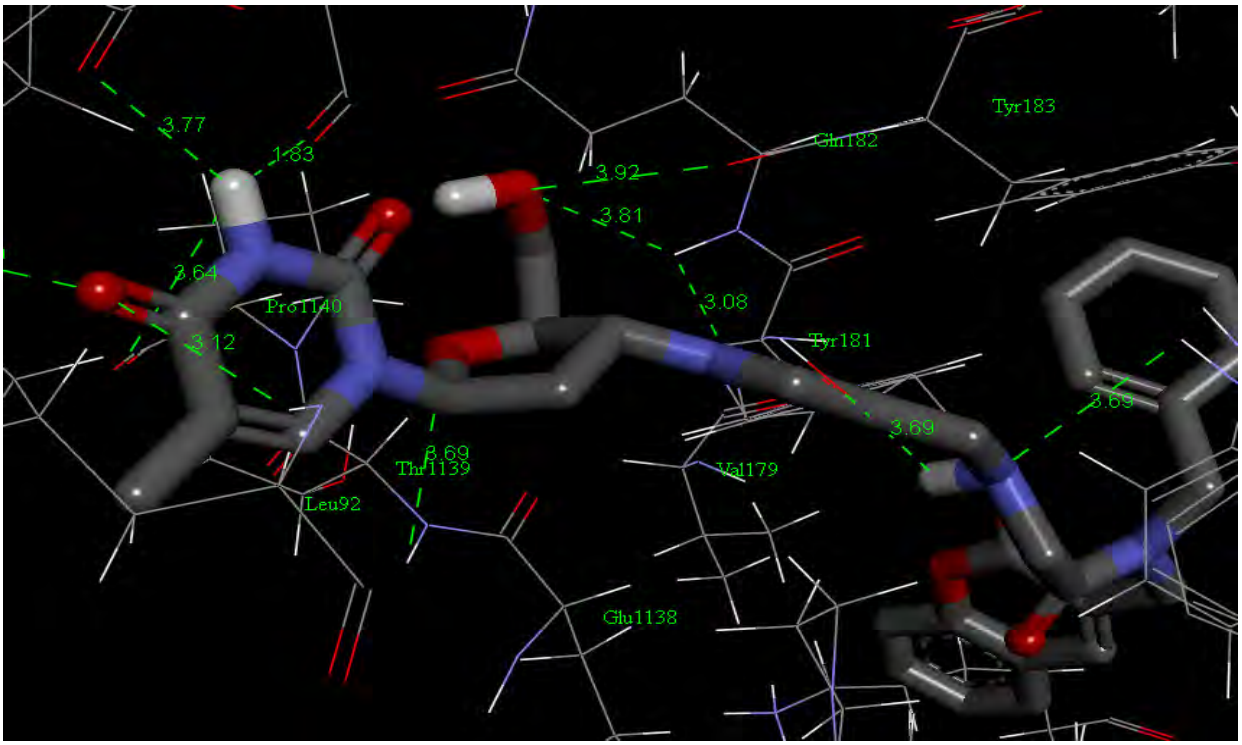

Figure 104. Docked conformation of the *N*-benzylated coumarin-AZT conjugate **169a** in the HIV-1 NNRT active site (PDB 1IKW).[269] Protein active-site residues are shown in wire-frame and coloured by atom type, and the ligand is shown as sticks coloured by atom type. Non-polar hydrogen atoms have been omitted for clarity and H-bonding interactions are shown as green dashed lines with distances in Å.

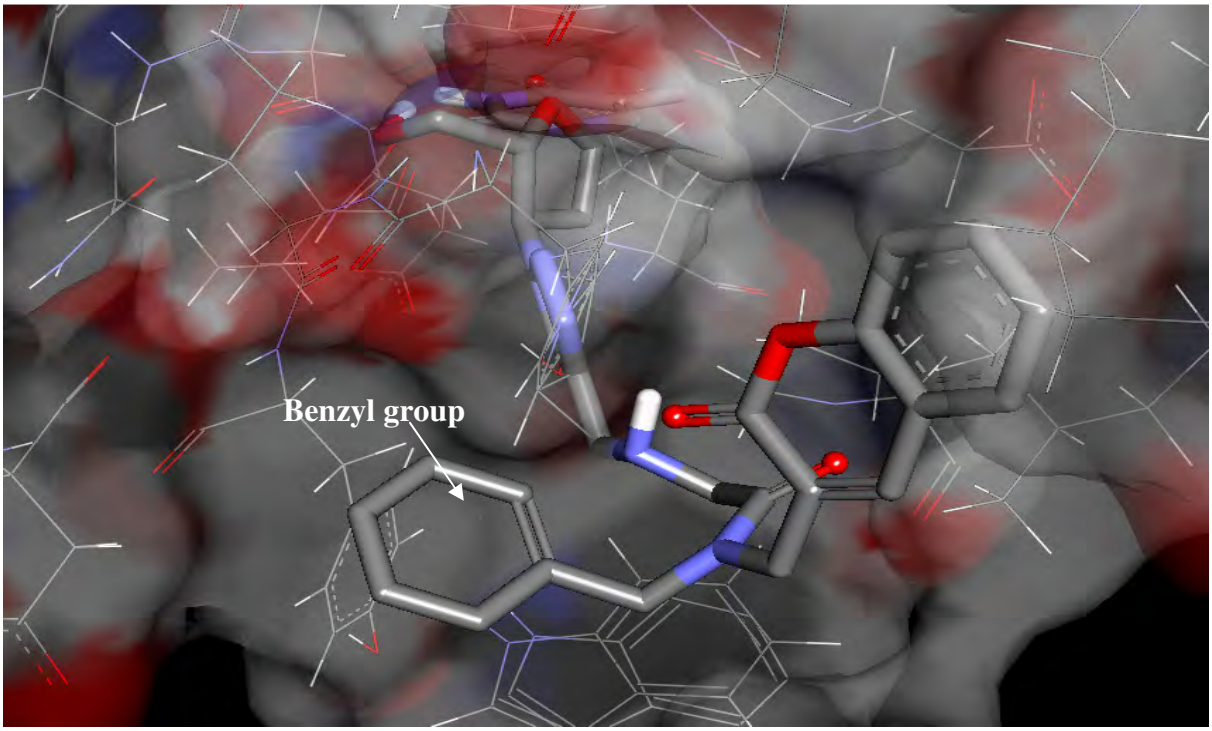

Figure 105. Active site of HIV-1 RT (PDB 1IKW),[269] showing the benzyl group of compound **169a** occupying a hydrophobic pocket. The surface zone is shown at 45% transparency and coloured by atom type. The ligand is shown as sticks and the protein residues in wire-frame, both coloured by atom type.

2.6.3.3. Modelling Studies of the Cinnamate Ester-AZT Conjugate 186a

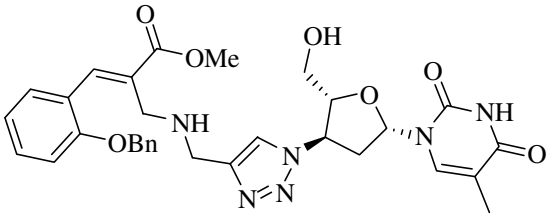

The parent cinnamate ester-AZT conjugate **186a** was docked into both the HIV-1 IN and the HIV-1 NNRT receptor cavities. The core domain structure of HIV-1 IN enzyme (PDB 1QS4),[271] containing the active site receptor cavity, was used as the full crystal structure of HIV-1 IN is not yet known. A charge of +2 was manually assigned to the Mg cation in the active site and residues Asp64 and Asp116 were defined as flexible residues for the simulated docking. The docked conformation of compound **186a** in the HIV-1 IN receptor cavity exhibits potential hydrogen-bonding interactions with amino acid residues Ser119, Lys156, Glu152 and Lys159 (Figure 106). The ligand adopts a conformation in which the OH group is close to the Mg co-factor (a distance of 3.09 Å) but does not displace the metal ion which remains complexed to the two aspartate residues. An overlay of the docked conformation of compound **186a** and the core domain crystal structure of the known inhibitor, 5CITEP **29**, in the active site of HIV-1 IN (Figure 107) shows reasonable overlap between the two ligands; however, compound **186a** extends beyond the binding limit of 5CITEP, and this might explain why these compounds exhibit comparatively low levels of HIV-1 IN inhibition.

Compound **186a** was also docked into the HIV-1 NNRT (PDB 1IKW)[269] active-site to explore its binding mode. As shown in Figure 108, the cinnamate ester-AZT conjugate **186a** fits well in the active-site showing potential hydrogen-bonding interactions between amino acid residues Lys101, Lys103, Lys172, Ile180, Tyr318, Thr1139 and Glu1138, and both the cinnamate ester and the AZT moieties. The *O*-benzyl group occupies a hydrophobic pocket next to Leu234 and Phe227 in the HIV-1 NNRT active site and this binding feature may contribute to the excellent RT enzyme inhibition data (comparable, in fact, with those of AZT) obtained for this class of compounds (Table 27). The proximity of other amino acid residues within the active site may favour interactions with substituents on the phenyl ring of the cinnamate group, and this is, perhaps, reflected in the bioassay data (Table 27).

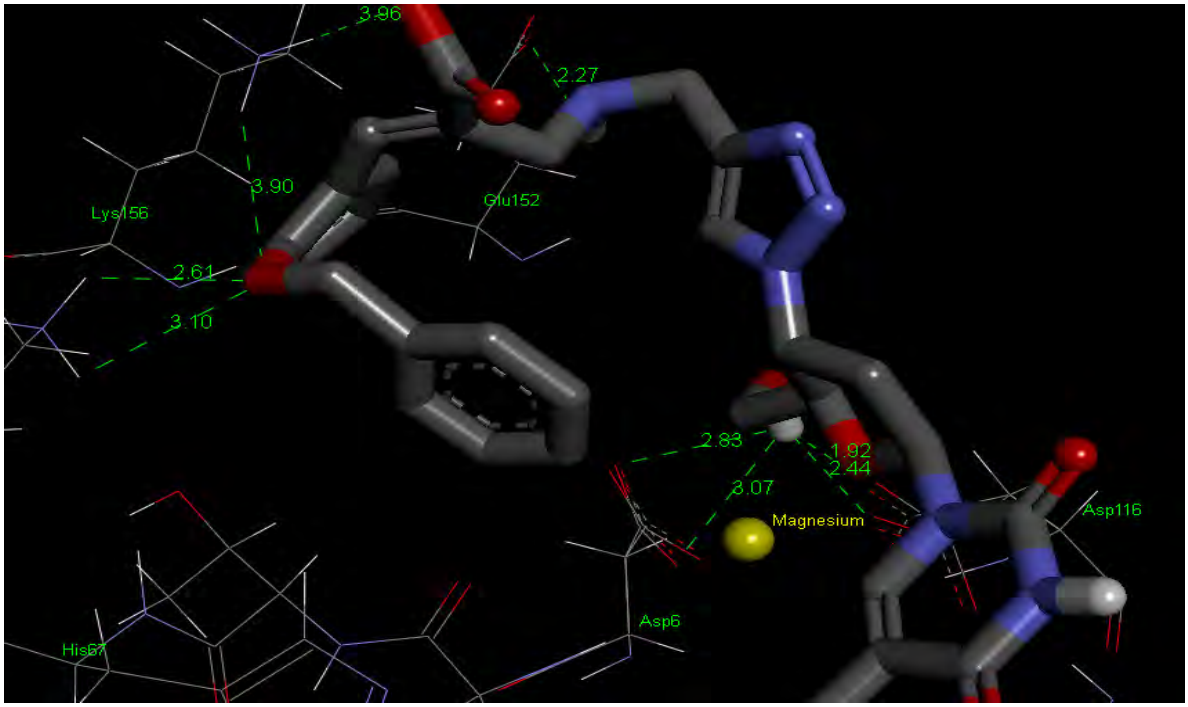

Figure 106. Docked conformation of cinnamate ester-AZT conjugate **186a** in the HIV-1 IN active-site (PDB 1QS4).[271] Protein active-site residues are shown in wire-frame and coloured by atom type, the ligand is shown as sticks coloured by atom type and Mg^{2+} as a yellow sphere. Non-polar hydrogen atoms have been omitted for clarity and H-bonding interactions are shown as green dashed lines with distances in Å.

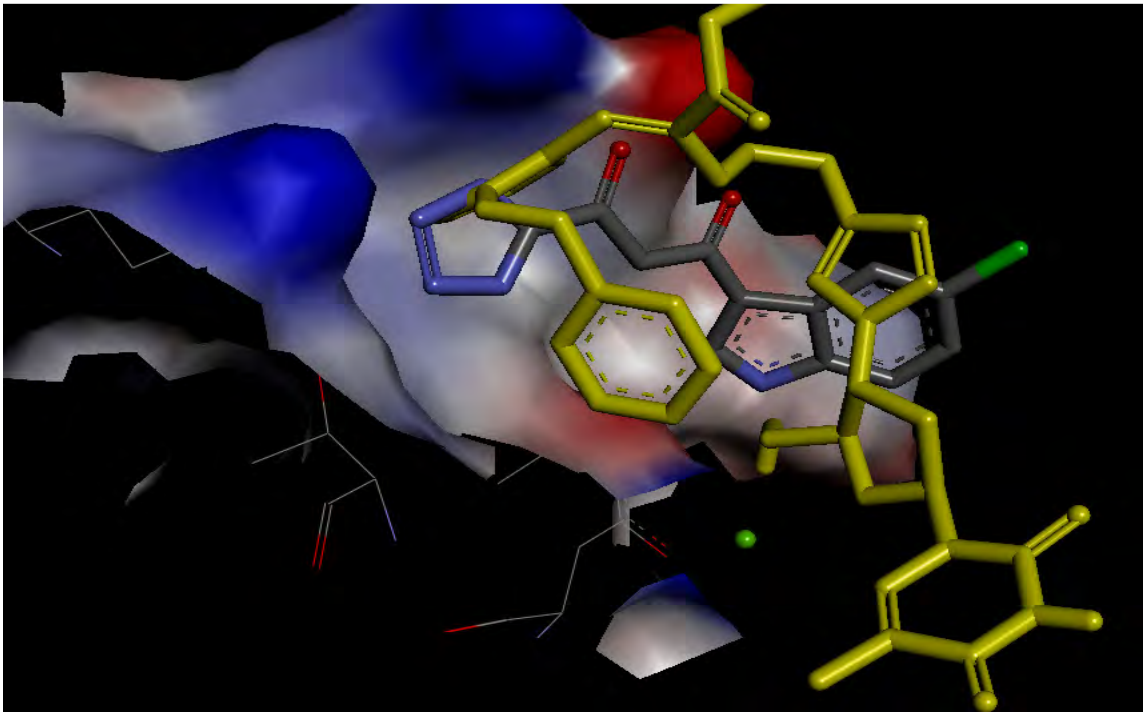

Figure 107. Overlay of the docked conformations of cinnamate ester-AZT conjugate **186a** (in yellow) and 5CITEP as found in the crystal structure, PDB 1QS4[271] (in atom type colours) in the HIV-1 IN active-site (surface zone coloured by atom types). Mg^{2+} is shown as a green sphere and protein residues are shown in wire-frame, coloured by atom type.

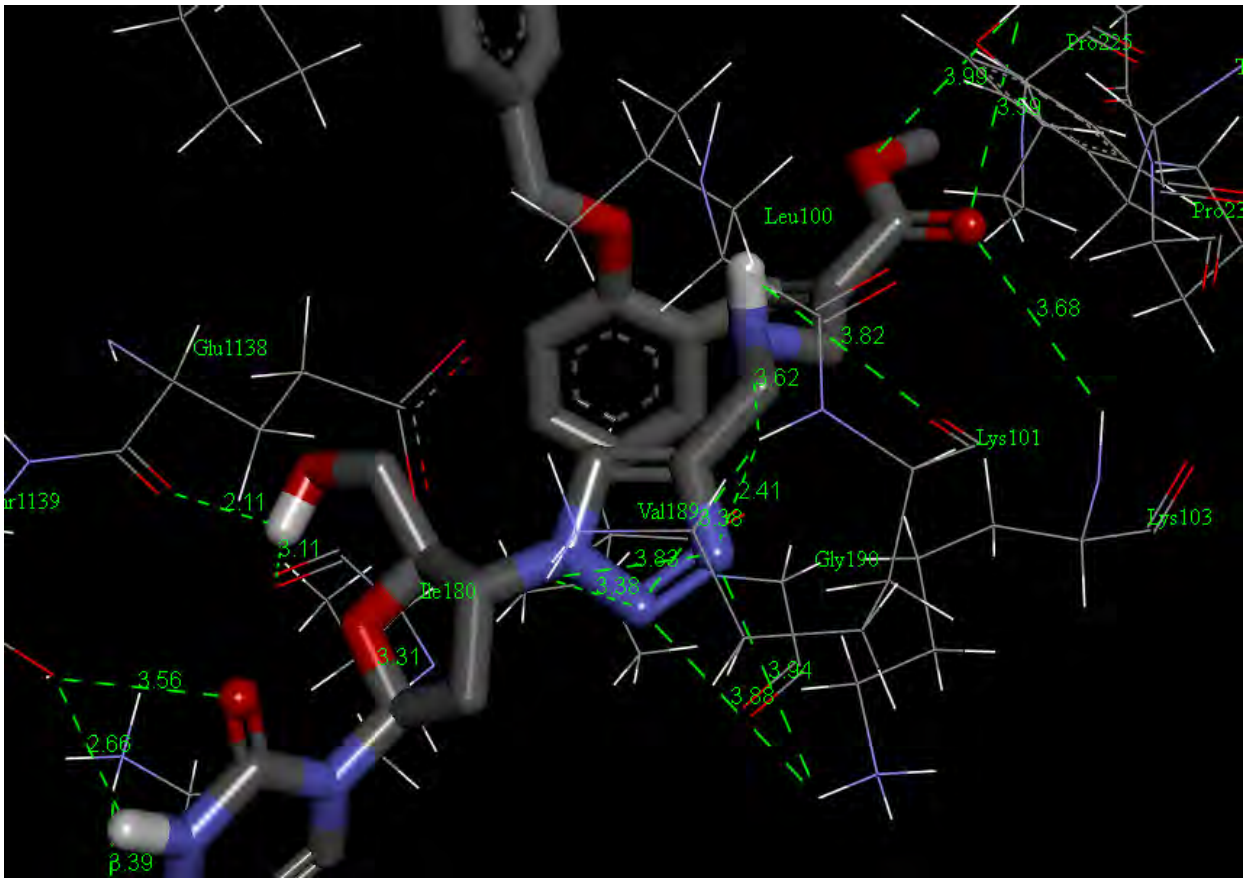

Figure 108. Docked conformation of cinnamate ester-AZT conjugate **186a** in the HIV-1 RT active-site (PDB 1IKW).[269] Protein active-site residues are shown in wire-frame and coloured by atom type, the ligand is shown as sticks coloured by atom type. Non-polar hydrogen atoms have been omitted for clarity and H-bonding interactions are shown as green dashed lines with distances in Å.

2.7. CONCLUSIONS

The present study has successfully extended the application of Baylis-Hillman methodology to the development of novel and complex coumarin and cinnamate ester derivatives. Areas such as kinetics, experimental / theoretical studies, computer modelling and bioassay have been covered in some form. Over seventy new compounds have been prepared and fully characterised using spectroscopic (IR and 1- and 2D-NMR), elemental (combustion or HRMS) and, where appropriate, X-ray crystallographic analysis.

DABCO-catalysed Baylis-Hillman reactions of a series of five salicylaldehyde derivatives with *tert*-butyl acrylate have been conducted out under both conventional and microwave-assisted conditions, and it has been shown that the latter methodology permits a significant reduction in reaction time but does not, in this case, lead to better yields. Cyclisation of the resulting Baylis-Hillman adducts was investigated using different reaction conditions. Under base-catalysed conditions, chromene-type products **163a** and **164a** were isolated. Under acid-catalysed conditions, on the other hand, cyclisation afforded coumarin derivatives, generally in excellent yield; HCl-catalysed reaction gave the 3-(chloromethyl)coumarin derivatives **148a-e**, while HI-catalysed reactions gave 3-methylcoumarin analogues **150a**,**b**,**d**,**f**, presumably due to HI-mediated reduction. I_2-catalysed cyclisation, under moist conditions, gave the 3-(hydroxyl-methyl)coumarin analogues, **192a**,**b**,**d**,**e**.

The 3-(chloromethyl)coumarin derivatives were reacted with propargylamine to afford the intermediates required for 'click' chemistry cycloaddition with AZT. These high-yielding reactions afforded the structurally complex coumarin-AZT conjugates in an overall, four-step sequence, and the results have been published.[218] A modification involving introduction of a benzyl group led to novel *N*-benzylated coumarin-AZT conjugates in a six-step sequence and, generally, in very good yields. These compounds were designed as potential bi-functional HIV-1 RT/PR inhibitors, with the coumarin moiety serving as the PR inhibitor and the AZT moiety as the RT inhibitor.

SeO_2 oxidation of selected 3-methylcoumarins, under microwave-assisted conditions, has afforded the corresponding coumarin-3-carbaldehydes in better yields than using conventional heating, permitting publication of an improved synthesis of these compounds.[246]

Attempts to prepare 4-hydroxy and / or 4-aminocoumarins proved to be frustrating, with various approaches being explored. Baylis-Hillman reactions of *N*-tosylaldimines with *tert*-butyl acrylate led to a number of products, noteworthy amongst them being the unexpected 2-[6-bromo-2-(tosylamino)-2*H*-chrome-3-yl]ethanol **202b** and its 8-ethoxy analogue **202d**. These compounds are apparently formed *via* ring-opening of 2,3-dihydrofuran present in the THF used as solvent. The structures assigned from the spectroscopic data were confirmed by X-ray crystallographic analysis of compound **202b**. Introduction of the phthalimide group prior to cyclisation has led to the 2,3-dihydro-4-phthalimidocoumarin analogue, which promises to provide access to the desired 4-aminocoumarins.

Conjugate addition of benzylamine and propargylamine to Baylis-Hillman adducts have afforded novel β-hydroxy hydrocinnamate derivatives which, surprisingly, have resisted dehydration. An alternative approach involving hydrochlorination of Baylis-Hillman adducts effected dehydration and novel, but unexpected, cinnamic acid analogues together with small quantities of the cyclised coumarin analogues. NMR based mechanistic and DFT [B3LYP 6/31G(d)] theoretical studies of this unusual reaction have been successfully completed and have established that the reaction proceeds sequentially through ester hydrolysis, conjugate addition and elimination steps to give as the major, kinetically controlled product, the cinnamic acid derivative **177a**. Reaction of benzyl-protected salicylaldehyde derivatives with methyl acrylate under Baylis-Hillman conditions afforded excellent yields of another set of Baylis-Hillman adducts, which were subsequently transformed into cinnamate ester analogues by acetylation followed by nucleophilic substitution, using step-wise or one-pot protocols. The propargylamine substituted cinnamate esters **184a-e** were used as substrates in 'click' reactions with AZT to afford cinnamate ester-AZT conjugates **186a-e** in very good yields. These compounds were designed to serve as potential HIV-1 RT-IN dual-action inhibitors.

Furocoumarin derivatives were successfully prepared as potential HIV-1 IN inhibitors in a four step synthesis. The critical furocoumarincarboxylic acid intermediate was prepared from the ether precursor *via* base-catalysed cyclisation. Activation of the carboxylic acid with *N*-hydroxysuccinimide followed by N,N′-diisocarbodiimide-mediated amidation with a series of amines **218a-g**, afforded compounds designed to act as HIV-1 IN inhibitors.

Finally, evaluation of the enzyme inhibition potential of the various ligands was explored using different techniques. STD NMR binding-, *in silico* modelling and bioassay studies have all been

used. The coumarin-AZT conjugates **167a-e** and their *N*-benzylated analogues **169a-e** were examined for both HIV-1 PR and RT inhibition activity, while the cinnamate ester-AZT conjugates **186a-e** were evaluated as HIV-1 IN and RT inhibitors. The bioassay results clearly indicate the potential of a number of these to serve as lead compounds in the development of novel dual-action inhibitors.

Overall, the study has successfully addressed the various initial objectives. Several series of potential dual-action HIV-1 RT/IN and HIV-1 RT/PR inhibitors have been prepared. Many of these compounds have shown significant inhibition potential and a number of lead compounds have been identified. Two papers on aspects of the research have already been published. Future research in this area is expected to include the following objectives.

1) Reaction of *N*-tosylaldimines and other possible substrates with 2,3-dihydrofuran
2) The use of base-catalysed cyclisation of Baylis-Hillman adducts to access chromone-3-carboxylic acid derivatives.
3) Optimising the structure of the cinnamate ester moiety to improve HIV-1 IN inhibition activity.
4) Exploring conformational effects in 4-phthalimidocoumarins and their application in accessing 4-aminocoumarins.

3. EXPERIMENTAL

3.1. GENERAL

Reagents were used without any further purification as supplied by Sigma-Aldrich or Fluka. Solvents were dried following the procedures prescribed by Perrin and Armarego.[272] Ethanol and methanol were dried by reaction with Mg turnings and iodine and then distilled from the resulting magnesium alkoxide under nitrogen. THF and diethyl ether were stored over CaH_2 and then distilled from Na wire in the presence of benzophenone under nitrogen. DCM was stored over $CaCl_2$ and distilled from CaH_2 under nitrogen. Acetone was distilled from and stored over 3 Å molecular sieves. Dioxane was treated with conc. HCl and water under reflux, neutralized with KOH and then distilled over sodium wire, stored away from light and passed through basic alumina before use.

Flash chromatography was carried out using Merck silica gel 60 [230-400 mesh (particle size 0.040-0.063 mm)]. Thin layer chromatography (TLC) was carried out on pre-coated Merck silica gel F254 plates, and viewed under UV light (254 / 365 nm) or following exposure to iodine vapour.

NMR spectra were recorded on Bruker AMX 400 and Biospin 600 spectrometers at 303 K (except where described otherwise for kinetics experiments) in DMSO-d_6, $CDCl_3$ or D_2O (for STD NMR experiments) and calibrated using solvent signals [δ_H: 7.26 ppm for residual $CHCl_3$, 2.50 ppm for residual DMSO and 4.79 ppm for residual H_2O; δ_C: 77.0 ppm ($CDCl_3$) and 39.5 (DMSO-d_6)]; coupling constants are given in Hertz (Hz). ^{31}P NMR spectral data was acquired using phosphoric acid (H_3PO_4) as an internal reference. Melting points were measured using a hot stage apparatus and are uncorrected. IR spectra were recorded on a Perkin Elmer Spectrum 100 FT-IR spectrometer with a diamond window, and compounds were analysed neat. High-resolution mass spectra (HRMS) were recorded on a Waters API Q-TOF Ultima spectrometer (University of Stellenbosch, Stellenbosch, South Africa). Elemental Analysis was done on a Vario MICRO VI.6.2 elemental analysen systeme GmbH. Microwave assisted reactions were conducted using a CEM Discover single-mode microwave apparatus, producing controlled irradiation at 2450 MHz, using standard 10-mL silicone-septum-sealed glass pressure vials. An extraction funnel was situated over the reaction vial during reactions with SeO_2 to remove noxious vapour.

Names of new compounds are italicized and literature references are cited for known compounds. For series of compounds with excessively long names, the parent analogue has been fully named as a footnote and abbreviated generic names have been used.

3.2. BAYLIS-HILLMAN REACTIONS WITH *TERT*-BUTYL ACRYLATE

tert-Butyl 3-hydroxy-3-(2-hydroxyphenyl)-2-methylenepropanoate 153a

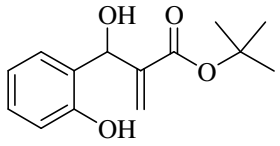

***Method* 1**. A mixture of salicylaldehyde (6.5 mL, 61 mmol), *tert*-butyl acrylate (14 mL, 97 mmol) and DABCO (5.7 g, 51 mmol) in $CHCl_3$ (21 mL) was sealed in a round-bottomed flask and stirred at r.t. for 18 d. The mixture was concentrated *in vacuo* and purified by flash chromatography [on silica gel; elution with hexane – EtOAc (9:1)] to afford *tert*-butyl 3-hydroxy-3-(2-hydroxyphenyl)-2-methylenepropanoate **153a** as a white solid (6.0 g, 39%), m.p. 108-110 °C (lit.[210] 108-110 °C); υ_{max} / cm^{-1} 3346 (OH) and 1687 (C=O); δ_H (400 MHz; $CDCl_3$) 1.51 [9H, s, $C(CH_3)_3$], 4.32 (1H, d, *J* = 3.8 Hz, OH), 5.48 and 6.23 (2H, 2 × s, $C=CH_2$), 5.69 (1H, d, *J* = 3.8 Hz, C*H*OH), 6.83 (1H, t, *J* = 7.4 Hz, ArH), 6.91-6.98 (2H, m, ArH), 7.21 (1H, t, *J* = 7.4 Hz, ArH) and 8.12 (1H, s, ArOH); δ_C (100 MHz; $CDCl_3$) 28.0 [$C(CH_3)_3$], 73.9 (CHOH), 82.6 [$C(CH_3)_3$], 117.6, 119.8 and 124.0 (Ar-C), 127.0 ($C=CH_2$), 127.8 and 129.5 (Ar-C), 140.8 ($C=CH_2$), 156.1 [ArC(OH)] and 166.8 (C=O).

***Method* 2**. A mixture of salicylaldehyde (1.3 mL, 12 mmol), *tert*-butyl acrylate (2.4 mL, 19 mmol) and DABCO (1.14 g, 10.2 mmol) in chloroform (2 mL) was sealed in a microwave vial and irradiated at 150 W and 30 °C for 1 hour, while monitoring the progress of the reaction using TLC and ^1H NMR analysis. The resulting mixture was concentrated *in vacuo* and purified using flash chromatography [on silica gel; elution with hexane – EtOAc (9:1)] to afford *tert*-butyl 3-hydroxy-3-(2-hydroxyphenyl)-2-methylenepropanoate **153a** as a white solid (0.82 g, 27%).

***tert*-Butyl 3-(5-bromo-2-hydroxyphenyl)-3-hydroxy-2-methylenepropanoate 153b**

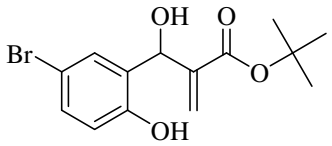

***Method* 1**. The procedure (method 1) described for the synthesis of *tert*-butyl 3-hydroxy-3-(2-hydroxyphenyl)-2-methylenepropanoate **153a** was followed, using 5-bromosalicylaldehyde (12 g, 61 mmol), *tert*-butyl acrylate (14 mL, 97 mmol) and DABCO (5.7 g, 51 mmol) in $CHCl_3$ (21 mL) and stirring for 4 d. The crude product was filtered and washed with $CHCl_3$ to afford *tert*-butyl 3-(5-bromo-2-hydroxyphenyl)-3-hydroxy-2-methylenepropanoate **153b** as a white solid (11.1 g, 55%), m.p. 185-187 °C (lit.[210] 186-188 °C); υ_{max} / cm^{-1} 3304 (OH) and 1690 (C=O); δ_H (400 MHz; DMSO-d_6) 1.32 [9H, s, $C(CH_3)_3$], 5.64 (1H, s, C*H*OH), 5.66 and 6.05 (2H, 2 × s, $C=CH_2$), 6.75 (1H, d, J = 8.4 Hz, ArH), 7.20 (1H, dd, J = 2.5 and 8.4 Hz, ArH), and 7.23 (1H, d, J = 2.5 Hz, ArH); δ_C (100 MHz; DMSO-d_6) 27.4 [$C(CH_3)_3$], 64.5 (CHOH), 80.0 [$C(CH_3)_3$], 109.6 and 117.1 (Ar-C), 122.9 ($C=CH_2$), 129.7, 130.4 and 131.8 (Ar-C), 144.8 ($C=CH_2$), 153.8 [ArC(OH)] and 164.9 (C=O).

***Method* 2**. The procedure (method 2) described for the synthesis of *tert*-butyl 3-hydroxy-3-(2-hydroxyphenyl)-2-methylenepropanoate **153a** was followed, using a mixture of 5-bromosalicylaldehyde (2.45 g, 12.2 mmol), *tert*-butyl acrylate (2.4 mL, 19 mmol) and DABCO (1.14 g, 10.2 mmol) in $CHCl_3$ (2 mL). The mixture was concentrated *in vacuo* and purified using flash chromatography [on silica gel; elution with hexane – EtOAc (9:1)] to afford *tert*-butyl 3-(5-bromo-2-hydroxyphenyl)-3-hydroxy-2-methylenepropanoate **153b** as a white solid (1.60 g, 40%).

***tert*-Butyl 3-hydroxy-3-(2-hydroxy-3-methoxyphenyl)-2-methylenepropanoate 153c**[210]

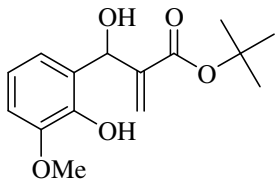

***Method* 1**. The procedure (method 1) described for the synthesis of *tert*-butyl 3-hydroxy-3-(2-hydroxyphenyl)-2-methylenepropanoate **153a** was followed, using 3-methoxysalicylaldehyde (10.1 g, 66.7 mmol), *tert*-butyl acrylate (14 mL, 97 mmol) and DABCO (5.7 g, 51 mmol) in $CHCl_3$ (21 mL) and stirring for 21 d. The mixture was concentrated *in vacuo* and purified using

flash chromatography [on silica gel; elution with hexane – EtOAc (9:1)] to afford *tert*-butyl 3-hydroxy-3-(2-hydroxy-3-methoxyphenyl)-2-methylenepropanoate **153c** as a yellow oil (5.42 g, 29%); υ_{max} / cm^{-1} 3460 (OH) and 1701 (C=O); δ_H (400 MHz; $CDCl_3$) 1.42 [9H, s, $C(CH_3)_3$], 3.77 (1H, d, *J* = 4.8 Hz, OH), 3.83 (3H, s, OCH_3), 5.80 (1H, d, *J* = 4.8 Hz, C*H*OH), 5.66 and 6.20 (2H, 2 × s, $C=CH_2$), 6.66 (1H, s, ArOH) and 6.78-6.84 (3H, overlapping m, ArH); δ_C (100 MHz; $CDCl_3$) 27.9 [$C(CH_3)_3$], 55.9 (OCH_3), 69.4 (CHOH), 81.5 [$C(CH_3)_3$], 110.4, 119.4 and 119.6 (Ar-C), 125.0 ($C=CH_2$), 126.5 (Ar-C), 142.1 ($C=CH_2$), 143.6 [ArC(OH)], 147.0 [ArC(OMe)] and 166.0 (C=O).

***Method* 2**. The procedure (method 2) described for the synthesis of *tert*-butyl 3-hydroxy-3-(2-hydroxyphenyl)-2-methylenepropanoate **153a** was followed, using a mixture of 3-methoxysalicylaldehyde (2.0 g, 13 mmol), *tert*-butyl acrylate (2.4 mL, 19 mmol) and DABCO (1.14 g, 10.2 mmol) in $CHCl_3$ (2 mL). The mixture was concentrated *in vacuo* and purified using flash chromatography [on silica gel; elution with hexane – EtOAc (9:1)] to afford *tert*-butyl 3-hydroxy-3-(2-hydroxy-3-methoxyphenyl)-2-methylenepropanoate **153c** as a yellow oil (1.18 g, 32%).

***tert*-Butyl 3-(3-ethoxy-2-hydroxyphenyl)-3-hydroxy-2-methylenepropanoate 153d**[210]

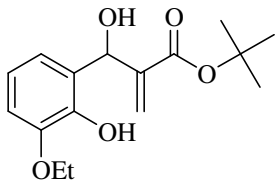

***Method* 1**. The procedure (method 1) described for the synthesis of *tert*-butyl 3-hydroxy-3-(2-hydroxyphenyl)-2-methylenepropanoate **153a** was followed, using 3-ethoxysalicylaldehyde (10.2 g, 61.5 mmol), *tert*-butyl acrylate (14 mL, 97 mmol) and DABCO (5.7 g, 51 mmol) in $CHCl_3$ (21 mL) and stirring for 21 d. The mixture was concentrated *in vacuo* and purified using flash chromatography [on silica gel; elution with hexane – EtOAc (9:1)] to afford *tert*-butyl 3-(3-ethoxy-2-hydroxyphenyl)-3-hydroxy-2-methylenepropanoate **153d** as a yellow oil (5.6 g, 31%); υ_{max} / cm^{-1} 3465 (OH) and 1712 (C=O); δ_H (400 MHz; $CDCl_3$) 1.41-1.44 [12H, overlapping s and t, $C(CH_3)_3$ and CH_2CH_3], 3.62 (1H, br s, OH) 4.08 (2H, q, *J* = 7.0 Hz, OCH_2CH_3), 5.83 (1H, s, C*H*OH), 5.67 and 6.22 (2H, 2 × s, $C=CH_2$), 6.44 (1H, br s, ArOH) and 6.77-6.85 (3H, overlapping m, ArH); δ_C (100 MHz; $CDCl_3$) 14.8 (CH_2CH_3) 28.0 [$C(CH_3)_3$], 64.6 (OCH_2CH_3),

69.3 (CHOH), 81.5 [*C*$(CH_3)_3$], 111.4, 119.5 and 119.7 (Ar-C), 124.9 (C=*C*H_2), 126.7 (Ar-C), 142.3 (*C*=CH_2), 143.7 [ArC(OH)], 146.1 [ArC(OEt)] and 166.1 (C=O).

***Method* 2**. The procedure (method 2) described for the synthesis of *tert*-butyl 3-hydroxy-3-(2-hydroxyphenyl)-2-methylenepropanoate **153a** under microwave irradiation was followed, using a mixture of 3-ethoxysalicylaldehyde (2.01 g, 12.1 mmol), *tert*-butyl acrylate (2.4 mL, 19 mmol) and DABCO (1.14 g, 10.2 mmol) in $CHCl_3$ (2 mL). The mixture was concentrated *in vacuo* and purified using flash chromatography [on silica gel; elution with hexane – EtOAc (9:1)] to afford *tert*-butyl 3-(3-ethoxy-2-hydroxyphenyl)-3-hydroxy-2-methylenepropanoate **153d** as a yellow oil (1.06 g, 30%).

***tert*-Butyl 3-(5-chloro-2-hydroxyphenyl)-3-hydroxy-2-methylenepropanoate 153e**

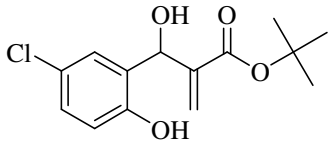

***Method* 1**. The procedure (method 1) described for the synthesis of *tert*-butyl 3-hydroxy-3-(2-hydroxyphenyl)-2-methylenepropanoate **153a** was followed, using 5-chlorosalicylaldehyde (10.1 g, 64.5 mmol), *tert*-butyl acrylate (14 mL, 97 mmol) and DABCO (5.7 g, 51 mmol) in $CHCl_3$ (21 mL) and stirring for 4 d. The crude product was filtered and washed with $CHCl_3$ to afford *tert*-butyl 3-(5-chloro-2-hydroxyphenyl)-3-hydroxy-2-methylenepropanoate **153e** as a white solid (10.05 g, 55%); m.p. 178-180 °C (lit.[273] 185-187 °C); υ_{max} / cm^{-1} 3300 and 1681 (C=O); δ_H (400 MHz; DMSO-d_6) 1.32 [9H, s, C$(CH_3)_3$], 5.67 (1H, s, C*H*OH), 5.64 and 6.06 (2H, 2 × s, C=CH_2), 6.79 (1H, d, *J* = 8.5 Hz, ArH), 7.06 (1H, d, *J* = 2.7 Hz, ArH) and 7.09 (1H, dd, *J* = 2.7 and 8.5 Hz, ArH); δ_C (100 MHz; DMSO-d_6) 27.4 [C(*C*$H_3)_3$], 64.5 (CHOH), 80.0 [*C*$(CH_3)_3$], 116.5 and 121.9 (Ar-C), 122.9 (C=*C*H_2), 126.8, 127.5 and 131.3 (Ar-C), 144.8 (*C*=CH_2), 153.3 [ArC(OH)] and 164.9 (C=O).

***Method* 2**. The procedure (method 2) described for the synthesis of *tert*-butyl 3-hydroxy-3-(2-hydroxyphenyl)-2-methylenepropanoate **153a** was followed, using a mixture of 5-chlorosalicylaldehyde (1.59 g, 10.2 mmol), *tert*-butyl acrylate (2.4 mL, 16 mmol) and DABCO (1.1 g, 8.1 mmol) in $CHCl_3$ (2 mL). The mixture was concentrated *in vacuo* and purified using flash chromatography [on silica gel; elution with hexane – EtOAc (9:1)] to afford *tert*-butyl 3-(5-

chloro-2-hydroxyphenyl)-3-hydroxy-2-methylenepropanoate **153e** as a white solid (1.03 g, 36%).

3.3. CYCLISATION OF BAYLIS-HILLMAN ADDUCTS

3.3.1. Base-Catalysed Cyclisation

tert-*Butyl 3,4-dihydro-4-hydroxy-2*H-*chromene-3-carboxylate* 163a

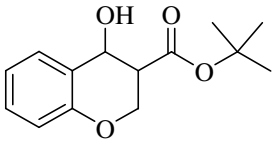

***tert*-Butyl 2*H*-chromene-3-carboxylate 164a**

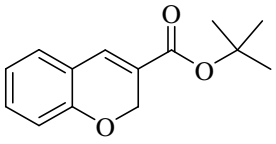

A solution of KOH (0.11 g, 2.0 mmol) in water (1 mL) was added to a solution of *tert*-butyl 3-hydroxy-3-(2-hydroxyphenyl)-2-methylenepropanoate **153a** (0.5 g, 2 mmol) in CH_3CN (5 mL) and the mixture was boiled under reflux for 5 hours. After cooling, the crude product was extracted with EtOAc, dried with anhydrous $MgSO_4$, concentrated *in vacuo* and flash chromatographed [on silica gel; elution with hexane – EtOAc – diethyl ether (8:1:1)] to afford two fractions.

***Fraction* 1**: tert-*Butyl 3,4-dihydro-4-hydroxy-2*H-*chromene-3-carboxylate* **163a** as a white solid (0.16 g, 32%); m.p. 75-76 °C (Found: C, 66.96; H, 7.09. $C_{14}H_{18}O_4$ requires: C, 67.18; H, 7.25%); υ_{max} / cm^{-1} 3225 (OH) and 1719 (C=O); δ_H (400 MHz; $CDCl_3$) 1.45 [9H, s, $C(CH_3)_3$], 2.86 (1H, dt, *J* = 7.6 and 3.3 Hz, 3-H), 3.07 (1H, br s, OH), 4.17-4.22 (1H, 2 × overlapping d, 2-CH_2), 4.38 (1H, dd, *J* = 9.7 and 3.3 Hz, 2-CH_2), 5.04 (1H, d, *J* = 7.6 Hz, 4-H), 6.81 (1H, d, *J* = 8.0 Hz, ArH), 6.94 (1H, t, *J* = 7.4 Hz, ArH), 7.17 (1H, t, *J* = 7.6 Hz, ArH) and 7.43 (1H, d, *J* = 7.6 Hz, ArH); δ_C (100 MHz; $CDCl_3$) 28.4 [$C(CH_3)_3$], 47.6 (C-3), 64.7 (C-2), 66.0 (C-4), 82.6 [$C(CH_3)_3$], 116.9, 121.5, 124.1, 128.8 and 130.0 (Ar-C), 154.2 [Ar$C(OCH_2)$] and 170.9 (C=O).

***Fraction* 2**: *tert*-Butyl 2*H*-chromene-3-carboxylate **164a** as a pale yellow solid (0.11 g, 24%), m.p. 25-26 °C (lit.[210] reported as an oil); υ_{max} / cm^{-1} 1689 (C=O); δ_H (400 MHz; $CDCl_3$) 1.54 [9H, s, $C(CH_3)_3$], 4.95 (2H, s, 2-CH_2), 6.83 (1H, d, *J* = 8.1 Hz, ArH), 6.90 (1H, t, *J* = 7.4 Hz, ArH), 7.11 (1H, d, *J* = 7.4 Hz, ArH), 7.20 (1H, t, *J* = 7.7 Hz, ArH) and 7.33 (1H, s, 4-H); δ_C

(100 MHz; $CDCl_3$) 28.6 [C(CH_3)$_3$], 65.1 (C-2), 81.6 [C(CH$_3$)$_3$], 116.5 (Ar-C), 121.6 (C-3), 122.1, 124.7, 129.2 and 132.0 (Ar-C), 133.0 (C-4), 155.5 [ArC(OCH$_2$)] and 164.3 (C=O).

3.3.2. Acid-Catalysed Cyclisation

3.3.2.1. HCl-Mediated Cyclisation

3-(Chloromethyl)coumarin 148a

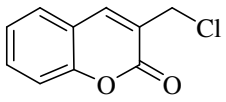

3-(Acetoxymethyl)coumarin 165a

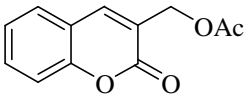

Conc. HCl (10 mL) was added to a solution of *tert*-butyl 3-hydroxy-3-(2-hydroxyphenyl)-2-methylenepropanoate **153a** (2.0 g, 8.2 mmol) in AcOH (10 mL). The mixture was refluxed for 2 h, allowed to cool to r.t. and then poured into ice-cooled water (30 mL). Stirring for 30 min gave a precipitate, which was filtered off, dried and then purified by flash chromatography [on silica gel; elution with hexane – EtOAc (9:1)] to afford two fractions.

***Fraction* 1**: 3-(Chloromethyl)coumarin **148a** as a white solid (1.11 g, 70%), m.p. 119-121 °C (lit.[208] 108-110 °C); υ_{max} / cm^{-1} 1712 (C=O); δ_H (400 MHz; $CDCl_3$) 4.56 (2H, s, 1′-CH_2), 7.31 (1H, t, J = 7.5 Hz, ArH), 7.34 (1H, d, J = 8.3 Hz, ArH), 7.52-7.58 (2H, m, ArH) and 7.89 (1H, s, 4-H); δ_C (100 MHz; $CDCl_3$) 41.0 (C-1′), 116.7, 118.8, 124.7, 125.1, 128.1, 132.0, 141.0 and 153.6 (Ar-C) and 160.0 (C=O).

***Fraction* 2**: 3-(Acetoxymethyl)coumarin **165a** as a pale yellow solid (0.11 g, 6%), m.p. 106-108 °C (lit.[210] 106-110 °C); υ_{max} / cm^{-1} 1732 and 1704 (C=O); δ_H (400 MHz; $CDCl_3$) 2.16 (3H, s, $COCH_3$), 5.08 (2H, s, 1′-CH_2), 7.29 (1H, t, J = 7.5 Hz, ArH), 7.35 (1H, d, J = 8.3 Hz, ArH), 7.50-7.56 (2H, m, ArH) and 7.75 (1H, s, 4-H); δ_C (100 MHz; $CDCl_3$) 20.9 (COCH$_3$), 61.2 (C-1′), 116.7, 118.8, 123.8, 124.6, 128.0, 131.8, 140.7 and 153.6 (Ar-C), 160.2 (C=O) and 170.5 (COCH$_3$).

6-Bromo-3-(chloromethyl)coumarin 148b

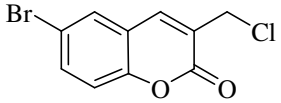

The procedure described for the synthesis of 3-(chloromethyl)coumarin **148a** was followed, using conc. HCl (10 mL) and a solution of *tert*-butyl 3-(5-bromo-2-hydroxyphenyl)-3-hydroxy-2-methylenepropanoate **153b** (2 g, 6 mmol) in AcOH (10 mL). Work-up and purification by flash chromatography [on silica gel; elution with hexane – EtOAc (9:1)] afforded 6-bromo-3-(chloromethyl)coumarin **148b** as a white solid (1.46 g, 88%), m.p. 114-115 °C (lit.[208] 116-118 °C); υ_{max} / cm^{-1} 1719 (C=O); δ_H (400 MHz; $CDCl_3$) 4.54 (2H, s, 1′-CH_2), 7.24 (1H, d, *J* = 8.8 Hz, ArH), 7.63 (1H, dd, *J* = 8.8 and 2.2 Hz, ArH), 7.67 (1H, d, *J* = 2.2 Hz, ArH), and 7.81 (1H, s, 4-H); δ_C (100 MHz, $CDCl_3$) 40.8 (C-1′), 117.3, 118.4, 120.3, 126.4, 130.3, 134.7, 139.5 and 152.3 (Ar-C) and 159.3 (C=O).

3-(Chloromethyl)-8-methoxycoumarin 148c

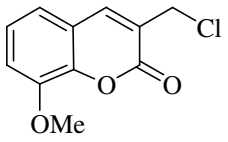

The procedure described for the synthesis of 3-(chloromethyl)coumarin **148a** was followed, using conc. HCl (10 mL) and a solution of *tert*-butyl 3-hydroxy-3-(2-hydroxy-3-methoxyphenyl)- 2-methylenepropanoate **153c** (2 g, 7 mmol) in AcOH (10 mL). Work-up and purification by flash chromatography [on silica gel; elution with hexane – EtOAc (9:1)] afforded 3-(chloromethyl)-8-methoxycoumarin **148c** as a grey solid (1.14 g, 71%), m.p. 146-148 °C (lit.[208] 146-148 °C); υ_{max} / cm^{-1} 1708 (C=O); δ_H (400 MHz; $CDCl_3$) 3.95 (3H, s, OCH_3), 4.53 (2H, s, 1′-CH_2), 7.06-7.09 (2H, m, ArH), 7.19-7.23 (1H, m, ArH) and 7.84 (1H, s, 4-H); δ_C (100 MHz; $CDCl_3$) 41.0 (C-1′), 56.3 (OCH_3), 113.9, 119.4, 119.5, 124.5, 125.1, 141.2, 143.2 and 147.1 (Ar-C) and 159.5 (C=O).

3-(Chloromethyl)-8-ethoxycoumarin 148d ***3-(Acetoxymethyl)-8-ethoxycoumarin*** **165d**

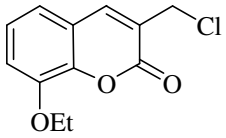

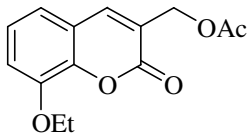

The procedure described for the synthesis of 3-(chloromethyl)coumarin **148a** was followed, using conc. HCl (10 mL) and a solution of *tert*-butyl 3-(3-ethoxy-2-hydroxyphenyl)-3-hydroxy-2-methylenepropanoate **153d** (2 g, 7 mmol) in AcOH (10 mL). Work-up and purification by flash chromatography [on silica gel; elution with hexane – EtOAc (9:1)] afforded two fractions.

***Fraction* 1**: 3-(Chloromethyl)-8-ethoxycoumarin **148d** as a brown solid (1.17 g, 72%), m.p. 121-123 °C (lit.[208] 122-124 °C); υ_{max} / cm^{-1} 1708 (C=O); δ_H (400 MHz; $CDCl_3$) 1.49 (3H, t, *J* = 7.0 Hz, CH_2CH_3), 4.19 (2H, q, *J* = 7.0 Hz, OCH_2CH_3) 4.54 (2H, s, 1′-CH_2), 7.07-7.10 (2H, overlapping m, ArH), 7.21 (1H, dd, *J* = 8.3 and 7.6 Hz, ArH) and 7.85 (1H, s, 4-H); δ_C (100 MHz; $CDCl_3$) 14.7 (CH_2CH_3), 41.0 (C-1′), 65.1 (OCH_2CH_3), 115.3, 119.4, 119.6, 124.5, 125.2, 141.2, 143.5, 146.5 (Ar-C) and 159.7 (C=O).

***Fraction* 2**: *3-(Acetoxymethyl)-8-ethoxycoumarin* **165d** as a beige solid (0.18 g, 10%); m.p. 108-110 °C (Found: C, 64.40; H, 5.59. $C_{14}H_{14}O_5$ requires: C, 64.22; H, 5.48%); υ_{max} / cm^{-1} 1740 and 1707 (C=O); δ_H (400 MHz; $CDCl_3$) 1.49 (3H, t, *J* = 7.0 Hz, CH_2CH_3), 2.15 (3H, s, $COCH_3$), 4.19 (2H, q, *J* = 7.0 Hz, OCH_2CH_3), 5.07 (2H, s, 1′-CH_2), 7.04-7.08 (2H, m, ArH), 7.17-7.20 (1H, m, ArH) and 7.71 (1H, s, 4-H); δ_C (100 MHz; $CDCl_3$) 14.7 (CH_2CH_3), 20.8 ($COCH_3$), 61.2 (C-1′), 65.1(OCH_2CH_3), 115.2, 119.4, 119.5, 123.9, 124.4, 140.8, 143.6 and 146.5 (Ar-C), 159.8 (C=O) and 170.4 ($COCH_3$).

6-Chloro-3-(chloromethyl)coumarin 148e

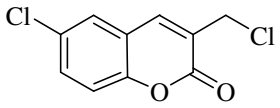

The procedure described for the synthesis of 3-(chloromethyl)coumarin **148a** was followed, using conc. HCl (10 mL) and a solution of *tert*-butyl 3-(5-chloro-2-hydroxyphenyl)-3-hydroxy-2-methylenepropanoate **153e** (2 g, 6 mmol) in AcOH (10 mL). Work-up and purification by flash chromatography [on silica gel; elution with hexane – EtOAc (9:1)] afforded 6-chloro-3-(chloromethyl)coumarin **148e** as a white solid (1.48 g, 92%), m.p. 111-112 °C (lit.[208] 112-114 °C); υ_{max} / cm^{-1} 1726 (C=O); δ_H (400 MHz; $CDCl_3$) 4.55 (2H, s, 1′-CH_2), 7.30 (1H, d, *J* = 7.1 Hz, ArH), 7.49 (1H, d, *J* = 2.4 Hz, ArH), 7.51 (1H, dd, *J* = 7.1 and 2.4 Hz, ArH) and 7.83 (1H, s, 4-H); δ_C (100 MHz; $CDCl_3$) 40.8 (C-1′), 118.1, 119.8, 126.3, 127.3, 130.0, 131.9, 139.7 and 151.8 (Ar-C) and 159.5 (C=O).

3.3.2.2. HI-Mediated Cyclisation

3-Methylcoumarin 150a

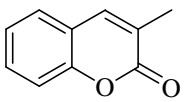

Conc. HI (10 mL) was added to a solution of *tert*-butyl 3-hydroxy-3-(2-hydroxyphenyl)-2-methylenepropanoate **153a** (0.50 g, 2.0 mmol) in a mixture of Ac_2O (5 mL) and AcOH (5 mL). The mixture was boiled under refluxed for 2 h at 150 °C (oil bath), cooled and then poured into ice-cooled water and left to stir for 1 h. The precipitate formed was filtered off and dried to afford 3-methylcoumarin **150a** as a light yellow solid (0.17 g, 53%), m.p. 92-94 °C (lit.[274] 90-92 °C) [HRMS: *m/z* calculated for $C_{10}H_9O_2$ (MH^+) 161.0603. Found 161.0611]; υ_{max} / cm^{-1} 1697 (C=O); δ_H (400 MHz; $CDCl_3$) 2.19 (3H, s, CH_3), 7.22 (1H, dt, *J* = 7.7 and 1.0 Hz, ArH), 7.27 (1H, d, *J* = 7.7 Hz, ArH), 7.38-7.45 (2H, m, ArH) and 7.49 (1H, s, 4-H); δ_C (100 MHz, $CDCl_3$) 17.1 (CH_3), 116.3, 119.4, 124.2, 125.7, 126.9, 130.4, 139.2 and 153.1 (Ar-C) and 162.1 (C=O).

6-Bromo-3-methylcoumarin **150b**

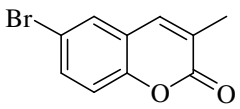

The procedure described for the synthesis of 3-methylcoumarin **150a** was followed, using conc. HI (10 mL) and *tert*-butyl 3-(5-bromo-2-hydroxyphenyl)-3-hydroxy-2-methylenepropanoate **153b** (0.50 g, 1.5 mmol) in a mixture of Ac_2O (5 mL) and AcOH (5 mL). Work up afforded *6-bromo-3-methylcoumarin* **150b** as a white solid (0.34 g, 94%), m.p. 156-158 °C (Found: C, 50.48; H, 3.01. $C_{10}H_7BrO_2$ requires: C, 50.24; H, 2.95%); υ_{max} / cm^{-1} 1717 (C=O); δ_H (400 MHz; $CDCl_3$) 2.21 (3H, s, CH_3), 7.17 (1H, d, *J* = 9.3 Hz, ArH), 7.40 (1H, s, ArH) and 7.51-7.54 (2H, m, ArH); δ_C (100 MHz; $CDCl_3$) 17.2 (CH_3), 116.7, 118.1, 121.1, 127.3, 129.2, 133.1, 137.7 and 152.1 (Ar-C) and 161.3 (C=O).

6-Chloro-3-methylcoumarin 150e

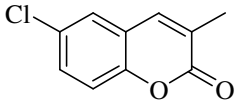

The procedure described for the synthesis of 3-methylcoumarin **150a** was followed, using conc. HI (10 mL) and *tert*-butyl 3-(5-chloro-2-hydroxyphenyl)-3-hydroxy-2-methylenepropanoate **153e** (0.50 g, 1.8 mmol) in a mixture of Ac_2O (5 mL) and AcOH (5 mL). Work up afforded 6-chloro-3-methylcoumarin **150e** as a white solid (0.31 g, 91%), m.p. 157-160 °C (dec.) (lit.[274] 158-160 °C); υ_{max} / cm^{-1} 1709 (C=O); δ_H (400 MHz; $CDCl_3$) 2.22 (3H, s, CH_3), 7.24 (1H, d, *J* = 9.0 Hz, ArH), 7.38-7.41 (2H, m, ArH) and 7.43 (1H, s, 4-H); δ_C (100 MHz; $CDCl_3$) 17.2 (CH_3), 117.9, 120.6, 126.2, 127.3, 129.5, 130.4, 137.8 and 151.6 (Ar-C) and 161.5 (C=O).

8-Hydroxy-3-methylcoumarin **150f**

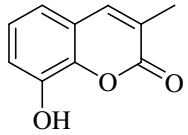

Method **1**. The procedure described for the synthesis of 3-methylcoumarin **150a** was followed, using conc. HI (10 mL) and *tert*-butyl 3-(3-ethoxy-2-hydroxyphenyl)-3-hydroxy-2-methylenepropanoate **153d** (0.50 g, 1.7 mmol) in a mixture of Ac_2O (5 mL) and AcOH (5 mL). Cooling in ice cold water followed by extraction with chloroform afforded *8-hydroxy-3-methylcoumarin* **150f** as a brown solid (0.26 g, 87%), m.p. 180-182 °C [HRMS: *m/z* calculated for $C_{10}H_7O_3$ $(M\text{-}H)^+$ 175.0395. Found 175.0406]; υ_{max} / cm^{-1} 3185 (OH) and 1674 (C=O); δ_H (400 MHz; $CDCl_3$) 2.22 (3H, s, CH_3), 6.95 (1H, dd, *J* = 7.4 and 1.2 Hz, ArH), 7.09 (1H, dd, *J* = 8.0 and 1.4 Hz, ArH) 7.12-7.16 (1H, m, ArH) and 7.53 (1H, d, *J* = 1.2 Hz, 4-H); δ_C (100 MHz; $CDCl_3$) 17.2 (CH_3), 116.9, 118.1, 119.8, 124.7, 125.5, 140.0, 141.0 and 143.2 (Ar-C) and 161.6 (C=O).

Method **2**. In a similar reaction using *tert*-butyl 3-hydroxy-3-(3-methoxy-2-hydroxyphenyl)-2-methylenepropanoate **153c**, 8-hydroxy-3-methylcoumarin **150f** was obtained as a brown solid (85%).

3.3.3. Iodine-Catalysed Cyclisation

3-(Hydroxymethyl)coumarin 192a

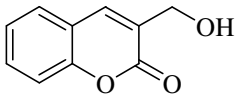

I_2 (0.08 g, 0.3 mmol) and then water (0.1 mL) were added to a solution of *tert*-butyl 3-hydroxy-3-(2-hydroxyphenyl)-2-methylenepropanoate **153a** (0.5 g, 2 mmol) in acetonitrile (5 mL) and the mixture was stirred under reflux for 5 hours. The reaction was then diluted with aq. $Na_2S_2O_3$ solution (5 mL) and extracted with EtOAc (2 × 25 mL). The combined organic layers were dried, concentrated *in vacuo* and purified using flash chromatography [on silica gel; elution with hexane – EtOAc (3:2)] to afford 3-(hydroxymethyl)coumarin **192a** as a yellow solid (0.31 g, 88%), m.p. 110-112 °C (lit.[275] m.p. not cited) [HRMS: *m/z* calculated for $C_{10}H_7O_3$ $(M\text{-}H)^+$ 175.0395. Found 175.0375]; υ_{max} / cm^{-1} 1666 (C=O); δ_H (400 MHz; DMSO-d_6) 4.90 (2H, s, 1′-CH_2), 6.84 (1H, d, *J* = 7.9 Hz, ArH), 6.95 (1H, t, *J* = 7.4 Hz, ArH), 7.26 (1H, t, *J* = 7.9 Hz,

ArH), 7.31 (1H, d, *J* = 7.4 Hz, ArH) and 7.43 (1H, s, 4-H); δ_C (100 MHz; DMSO-d_6) 64.1 (C-1′), 115.6, 120.8, 121.7, 123.4, 129.1, 131.8, 132.2 and 154.4 (Ar-C) and 165.4 (C=O).

6-Bromo-3-(hydroxymethyl)coumarin 192b

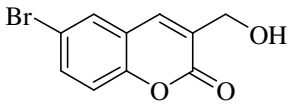

The procedure described for the synthesis of 3-(hydroxymethyl)coumarin **192a** was followed, using a mixture of I_2 (0.08 g, 0.3 mmol), *tert*-butyl 3-(5-bromo-2-hydroxyphenyl)-3-hydroxy-2-methylenepropanoate **153b** (0.50 g, 1.5 mmol), water (0.1 mL) and acetonitrile (5 mL) under reflux for 5 hours. Work up afforded 6-bromo-3-(hydroxymethyl)coumarin **192b** as a yellow solid (0.27 g, 69%), m.p. 163-165 °C (lit.[276] 147-149 °C); υ_{max} / cm^{-1} 1670 (C=O); δ_H (400 MHz; DMSO-d_6) 4.93 (2H, s, 1′-CH_2), 6.81 (1H, d, *J* = 8.6 Hz, ArH), 7.41 (1H, dd, *J* = 1.8 and 8.6 Hz, ArH), 7.43 (1H, s, 4-H), 7.57 (1H, d, *J* = 1.8 Hz, ArH) and 13.00 (1H, br s, OH); δ_C (100 MHz; DMSO-d_6) 64.4 (C-1′), 112.8, 117.9, 123.0, 124.7, 130.9, 131.0, 133.9 and 153.6 (Ar-C) and 165.2 (C=O).

***8-Ethoxy-3-(hydroxymethyl)coumarin* 192d**

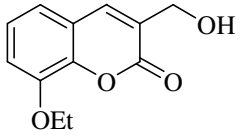

The procedure described for the synthesis of 3-(hydroxymethyl)coumarin **192a** was followed, using a mixture of I_2 (0.08 g, 0.3 mmol), *tert*-butyl 3-(3-ethoxy-2-hydroxyphenyl)-3-hydroxy-2-methylenepropanoate **153d** (0.50 g, 1.7 mmol), water (0.1 mL) and acetonitrile (5 mL) under reflux for 5 hours. Work up afforded *8-ethoxy-3-(hydroxymethyl)coumarin* **192d** as a yellow solid (0.24 g, 65%), m.p. 143-145 °C (Found: C, 65.30; H, 5.55. $C_{12}H_{12}O_4$ requires: C, 65.45; H, 5.49%); υ_{max} / cm^{-1} 1661 (C=O); δ_H (400 MHz; DMSO-d_6) 1.31 (3H, t, *J* = 6.9 Hz, OCH_2CH_3), 4.02 (2H, q, *J* = 6.9 Hz, OCH_2CH_3), 4.88 (2H, s, 1′-CH_2), 6.85-6.93 (2H, overlapping m, ArH), 6.98 (1H, d, *J* = 7.6 Hz, ArH) and 7.41 (1H, s, 4-H); δ_C (100 MHz; DMSO-d_6) 14.7 (CH_3), 64.0 (C-1′ and OCH_2CH_3), 116.2, 120.8, 121.4, 121.6, 123.4, 132.5, 143.6 and 146.8 (Ar-C) and 165.5 (C=O).

6-Chloro-3-(hydroxymethyl)coumarin **192e**

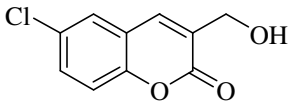

The procedure described for the synthesis of 3-(hydroxymethyl)coumarin **192a** was followed, using a mixture of I_2 (0.08 g, 0.3 mmol), *tert*-butyl 3-(5-chloro-2-hydroxyphenyl)-3-hydroxy-2-methylenepropanoate **153e** (0.50 g, 1.8 mmol), water (0.1 mL) and acetonitrile (5 mL) under reflux for 5 hours. Work up afforded *6-chloro-3-(hydroxymethyl)coumarin* **192e** as a yellow solid (0.23 g, 60%), m.p. 125-127 °C (Found: C, 57.20; H, 3.41. $C_{10}H_7ClO_3$ requires: C, 57.03; H, 3.35%); υ_{max} / cm^{-1} 1669 (C=O); δ_H (400 MHz; DMSO-d_6) 4.93 (2H, s, 1′-CH_2), 6.86 (1H, d, *J* = 8.6 Hz, ArH), 7.27 (1H, dd, *J* = 8.6 and 2.3 Hz, ArH) and 7.42-7.44 (2H, overlapping m, ArH); δ_C (100 MHz; DMSO-d_6) 64.4 (C-1′), 117.3, 122.4, 124.8, 125.2, 128.1, 130.9, 131.0 and 153.1 (Ar-C) and 165.2 (C=O).

3.4. NUCLEOPHILIC SUBSTITUTION OF 3-(CHLOROMETHYL)COUMARINS

3.4.1. Reaction of 3-(Chloromethyl)coumarins with Propargylamine

3-[(2-Propynylamino)methyl]coumarin **166a**

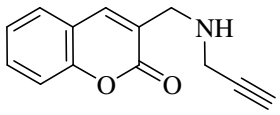

Propargylamine (0.60 mL, 8.8 mmol) was added to a solution of 3-(chloromethyl)coumarin **148a** (0.80 g, 4.1 mmol) in dry THF (5 mL). After stirring at r.t. for 48 h, the reaction mixture was concentrated *in vacuo* and flash chromatographed [on silica gel; elution with hexane – EtOAc (3:2)] to afford *3-[(2-propynylamino)methyl]coumarin* **166a** as an off-white solid (0.7 g, 80%), m.p. 107-108 °C [HRMS: *m/z* calculated for $C_{13}H_{12}NO_2$ (MH^+) 214.0868. Found 214.0860]; υ_{max} / cm^{-1} 1694 (C=O); δ_H (400 MHz; $CDCl_3$) 1.78 (1H, s, NH), 2.24 (1H, t, *J* = 2.4 Hz, C≡CH), 3.48 (2H, d, *J* = 2.4 Hz, CH_2–C≡CH), 3.82 (2H, s, CH_2NH), 7.26 (1H, m, ArH), 7.32 (1H, d, *J* = 8.1 Hz, ArH), 7.48 (2H, m, ArH) and 7.73 (1H, s, 4-H); δ_C (100 MHz; $CDCl_3$) 38.1 and 48.2 (CH_2N), 72.4 and 82.0 (C≡CH), 117.0, 119.6, 124.9, 127.3, 128.1, 131.6, 139.9 and 153.7 (Ar-C) and 161.8 (C=O).

6-Bromo-3-[(2-propynylamino)methyl]coumarin **166b**

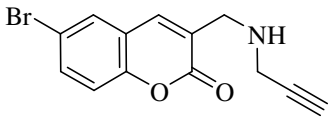

The procedure described for the synthesis of 3-[(2-propynylamino)methyl]coumarin **166a** was followed, using propargylamine (0.60 mL, 8.8 mmol) and 6-bromo-3-(chloromethyl)coumarin **148b** (1.0 g, 3.7 mmol) in dry THF (5 mL). Work-up afforded *6-bromo-3-[(2-propynylamino)-methyl]coumarin* **166b** as an off-white solid (0.55 g, 52%), m.p. 136-137 °C [HRMS: *m/z* calculated for $C_{13}H_{11}BrNO_2$ (MH^+) 291.9973. Found 291.9966]; υ_{max} / cm^{-1} 1712 (C=O); δ_H (400 MHz; $CDCl_3$) 1.76 (1H, br s, NH), 2.23 (1H, s, C≡CH), 3.46 (2H, s, CH_2-C≡CH), 3.80 (2H, s, CH_2NH), 7.18 (1H, d, *J* = 8.7 Hz, ArH), 7.54 (1H, d, *J* = 8.8 Hz, ArH), 7.58 (1H, s, ArH) and 7.64 (1H, s, 4-H); δ_C (100 MHz; $CDCl_3$) 38.1 and 48.0 (CH_2N), 72.5 and 81.9 (C≡CH), 117.4, 118.6, 121.2, 128.8, 130.3, 134.2, 138.3 and 152.5 (Ar-C) and 161.0 (C=O).

8-Methoxy-3-[(2-propynylamino)methyl]coumarin **166c**

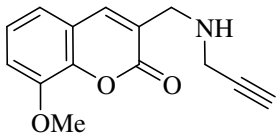

The procedure described for the synthesis of 3-[(2-propynylamino)methyl]coumarin **166a** was followed, using propargylamine (0.60 mL, 9 mmol) and 3-(chloromethyl)-8-methoxycoumarin **148c** (1.0 g, 4.5 mmol) in dry THF (5 mL). Work-up afforded *8-methoxy-3-[(2-propynylamino)methyl]coumarin* **166c** as a pale yellow solid (0.70 g, 65%), m.p. 89-91 °C [HRMS: *m/z* calculated for $C_{14}H_{14}NO_3$ (MH^+) 244.0974. Found 244.0973]; υ_{max} / cm^{-1} 1702 (C=O); δ_H (400 MHz; $CDCl_3$) 1.83 (1H, br s, NH), 2.21 (1H, s, C≡CH), 3.45 (2H, s, CH_2-C≡CH), 3.78 (2H, s, CH_2NH), 3.91 (3H, s, OCH_3), 7.01 (2H, d, *J* = 7.9 Hz, ArH), 7.15 (1H, t, *J* = 7.9 Hz, ArH) and 7.67 (1H, s, 4-H); δ_C (100 MHz; $CDCl_3$) 38.0 and 48.2 (CH_2N), 56.7 (OCH_3), 72.4 and 82.0 (C≡CH), 113.5, 119.5, 120.3, 124.7, 127.5, 139.9, 143.3 and 147.5 (Ar-C) and 161.2 (C=O).

8-Ethoxy-3-[(2-propynylamino)methyl]coumarin **166d**

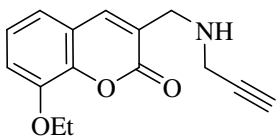

The procedure described for the synthesis of 3-[(2-propynylamino)methyl]coumarin **166a** was followed, using propargylamine (0.60 mL, 8.8 mmol) and 3-(chloromethyl)-8-ethoxycoumarin **148d** (1.0 g, 4.2 mmol) in dry THF (5 mL). Work-up afforded *8-ethoxy-3-[(2-propynylamino)-methyl]coumarin* **166d** as a pale yellow solid (0.75 g, 70%), m.p. 120-121 °C [HRMS: *m/z* calculated for $C_{15}H_{16}NO_3$ (MH^+) 258.1130. Found 258.1124]; υ_{max} / cm^{-1} 1699 (C=O); δ_H (400 MHz; $CDCl_3$) 1.46 (3H, t, *J* = 7.0 Hz, OCH_2CH_3), 1.85 (1H, br s, NH), 2.23 (1H, t, *J* = 2.4 Hz, C≡CH), 3.46 (2H, d, *J* = 2.4 Hz, CH_2-C≡CH), 3.79 (2H, s, CH_2NH), 4.15 (2H, q, *J* = 7.0 Hz, OCH_2CH_3), 7.01 (2 × overlapping d, ArH), 7.15 (1H, dd, *J* = 8.5 and 7.4 Hz, ArH) and 7.68 (1H, s, 4-H); δ_C (100 MHz; $CDCl_3$) 15.2 (CH_3), 38.0 and 48.2 (CH_2N), 65.4 (CH_2O), 72.4 and 82.0 (C≡CH), 114.8, 119.5, 120.4, 124.7, 127.4, 140.1, 143.6 and 146.8 (Ar-C) and 161.4 (C=O).

***6-Chloro-3-[(2-propynylamino)methyl]coumarin* 166e**

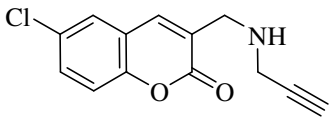

The procedure described for the synthesis of 3-[(2-propynylamino)methyl]coumarin **166a** was followed, using propargylamine (0.60 mL, 8.8 mmol) and 6-chloro-3-(chloromethyl)coumarin **148e** (1.00 g, 4.4 mmol) in dry THF (5 mL). Work-up afforded *6-chloro-3-[(2-propynyl-amino)methyl]coumarin* **166e** as a pale yellow solid (0.76 g, 70%), m.p. 116-117 °C [HRMS: *m/z* calculated for $C_{13}H_{11}ClNO_2$ (MH^+) 248.0478. Found 248.0460]; υ_{max} / cm^{-1} 1702 (C=O); δ_H (400 MHz; $CDCl_3$) 1.76 (1H, br s, NH), 2.27 (1H, t, *J* = 2.4 Hz, C≡CH), 3.50 (2H, d, *J* = 2.4 Hz, CH_2-C≡CH), 3.84 (2H, s, CH_2NH), 7.28 (1H, d, *J* = 8.5 Hz, ArH), 7.45 (2H, m, ArH) and 7.69 (1H, s, 4-H); δ_C (100 MHz; $CDCl_3$) 38.1 and 48.0 (CH_2N), 72.6 and 81.8 (C≡CH), 118.4, 120.7, 127.3, 128.7, 130.1, 131.5, 138.5 and 152.0 (Ar-C) and 161.2 (C=O).

3.4.2. Reaction of 3-(Chloromethyl)coumarins with Benzylamine

3-[(Benzylamino)methyl]coumarin 156a

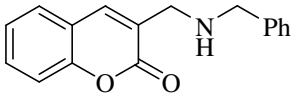

A mixture of 3-(chloromethyl)coumarin **148a** (0.31 g, 1.2 mmol) and benzylamine (0.4 mL, 4 mmol) in dry THF (6 mL) was stirred in a stoppered reaction flask at r.t. for 4 hours. The mixture

was then concentrated *in vacuo* and purified by flash chromatography (on silica gel; elution with chloroform) to afford 3-[(benzylamino)methyl]coumarin **156a** as a pale yellow solid (0.36 g, 85%), m.p. 71-74 °C (lit.[273] 70-74 °C); υ_{max} / cm^{-1} 3320 (N-H) and 1717 (C=O); δ_H (400 MHz; $CDCl_3$) 1.83 (1H, br s, NH), 3.74 (2H, s, 1′-CH_2), 3.83 (2H, s, CH_2Ph), 7.21-7.36 (7H, overlapping m, ArH), 7.43-7.48 (2H, m, ArH) and 7.69 (1H, s, 4-H); δ_C (100 MHz; $CDCl_3$) 48.4 and 53.2 (CH_2), 116.5, 119.3, 124.4, 127.1, 127.4, 127.5, 128.1, 128.5, 131.0, 139.1, 139.8 and 153.2 (Ar-C) and 161.4 (C=O).

3-[(Benzylamino)methyl]-6-bromocoumarin 156b

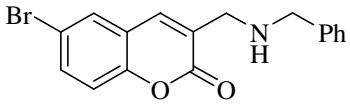

The procedure described for the synthesis of 3-[(benzylamino)methyl]coumarin **156a** was followed, using 6-bromo-3-(chloromethyl)coumarin **148b** (0.33 g, 1.2 mmol) and benzylamine (0.4 mL, 4 mmol) in dry THF (6 mL). Work-up afforded 3-[(benzylamino)methyl]-6-bromocoumarin **156b** as a pale yellow solid (0.30 g, 73%), m.p. 106-108 °C (lit.[273] 107-110 °C); υ_{max} / cm^{-1} 3325 (N-H) and 1722 (C=O); δ_H (400 MHz; $CDCl_3$) 1.75 (1H, br s, NH), 3.76 (2H, s, 1′-CH_2), 3.86 (2H, s, CH_2Ph), 7.21 (1H, d, *J* = 8.7 Hz, Ar-H), 7.27-7.36 (5H, overlapping m, ArH), 7.57 (1H, dd, *J* = 8.7 and 2.3 Hz, ArH), 7.61 (1H, d, *J* = 2.3 Hz, ArH) and 7.65 (1H, s, 4-H); δ_C (100 MHz; $CDCl_3$) 48.2 and 53.3 (CH_2), 117.0, 118.2, 120.9, 127.2, 128.1, 128.5, 129.0, 129.8, 133.7, 137.6, 139.7 and 152.0 (Ar-C) and 160.7 (C=O).

3-[(Benzylamino)methyl]-8-methoxycoumarin 156c[273]

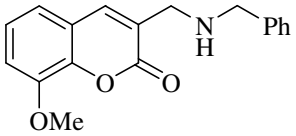

The procedure described for the synthesis of 3-[(benzylamino)methyl]coumarin **156a** was followed, using 3-(chloromethyl)-8-methoxycoumarin **148c** (0.33 g, 1.5 mmol) and benzylamine (0.4 mL, 4 mmol) in dry THF (6 mL). Work-up afforded 3-[(benzylamino)methyl]-8-methoxy-coumarin **156c** as a yellow oil (0.37 g, 83%); υ_{max} / cm^{-1} 3380 (N-H) and 1717 (C=O); δ_H (400 MHz; $CDCl_3$) 1.97 (1H, br s, NH), 3.72 (2H, s, 1′-CH_2), 3.81 (2H, s, CH_2Ph), 3.91 (3H, s, OCH_3), 7.01 (2H, d, *J* = 7.9 Hz, Ar-H), 7.16 (1H, t, *J* = 7.9 Hz, ArH), 7.23-7.34 (5H, overlapping m, Ar-H) and 7.66 (1H, s, 4-H); δ_C (100 MHz; $CDCl_3$) 48.1 and 53.0 (CH_2), 56.0

(OCH_3), 112.7, 118.8, 119.7, 124.0, 126.8, 127.4, 127.9, 128.2, 139.0, 139.6, 142.5 and 146.7 (Ar-C) and 160.6 (C=O).

3-[(Benzylamino)methyl]-8-ethoxycoumarin 156d

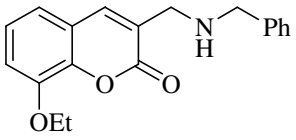

The procedure described for the synthesis of 3-[(benzylamino)methyl]coumarin **156a** was followed, using 3-(chloromethyl)-8-ethoxycoumarin **148d** (0.33 g, 1.4 mmol) and benzylamine (0.4 mL, 4 mmol) in dry THF (6 mL). Work-up afforded 3-[(benzylamino)methyl]-8-ethoxycoumarin **156d** as a pale yellow solid (0.34 g, 78%), m.p. 97-99 °C (lit.[273] 98-102 °C); υ_{max} / cm^{-1} 3400 (N-H) and 1713 (C=O); δ_H (400 MHz; $CDCl_3$) 1.50 (3H, t, *J* = 7.0 Hz, OCH_2CH_3), 1.86 (1H, br s, NH), 3.76 (2H, s, 1′-CH_2), 3.85 (2H, s, CH_2Ph), 4.19 (2H, q, *J* = 7.0 Hz, OCH_2CH_3), 7.04 (2H, d, *J* = 8.0 Hz, Ar-H), 7.17 (1H, t, *J* = 8.0 Hz, ArH), 7.23-7.37 (5H, overlapping m, Ar-H) and 7.68 (1H, s, 4-H); δ_C (100 MHz; $CDCl_3$) 14.8 (CH_3), 48.4 and 53.2 (CH_2N), 65.0 (OCH_2), 114.4, 119.0, 120.1, 124.2, 127.1, 127.7, 128.1, 128.4, 139.3, 139.9, 143.2 and 146.4 (Ar-C) and 161.0 (C=O).

3-[(Benzylamino)methyl]-6-chlorocoumarin 156e

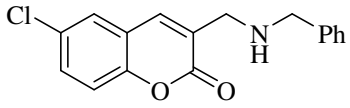

The procedure described for the synthesis of 3-[(benzylamino)methyl]coumarin **156a** was followed, using 6-chloro-3-(chloromethyl)coumarin **148e** (0.33 g, 1.5 mmol) and benzylamine (0.4 mL, 3.7 mmol) in dry THF (6 mL). Work-up afforded 3-[(benzylamino)methyl]-6-chlorocoumarin **156e** as a yellow solid (0.35 g, 80%), m.p. 106-108 °C (lit.[273] 106-110 °C); υ_{max} / cm^{-1} 3355 (N-H) and 1711 (C=O); δ_H (400 MHz; $CDCl_3$) 1.78 (1H, br s, NH), 3.76 (2H, s, 1′-CH_2), 3.86 (2H, s, CH_2Ph), 7.24-7.37 (6H, overlapping m, ArH), 7.42-7.46 (2H, m, ArH) and 7.66 (1H, s, 4-H); δ_C (100 MHz; $CDCl_3$) 48.2 and 53.3 (CH_2), 117.9, 120.4, 126.8, 127.2, 128.1, 128.5, 129.0, 129.7, 130.9, 137.7, 139.7 and 151.5 (Ar-C) and 160.8 (C=O).

3.5. CHLOROACETYLATION OF 3-[(BENZYLAMINO)METHYL]COUMARINS

N-Benzyl-2-chloro-*N*-[(coumarin-3-yl)methyl]acetamide 157a*

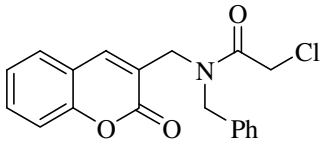

A mixture of 3-[(benzylamino)methyl]coumarin **156a** (0.35 g, 1.3 mmol) and chloroacetyl chloride (0.30 mL, 3.8 mmol) in dry THF (6 mL) was stirred under reflux for 45 minutes at 110 °C (oil bath). On cooling, the resulting mixture was crystallised from ethanol to afford *N*-benzyl-2-chloro-*N*-[(coumarin-3-yl)methyl]acetamide **157a** as a white solid (0.41 g, 91%), m.p. 98-99 °C (lit.[213] 98-100 °C); υ_{max} / cm^{-1} 1709 (O-C=O) and 1650 (N-C=O); δ_H (400 MHz; $CDCl_3$) 4.14-4.85 (6H, series of signals, 3 × CH_2), 7.24-7.58 (9H, overlapping m, ArH) and 7.84 (1H, s, 4-H).

N-Benzyl-*N*-[(6-bromocoumarin-3-yl)methyl]-2-chloroacetamide 157b*

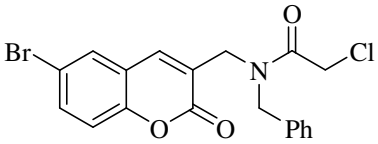

The procedure described for the synthesis of *N*-benzyl-2-chloro-*N*-[(coumarin-3-yl)methyl]acetamide **157a** was followed, using 3-[(benzylamino)methyl]-6-bromocoumarin **156b** (0.25 g, 0.73 mmol) and chloroacetyl chloride (0.20 mL, 2.5 mmol) in dry THF (6 mL). Crystallisation from ethanol afforded *N*-benzyl-*N*-[(6-bromocoumarin-3-yl)methyl]-2-chloroacetamide **157b** as a white solid (0.24 g, 78%), m.p. 109-111 °C (lit.[213] 109-111 °C); υ_{max} / cm^{-1} 1702 (O-C=O) and 1655 (N-C=O); δ_H (400 MHz; $CDCl_3$) 4.28-4.72 (6H, series of signals, 3 × CH_2), 7.24-7.39 and 7.72-7.80 (8H, overlapping m, ArH) and 7.95-7.80 (1H, series of signals, 4-H).

N-*Benzyl-2-chloro*-N-*[(8-methoxycoumarin-3-yl)methyl]acetamide* 157c*

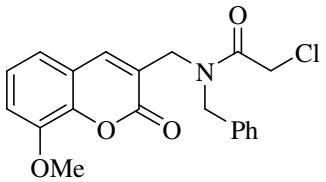

* *[13]C data not cited due to multiplicity of signals arising from rotamers at 303K.*

The procedure described for the synthesis of *N*-benzyl-2-chloro-*N*-[(coumarin-3-yl)methyl]acetamide **157a** was followed, using 3-[(benzylamino)methyl]-8-methoxycoumarin **156c** (0.38 g, 1.3 mmol) and chloroacetyl chloride (0.30 mL, 3.8 mmol) in dry THF (6 mL). Work-up afforded N-*benzyl-2-chloro*-N-*[(8-methoxycoumarin-3-yl)methyl]acetamide* **157c** as a white solid (0.41 g, 85%), m.p. 98-100 °C [HRMS: *m/z* calculated for $C_{20}H_{18}ClNO_4Na$ (MNa^+) 394.0822. Found 394.0836]; υ_{max} / cm^{-1}: 1716 (O-C=O) and 1649 (N-C=O); δ_H (400 MHz; $CDCl_3$) 3.93 (3H, s, OMe), 4.14-4.82 (6H, series of signals, 3 × CH_2), 7.00-7.45 (8H, overlapping m, ArH) and 7.77 (1H, s, 4-H).

_N_-Benzyl-2-chloro-_N_-[(8-ethoxycoumarin-3-yl)methyl]acetamide 157d[*,213]

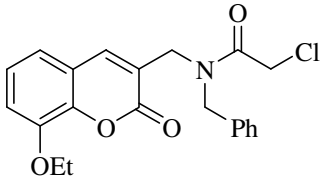

The procedure described for the synthesis of *N*-benzyl-2-chloro-*N*-[(coumarin-3-yl)methyl]acetamide **157a** was followed, using 3-[(benzylamino)methyl]-8-ethoxycoumarin **156d** (0.40 g, 1.3 mmol) and chloroacetyl chloride (0.30 mL, 3.8 mmol) in dry THF (6 mL). The mixture was then concentrated *in vacuo* and flash chromatographed [on silica gel; elution with hexane – EtOAc (3:2)] to afford *N*-benzyl-2-chloro-*N*-[(8-ethoxycoumarin-3-yl)methyl]-acetamide **157d** as a brown oil (0.49 g, 98%); υ_{max} / cm^{-1} 1721 (O-C=O) and 1648 (N-C=O); δ_H (400 MHz; $CDCl_3$) 1.48 (3H, t, *J* = 6.7 Hz, $OCH_2C\mathit{H}_3$), 4.09-4.86 (8H, series of signals, 4 × CH_2), 6.98-7.41 (8H, overlapping m, ArH) and 7.79 (1H, s, 4-H).

_N_-Benzyl-2-chloro-_N_-[(6-chlorocoumarin-3-yl)methyl]acetamide 157e[*]

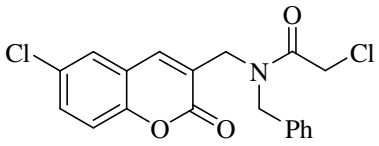

The procedure described for the synthesis of *N*-benzyl-2-chloro-*N*-[(coumarin-3-yl)methyl]acetamide **157a** was followed, using 3-[(benzylamino)methyl]-6-chlorocoumarin **156e** (0.40 g, 1.3 mmol) and chloroacetyl chloride (0.30 mL, 3.8 mmol) in dry THF (6 mL). Crystallisation from ethanol afforded *N*-benzyl-2-chloro-*N*-[(6-chlorocoumarin-3-yl)methyl]acetamide **157e** as a white solid (0.48 g, 96%), m.p. 109-111 °C (lit.[213] 109-111 °C);

υ_{max} / cm^{-1} 1699 (O-C=O) and 1664 (N-C=O); δ_H (400 MHz; $CDCl_3$) 4.14-4.83 (6H, series of signals, 3 × CH_2), 7.22-7.50 (8H, overlapping m, ArH) and 7.73 (1H, s, 4-H).

3.6. PROPARGYLATION OF CHLOROACETAMIDE DERIVATIVES

N-*Benzyl*-N-*[(coumarin-3-yl)methyl]-2-(2-propynylamino)acetamide* 168a[†]

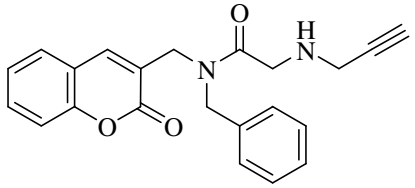

Propargylamine (0.3 mL, 4 mmol) was added to a solution of *N*-benzyl-2-chloro-*N*-[(coumarin-3-yl)methyl]acetamide **157a** (0.41 g, 1.2 mmol) in dry THF (5 mL) and the mixture stirred at r.t. for 48 h. The reaction mixture was then concentrated *in vacuo* and flash chromatographed [on silica gel; elution with hexane – EtOAc (3:2)] to afford N-*benzyl*-N-*[(coumarin-3-yl)methyl]-2-(2-propynylamino)acetamide* **168a** as a yellow oil (0.34 g, 79%) [HRMS: *m/z* calculated for $C_{22}H_{21}N_2O_3$ (MH^+) 361.1552. Found 361.1553]; υ_{max} / cm^{-1} 3195 (NH), 1708 (O-C=O) and 1630 (N-C=O); δ_H (600 MHz; $CDCl_3$) 2.02 (1H, br s, NH), 2.09-2.18 (1H, series of signals, C≡CH), 3.45-4.77 (8H, series of signals, 4 × CH_2), 7.18-7.56 (9H, overlapping m, ArH) and 7.82 (1H, s, 4-H).

N-*Benzyl*-N-*[(6-bromocoumarin-3-yl)methyl]-2-(2-propynylamino)acetamide* 168b[†]

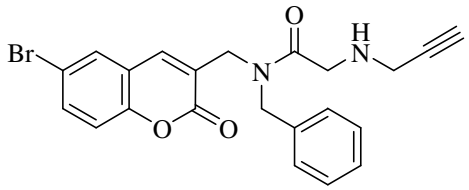

The procedure described for the synthesis of *N*-benzyl-*N*-[(coumarin-3-yl)methyl]-2-(2-propynylamino)acetamide **168a** was followed, using propargylamine (0.3 mL, 4 mmol) and *N*-benzyl-2-chloro-*N*-[(6-bromocoumarin-3-yl)methyl]acetamide **157b** (0.50 g, 1.2 mmol) in dry THF (5 mL). Work-up afforded N-*benzyl*-N-*[(6-bromocoumarin-3-yl)methyl]-2-(2-propynylamino)acetamide* **168b** as a light brown solid (0.45 g, 86%), m.p. 130-131 °C [HRMS: *m/z*

[†] *^{13}C data not cited due to multiplicity of signals arising from rotamers at 303 K.*

calculated for $C_{22}H_{20}BrN_2O_3$ (MH^+) 439.0657. Found 439.0661]; υ_{max} / cm^{-1} 3281 (NH), 1712 (O-C=O) and 1633 (N-C=O); δ_H (400 MHz; $CDCl_3$) 2.03 (1H, br s, NH), 2.12-2.16 (1H, series of signals, C≡CH), 3.47-4.72 (8H, series of signals, 4 × CH_2), 7.17-7.37 and 7.54-7.61 (8H, overlapping m, ArH) and 7.71 (1H, s, 4-H).

N-*Benzyl*-N-*[(8-methoxycoumarin-3-yl)methyl]-2-(2-propynylamino)acetamide* 168c[†]

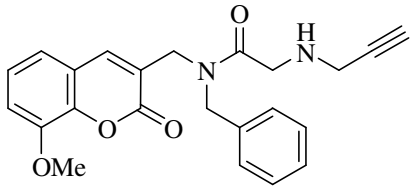

The procedure described for the synthesis of *N*-benzyl-*N*-[(coumarin-3-yl)methyl]-2-(2-propynylamino)acetamide **168a** was followed, using propargylamine (0.3 mL, 4 mmol) and *N*-benzyl-2-chloro-*N*-[(8-methoxycoumarin-3-yl)methyl]acetamide **157c** (0.45 g, 1.2 mmol) in dry THF (5 mL). Work-up afforded N-*benzyl*-N-*[(8-methoxycoumarin-3-yl)methyl]-2-(2-propynyl-amino)acetamide* **168c** as a brown solid (0.40 g, 86%), m.p. 104-106 °C [HRMS: *m/z* calculated for $C_{23}H_{23}N_2O_4$ (MH^+) 391.1658. Found 391.1661]; υ_{max} / cm^{-1} 3200 (NH), 1687 (O-C=O) and 1641 (N-C=O); δ_H (400 MHz; $CDCl_3$) 2.09-2.14 (1H, series of signals, C≡CH), 2.21 (1H, br s, NH), 3.43-3.61 and 4.33-4.70 (8H, series of signals, 4 × CH_2), 3.90 (3H, s, OCH_3), 6.94-7.34 (8H, overlapping m, ArH) and 7.72 (1H, s, 4-H).

N-*Benzyl*-N-*[(8-ethoxycoumarin-3-yl)methyl]-2-(2-propynylamino)acetamide* 168d[†]

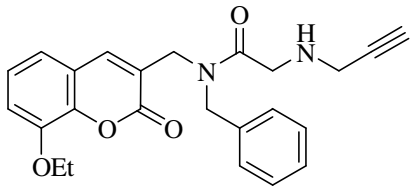

The procedure described for the synthesis of *N*-benzyl-*N*-[(coumarin-3-yl)methyl]-2-(prop-2-ynylamino)acetamide **168a** was followed, using propargylamine (0.3 mL, 4 mmol) and *N*-benzyl-2-chloro-*N*-[(8-ethoxycoumarin-3-yl)methyl]acetamide **157d** (0.46 g, 1.2 mmol) in dry THF (5 mL). Work-up afforded N-*benzyl*-N-*[(8-ethoxycoumarin-3-yl)methyl]-2-(2-propynyl-amino)acetamide* **168d** as a brown oil (0.40 g, 82%) [HRMS: *m/z* calculated for $C_{24}H_{25}N_2O_4$ (MH^+) 405.1814. Found 405.1823]; υ_{max} / cm^{-1} 3286 (NH), 1707 (O-C=O) and 1643 (N-C=O); δ_H (400 MHz; $CDCl_3$) 1.33 (3H, t, *J* = 6.8 Hz, OCH_2CH_3), 2.05-2.12 (1H, series of signals,

C≡CH), 2.49 (1H, br s, NH), 3.33-4.61 (10H, series of signals, 5 × CH_2), 6.86-7.31 (8H, overlapping m, ArH) and 7.61 (1H, s, 4-H).

N-*Benzyl*-N-*[(6-chlorocoumarin-3-yl)methyl]-2-(2-propynylamino)acetamide* 168e[†]

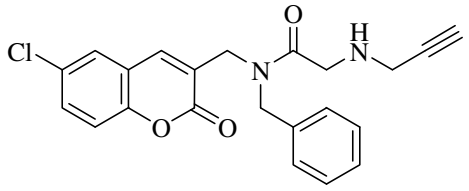

The procedure described for the synthesis of *N*-benzyl-*N*-[(coumarin-3-yl)methyl]-2-(2-propynylamino)acetamide **168a** was followed, using propargylamine (0.3 mL, 4.4 mmol) and *N*-benzyl-2-chloro-*N*-[(6-chlorocoumarin-3-yl)methyl]acetamide **157e** (0.45 g, 1.2 mmol) in dry THF (5 mL). Work-up afforded N-*benzyl*-N-*[(6-chlorocoumarin-3-yl)methyl]-2-(2-propynylamino)acetamide* **168e** as a pale yellow solid (0.40 g, 85%), m.p. 133-135 °C [HRMS: *m/z* calculated for $C_{22}H_{20}ClN_2O_3$ (MH^+) 395.1162. Found 395.1169]; υ_{max} / cm^{-1} 3230 (NH), 1714 (O-C=O) and 1633 (N-C=O); δ_H (400 MHz; $CDCl_3$) 2.05-2.20 (2H, series of signals, NH and C≡CH), 3.46-4.71 (8H, series of signals, 4 × CH_2), 7.20-7.47 (8H, overlapping m, ArH) and 7.71 (1H, s, 4-H).

3.7. CLICK REACTIONS OF COUMARIN DERIVATIVES

***Coumarin-AZT Conjugate* 167a**[‡]

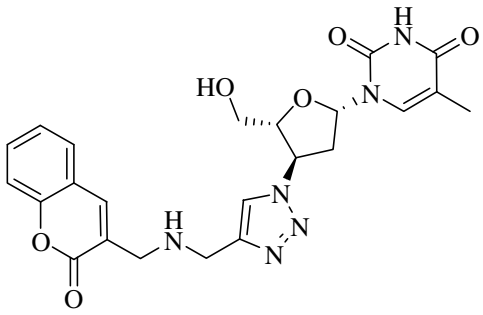

3'-Azido-3'-deoxythymidine (AZT) **2** (0.61 g, 2.3 mmol) was dissolved in H_2O-THF (1:1; 12 mL) and 3-[(2-propynylamino)methyl]coumarin **166a** (0.49 g, 2.3 mmol), sodium ascorbate (96 mg, 0.49 mmol) and $CuSO_4 \cdot 5H_2O$ (17 mg, 68 μmol) were added to the solution. After stirring

[‡] *4-{[(2*H*-1-Benzopyran-2-on-3-yl)methylamino]methyl}-1-[(2*R*,3*R*,5*S*)-5-(5-methyl-2,4-dioxo-1,2,3,4-tetrahydro-pyrimidin-1-yl)-2-(hydroxymethyl)tetrahydrofuran-3-yl]-1*H*-1,2,3-triazole* **167a**

for 24 h at room temperature, the mixture was extracted with CH_2Cl_2 (2 × 100 mL) and washed sequentially with H_2O (50 mL) and brine (30 mL). The organic layers were combined, dried over anhydrous $MgSO_4$, filtered and concentrated *in vacuo*. The crude material was purified by flash chromatography [on silica gel; elution with EtOAc and then with methanol – EtOAc (2:3)] to afford the *coumarin-AZT conjugate* **167a** (0.72 g, 65%) as a light brown solid, m.p. 125-127 °C [HRMS: *m/z* calculated for $C_{23}H_{25}N_6O_6$ (MH^+) 481.1836. Found 481.1823]; υ_{max} / cm^{-1} 3291 (OH) and 1684 (C=O); δ_H (400 MHz; methanol-d_4) 1.90 (3H, s, CH_3), 2.70 and 2.85 (2H, m, CH_2CHN), 3.72 and 3.95 (4H, s, 2 × NCH_2), 3.76 (1H, dd, *J* = 3.2 and 12.3 Hz, CH_aOH) 3.89 (1H, dd, *J* = 2.9 and 12.2 Hz, CH_bOH), 4.30-4.34 (1H, m, OCHC*H*N), 5.37-5.42 (1H, m, OC*H*CH_2OH), 6.47 (1H, t, *J* = 6.5 Hz, OCHN), 7.32-7.35 (2H, m, ArH), 7.54-7.59 (1H, m, ArH), 7.63 (1H, dd, *J* = 1.3 and 7.9 Hz, ArH), 7.90 (1H, s, ArH), 7.93 (1H, s, ArH) and 8.05 (1H, s, ArH); δ_C (100 MHz; methanol-d_4) 10.0 (CH_3), 36.5 (*C*H_2CHN), 41.8 and 46.4 (CH_2N), 58.5 (CHN), 59.6 (CH_2O), 83.9 ($HOCH_2$*C*HO), 84.2 (NCHO), 109.2, 114.8, 118.2, 121.6, 123.3, 125.0, 126.8, 130.1, 135.7, 139.3, 144.9, 150.0, 152.1, 160.6 and 164.2 (Ar-C and C=O).

***Coumarin-AZT Conjugate* 167b**

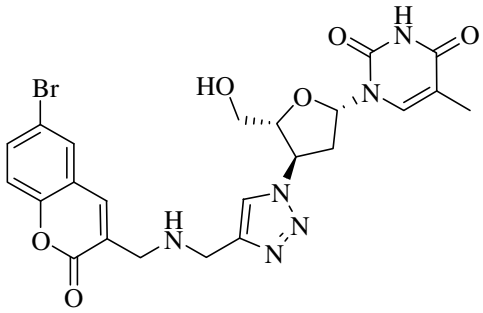

The procedure described for the synthesis of coumarin-AZT conjugate **167a** was followed, using AZT **2** (0.32 g, 1.2 mmol), 6-bromo-3-[(2-propynylamino)methyl]coumarin **166b** (0.35 g, 1.2 mmol), sodium ascorbate (96 mg, 0.49 mmol) and $CuSO_4 \cdot 5H_2O$ (17 mg, 68 μmol) in H_2O-THF (1:1; 12 mL). Work-up afforded the *coumarin-AZT conjugate* **167b** (0.51 g, 76%) as an off-white solid, m.p. 129-130 °C [HRMS: *m/z* calculated for $C_{23}H_{24}BrN_6O_6$ (MH^+) 559.0941. Found 559.0922]; υ_{max} / cm^{-1} 3367 (OH) and 1674 (C=O); δ_H (400 MHz; DMSO-d_6) 1.82 (3H, s, CH_3), 2.60-2.72 (2H, m, CH_2CHN), 3.59-3.72 (4H, overlapping s and dd, CH_2OH and NCH_2CC=O), 3.84 (2H, s, NCH_2CN), 4.16-4.22 (1H, m, OCHC*H*N), 5.33-5.39 (1H, m, OC*H*CH_2OH), 6.42 (1H, t, *J* = 6.5 Hz, OCHN), 7.38 (1H, d, *J* = 8.8 Hz, ArH), 7.72 (1H, d, *J* = 8.8 Hz, ArH), 7.83 (1H, s, ArH), 7.98 (2H, overlapping s, ArH), 8.21 (1H, s, ArH) and 11.38 (1H, br s, NHC=O); δ_C

(100 MHz; DMSO-d_6) 13.2 (CH_3), 38.0 (CH_2CHN), 44.4 and 48.0 (CH_2N), 60.0 (CHN), 61.6 (CH_2O), 84.8 (HOCH_2CHO), 85.4 (NCHO), 110.5, 117.0, 119.1, 122.0, 123.4, 129.5, 131.0, 134.2, 137.1, 138.1, 147.3, 151.4, 152.4, 160.9 and 164.7 (Ar-C and C=O).

***Coumarin-AZT Conjugate* 167c**

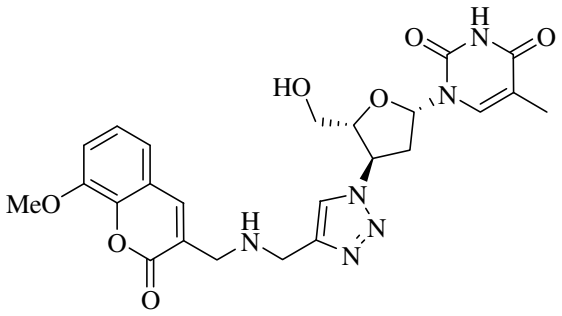

The procedure described for the synthesis of coumarin-AZT conjugate **167a** was followed, using AZT **2** (0.32 g, 1.2 mmol), 8-methoxy-3-[(2-propynylamino)methyl]coumarin **166c** (0.29 g, 1.2 mmol), sodium ascorbate (96 mg, 0.49 mmol) and $CuSO_4 \cdot 5H_2O$ (17 mg, 68 μmol) in H_2O-THF (1:1; 12 mL). Work-up afforded the *coumarin-AZT conjugate* **167c** (0.45 g, 75%) as a yellow solid, m.p. 126-127 °C [HRMS: *m/z* calculated for $C_{24}H_{27}N_6O_7$ (MH^+) 511.1941. Found 511.1940]; υ_{max} / cm^{-1} 3291 (OH) and 1671 (C=O); δ_H (400 MHz; DMSO-d_6) 1.81 (3H, s, CH_3), 2.58-2.75 (2H, m, CH_2CHN), 3.59-3.71 (4H, overlapping s and dd, CH_2OH and NCH_2CC=O), 3.83 (2H, s, NCH_2CN), 3.90 (3H, s, OMe), 4.16-4.21 (1H, m, OCHC*H*N), 5.27-5.37 (2H, m, OC*H*CH_2OH and OH), 6.41 (1H, t, J = 5.6 Hz, OCHN), 7.23-7.32 (3H, m, ArH), 7.81 (1H, s, ArH), 7.95 (1H, s, ArH), 8.18 (1H, s, ArH) and 11.36 (1H, br s, NHC=O); δ_C (100 MHz; DMSO-d_6) 13.1 (CH_3), 38.0 (CH_2CHN), 44.4 and 48.0 (CH_2N), 56.9 (OCH_3), 59.9 (CHN), 61.6 (CH_2O), 84.7 (HOCH_2CHO), 85.4 (NCHO), 110.5, 114.2, 120.1, 120.6, 123.3, 125.3, 128.3, 137.1, 139.7, 142.7, 147.3, 147.4, 151.3, 161.1 and 164.7 (Ar-C and C=O).

***Coumarin-AZT Conjugate* 167d**

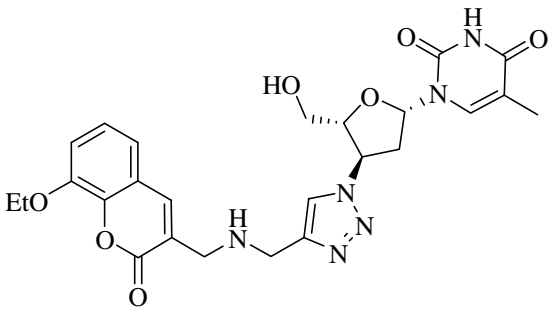

The procedure described for the synthesis of coumarin-AZT conjugate **167a** was followed, using AZT **2** (0.32 g, 1.2 mmol), 8-ethoxy-3-[(2-propynylamino)methyl]coumarin **166d** (0.31 g, 1.2 mmol), sodium ascorbate (96 mg, 0.49 mmol) and $CuSO_4 \cdot 5H_2O$ (17 mg, 68 μmol) in H_2O-THF (1:1; 12 mL). Work-up afforded the *coumarin-AZT conjugate* **167d** (0.44 g, 70%) as a yellow solid, m.p. 114-116 °C [HRMS: *m/z* calculated for $C_{25}H_{29}N_6O_7$ (MH^+) 525.2079. Found 525.2077]; υ_{max} / cm^{-1} 3306 (OH) and 1679 (C=O); δ_H (400 MHz; DMSO-d_6) 1.40 (3H, t, *J* = 6.9 Hz, OCH_2CH_3), 1.81 (3H, s, CH_3), 2.58-2.73 (2H, m, CH_2CHN), 3.60-3.71 (4H, overlapping s and dd, CH_2OH and $NCH_2CC{=}O$), 3.83 (2H, s, NCH_2CN), 4.14-4.20 (3H, overlapping m and q, OCHCHN and OCH_2CH_3), 5.31-5.38 (2H, m, $OCHCH_2OH$ and OH), 6.41 (1H, t, *J* = 6.5 Hz, OCHN), 7.23-7.28 (3H, m, ArH), 7.82 (1H, s, ArH), 7.94 (1H, s, ArH), 8.19 (1H, s, ArH) and 11.43 (1H, br s, NHC=O); δ_C (100 MHz; DMSO-d_6) 13.1 and 15.5 (2 × CH_3), 38.0 (CH_2CHN), 44.5 and 48.0 (CH_2N), 59.9 (CHN), 61.6 and 65.2 (2 × CH_2O), 84.8 ($HOCH_2CHO$), 85.4 (NCHO), 110.5, 115.1, 120.1, 120.6, 123.3, 125.3, 128.2, 137.1, 139.8, 142.8, 146.5, 147.4, 151.3, 161.2 and 164.6 (Ar-C and C=O).

***Coumarin-AZT Conjugate* 167e**

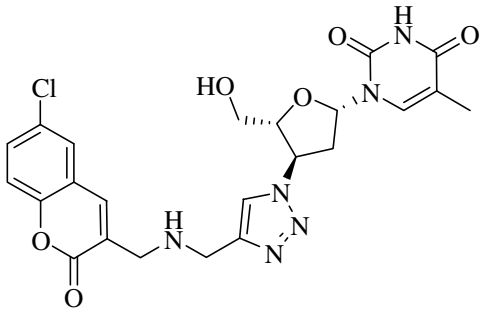

The procedure described for the synthesis of coumarin-AZT conjugate **167a** was followed, using AZT **2** (0.32 g, 1.2 mmol), 6-chloro-3-[(2-propynylamino)methyl]coumarin **166e** (0.30 g, 1.2 mmol), sodium ascorbate (96 mg, 0.49 mmol) and $CuSO_4 \cdot 5H_2O$ (17 mg, 68 μmol) in H_2O-THF (1:1; 12 mL). Work-up afforded the *coumarin-AZT conjugate* **167e** (0.40 g, 64%) as an off-white solid, m.p. 103-105 °C [HRMS: *m/z* calculated for $C_{23}H_{24}ClN_6O_6$ (MH^+) 515.1446. Found 515.1435]; υ_{max} / cm^{-1} 3260 (OH) and 1679 (C=O); δ_H (400 MHz; DMSO-d_6) 1.80 (3H, s, CH_3), 2.58-2.74 (2H, m, CH_2CHN), 3.60-3.71 (4H, overlapping s and dd, CH_2OH and $NCH_2CC{=}O$), 3.82 (2H, s, NCH_2CN), 4.16 (1H, dd, *J* = 8.2 and 3.5 Hz, OCHCHN), 5.37-5.43 (1H, m, $OCHCH_2OH$), 5.46 (1H, t, *J* = 4.60 Hz, OH), 6.41 (1H, t, *J* = 6.6 Hz, OCHN), 7.43 (1H, d, *J* = 8.8 Hz, ArH), 7.59 (1H, dd, *J* = 8.8 and 2.4 Hz, ArH), 7.86 (2H, d, *J* = 2.6 Hz, ArH), 7.98 (1H,

s, ArH), 8.23 (1H, s, ArH) and 11.34 (1H, br s, NHC=O); δ_C (100 MHz; DMSO-d_6) 13.1 (CH_3), 38.0 (CH_2CHN), 44.4 and 48.0 (CH_2N), 60.0 (CHN), 61.6 (CH_2O), 84.8 ($HOCH_2CHO$), 85.4 (NCHO), 110.5, 118.8, 121.5, 123.5, 128.0, 129.1, 129.4, 131.5, 137.1, 138.3, 147.2, 151.3, 151.9, 160.9 and 164.6 (Ar-C and C=O).

N-*Benzylated Coumarin-AZT Conjugate* 169a[§]

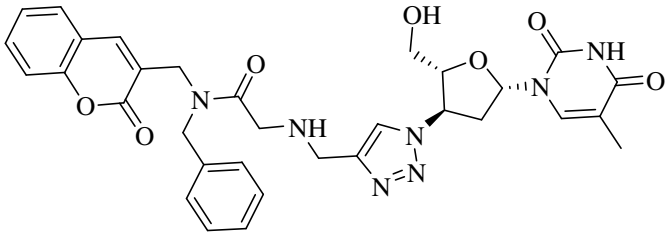

3'-Azido-3'-deoxythymidine **2** (0.25 g, 0.90 mmol) was dissolved in H_2O-THF (1:1; 12 mL) and *N*-benzyl-*N*-[(coumarin-3-yl)methyl]-2-(2-propynylamino)acetamide **168a** (0.29 g, 0.80 mmol), sodium ascorbate (96 mg, 0.49 mmol) and $CuSO_4 \cdot 5H_2O$ (17 mg, 68 μmol) were added to the solution. After stirring for 24 h at room temperature, the mixture was extracted with CH_2Cl_2 (2 × 100 mL) and washed sequentially with H_2O (50 mL) and brine (30 mL). The organic layers were combined, dried over anhydrous $MgSO_4$, filtered and concentrated *in vacuo*. The crude material was purified by flash chromatography [on silica gel; elution with EtOAc and then with methanol – DCM (1:4)] to afford the N-*benzylated coumarin-AZT conjugate* **169a** (0.35 g, 70%) as a yellow solid, m.p. 160-162 °C [HRMS: *m/z* calculated for $C_{32}H_{34}N_7O_7$ (MH^+) 628.2520. Found 628.2523]; υ_{max} / cm^{-1} 3327 (OH), 1707 and 1661 (C=O); δ_H (400 MHz; DMSO-d_6) 1.22 (1H, br s, CH_2NH), 1.81 (3H, s, CH_3), 2.08 (4H, s, 2 × CH_2NH), 2.53-2.71 (2H, m, CH_2CHN), 3.58-3.79 (4H, series of signals, CH_2OH and NCH_2CC=O), 4.14 (1H, br s, OH), 4.29-4.35 (1H, m, OCHCHN), 4.55-4.70 (2H, series of signals, NCH_2Ph), 5.35-5.48 (1H, m, $OCHCH_2OH$), 6.35-6.44 (1H, m, OCHN), 7.20-7.87 (11H, overlapping m, ArH), 8.14 (1H, s, ArH) and 11.32 (1H, br s, NHC=O).

[§] *4-[6-(2H-1-Benzopyran-2-on-3-yl)-5-benzyl-4-oxo-3,5-diazahexyl]methyl}-1-[(2R,3R,5S)-5-(5-methyl-2,4-dioxo-1,2,3,4-tetrahydro-pyrimidin-1-yl)-2-(hydroxymethyl)tetrahydrofuran-3-yl]-1H-1,2,3-triazole* **169a**.
[13]C data not cited due to multiplicity of signals arising from rotamers at 30 °C.

N-*Benzylated Coumarin-AZT Conjugate* 169b[§]

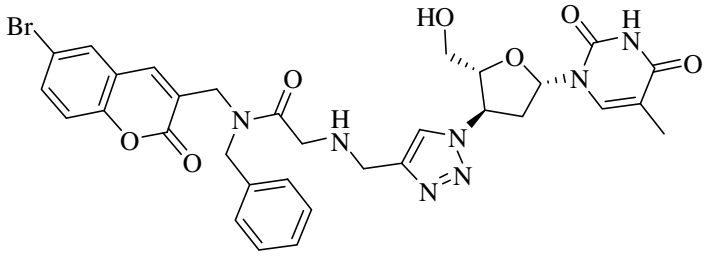

The procedure described for the synthesis of *N*-benzylated coumarin-AZT conjugate **169a** was followed, using AZT **2** (0.25 g, 0.90 mmol), *N*-benzyl-*N*-[(6-bromocoumarin-3-yl)methyl]-2-(2-propynylamino)acetamide **168b** (0.35 g, 0.80 mmol), sodium ascorbate (96 mg, 0.49 mmol) and $CuSO_4 \cdot 5H_2O$ (17 mg, 68 μmol) in H_2O-THF (1:1; 12 mL). Work-up afforded the N-*benzylated coumarin-AZT conjugate* **169b** (0.45 g, 80%) as a yellow solid, m.p. 171-173 °C [HRMS: *m/z* calculated for $C_{32}H_{33}BrN_7O_7$ (MH^+) 706.1625. Found 706.1654]; υ_{max} / cm^{-1} 3372 (OH), 1656 (C=O); δ_H (400 MHz; DMSO-d_6) 1.20 (1H, br s, CH_2NH), 1.82 (3H, s, CH_3), 1. 98 (2H, s, CH_2CO), 2.53-2.72 (2H, m, CH_2CHN), 3.17 (2H, s, $NHCH_2CN$), 3.57-3.80 (4H, series of signals, CH_2OH and $NCH_2CC{=}O$), 4.16 (1H, br s, OH), 4.28-4.36 (1H, m, $OCHCHN$), 4.52-4.69 (2H, series of signals, NCH_2Ph), 5.22-5.39 (1H, m, $OCHCH_2OH$), 6.36-6.42 (1H, m, OCHN), 7.20-7.38 (6H, overlapping m, ArH), 7.70-7.81 (3H, overlapping m, ArH), 7.99 (1H, s, ArH), 8.10 (1H, s, ArH) and 11.32 (1H, br s, NHC=O).

N-*Benzylated Coumarin-AZT Conjugate* 169c[§]

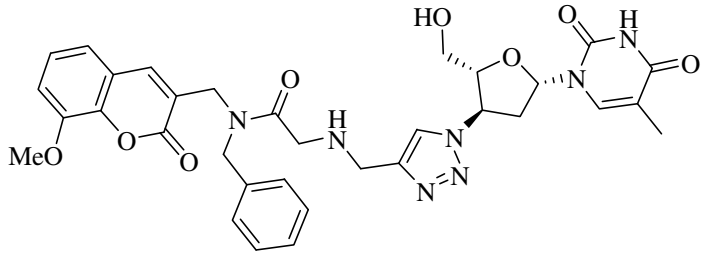

The procedure described for the synthesis of *N*-benzylated coumarin-AZT conjugate **169a** was followed, using AZT **2** (0.25 g, 0.90 mmol), *N*-benzyl-*N*-[(8-methoxycoumarin-3-yl)methyl]-2-(2-propynylamino)acetamide **168c** (0.31 g, 0.80 mmol), sodium ascorbate (96 mg, 0.49 mmol) and $CuSO_4 \cdot 5H_2O$ (17 mg, 68 μmol) in H_2O-THF (1:1; 12 mL). Work-up afforded the N-*benzylated coumarin-AZT conjugate* **169c** (0.38 g, 72%) as a yellow solid, m.p. 122-124 °C [HRMS: *m/z* calculated for $C_{33}H_{36}N_7O_8$ (MH^+) 658.2625. Found 658.2616]; υ_{max} / cm^{-1} 3281 (OH), 1684 and 1651 (C=O); δ_H (400 MHz; DMSO-d_6) 1.22 (1H, br s, CH_2NH), 1.81 (3H, s,

CH_3), 1.98 (2H, s, CH_2CO), 2.56-2.73 (2H, m, CH_2CHN), 3.25 (2H, s, NHCH_2CN), 3.58-3.75 (4H, series of signals, CH_2OH and NCH_2CC=O), 3.80-3.91 (3H, series of signals, OCH_3), 4.16 (1H, br s, OH), 4.31-4.33 (1H, m, OCHC*H*N), 4.52-4.69 (2H, series of signals, NCH_2Ph), 5.25-5.39 (1H, m, OC*H*CH_2OH), 6.37-6.44 (1H, m, OCHN), 7.15-7.37 (9H, overlapping m, ArH), 7.80-7.82 (1H, m, ArH), 8.11 (1H, s, ArH) and 11.35 (1H, br s, NHC=O).

N-*Benzylated Coumarin-AZT Conjugate* 169d[§]

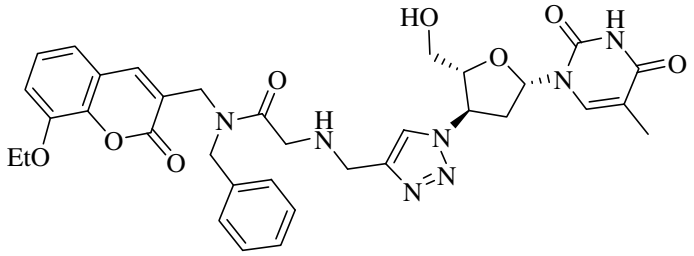

The procedure described for the synthesis of *N*-benzylated coumarin-AZT conjugate **169a** was followed, using AZT **2** (0.25 g, 0.9 mmol), *N*-benzyl-*N*-[(8-ethoxycoumarin-3-yl)methyl]-2-(2-propynylamino)acetamide **168d** (0.32 g, 0.8 mmol), sodium ascorbate (96 mg, 0.49 mmol) and $CuSO_4 \cdot 5H_2O$ (17 mg, 68 μmol) in H_2O-THF (1:1; 12 mL). Work-up afforded the N-*benzylated coumarin-AZT conjugate* **169d** (0.41 g, 78%) as a yellow solid, m.p. 144-146 °C [HRMS: *m/z* calculated for $C_{34}H_{38}N_7O_8$ (MH^+) 672.2782. Found 672.2753]; υ_{max} / cm^{-1} 3362 (OH), 1692 and 1659 (C=O); δ_H (400 MHz; DMSO-d_6) 1.21 (1H, br s, CH_2NH), 1.37 (3H, series of signals, OCH_2CH_3), 1.81 (3H, s, $ArCH_3$), 2.07 (4H, s, 2 × CH_2N), 2.53-2.72 (2H, m, CH_2CHN), 3.58-3.79 (4H, series of signals, CH_2OH and NCH_2CC=O), 4.14-4.17 (3H, series of signals, OH and OCH_2CH_3), 4.31-4.33 (1H, m, OCHC*H*N), 4.50-4.69 (2H, series of signals, NCH_2Ph), 5.32-5.41 (1H, m, OC*H*CH_2OH), 6.37-6.43 (1H, m, OCHN), 7.14-7.37 (8H, overlapping m, ArH), 7.71-7.86 (2H, m, ArH), 8.14 (1H, s, ArH) and 11.35 (1H, br s, NHC=O).

N-*Benzylated Coumarin-AZT Conjugate* 169e[§]

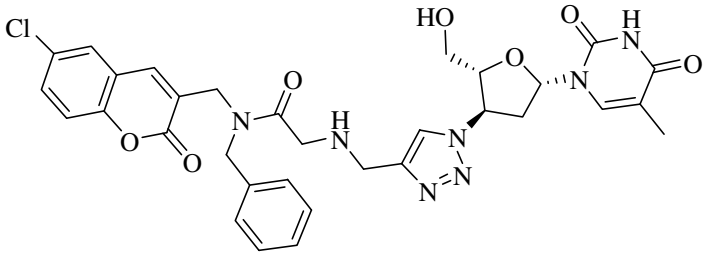

The procedure described for the synthesis of N-*benzylated coumarin-AZT conjugate* **169a** was followed, using AZT **2** (0.25 g, 0.90 mmol), N-*benzyl*-N-*[(6-bromocoumarin-3-yl)methyl]-2-(2-propynylamino)acetamide* **168e** (0.32 g, 0.80 mmol), sodium ascorbate (96 mg, 0.49 mmol) and $CuSO_4 \cdot 5H_2O$ (17 mg, 68 μmol) in H_2O-THF (1:1; 12 mL) mixture. Work-up afforded the N-*benzylated coumarin-AZT conjugate* **169e** (0.40 g, 74%) as a yellow solid, m.p. 140-142 °C [HRMS: *m/z* calculated for $C_{32}H_{33}ClN_7O_7$ (MH^+) 662.2130. Found 662.2115]; υ_{max} / cm^{-1} 3341 (OH), 1687 and 1649 (C=O); δ_H (400 MHz; DMSO-d_6) 1.18 (1H, br s, CH_2NH), 1.81 (3H, s, CH_3), 2.08 (4H, s, 2 × CH_2N), 2.58-2.72 (2H, m, CH_2CHN), 3.61-3.84 (4H, series of signals, CH_2OH and $NCH_2CC{=}O$), 4.16 (1H, br s, OH), 4.29-4.36 (1H, m, OCHCHN), 4.54-4.65 (2H, series of signals, NCH_2Ph), 5.23-5.37 (1H, m, $OCHCH_2OH$), 6.38-6.43 (1H, m, OCHN), 7.14-7.87 (10H, overlapping m, ArH), 8.14 (1H, series of signals, ArH) and 11.33 (1H, br s, NHC=O).

3.8. SYNTHESIS OF CINNAMATE DERIVATIVES

3.8.1. Aza-Michael Reaction of Baylis-Hillman Adducts with Piperidine

tert-*Butyl 3-hydroxy-3-(2-hydroxyphenyl)-2-[(piperidin-1-yl)methyl]propanoate* 170a

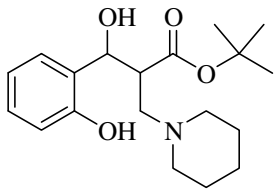

Piperidine (0.4 mL, 4.4 mmol) was added to a solution of *tert*-butyl 3-hydroxy-3-(2-hydroxyphenyl)-2-methylenepropanoate **153a** (0.55 g, 2.2 mmol) in dry THF (5 mL) and the mixture stirred at r.t. for 48 h. The reaction mixture was then concentrated *in vacuo* and flash chromatographed [on silica gel; elution with hexane – EtOAc (1:1)] to afford tert-*butyl 3-hydroxy-3-(2-hydroxyphenyl)-2-[(piperidin-1-yl)methyl]propanoate* **170a** as a pale yellow solid (0.62 g, 84%), m.p. 67-69 °C [HRMS: *m/z* calculated for $C_{19}H_{28}NO_4$ $(M-H)^+$ 334.2018. Found 334.2018]; υ_{max} / cm^{-1} 3276 (OH) and 1719 (C=O); δ_H (400 MHz; $CDCl_3$) 1.20 [9H, s, $C(CH_3)_3$], 1.48-1.52 (2H, m, $CH_2CH_2CH_2N$), 1.60-1.68 (4H, m, 2 × CH_2CH_2N), 2.39-2.52 (2H, series of signals, CH_aCH_2N), 2.66-2.78 (3H, series of signals, CH_bCH_2N and $CHCH_cN$), 2.98 (1H, t, J = 12.3 Hz, $CHCH_dN$), 3.14 (1H, ddd, J =12.3, 9.4 and 3.0 Hz, CHCO), 5.10 (1H, d, J = 9.4 Hz, CHOH), 6.74 (1H, t, J = 7.4 Hz, ArH), 6.86 (1H, d, J = 7.9 Hz, ArH), 6.95 (1H, d, J = 7.4 Hz,

ArH) and 7.15 (1H, t, J = 7.9 Hz, ArH); δ_C (100 MHz; $CDCl_3$) 23.8, 25.6 and 54.6 ($CH_2CH_2CH_2N$), 27.7 [$C(CH_3)_3$], 47.6 ($CHCO$), 60.9 ($CHCH_2N$), 79.1 (CHOH), 81.2 [$C(CH_3)_3$], 117.0, 119.1, 124.9, 128.2 and 129.0 (Ar-C), 156.6 [ArC(OH)] and 170.3 (C=O).

tert-*Butyl 3-(5-bromo-2-hydroxyphenyl)-3-hydroxy-2-[(piperidin-1-yl)methyl]propanoate* 170b

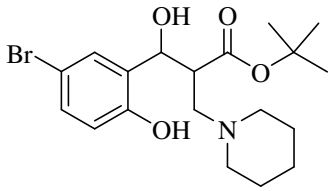

The procedure described for the synthesis of *tert*-butyl 3-hydroxy-3-(2-hydroxyphenyl)-2-[(piperidin-1-yl)methyl]propanoate **170a** was followed, using piperidine (0.4 mL, 4 mmol) and *tert*-butyl 3-(5-bromo-2-hydroxyphenyl)-3-hydroxy-2-methylenepropanoate **153b** (0.72 g, 2.2 mmol) in dry THF (5 mL). Work-up afforded tert-*butyl 3-(5-bromo-2-hydroxyphenyl)-3-hydroxy-2-[(piperidin-1-yl)methyl]propanoate* **170b** as a yellow solid (0.89 g, 97%), m.p. 89-91 °C [HRMS: *m/z* calculated for $C_{19}H_{27}BrNO_4$ $(M-H)^+$ 412.1123. Found 412.1138]; υ_{max} / cm^{-1} 3200 (OH) and 1719 (C=O); δ_H (400 MHz; $CDCl_3$) 1.28 [9H, s, $C(CH_3)_3$], 1.46-1.53 (2H, m, $CH_2CH_2CH_2N$), 1.59-1.69 (4H, m, 2 × CH_2CH_2N), 2.38-2.51 (2H, series of signals, CH_aCH_2N), 2.66-2.75 (3H, series of signals, CH_bCH_2N and $CHCH_cN$), 2.96 (1H, t, J = 12.3 Hz, $CHCH_dN$), 3.08 (1H, ddd, J = 12.3, 9.3 and 3.0 Hz, CHCO), 5.05 (1H, d, J = 9.3 Hz, $CHOH$), 6.74 (1H, d, J = 8.6 Hz, ArH), 7.06 (1H, d, J = 2.4 Hz, ArH) and 7.24 (1H, dd, J = 8.6 and 2.4 Hz, ArH); δ_C (100 MHz; $CDCl_3$) 23.7, 25.7 and 54.8 ($CH_2CH_2CH_2N$), 27.7 [$C(CH_3)_3$], 47.6 ($CHCO$), 60.8 ($CHCH_2N$), 78.3 (CHOH), 81.9 [$C(CH_3)_3$], 111.1, 119.1, 126.9, 130.7 and 131.8 (Ar-C), 155.9 [ArC(OH)] and 170.0 (C=O).

tert-*Butyl 3-(3-ethoxy-2-hydroxyphenyl)-3-hydroxy-2-[(piperidin-1-yl)methyl]propanoate* 170d

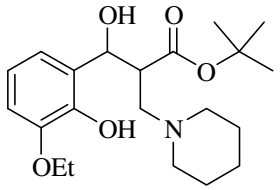

The procedure described for the synthesis of *tert*-butyl 3-hydroxy-3-(2-hydroxyphenyl)-2-[(piperidin-1-yl)methyl]propanoate **170a** was followed, using piperidine (0.4 mL, 4 mmol) and *tert*-butyl 3-(3-ethoxy-2-hydroxyphenyl)-3-hydroxy-2-methylenepropanoate **153d** (0.65 g, 2.2 mmol) in dry THF (5 mL). Work-up afforded tert-*butyl 3-(3-ethoxy-2-hydroxyphenyl)-3-*

hydroxy-2-[(piperidin-1-yl)methyl]propanoate **170d** as a brown oil (0.77 g, 93%), [HRMS: *m/z* calculated for $C_{21}H_{32}NO_5$ $(M-H)^+$ 378.2280. Found 378.2285]; υ_{max} / cm^{-1} 3422 (OH) and 1712 (C=O); δ_H (400 MHz; $CDCl_3$) 1.20 [9H, s, $C(CH_3)_3$], 1.42-1.50 (5H, overlapping t and m, $CH_2CH_2CH_2N$ and OCH_2CH_3), 1.56-1.70 (4H, m, 2 × CH_2CH_2N), 2.37-2.53 (2H, series of signals, CH_aCH_2N), 2.62-2.77 (3H, series of signals, CH_bCH_2N and $CHCH_cN$), 2.99 (1H, t, *J* = 12.3 Hz, $CHCH_dN$), 3.18 (1H, ddd, *J* = 12.3, 9.5 and 3.2 Hz, CHCO), 4.09 (2H, q, *J* = 6.9 Hz, OCH_2CH_3), 5.15 (1H, d, *J* = 9.5 Hz, CHOH), 6.66-6.72 (2H, m, ArH) and 6.79 (1H, dd, *J* = 1.8 and 7.4 Hz, ArH); δ_C (100 MHz; $CDCl_3$) 14.9 (OCH_2CH_3), 23.9, 25.8 and 54.7 ($CH_2CH_2CH_2N$), 27.8 [$C(CH_3)_3$], 47.5 (*C*HCO), 61.1 ($CHCH_2N$), 64.5 (OCH_2), 77.8 (CHOH), 81.0 [$C(CH_3)_3$], 112.7, 118.9, 120.6 and 126.1(Ar-C), 145.8 and 147.3 [ArC(OH) and ArC(OEt)] and 170.6 (C=O).

tert-*Butyl 3-(5-chloro-2-hydroxyphenyl)-3-hydroxy-2-[(piperidin-1-yl)methyl]propanoate* 170e

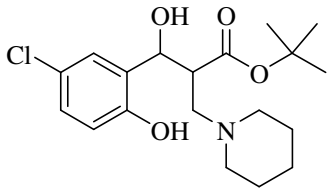

The procedure described for the synthesis of *tert*-butyl 3-hydroxy-3-(2-hydroxyphenyl)-2-[(piperidin-1-yl)methyl]propanoate **170a** was followed, using piperidine (0.4 mL, 4 mmol) and *tert*-butyl 3-(5-chloro-2-hydroxyphenyl)-3-hydroxy-2-methylenepropanoate **153e** (0.63 g, 2.2 mmol) in dry THF (5 mL). Work-up afforded tert-*butyl 3-(5-chloro-2-hydroxyphenyl)-3-hydroxy-2-[(piperidin-1-yl)methyl]propanoate* **170e** as a yellow solid (0.77 g, 95%), m.p. 81-82 °C [HRMS: *m/z* calculated for $C_{19}H_{27}ClNO_4$ $(M-H)^+$ 368.1629. Found 368.1644]; υ_{max} / cm^{-1} 3423 (OH) and 1719 (C=O); δ_H (400 MHz; $CDCl_3$) 1.27 [9H, s, $C(CH_3)_3$], 1.46-1.52 (2H, m, $CH_2CH_2CH_2N$), 1.58-1.70 (4H, m, 2 × CH_2CH_2N), 2.40-2.51 (2H, series of signals, CH_aCH_2N), 2.65-2.77 (3H, series of signals, CH_bCH_2N and $CHCH_cN$), 2.96 (1H, t, *J* = 12.3 Hz, $CHCH_dN$), 3.09 (1H, ddd, *J* = 12.3, 9.2 and 3.1Hz, CHCO), 5.05 (1H, d, *J* = 9.2 Hz, CHOH), 6.79 (1H, d, *J* = 8.6 Hz, ArH), 6.93 (1H, d, *J* = 2.6 Hz, ArH) and 7.10 (1H, dd, *J* = 8.6 and 2.6 Hz, ArH); δ_C (100 MHz; $CDCl_3$) 23.8, 25.7 and 54.8 ($CH_2CH_2CH_2N$), 27.8 [$C(CH_3)_3$], 47.6 (*C*HCO), 60.7 ($CHCH_2N$), 78.3 (CHOH), 81.9 [$C(CH_3)_3$], 118.6, 123.8, 126.3, 127.8 and 128.8 (Ar-C), 155.3 [ArC(OH)] and 170.1 (C=O).

3.8.2. Aza-Michael Reaction of Baylis-Hillman Adducts with Propargylamine

tert-*Butyl 3-hydroxy-3-(2-hydroxyphenyl)-2-[(2-propynylamino)methyl]propanoate* 171a

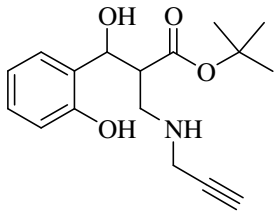

Propargylamine (0.3 mL, 4 mmol) was added to a solution of *tert*-butyl 3-hydroxy-3-(2-hydroxyphenyl)-2-methylenepropanoate **153a** (0.55 g, 2.2 mmol) in dry THF (5 mL) and the mixture stirred at r.t. for 48 h. The reaction mixture was then concentrated *in vacuo* and flash chromatographed [on silica gel; elution with hexane – EtOAc (1:1)] to afford tert-*butyl 3-hydroxy-3-(2-hydroxyphenyl)-2-[(2-propynylamino)methyl]propanoate* **171a** as a white solid (0.67 g, 99%), m.p. 68-70 °C [HRMS: *m/z* calculated for $C_{17}H_{24}NO_4$ (MH^+) 306.1705. Found 306.1698]; υ_{max} / cm^{-1} 3458 (OH) and 1709 (C=O); δ_H (400 MHz; $CDCl_3$) 1.28 [9H, s, $C(CH_3)_3$], 2.26 (1H, t, *J* = 2.4 Hz, C≡CH), 3.03 (1H, dt, *J* = 7.4 and 4.6 Hz, CHCO), 3.08-3.18 (2H, series of signals, CHCH_2), 3.41 (2H, d, *J* = 2.4 Hz, CH_2C≡CH), 5.21 (1H, d, *J* = 7.4 Hz, C*H*OH), 6.77 (1H, dt, *J* = 7.5 and 1.0 Hz, ArH), 6.82 (1H, dd, *J* = 8.1 and 1.0 Hz, ArH), 6.98 (1H, dd, *J* = 1.6 and 7.5 Hz, ArH) and 7.13 (1H, dt, *J* = 8.1 and 1.6 Hz, ArH); δ_C (100 MHz; $CDCl_3$) 27.8 [C(*C*H_3)$_3$], 37.8 and 48.7 (CH_2), 50.1 (*C*HCO), 72.8 and 81.5 (C≡CH), 77.2 (CHOH), 80.0 [*C*(CH_3)$_3$], 117.0, 119.3, 125.3, 127.9 and 129.0 (Ar-C), 156.0 [ArC(OH)] and 171.1 (C=O).

tert-*Butyl 3-(5-bromo-2-hydroxyphenyl)-3-hydroxy-2-[(2-propynylamino)methyl]propanoate* 171b

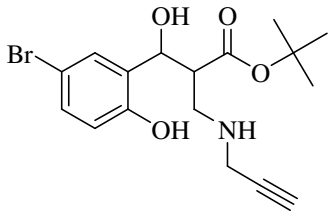

The procedure described for the synthesis of *tert*-butyl 3-hydroxy-3-(2-hydroxyphenyl)-2-[(2-propynylamino)methyl]propanoate **171a** was followed, using propargylamine (0.3 mL, 4 mmol) and *tert*-butyl 3-(5-bromo-2-hydroxyphenyl)-3-hydroxy-2-methylenepropanoate **153b** (0.72 g, 2.2 mmol) in dry THF (5 mL). Work-up afforded tert-*butyl 3-(5-bromo-2-hydroxyphenyl)-3-hydroxy-2-[(2-propynylamino)methyl]propanoate* **171b** as a white solid (0.76 g, 90%), m.p.

136-138 °C [HRMS: *m/z* calculated for $C_{17}H_{21}BrNO_4$ $(M-H)^+$ 382.0654. Found 382.0660]; υ_{max} / cm^{-1} 3260 (OH) and 1724 (C=O); δ_H (400 MHz; DMSO-d_6) 1.24 [9H, s, $C(CH_3)_3$], 2.71 (1H, dd, J = 14.9 and 8.4 Hz, CHCH_a), 2.81 (2H, q, J = 8.4 Hz, CHCO and CHCH_b), 3.04 (1H, s, C≡CH), 3.25 (2H, s, CH_2C≡CH), 5.01 (1H, d, J = 5.7 Hz, CHOH), 6.71 (1H, d, J = 8.6 Hz, ArH), 7.20 (1H, dd, J = 8.6 and 2.3 Hz, ArH) and 7.35 (1H, d, J = 2.3 Hz, ArH); δ_C (100 MHz; DMSO-d_6) 27.6 [C(CH_3)$_3$], 37.5 and 46.9 (CH_2), 51.8 (CHCO), 67.4 (CHOH), 73.8 and 82.7 (C≡CH), 79.5 [C(CH_3)$_3$], 109.9, 117.3, 130.4, 130.6 and 131.8 (Ar-C), 153.6 [ArC(OH)] and 171.4 (C=O).

tert-*Butyl 3-hydroxy-3-(2-hydroxy-3-methoxyphenyl)-2-[(prop-2-ynylamino)methyl]-propanoate* 171c

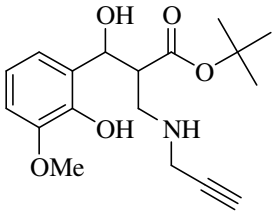

The procedure described for the synthesis of *tert*-butyl 3-hydroxy-3-(2-hydroxyphenyl)-2-[(2-propynylamino)methyl]propanoate **171a** was followed, using propargylamine (0.3 mL, 4 mmol) and *tert*-butyl 3-hydroxy-3-(2-hydroxy-3-methoxyphenyl)-2-methylenepropanoate **153c** (0.62 g, 2.2 mmol) in dry THF (5 mL). Work-up afforded tert-*butyl 3-hydroxy-3-(2-hydroxy-3-methoxyphenyl)-2-[(2-propynylamino)methyl]propanoate* **171c** as a yellow solid (0.65 g, 88%), m.p. 67-69 °C [HRMS: *m/z* calculated for $C_{18}H_{26}NO_5$ (MH^+) 336.1811. Found 336.1827 υ_{max} / cm^{-1} 3356 (OH) and 1714 (C=O); δ_H (400 MHz; $CDCl_3$) 1.24 [9H, s, $C(CH_3)_3$], 2.14 (1H, s, C≡CH), 2.67-2.72 (1H, m, CHCH_a), 2.94-3.02 (2H, m, CHCO and CHCH_b), 3.22 (2H, q, J = 17.1 Hz, CH_2C≡CH), 3.69 (3H, s, OCH_3), 5.22 (1H, s, CHOH), 6.61-6.68 (2H, m, ArH), and 6.75-6.78 (1H, m, ArH); δ_C (100 MHz; $CDCl_3$) 27.4 [C(CH_3)$_3$], 37.6 and 46.9 (CH_2), 49.2 (CHCO), 55.5 (OCH_3), 71.8 (CHOH), 72.8 and 80.5 (C≡CH), 73.0 [C(CH_3)$_3$], 109.7, 118.6, 119.3 and 127.4 (Ar-C), 142.9 and 146.6 [ArC(OH) and ArC(OMe)] and 171.8 (C=O).

tert-*Butyl 3-(3-ethoxy-2-hydroxyphenyl)-3-hydroxy-2-[(2-propynylamino)methyl]propanoate* 171d

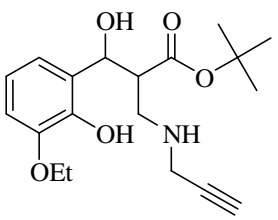

The procedure described for the synthesis of *tert*-butyl 3-hydroxy-3-(2-hydroxyphenyl)-2-[(2-propynylamino)methyl]propanoate **171a** was followed, using propargylamine (0.3 mL, 4 mmol) and *tert*-butyl 3-(3-ethoxy-2-hydroxyphenyl)-3-hydroxy-2-methylenepropanoate **153d** (0.65 g, 2.2 mmol) in dry THF (5 mL). Work-up afforded tert-*butyl 3-(3-ethoxy-2-hydroxyphenyl)-3-hydroxy-2-[(2-propynylamino)methyl]propanoate* **171d** as a brown solid (0.73 g, 95%), m.p. 48-50 °C [HRMS: *m/z* calculated for $C_{19}H_{28}NO_5$ (MH^+) 350.1967. Found 350.1953]; υ_{max} / cm^{-1} 3356 (OH) and 1740 (C=O); δ_H (400 MHz; $CDCl_3$) 1.41-1.45 [12H, overlapping s and t, $C(CH_3)_3$ and OCH_2CH_3], 2.20 (1H, t, *J* = 2.3 Hz, C≡CH), 2.72 (1H, dd, *J* = 12.2 and 3.9 Hz, $CHCH_a$), 3.05 (1H, dd, *J* = 9.1 and 5.0 Hz, CHCO), 3.19 (1H, dd, *J* = 12.2 and 5.0 Hz, $CHCH_b$), 3.30 (1H, dd, , *J* = 17.1 and 2.3 Hz, $CH_aC{\equiv}CH$), 3.43 (1H, dd, *J* = 2.3 and 17.1 Hz, $CH_bC{\equiv}CH$), 3.69 (3H, s, OCH_3), 4.09 (2H, q, *J* = 7.0 Hz, OCH_2), 5.44 (1H, d, *J* = 5.0 Hz, CHOH), 6.76-6.83 (2H, m, ArH), and 6.94 (1H, dd, *J* = 7.2 and 1.8 Hz, ArH); δ_C (100 MHz; $CDCl_3$) 14.4 (OCH_2CH_3), 27.9 [$C(CH_3)_3$], 38.1 and 47.3 (CH_2), 48.9 (CHCO), 64.5 (OCH_2), 72.1 and 80.8 (C≡CH), 73.5 (CHOH), 81.2 [$C(CH_3)_3$], 110.9, 119.2, 119.4 and 127.8 (Ar-C), 142.9 and 145.9 [ArC(OH) and ArC(OEt)] and 172.3 (C=O).

tert-*Butyl 3-(5-chloro-2-hydroxyphenyl)-3-hydroxy-2-[(2-propynylamino)methyl]propanoate* 171e

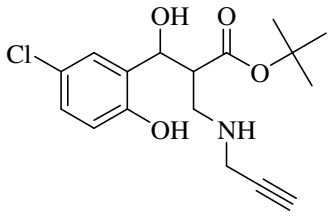

The procedure described for the synthesis of *tert*-butyl 3-hydroxy-3-(2-hydroxyphenyl)-2-[(2-propynylamino)methyl]propanoate **171a** was followed, using propargylamine (0.3 mL, 4 mmol) and *tert*-butyl 3-(5-chloro-2-hydroxyphenyl)-3-hydroxy-2-methylenepropanoate **153e** (0.63 g, 2.2 mmol) in dry THF (5 mL). Work-up afforded tert-*butyl 3-(5-chloro-2-hydroxyphenyl)-3-hydroxy-2-[(2-propynylamino)methyl]propanoate* **171e** as a white solid (0.68 g, 91%), m.p. 125-126 °C [HRMS: *m/z* calculated for $C_{17}H_{23}ClNO_4$ (MH^+) 340.1316. Found 340.1331]; υ_{max} / cm^{-1} 3549 (OH) and 1697 (C=O); δ_H (400 MHz; DMSO-d_6) 1.25 [9H, s, $C(CH_3)_3$], 2.70 (1H, q, *J* = 8.8 Hz, $CHCH_a$), 2.78-2.84 (2H, m, CHCO and $CHCH_b$), 3.04 (1H, t, *J* = 2.3 Hz, C≡CH), 3.25 (2H, t, *J* = 2.3 Hz, $CH_2C{\equiv}CH$), 5.02 (1H, d, *J* = 5.7 Hz, CHOH), 6.77 (1H, s, ArH), 7.09 (1H, dd, *J* = 8.6 and 2.7 Hz, ArH) and 7.23 (1H, d, *J* = 2.7 Hz, ArH); δ_C (100 MHz; DMSO-d_6) 27.6

[C(CH_3)$_3$], 37.5 and 46.8 (CH_2), 51.7 (*C*HCO), 67.4 (CHOH), 73.8 and 82.7 (C≡CH), 79.5 [*C*(CH_3)$_3$], 116.7, 122.2, 127.5, 127.7 and 131.3 (Ar-C), 153.1 [ArC(OH)] and 171.4 (C=O).

3.8.3. Synthesis of Cinnamic Acid Derivatives

(Z)-*2-(Chloromethyl)-3-(2-hydroxyphenyl)-2-propenoic acid* 177a

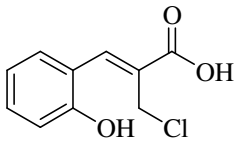

3-(Chloromethyl)coumarin 148a

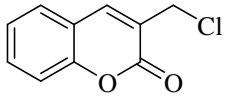

Acetyl chloride (1.2 mL) was added drop-wise to dry methanol (1.0 mL) cooled in an ice bath. The mixture was left to stir for 30 minutes and *tert*-butyl 3-hydroxy-3-(2-hydroxyphenyl)-2-methylenepropanoate **153a** (0.50 g, 2.0 mmol) dissolved in dry methanol (2 mL) was then added and the mixture left to stir overnight. Water (20 mL) was added to the crude mixture, which was then extracted with $CHCl_3$ (2 × 20 mL) and concentrated *in vacuo*. Fractional recrystallisation from chloroform afforded two products.

***Product* 1**. (Z)-*2-(Chloromethyl)-3-(2-hydroxyphenyl)-2-propenoic acid* **177a** as a pink solid (0.35 g, 83%), m.p. 129-131 °C (Found: C, 56.22; H, 4.40. $C_{10}H_9ClO_3$ requires C, 56.49; H, 4.27%); υ_{max} / cm^{-1} 3453 (OH) and 1666 (C=O); δ_H (400 MHz; DMSO-d_6) 4.47 (2H, s, CH_2), 6.90-6.96 (2H, m, ArH), 7.28 (1H, t, *J* = 7.7 Hz, ArH), 7.46 (1H, m, ArH), 7.95 (1H, s, C=CH) and 10.22 (1H, br s, OH); δ_C (100 MHz; DMSO-d_6) 41.1 (CH_2), 116.7, 120.1, 121.8, 128.2, 130.0, 132.3, 139.5 and 157.4 (Ar-C and C=C) and 168.2 (C=O).

***Product* 2**. 3-(Chloromethyl)coumarin **148a** as a pale yellow solid (0.05 g, 13%).

(Z)-*3-(5-Bromo-2-hydroxyphenyl)-2-(chloromethyl)-2-propenoic acid* 177b

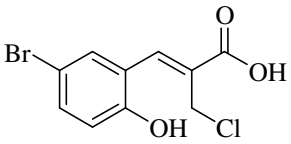

6-Bromo-3-(chloromethyl)coumarin 148b

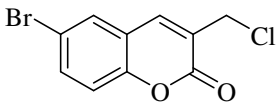

The procedure described for the synthesis of (Z)-2-(chloromethyl)-3-(2-hydroxyphenyl)-2-propenoic acid **177a** was followed, using acetyl chloride (1.2 mL), dry methanol (1.0 mL) and *tert*-butyl 3-(5-bromo-2-hydroxyphenyl)-3-hydroxy-2-methylenepropanoate **153b** (0.50 g, 1.5

mmol) in dry methanol (2 mL). Work-up afforded (Z)-*3-(5-bromo-2-hydroxyphenyl)-2-(chloromethyl)-2-propenoic acid* **177a** as a pale yellow solid (0.37 g, 84%), m.p. 146-148 °C (Found: C, 41.29; H, 2.88. $C_{10}H_8BrClO_3$ requires C, 41.20; H, 2.77%); υ_{max} / cm^{-1} 3421 (OH) and 1669 (C=O); δ_H (400 MHz; DMSO-d_6) 4.44 (2H, s, CH_2), 6.90 (1H, d, *J* = 8.7 Hz ArH), 7.45 (1H, dd, *J* = 8.7, 2.4 Hz, ArH), 7.62 (1H, d, *J* = 2.3 Hz, ArH), 7.83 (1H, s, C=CH) and 10.56 (1H, br s, OH); δ_C (100 MHz; DMSO-d_6) 40.7 (CH_2), 110.0, 118.7, 124.0, 129.5, 132.1, 134.6, 138.0 and 156.6 (Ar-C and C=C) and 167.9 (C=O).

***Product* 2**. 6-Bromo-3-(chloromethyl)coumarin (14% estimated by ^{1}H NMR analysis).

(Z)-*2-(Chloromethyl)-3-(2-hydroxy-3-methoxyphenyl)-2-propenoic acid* 177c

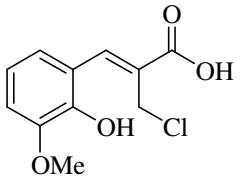

3-(Chloromethyl)-8-methoxycoumarin 148c

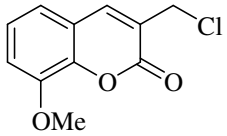

The procedure described for the synthesis of (*Z*)-2-(chloromethyl)-3-(2-hydroxyphenyl)-2-propenoic acid **177a** was followed, using acetyl chloride (1.2 mL), dry methanol (1.0 mL) and *tert*-butyl 3-hydroxy-3-(2-hydroxy-3-methoxyphenyl)-2-methylenepropanoate **153c** (0.50 g, 1.8 mmol) in dry methanol (2 mL). Work-up afforded two products.

***Product* 1**. (Z)-*2-(Chloromethyl)-3-(2-hydroxy-3-methoxyphenyl)-2-propenoic acid* **177c** as a lilac solid (0.39 g, 90%), m.p. 137-139 °C (Found: C, 54.63; H, 4.80%. $C_{11}H_{11}ClO_4$ requires C, 54.45; H, 4.57%); υ_{max} / cm^{-1} 3499 (OH), 1671 (C=O); δ_H (400 MHz; methanol-d_4) 3.87 (3H, s, OCH_3), 4.47 (2H, s, CH_2), 6.88 (1H, t, *J* = 8.0 Hz, ArH), 7.00 (1H, d, *J* = 8.0 Hz, ArH), 7.20 (1H, d, *J* = 7.8 Hz, ArH) and 8.10 (1H, s, C=CH); δ_C (100 MHz; methanol-d_4) 40.7 (CH_2), 56.6 (OCH_3), 113.8, 120.3, 122.2, 122.6, 129.2, 140.5, 147.3 and 149.1 (Ar-C and C=C) and 169.8 (C=O).

***Product* 2**. 3-(Chloromethyl)-8-methoxycoumarin **148d** as a brown solid (0.04 g, 10%).

(Z)-*2-(Chloromethyl)-3-(3-ethoxy-2-hydroxyphenyl)-2-propenoic acid* 177d

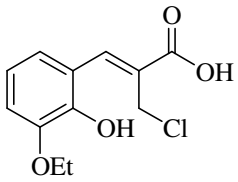

3-(Chloromethyl)-8-ethoxycoumarin 148d

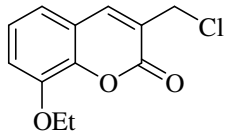

The procedure described for the synthesis of (*Z*)-2-(chloromethyl)-3-(2-hydroxyphenyl)-2-propenoic acid **177a** was followed, using acetyl chloride (1.2 mL), dry methanol (1.0 mL) and *tert*-butyl 3-(3-ethoxy-2-hydroxyphenyl)-3-hydroxy-2-methylenepropanoate **153d** (0.50 g, 1.7 mmol) in dry methanol (2 mL). Work-up afforded (Z)-*2-(chloromethyl)-3-(3-ethoxy-2-hydroxyphenyl)-2-propenoic acid* as a purple solid (0.37 g, 85%), m.p. 128-130 °C (Found: C, 56.27; H, 5.10. $C_{12}H_{13}ClO_4$ requires C, 56.15; H, 5.10%); υ_{max} / cm^{-1} 3489 (OH) and 1674 (C=O); δ_H (400 MHz; methanol-d_4) 1.46 (3H, t, *J* = 6.9 Hz, CH_3),4.14 (2H, q, *J* = 6.9 Hz, OCH_2), 4.49 (2H, s, CH_2), 6.06 (1H, br s, OH), 6.91 (2H, m, ArH), 7.27 (1H, m, ArH) and 8.24 (1H, s, C=CH); δ_C (100 MHz; methanol-d_4) 14.8 (CH_3), 39.3 (CH_2), 64.8 (OCH_2), 113.1, 119.9, 120.4, 121.4, 127.3, 140.7, 145.1 and 145.8 (Ar-C and C=C) and 171.3 (C=O).

***Product* 2**. 3-(Chloromethyl)-8-ethoxycoumarin (10% estimated by ^{1}H NMR analysis).

(Z)-*3-(5-Chloro-2-hydroxyphenyl)-2-(chloromethyl)-2-propenoic acid* 177e

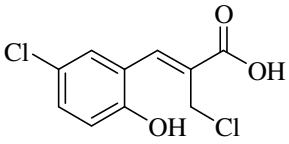

6-Chloro-3-(chloromethyl)coumarin 148e

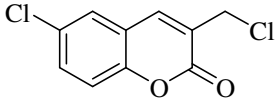

The procedure described for the synthesis of (*Z*)-2-(chloromethyl)-3-(2-hydroxyphenyl)-2-propenoic acid **177a** was followed, using acetyl chloride (1.2 mL), dry methanol (1.0 mL) and *tert*-butyl 3-(5-chloro-2-hydroxyphenyl)-3-hydroxy-2-methylenepropanoate **153e** (0.50 g, 1.8 mmol) in dry methanol (2 mL). Work-up afforded (Z)-*3-(5-chloro-2-hydroxyphenyl)-2-(chloromethyl)-2-propenoic acid* **177e** as a pale yellow solid (0.39 g, 89%), m.p. 126-128 °C (Found: C, 48.48; H, 3.48. $C_{10}H_8Cl_2O_3$ requires C, 48.61; H, 3.26%); υ_{max} / cm^{-1} 3408 (OH) and 1666 (C=O); δ_H (400 MHz; methanol-d_4) 4.43 (2H, s, CH_2), 6.84 (1H, d, *J* = 8.7 Hz, ArH), 7.23 (1H, dd, *J* = 2.5, 8.7 Hz, ArH), 7.56 (1H, d, *J* = 2.4 Hz, ArH) and 7.97 (1H, s, C=CH); δ_C (100

MHz; methanol-d_4) 40.2(CH_2), 118.0, 124.4, 125.2, 130.0, 130.3, 132.0, 139.4 and 156.5 (Ar-C and C=C) and 169.3 (C=O).

***Product* 2**. 6-Chloro-3-(chloromethyl)coumarin **148e** (10% estimated by ^{1}H NMR analysis).

3.9. PREPARATION OF SALICYLALDEHYDE BENZYL ETHERS

2-(Benzyloxy)benzaldehyde 145a

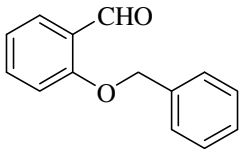

Absolute EtOH (100 mL) was added to a mixture of salicylaldehyde (2.8 mL, 26 mmol), benzyl bromide (3.1 mL, 26 mmol), anhydrous K_2CO_3 (21 g, 0.15 mol) and NaI (23 g, 0.15 mol), and the mixture was boiled under reflux for 12 h. Water (50 mL) was then added and the aqueous layer extracted with $CHCl_3$ (2 x 100 mL). The combined organic extracts were washed with brine and dried (anhydrous $MgSO_4$), filtered and concentrated *in vacuo* to give a dark brown oil. Crystallisation from hexane afforded 2-benzyloxybenzaldehyde **145a** as a yellow solid (5.46 g, 99%), m.p. 42-44 ^oC (lit.[277] reported as an oil); υ_{max} / cm^{-1} 1679 (C=O); δ_H (400 MHz; $CDCl_3$) 5.19 (2H, s, OCH_2Ph), 7.06 (2H, d, J = 8.8 Hz, ArH), 7.34-7.47 (5H, overlapping m, ArH), 7.53 (1H, t, 7.7 Hz, ArH), 7.88 (1H, d, J = 7.7 Hz, ArH) and 10.59 (1H, s, CHO); δ_C (100 MHz; $CDCl_3$) 70.3 (OCH_2Ph), 112.9, 120.9, 125.1, 127.2, 128.1, 128.3, 128.6, 135.8 and 136.0 (Ar-C), 160.9 [ArC(OBn)] and 189.5 (C=O).

2-(Benzyloxy)-5-bromobenzaldehyde 145b

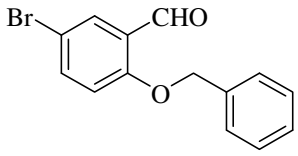

The procedure described for the synthesis of 2-benzyloxybenzaldehyde **145a** was followed, using 5-bromosalicylaldehyde (5.2 g, 26 mmol), benzyl bromide (3.1 mL, 26 mmol), anhydrous K_2CO_3 (21 g, 0.15 mol) and NaI (23 g, 0.15 mol) in absolute ethanol (100 mL). Work-up afforded 2-benzyloxy-5-bromobenzaldehyde **145b** as a light yellow solid (6.81 g, 90%), m.p. 73-74 ^oC (lit.[278] 73-74 ^oC); υ_{max} / cm^{-1} 1682 (C=O); δ_H (400 MHz; $CDCl_3$) 5.18 (2H, s, OCH_2Ph),

6.95 (1H, d, *J* = 8.8 Hz, ArH), 7.35-7.42 (5H, overlapping m, ArH), 7.60 (1H, dd, *J* = 8.8 and 2.3 Hz, ArH), 7.95 (1H, d, *J* = 2.3 Hz, ArH) and 10.46 (1H, s, CHO); δ_C (100 MHz: $CDCl_3$) 70.8 (OCH_2Ph), 113.8, 115.1, 126.4, 127.3, 128.5, 128.8, 131.0, 135.5 and 138.2 (Ar-C), 159.8 [ArC(OBn)] and 188.3 (C=O).

2-(Benzyloxy)-3-methoxybenzaldehyde 145c

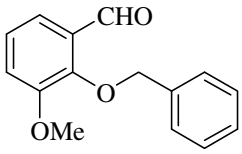

The procedure described for the synthesis of 2-benzyloxybenzaldehyde **145a** was followed, using 3-methoxysalicylaldehyde (4.0 g, 26 mmol), benzyl bromide (3.1 mL, 26 mmol), anhydrous K_2CO_3 (21 g, 0.15 mol) and NaI (23 g, 0.15 mol) in absolute ethanol (100 mL). Work-up afforded 2-benzyloxy-3-methoxybenzaldehyde **145c** as a white solid (5.54 g, 88%), m.p. 40-41 ^oC (lit.[279] 45 ^oC); υ_{max} / cm^{-1} 1689 (C=O); δ_H (400 MHz; $CDCl_3$) 3.91 (3H, s, OCH_3), 5.19 (2H, s, OCH_2Ph), 7.10-7.18 (2H, overlapping m, ArH), 7.33-7.41 (6H, series of overlapping signals, ArH) and 10.27 (1H, s, CHO); δ_C (100 MHz; $CDCl_3$) 55.8 (OCH_3), 76.1 (OCH_2Ph), 117.8, 118.8, 124.0, 128.3, 128.4, 128.5, 130.1 and 136.2 (Ar-C), 150.8 and 152.8 [ArC(OBn) and ArC(OMe)] and 189.9 (C=O).

2-(Benzyloxy)-3-ethoxybenzaldehyde 145d

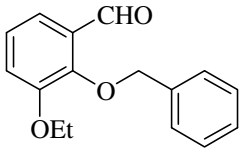

The procedure described for the synthesis of 2-benzyloxybenzaldehyde **145a** was followed, using 3-ethoxysalicylaldehyde (4.32 g, 26 mmol), benzyl bromide (3.1 mL, 26 mmol), anhydrous K_2CO_3 (20.7 g, 0.15 mol) and NaI (22.5 g, 0.15 mol) in absolute ethanol (100 mL). Work-up afforded 2-benzyloxy-3-ethoxybenzaldehyde **145d** as a grey solid (6.33 g, 95%), m.p. 38-39 ^oC (lit.[280] 39-40 ^oC); υ_{max} / cm^{-1} 1680 (C=O); δ_H (400 MHz; $CDCl_3$) 1.51 (3H, t, *J* = 6.9 Hz, CH_3), 4.15 (2H, q, *J* = 6.9 Hz, OCH_2CH_3), 5.20 (2H, s, OCH_2Ph), 7.11 (1H, t, *J* = 7.8 Hz, ArH), 7.17 (1H, d, *J* = 7.8 Hz, ArH), 7.31-7.41 (6H, overlapping m, ArH) and 10.27 (1H, s, CHO); δ_C (100 MHz; $CDCl_3$) 14.9 (CH_3), 64.7 (OCH_2CH_3), 76.2 (OCH_2Ph), 119.0, 119.2, 124.1, 128.4, 128.5, 128.6, 130.4 and 136.5 (Ar-C), 151.3 and 152.3 [ArC(OBn) and ArC(OEt)] and 190.2 (C=O).

2-(Benzyloxy)-5-chlorobenzaldehyde 145e

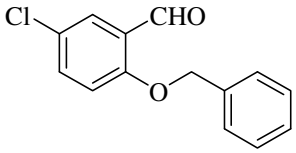

The procedure described for the synthesis of 2-benzyloxybenzaldehyde **145a** was followed, using 5-chlorosalicylaldehyde (4.1 g, 26 mmol), benzyl bromide (3.1 mL, 26 mmol), anhydrous K_2CO_3 (21 g, 0.15 mol) and NaI (23 g, 0.15 mol) in absolute ethanol (100 mL). Work-up afforded 2-benzyloxy-5-chlorobenzaldehyde **145e** as a yellow solid (5.84 g, 91%), m.p. 70-72 ^oC (lit.[208] 70-72 ^oC); υ_{max} / cm^{-1} 1685 (C=O); δ_H (400 MHz; $CDCl_3$) 5.18 (2H, s, OCH_2Ph), 7.00 (1H, d, *J* = 8.8 Hz, ArH), 7.34-7.42 (5H, overlapping m, ArH), 7.45 (1H, dd, *J* = 2.7 and 8.8 Hz, ArH), 7.79 (1H, d, *J* = 2.7 Hz, ArH) and 10.47 (1H, s, CHO); δ_C (100 MHz: $CDCl_3$) 70.8 (OCH_2Ph), 114.6, 125.9, 126.6, 127.3, 127.9, 128.4, 128.7, 135.3 and 135.5 (Ar-C), 159.3 [ArC(OBn)] and 188.3 (C=O).

***4-[2-(Benzyloxy)phenyl]-4-hydroxybutan-2-one* 220a**

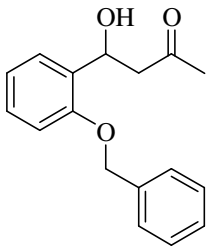

Dry acetone (100 mL) was added to a mixture of salicylaldehyde (2.8 mL, 26 mmol), benzyl bromide (3.1 mL, 26 mmol), anhydrous K_2CO_3 (21 g, 0.15 mol) and NaI (23 g, 0.15 mol), and the mixture was boiled under reflux for 12 h. Water (50 mL) was then added and the aqueous layer extracted with $CHCl_3$ (2 x 100 mL). The combined organic extracts were washed with brine and dried (anhydrous $MgSO_4$), filtered and concentrated *in vacuo* to give a brown solid. Crystallisation from diethyl ether afforded *4-[2-(benzyloxy)phenyl]-4-hydroxybutan-2-one* **220a** as a brown solid (6.5 g, 92%), m.p. 70-72 ^oC [HRMS: *m/z* calculated for $C_{17}H_{18}O_3Na$ (MNa^+) 293.1154. Found 293.1159]; υ_{max} / cm^{-1} 3418 (OH) and 1684 (C=O); δ_H (400 MHz; $CDCl_3$) 2.16 (3H, s, CH_3), 2.82 (1H, dd, *J* = 16.9 and 9.0 Hz, CH_a.$COCH_3$), 3.00 (1H, d, *J* = 16.9 Hz, CH_b.$COCH_3$), 3.75 (1H, br s, OH), 5.13 (2H, s, OCH_2Ph), 5.58 (1H, d, 9.0 Hz, C*H*OH), 6.98 (1H, d, *J* = 8.0 Hz, ArH), 7.06 (1H, t, *J* = 7.5 Hz, ArH), 7.29 (1H, t, *J* = 8.0 Hz, ArH), 7.38-7.50 (5H, overlapping m, ArH) and 7.58 (1H, d, *J* = 7.5, ArH); δ_C (100 MHz; $CDCl_3$) 30.2 (CH_3),

50.2 (CH_2.$COCH_3$), 65.2 (OCH_2Ph), 69.7 (CHOH), 111.3, 120.9, 126.2, 126.9, 127.7, 128.1, 128.4, 131.2 and 136.6 (Ar-C) and 154.5 [ArC(OBn)] and 209.1 (C=O).

***4-(2-(Benzyloxy)-5-bromophenyl)-4-hydroxybutan-2-one* 220b**

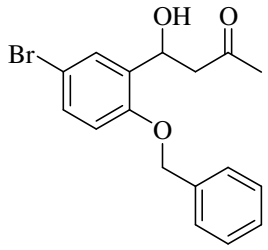

The procedure described for the synthesis of 4-[2-(benzyloxy)phenyl]-4-hydroxybutan-2-one **220a** was followed, using 5-bromosalicylaldehyde (5.2 g, 26 mmol), benzyl bromide (3.1 mL, 26 mmol), anhydrous K_2CO_3 (21 g, 0.15 mol) and NaI (23 g, 0.15 mol) in dry acetone (100 mL). Work-up afforded *4-(2-(benzyloxy)-5-bromophenyl)-4-hydroxybutan-2-one* **220b** as a pale yellow solid (8.6 g, 95%), m.p. 113-115 ^oC [HRMS: *m/z* calculated for $C_{17}H_{17}BrO_3Na$ (MNa^+) 371.0259. Found 371.0241]; υ_{max} / cm^{-1} 3549 (OH) and 1697 (C=O); δ_H (400 MHz; $CDCl_3$) 2.13 (3H, s, CH_3), 2.69 (1H, dd, *J* = 17.4 and 9.4 Hz, CH_a.$COCH_3$), 2.94 (1H, d, *J* = 17.4 Hz, CH_b.$COCH_3$), 3.62 (1H, br s, OH), 5.06 (2H, s, OCH_2Ph), 5.44 (1H, d, 9.0 Hz, C*H*OH), 6.78 (1H, d, *J* = 8.7 Hz, ArH), 7.29-7.41 (6H, m, ArH) and 7.64 (1H, s, ArH); δ_C (100 MHz; $CDCl_3$) 30.5 (CH_3), 49.9 (CH_2.$COCH_3$), 64.6 (OCH_2Ph), 70.2 (CHOH), 113.2, 113.6, 127.0, 128.1, 128.6, 129.3, 130.8, 133.5 and 136.2 (Ar-C) and 153.5 [ArC(OBn)] and 209.3 (C=O).

3.10. BAYLIS-HILLMAN REACTION OF SALICYLALDEHYDE BENZYL ETHERS

Methyl 3-(2-benzyloxyphenyl)-3-hydroxy-2-methylenepropanoate 146a[275]

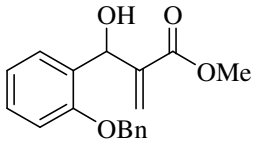

A mixture of 2-benzyloxybenzaldehyde **145a** (2.1 g, 10 mmol), methyl acrylate (1.8 mL, 20 mmol) and DABCO (0.29 g, 2.6 mmol) in $CHCl_3$ (5 mL) was sealed in a round-bottomed flask and stirred at room temperature for 21 d. The mixture was concentrated *in vacuo* and purified by flash chromatography [on silica gel; elution with hexane – EtOAc (9:1)] to afford methyl 3-(2-benzyloxyphenyl)-3-hydroxy-2-methylenepropanoate **146a** as a yellow oil (2.45 g, 82%); υ_{max} /

cm^{-1} 3448 (OH) and 1717 (C=O); δ_H (400 MHz; $CDCl_3$) 3.41 (1H, d, *J* = 6.3 Hz, OH), 3.72 (3H, s, OCH_3), 5.09 (2H, s, OCH_2Ph), 5.70 and 6.29 (2H, 2 × s, $C=CH_2$), 5.95 (1H, d, *J* = 6.3 Hz, C*H*OH), 6.94 (1H, d, *J* = 7.8, ArH), 6.99 (1H, t, *J* = 7.8 Hz, ArH), 7.26 (1H, t, *J* = 7.1 Hz, ArH) and 7.33-7.42 (6H, overlapping m, ArH); δ_C (100 MHz; $CDCl_3$) 51.8 (OCH_3), 68.3 (CHOH), 70.1 (OCH_2Ph), 125.8 ($C=CH_2$), 111.8, 120.9, 127.3, 127.7, 127.9, 128.5, 128.8, 129.5, 136.4, 141.3 and 155.7 (*C*=CH_2 and Ar-C) and 166.9 (C=O).

Methyl 3-(2-benzyloxy-5-bromophenyl)-3-hydroxy-2-methylenepropanoate 146b

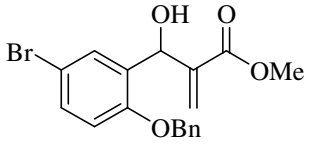

The procedure described for the synthesis of methyl 3-(2-benzyloxyphenyl)-3-hydroxy-2-methylenepropanoate **146a** was followed, using 2-benzyloxy-5-bromobenzaldehyde **145b** (2.91 g, 10 mmol), methyl acrylate (1.8 mL, 20 mmol) and DABCO (0.29 g, 2.6 mmol) in $CHCl_3$ (5 mL). Work-up afforded methyl 3-(2-benzyloxy-5-bromophenyl)-3-hydroxy-2-methylene-propanonate **146b** as a yellow solid (3.55 g, 94%), m.p. 115-117 ^oC (lit.[208] 114-116 ^oC); υ_{max} / cm^{-1} 3202 (OH) and 1711 (C=O); δ_H (400 MHz; $CDCl_3$) 3.48 (1H, d, *J* = 5.8 Hz, OH), 3.72 (3H, s, OCH_3), 5.04 (2H, s, OCH_2Ph), 5.67 and 6.30 (2H, 2 x s, $C=CH_2$), 5.91 (1H, d, *J* = 5.8 Hz, C*H*OH), 6.79 (1H, d, *J* = 8.7 Hz, ArH), 7.32-7.39 (6H, overlapping m, ArH) and 7.57 (1H, s, ArH); δ_C (100 MHz; $CDCl_3$) 51.9 (OCH_3), 67.4 (CHOH), 70.3 (OCH_2Ph), 126.3 ($C=CH_2$), 113.4, 113.5, 127.2, 128.0, 128.5, 130.4, 131.3, 131.9, 136.1, 140.8 and 154.5 (*C*=CH_2 and Ar-C) and 166.7 (C=O).

Methyl 3-(2-benzyloxy-3-methoxyphenyl)-3-hydroxy-2-methylenepropanoate 146c[208]

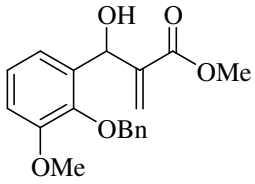

The procedure described for the synthesis of methyl 3-(2-benzyloxyphenyl)-3-hydroxy-2-methylenepropanoate **146a** was followed, using 2-benzyloxy-3-methoxybenzaldehyde **145c** (2.4 g, 10 mmol), methyl acrylate (1.8 mL, 20 mmol) and DABCO (0.29 g, 2.6 mmol) in $CHCl_3$ (5 mL). Work-up afforded methyl 3-(2-benzyloxy-3-methoxyphenyl)-3-hydroxy-2-methylene-propanoate **146c** as a yellow oil (2.89 g, 88%); υ_{max} / cm^{-1} 3451 (OH) and 1718 (C=O); δ_H (400

MHz; $CDCl_3$) 2.94 (1H, s, OH), 3.70 and 3.90 (6H, 2 x s, 2 x OCH_3), 5.08 (2H, s, OCH_2), 5.74 and 6.29 (2H, 2 x s, C=CH_2), 5.87 (1H, s, C*H*OH), 6.90-6.95 (2H, series of signals, ArH), 7.08 (1H, t, *J* = 7.7 Hz, ArH), 7.33- 7.40 (3H, overlapping m, ArH) and 7.45 (2H, d, *J* = 7.7 Hz, ArH); δ_C (100 MHz; $CDCl_3$) 51.8 and 55.8 (2 x OCH_3), 67.7 (CHOH), 74.7 (OCH_2Ph), 125.9 (C=*C*H_2), 112.0, 119.3, 124.2, 128.0, 128.3, 128.4, 135.1, 137.6, 141.6, 145.2 and 152.5 (*C*=CH_2 and Ar-C) and 166.8 (C=O).

Methyl 3-(2-benzyloxy-3-ethoxyphenyl)-3-hydroxy-2-methylenepropanoate 146d[208]

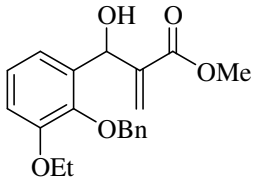

The procedure described for the synthesis of methyl 3-(2-benzyloxyphenyl)-3-hydroxy-2-methylenepropanoate **146a** was followed, using 2-benzyloxy-3-ethoxybenzaldehyde **146d** (2.6 g, 10 mmol), methyl acrylate (1.8 mL, 20 mmol) and DABCO (0.29 g, 2.6 mmol) in $CHCl_3$ (5 mL). Work-up afforded methyl 3-(2-benzyloxy-3-ethoxyphenyl)-3-hydroxy-2-methylenepropanoate **146d** as a yellow oil (2.94 g, 86%); υ_{max} / cm^{-1} 3460 (OH) and 1715 (C=O); δ_H (400 MHz; $CDCl_3$) 1.48 (3H, t, *J* = 6.9 Hz, CH_3), 3.07 (1H, d, *J* = 5.2 Hz, OH), 3.69 (3H, s, OCH_3), 4.11 (2H, q, *J* = 6.9 Hz, O*C*H_2CH_3), 5.11 (2H, s, OCH_2Ph), 5.75 and 6.30 (2H, 2 x s, C=CH_2) 5.90 (1H, d, *J* = 5.2 Hz, C*H*OH), 6.89-6.95 (2H, series of signals, ArH), 7.05 (1H, t, *J* = 7.5 Hz, ArH), 7.32- 7.40 (3H, overlapping m, ArH) and 7.48 (2H, d, *J* = 7.5 Hz, ArH); δ_C (100 MHz; $CDCl_3$) 14.9 (OCH_2CH_3), 51.7 (OCH_3), 64.2 (OCH_2CH_3), 67.8 (CHOH), 74.6 (OCH_2Ph), 125.7 (C=*C*H_2), 113.2, 119.3, 124.0, 127.9, 128.2, 128.3, 135.1, 137.7, 141.7, 145.4 and 151.8 (*C*=CH_2 and Ar-C) and 166.8 (C=O).

Methyl 3-(2-benzyloxy-5-chlorophenyl)-3-hydroxy-2-methylenepropanoate 146e[208]

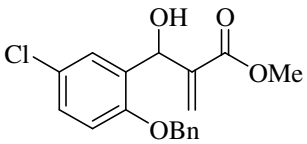

The procedure described for the synthesis of methyl 3-(2-benzyloxyphenyl)-3-hydroxy-2-methylenepropanoate **146a** was followed, using 2-benzyloxy-5-chlorobenzaldehyde **145e** (2.47 g, 10 mmol), methyl acrylate (1.8 mL, 20 mmol) and DABCO (0.29 g, 2.6 mmol) in $CHCl_3$ (5 mL). Work-up afforded methyl 3-(2-benzyloxy-5-chlorophenyl)-3-hydroxy-2-methylene-

propanonate **146e** as a yellow oil (3.00 g, 90%); υ_{max} / cm^{-1} 3402 (OH) and 1710 (C=O); δ_H (400 MHz; $CDCl_3$) 3.36 (1H, br s, OH), 3.74 (3H, s, OCH_3), 5.06 (2H, s, OCH_2Ph), 5.67 and 6.30 (2H, 2 x s, $C=CH_2$), 5.89 (1H, s, C*H*OH), 6.85 (1H, d, *J* = 8.7 Hz, ArH), 7.20 (1H, d, *J* = 8.7 Hz, ArH) and 7.30-7.41 (6H, overlapping m, ArH); δ_C (100 MHz; $CDCl_3$) 51.9 (OCH_3), 67.8 (CHOH), 70.6 (OCH_2Ph), 126.4 ($C=CH_2$), 113.2, 126.2, 127.3, 127.8, 128.1, 128.5, 128.6, 131.5, 136.3, 140.8 and 154.2 ($C=CH_2$ and Ar-C) and 166.8 (C=O).

3.11. SYNTHESIS OF BENZYLATED CINNAMATE ESTER DERIVATIVES

***Methyl 3-(2-(benzyloxy)-5-bromophenyl)-3-hydroxy-2-[(2-propynylamino)methyl]propanoate* 219b**

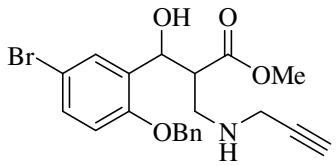

Propargylamine (0.3 mL, 4.4 mmol) was added to a solution of methyl 3-(2-benzyloxy-5-bromophenyl)-3-hydroxy-2-methylenepropanonate **146b** (0.83 g, 2.2 mmol) in dry THF (5 mL) and the mixture was stirred at r.t. for 48 h. The reaction mixture was then concentrated *in vacuo* and flash chromatographed [on silica gel; elution with hexane – EtOAc (1:1)] to afford *methyl 3-(2-(benzyloxy)-5-bromophenyl)-3-hydroxy-2-[(2-propynylamino)methyl]propanoate* **219b** as a white solid (0.87 g, 92%), m.p. 97-99 °C [HRMS: *m/z* calculated for $C_{21}H_{23}BrNO_4$ (MH^+) 432.0810. Found 432.0809]; υ_{max} / cm^{-1} 1719 (C=O); δ_H (400 MHz; $CDCl_3$) 2.19 (1H, s, C≡CH), 3.03 (1H, dd, *J* = 4.5 and 11.9 Hz, CHCO), 3.10 (1H, dd, *J* = 4.1 and 8.6 Hz, $CHCH_a$), 3.16 (1H, dd, *J* = 4.1 and 11.9 Hz, $CHCH_b$), 3.36 (2H, q, *J* = 17.1 Hz, CH_2-C≡CH), 3.54 (3H, s, OCH_3), 5.08 (2H, q, *J* = 11.7 Hz, OCH_2), 5.34 (1H, d, *J* = 4.5 Hz, C*H*OH), 6.79 (1H, d, *J* = 8.6 Hz, ArH), 7.31-7.42 (6H, overlapping m, ArH) and 7.56 (1H, s, ArH); δ_C (100 MHz; $CDCl_3$) 37.9 and 48.4 (NCH_2), 49.7 (*C*HCO), 51.3 (CH_3), 69.3 (CHOH), 71.8 (OCH_2), 72.4 and 81.2 (C≡CH), 113.0, 113.3, 127.1, 128.0, 128.6, 129.9, 130.8, 132.7 and 136.2 (Ar-C), 153.9 [ArC(OBn)] and 173.4 (C=O).

Methyl 3-acetoxy-3-[(2-benzyloxy-5-bromophenyl)-2-methylene]propanoate 182b[290]

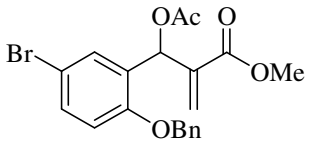

Acetyl chloride (0.3 mL, 4 mmol) was slowly added to a solution of methyl 3-(2-benzyloxy-5-bromophenyl)-3-hydroxy-2-methylenepropanoate **146b** (0.50 g, 1.3 mmol) in dry DCM (10 mL). Pyridine (0.1 mL) was then added and the mixture left to stir at r.t. for 4 h. The crude mixture was concentrated *in vacuo* and flash chromatographed [on silica gel; elution with hexane – EtOAc (9:1)] to afford methyl 3-acetoxy-3-[(2-benzyloxy-5-bromophenyl)-2-methylene]-propanoate **182b** as a light brown oil (0.31 g, 55%) [HRMS: *m/z* calculated for $C_{20}H_{19}BrO_5Na$ (MNa^+) 441.0314. Found 441.0313]; υ_{max} / cm^{-1} 1719 (C=O); δ_H (400 MHz; $CDCl_3$) 2.10 (3H, s, CH_3CO), 3.69 (3H, s, OCH_3), 5.08 (2H, s, OCH_2Ph), 5.68 and 6.43 (2H, 2 x s, $C=CH_2$), 6.80 (1H, d, *J* = 8.7 Hz, ArH), 7.11 (1H, s, CHOAc) and 7.30-7.42 (7H, overlapping m, ArH); δ_C (100 MHz; $CDCl_3$) 20.8 (CH_3CO), 51.8 (OCH_3), 67.4 (CHOAc), 70.2 (OCH_2Ph), 127.6 ($C=CH_2$), 112.9, 113.9, 126.9, 127.8, 128.4, 128.7, 130.4, 132.0, 136.2, 138.4 and 154.7 ($C=CH_2$ and Ar-C), 165.2 and 169.1 (C=O).

***Methyl* (Z)-*3-[2-(benzyloxy)phenyl]-2-(bromomethyl)-2-propenoate* 183a**

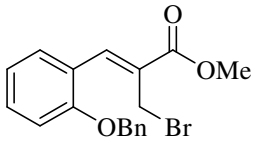

Acetyl bromide (0.3 mL, 4.1 mmol) was slowly added to a solution of methyl 3-(2-benzyloxyphenyl)-3-hydroxy-2-methylenepropanoate **146a** (0.39 g, 1.3 mmol) in dry DCM (10 mL) on an ice bath. Pyridine (0.1 mL) was then added and the mixture left to stir at r.t. for 4 h. The crude mixture was concentrated *in vacuo* and flash chromatographed [on silica gel; elution with hexane – EtOAc (9:1)] to afford *methyl* (Z)-*3-[2-(benzyloxy)phenyl]-2-(bromomethyl)-2-propenoate* **183a** as a yellow oil (0.39 g, 83%) (Found: C, 59.65; H, 4.74. $C_{18}H_{17}BrO_3$ requires: C, 59.85; H, 4.74%); υ_{max} / cm^{-1} 1711 (C=O); δ_H (400 MHz; $CDCl_3$) 3.87 (3H, s, OCH_3), 4.39 (2H, s, CH_2Br), 5.15 (2H, s, OCH_2Ph), 6.98 (1H, d, *J* = 8.3 Hz, ArH), 7.08 (1H, t, *J* = 7.5 Hz, ArH), 7.33-7.42 (6H, overlapping m, ArH), 7.72 (1H, d, *J* = 7.5 Hz) and 8.12 (1H, s, 1′-H); δ_C (100 MHz; $CDCl_3$) 27.4 and 70.3 (CH_2), 52.3 (OCH_3), 112.5, 121.0, 123.9, 127.0, 128.0, 128.4, 128.6, 129.6, 131.1, 136.5 and 138.9 (C=CH and Ar-C), 157.1 [ArC(OBn)] and 166.6 (C=O).

***Methyl* (Z)-*3-[2-(benzyloxy)-5-bromophenyl]-2-(bromomethyl)-2-propenoate* 183b**

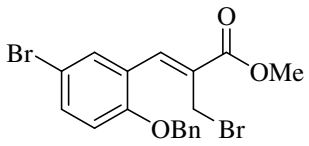

Conc. H_2SO_4 (3.1 mL) was slowly added to a cooled mixture of 3-(2-benzyloxy-5-bromophenyl)-3-hydroxy-2-methylene-propanonate **146b** (0.8 g, 2 mmol) and LiBr (0.37 g, 4.3 mmol) in acetonitrile (10 mL) and stirred at 0 °C for 30 minutes and allowed to warm up to r.t. and stirred for another 1 h. The crude mixture was dissolved in DCM, washed sequentially with water (30 mL), saturated $NaHCO_3$ (30 mL) and brine (30 mL), dried over anhydrous $MgSO_4$, concentrated *in vacuo* and flash chromatographed [on silica gel; elution with hexane – EtOAc (1:1)] to afford *methyl* (Z)-*3-[2-(benzyloxy)-5-bromophenyl]-2-(bromomethyl)-2-propenoate* **183b** as a yellow solid (0.56 g, 60%), m.p. 90-91 °C (Found: C, 49.18; H, 3.65. $C_{18}H_{16}Br_2O_3$ requires: C, 49.12; H, 3.66%); υ_{max} / cm^{-1} 1694 (C=O); δ_H (400 MHz; $CDCl_3$) 3.94 (3H, s, OCH_3), 4.42 (2H, s, CH_2Br), 5.16 (2H, s, OCH_2Ph), 6.90 (1H, d, *J* = 8.7 Hz, ArH), 7.39-7.50 (6H, overlapping m, ArH), 7.93 (1H, s, ArH) and 8.09 (1H, s, 1′-H); δ_C (100 MHz; $CDCl_3$) 26.4 and 70.3 (CH_2), 52.2 (OCH_3), 112.9, 114.0, 125.5, 126.8, 127.9, 128.4, 129.3, 131.7, 133.4, 135.8 and 137.0 (C=CH and Ar-C), 155.8 [ArC(OBn)] and 166.0 (C=O).

***Methyl* (Z)-*3-[2-(benzyloxy)-3-methoxyphenyl]-2-(bromomethyl)-2-propenoate* 183c**

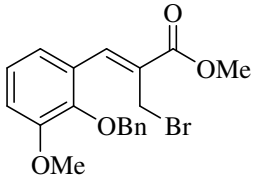

The procedure described for the synthesis of methyl (*Z*)-3-[2-(benzyloxy)phenyl]-2-(bromomethyl)-2-propenoate **183a** was followed, using acetyl bromide (0.3 mL, 4 mmol), methyl 3-(2-benzyloxy-3-methoxyphenyl)-3-hydroxy-2-methylenepropanoate **146c** (0.43 g, 1.3 mmol) and pyridine (0.1 mL) in dry DCM (10 mL). Work-up afforded *methyl* (Z)-*3-[2-(benzyloxy)-3-methoxyphenyl]-2-(bromomethyl)-2-propenoate* **183c** as a brown oil (0.48 g, 94%) (Found: C, 58.33; H, 4.89. $C_{19}H_{19}BrO_4$ requires: C, 58.45; H, 4.99%); υ_{max} / cm^{-1} 1712 (C=O); δ_H (400 MHz; $CDCl_3$) 3.88 and 3.94 (6H, 2 × s, 2 × OCH_3), 4.24 (2H, s, CH_2Br), 5.05 (2H, s, OCH_2Ph), 7.05 (1H, d, *J* = 7.9 Hz, ArH), 7.19 (1H, t, *J* = 8.0 Hz, ArH), 7.27 (1H, d, *J* = 7.7 Hz), 7.32-7.39 (5H, overlapping m, ArH) and 7.90 (1H, s, 1′-H); δ_C (100 MHz; $CDCl_3$) 26.9 and 75.2 (CH_2), 52.1 and

55.7 (OCH_3), 113.6, 120.5, 124.3, 128.06, 128.09, 128.7, 128.8, 129.3, 136.6 and 139.1 (C=CH and Ar-C), 146.1 and 152.7{[ArC(OBn)] and [ArC(OMe)]} and 166.1 (C=O).

***Methyl* (Z)-*3-[2-(benzyloxy)-3-ethoxyphenyl]-2-(bromomethyl)-2-propenoate* 183d**

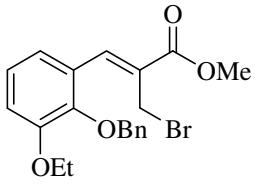

The procedure described for the synthesis of methyl (*Z*)-3-[2-(benzyloxy)phenyl]-2-(bromomethyl)-2-propenoate **183a** was followed, using acetyl bromide (0.3 mL, 4 mmol), methyl 3-(2-benzyloxy-3-ethoxyphenyl)-3-hydroxy-2-methylenepropanoate **146d** (0.45 g, 1.3 mmol) and pyridine (0.1 mL) in dry DCM (10 mL). Work-up afforded *methyl* (Z)-*3-[2-(benzyloxy)-3-ethoxyphenyl]-2-(bromomethyl)-2-propenoate* **183d** as a brown oil (0.46 g, 88%), (Found: C, 59.66; H, 5.42. $C_{20}H_{21}BrO_4$ requires: C, 59.27; H, 5.22%); υ_{max} / cm^{-1} 1712 (C=O); δ_H (400 MHz; $CDCl_3$) 1.50 (3H, t, *J* = 7.0 Hz, CH_2CH_3), 3.85 (3H, s, OCH_3), 4.14 (2H, q, *J* = 7.0 Hz, CH_2CH_3), 4.21 (2H, s, CH_2Br), 5.03 (2H, s, OCH_2Ph), 7.00 (1H, d, *J* = 8.0 Hz, ArH), 7.13 (1H, t, *J* = 8.0 Hz, ArH), 7.22 (1H, d, *J* = 7.6 Hz), 7.29-7.36 (5H, overlapping m, ArH) and 7.87 (1H, s, 1′-H); δ_C (100 MHz; $CDCl_3$) 14.9 (CH_2CH_3), 27.0, 64.4 and 75.3 (CH_2), 52.2 (OCH_3), 114.9, 120.7, 124.3, 128.2, 128.9, 129.5, 137.0 and 139.3 (C=CH and Ar-C), 146.5 and 152.2 {[ArC(OBn)] and [ArC(OEt)]} and 166.4 (C=O).

***Methyl* (Z)-*3-[2-(benzyloxy)-5-chlorophenyl]-2-(bromomethyl)-2-propenoate* 183e**

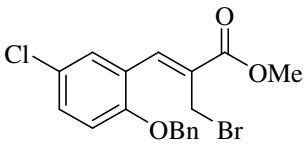

The procedure described for the synthesis of methyl (*Z*)-3-[2-(benzyloxy)phenyl]-2-(bromomethyl)-2-propenoate **183a** was followed, using acetyl bromide (0.3 mL, 4 mmol), methyl 3-(2-benzyloxy-5-chlorophenyl)-3-hydroxy-2-methylenepropanoate **146e** (0.43 g, 1.3 mmol) and pyridine (0.1 mL) in dry DCM (10 mL). Work-up afforded *methyl* (Z)-*3-[2-(benzyloxy)-5-chlorophenyl]-2-(bromomethyl)-2-propenoate* **183e** as a yellow solid (0.47 g, 91%), m.p. 80-81 °C (Found: C, 54.40; H, 4.24. $C_{18}H_{16}BrClO_3$ requires: C, 54.64; H, 4.08%); υ_{max} / cm^{-1}1697 (C=O); δ_H (600 MHz; $CDCl_3$) 3.88 (3H, s, OCH_3), 4.33 (2H, s, CH_2Br), 5.13 (2H, s, OCH_2Ph), 6.89 (1H, d, *J* = 8.8 Hz, ArH), 7.29 (1H, d, *J* = 8.8 Hz), 7.33-7.39 (5H, overlapping m, ArH),

7.68 (1H, s, ArH) and 7.97 (1H, s, 1′-H); δ_C (150 MHz; $CDCl_3$) 26.5 and 70.8 (CH_2), 52.5 (OCH_3), 113.8, 125.4, 126.1, 127.0, 128.2, 128.7, 129.1, 129.6, 130.6, 136.1 and 137.4 (C=CH and Ar-C), 155.6 [ArC(OBn)] and 166.3 (C=O).

***Methyl* (E)-*3-[2-(benzyloxy)phenyl]-2-[(2-propynylamino)methyl]-2-propenoate* 184a**

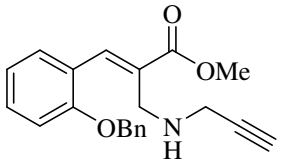

Propargylamine (0.3 mL, 4 mmol) was added to a solution of methyl (*Z*)-3-[2-(benzyloxy)-phenyl]-2-(bromomethyl)-2-propenoate **183a** (0.79 g, 2.2 mmol) in dry THF (5 mL) and the mixture stirred at r.t. for 24 h. The reaction mixture was then concentrated *in vacuo* and flash chromatographed [on silica gel; elution with hexane – EtOAc (3:1)] to afford *methyl* (E)-*3-[2-(benzyloxy)phenyl]-2-[(2-propynylamino)methyl]-2-propenoate* **184a** as a yellow oil (0.57 g, 77%) [HRMS: *m/z* calculated for $C_{21}H_{22}NO_3$ (MH^+) 336.1600. Found 336.1602]; υ_{max} / cm^{-1} 3291 (NH) and 1709 (C=O); δ_H (600 MHz; $CDCl_3$) 1.66 (1H, br s, NH), 2.16 (1H, t, *J* = 2.4 Hz, C≡CH), 3.42 (2H, d, *J* = 2.4 Hz, $CH_2C{\equiv}C$), 3.64 (2H, s, NCH_2), 3.82 (3H, s, OCH_3), 5.14 (2H, s, OCH_2), 6.94 (1H, d, *J* = 8.3 Hz, ArH), 6.98 (1H, t, *J* = 7.5 Hz, ArH), 7.28-7.42 (6H, series of signals, ArH), 7.54 (1H, d, *J* = 7.5 Hz, ArH) and 8.06 (1H, s, 1′-H); δ_C (150 MHz; $CDCl_3$) 38.0 and 45.4 (NCH_2), 52.0 (CH_3), 70.3 (OCH_2), 71.3 and 81.9 (C≡CH), 112.3, 120.8, 124.6, 127.0, 127.9, 128.6, 129.9, 130.4, 130.6, 130.8 and 138.4 (C=CH and Ar-C), 156.8 [ArC(OBn)] and 168.4 (C=O).

***Methyl* (E)-*3-[2-(benzyloxy)-5-bromophenyl]-2-[(2-propynylamino)methyl]-2-propenoate* 184b**

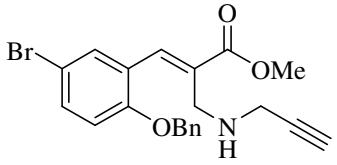

Propargylamine (0.3 mL, 4 mmol) was added to a solution of methyl 3-acetoxy-3-[(2-benzyloxy-5-bromophenyl)-2-methylene]propanoate **182b** (0.92 g, 2.2 mmol) and K_2CO_3 (0.35 g, 2.5 mmol) in CH_3CN (5 mL) and the mixture stirred at r.t. for 12 h. The reaction mixture was then neutralised by pouring into 0.5N-HCl (20 mL) and extracted using $CHCl_3$ (3 × 20 mL). The extracts were combined, washed with brine (2 × 20 mL), concentrated *in vacuo* and flash chromatographed [on silica gel; elution with hexane – EtOAc (4:1)] to afford *methyl* (E)-*3-[2-*

(benzyloxy)-5-bromophenyl]-2-[(2-propynylamino)methyl]-2-propenoate **184b** as a yellow solid (0.75 g, 82%), m.p. 53-54 °C [HRMS: *m/z* calculated for $C_{21}H_{21}BrNO_3$ (MH^+) 414.0705. Found 414.0700]; υ_{max} / cm^{-1} 3296 (NH) and 1697 (C=O); δ_H (400 MHz; $CDCl_3$) 1.82 (1H, br s, NH), 2.22 (1H, s, C≡CH), 3.44 (2H, s, $CH_2C{\equiv}C$), 3.61 (2H, s, NCH_2), 3.82 (3H, s, OCH_3), 5.10 (2H, s, OCH_2), 6.80 (1H, d, *J* = 8.7 Hz, ArH), 7.30-7.40 (6H, overlapping m, ArH), 7.74 (1H, s, ArH) and 7.95 (1H, s, 1′-H); δ_C (100 MHz; $CDCl_3$) 37.7 and 45.0 (NCH_2), 52.0 (CH_3), 70.4 (OCH_2), 71.6 and 81.6 (C≡CH), 113.0, 113.8, 126.5, 126.9, 128.0, 128.5, 131.0, 132.8, 133.0, 136.2 and 136.7 (C=CH and Ar-C), 155.7 [ArC(OBn)] and 167.9 (C=O).

***Methyl* (E)-*3-[2-(benzyloxy)-3-methoxyphenyl]-2-[(2-propynylamino)methyl]-2-propenoate* 184c**

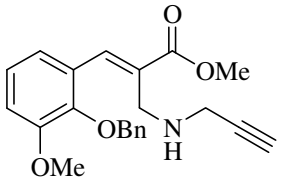

The procedure described for the synthesis of methyl (*E*)-3-[2-(benzyloxy)phenyl]-2-[(2-propynylamino)methyl]-2-propenoate **184a** was followed, using propargylamine (0.3 mL, 4 mmol) and methyl (*Z*)-3-[2-(benzyloxy)-3-methoxyphenyl]-2-(bromomethyl)-2-propenoate **183c** (0.86 g, 2.2 mmol) in dry THF (5 mL). Work-up afforded *methyl* (E)-*3-[2-(benzyloxy)-3-methoxyphenyl]-2-[(2-propynylamino)methyl]-2-propenoate* **184c** as a white solid (0.68 g, 85%), m.p. 54-56 °C [HRMS: *m/z* calculated for $C_{22}H_{24}NO_4$ (MH^+) 366.1705. Found 366.1710]; υ_{max} / cm^{-1} 3296 (NH) and 1709 (C=O); δ_H (600 MHz; $CDCl_3$) 1.72 (1H, br s, NH), 2.17 (1H, s, C≡CH), 3.40 (2H, s, $CH_2C{\equiv}C$), 3.53 (2H, s, NCH_2), 3.80 and 3.90 (6H, s, 2 × OCH_3), 4.99 (2H, s, OCH_2), 6.96 (1H, d, *J* = 7.9 Hz, ArH), 7.07 (1H, t, *J* = 7.9 Hz, ArH), 7.11 (1H, d, *J* = 7.7 Hz, ArH), 7.29-7.41 (5H, series of signals, ArH) and 7.87 (1H, s, 1′-H); δ_C (150 MHz; $CDCl_3$) 38.1 and 45.3 (NCH_2), 51.9 and 55.9 (OCH_3), 71.3 and 81.9 (C≡CH), 75.3 (OCH_2), 113.3, 122.0, 124.0, 128.1, 128.3, 128.7, 130.0, 130.7, 137.2, 138.3 and 146.3 (C=CH and Ar-C), 152.8 [ArC(OBn)] and 168.2 (C=O).

***Methyl* (E)-*3-[2-(benzyloxy)-3-ethoxyphenyl]-2-[(2-propynylamino)methyl]-2-propenoate* 184d**

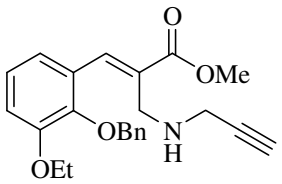

The procedure described for the synthesis of methyl (*E*)-3-[2-(benzyloxy)phenyl]-2-[(2-propynylamino)methyl]-2-propenoate **184a** was followed, using propargylamine (0.3 mL, 4 mmol) and methyl (*Z*)-3-[2-(benzyloxy)-3-ethoxyphenyl]-2-(bromomethyl)-2-propenoate **183d** (0.89 g, 2.2 mmol) in dry THF (5 mL). Work-up afforded *methyl* (E)-*3-[2-(benzyloxy)-3-ethoxyphenyl]-2-[(2-propynylamino)methyl]-2-propenoate* **184d** as a yellow solid (0.74 g, 89%), m.p. 52-53 °C [HRMS: *m/z* calculated for $C_{23}H_{26}NO_4$ (MH^+) 380.1862. Found 380.1861]; υ_{max} / cm^{-1} 3180 (NH) and 1707 (C=O); δ_H (600 MHz; $CDCl_3$) 1.48 (3H, t, *J* = 7.0 Hz, OCH_2CH_3), 1.77 (1H, br s, NH), 2.17 (1H, t, *J* = 2.4 Hz, C≡CH), 3.40 (2H, d, *J* = 2.4 Hz, $CH_2C{\equiv}C$), 3.55 (2H, s, NCH_2), 3.81 (3H, s, OCH_3), 4.11 (2H, q, *J* = 7.0 Hz, OCH_2CH_3), 5.02 (2H, s, OCH_2Ph), 6.95 (1H, d, *J* = 8.0 Hz, ArH), 7.05 (1H, t, *J* = 8.0 Hz, ArH), 7.10 (1H, d, *J* = 7.5 Hz, ArH), 7.30-7.43 (5H, series of signals, ArH) and 7.90 (1H, s, 1′-H); δ_C (150 MHz; $CDCl_3$) 14.9 (CH_2CH_3), 38.0 and 45.3 (NCH_2), 51.9 (OCH_3), 64.4 and 75.2 (OCH_2), 71.3 and 81.9 (C≡CH), 114.4, 121.9, 123.9, 128.0, 128.2, 128.6, 130.0, 130.6, 137.3, 138.4 and 146.5 (C=CH and Ar-C), 152.0 [ArC(OBn)] and 168.2 (C=O).

***Methyl* (E)*-3-[2-(benzyloxy)-5-chloro-phenyl]-2-[(2-propynylamino)methyl]-2-propenoate* 184e**

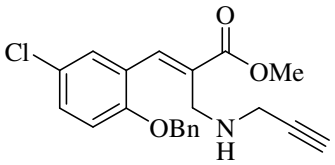

***Methyl 3-[2-(benzyloxy)-5-chlorophenyl]-3-(2-propynylamino)-2-methylenepropanoate* 185e**

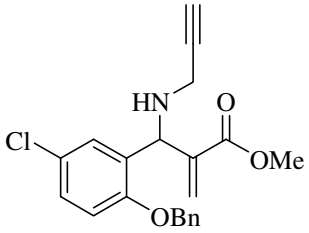

The procedure described for the synthesis of methyl (*E*)-3-[2-(benzyloxy)phenyl]-2-[(2-propynylamino)methyl]-2-propenoate **184a** was followed, using propargylamine (0.3 mL, 4 mmol) and methyl (*Z*)-3-[2-(benzyloxy)-5-chlorophenyl]-2-(bromomethyl)-2-propenoate **183e** (0.87 g, 2.2 mmol) in dry THF (5 mL). Work-up afforded two products.

***Product* 1**. *Methyl* (E)*-3-[2-(benzyloxy)-5-chlorophenyl]-2-[(2-propynylamino)methyl]-2-propenoate* **184e** as a yellow solid (0.61 g, 75%), m.p. 51-53 °C [HRMS: *m/z* calculated for $C_{21}H_{21}ClNO_3$ (MH^+) 370.1210. Found 370.1205]; υ_{max} / cm^{-1} 3301 (NH) and 1697 (C=O); δ_H (600 MHz; $CDCl_3$) 1.77 (1H, br s, NH), 2.20 (1H, s, C≡CH), 3.44 (2H, s, $CH_2C{\equiv}C$), 3.61 (2H, s, NCH_2), 3.83 (3H, s, OCH_3), 5.11 (2H, s, OCH_2), 6.85 (1H, d, *J* = 8.8 Hz, ArH), 7.24 (1H, d, *J* = 8.8 Hz, ArH), 7.32-7.48 (5H, series of signals, ArH), 7.60 (1H, s, ArH) and 7.95 (1H, s, 1′-H); δ_C

(150 MHz; $CDCl_3$) 37.8 and 45.1 (NCH_2), 52.1 (CH_3), 70.6 (OCH_2), 71.6 and 81.6 (C≡CH), 113.5, 125.8, 126.1, 127.0, 128.0, 128.6, 129.9, 130.2, 131.0, 136.3 and 136.9 (C=CH and Ar-C), 155.3 [ArC(OBn)] and 168.1 (C=O).

***Product* 2**. *Methyl 3-[2-(benzyloxy)-5-chlorophenyl]-3-(2-propynylamino)-2-methylenepropanoate* **185e** as a yellow solid (0.16 g, 20%), m.p. 66-68 °C [HRMS: *m/z* calculated for $C_{21}H_{21}ClNO_3$ (MH^+) 370.1210. Found 370.1209]; υ_{max} / cm^{-1} 3271 (NH) and 1707 (C=O).; δ_H (600 MHz; $CDCl_3$) 1.84 (1H, br s, NH), 2.11 (1H, s, C≡CH), 3.34 (2H, s, $CH_2C{\equiv}C$), 3.67 (3H, s, OCH_3), 5.07 (2H, s, OCH_2), 5.29 (1H, s, C*H*NH), 5.80 and 6.36 (2H, 2 × s, $C{=}CH_2$), 6.84 (1H, d, *J* = 8.7 Hz, ArH), 7.16 (1H, d, *J* = 8.7 Hz, ArH), 7.31-7.43 (5H, series of signals, ArH), 7.60 (1H, s, ArH) and 7.95 (1H, s, 1′-H); δ_C (150 MHz; $CDCl_3$) 36.5 (NCH_2), 51.8 (CH_3), 55.0 (CHN), 70.6 (OCH_2), 71.5 and 81.7 (C≡CH), 113.4 and 126.0 (Ar-C), 126.7 ($C{=}CH_2$), 127.4, 128.0, 128.2, 128.4, 128.5, 131.0 and 136.5 (Ar-C), 140.3 ($C{=}CH_2$), 154.9 [ArC(OBn)] and 166.6 (C=O).

***Cinnamate Ester-AZT Conjugate* 186a**[**]

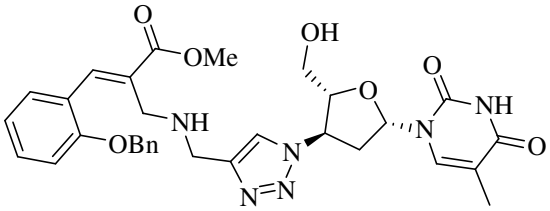

3'-Azido-3'-deoxythymidine **2** (0.61 g, 2.3 mmol) was dissolved in H_2O-THF (1:1; 12 mL) and methyl (*E*)-3-[2-(benzyloxy)phenyl]-2-[(2-propynylamino)methyl]-2-propenoate **184a** (0.77 g, 2.3 mmol), sodium ascorbate (96 mg, 0.49 mmol) and $CuSO_4{\cdot}5H_2O$ (17 mg, 68 μmol) were added to the solution. After stirring for 24 h at r.t., the mixture was extracted with CH_2Cl_2 (2 × 100 mL) and washed sequentially with H_2O (50 mL) and brine (30 mL). The organic layers were combined, dried over anhydrous $MgSO_4$, filtered and concentrated *in vacuo*. The crude material was purified by flash chromatography [on silica gel; elution with EtOAc and then with methanol – DCM (1:4)] to afford the *cinnamate ester-AZT conjugate* **186a** (1.21 g, 87%) as a pale yellow solid, m.p. 92-94 °C [HRMS: *m/z* calculated for $C_{31}H_{35}N_6O_7$ (MH^+) 603.2567. Found 603.2574]; υ_{max} / cm^{-1} 1681 (C=O); δ_H (600 MHz; $CDCl_3$) 1.87 (3H, s, CH_3), 2.78-2.87 (2H, m, C*H*$_2$CHN),

[**] *4-{(*E*)-5-[2-(Benzyloxy)phenyl]-4-methoxycarbonyl-2-aza-4-pentenyl}-1-[(2R,3R,5S)-5-(5-methyl-2,4-dioxo-1,2,3,4-tetrahydro-pyrimidin-1-yl)-2-(hydroxymethyl)tetrahydrofuran-3-yl]-1H-1,2,3-triazole* **186a**

3.63 and 3.87 (4H, s, 2 × NCH_2), 3.72 (1H, dd, *J* = 10.3 and 1.8 Hz, C*H*$_a$OH), 3.81 (3H, s, OCH_3), 3.93 (1H, dd, *J* = 10.3 and 1.8 Hz, C*H*$_b$OH), 4.29-4.31 (1H, m, OCHC*H*N), 5.13 (2H, s, OCH_2Ph), 5.34-5.38 (1H, m, OC*H*CH_2OH), 6.26 (1H, t, *J* = 6.4 Hz, OCHN), 6.94 (2H, t, *J* = 8.0 Hz, ArH), 7.27-7.31 (2H, overlapping m, ArH), 7.34-7.41 (5H, series of signals, ArH), 7.53 (1H, s, ArH), 7.57 (1H, s, ArH) and 8.05 (1H, s, 1′-H); δ_C (150 MHz; $CDCl_3$) 14.5 (CH_3Ar), 37.6 (*C*H_2CHN), 43.7 and 45.3 (CH_2N), 52.1 (OCH_3), 59.0 (CHN), 61.1 (CH_2OH), 70.2 (OCH_2Ph), 85.1 ($HOCH_2$*C*HO), 87.4 (NCHO), 111.0, 112.4, 120.6, 121.8, 124.4, 127.0, 127.8, 128.5, 129.6, 130.3, 130.4, 136.6, 137.3, 138.7, 146.6, 150.5, 156.6, 164.1 and 168.3 (Ar-C, C=C and C=O).

***Cinnamate Ester-AZT Conjugate* 186b**[**]

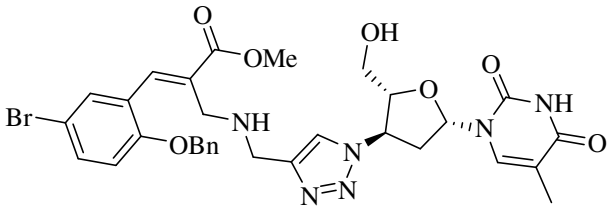

The procedure described for the synthesis of cinnamate ester-AZT conjugate **186a** was followed, using AZT **2** (0.32 g, 1.2 mmol), methyl (*E*)-3-[2-(benzyloxy)-5-bromophenyl]-2-[(2-propynyl-amino)methyl]-2-propenoate **184b** (0.50 g, 1.2 mmol), sodium ascorbate (96 mg, 0.49 mmol) and $CuSO_4 \cdot 5H_2O$ (17 mg, 68 μmol) in H_2O-THF (1:1; 12 mL) mixture. Work-up afforded the *cinnamate ester-AZT conjugate* **186b** (0.75 g, 92%) as a pale yellow solid, m.p. 96-97 °C [HRMS: *m/z* calculated for $C_{31}H_{34}BrN_6O_7$ (MH^+) 681.1672. Found 681.1669]; υ_{max} / cm^{-1} 1681 (C=O); δ_H (600 MHz; $CDCl_3$) 1.90 (3H, s, CH_3), 2.88 (2H, t, *J* = 6.5 Hz, C*H*$_2$CHN), 3.56 and 3.91 (4H, s, 2 × NCH_2), 3.72 (1H, d, *J* = 11.9 Hz, C*H*$_a$OH), 3.81 (3H, s, OCH_3), 3.96 (1H, d, *J* = 11.9 Hz, C*H*$_b$OH), 4.33-4.35 (1H, m, OCHC*H*N), 5.11 (2H, s, OCH_2Ph), 5.37 (1H, dd, *J* = 11.9 and 6.7 Hz, OC*H*CH_2OH), 6.22 (1H, t, *J* = 6.4 Hz, OCHN), 6.82 (1H, d, *J* = 8.8 Hz, ArH), 7.29-7.36 (6H, series of signals, ArH), 7.48 (1H, s, ArH), 7.61 (1H, s, ArH), 7.67 (1H, s, ArH) and 7.93 (1H, s, 1′-H); δ_C (150 MHz; $CDCl_3$) 12.4 (CH_3Ar), 37.5 (*C*H_2CHN), 44.0 and 45.6 (CH_2N), 52.2 (OCH_3), 59.1 (CHN), 61.4 (CH_2OH), 70.6 (OCH_2Ph), 85.2 ($HOCH_2$*C*HO), 88.2 (NCHO), 111.2, 112.8, 114.1, 121.9, 126.6, 127.0, 128.1, 128.6, 130.8, 132.8, 133.0, 136.2, 137.2, 137.6, 146.9, 150.4, 155.8, 163.8 and 168.0 (Ar-C, C=C and C=O).

***Cinnamate Ester-AZT Conjugate* 186c**[**]

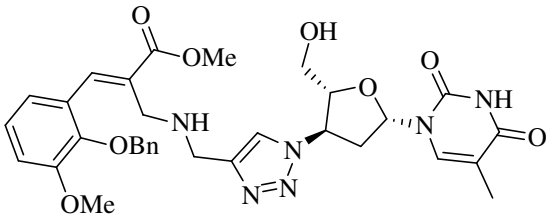

The procedure described for the synthesis of cinnamate ester-AZT conjugate **186a** was followed, using AZT **2** (0.32 g, 1.2 mmol), methyl (*E*)-3-[2-(benzyloxy)-3-methoxyphenyl]-2-[(2-propynylamino)methyl]-2-propenoate **184c** (0.44 g, 1.2 mmol), sodium ascorbate (96 mg, 0.49 mmol) and $CuSO_4 \cdot 5H_2O$ (17 mg, 68 μmol) in H_2O-THF (1:1; 12 mL) mixture. Work-up afforded the *cinnamate ester-AZT conjugate* **186c** (0.68 g, 89%) as a light brown solid, m.p. 82-84 °C [HRMS: *m/z* calculated for $C_{32}H_{37}N_6O_8$ (MH^+) 633.2673. Found 633.2670]; υ_{max} / cm^{-1} 1681 (C=O); δ_H (600 MHz; $CDCl_3$) 1.89 (3H, s, CH_3), 2.84-2.88 (2H, m, CH_2CHN), 3.52 and 3.85 (4H, s, 2 × NCH_2), 3.71 (1H, d, *J* = 12.4 Hz, CH_aOH), 3.79 and 3.89 (6H, s, 2 × OCH_3), 3.93 (1H, d, *J* = 12.4 Hz, CH_bOH), 4.29-4.31 (1H, m, OCHC*H*N), 4.98 (2H, s, OCH_2Ph), 5.35 (1H, dd, *J* = 12.4 and 6.3 Hz, OC*H*CH_2OH), 6.21 (1H, t, *J* = 6.4 Hz, OCHN), 6.93-6.96 (2H, series of signals, ArH), 7.04 (1H, t, *J* = 7.9 Hz, ArH), 7.28-7.38 (5H, series of signals, ArH), 7.48 (1H, s, ArH), 7.58 (1H, s, ArH) and 7.81 (1H, s, 1′-H); δ_C (150 MHz; $CDCl_3$) 12.4 (CH_3Ar), 37.5 (*C*H_2CHN), 44.0 and 45.4 (CH_2N), 52.1 and 55.9 (OCH_3), 59.0 (CHN), 61.3 (CH_2OH), 75.3 (OCH_2Ph), 85.2 ($HOCH_2$*C*HO), 88.2 (NCHO), 111.1, 113.2, 121.6, 122.0, 124.1, 128.1, 128.3, 128.7, 129.8, 130.5, 137.1, 137.6, 138.7, 146.0, 146.6, 150.4, 152.8, 163.8 and 168.1 (Ar-C, C=C and C=O).

***Cinnamate Ester-AZT Conjugate* 186d**[**]

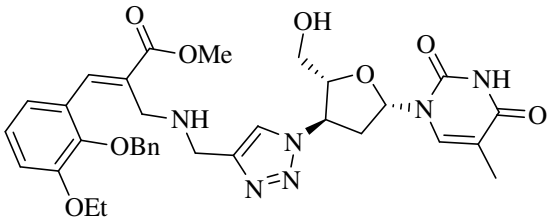

The procedure described for the synthesis of cinnamate ester-AZT conjugate **186a** was followed, using AZT **2** (0.32 g, 1.2 mmol), methyl (*E*)-3-[2-(benzyloxy)-3-ethoxyphenyl]-2-[(2-propynyl-amino)methyl]-2-propenoate **184d** (0.46 g, 1.2 mmol), sodium ascorbate (96 mg, 0.49 mmol) and $CuSO_4 \cdot 5H_2O$ (17 mg, 68 μmol) in H_2O-THF (1:1; 12 mL) mixture. Work-up afforded the

cinnamate ester-AZT conjugate **186d** (0.69 g, 89%) as a light brown solid, m.p. 91-93 °C [HRMS: *m/z* calculated for $C_{33}H_{39}N_6O_8$ (MH^+) 647.2829. Found 647.2833]; υ_{max} / cm^{-1} 1684 (C=O); δ_H (600 MHz; $CDCl_3$) 1.45 (3H, t, *J* = 7.0 Hz, OCH_2CH_3), 1.85 (3H, s, CH_3), 2.78-2.87 (2H, m, CH_2CHN), 3.52 and 3.83 (4H, s, 2 × NCH_2), 3.70 (1H, d, *J* = 2.1 and 12.1Hz, CH_aOH), 3.78 (3H, s, OCH_3), 3.91 (1H, d, *J* = 2.1 and 12.1 Hz, CH_bOH), 4.08 (2H, q, *J* = 7.0 Hz, OCH_2CH_3), 4.28-4.30 (1H, m, OCHC*H*N), 4.98 (2H, s, OCH_2Ph), 5.36 (1H, dd, *J* = 8.4 and 5.8 Hz, $OCHCH_2OH$), 6.24 (1H, t, *J* = 6.4 Hz, OCHN), 6.93 (2H, d, *J* = 7.9 Hz, ArH), 7.00 (1H, m, ArH), 7.27-7.39 (5H, series of signals, ArH), 7.54 (1H, s, ArH), 7.60 (1H, s, ArH) and 7.83 (1H, s, 1′-H); δ_C (150 MHz; $CDCl_3$) 12.4 (CH_3Ar), 15.0 (CH_2CH_3), 37.7 (CH_2CHN), 44.1 and 45.5 (CH_2N), 52.1 (OCH_3), 59.1 (CHN), 61.2 (CH_2OH), 64.4 (OCH_2CH_3), 75.2 (OCH_2Ph), 85.3 ($HOCH_2CHO$), 87.6 (NCHO), 111.0, 114.4, 121.6, 122.0, 124.1, 128.1, 128.3, 128.7, 129.8, 130.5, 137.3, 137.5, 138.7, 146.3, 146.9, 150.6, 152.2, 164.2 and 168.3 (Ar-C, C=C and C=O).

***Cinnamate Ester-AZT Conjugate* 186e**[**]

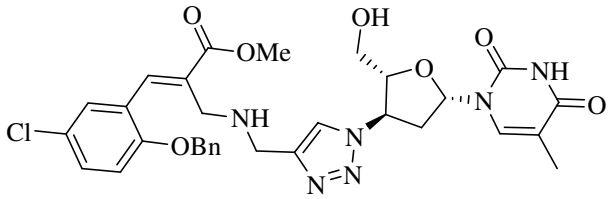

The procedure described for the synthesis of cinnamate ester-AZT conjugate **186a** was followed, using AZT **2** (0.32 g, 1.2 mmol), methyl (*E*)-3-[2-(benzyloxy)-5-chlorophenyl]-2-[(2-propynyl-amino)methyl]-2-propenoate **184e** (0.44 g, 1.2 mmol), sodium ascorbate (96 mg, 0.49 mmol) and $CuSO_4 \cdot 5H_2O$ (17 mg, 68 μmol) in H_2O-THF (1:1; 12 mL) mixture. Work-up afforded the *cinnamate ester-AZT conjugate* **186e** (0.69 g, 90%) as an off white solid, m.p. 92-93 °C [HRMS: *m/z* calculated for $C_{31}H_{34}ClN_6O_7$ (MH^+) 637.2178. Found 637.2180]; υ_{max} / cm^{-1} 1689 (C=O); δ_H (600 MHz; $CDCl_3$) 1.85 (3H, s, CH_3), 2.77-2.88 (2H, m, CH_2CHN), 3.56 and 3.89 (4H, s, 2 × NCH_2), 3.73 (1H, d, *J* = 11.9 Hz, CH_aOH), 3.79 (3H, s, OCH_3), 3.92 (1H, d, *J* = 11.9 Hz, CH_bOH), 4.29-4.31 (1H, m, OCHC*H*N), 5.09 (2H, s, OCH_2Ph), 5.35-5.39 (1H, m, $OCHCH_2OH$), 6.26 (1H, t, *J* = 5.7 Hz, OCHN), 6.85 (1H, d, *J* = 8.9 Hz, ArH), 7.20 (1H, d, *J* = 7.5 Hz, ArH), 7.27-7.36 (5H, series of signals, ArH), 7.47 (1H, s, ArH), 7.57 (1H, s, ArH), 7.65 (1H, s, ArH) and 7.92 (1H, s, 1′-H); δ_C (150 MHz; $CDCl_3$) 12.3 (CH_3Ar), 37.6 (CH_2CHN), 43.9 and 45.4 (CH_2N), 50.4 (OCH_3), 59.1 (CHN), 61.1 (CH_2OH), 70.6 (OCH_2Ph), 85.2

($HOCH_2CHO$), 87.3 (NCHO), 111.0, 113.7, 122.0, 125.4, 126.0, 127.0, 127.1, 128.0, 128.6, 129.9, 130.0, 130.5, 136.2, 137.3, 146.5, 150.6, 155.2, 164.1 and 168.0 (Ar-C, C=C and C=O).

***1-[(2*S*,4*R*,5*R*)-4-Azido-5-(bromomethyl)tetrahydrofuran-2-yl]-5-methylpyrimidine-2,4(1*H*,3*H*)-dione* 187**

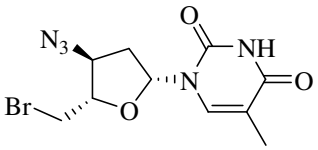

Br_2 (0.25 mL, 4.8 mmol) was added dropwise to a solution of PPh_3 (1.25 g, 4.8 mmol) in dry DCM (10 mL) at 0 °C until an orange colour persisted. Solution was then stirred for 30 minutes. 3'-azido-3'-deoxythymidine **2** (1.2 g, 4.6 mmol) dissolved in THF (5 mL) was then added and the mixture was stirred for 3 h at 0 °C. The crude product was washed with saturated aq. Na_2SO_3 (15 mL) and aq. Na_2CO_3 (15 mL), and the organic layer was dried over anhydrous $MgSO_4$, concentrated *in vacuo* and purified by flash chromatography [on silica gel; elution with hexane – EtOAc (3:1)] to afford *1-[(2*S*,4*R*,5*R*)-4-azido-5-(bromomethyl)tetrahydrofuran-2-yl]-5-methylpyrimidine-2,4(1*H*,3*H*)-dione* **187** (0.99 g, 65%) as a brown solid, m.p. 90-92 °C [HRMS: *m/z* calculated for $C_{10}H_{13}BrN_5O_3$ (MH^+) 330.0202. Found 330.0203]; υ_{max} / cm^{-1} 2096 (N≡N) and 1697 (C=O); δ_H (400 MHz; $CDCl_3$) 1.90 (3H, s, CH_3), 2.36-2.48 (2H, m, CH_2CHN), 3.65 (2H, dd, *J* = 11.3 and 4.5 Hz, CH_2Br), 4.05 (1H, dd, *J* = 7.9 and 4.3 Hz, OCHC*H*N), 4.28 (1H, dd, *J* = 7.9 and 4.5 Hz, OC*H*CH_2Br), 6.14 (1H, t, *J* = 6.6 Hz, OCHN) and 7.36 (1H, s, ArH); δ_C (100 MHz; $CDCl_3$) 12.5 (CH_3), 32.7 and 37.2 (CH_2), 62.2 (CHN), 82.1 ($BrCH_2CHO$), 85.1 (NCHO), 111.4, 135.6, 150.3 and 164.0 (Ar-C and C=O).

3'-Azido-3'-deoxythymidine diethyl phosphate 189[281]

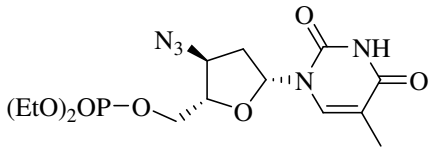

n-BuLi (2.5 M, 1.0 mL) was added to a solution of 3'-azido-3'-deoxythymidine **2** (0.64 g, 2.4 mmol) dissolved in THF (10 mL) at 0 °C under Ar and stirred for 30 min. Diethyl chlorophosphate (0.4 mL, 3 mmol) was then introduced into the mixture, which was then stirred for 3 h at 0 °C and then overnight at r.t. Saturated aq. NH_4Cl (25 mL) was added to quench the reaction and the product was extracted with DCM (30 mL × 3). The combined organic extracts were washed with brine, dried over anhydrous $MgSO_4$, concentrated *in vacuo* and flash

chromatographed [on silica gel; elution with hexane – EtOAc (1:1)] to afford 3'-azido-3'-deoxythymidine diethyl phosphate **189** (0.67 g, 72%) as a yellow oil [HRMS: *m/z* calculated for $C_{14}H_{23}N_5O_6P$ (MH^+) 388.1386. Found 388.1389]; υ_{max} / cm^{-1} 2101 (N≡N) and 1681 (C=O); δ_H (600 MHz; $CDCl_3$) 1.34 (6H, dt, J = 7.1 and 4.4 Hz, 2 × OCH_2CH_3), 1.92 (3H, s, CH_3Ar), 2.31 and 2.44 (2H, m, CH_2CHN), 4.02 (1H, m, OCHCHN), 4.15 (4H, m, 2 × OCH_2CH_3), 4.24 (1H, ddd, J = 11.5, 6.1 and 2.9 Hz, CH_aOP), 4.29 (1H, ddd, J = 11.5, 5.8 and 2.9 Hz, OCH_bOP) 4.34 (1H, td, J = 7.4 and 4.6 Hz, $OCHCH_2OP$), 6.24 (1H, t, J = 6.5 Hz, OCHN), 7.39 (1H, s, ArH) and 9.76 (1H, br s, NH); δ_C (150 MHz; $CDCl_3$) 12.3 (CH_3Ar), 16.0 (d, $J_{P,C}$ = 6.5 Hz, OCH_2CH_3), 37.4 (CH_2CHN), 60.0 (CHN), 64.3 (d, $J_{P,C}$ = 6.0 Hz, OCH_2CH_3), 66.0 (d, $J_{P,C}$ = 5.5 Hz, CH_2OP), 82.2 (d, $J_{P,C}$ = 7.8 Hz, $POCH_2CHO$), 84.6 (NCHO), 111.4, 135.0, 150.4 and 163.9 (Ar-C and C=O).

Phosphorylated Cinnamate Ester-AZT conjugate **190a**[††]

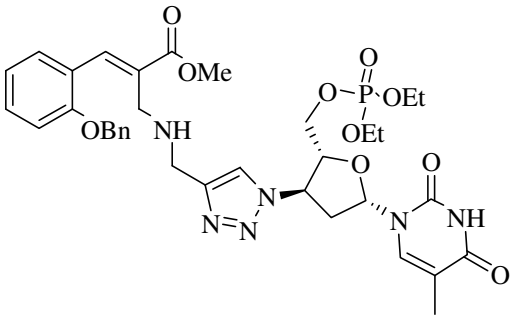

3'-Azido-3'-deoxythymidine diethyl phosphate **189** (0.93 g, 2.3 mmol) was dissolved in H_2O-THF (1:1; 12 mL) and methyl (*E*)-3-[2-(benzyloxy)phenyl]-2-[(2-propynylamino)methyl]-2-propenoate **184a** (0.77 g, 2.3 mmol), sodium ascorbate (96 mg, 0.49 mmol) and $CuSO_4 \cdot 5H_2O$ (17 mg, 68 μmol) were added to the solution. After stirring for 24 h at r.t., the mixture was extracted with CH_2Cl_2 (2 × 100 mL) and the combined extracts were washed sequentially with H_2O (50 mL) and brine (30 mL), dried over anhydrous $MgSO_4$, filtered and concentrated *in vacuo*. The crude material was purified by flash chromatography [on silica gel; elution with EtOAc and then with methanol – DCM (1:4)] to afford the *phosphorylated cinnamate ester-AZT conjugate* **190a** (1.31 g, 82%) as a pale yellow solid, m.p. 74-76 °C [HRMS: *m/z* calculated for $C_{33}H_{39}N_6O_9P$ (MH^+) 694.2516. Found 694.2519]; υ_{max} / cm^{-1} 1689 (C=O); δ_H (600 MHz; $CDCl_3$) 1.32 (6H, dt, J = 11.9 and 7.0 Hz, OCH_2CH_3), 1.95 (3H, s, CH_3Ar), 2.58-2.92 (2H, m,

[††] *4-{(E)-5-[2-(Benzyloxy)phenyl]-4-methoxycarbonyl-2-aza-4-pentenyl}-1-{[(2R,3R,5S)-5-(5-methyl-2,4-dioxo-1,2,3,4-tetrahydro-pyrimidin-1-yl)-2-[(diethoxyphosphonyl)methyl]tetrahydrofuran-3-yl]-1H-1,2,3-triazole* **190a**

C*H*$_2$CHN), 3.62 and 3.87 (4H, s, 2 × NCH$_2$), 3.80 (3H, s, OCH$_3$), 4.17 (4H, m, OCH$_2$CH$_3$), 4.25 (1H, ddd, *J* = 11.5, 6.0 and 2.6 Hz, C*H*$_a$OH), 4.36 (1H, ddd, *J* = 11.5, 6.0 and 2.6 Hz, C*H*$_b$OH), 4.46 (1H, m, OCHC*H*N), 5.13 (2H, s, OCH$_2$Ph), 5.29-5.31 (1H, m, OC*H*CH$_2$OH), 6.40 (1H, t, *J* = 6.0 Hz, OCHN), 6.94 (2H, t, *J* = 6.9 Hz, ArH), 7.26-7.40 (7H, series of signals, ArH), 7.47 (1H, s, ArH), 7.55 (1H, s, ArH) and 8.04 (1H, s, 1′-H); δ_C (150 MHz; CDCl$_3$) 12.3 (CH$_3$Ar), 16.1 (d, J_{PC} = 6.4 Hz, OCH$_2$*C*H$_3$), 38.0 (*C*H$_2$CHN), 43.6 and 45.2 (CH$_2$N), 52.0 (OCH$_3$), 58.8 (CHN), 64.4 (d, $J_{P,C}$ = 5.0 Hz, O*C*H$_2$CH$_3$), 65.7 (d, $J_{P,C}$ = 5.0 Hz, CH$_2$OH), 70.3 (OCH$_2$Ph), 82.5 (d, $J_{P,C}$ = 7.9 Hz, POCH$_2$*C*HO), 85.6 (NCHO), 111.5, 112.5, 120.7, 122.0, 124.4, 127.0, 127.9, 128.47, 128.50, 128.54, 130.39, 130.44, 135.6, 136.9, 139.1, 150.2, 156.7, 163.7 and 168.2 (Ar-C, C=C and C=O).

3.12. SYNTHESIS AND REACTIONS OF COUMARIN-3-CARBALDEHYDES

Coumarin-3-carbaldehyde 191a

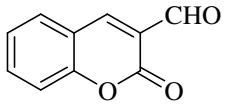

Method 1. *Microwave-assisted reaction.* A mixture of 3-methylcoumarin **150a** (0.50 g, 3.1 mmol) and SeO_2 (0.69 g, 6.2 mmol) was ground in a mortar and transferred into a microwave vial, sealed and irradiated at 150 W and 170 °C for 1 hour. (An extraction funnel was situated over the reaction vial during the reaction with SeO_2.) The product was then extracted into EtOAc and the solution was concentrated *in vacuo*. Flash chromatography [on silica gel; elution with hexane – EtOAc (3:1)] afforded brown crystals of coumarin-3-carbaldehyde **191a** (0.28 g, 52%), m.p. 133-135 °C (lit.[245] 132-133 °C) [HRMS: *m/z* calculated for $C_{10}H_7O_3$ (MH^+) 175.0395. Found 175.0381]; υ_{max} / cm^{-1} 1717 and 1687 (C=O); δ_H (400 MHz, $CDCl_3$) 7.37 (2H, overlapping d and t, ArH), 7.68 (2H, m, ArH), 8.42 (1H, s, ArH) and 10.24 (1H, s, CHO); δ_C (100 MHz, $CDCl_3$) 117.6, 118.6, 122.2, 125.8, 131.3, 135.5, 146.1, 160.0, (Ar-C), 160.6 and 188.2 (C=O).

Method 2. *Conventional thermal reaction.* A mixture of 3-methylcoumarin **150a** (0.50 g, 3.1 mmol) and selenium dioxide (0.69 g, 6.2 mmol) was heated at 170 °C for 3 h initially and then for a further 6 h. The product was then extracted into EtOAc and the solution was concentrated

in vacuo. Flash chromatography [on silica gel; elution with hexane – EtOAc (3:1)] afforded brown crystals of coumarin-3-carbaldehyde **191a** (0.13 g, 24%).

6-Bromocoumarin-3-carbaldehyde 191b

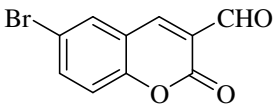

The procedure described for the synthesis of coumarin-3-carbaldehyde **191a** (*Method 1*) was followed, using 6-bromo-3-methylcoumarin **150b** (0.74 g, 3.1 mmol) and SeO_2 (0.69 g, 6.2 mmol). Work-up afforded 6-bromocoumarin-3-carbaldehyde **191b** (0.47 g, 60%) as a yellow solid, m.p. 189-190 °C (lit.[282] 195 °C) [HRMS: *m/z* calculated for $C_{10}H_6BrO_3$ (MH^+) 252.9500. Found 252.9481]; υ_{max} / cm^{-1} 1732 and 1687 (C=O); δ_H (400 MHz, $CDCl_3$) 7.29 (1H, d, *J* = 8.83 Hz, ArH), 7.76 (1H, dd, *J* = 8.83 and 2.30 Hz, ArH), 7.81 (1H, d, *J* = 2.24 Hz, ArH), 8.32 (1H, s, ArH) and 10.24 (1H, s, CHO); δ_C (100 MHz, $CDCl_3$) 118.3, 119.3, 120.0, 122.9, 133.2, 138.1, 144.5, 154.7, (Ar-C), 159.8 and 187.7 (C=O).

6-Chlorocoumarin-3-carbaldehyde 191e

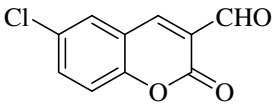

The procedure described for the synthesis of coumarin-3-carbaldehyde **191a** (*Method 1*) was followed, using 6-chloro-3-methylcoumarin **150e** (0.60 g, 3.1 mmol) and SeO_2 (0.69 g, 6.2 mmol). Work-up afforded 6-chlorocoumarin-3-carbaldehyde **191e** (0.36 g, 56%) as a yellow solid, m.p. 179-180 °C (lit.[282] 179 °C) [HRMS: *m/z* calculated for $C_{10}H_6ClO_3$ (MH^+) 209.0005. Found 209.0002]; υ_{max} / cm^{-1} 1740 and 1689 (C=O); δ_H (400 MHz, $CDCl_3$) 7.35 (1H, d, *J* = 8.81 Hz, ArH), 7.62 (1H, d, *J* = 8.89, ArH), 7.66 (1H, s, ArH), 8.33 (1H, s, ArH) and 10.24 (1H, s, CHO); δ_C (100 MHz, $CDCl_3$) 119.0, 119.5, 122.9, 130.1, 131.1, 135.3, 144.7, 154.3, (Ar-C), 159.9 and 187.8 (C=O).

***Methyl 3-(6-bromocoumarin-3-yl)-3-hydroxy-2-methylenepropanoate* 196b**

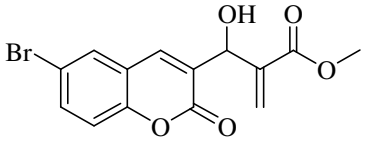

A mixture of 6-bromocoumarin-3-carbaldehyde **191b** (0.25 g, 1.0 mmol), methyl acrylate (0.18 mL, 2.0 mmol) and DABCO (0.03 g, 0.3 mmol) in $CHCl_3$ (5 mL) was sealed in a round-bottomed flask and stirred at r.t. for 4 d. The mixture was concentrated *in vacuo* and purified by flash chromatography [on silica gel; elution with hexane – EtOAc (9:1)] to afford *methyl 3-(6-bromocoumarin-3-yl)-3-hydroxy-2-methylenepropanoate* **196b** as a white solid (0.15 g, 45%), m.p. 105-106 °C [HRMS: *m/z* calculated for $C_{14}H_{11}BrO_5Na$ (MNa^+) 360.9688. Found 360.9690]; υ_{max} / cm^{-1} 3413 (OH) and 1702 (C=O); δ_H (400 MHz; $CDCl_3$) 3.76 (3H, s, OCH_3), 4.01 (1H, d, *J* = 7.1 Hz, OH), 5.61 (1H, d, *J* = 7.1 Hz, C*H*OH), 6.08 and 6.45 (2H, 2 × s, C=CH_2), 7.22 (1H, d, *J* = 8.8 Hz, ArH), 7.61 (1H, dd, *J* = 8.8 and 2.0 Hz, ArH), 7.67 (1H, d, *J* = 2.0 Hz, ArH) and 7.78 (1H, s, 4-H); δ_C (100 MHz; $CDCl_3$) 52.2 (OCH_3), 69.1 (CHOH), 128.2 (C=*C*H_2), 117.2, 118.2, 120.5, 129.3, 130.5, 134.4, 138.2, 138.5 and 152.1 (*C*=CH_2 and Ar-C), 160.0 and 166.5 (C=O).

4-(6-Bromocoumarin-3-yl)-4-hydroxy-3-methylene-2-butanone **195b**

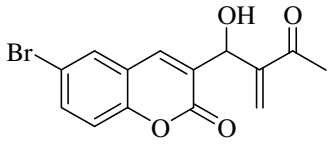

A mixture of 6-bromocoumarin-3-carbaldehyde **191b** (0.25 g, 1.0 mmol), methyl vinyl ketone (0.17 mL, 2.0 mmol) and DABCO (0.03 g, 0.3 mmol) in $CHCl_3$ (5 mL) was sealed in a round-bottomed flask and stirred at r.t. for 4 d. The mixture was concentrated *in vacuo* and purified by flash chromatography [on silica gel; elution with hexane – EtOAc (9:1)] to afford *4-(6-bromocoumarin-3-yl)-4-hydroxy-3-methylene-2-butanone* **195b** as a white solid (0.14 g, 42%), m.p. 122-124 °C [HRMS: *m/z* calculated for $C_{14}H_{11}BrO_4Na$ (MNa^+) 344.9738. Found 344.9734]; υ_{max} / cm^{-1} 3413 (OH), 1699 and 1712 (C=O); δ_H (400 MHz; $CDCl_3$) 2.37 (3H, s, CH_3), 4.12 (1H, d, *J* = 7.9 Hz, OH), 5.60 (1H, d, *J* = 7.9 Hz, C*H*OH), 6.25 and 6.31 (2H, 2 × s, C=CH_2), 7.22 (1H, d, *J* = 8.8 Hz, ArH), 7.61 (1H, d, *J* = 8.8 Hz, ArH), 7.67 (1H, s, ArH) and 7.80 (1H, s, 4-H); δ_C (100 MHz; $CDCl_3$) 26.3 (CH_3), 69.2 (CHOH), 128.7 (C=*C*H_2), 117.2, 118.2, 120.6, 129.4, 130.5, 134.3, 138.7, 146.2 and 152.0 (*C*=CH_2 and Ar-C), 160.0 and 200.3 (C=O).

3.13. 4-SUBSTITUTED COUMARINS

2-(Tosyliminomethyl)phenol 198a

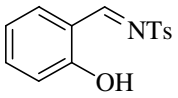

p-Toluenesulphonamide (2.98 g, 17.4 mmol), tetraethyl orthosilicate (4.2 mL, 19 mmol) and salicylaldehyde **142a** (2.12 g, 17.4 mmol) were added to a 50 mL round-bottomed flask equipped with a magnetic stirrer, a positive flow of nitrogen and a short still-head connected to a receiving flask. The reaction mixture was heated for 12 h. at 150 °C (oil bath), and ethanol, upon formation, was collected in the receiving flask. After cooling, the reaction mixture was diluted with ether and the precipitate was filtered off and washed with cold ether (3 × 15 mL). Recrystallisation from ether afforded 2-(tosyliminomethyl)phenol **198a** as a yellow solid (4.2 g, 87%), m.p. 119-120 °C (lit.[283] 120 °C); υ_{max} / cm^{-1} 1621 (C=N); δ_H (400 MHz; $CDCl_3$) 2.43 (3H, s, CH_3), 6.99 (2H, d, *J* = 8.6 Hz, ArH), 7.34 (2H, d, *J* = 8.0 Hz, ArH), 7.50 (2H, d, *J* = 8.6 Hz, ArH), 7.85 (2H, d, *J* = 8.0 Hz, ArH), 9.08 (1H, s, HCN) and 10.82 (1H, s, OH); δ_C (100 MHz; $CDCl_3$) 21.6 (CH_3), 116.5, 117.8, 120.2, 127.8, 129.9, 134.9, 135.3, 137.3, 145.0 and 162.0 (Ar-C) and 171.4 (C=N).

4-Bromo-2-(tosyliminomethyl)phenol 198b

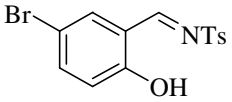

The procedure described for the synthesis of 2-(tosyliminomethyl)phenol **198a** was followed, using *p*-toluenesulphonamide (2.98 g, 17.4 mmol), tetraethyl orthosilicate (4.2 mL, 19 mmol) and 5-bromosalicylaldehyde **142b** (3.50 g, 17.4 mmol). Work-up afforded 4-bromo-2-(tosylimino-methyl)phenol **198b** as a yellow solid (5.7 g, 93%), m.p. 185-187 °C (lit.[284] 183-185 °C); υ_{max} / cm^{-1} 1613 (C=N); δ_H (400 MHz; $CDCl_3$) 2.44 (3H, s, CH_3), 6.89 (1H, d, *J* = 8.9 Hz, ArH), 7.35 (2H, d, *J* = 8.1 Hz, ArH), 7.55 (1H, dd, *J* = 8.5 and 2.0 Hz, ArH), 7.60 (1H, d, *J* = 2.0 Hz, ArH), 7.85 (2H, d, *J* = 8.5 Hz, ArH), 9.00 (1H, s, HCN) and 10.80 (1H, s, OH); δ_C (100 MHz; $CDCl_3$) 21.6 (CH_3), 111.6, 117.9, 119.8, 128.0, 130.1, 134.4, 136.8, 139.6, 145.3 and 160.9 (Ar-C) and 170.1 (C=N).

2-Methoxy-6-(tosyliminomethyl)phenol 198c

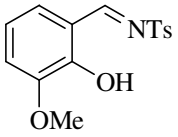

The procedure described for the synthesis of 2-(tosyliminomethyl)phenol **198a** was followed, using *p*-toluenesulphonamide (2.98 g, 17.4 mmol), tetraethyl orthosilicate (4.2 mL, 19 mmol) and 3-methoxysalicylaldehyde **142c** (2.65 g, 17.4 mmol). Work-up afforded 2-methoxy-6-(tosyl-iminomethyl)phenol **198c** as a yellow solid (4.8 g, 90%), m.p. 110-112 °C (lit.[284] 115-117 °C); υ_{max} / cm^{-1} 1593 (C=N); δ_H (400 MHz; $CDCl_3$) 2.41 (3H, s, CH_3Ar), 3.87 (3H, s, OCH_3), 6.92 (1H, t, *J* = 7.8 Hz, ArH), 7.08 (1H, d, *J* = 7.8 Hz, ArH), 7.12 (1H, d, *J* = 7.8 Hz, ArH), 7.32 (2H, d, *J* = 7.6 Hz, ArH), 7.84 (2H, d, *J* = 7.6 Hz, ArH), 9.10 (1H, s, HCN) and 10.71 (1H, s, OH); δ_C (100 MHz; $CDCl_3$) 21.6 (CH_3Ar), 56.2 (OCH_3), 116.7, 118.0, 119.9, 125.7, 127.8, 129.9, 134.9, 145.0, 148.3 and 152.0 (Ar-C) and 171.0 (C=N).

***2-Ethoxy-6-(tosyliminomethyl)phenol* 198d**

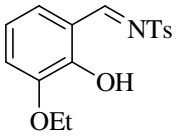

The procedure described for the synthesis of 2-(tosyliminomethyl)phenol **198a** was followed, using *p*-toluenesulphonamide (2.98 g, 17.4 mmol), tetraethyl orthosilicate (4.2 mL, 19 mmol) and 3-ethoxysalicylaldehyde **142d** (2.89 g, 17.4 mmol). Work-up afforded *2-ethoxy-6-(tosylimino-methyl)phenol* **198d** as a yellow solid (5.1 g, 92%), m.p. 119-121 °C [HRMS: *m/z* calculated for $C_{16}H_{16}NO_4S$ $(M-H)^+$ 318.0800. Found 318.0804]; υ_{max} / cm^{-1} 1570 (C=N); δ_H (400 MHz; $CDCl_3$) 1.42 (3H, t, *J* = 7.0 Hz, $OCH_2C\mathit{H}_3$), 2.39 (3H, s, CH_3Ar), 4.06 (2H, q, *J* = 7.0 Hz, $OC\mathit{H}_2CH_3$), 6.89 (1H, t, *J* = 6.6 Hz, ArH), 7.05 (1H, d, *J* = 6.6 Hz, ArH), 7.12 (1H, d, *J* = 6.6 Hz, ArH), 7.30 (2H, d, *J* = 5.9 Hz, ArH), 7.82 (2H, d, *J* = 5.9 Hz, ArH), 9.10 (1H, s, HCN) and 10.61 (1H, s, OH); δ_C (100 MHz; $CDCl_3$) 15.2 ($OCH_2\mathit{C}H_3$), 22.1 (CH_3Ar), 65.3 (OCH_2), 117.3, 119.8, 120.4, 126.0, 128.3, 130.4, 135.6, 145.4, 148.1 and 152.7 (Ar-C) and 171.3 (C=N).

4-Chloro-2-(tosyliminomethyl)phenol 198e[285]

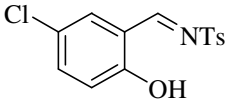

The procedure described for the synthesis of 2-(tosyliminomethyl)phenol **198a** was followed, using *p*-toluenesulphonamide (2.98 g, 17.4 mmol), tetraethyl orthosilicate (4.2 mL, 19 mmol) and 5-chlorosalicylaldehyde **142e** (2.72 g, 17.4 mmol). Work-up afforded 4-bromo-2-(tosylimino-methyl)phenol **198e** as a yellow solid (5.0 g, 93%), m.p. 174-175 °C (lit.[285] m.p. not cited); υ_{max} / cm^{-1} 1618 (C=N); δ_H (400 MHz; $CDCl_3$) 2.43 (3H, s, CH_3), 6.93 (1H, d, *J* = 8.8 Hz, ArH), 7.35 (2H, d, *J* = 7.5 Hz, ArH), 7.42 (1H, d, *J* = 8.8 and 2.0 Hz, ArH), 7.45 (1H, s, ArH), 7.84 (2H, d, *J* = 7.5 Hz, ArH), 9.00 (1H, s, HCN) and 10.78 (1H, s, OH); δ_C (100 MHz; $CDCl_3$) 21.6 (CH_3), 117.2, 119.5, 124.9, 128.0, 130.0, 133.7, 134.4, 136.9, 145.3 and 160.5 (Ar-C) and 170.2 (C=N).

***2-[6-Bromo-2-(tosylamino)-2*H*-chromen-3-yl]ethanol* 202b**

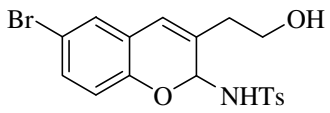

tert-*Butyl 3-(5-bromo-2-hydroxyphenyl)-3-tosylamino-2-methylenepropanoate* 199b

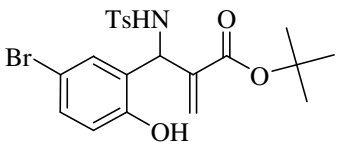

A mixture of 4-bromo-2-(tosyliminomethyl)phenol **198b** (0.7 g, 2 mmol), *tert*-butyl acrylate (0.7 mL, 5 mmol) and DABCO (0.9 g, 9 mmol) in $CHCl_3$–THF (1:1; 10 mL) was sealed in a round-bottomed flask and stirred at room temperature for 2 d. The mixture was concentrated *in vacuo* and purified by flash chromatography [on silica gel; elution with hexane – EtOAc (9:1)] to afford three products.

Product 1. *2-[6-Bromo-2-(tosylamino)-2*H*-chromen-3-yl]ethanol* **202b** as a white solid (0.24 g, 28%), m.p. 116-117 °C [HRMS: *m/z* calculated for $C_{18}H_{17}BrNO_4S$ $(M-H)^+$ 422.0062. Found 422.0079]; υ_{max} / cm^{-1} 3478 (OH); δ_H (400 MHz; $CDCl_3$) 2.43-2.55 (6H, overlapping signals, CH_3, 1′-CH_2 and OH), 3.83 (2H, m, 2′-CH_2), 5.94 (1H, d, *J* = 8.6 Hz, ArH), 6.01 (1H, d, *J* = 9.3 Hz, 2-H), 6.16 (1H, d, *J* = 9.3 Hz, NH), 6.39 (1H, s, 4-H), 7.04 (1H, dd, *J* = 8.6 and 2.4 Hz, ArH), 7.10 (1H, d, *J* = 2.4 Hz, ArH), 7.28 (2H, d, *J* = 8.2 Hz, ArH) and 7.70 (2H, d, *J* = 8.2 Hz, ArH); δ_C (100 MHz; $CDCl_3$) 21.6 (CH_3), 35.6 (C-1′), 60.2 (C-2′), 80.0 (C-2), 114.2, 118.1, 122.5, 122.9, 127.3, 128.7, 129.5, 130.8, 131.3, 138.3, 143.6 and 147.6 (Ar-C).

Product 2. *tert-Butyl 3-(5-bromo-2-hydroxyphenyl)-3-tosylamino-2-methylenepropanoate* **199b** as an off-white solid (0.24 g, 28%), m.p. 155-157 °C [HRMS: *m/z* calculated for $C_{21}H_{23}BrNO_5S$ $(M-H)^+$ 480.0480. Found 480.0472]; υ_{max} / cm^{-1} 3394 (OH) and 1685 (C=O); δ_H (400 MHz;

$CDCl_3$) 1.41 [9H, s, $C(CH_3)_3$], 2.37 (3H, s, CH_3Ar), 5.35 (1H, d, *J* = 9.0 Hz, NH), 5.72 and 6.11 (2H, 2 × s, $C=CH_2$), 5.94 (1H, d, *J* = 9.0 Hz, C*H*N), 6.60 (1H, d, *J* = 8.6 Hz, ArH), 6.91 (1H, d, *J* = 2.4 Hz, ArH), 7.11 (1H, dd, *J* = 8.6 and 2.4 Hz, ArH), 7.15 (1H, d, *J* = 8.2 Hz, ArH) and 7.57 (1H, d, *J* = 8.2 Hz, ArH); δ_C (100 MHz; DMSO-d_6) 21.5 (CH_3Ar), 27.9 [$C(CH_3)_3$], 54.7 (CHN), 82.8 [$C(CH_3)_3$], 126.3 ($C=CH_2$), 112.3, 118.8, 126.9, 127.1, 129.5, 131.2, 131.7, 136.5, 139.2 and 143.7 (Ar-C and $C=CH_2$), 152.8 [ArC(OH)] and 165.7 (C=O).

***Product* 3**. *tert*-butyl 3-(5-bromo-2-hydroxyphenyl)-3-hydroxy-2-methylenepropanoate **153b** as a white solid (0.08 g, 12%).

***2-[8-Ethoxy-2-(tosylamino)-2*H*-chromen-3-yl]ethanol* 202d**

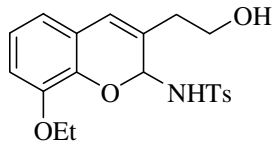

tert-*Butyl 8-ethoxy-2*H-*chromene-3-carboxylate* 164d

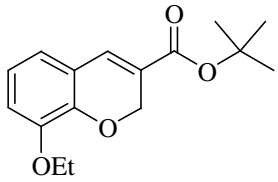

The procedure described for the synthesis of 2-[6-bromo-2-(tosylamino)-2*H*-chromen-3-yl]ethanol **202b** was followed, using 2-ethoxy-6-(tosylimino-methyl)phenol **198d** (0.64 g, 2.0 mmol), *tert*-butyl acrylate (0.7 mL, 5 mmol) and DABCO (0.9 g, 9 mmol) in $CHCl_3$–THF (1:1; 10 mL). Work-up afforded a mixture from which the following two products were isolated.

Product 1. *2-[8-Ethoxy-2-(tosylamino)-2*H*-chromen-3-yl]ethanol* **202d** as a brown oil (0.17 g, 22%) [HRMS: *m/z* calculated for $C_{20}H_{23}NO_5SNa$ (MNa^+) 412.1195. Found 412.1211]; υ_{max} / cm^{-1} 3357 (OH); δ_H (400 MHz; $CDCl_3$) 1.27 (3H, t, *J* = 7.0 Hz, OCH_2CH_3), 2.34-2.48 (6H, overlapping signals, CH_3Ar, 1′-CH_2 and OH), 3.80-3.88 (4H, series of signals, 2′-CH_2 and OCH_2CH_3), 6.12 (1H, s, 2-H), 6.43 (1H, s, 4-H), 6.64 (1H, d, *J* = 7.7 Hz, ArH), 6.69 (1H, d, *J* = 7.7 Hz, ArH), 6.79 (1H, t, *J* = 7.7 Hz, ArH), 7.21 (2H, d, *J* = 8.0 Hz, ArH) and 7.77 (2H, d, *J* = 8.0 Hz, ArH); δ_C (100 MHz; $CDCl_3$) 14.7 (OCH_2CH_3), 21.4 (CH_3Ar), 35.4 (C-1′), 60.2 (C-2′), 64.3 (OCH_2CH_3), 79.8 (C-2), 113.7, 118.7, 121.5, 121.8, 123.2, 126.9, 129.2, 129.3, 138.5, 138.7, 142.9 and 147.5 (Ar-C).

Product 2. tert-*Butyl 8-ethoxy-2*H*-chromene-3-carboxylate* **164d** as a yellow oil (0.066 g, 12%) (Found: C, 69.54; H, 7.30; $C_{16}H_{20}O_4$ requires: C, 69.61; H, 7.27%); υ_{max} / cm^{-1} 3290 (OH) and 1714 (C=O); δ_H (400 MHz; $CDCl_3$) 1.43 (3H, t, *J* = 7.0 Hz, OCH_2CH_3), 1.52 [9H, s, $C(CH_3)_3$],

4.08 (2H, q, J = 7.0 Hz, OCH_2CH$_3$), 5.00 (2H, s, 2-CH$_2$), 6.75 (1H, d, J = 7.1 Hz, ArH), 6.84 (2H, overlapping m, ArH) and 7.30 (1H, s, 4-H); δ_C (100 MHz; $CDCl_3$) 14.8 (OCH$_2$*C*H$_3$), 28.1 [C(*C*H$_3$)$_3$], 65.2 and 65.3 (CH$_2$), 81.1 [*C*(CH$_3$)$_3$], 116.0, 120.9, 121.2, 121.9, 124.2 and 132.5 (Ar-C and C=C), 144.4 and 147.1 [Ar*C*(OCH$_2$) and 163.8 (C=O).

1-(Benzyloxy)-4-chloro-2-(tosyliminomethyl)benzene **204e**

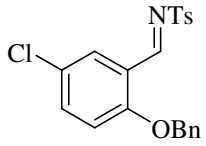

p-Toluenesulphonamide (0.29 g, 1.7 mmol), tetraethyl orthosilicate (0.4 mL, 2 mmol) and 2-(benzyloxy)-5-chlorobenzaldehyde **145e** (0.70 g, 1.7 mmol) were added to a 50 mL round-bottomed flask equipped with a magnetic stirrer, a positive flow of nitrogen and a short still-head connected to a receiving flask. The reaction mixture was heated for 8 h. at 150 °C (oil bath), and ethanol, upon formation, was collected in the receiving flask. After cooling, the reaction mixture was diluted with ether and the precipitate was filtered off and washed with cold ether (3 × 15 mL) to afford *1-(benzyloxy)-4-chloro-2-(tosyliminomethyl)benzene* **204e** as a yellow solid (0.67 g, 98%), m.p. 130-132 °C [HRMS: *m/z* calculated for $C_{21}H_{19}ClNO_3S$ (MH^+) 400.0774. Found 400.0760]; υ_{max} / cm^{-1} 1585 (C=N); δ_H (400 MHz; $CDCl_3$) 2.43 (3H, s, CH$_3$), 5.18 (2H, s, OCH$_2$), 6.94 (1H, d, J = 8.9 Hz, ArH), 7.32-7.45 (8H, overlapping m, ArH), 7.87 (2H, d, J = 7.9 Hz, ArH), 8.02 (1H, s, ArH) and 9.46 (1H, s, HCN); δ_C (100 MHz; $CDCl_3$) 21.6 (CH$_3$), 71.1 (OCH$_2$), 114.6, 122.4, 126.7, 127.2, 128.1, 128.5, 128.7, 128.8, 129.8, 134.9, 135.3, 136.1, 144.6 and 159.1 (Ar-C) and 164.6 (C=N).

tert-*Butyl 3-[2-(benzyloxy)-5-chlorophenyl]-3-tosylamino-2-methylenepropanoate* **205e**

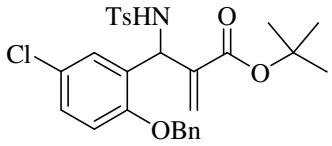

A mixture of *1-(benzyloxy)-4-chloro-2-(tosyliminomethyl)benzene* **204e** (0.50 g, 1.3 mmol), *tert*-butyl acrylate (0.4 mL, 3 mmol) and DABCO (0.05 g, 0.4 mmol) in $CHCl_3$ (5 mL) was sealed in a round-bottomed flask and stirred at room temperature for 6 d. The mixture was concentrated *in vacuo* and purified by flash chromatography [on silica gel; elution with hexane – EtOAc (9:1)] to afford tert-*butyl 3-[2-(benzyloxy)-5-chlorophenyl]-3-tosylamino-2-methylenepropanoate* **205e** as

a white solid (0.32 g, 48%), m.p. 157-158 °C [HRMS: *m/z* calculated for $C_{28}H_{31}ClNO_5S$ (MH^+) 528.1611. Found 528.1591]; υ_{max} / cm^{-1} 3194 (NH) and 1689 (C=O); δ_H (400 MHz; $CDCl_3$) 1.38 [9H, s, $C(CH_3)_3$], 2.33 (3H, s, CH_3Ar), 4.95 (2H, s, OCH_2Ph), 5.51 (1H, d, *J* = 10.0 Hz, NH), 5.53 and 6.04 (2H, 2 x s, $C=CH_2$), 5.82 (1H, d, *J* = 10.0 Hz, CHN), 6.67 (1H, d, *J* = 8.7 Hz, ArH), 6.96 (1H, d, *J* = 2.1 Hz, ArH), 7.03 (1H, dd, *J* = 8.7 and 2.1 Hz, ArH), 7.07 (2H, d, *J* = 8.0 Hz, ArH), 7.34-7.42 (5H, overlapping m, ArH) and 7.51 (2H, d, *J* = 8.0 Hz, ArH); δ_C (100 MHz; $CDCl_3$) 21.4 (CH_3), 27.9 [$C(CH_3)_3$], 54.8 (CHN), 70.6 (OCH_2Ph), 81.9 [$C(CH_3)_3$], 126.1 ($C=CH_2$), 113.1, 125.5, 126.9, 127.6, 128.1, 128.2, 128.4, 128.7, 129.2, 129.4, 135.9, 137.5, 139.4 and 143.2 ($C=CH_2$ and Ar-C), 154.0 [ArC(OBn)] and 164.8 (C=O).

N-*[(6-Chlorocoumarin-3-yl)methyl]phthalimide* 208e

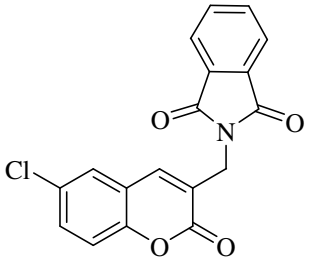

6-Chloro-3-(chloromethyl)coumarin **148e** (0.23 g, 1.0 mmol) was added to a well-ground mixture of potassium phthalimide (0.19 g, 1.0 mmol), TBAB (0.16 g, 0.50 mmol) and DABCO (0.11 g, 1.0 mmol) and heated under reflux for 10 h at 100 °C (oil bath). After cooling, the mixture was dissolved in chloroform (25 mL), washed with water (2 × 25 mL), dried over anhydrous $MgSO_4$, concentrated *in vacuo* and flash chromatographed [on silica gel; elution with hexane – EtOAc (5:1)] to afford N-*[(6-chlorocoumarin-3-yl)methyl]phthalimide* **208e** as a white solid (0.26 g, 78%), m.p. 206-208 °C [HRMS: *m/z* calculated for $C_{18}H_{11}ClNO_4$ (MH^+) 340.0377. Found 340.0360]; υ_{max} / cm^{-1} 1702 (C=O); δ_H (400 MHz; $CDCl_3$) 4.82 (2H, s, NCH_2), 7.28 (1H, s, ArH), 7.42 (3H, overlapping s and d, ArH), 7.78 (2H, s, ArH) and 7.91 (2H, s, ArH); δ_C (100 MHz; $CDCl_3$) 37.2 (NCH_2), 118.0, 119.7, 123.7, 124.6, 127.0, 129.8, 131.5, 131.8, 134.4, 138.0 and 151.6 (Ar-C), 159.6 and 167.6 (C=O).

***Methyl 3-[2-(benzyloxy)-5-bromophenyl]-3-phthalimido-2-methylenepropanoate* 209b**

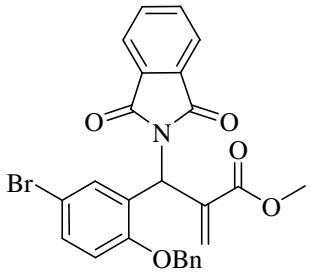

DABCO (0.08 g, 0.7 mmol) was added to a solution of methyl (*Z*)-3-[2-(benzyloxy)-5-bromophenyl]-2-(bromomethyl)-2-propenoate **183b** (0.25 g, 0.57 mmol) in CH_3CN (5 mL). After stirring for 30 minutes, potassium phthalimide (0.12 g, 0.65 mmol) was then added and the mixture left to stir at r.t. for 2 d. The crude mixture was concentrated *in vacuo* and flash chromatographed [on silica gel; elution with hexane – EtOAc (3:1)] to afford *methyl 3-[2-(benzyloxy)-5-bromophenyl]-3-phthalimido-2-methylenepropanoate* **209b** as a yellow oil (0.18 g, 62%) [HRMS: *m/z* calculated for $C_{26}H_{21}BrNO_5$ (MH^+) 506.0603. Found 506.0598]; υ_{max} / cm^{-1} 1721 and 1698 (C=O); δ_H (400 MHz; $CDCl_3$) 3.70 (3H, s, OCH_3), 5.05 (2H, s, OCH_2Ph), 5.71 (1H, s, CHN), 6.58 and 6.84 (2H, 2 × s, $C=CH_2$), 6.80 (1H, d, *J* = 8.7 Hz, ArH), 7.25-7.30 (5H, overlapping m, ArH), 7.34 (1H, d, *J* = 8.7 Hz), 7.70 (2H, s, ArH) and 7.79 (2H, s, ArH); δ_C (100 MHz; $CDCl_3$) 48.8 (CHN) 52.1 (OCH_3), 70.3 (CH_2), 112.9, 113.7, 123.3, 127.1, 127.76, 127.82, 128.4, 128.9, 131.7, 131.9, 132.1, 133.9, 136.0 and 136.5 (C=CH and Ar-C), 154.7 [ArC(OBn)], 165.7 and 167.6 (C=O).

***4-Phthalimido-3-methyl-3,4-dihydrocoumarin* 210a**

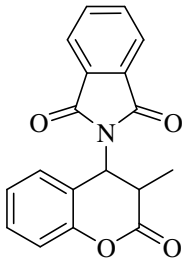

A mixture of methyl 3-[2-(benzyloxy)-5-bromophenyl]-3-phthalimido-2-methylenepropanoate **209b** (0.2 g, 0.4 mmol) and pre-equilibrated 10% Pd/C catalyst (0.04 g) in absolute ethanol (10 mL) was hydrogenated at r.t. and atmospheric pressure. The mixture was filtered and the filtrate was concentrated *in vacuo* and flash chromatographed [on silica gel; elution with hexane – EtOAc (3:1)] to afford *4-phthalimido-3-methyl-3,4-dihydrocoumarin* **210a** as a brown solid

(0.068 g, 56%), m.p. 172-174 °C [HRMS: *m/z* calculated for $C_{18}H_{14}NO_4$ (MH^+) 308.0923. Found 308.0919]; υ_{max} / cm^{-1} 1768 and 1698 (C=O); δ_H (600 MHz; $CDCl_3$) 1.33 (3H, d, *J* = 7.3 Hz, CH_3), 3.22 (1H, m, 3-H), 5.64 (1H, d, *J* = 7.3 Hz, 4-H), 7.09 (1H, t, *J* = 7.9 Hz, ArH) 7.13 (1H, d, *J* = 7.9 Hz, ArH), 7.13 (1H, d, *J* = 7.7 Hz, ArH), 7.35 (1H, t, *J* = 7.7 Hz, ArH) , 7.73 (2H, s, ArH) and 7.81-7.88 (2H, s, ArH); δ_C (150 MHz; $CDCl_3$) 11.4 (CH_3), 36.8 (C-3), 48.4 (CHN), 117.4, 119.1, 123.8, 124.4, 128.8, 130.6, 134.4 and 152.4 (Ar-C), 167.7 and 168.1 (C=O).

3.14. SYNTHESIS OF FUROCOUMARIN CARBOXAMIDES

Ethyl 3-(7-hydroxy-4-methylcoumarin-3-yl)propanoate 215

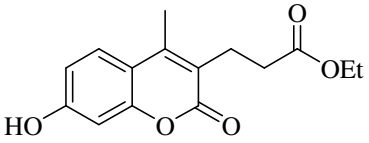

Acetyl chloride (90 mL, 1.3 mol) was added slowly to EtOH (70 mL, 1.2 mol) at 0 °C. The mixture was stirred for 30 minutes and was transferred slowly through a dropping funnel into a stirred mixture of diethyl acetylglutarate (54 mL, 0.37 mol), resorcinol (28 g, 0.25 mol) and ethanol (50 mL) at 0 °C over a 90 min period. The reaction mixture was then allowed to stir at r.t. overnight, after which it was concentrated *in vacuo*. Ice-cold water was added to the sticky residue, which was extracted into DCM. Evaporation of the solvent gave brown crystals, which were recrystallised from diethyl ether - hexane (1:1) to give ethyl 3-(7-hydroxy-4-methylcoumarin-3-yl)propanoate **215** as a pale yellow solid (44.2 g, 64%), m.p. 126-127 °C (lit.[286] 124 °C); δ_H (400 MHz; $CDCl_3$) 1.19 (3H, t, *J* = 7.1 Hz, $OCH_2C\mathit{H}_3$), 2.34 (3H, s, $ArCH_3$), 2.55 and 2.89 (4H, 2 × t, *J* = 7.6 Hz, $ArCH_2$ and CH_2CO), 4.09 (2H, q, *J* = 7.1 Hz, $OC\mathit{H}_2CH_3$), 6.77 (1H, dd, *J* = 8.7 and 2.2 Hz, ArH), 6.80 (1H, d, *J* = 2.2 Hz, ArH), 7.36 (1H, d, *J* = 8.7 Hz, ArH) and 8.98 (1H, br s, OH); δ_C (100 MHz; $CDCl_3$) 14.0 and 14.7 (CH_3), 22.9, 32.7 and 60.7 (CH_2), 102.6, 113.2, 113.3, 119.9, 125.8, 148.9, 153.3 and 159.8 (Ar-C), 162.8 and 173.4 (C=O).

Ethyl 3-[7-(2-oxopropoxy)-4-methylcoumarin-3-yl]propanoate 216

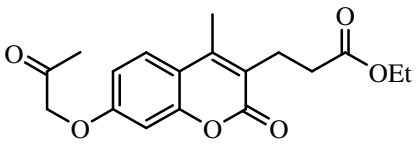

Dry acetone (300 mL) was added to ethyl 3-(7-hydroxy-4-methylcoumarin-3-yl)propanoate **215** (32 g, 0.12 mol) and the mixture was heated to 60 °C under N_2. Freshly calcined K_2CO_3 (48 g, 0.35 mol) was then introduced and, after further stirring for 15 min, chloroacetone (10 mL, 0.13 mol; **CAUTION!** Lachrymatory compound) was added and the mixture stirred vigorously for 3 h. The solution was then allowed to cool and poured into 4M-H_2SO_4 (280 mL). The precipitate was recrystallised from ethanol to afford ethyl 3-[7-(2-oxopropoxy)-4-methylcoumarin-3-yl]propanoate **216** as white crystals (28.1 g, 73%), m.p. 122-123 °C (lit.[287] 115-116 °C); δ_H (400 MHz; $CDCl_3$) 1.17 (3H, t, *J* = 7.1 Hz, OCH_2CH_3), 2.24 (3H, s, CH_3CO), 2.37 (3H, s, $ArCH_3$), 2.53 and 2.88 (4H, 2 × t, *J* = 7.6 Hz, $ArCH_2$ and CH_2CO), 4.06 (2H, q, *J* = 7.1 Hz, OCH_2CH_3), 4.59 (2H, s, OCH_2), 6.66 (1H, d, *J* = 2.4 Hz, ArH), 6.82 (1H, dd, *J* = 8.9 and 2.4 Hz, ArH) and 7.48 (1H, d, *J* = 8.9 Hz, ArH); δ_C (100 MHz; $CDCl_3$) 14.0, 14.7 and 26.3 (CH_3), 23.0, 32.4, 60.3 and 72.7 (CH_2), 101.3, 112.0, 114.7, 121.8, 125.9, 147.1, 153.4 and 159.6 (Ar-C), 161.2, 172.6 and 203.5 (C=O).

3-[3,5-dimethylfuro[3,2-g]coumarin-6-yl]propanoic acid 217

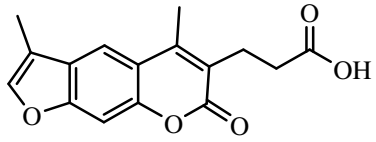

A solution of ethyl 3-[7-(2-oxopropoxy)-4-methylcoumarin-3-yl]propanoate **216** (25 g, 75 mmol) in 2-propanol (200 mL) was treated with 2N-NaOH (200 mL), and the resulting mixture then heated for 3 h at 68 °C (oil bath). On cooling, the solution was poured into 4M-H_2SO_4 (1 L) to afford a brown precipitate, which was recrystallised from 2-propanol to give 3-{3,5-dimethyl-furo[3,2-*g*]coumarin-6-yl}propanoic acid **217** as a yellow solid (16.9 g, 79%), m.p. 220-221 °C (lit.[287] 215-216 °C); δ_H (400 MHz; DMSO-d_6) 2.20 (3H, s, 3-CH_3), 2.42 (5H, overlapping s and t, 5-CH_3 and CH_2Ar), 2.77 (2H, t, *J* = 7.7 Hz, CH_2CO), 7.42 (1H, s, ArH) and 7.75-7.76 (2H, overlapping s, ArH); δ_C (100 MHz; DMSO-d_6) 7.4 and 15.0 (CH_3), 23.0 and 32.3 (CH_2), 98.5, 115.5, 115.6, 116.1, 121.8, 125.7, 143.4, 147.8, 149.6 and 155.1 (Ar-C), 160.5 and 173.7 (C=O).

***3-{3,5-Dimethylfuro[3,2-g]coumarin-6-yl}*-N-*[(pyridin-2-yl)methyl]propanamide* 212a**

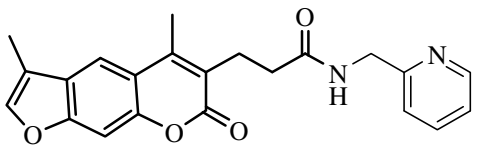

3-{3,5-dimethyl-furo[3,2-*g*]coumarin-6-yl}propanoic acid **217** (1.0 g, 3.5 mmol) was dissolved in dry dioxane (50 mL) in a 2-necked round-bottomed flask and *N*-hydroxysuccinimide (0.44 g, 3.8 mmol) was added. The solution was stirred under N_2 for 20 min.; *N,N′*-diisopropylcarbodiimide (0.6 mL, 4 mmol) was then added through a septum and the solution stirred vigorously for 2 h. 2-Picolylamine **218a** (0.4 mL, 4 mmol) was then introduced through the septum and the mixture stirred for 4 h at r.t. under N_2. Ice-cooled water was then added to the mixture and the resulting precipitate was filtered off. Recrystallisation from 2-propanol gave *3-{3,5-dimethylfuro[3,2-g]coumarin-6-yl}*-N-*[(pyridin-2-yl)methyl]propanamide* **212a** as a yellow solid (1.03 g, 78%), m.p. 212-213 °C [HRMS: *m/z* calculated for $C_{22}H_{21}N_2O_4$ (MH^+) 377.1501. Found 377.1498]; δ_H (400 MHz; DMSO-d_6) 2.26 (3H, s, 3-CH_3), 2.41 (2H, t, *J* = 7.5 Hz, CH_2Ar), 2.45 (3H, s, 5-CH_3), 2.85 (2H, t, *J* = 7.5 Hz, CH_2CO), 4.32 (2H, d, *J* = 5.7 Hz, NCH_2), 7.18 (2H, t, *J* = 7.6 Hz, ArH), 7.56-7.59 (2H, m, ArH), 7.83 (1H, s, ArH), 7.90 (1H, s, ArH), 8.42 (1H, d, *J* = 4.3, ArH) and 8.51 (1H, t, *J* = 5.7 Hz, NH); δ_C (100 MHz; DMSO-d_6) 7.6 and 15.2 (CH_3), 23.7, 33.9 and 44.2 (CH_2), 98.8, 115.6, 116.0, 116.3, 120.9, 122.0, 122.4, 125.9, 136.5, 143.6, 147.9, 148.8, 149.7, 155.2 and 158.6 (Ar-C), 160.7 and 171.5 (C=O).

***3-{3,5-Dimethylfuro[3,2-g]coumarin-6-yl}*-N-*[(furan-2-yl)methyl]propanamide* 212b**

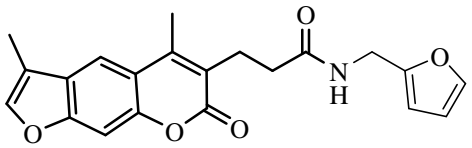

The procedure described for the synthesis of 3-{3,5-dimethylfuro[3,2-g]coumarin-6-yl}-*N*-[(pyridin-2-yl)methyl]propanamide **212a** was followed, using 3-{3,5-dimethylfuro[3,2-*g*]coumarin-6-yl}propanoic acid **217** (1.0 g, 3.5 mmol), *N*-hydroxysuccinimide (0.44 g, 3.8 mmol) and *N,N′*-diisopropylcarbodiimide (0.6 mL, 4 mmol) in dry dioxane (50 mL) and furfurylamine **218b** (0.3 mL, 4 mmol). Work-up afforded *3-{3,5-dimethylfuro[3,2-g]coumarin-6-yl}*-N-*[(furan-2-yl)methyl]propanamide* **212b** as a yellow solid (1.02 g, 80%), m.p. 215-217 °C [HRMS: *m/z* calculated for $C_{21}H_{20}NO_5$ (MH^+) 366.1341. Found 366.1331]; δ_H (400 MHz; $CDCl_3$) 2.28 (3H, s, 3-CH_3), 2.53 (5H, overlapping s and t, 5-CH_3 and CH_2Ar), 3.02 (2H, t, *J* = 7.4 Hz, CH_2CO), 4.39 (2H, d, *J* = 5.5 Hz, NCH_2), 6.14 (1H, d, *J* = 2.1 Hz, ArH), 6.20 (1H, t, *J* = 2.1 Hz, ArH), 6.24 (1H, br s, NH), 7.17 (1H, s, ArH), 7.29 (1H, s, ArH), 7.43 (1H, s, ArH) and 7.66 (1H, s, ArH); δ_C (100 MHz; $CDCl_3$) 7.9 and 15.5 (CH_3), 24.1, 34.9 and 36.4 (CH_2), 99.2,

107.3, 110.2, 114.9, 115.6, 116.6, 122.4, 126.3, 142.0, 142.9, 148.3, 150.2, 151.2 and 155.9 (Ar-C), 162.0 and 171.8 (C=O).

N-*[5-(Diethylamino)pent-2-yl]-3-{3,5-dimethylfuro[3,2-g]coumarin-6-yl}propanamide* 212c

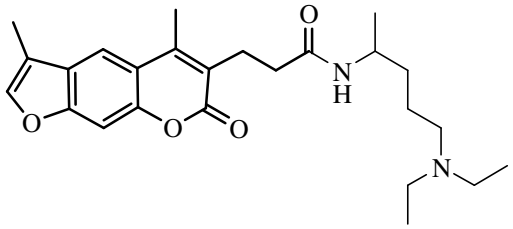

The procedure described for the synthesis of 3-{3,5-dimethylfuro[3,2-g]coumarin-6-yl}-*N*-[(pyridin-2-yl)methyl]propanamide **212a** was followed, using 3-{3,5-dimethylfuro[3,2-*g*]coumarin-6-yl}propanoic acid **217** (1.0 g, 3.5 mmol), *N*-hydroxysuccinimide (0.44 g, 3.8 mmol) and *N,N′*-diisopropylcarbodiimide (0.6 mL, 4 mmol) in dry dioxane (50 mL) and 5-diethylamino-2-pentylamine **218c** (0.8 mL, 4 mmol). Work-up afforded N-*[5-(diethylamino)pent-2-yl]-3-{3,5-dimethylfuro[3,2-g]coumarin-6-yl}propanamide* **212c** as a yellow solid (1.02 g, 76%), m.p. 59-60 °C [HRMS: *m/z* calculated for $C_{25}H_{35}N_2O_4$ (MH^+) 427.2597. Found 427.2611]; δ_H (400 MHz; $CDCl_3$) 0.93 (6H, t, J = 6.5 Hz, 2 × CH_2CH_3), 1.04 (3H, d, J = 5.9 Hz, $CHCH_3$), 1.37 (4H, s, $CHCH_2CH_2$), 2.25 (5H, overlapping s and t, 3-CH_3 and CH_2Ar), 2.39-2.48 (6H, series of signals, 3 × NCH_2), 2.54 (3H, s, 5-CH_3), 2.99 (2H, t, J = 6.5 Hz, CH_2CO), 3.87-3.92 (1H, overlapping signals, NCH), 6.22 (1H, d, J = 6.7 Hz, ArH), 7.29 (1H, s, ArH), 7.41 (1H, s, ArH) and 7.65 (1H, s, ArH); δ_C (100 MHz; $CDCl_3$) 7.8, 11.2, 15.4 and 20.6 (CH_3), 23.3, 24.3, 34.6, 35.3, 46.6 and 52.6 (CH_2), 45.0 (NCH), 99.2, 114.8, 115.6, 116.6, 122.7, 126.3, 142.9, 148.1, 150.1 and 155.9 (Ar-C), 162.0 and 171.3 (C=O).

***3-{3,5-Dimethylfuro[3,2-g]coumarin-6-yl}*-N-*[(pyridin-3-yl)methyl]propanamide* 212d**

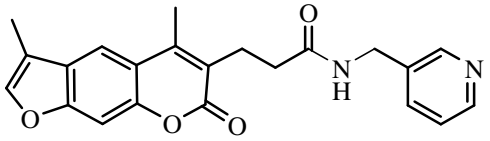

The procedure described for the synthesis of 3-{3,5-dimethylfuro[3,2-g]coumarin-6-yl}-*N*-[(pyridin-2-yl)methyl]propanamide **212a** was followed, using 3-{3,5-dimethylfuro[3,2-*g*]coumarin-6-yl}propanoic acid **217** (1.0 g, 3.5 mmol), *N*-hydroxysuccinimide (0.44 g, 3.8 mmol) and *N,N′*-diisopropylcarbodiimide (0.6 mL, 4 mmol) in dry dioxane (50 mL) and 3-picolylamine **218d** (0.4 mL, 4 mmol). Work-up afforded *3-{3,5-dimethylfuro[3,2-g]coumarin-6-*

yl}-N-*[(pyridin-3-yl)methyl]propanamide* **212d** as an off-white solid (1.07 g, 81%), m.p. 234-236 °C [HRMS: *m/z* calculated for $C_{22}H_{21}N_2O_4$ (MH^+) 377.1501. Found 377.1513]; δ_H (400 MHz; DMSO-d_6) 2.25 (3H, s, 3-CH_3), 2.37 (2H, t, *J* = 7.5 Hz, CH_2Ar), 2.43 (3H, s, 5-CH_3), 2.83 (2H, t, *J* = 7.5 Hz, CH_2CO), 4.25 (2H, d, *J* = 5.7 Hz, NCH_2), 7.17 (1H, td, *J* = 11.0 and 5.5 Hz, ArH), 7.51 (1H, s, ArH), 7.80 (2H, s, ArH), 7.86 (1H, s, ArH), 8.37 (1H, d, *J* = 3.9, ArH), 8.43 (1H, s, ArH) and 8.45 (1H, d, *J* = 5.7 Hz, NH); δ_C (100 MHz; DMSO-d_6) 7.5 and 15.1 (CH_3), 23.7, 33.9 and 39.9 (CH_2), 98.7, 115.5, 115.9, 116.2, 122.3, 123.3, 125.8, 134.9, 135.0, 143.5, 147.8, 147.9, 148.7, 149.7 and 155.2 (Ar-C), 160.6 and 171.4 (C=O).

N-*Benzyl-3-{3,5-dimethylfuro[3,2-g]coumarin-6-yl}propanamide* 212e

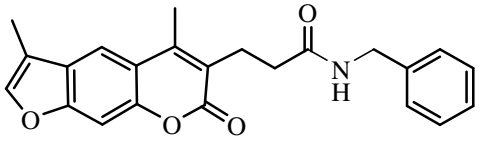

The procedure described for the synthesis of 3-{3,5-dimethylfuro[3,2-g]coumarin-6-yl}-*N*-[(pyridin-2-yl)methyl]propanamide **212a** was followed, using 3-{3,5-dimethylfuro[3,2-*g*]coumarin-6-yl}propanoic acid **217 (**1.0 g, 3.5 mmol), *N*-hydroxysuccinimide (0.44 g, 3.8 mmol) and *N,N′*-diisopropylcarbodiimide (0.6 mL, 4 mmol) in dry dioxane (50 mL) and benzylamine **218e** (0.4 mL, 4 mmol). Work-up afforded N-*benzyl-3-{3,5-dimethyl-furo[3,2-g]coumarin-6-yl}propanamide* **212e** as an off-white solid (1.07 g, 82%), m.p. 230-232 °C [HRMS: *m/z* calculated for $C_{23}H_{22}NO_4$ (MH^+) 376.1549. Found 376.1565]; δ_H (400 MHz; DMSO-d_6) 2.26 (3H, s, 3-CH_3), 2.37 (2H, t, *J* = 7.5 Hz, CH_2Ar), 2.45 (3H, s, 5-CH_3), 2.84 (2H, t, *J* = 7.5 Hz, CH_2CO), 4.21 (2H, s, NCH_2), 7.15 (5H, s, ArH), 7.58 (1H, s, ArH), 7.85 (1H, s, ArH), 7.92 (1H, s, ArH) and 8.42 (1H, br s, NH); δ_C (100 MHz; DMSO-d_6) 7.6 and 15.2 (CH_3), 23.8, 34.0 and 42.1 (CH_2), 98.8, 115.7, 116.1, 116.4, 122.5, 125.9, 126.7, 127.2, 128.2, 139.5, 143.7, 148.0, 149.8 and 155.2 (Ar-C), 160.7 and 171.3 (C=O).

N-tert-*Butyl-3-{3,5-dimethylfuro[3,2-g]coumarin-6-yl}propanamide* 212f

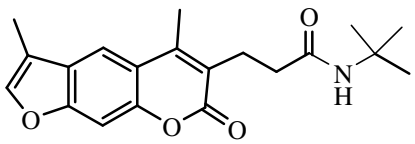

The procedure described for the synthesis of 3-{3,5-dimethylfuro[3,2-g]coumarin-6-yl}-*N*-[(pyridin-2-yl)methyl]propanamide **212a** was followed, using 3-{3,5-dimethylfuro[3,2-*g*]coumarin-6-yl}propanoic acid **217 (**1.0 g, 3.5 mmol), *N*-hydroxysuccinimide (0.44 g, 3.8

mmol) and *N,N′*-diisopropylcarbodiimide (0.6 mL, 4 mmol) in dry dioxane (50 mL) and *tert*-butylamine **218f** (0.4 mL, 4 mmol). Work-up afforded N-tert-*butyl-3-{3,5-dimethylfuro[3,2-g]coumarin-6-yl}propanamide* **212f** as a white solid (0.75 g, 63%), m.p. 84-85 °C [HRMS: *m/z* calculated for $C_{20}H_{24}NO_4$ (MH^+) 342.1705. Found 342.1698]; δ_H (400 MHz; $CDCl_3$) 1.28 [9H, s, $C(CH_3)_3$], 2.26 (3H, s, 3-CH_3), 2.39 (2H, t, J = 7.5 Hz, CH_2Ar), 2.54 (3H, s, 5-CH_3), 2.97 (2H, t, J = 7.5 Hz, CH_2CO), 5.67 (1H, br s, NH), 7.28 (1H, s, ArH), 7.41 (1H, s, ArH) and 7.65 (1H, s, ArH); δ_C (100 MHz; $CDCl_3$) 7.8, 15.5 and 28.6 (CH_3), 24.2 and 36.0 (CH_2), 51.0 [$C(CH_3)_3$], 99.1, 114.8, 115.6, 116.6, 122.8, 126.3, 142.8, 148.0, 150.1 and 155.8 (Ar-C), 162.0 and 171.3 (C=O).

***3-{3,5-Dimethylfuro[3,2-g]coumarin-6-yl}*-N-*propylpropanamide* 212g**

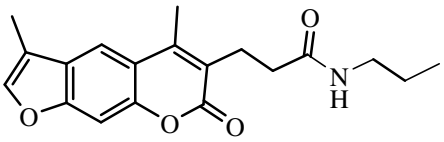

The procedure described for the synthesis of 3-{3,5-dimethylfuro[3,2-g]coumarin-6-yl}-*N*-[(pyridin-2-yl)methyl]propanamide **212a** was followed, using 3-{3,5-dimethylfuro[3,2-*g*]coumarin-6-yl}propanoic acid **217 (**1.0 g, 3.5 mmol), *N*-hydroxysuccinimide (0.44 g, 3.8 mmol) and *N,N′*-diisopropylcarbodiimide (0.6 mL, 4 mmol) in dry dioxane (50 mL) and propylamine **218g** (0.30 mL, 3.9 mmol). Work-up afforded *3-{3,5-dimethylfuro[3,2-g]coumarin-6-yl}*-N-*propylpropanamide* **212g** as a yellow solid (0.95 g, 83%), m.p. 211-213 °C [HRMS: *m/z* calculated for $C_{19}H_{22}NO_4$ (MH^+) 328.1549. Found 328.1561]; δ_H (400 MHz; DMSO-d_6) 0.75 (3H, t, J = 7.2 Hz, CH_3), 1.33 (2H, m, CH_2CH_3), 2.24-2.29 (5H, overlapping s and t, 3-CH_3 and CH_2Ar), 2.47 (3H, s, 5-CH_3), 2.79 (2H, t, J = 7.2 Hz, CH_2CO), 2.95 (2H, dd, J = 12.1 and 5.9 Hz, NCH_2), 7.55 (1H, s, ArH), 7.82 (1H, s, ArH) 7.88 (1H, t, J = 5.9, NH) and 7.92 (1H, s, ArH); δ_C (100 MHz; DMSO-d_6) 7.6, 11.4 and 15.3 (CH_3), 23.9, 34.1, 39.5 and 40.4 (CH_2), 51.0 [$C(CH_3)_3$], 98.8, 115.7, 116.0, 122.6, 125.9, 143.7, 147.9, 149.8 and 155.2 (Ar-C), 160.8 and 171.2 (C=O).

3.15. X-RAY CRYSTAL STRUCTURE DATA

(As provided by Professor M. Caira, University of Cape Town).

X-ray data for Cinnamic acid derivative 177a

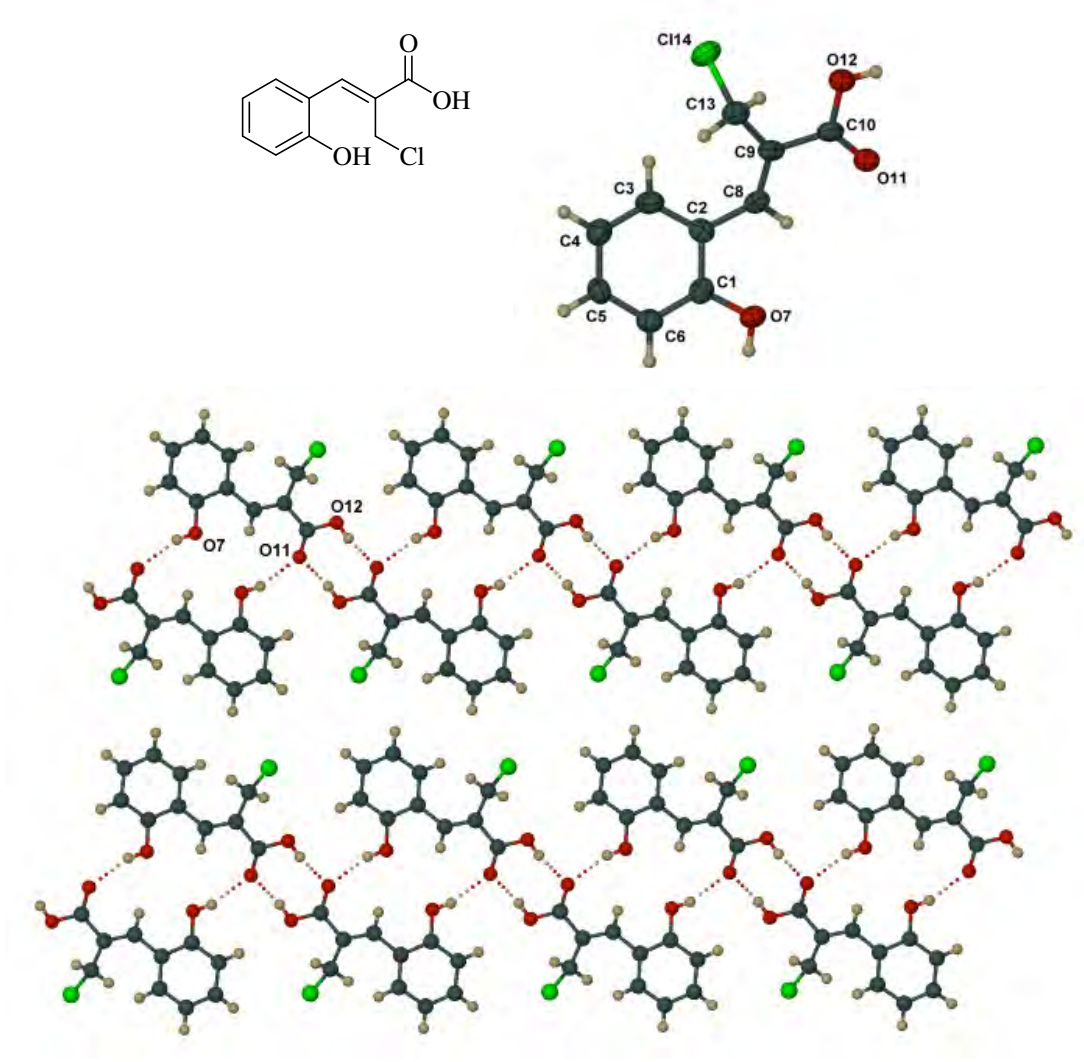

Figure 109. ORTEP diagram of crystal structure of compound **177a** and the topology of the crystal packing. [C8-C9 1.347(5) Å, C13-Cl14 1.814(4) Å; dihedral angle C3-C2-C8-C9 29.8(6)°].

The layer comprises hydrogen bonded ribbons with alternating centrosymmetric $R_2^2(8)$ H-bonded motifs (the carboxylic acid dimers) and centrosymmetric $R_2^2(16)$ H-bonded motifs. Portions of two ribbons are illustrated. There is no π-π stacking between phenyl rings of successive layers. Crystal data: Formula, $C_{10}H_9ClO_3$; Formula Weight, 212.62; Crystal System, Triclinic; Space group P-1(No. 2); a, b, c [Angstrom] 5.1208(4) 7.8498(8) 11.9863(12); alpha, beta, gamma [deg] 99.256(4) 91.114(7) 100.217(7); V [Ang**3] 467.43(8); Z 2; D(calc) [g/cm^3] 1.511;

Mu(MoKa) [/mm] 0.383; F(000) 220; Crystal Size [mm] 0.09 x 0.13 x 0.25; Data Collection: Temperature (K) 173; Radiation [Angstrom] MoKa 0.71073; Theta Min-Max [Deg] 3.4, 27.5; Dataset -6: 6 ; -10: 10 ; -15: 15; Tot., Uniq. Data, R(int) 25716, 2115, 0.043; Observed data [I > 2.0 sigma(I)] 1552; Refinement: Nref, Npar 2115, 129; R, wR2, S 0.0765, 0.2285, 1.04; w = 1/[\s^2^(Fo^2^) + (0.1184P)^2^ + 0.7230P] where P = (Fo^2^ + 2Fc^2^)/3; Max. and Av. Shift/Error 0.00, 0.00; Min. and Max. Resd. Dens. [e/Ang^3] -0.29, 0.82.

Table 29. Atomic coordinates and equivalent isotropic displacement parameters for non-hydrogen atoms for compound **177a** (R = 0.08)

Atom	x	y	z	U(eq) [Ang^2]
Cl14	0.4410(2)	0.66520(14)	0.37189(8)	0.0595(4)
O7	0.7799(6)	0.0092(4)	0.0769(2)	0.0522(9)
O11	0.1634(5)	0.3440(3)	0.0218(2)	0.0465(8)
O12	0.2236(6)	0.6221(3)	0.1089(2)	0.0536(10)
C1	0.8569(7)	0.0776(5)	0.1863(3)	0.0421(10)
C2	0.7451(7)	0.2220(4)	0.2362(3)	0.0400(10)
C3	0.8132(8)	0.2915(5)	0.3491(3)	0.0487(11)
C4	0.9923(8)	0.2264(5)	0.4099(3)	0.0506(12)
C5	1.1068(7)	0.0893(5)	0.3599(3)	0.0451(11)
C6	1.0419(7)	0.0126(5)	0.2485(3)	0.0432(11)
C8	0.5531(7)	0.2816(5)	0.1670(3)	0.0406(10)
C9	0.4918(7)	0.4430(4)	0.1756(3)	0.0395(10)
C10	0.2796(7)	0.4627(5)	0.0953(3)	0.0419(11)
C13	0.6287(8)	0.6049(5)	0.2496(3)	0.0459(11)

Table 30. Bond distances (Angstrom) for compound **177a** (R = 0.08)

Atoms	Bond length	Atoms	Bond length
Cl14 - C13	1.814(4)	C5 - C6	1.382(5)
O7 - C1	1.357(4)	C8 - C9	1.347(5)
O11 - C10	1.232(4)	C9 - C13	1.480(5)
O12 - C10	1.318(5)	C9 - C10	1.483(5)
O7 - H7	0.8400	C3 - H3	0.9500
O12 - H12	0.8400	C4 - H4	0.9500
C1 - C2	1.413(5)	C5 - H5	0.9500
C1 - C6	1.407(5)	C6 - H6	0.9500
C2 - C3	1.388(5)	C8 - H8	0.9500
C2 - C8	1.459(5)	C13 - H13A	0.9900
C3 - C4	1.376(6)	C13 - H13B	0.9900
C4 - C5	1.375(5)		

Table 31. Bond angles (degrees) for compound **177a** (R = 0.08)

Atoms	Bond angle	Atoms	Bond Angle
C1 - O7 - H7	109.00	O12 - C10 - C9	113.7(3)
C10 - O12 - H12	109.00	Cl14 - C13 - C9	112.2(3)
C2 - C1 - C6	120.4(3)	C2 - C3 - H3	119.00
O7 - C1 - C2	116.7(3)	C4 - C3 - H3	119.00
O7 - C1 - C6	122.9(3)	C3 - C4 - H4	120.00
C3 - C2 - C8	124.3(3)	C5 - C4 - H4	120.00
C1 - C2 - C8	117.5(3)	C4 - C5 - H5	120.00
C1 - C2 - C3	118.2(3)	C6 - C5 - H5	120.00
C2 - C3 - C4	121.2(4)	C1 - C6 - H6	121.00
C3 - C4 - C5	120.4(3)	C5 - C6 - H6	121.00
C4 - C5 - C6	120.9(3)	C2 - C8 - H8	116.00
C1 - C6 - C5	118.9(3)	C9 - C8 - H8	116.00
C2 - C8 - C9	128.4(3)	Cl14 - C13- H13A	109.00
C10 - C9 - C13	116.7(3)	Cl14 - C13 - H13B	109.00
C8 - C9 - C10	116.2(3)	C9 - C13 - H13A	109.00
C8 - C9 - C13	126.9(3)	C9 - C13 - H13B	109.00
O11 - C10 - O12	121.8(3)	H13A - C13 - H13B	108.00
O11 - C10 - C9	124.5(3)		

X-ray data for Chromene derivative 202b

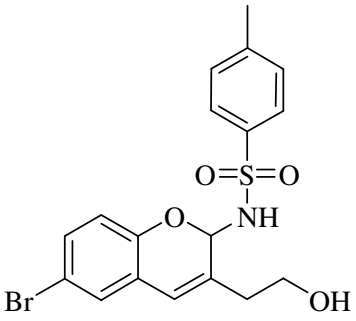

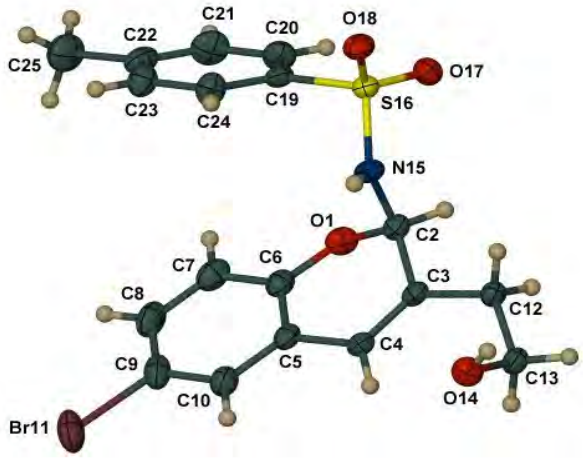

Figure 110. ORTEP diagram of crystal structure of compound **202b** showing crystallographic numbering.

As shown in Figure 110, compound **202b** has an *R*-configuration at chiral centre C2. (The crystal is centrosymmetric and therefore racemic). Its overall conformation is accurately described by citing several key torsion angles: O1-C2-N15-S16 = -72.2°, C2-N15-C16-C19 82.4°, N15-S16-C19-C20 = -117.6°. The heterocyclic ring is puckered, atoms O1, C6, C5 and C4 being practically coplanar (dihedral angle around C5-C6 = 1.6°) but two endocyclic torsion angles

deviating significantly from zero, as follows: C6-O1-C2-C3 = 43.1°, O1-C2-C3-C4 = -29.6°. Torsion angle C2-C3-C4-C5 is only 2.7° (all e.s.d.s in the range 0.2-0.3°).

Hydrogen bonding (primarily O-H···O and N-H···O, supported by C-H···O) stabilises the crystal structure. Cyclic, centrosymmetric arrays comprising four molecules are generated by classical hydrogen bonding, as shown in Figure 111. Repetition of such arrays by the space group symmetry generates the full crystal structure. There are no significant π-stacking interactions in the crystal.

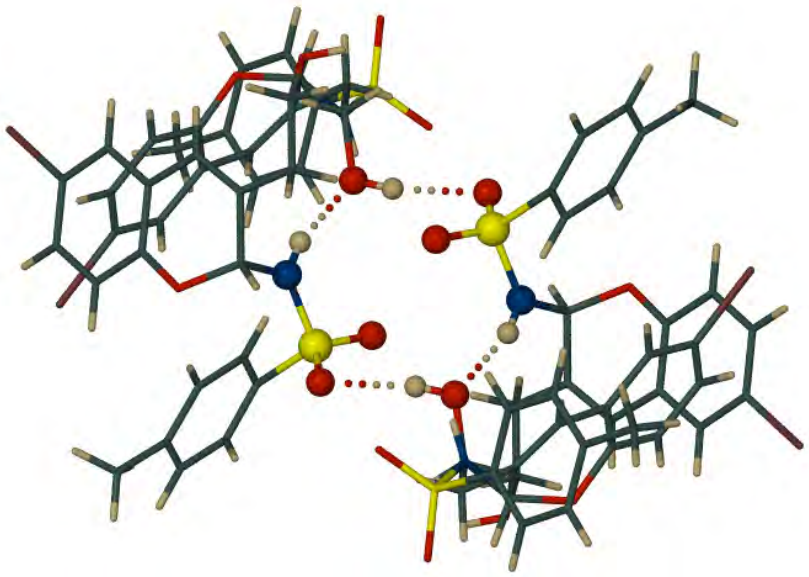

Figure 111. Showing the crystal structure H-bonding interactions in compound **202b**.

Crystal data: Formula, $C_{18}H_{18}BrNO_4S$; Formula Weight, 424.30; Crystal System, Monoclinic; Space group P21/c (No. 14); a, b, c [Angstrom] 18.060(3) 12.342(2) 7.9922(14); alpha, beta, gamma [deg] 90 92.905(3) 90; V [Ang**3] 1779.1(5); Z 4; D(calc) [g/cm^3] 1.584; Mu(MoKa) [/mm] 2.451; F(000) 864; Crystal Size [mm] 0.05 x 0.23 x 0.26; Data Collection: Temperature (K) 173; Radiation [Angstrom] MoKa 0.71073; Theta Min-Max [Deg] 2.0, 26.4; Dataset -22: 22 ; -15: 15 ; -9: 9; Tot., Uniq. Data, R(int) 26000, 3637, 0.045; Observed data [I > 2.0 sigma(I)] 2828; Refinement: Nref, Npar 3637, 228; R, wR2, S 0.0346, 0.0897, 1.03; w = 1/[\s^2^(Fo^2^) + (0.1184P)^2^ + 0.7230P] where P=(Fo^2^ + 2Fc^2^)/3; Max. and Av. Shift/Error 0.00, 0.00; Min. and Max. Resd. Dens. [e/Ang^3] -0.38, 0.59.

Table 32. Atomic coordinates and equivalent isotropic displacement parameters for non-hydrogen atoms for compound **202b** (R = 0.03)

Atom	x	y	z	U(eq) [Ang^2]
Br11	0.04132(2)	0.16606(3)	0.31186(4)	0.0517(1)
S16	0.38936(3)	0.57519(5)	0.53540(8)	0.0256(2)
O1	0.25866(10)	0.53236(14)	0.2476(2)	0.0298(6)
O14	0.43595(10)	0.21526(14)	-0.0010(2)	0.0305(5)
O17	0.40709(10)	0.67453(14)	0.4512(2)	0.0335(6)
O18	0.44243(10)	0.52845(15)	0.6542(2)	0.0318(6)
N15	0.37104(11)	0.48243(16)	0.3969(2)	0.0257(6)
C2	0.33572(14)	0.5060(2)	0.2340(3)	0.0256(8)
C3	0.34792(13)	0.41012(19)	0.1197(3)	0.0238(7)
C4	0.29530(13)	0.33430(19)	0.1073(3)	0.0243(7)
C5	0.22660(14)	0.3458(2)	0.1953(3)	0.0257(8)
C6	0.21117(14)	0.4471(2)	0.2656(3)	0.0281(8)
C7	0.14573(15)	0.4652(2)	0.3451(3)	0.0360(9)
C8	0.09484(16)	0.3818(3)	0.3575(4)	0.0410(10)
C9	0.11012(15)	0.2817(2)	0.2893(4)	0.0358(9)
C10	0.17482(14)	0.2627(2)	0.2082(3)	0.0316(8)
C12	0.42077(14)	0.4106(2)	0.0368(3)	0.0264(8)
C13	0.43375(14)	0.31863(19)	-0.0831(3)	0.0269(8)
C19	0.30608(13)	0.59645(19)	0.6379(3)	0.0247(7)
C20	0.27035(16)	0.6959(2)	0.6312(4)	0.0350(9)
C21	0.20560(17)	0.7084(2)	0.7156(4)	0.0416(10)
C22	0.17604(15)	0.6242(2)	0.8051(3)	0.0343(8)
C23	0.21319(15)	0.5255(2)	0.8106(3)	0.0333(8)
C24	0.27751(15)	0.5115(2)	0.7276(3)	0.0325(8)
C25	0.10493(18)	0.6368(3)	0.8949(4)	0.0497(11)

Table 33. Bond distances (Angstrom) for compound **202b** (R = 0.03)

Atoms	Bond length	Atoms	Bond length
Br11 - C9	1.907(3)	C19 - C20	1.387(3)
S16 - O17	1.4424(18)	C20 - C21	1.388(4)
S16 - O18	1.4355(18)	C21- C22	1.384(4)
S16 - N15	1.6150(19)	C22 - C23	1.390(4)
S16 - C19	1.768(2)	C22 - C25	1.511(4)
O1 - C2	1.439(3)	C23 - C24	1.377(4)
O1- C6	1.370(3)	C2 - H2	1.0000
O14 - C13	1.434(3)	C4 - H4	0.9500
O14 - H14	0.8400	C7 - H7	0.9500
N15 - C2	1.450(3)	C8 - H8	0.9500
N15 - H15	0.8800	C10 - H10	0.9500
C2 - C3	1.518(3)	C12 - H12A	0.9900
C3 - C12	1.503(3)	C12 - H12B	0.9900
C3 - C4	1.334(3)	C13 - H13A	0.9900
C4 - C5	1.464(3)	C13 - H13B	0.9900
C5 - C6	1.404(3)	C20 - H20	0.9500
C5 - C10	1.395(4)	C21 - H21	0.9500
C6 - C7	1.388(4)	C23 - H23	0.9500
C7 - C8	1.387(4)	C24 - H24	0.9500
C8 - C9	1.384(4)	C25 - H25A	0.9800
C9 - C10	1.385(4)	C25 - H25B	0.9800
C12 - C13	1.511(3)	C25 - H25C	0.9800
C19 - C24	1.385(3)		

Table 34. Bond angles (degrees) for compound **202b** (R = 0.03)

Atoms	Bond angle	Atoms	Bond Angle
O17 - S16 - O18	119.58(11)	Br11 - C9 - C10	119.14(19)
O17 - S16 - N15	108.99(10)	C5 - C10 - C9	119.7(2)
O17 - S16 - C19	107.71(11)	C3 - C12 - C13	116.4(2)
O18 - S16 - N15	105.97(10)	O14 - C13 - C12	112.31(19)
O18 - S16 - C19	107.96(11)	S16 - C19 - C20	121.2(2)
N15 - S16 - C19	105.85(11)	S16 - C19 - C24	118.40(19)
C2 - O1 -C6	116.58(19)	C20 - C19 - C24	120.4(2)
C13 - O14 - H14	109.00	C19 - C20 - C21	118.8(2)
S16 - N15 - C2	122.60(16)	C20 - C21 - C22	121.6(2)
S16 - N15 - H15	119.00	C21 - C22 - C25	121.9(3)
C2 - N15 - H15	119.00	C21 - C22 - C23	118.4(2)
N15 - C2 - C3	108.26(19)	C23 -C22 -C25	119.7(2)
O1 - C2 - C3	113.1(2)	C22 - C23 - C24	120.8(2)
O1 - C2 - N15	111.15(19)	C19 - C24 - C23	120.0(2)
C4 - C3 - C12	127.3(2)	O1 - C2 - H2	108.00
C2 - C3 - C12	114.8(2)	N15 - C2 - H2	108.00
C2 - C3 - C4	117.9(2)	C3 - C2 - H2	108.00
C3 - C4 - C5	121.0(2)	C3 - C4 - H4	120.00
C4 - C5 - C6	118.0(2)	C5 - C4 - H4	120.00
C4 - C5 - C10	123.5(2)	C6 - C7 - H7	120.00
C6 - C5 - C10	118.5(2)	C8 - C7 - H7	120.00
C5 - C6 - C7	121.2(2)	C7 - C8 - H8	120.00
O1 - C6 - C5	120.3(2)	C9 - C8 - H8	120.00
O1 - C6 - C7	118.5(2)	C5 - C10 - H10	120.00
C6 - C7 - C8	119.7(2)	C9 - C10 - H10	120.00
C7 - C8 - C9	119.2(3)	C3 -C12 - H12A	108.00
Br11 - C9 - C8	119.2(2)	C3 - C12 - H12B	108.00
C8 - C9 - C10	121.7(2)	C13 - C12 - H12A	108.00
C13 - C12 - H12B	108.00	C22 - C23 - H23	120.00
H12A - C12 - H12B	107.00	C24 - C23 - H23	120.00
O14 - C13 - H13A	109.00	C19 -C24 - H24	120.00
O14 - C13 - H13B	109.00	C23 - C24 - H24	120.00
C12 - C13 - H13A	109.00	C22 - C25 - H25A	109.00
C12 - C13 - H13B	109.00	C22 - C25 - H25B	109.00
H13A - C13 - H13B	108.00	C22 - C25 - H25C	109.00
C19 - C20 - H20	121.00	H25A - C25 - H25B	110.00
C21 - C20 - H20	121.00	H25A - C25 - H25C	110.00
C20 - C21 -H21	119.00	H25B - C25 - H25C	109.00
C22 - C21 - H21	119.00		

3.16. COMPUTATIONAL ANALYSIS PROCEDURE

Energy level calculations. Energy minimization of structures to determine the global minimum conformation was achieved using the Universal Force Field on Cerius 2. The resulting structures were then optimised at the B3LYP level with basis set 6-31G(d), which employs Becke's method using Lee–Yang–Parr's gradient-correction, exchange-correlation density function, which includes a hybrid of the Hartree-Fock exchange and the DFT exchange. DFT and UHF (for transition state) calculations were done using the Gaussian 03 programme[229] running on an Intel/Linux cluster and Gaussview 4.1 program was used for all visualization. Approximate transition structure was obtained by the quadratic synchronous transit method of Halgren and Lipscomb[231] and optimized at the B3LYP level with basis set 6-31G(d). Transition states were characterized by the presence of a single imaginary frequency.

Table 35. Total electronic and free energies, gas phase enthalpies and entropies for molecules depicted in Figure 44, calculated at the B3LYP level of theory.

Molecule	G (Hartrees)	H (Hartrees)	S (cal/mol.K)
178a	-845.464278	-845.38332	139.669
178a → 179a (TS1)	-845.434619	-845.357882	161.507
179a	-687.802858	-687.749685	111.912
177a	-1072.203164	-1072.148900	114.210
179a → 180a (TS2)	-687.772697	-687.692510	105.627
180a	-687.786343	-687.736304	106.316
180a → 181a (TS3)	-687.782089	-687.745893	118.274
181a	-611.400274	-611.353012	99.470
181a → 148a (TS4)	-1072.136561	-1072.084656	109.244
148a	-995.825413	-995.776829	102.255

Fukui Functions. The Fukui function is a local reactivity descriptor within the DFT framework that is useful in determining the variation in electron density within a molecule when accepting or donating an electron. In this study, the interest was in the local softness of the two carbon centres next to the vinylic carbon in compound **179a**. The local softness (S^+) was determined in each case by multiplying the Fukui function for nucleophilic attack (F^+) by the absolute softness value (calculated from the ionization potential and electron affinities of the system). Single point energy calculation for the ground state of molecule **179a** was achieved at the B3LYP 6-31G(d) level, thereby permitting access to the Mulliken charges on the atoms. Single point energy calculations were also performed on molecule **179a** for cases involving the gain and the loss of a

single electron. Results are shown in Table 36 with the red highlighted carbon atoms as those of interest in this study (Figure 38).

Table 36. Fukui parameters used in determination of local softness of compound **179a**.

		Mulliken charges					
Atom	**Atom #**	**-ve**	**+ve**	**neutral**	F^+	F^-	S^+
C	1	-0.123511	0.026858	-0.07897	-0.04454	0.105832	0.628605
C	2	0.278681	0.480226	0.300184	-0.0215	0.180042	1.069386
C	3	0.168529	0.337418	0.087941	0.080588	0.249477	1.481806
C	4	-0.040075	-0.27675	0.009918	-0.04999	-0.28667	-1.7027
C	5	-0.052525	0.311117	-0.01193	-0.0406	0.323042	1.918756
C	6	-0.061245	0.203436	-0.00502	-0.05622	0.20846	1.238179
H	7	0	0	0	0	0	0
H	8	0	0	0	0	0	0
H	9	0	0	0	0	0	0
H	10	0	0	0	0	0	0
C	11	0.087902	0.330459	0.176531	-0.08863	0.153928	0.914278
H	12	0	0	0	0	0	0
O	13	-0.280669	-0.25815	-0.23294	-0.04773	-0.0252	-0.1497
H	14	0	0	0	0	0	0
C	15	0.123506	-0.20523	0.113239	0.010267	-0.31847	-1.89158
C	16	0.454325	1.218707	0.550362	-0.09604	0.668345	3.969735
O	17	-0.67351	-0.80048	-0.45577	-0.21775	-0.34472	-2.04749
O	18	-0.294299	-0.41099	-0.17727	-0.11703	-0.23373	-1.38826
O	19	-0.264665	-0.16319	-0.24675	-0.01791	0.083558	0.496305
H	20	0	0	0	0	0	0
C	21	-0.322445	0.206566	-0.02953	-0.29292	0.236094	1.402316
H	22	0	0	0	0	0	0
H	23	0	0	0	0	0	0
H	24	0	0	0	0	0	0

Computer docking studies. The structures of the compounds and the protein were prepared using Discovery Studio Visualiser.[266] The protease, integrase and reverse transcriptase structures were obtained using the HIV-1 PR, IN and RT coordinates taken from the RCSB Protein Data Base (PDB entry code 1HXW,[265] 1QS4[269] and 1IKW,[271] respectively); all water molecules were removed from the original PDB file, hydrogen atoms were added and each atom assigned an Autodock Type using AutoDock Tools (ADT). The Autodock 4.2 programme[267] was used to explore the binding mode of selected compounds when docked in the binding site. For docking calculations, Gasteiger partial charges[268] were assigned to the ligands and non-polar hydrogen atoms were merged. All torsions were allowed to rotate during docking. Autogrid calculations were carried out after carefully locating the grid box over the active site of each enzyme. In the specific case of HIV-1 IN, the Mg atom was assigned a charge of +2 prior to docking. The dockings were simulated using a Lamarckian genetic algorithm in Autodock 4.2 and 100 docking

runs were carried out for each ligand using: a population size of 150; mutation rate of 0.02; cross-over rate of 0.8; and allowing a maximum of 27 000 generations and 2.5×10^7 energy evaluations.

3.17. SATURATION TRANSFER DIFFERENCE (STD) NMR ANALYSIS

Saturation Transfer Difference (STD) NMR studies using HIV-1 subtype C protease.[258] The over-expression and purification of the wild-type PR has been described previously.[288]

A buffered, aqueous solution of HIV-1 subtype C protease (0.35 mL), provided by Dr. Yasien Sayed (Department of Biochemistry, University of the Witwatersrand), was freeze-dried and then re-constituted in an equal volume of D_2O. The five ligands **167a-e** (2 mg of each) were dissolved together in D_2O (0.25 ml) and the resulting solution was added to the protein solution. Magnetic resonance saturation of the protein was achieved using a train of four Gaussian bell-shaped pulses separated by a 1 ms delay at a power level of 40 dB and a WATERGATE (water suppression by gradient-tailored excitation) pulse sequence was used to suppress the residual water signal.[289] The frequency of the saturating on-resonance pulse was at 1.64 ppm and the off-resonance pulse at 20 ppm.

3.18. BIOASSAY PROCEDURE

Unless indicated otherwise, the assays were conducted for the author by Dr. Nicodemus Mautsa (Rhodes Centre for Chemico- and Biomedicinal Research).

HIV-1 RT assay. Quantification of the inhibitory effect of the synthesised ligands was performed, for the author using the HIV-RT kit (Roche Applied Science, USA) as per manufacturer's instruction. The inhibitory activity of the reverse transcriptase inhibitors was calculated as the percentage of the enzyme activity compared to a sample that does not contain any inhibitor.

HIV-1 IN assay used for cinnamate ester derivatives. The HIV-1 Integrase assay was performed using the Auropure HIV-1 IN kit (Biocom Biotech) as per the manufacturer's instruction.

HIV-1 IN assay used for furocoumarins. The assays for detection of HIV-1 strand transfer inhibitors was adapted from previously described methods,[262] and were conducted by Mintek.

HIV-1 PR assay: The assay was performed according to the manufacturer's (Anaspec) instruction of Protocol A.

3.19. KINETIC STUDY OF THE REACTION OF BAYLIS-HILLMAN ADDUCT 153a WITH HCl

The study was conducted on a Bruker Biospin 600 MHz NMR spectrometer. Temperature calibration of the spectrometer was carried out between 273 and 333K, and temperatures reported for each kinetic run are the corrected values.

For each kinetic run, acetyl chloride (0.1 mL) was added to cooled CD_3OD (0.4 mL) in graduated NMR tube sealed with a septum, and the initial ^1H spectrum was obtained. (1,3,5-trimethoxybenzene was initially used as a standard, but was found to be reactive under the reaction conditions and therefore excluded). Compound **153a** (0.020 g, 80 μmol) dissolved in CD_3OD (0.1 mL) was then added, the total volume of reaction mixture noted and the tube replaced in the NMR probe. ^1H spectra were recorded automatically with a delay of 40 s between acquisitions. Experimental data obtained and used in the plot of the graph in Figure 41 is shown in Table 38. Experiments were repeated at different temperatures between 273 and 295 K and the rate constant determined at each temperature is reported in Table 37.

Table 37. Data used for the Arrhenius (Figure 43) and Erring plots for the formation of compound **177a**.

T/ K	K_{obs}	K	1/T	lnK	ln(K/T)
276.21	0.000017	7.23401E-06	0.003620434	-11.83671704	-17.45787849
280.05	0.000023	9.78719E-06	0.003570791	-11.53443617	-17.16940433
282.61	0.000059	2.51063E-05	0.003538445	-10.59239294	-16.2364608
286.45	0.000077	3.27658E-05	0.003491011	-10.32612496	-15.98368897
289.00	0.000102	4.34041E-05	0.003460208	-10.04495757	-15.71138426
293.40	0.000107	4.55317E-05	0.003408316	-9.997101552	-15.67863842

Table 38. Data used to plot graph in Figure 41.

Time (s)	[148a]	[179a]	[153]	[180a]	[177a]
0	0.000179	0.004677	0.033277	0.000742	0.000528
73	0.000172	0.005758	0.030767	0.000939	0.000701
145	0.000216	0.006922	0.028427	0.001188	0.000855
217	0.000355	0.007961	0.026148	0.001255	0.001058
289	0.000441	0.009054	0.024156	0.00137	0.001244
361	0.000512	0.009951	0.022276	0.001625	0.001453
433	0.000535	0.010848	0.020544	0.001742	0.001626
505	0.000642	0.011806	0.018913	0.001822	0.001821
577	0.00073	0.01266	0.017512	0.001975	0.001977
649	0.000791	0.013552	0.016059	0.002121	0.002192
721	0.000976	0.014387	0.014839	0.002064	0.002364
793	0.000982	0.015122	0.013584	0.002205	0.002568
865	0.001067	0.015843	0.012598	0.002353	0.002781
937	0.001177	0.016536	0.011549	0.00232	0.003046
1009	0.001306	0.017259	0.010637	0.002497	0.003185
1081	0.001324	0.017853	0.009814	0.002493	0.003404
1153	0.00149	0.018499	0.008977	0.00255	0.003608
1227	0.001453	0.018963	0.008345	0.002577	0.00386
1299	0.001559	0.019641	0.007539	0.002591	0.004084
1371	0.00173	0.020122	0.007099	0.002716	0.004268
1443	0.001641	0.020638	0.006461	0.002661	0.004488
1515	0.001836	0.02098	0.005894	0.002783	0.00473
1587	0.001827	0.021546	0.005375	0.002586	0.004922
1659	0.001928	0.021946	0.004881	0.002699	0.005174
1732	0.001934	0.022259	0.004594	0.002588	0.005371
1803	0.001994	0.022655	0.004142	0.002692	0.005562
1876	0.002116	0.023082	0.003793	0.002701	0.005783
1948	0.002127	0.023377	0.003581	0.002601	0.006022
2020	0.002118	0.023682	0.00323	0.002574	0.006238
2092	0.002182	0.023976	0.003018	0.002572	0.006441
2166	0.002322	0.02413	0.002752	0.0025	0.006687
2242	0.002212	0.024432	0.002571	0.002558	0.006896
2315	0.002307	0.02462	0.002258	0.00245	0.007147
2393	0.002312	0.024883	0.002089	0.00239	0.007307
2467	0.002352	0.025101	0.00185	0.002417	0.007567
2546	0.002464	0.025175	0.001749	0.00236	0.00777
2618	0.002528	0.025495	0.001586	0.002347	0.00798
2692	0.002557	0.025613	0.001444	0.002421	0.008159
2765	0.002562	0.025672	0.001338	0.002343	0.00844
2838	0.002612	0.025881	0.001181	0.002184	0.008556
2911	0.002613	0.025915	0.001166	0.002299	0.008792
2984	0.002574	0.026067	0.000985	0.002234	0.009033
3056	0.002658	0.026099	0.000918	0.002181	0.009198
3128	0.002686	0.026079	0.000886	0.002247	0.009458
3200	0.002755	0.026143	0.000778	0.002178	0.009643
3272	0.002809	0.026324	0.000711	0.002075	0.009774
3344	0.002803	0.026416	0.000716	0.002001	0.009989
3416	0.00286	0.026395	0.000629	0.001898	0.010172
3488	0.002878	0.026449	0.000575	0.00195	0.010383
3560	0.002834	0.026463	0.000537	0.001897	0.010587
3632	0.002849	0.02645	0.00041	0.001819	0.010758
3705	0.002882	0.026503	0.000338	0.001827	0.011042

3777	0.002893	0.026529	0.000294	0.001727	0.011217
3849	0.002934	0.026505	0.000202	0.001694	0.011383
3921	0.002949	0.026469	0.000247	0.001637	0.011579
3993	0.002933	0.026408	0.000223	0.001641	0.011774
4065	0.003051	0.02636	0.000211	0.001669	0.0118
4137	0.002975	0.02627	0.000296	0.001544	0.012075
4209	0.002971	0.026311	0.000262	0.001496	0.012254
4281	0.003083	0.026174	0.000346	0.001491	0.012346
4353	0.002972	0.026148	0.000162	0.001372	0.012574
4425	0.002994	0.026052	0.000176	0.001425	0.012723
4497	0.003051	0.026027	0.000117	0.001488	0.012882
4569	0.003036	0.025952	0.000142	0.00136	0.013069
4641	0.003043	0.026036	-2.5E-05	0.001273	0.013279
4713	0.003071	0.025798	4.86E-05	0.001257	0.013403
4785	0.00306	0.025714	6.41E-05	0.001298	0.013635
4857	0.003013	0.025717	3.9E-07	0.001277	0.013817
4930	0.003044	0.025721	7.15E-05	0.001185	0.01387
5002	0.003027	0.025603	3.83E-05	0.001116	0.014085
5074	0.003065	0.025713	-7.6E-06	0.001011	0.014317
5146	0.003073	0.025515	2.91E-05	0.001046	0.014397
5218	0.002999	0.025398	-6.8E-05	0.001042	0.01458
5290	0.003126	0.025241	-8.1E-06	0.001013	0.014756
5362	0.003094	0.025094	9.06E-05	0.001019	0.014829
5434	0.00322	0.025079	-8.9E-05	0.000996	0.015059
5506	0.00314	0.024983	5.38E-06	0.000975	0.015084
5578	0.003099	0.024861	-1.1E-05	0.001012	0.015307
5650	0.00314	0.024779	-9.4E-05	0.000947	0.015541
5722	0.003142	0.024717	-5.7E-05	0.000903	0.015611
5794	0.00312	0.02453	-0.00011	0.000856	0.015844
5866	0.003176	0.024513	-0.0001	0.000833	0.015871
5938	0.003158	0.024393	1.26E-05	0.000832	0.016117
6010	0.003192	0.024195	-2E-05	0.000861	0.016156
6082	0.003304	0.02418	-0.00016	0.000791	0.016359
6155	0.003169	0.024058	-1.9E-05	0.000732	0.016554
6227	0.003225	0.023872	-2.7E-05	0.000772	0.01654
6299	0.003237	0.023875	-0.00014	0.000566	0.016765
6371	0.003177	0.023687	-6.6E-05	0.000696	0.016859
6443	0.003194	0.023708	-0.00017	0.000679	0.017088
6515	0.00323	0.023395	-0.00011	0.00064	0.017229
6587	0.003274	0.023368	-0.00014	0.000613	0.017321
6659	0.003268	0.02323	-6.8E-05	0.00056	0.017489
6731	0.003313	0.023194	-4.5E-05	0.000637	0.017556
6803	0.003214	0.023099	-0.00012	0.000649	0.017742
6875	0.003373	0.022908	-9.1E-06	0.000523	0.017858
6947	0.003314	0.022818	9.07E-06	0.000573	0.017888
7019	0.003329	0.022701	-3.8E-05	0.000568	0.018109
7091	0.003211	0.022592	-5.7E-05	0.000613	0.018254
7163	0.003324	0.022461	2.27E-05	0.000429	0.018338
7235	0.00334	0.022294	1.71E-06	0.000519	0.018502
7307	0.003335	0.022171	2.17E-05	0.000567	0.018454
7379	0.003243	0.02211	-0.00013	0.000554	0.018698
7451	0.003337	0.022044	0.000101	0.000404	0.018843
7523	0.003294	0.021862	5.76E-05	0.000444	0.018908
7595	0.003385	0.021667	-3.2E-05	0.000525	0.019038
7667	0.003413	0.021674	-4.7E-05	0.000341	0.019157

7739	0.003307	0.021435	-0.0001	0.000492	0.019341
7811	0.003381	0.021434	-4.9E-05	0.000428	0.019423
7883	0.003431	0.021327	-9.1E-05	0.000336	0.019518
7955	0.003399	0.021105	-8.3E-05	0.000434	0.019677
8027	0.003327	0.021014	-1.9E-05	0.000405	0.019777
8100	0.003381	0.020959	-8.2E-05	0.000381	0.019937
8172	0.003251	0.020823	-0.00017	0.000328	0.020115
8244	0.003321	0.020769	-2.8E-05	0.000308	0.020164
8316	0.00346	0.020576	-3.3E-05	0.000296	0.020225
8388	0.003342	0.020576	-6.6E-05	0.000353	0.020355
8460	0.003412	0.020312	7.55E-05	0.000321	0.020466
8532	0.003392	0.020274	-0.00012	0.000305	0.020625
8604	0.003438	0.02014	-8.3E-05	0.000245	0.020709
8677	0.003309	0.019934	-6.9E-05	0.000277	0.02087
8749	0.003408	0.019905	-0.00012	0.000254	0.020968
8821	0.003274	0.019745	-1.6E-05	0.000234	0.021146
8893	0.003417	0.019716	-6.3E-05	0.000249	0.021159
8965	0.003412	0.019571	-8.9E-06	0.000138	0.021265
9037	0.0034	0.019534	-7.2E-05	0.000154	0.021373
9109	0.003379	0.019376	-4.2E-05	0.000229	0.021501
9181	0.003472	0.019252	-0.00011	0.000246	0.021578
9253	0.003395	0.019067	-4.7E-05	0.000131	0.021747
9325	0.003365	0.018997	-7.8E-06	0.000205	0.021754
9397	0.003397	0.018844	-6.6E-05	0.000202	0.021944
9469	0.003373	0.018768	-1.2E-05	0.000212	0.022037
9541	0.003465	0.018722	-0.00011	0.00017	0.022091
9613	0.003414	0.018531	-4.5E-05	0.000229	0.022184
9685	0.00345	0.018532	-3.5E-05	0.00014	0.022289
9757	0.003464	0.018457	-6.2E-05	0.000219	0.022384
9829	0.003381	0.018199	-5.4E-05	0.000164	0.02255
9901	0.003303	0.018063	-4.5E-05	0.000183	0.022684
9973	0.003391	0.018128	-7.8E-05	7.34E-05	0.022781
10045	0.003409	0.017944	-9.1E-05	0.000176	0.022872
10117	0.003386	0.017745	-2.9E-05	8.44E-05	0.022892
10189	0.003321	0.017776	3.33E-05	0.000142	0.022957
10261	0.003331	0.017655	-8.6E-05	0.0002	0.023136
10333	0.003352	0.017453	-7.7E-05	0.00017	0.023244
10405	0.003406	0.017295	-0.00011	0.000141	0.023367
10477	0.003328	0.017354	-0.00013	7.7E-05	0.023463
10549	0.003537	0.017183	-0.00015	7.76E-05	0.023519
10621	0.003363	0.017169	2.36E-05	0.000124	0.023478
10693	0.003413	0.016923	-8.2E-05	0.000104	0.023698

10765	0.003374	0.01692	-9.4E-05	-3.5E-05	0.023861
10837	0.003411	0.01681	-0.00011	2.92E-05	0.023831
10909	0.00335	0.016686	-0.00012	0.000115	0.024057
10981	0.003401	0.016558	-3.2E-05	0.000112	0.024017
11053	0.00348	0.016534	-0.00013	2.26E-05	0.02414
11125	0.003368	0.01645	6.1E-06	8.94E-06	0.024196
11197	0.003365	0.016297	-4E-05	5.23E-05	0.02437
11269	0.003328	0.016209	-0.00011	1.77E-05	0.024446
11341	0.003462	0.016212	-6E-05	4.78E-05	0.024467
11413	0.00349	0.016101	-0.00013	9.71E-05	0.024586
11485	0.003456	0.015974	-5.7E-05	8.01E-05	0.024616
11557	0.003422	0.015776	-0.0001	2.22E-05	0.024823
11629	0.00344	0.015756	-6.9E-05	2.87E-05	0.024816
11701	0.003484	0.01564	-8.4E-05	-1.4E-05	0.024939
11773	0.003493	0.015604	-6.7E-05	5.76E-05	0.024999
11846	0.003442	0.015469	-2.6E-05	-3.7E-05	0.025129
11918	0.003364	0.015368	-8.2E-05	1.85E-05	0.025236
11990	0.003432	0.015272	-5.3E-05	-4.4E-07	0.025261
12062	0.003412	0.015155	-1.3E-05	-7.2E-05	0.025358
12134	0.00343	0.015036	-4.1E-05	-3.5E-05	0.025434
12206	0.003419	0.015056	-5.7E-05	1.4E-05	0.025464
12278	0.003324	0.015008	7.71E-07	-0.00011	0.025629
12350	0.003432	0.014867	-1.2E-05	5.98E-05	0.025634
12422	0.003413	0.014739	-0.00011	-1.3E-05	0.02571
12494	0.003362	0.014798	-1E-04	-7.6E-05	0.025868
12566	0.003441	0.014527	4.86E-06	-1.5E-05	0.025848
12638	0.003328	0.014518	6.96E-05	-2.3E-05	0.025901
12710	0.00339	0.014449	-0.00011	-9.2E-05	0.026103
12782	0.003339	0.01427	-0.00011	1.2E-05	0.026198
12854	0.003323	0.014261	-3.9E-05	-7.3E-05	0.0262
12926	0.003432	0.014069	5.53E-05	-2.6E-05	0.026325
12998	0.003395	0.014021	-5.4E-05	-1.9E-05	0.026447
13070	0.003428	0.014038	-0.00011	-6.6E-05	0.026476
13142	0.003463	0.013852	-0.00015	3.96E-06	0.02659
13214	0.003465	0.013732	-6.9E-05	6.4E-05	0.026636
13286	0.003337	0.013673	-8E-05	4.98E-05	0.026617
13358	0.003349	0.013668	-2.4E-05	5.45E-06	0.026709
13430	0.003367	0.013537	-0.0001	-7.5E-06	0.026841
13502	0.00342	0.013546	-0.00014	-3.1E-05	0.026902
13574	0.003409	0.013384	1.48E-05	-5.8E-05	0.026914
13646	0.003325	0.013387	-4.9E-05	3.98E-05	0.027006
13718	0.003442	0.013265	-0.0001	1.68E-05	0.027042

13790	0.003394	0.013206	1.15E-05	-2.6E-05	0.027156
13863	0.003438	0.013093	1.94E-05	-0.00012	0.027231
13935	0.003321	0.012984	-0.00011	-2.7E-05	0.027365
14006	0.003525	0.012879	-6.3E-05	6.02E-05	0.027355
14078	0.003298	0.0128	-6.1E-05	2.35E-05	0.027394
14151	0.003335	0.012765	-0.0001	-1.2E-05	0.027573
14223	0.003354	0.012723	-0.00012	-1.9E-05	0.02758
14295	0.003286	0.012652	-0.00012	-6.3E-05	0.027639
14367	0.003525	0.01253	1.13E-05	-9.7E-05	0.027625
14439	0.003444	0.012372	-0.0001	3.68E-05	0.027785
14511	0.003439	0.012482	2.07E-06	-0.00017	0.027772
14583	0.003379	0.0123	-0.00013	-6.4E-05	0.028031
14655	0.003527	0.012234	-7.4E-05	-4.4E-05	0.027961
14727	0.003283	0.012178	-5.1E-06	-1.5E-05	0.028087
14799	0.0034	0.012153	-4E-05	-1.4E-05	0.028159
14871	0.003464	0.012019	-9.7E-05	1.4E-05	0.028161
14943	0.003355	0.011954	-0.00015	-9.6E-05	0.0283
15015	0.003344	0.011858	-9.3E-05	-0.00017	0.028404
15087	0.003441	0.011655	-9.1E-05	8.8E-05	0.028355
15159	0.003324	0.01175	-5.2E-05	-4.7E-05	0.028418
15231	0.003488	0.011692	-5E-05	-0.00014	0.028495
15303	0.00328	0.01161	-0.00011	-9.5E-05	0.0286
15375	0.003457	0.011509	-3.6E-05	-3.6E-05	0.028648
15447	0.003443	0.011502	-8.5E-05	-8.1E-05	0.028643
15519	0.003528	0.011378	2.2E-05	-5.7E-06	0.02873
15591	0.003369	0.01128	-6.8E-05	-2.2E-05	0.028877
15663	0.00344	0.011222	-4.3E-05	-7.2E-05	0.028861
15735	0.003432	0.01118	-4.7E-05	-6.7E-05	0.028879
15807	0.003343	0.011052	-9.8E-05	-3.2E-07	0.028959
15879	0.003373	0.010927	-9.1E-05	-3.8E-05	0.02914
15951	0.003464	0.010959	-4.5E-05	-8.7E-05	0.029036
16023	0.003495	0.010879	-0.0001	-6.6E-06	0.029168
16095	0.003439	0.01087	0.000105	1.83E-05	0.029144
16167	0.003352	0.010756	-8.3E-05	-2.2E-05	0.029221
16239	0.003335	0.010752	-9.4E-05	1.73E-07	0.029315
16312	0.003297	0.010529	-0.00012	-8.7E-05	0.029507
16384	0.00352	0.010529	-1.5E-05	-6E-05	0.029395
16456	0.00341	0.010442	7.91E-06	-4.7E-05	0.029506
16528	0.003309	0.010464	-0.0001	-0.00011	0.029609
16600	0.003489	0.010468	-8E-05	-6.3E-05	0.029515
16672	0.003358	0.01035	-0.00011	-2.9E-05	0.029696
16744	0.003275	0.010228	-0.00011	-6.9E-05	0.029849

16816	0.003317	0.010211	-5.3E-05	-5.6E-05	0.029828
16888	0.003434	0.010081	-1.5E-05	-8.9E-05	0.029845
16960	0.003329	0.010003	-0.00012	-3.4E-05	0.029986
17032	0.003255	0.010082	-7.9E-06	-0.00014	0.030072
17104	0.003435	0.009916	-9.1E-05	-3.2E-05	0.030023
17176	0.003295	0.00982	-0.00021	-0.00013	0.030176
17248	0.003472	0.009911	-1.8E-05	-8.8E-05	0.030045
17320	0.003303	0.00976	-0.00015	-0.00011	0.030368
17392	0.003355	0.009679	-0.00016	5.85E-06	0.030259
17464	0.003544	0.00971	-3.7E-05	-7.3E-05	0.030188
17536	0.003292	0.009552	-0.00017	-0.00011	0.030476
17608	0.003301	0.009517	-0.00014	-0.00014	0.030516
17680	0.0033	0.009477	-0.0001	-0.00019	0.030573
17752	0.003261	0.009449	-0.00014	-8.9E-05	0.030608
17824	0.003247	0.009427	-0.00012	-0.00017	0.03064
17896	0.003347	0.00929	-8.5E-05	-8.2E-05	0.030666
17968	0.003288	0.009257	-0.00024	-7.5E-06	0.030772
18040	0.003311	0.009142	-0.00021	-0.00012	0.030858
18112	0.003336	0.009193	-9.2E-05	-2.1E-05	0.03076
18184	0.003281	0.009129	-0.00017	-9.9E-05	0.030864
18256	0.003265	0.009035	-7.1E-05	-0.00013	0.030862
18328	0.003254	0.009028	-0.00015	-0.00015	0.031025
18400	0.003342	0.008997	-0.00019	-0.00013	0.031063
18472	0.003331	0.008821	3.02E-05	9.53E-06	0.030999
18544	0.003403	0.008797	-0.00011	-0.00013	0.031128
18616	0.003298	0.008825	-0.00022	-9.4E-05	0.03117
18688	0.003225	0.008772	-0.00018	-0.00018	0.031255
18760	0.003212	0.00865	-0.00013	-0.00013	0.031299
18833	0.003277	0.008564	-0.00016	-0.00014	0.031271
18905	0.00326	0.008538	-0.00019	6.49E-06	0.031413
18977	0.003303	0.008499	-0.00015	-4.7E-05	0.031361
19049	0.003311	0.008502	-0.0002	-0.00019	0.031523
19121	0.00331	0.008502	-0.00013	-0.0001	0.031463
19193	0.003289	0.00835	-0.0002	-6.4E-05	0.031593
19265	0.003313	0.008319	-8.6E-05	-0.00015	0.031611
19337	0.003246	0.008331	-7.6E-05	-0.00013	0.031582
19409	0.003296	0.008224	-0.00021	-0.00018	0.031679
19481	0.00329	0.008094	-0.00025	1.66E-05	0.031724
19554	0.00329	0.008111	-0.00016	-0.00015	0.031811
19626	0.003365	0.008119	-0.00013	-9.6E-05	0.031762
19698	0.00328	0.008002	-0.00026	-0.0001	0.031899
19770	0.0033	0.008026	-0.00014	-0.00018	0.031855

19842	0.003289	0.007932	-0.00021	-0.00013	0.031907
19914	0.003282	0.007895	-0.00023	-0.0002	0.032031
19986	0.00324	0.007764	-0.00015	-4E-05	0.03208
20059	0.003279	0.007835	-0.00011	-0.0001	0.032099
20130	0.003241	0.007764	-0.00011	-0.00017	0.032152
20203	0.003307	0.007557	-0.00012	-0.00016	0.032184
20275	0.00326	0.007654	-0.00015	-0.00025	0.0322
20347	0.003294	0.007578	-0.00021	-0.00019	0.032245
20419	0.003325	0.007567	-0.00014	-0.00021	0.032272
20491	0.003311	0.007542	-0.00022	-1E-04	0.032351
20563	0.003286	0.007507	-0.00019	-0.00012	0.032347
20635	0.003241	0.007447	-0.00014	-0.00019	0.032406
20707	0.003289	0.007385	-0.00022	-0.00014	0.032474
20779	0.003252	0.007319	-0.00013	-0.00013	0.032529
20851	0.003344	0.007266	-0.00015	-0.00019	0.032509
20923	0.003336	0.00728	-0.00019	-0.00012	0.032544
20995	0.003242	0.007204	-0.00013	-0.00016	0.032615
21067	0.003283	0.007189	-0.00016	-0.00012	0.03265
21139	0.003281	0.007043	-8.4E-05	-0.00014	0.032654
21211	0.003299	0.007096	-0.00023	-9.5E-05	0.032709
21283	0.003222	0.007063	-0.00017	-0.00011	0.03277
21355	0.00326	0.00709	-0.00015	-0.00012	0.032808
21427	0.003272	0.007007	-0.00017	-9.2E-05	0.032811
21499	0.003298	0.006872	-0.0002	-0.00025	0.032855
21571	0.003285	0.006902	-5.9E-05	-8.3E-05	0.032773
21643	0.003331	0.006866	-0.00016	-0.00011	0.03289
21715	0.003281	0.006831	-0.00016	-0.00018	0.03301
21787	0.003268	0.006733	-0.00025	-6.9E-05	0.033022
21859	0.003332	0.006692	-0.00013	-0.00016	0.033037
21931	0.003203	0.006673	-0.00027	2.06E-05	0.033046
22003	0.003258	0.006657	-9.7E-05	-7.6E-05	0.033071
22075	0.003288	0.006629	-0.00016	-7.4E-05	0.033107
22147	0.003194	0.006656	-0.00023	-8.9E-05	0.033193
22219	0.003296	0.006603	-0.0001	-6.8E-05	0.033146
22291	0.003233	0.006414	-0.00014	-0.00019	0.03328
22363	0.003263	0.006377	-0.00016	-8.2E-05	0.03327
22435	0.003221	0.00638	-0.00011	-8.7E-05	0.033307
22507	0.003259	0.006435	-0.00012	-0.00011	0.03328
22579	0.003291	0.006369	-6.7E-05	-0.00019	0.033395
22651	0.003277	0.0062	-0.00015	-0.00015	0.033436
22723	0.00328	0.006335	-4.2E-05	-0.00015	0.033395
22795	0.003277	0.006318	-0.00022	-0.0001	0.033416

22867	0.003207	0.006237	-0.00011	-9.9E-05	0.033497
22939	0.003289	0.006148	-0.00014	-0.00016	0.033524
23012	0.003292	0.006112	-0.00015	-0.00016	0.033587
23083	0.003287	0.006196	-4.2E-06	-0.00011	0.033532
23156	0.003242	0.006126	-0.00015	-9.6E-05	0.033643
23227	0.003288	0.00608	-0.00015	-0.00021	0.033599
23300	0.003285	0.005946	-0.00011	-0.00012	0.033657
23372	0.003284	0.006026	-0.00014	-0.00027	0.033682
23444	0.003261	0.00594	-0.00014	-0.00022	0.033753
23516	0.003319	0.005974	-0.00014	-0.00019	0.033745
23588	0.003262	0.00585	-0.00017	-2.6E-05	0.033776
23660	0.003177	0.005792	-0.00012	-0.00018	0.033872
23732	0.003298	0.005759	-0.00013	-0.00019	0.033881
23804	0.003299	0.005748	-0.00017	-9.2E-05	0.033873
23876	0.003235	0.005687	-0.00018	-0.00017	0.033918
23948	0.003263	0.005686	-0.00012	-0.00015	0.033988
24020	0.003283	0.005745	-0.00013	-0.00012	0.034008
24092	0.003334	0.005608	-0.00014	-0.0001	0.034033
24164	0.003294	0.005593	-7.6E-05	-0.00015	0.034041
24236	0.003317	0.005591	-0.00021	-0.00019	0.03406
24308	0.003273	0.005626	-5.2E-05	-0.0002	0.034132
24380	0.003218	0.005451	-0.00019	-0.00018	0.034162
24452	0.003291	0.005431	-0.00019	-5.7E-05	0.034187
24524	0.003259	0.005454	-0.00011	-0.00026	0.03422
24596	0.00325	0.005348	-0.00017	-7.8E-05	0.034241
24668	0.003272	0.005341	-0.00017	-0.00015	0.034316
24740	0.003284	0.005319	-0.00012	-8.5E-05	0.034227
24812	0.003317	0.005342	-0.00023	-0.00021	0.03435
24884	0.003319	0.005203	-5.4E-05	-7.4E-05	0.034301
24956	0.003244	0.005276	-0.00015	-0.00015	0.034314
25028	0.003267	0.005141	-0.0002	-0.00021	0.03443
25100	0.00322	0.005229	-0.00011	-8E-05	0.03444
25172	0.003282	0.005131	-0.00014	-7.8E-05	0.034412
25244	0.003335	0.00511	-0.00019	-0.00015	0.034449
25316	0.003199	0.005117	-0.00023	-0.00012	0.034557
25388	0.003277	0.00504	-0.00011	-0.00022	0.034548
25460	0.003206	0.005015	-0.00013	-8E-05	0.034541
25532	0.00333	0.005076	-0.00018	-0.00011	0.034565
25604	0.003274	0.005006	-9.6E-05	-6.9E-05	0.034525
25676	0.003286	0.004961	-0.00014	-0.00013	0.034577
25748	0.003201	0.004872	-0.00013	-0.00014	0.034603
25820	0.003285	0.004821	-0.00027	-6.8E-05	0.034594

25892	0.003285	0.004918	-0.00021	-0.00018	0.03465
25964	0.003288	0.004871	-0.00022	-0.00014	0.034806
26036	0.00325	0.004822	-0.00014	-5.6E-05	0.034725
26109	0.003226	0.004791	-0.00023	-0.00013	0.034784
26181	0.003295	0.004754	-0.00019	-8.4E-05	0.03471
26253	0.003339	0.00478	-0.00016	-9.6E-05	0.034816
26325	0.003226	0.004915	-0.00018	-9.8E-05	0.034758
26397	0.00331	0.004717	-0.00013	-0.0002	0.034872
26469	0.003261	0.004681	-0.00027	-9.7E-05	0.034918
26541	0.00321	0.004698	-0.00027	-0.00011	0.034911
26613	0.003253	0.004687	-0.00019	-0.00013	0.034955
26685	0.003307	0.004591	-0.00025	-0.00017	0.035032
26757	0.003258	0.004543	-0.00016	-0.00014	0.035048
26829	0.003239	0.004552	-0.00017	-0.00015	0.035052
26901	0.003195	0.004507	-0.00014	-4.9E-05	0.035122
26973	0.003243	0.00467	-0.00029	-0.0002	0.035083
27045	0.003297	0.004465	-0.00023	-0.00026	0.035209
27117	0.003223	0.004352	-0.00026	-0.0003	0.035294
27189	0.003252	0.004314	-0.00019	-5.8E-05	0.035197
27261	0.003315	0.004456	-0.00011	-0.00014	0.035121
27333	0.003163	0.004351	-0.00023	-0.00017	0.035235
27405	0.00328	0.0042	-9.3E-05	-0.00018	0.035299
27477	0.003279	0.004274	-0.00018	-0.0001	0.035209
27549	0.003269	0.004244	-0.00018	-0.00017	0.035301
27621	0.003251	0.00419	-0.00022	-9.3E-05	0.035331
27693	0.003286	0.0041	-0.00011	-2.7E-06	0.035302
27765	0.003314	0.004179	-0.00031	-6.1E-05	0.035404
27837	0.003306	0.004164	-0.00026	-0.00019	0.035405
27909	0.003215	0.004198	-0.0002	-9.9E-05	0.035421
27981	0.003271	0.004078	-0.00016	-0.00011	0.035395
28053	0.003255	0.004009	-4.8E-05	-0.00011	0.035401
28125	0.003257	0.004074	-0.00024	-6.8E-05	0.035535
28197	0.003137	0.004019	-0.0002	-0.0001	0.035516
28269	0.003293	0.004082	-7.3E-05	-0.0001	0.035362
28341	0.00321	0.00395	-0.00019	-4.7E-05	0.035512
28413	0.003267	0.003968	-0.00026	-0.00016	0.03557
28485	0.003236	0.003958	-0.00016	-0.00015	0.03561
28557	0.003266	0.003946	-0.0001	-0.00012	0.035506
28629	0.003197	0.003971	-0.00023	-0.00014	0.035645
28701	0.003237	0.003878	-0.00018	-8.8E-05	0.03553
28773	0.003171	0.003911	-0.00019	-0.00017	0.035676
28846	0.003257	0.003922	-0.0002	-0.0002	0.035658

28918	0.00328	0.003875	-0.00013	-0.00018	0.035673
28990	0.003248	0.003912	-0.00032	-0.00015	0.035721
29062	0.003258	0.003716	-0.0002	-0.00012	0.035677
29134	0.003207	0.003836	-0.00027	-0.00011	0.035728
29206	0.0032	0.003783	-0.00019	-5.7E-05	0.035707
29278	0.003274	0.00383	-0.00025	-0.00012	0.035758
29350	0.003308	0.003801	-0.00013	-0.00018	0.035709
29422	0.003241	0.003752	-0.00022	-0.0002	0.035805
29494	0.0033	0.003654	-0.00021	-0.00012	0.035793
29566	0.003337	0.003671	-0.00026	-0.00012	0.035821
29638	0.003241	0.003635	-0.00015	-0.00013	0.035839
29710	0.003342	0.003586	-0.00023	-0.00013	0.035935
29782	0.00318	0.003589	-0.00019	-0.00022	0.035899
29854	0.003247	0.003636	-0.00026	-0.00011	0.035943
29926	0.003203	0.003568	-0.0002	-0.00013	0.035972
29998	0.003199	0.00366	-0.00027	-0.00027	0.035966
30070	0.003263	0.003505	-0.00033	-0.00017	0.036064
30142	0.003228	0.003517	-0.0001	-0.00018	0.035945
30214	0.003186	0.003533	-0.00018	-0.00019	0.035938
30286	0.003285	0.003454	-0.00022	-4.8E-05	0.035907
30358	0.003269	0.003361	-0.00016	-0.00012	0.036103
30430	0.003216	0.003336	-0.00028	-8.7E-05	0.03609
30502	0.003261	0.003389	-0.00013	-0.00016	0.036033
30574	0.00326	0.003433	-0.00019	-0.0002	0.036075
30646	0.003241	0.003457	-0.00015	-0.00021	0.03612
30718	0.00316	0.003357	-3.2E-05	-0.00017	0.0361
30790	0.003224	0.00333	-0.00022	-0.00021	0.036161
30862	0.00321	0.003332	-0.00012	-0.00013	0.036127
30934	0.003247	0.003275	-0.00024	-4.3E-05	0.03617
31006	0.003273	0.003319	-0.00024	-0.00017	0.03618
31078	0.003248	0.003249	-0.00014	-0.00017	0.03621
31150	0.003218	0.003234	-0.00014	-0.00015	0.036243
31222	0.003244	0.003377	-0.00019	-6.7E-05	0.036145
31294	0.00322	0.003179	-0.0001	-0.00012	0.036213
31366	0.003266	0.003208	-0.00023	-0.0001	0.036247
31438	0.003255	0.003191	-0.00023	-0.00018	0.036302
31510	0.003302	0.003172	-0.00021	-0.00021	0.036306
31582	0.003317	0.003206	-0.00019	-0.00016	0.036254
31654	0.003244	0.003033	-0.00019	-0.00014	0.036327
31726	0.003213	0.003248	-0.00023	-0.0001	0.036318
31798	0.003275	0.003095	-0.00017	-0.00018	0.036304
31870	0.003285	0.003054	-0.00011	-0.00011	0.036309

31943	0.003195	0.003038	-0.00013	-0.00022	0.036377
32014	0.003192	0.003017	-0.00024	-0.00015	0.03646
32087	0.003261	0.003122	-0.0002	-8.3E-05	0.036367
32158	0.00322	0.003125	-0.00018	-0.00019	0.036376
32231	0.003292	0.003003	-0.00023	-0.00024	0.036473
32302	0.003291	0.00308	-0.00014	-0.00017	0.03636
32374	0.003226	0.003023	-0.00029	-0.00011	0.036509
32446	0.003151	0.002941	-0.00015	-0.00022	0.03652
32518	0.003224	0.002916	-0.00021	-0.00016	0.036469
32590	0.003165	0.002899	-0.00016	-2.6E-05	0.03656
32663	0.003167	0.002968	-0.00025	-0.00011	0.036536
32734	0.003236	0.00301	-0.00035	-0.00018	0.036653
32806	0.003245	0.002894	-0.00023	-0.00021	0.036547
32879	0.003233	0.002864	-0.00024	-0.00013	0.036528
32950	0.003231	0.002909	-0.00029	-0.00014	0.036562
33023	0.003237	0.002942	-0.00027	-0.00015	0.036658
33095	0.003207	0.002898	-0.0003	-0.00015	0.036681
33167	0.003278	0.002829	-0.00013	-0.00015	0.036617
33239	0.00326	0.00286	-0.00022	-0.00016	0.036592
33311	0.003232	0.002768	-0.00027	-0.00012	0.0367
33383	0.003305	0.002859	-0.00029	-0.00011	0.036586
33455	0.003291	0.002831	-0.00014	-0.00017	0.036621
33527	0.003186	0.002874	-0.00023	-0.00021	0.036708
33599	0.003278	0.002764	-0.00011	-0.00013	0.03672
33671	0.003253	0.002804	-7.7E-05	-0.00019	0.036623
33743	0.003288	0.002667	-9E-05	-0.0003	0.036742
33815	0.003296	0.002866	-0.00018	-8.4E-05	0.03662
33887	0.003248	0.002736	-0.0002	-0.00017	0.036766
33959	0.003297	0.002758	-0.00029	-0.00013	0.036696
34031	0.003247	0.002642	-0.00018	-0.00013	0.036742
34103	0.003284	0.002697	-0.00016	-0.00011	0.036706
34175	0.003246	0.002613	-0.0002	-0.00011	0.036801
34247	0.00329	0.002703	-0.00018	-0.00014	0.036734
34319	0.003218	0.002719	-0.00028	-0.00018	0.036794
34391	0.003284	0.002577	-0.00031	-0.00021	0.036884
34463	0.003223	0.002777	-0.00024	-0.00022	0.036822
34535	0.003236	0.002512	-0.00024	-0.00011	0.036883
34607	0.003191	0.002594	-0.00025	-0.00019	0.036835
34679	0.003207	0.002505	-0.00021	-0.00014	0.036928
34751	0.00326	0.002526	-0.00014	-9.6E-05	0.036932
34823	0.00317	0.002564	-0.00017	-0.00028	0.036899
34895	0.003325	0.002542	-0.00024	-0.00017	0.036903

34967	0.003259	0.002657	-0.00018	-0.00015	0.036884
35039	0.003291	0.002534	-0.00027	-0.00015	0.036904
35111	0.003184	0.002615	-0.00012	-0.00011	0.036862
35183	0.003229	0.002447	-9.4E-05	-8.4E-05	0.036957
35255	0.00326	0.002452	-0.00018	-0.00011	0.036961
35327	0.003227	0.002461	-0.00027	-0.00031	0.037042
35399	0.003239	0.002435	-0.0002	-0.00015	0.037021
35471	0.003253	0.00251	-0.00028	-0.00027	0.037108
35543	0.003281	0.002442	-0.0002	-0.00019	0.037065
35615	0.003302	0.002483	-0.0003	-0.00025	0.03702
35687	0.003321	0.00245	-0.0002	-0.00019	0.036962
35759	0.003188	0.002405	-0.00024	-1.2E-05	0.037008
35831	0.003227	0.002484	-0.00021	-0.00033	0.037094
35903	0.00328	0.002289	-0.00015	-0.00019	0.037013
35975	0.003258	0.002301	-0.00017	-0.00013	0.037072
36047	0.003181	0.00236	-0.00021	-0.00015	0.037025
36119	0.003208	0.00237	-0.00026	-0.00017	0.037188
36191	0.003265	0.002321	-0.0002	-0.00014	0.037052
36263	0.003263	0.002324	-0.00022	-0.00024	0.037107
36335	0.003232	0.002357	-0.00015	-0.0001	0.037089
36407	0.003288	0.002404	-0.00026	-7.1E-05	0.037066
36479	0.003253	0.002446	-0.0002	-0.00014	0.037059
36551	0.003215	0.002344	-0.00019	-0.0002	0.037099
36623	0.0033	0.002328	-0.00013	-0.0002	0.037136
36695	0.003285	0.002335	-0.00023	-0.00018	0.037122
36767	0.003246	0.002208	-0.00024	-6E-05	0.037212
36839	0.00329	0.002206	-0.00031	-0.00015	0.037241
36911	0.003206	0.002186	-0.00028	-0.00032	0.037369
36983	0.003202	0.002195	-0.00022	-0.00018	0.037214
37055	0.003272	0.002212	-0.00015	-0.00014	0.037166
37127	0.00326	0.002228	-0.00027	-0.00016	0.037263
37199	0.003231	0.00214	-0.00018	-0.00014	0.037179
37271	0.003231	0.00224	-0.00025	-0.00016	0.037167
37343	0.003252	0.002106	-0.00018	-0.00018	0.037258
37415	0.003202	0.002163	-0.00011	-0.00019	0.037237
37487	0.003163	0.002165	-0.00026	-0.00019	0.037228
37559	0.003168	0.00209	-0.0001	-8.7E-05	0.037187
37631	0.00328	0.002072	-0.00023	-0.00017	0.037288
37703	0.003221	0.002147	-0.00032	-0.00015	0.037342
37775	0.003336	0.002047	-0.00021	-0.00011	0.037322
37847	0.003171	0.002101	-0.00027	-0.0002	0.037324
37919	0.003319	0.002155	-0.00019	-0.0002	0.037288

37991	0.003154	0.002114	-0.00018	-0.00023	0.037371
38063	0.003265	0.002154	-0.00021	-0.00016	0.037303
38135	0.00336	0.002057	-0.00033	-0.00014	0.037372
38207	0.003237	0.002021	-0.00022	-0.00022	0.037403
38279	0.003207	0.002115	-0.00029	-0.00011	0.037396
38351	0.003222	0.002151	-0.00022	-0.00019	0.037331
38423	0.003157	0.002042	-0.00023	-0.00018	0.037469
38495	0.003281	0.002005	-0.00013	-0.00013	0.037307
38567	0.003223	0.002107	-0.00023	-0.00015	0.037429
38639	0.003331	0.002011	-0.00024	-0.00025	0.037425
38711	0.003225	0.002016	-8E-05	-0.00013	0.037329
38783	0.003293	0.001989	-0.00021	-0.00019	0.037404
38855	0.003342	0.001977	-8.9E-05	-0.0002	0.037425
38927	0.003252	0.002075	-0.00021	-0.00017	0.037446
38999	0.003244	0.001987	-0.00025	-0.00022	0.037393
39071	0.003238	0.002015	-0.00024	-0.0002	0.037421
39143	0.003315	0.00193	-0.00019	-0.00016	0.037435
39215	0.003226	0.001916	-0.00023	-0.00017	0.037472
39287	0.003118	0.001773	-0.00025	-0.00011	0.037625
39359	0.003201	0.001914	-0.00026	-7.4E-05	0.037522
39431	0.003257	0.001959	-0.00023	-0.00017	0.037481
39503	0.003293	0.001967	-0.00023	-0.0002	0.037442
39575	0.003329	0.001897	-0.00021	-0.00018	0.037478
39647	0.003261	0.001943	-0.00027	-0.00022	0.03751
39719	0.00326	0.001898	-0.00025	-0.00015	0.037557
39791	0.003275	0.001917	-0.0002	-0.00011	0.037441
39863	0.003199	0.001913	-0.00017	-0.00023	0.03754
39935	0.003199	0.001866	-0.00021	-0.00015	0.037554
40007	0.003249	0.001934	-0.0003	-0.00012	0.037547
40079	0.003293	0.001848	-0.00032	-0.00026	0.037617
40151	0.003228	0.001887	-0.00022	-0.00023	0.037555
40223	0.003232	0.001849	-0.00017	-8.4E-05	0.037438
40295	0.003297	0.001877	-0.00017	-0.00017	0.037499
40367	0.003277	0.001858	-0.00027	-5.7E-05	0.037558
40439	0.003328	0.001915	-0.00014	-0.0001	0.037541
40511	0.003241	0.001834	-0.0003	-0.0002	0.037674
40583	0.003284	0.00187	-0.00012	-4.5E-06	0.037403
40655	0.003294	0.001775	-0.0002	-7.9E-05	0.037617
40727	0.003218	0.001832	-0.00028	-0.0001	0.037659
40799	0.003192	0.001807	-0.00015	-6.4E-07	0.037582
40871	0.003192	0.001727	-0.00011	-0.00018	0.037648
40943	0.003315	0.001836	-0.00014	-9.9E-05	0.037515

41015	0.003298	0.001686	-0.00031	-0.00026	0.037733
41087	0.003241	0.001697	-0.00028	-0.0001	0.037625
41159	0.003274	0.001726	-0.00029	-0.00014	0.037767
41231	0.003277	0.001673	-0.00027	-9.5E-05	0.037654
41303	0.003234	0.001826	-0.0002	-0.00017	0.037624
41375	0.003348	0.001739	-0.00024	-0.00017	0.037615
41447	0.003259	0.001643	-0.00029	-0.00015	0.037747
41519	0.003267	0.001798	-0.00029	-6E-05	0.037609
41591	0.003302	0.001724	-0.00017	-0.00013	0.037628
41663	0.003162	0.00174	-6.5E-05	-8.4E-05	0.037655
41735	0.003258	0.001746	-0.0002	-0.00019	0.03764
41807	0.0033	0.001691	-0.0003	-9.2E-05	0.03776
41879	0.003313	0.001651	-0.00018	-0.00015	0.037646
41951	0.003295	0.001836	-0.00027	-5.7E-05	0.037617
42023	0.003276	0.001723	-0.0002	-0.0002	0.037713
42095	0.003306	0.001613	-0.00021	-0.00017	0.037726
42167	0.003266	0.001627	-0.0002	-7.7E-05	0.037768
42239	0.003264	0.001688	-0.00025	-0.0002	0.037804
42311	0.003245	0.001525	-0.00027	-0.00014	0.037815
42383	0.003285	0.00167	-0.00015	-0.00014	0.03773
42455	0.003278	0.001592	-0.00019	-0.00024	0.037771
42527	0.003216	0.001578	-0.00024	-0.00024	0.037799
42599	0.003217	0.001696	-0.00025	-9.5E-05	0.037727
42671	0.003273	0.001599	-0.00026	-0.0001	0.037767
42743	0.003274	0.001617	-0.00021	-0.00013	0.03782
42815	0.003345	0.001665	-0.00026	-3.5E-06	0.037748
42887	0.00328	0.001475	-0.0002	-0.00018	0.037881
42959	0.003236	0.001631	-0.00023	-0.00016	0.037779
43031	0.003295	0.001614	-0.0002	-0.00014	0.037733
43103	0.00324	0.001548	-0.00021	-0.00025	0.037828
43175	0.003254	0.001596	-0.00019	-0.00012	0.03775

4. REFERENCES

1. M. Camarasa, S. Velazquez, A. San-Felix, M-J. Perez-Perez and F. Gago. *Antiviral Res.* **2006,** *71,* 260-267.

2. International Committee on Taxonomy of Viruses. "61.0.6. Lentivirus". National Institutes of Health. http://www.ictvdb.org/MCM8.pdf (accessed February 28, 2011).

3. Z. Chen, P. Telfer, A. Gettie, P. Reed, L. Zhang, D.D. Ho and P.A. Marx. *J. Virol.* **1996,** *70,* 3617-3627.

4. F. Gao, E. Bailes, D.L. Robertson, Y. Chen, C.M. Rodenburg, S.F. Michael, L.B. Cummins, L.O. Arthur, M. Peeters, G.M. Shaw, P.M. Sharp and B.H. Hahn. *Nature* **1999,** *397,* 436-441.

5. V.M. Hirsch, R.A. Olmsted, M. Murphey-Corb, R.H. Purcell and P.R. Johnson. *Nature* **1989,** *339,* 389-392.

6. T. Huet, R. Cheynier, A. Meyerhans, G. Roelants and S. Wain-Hobson. *Nature* **1990,** *345,* 356-359.

7. K.A. Sepkowitz. *N. Engl. J. Med.* **2001,** *344,* 1764-1772.

8. R.A. Weiss. *Science* **1993,** *260,* 1273-1279.

9. UNAIDS. UNAIDS report on the global AIDS epidemic, 2010. http://www.unaids.org/globalreport/Global_report.htm.

10. J. Hemelaar, E. Gouws, P.D. Ghys and S. Osmanov. *AIDS* **2006,** *20,* W13-23.

11. H.M. Jackson. Foundation for the Advancement of Military Medicine. 2008. http://www.sciencedaily.com /releases/2008/05/080521133456.htm. (accessed Feb 28, 2011).

12. D.L. Robertson, J.P. Anderson, J.A. Badac. J.K. Carr, B. Foley, R.K. Funkhouser, F.Gao, B.H. Hahn, M.L. Kalish, C. Kuiken, G.H. Learn, T.Leitner, F. McCutchan, S. Osmanov, M. Peeters, D. Pieniazek, M. Salminen, P.M. Sharp, S.Wolinsky and B. Korber. *Science* **2000,** *288,* 55-56.

13. K. Chalmet, D. Staelens, S. Blot, S. Dinakis, J. Pelgrom, J. Plum, D. Vogelaers, L. Vandekerckhove and C. Verhofstede. *BMC Infect. dis.* **2010,** *10,* 1-9.

14. D.S. Burke. *Emerg. Infect. Dis.* **1997,** *3,* 253-259.

15. F. Gao, D.L. Robertson, C.D. Carruthers, Y. Li, E. Bailes, L.G. Kostrikis, M.O. Salminen, F. Bibollet-Ruche, M. Peeters, D.D. Ho, G.M.Shaw, P.M. Sharp and B.H. Hahn. *J. Virol.* **1998,** *72,* 10234-10241.

16. H.B. Bernstein, S.P. Tucker, S.R. Kar, S.A. McPherson, D.T. McPherson, J.W. Dubay, J. Lebowitz, R.W. Compans, and E. Hunter. *J. Virol.* **1995,** *69,* 2745-2750.

17. W.C. Greene. *Scientific American* **1993,** *269*, 98-105.

18. D.I. Watkins. *Top. HIV Med.* **2008,** *16,* 7-8.

19. Avert website. http://www.avert.org/hiv-virus.htm (accessed March 01, 2011).

20. R. Gallo, F. Wong-Staal, L. Montagnier, W.A. Haseltine and M. Yoshida. *Nature* **1988,** *333,* 504-505.

21. M. Ottman, C. Gabus and J.L. Darlix. *J. Virol.* **1995,** *69,* 1778-1784.

22. R. Welker, H. Hohenberg, U. Tessmer, C. Huckhagel and H. Kräusslich. *J.Virol.* **2000,** *74,* 1168-1169.

23. D. Chan and P. Kim. *Cell* **1998,** *93,* 681- 684.

24. R. Wyatt and J. Sodroski. *Science* **1998,** *280,* 1884-1888.

25. S. Nisole and A. Saib. *Retrovirology* **2004,** *1,* 9.

26. M.H. Nielsen, F.S. Pedersen and J. Kjems. *Retrovirology* **2005,** *2,* 10-29.

27. NIAID. http://www.niaid.nih.gov/topics/HIVAIDS/Understanding/Biology/pages/hivreplicationcycle.aspx (accessed March 02, 2011).

28. P. Luciw. Fundamental Virology. Fields, B. N., Knipe, D. M., Howley, P. M., Eds.; Lippincott-Raven: New York, 1996; pp 845-916.

29. S.G. Sarafianos, K. Das, C. Tantillo, A.D. Clark, Jr., J. Ding, J.M. Whitcomb, P.L. Boyer, S.H. Hughes and E. Arnold. *EMBO J.* **2001,** *20,* 1449-1461.

30. S.G. Sarafianos, B. Marchand, K. Das, D.M. Himmel, M.A. Parniak, S.H. Hughes and E. Arnold. *J. Mol. Biol.* **2009,** *385,* 693-713.

31. L.A. Kohlstaedt, J. Wang, J.M. Friedman, P.A. Rice and T.A. Steitz. *Science* **1992,** *256,* 1783-1790.

32. A. Jacobo-Molina, J. Ding, R.G. Nanni, A.D. Clark, Jr., X. Lu, C. Tantillo, R.L. Williams, G. Kamer, A.L. Ferris, and P. Clark. *Proc. Natl. Acad. Sci. USA* **1993,** *90,* 6320-6324.

33. Y. Xiong and T.H. Eickbush. *EMBO J.* **1990,** *9,* 3353-3362.

34. J. Colicelli and S.P. Goff. *J. Mol. Biol.* **1988,** *199,* 47-59.

35. P.O. Brown. Retroviruses. Coffin, J. M., Hughes, S. H., Varmus, H. E., Eds.; Cold Spring Harbor Lab. Press, Plainview, NY, 1997; pp 161-203.

36. D. Esposito and R. Craigie . *Adv. Virus Res.* **1999,** *52,* 319-333.

37. S. Maignan, J.P. Guilloteau, Q. Zhou-Liu, C. Clement-Mella and V. Mikol. *J. Mol. Biol.* **1998,** *282,* 359-368.

38. Y. Goldgur, F. Dyda, A.B. Hickman, T.M. Jenkins, R. Craigie and D.R. Davies. *Proc. Natl. Acad. Sci. USA* **1998,** *95,* 9150-9154.

39. E. Deprez, P. Tauc, H. Leh, J-F. Mouscadet, C. Auclair and J-C. Brochon. *Biochemistry* **2000,** *39,* 9275-9284.

40. A. Faure, C. Calmels, C. Desjobert, M. Castroviejo, A. Caumont-Sarcos, L. Tarrago-Litvak, S. Litvak, and V. Parissi. *Nucleic Acids Res.* **2005,** *33,* 977-986.

41. F. Dyda, A.B. Hickman, T.M. Jenkins, A. Engelman, R. Craigie and D.R. Davies. *Science* **1994,** *266,* 1981-1986.

42. T.M. Fletcher III, M.A. Soares, S. McPhearson, H. Hui, M. Wiskerchen, M.A. Muesing, G.M. Shaw, A.D. Leavitt, J.D. Boeke and B.H. Hahn. *EMBO J.* **1997,** *16,* 5123-5138.

43. J. Kulkosky, K.S. Jones, R.A. Katz, J.P. Mack and A.M. Skalka. *Mol. Cell. Biol.* **1992,** *12,* 2331-2338.

44. F.D. Bushman and R. Craigie. *Proc. Natl. Acad. Sci. USA* **1991,** *88,* 1339-1343.

45. C. Vink, D.C. van Gent, Y. Elgersma and R.H. Plasterk. *J. Virol.* **1991,** *65,* 4636-4644.

46. C. Vink, M. Groenink, Y. Elgersma, R.A. Fouchier, M. Tersmette and R.H. Plasterk. *J. Virol.* **1990,** *64,* 5626-5627.

47. Y. Pommier and N. Neamati. *Adv. Virus Res.* **1999,** *52,* 427-458.

48. M.A. Muesing, D.H. Smith, C.D. Cabradilla, C.V. Benton, L.A. Lasky and D.J. Capon. *Nature* **1985,** *313,* 450-458.

49. R. Craigie. *J. Biol. Chem* **2001,** *276*, 23213-23216.

50. N.E. Kohl, E.A. Emini, W.A. Schleif, L.J. Davis, J.C. Heimbach, R.A. Dixon, E.M. Scolnick and I.S. Sigal. *Proc. Natl. Acad. Sci. USA* **1988,** *85,* 4686-4690.

51. S. Oroszlan and R.B. Luftig. *Curr. Top. Microbiol. Immunol.* **1990,** *157,* 153-185.

52. J. Schneider and S.B. Kent . *Cell* **1988,** *54,* 363-368.

53. T.D. Meek, B.D. Dayton, B.W. Metcalf, G.B. Dreyer, J.E. Strickler, J.G. Gorniak, M. Rosenberg, M.L. Moore, V.W. Magaard and C. Debouck. *Proc. Natl. Acad. Sci., U.S.A.* **1989,** *86,* 1841-1845.

54. R. Ishima, R. Ghirlando, J. Tozser, A.M. Gronenborn, D.A. Torchia and J.M. Louis. *J. Biol. Chem.* **2001,** *276,* 49110-49116.

55. V. Hornak, A. Okur, R.C. Rizzo and C. Simmerling. *J. Am. Chem. Soc.* **2006,** *128,* 2812-2813.

56. J.P. Vacca and J.H. Condra. *Drug Des. Discov.* **1997,** *2,* 261-262.

57. A. Friedler, I. Blumenzweig, L. Baraz, M. Steinitz, M. Kotler and C. Gilon. *J. Mol. Biol.* **1999,** *287,* 93-101.

58. M. Prabu-Jeyabalan, E. Nalivaika and C.A. Schiffer. *Structure* **2002,** *10,* 369-381.

59. I. Schechter and A. Berger. *Biochem. Biophys. Res. Commun.* **1967,** *27,* 157-162.

60. A. Wlodawer and J. Vondrasek. *Annu. Rev. Biophys. Biomol. Struct.* **1998,** *27,* 249-284.

61. E. De Clercq. Virus replication: target functions and events for virus-specific inhibitors. In *Antiviral Agents and Human Viral Diseases;* Galasso, G. J., Whitley, R. J., Merigan, T. C., Eds.; Philadelphia: Lippincott-Raven, 1997; pp 1-44.

62. E. De Clercq. *Pure & Appl. Chem.* **1998,** *70*, 567-577.

63. E. De Clercq. *Rev. Med. Virol.* **1996,** *6,* 97-117.

64. H. van de Waterbeemd, R.E. Carter, G. Grassy, H. Kubinyi, Y.C. Martin,M.S. Tute and P. Willett. In *Glossary of Terms Used in Computational Drug Design (IUPAC Recommendations 1997);* Academic P: San Diego, 1998.

65. N. Prakash and P. Devangi. *J. Antivir. Antiretrovir.* **2010,** *2,* 63-68.

66. K.H. Bleicher, H-J. Böhm, K. Muller and A.I. Alanine. *Nat. Rev. Drug. Discov.* **2003,** *2,* 369-378.

67. W.G. Richards. *Pure & Appl. Chem.* **1994,** *66,* 1589-1596.

68. T. Lengauer and M. Rarey. *Curr. Opin. Struct. Biol.* **1996,** *6,* 402-406.

69. D.B. Kitchen, H. Decornez, J.R. Furr and J. Bajorath. *Nat. Rev. Drug Discov.* **2004,** *3,* 935-949.

70. G. Schneider and U. Fechner. *Nat. Rev. Drug Discov.* **2005,** *4,* 649-663.

71. A. Oda, K. Tsuchida, T. Takakura, N. Yamaotsu and S. Hirono. *J. Chem. Inf. Model* **2006,** *46,* 380-391.

72. Z. Deng, C. Chuaqui and J. Singh. *J. Med. Chem.* **2004,** *47,* 337-344.

73. O. Nicolotti, T.F. Miscioscia, A. Carotti, F. Leonetti and A. Carotti. *J. Chem. Inf. Model.* **2008,** *48,* 1211-1226.

74. L. Peltason and J. Bajorath. *Chem. Biol.* **2007,** *14,* 489-497.

75. T.I. Oprea and H. Matter. *Curr. Opin. Chem. Biol.* **2004,** *8,* 349-358.

76. R.S. Goody, B. Müller and T. Restle. *FEBS Lett.* **1991,** *291,* 1-5.

77. C. Loveday. *JAIDS* **2001,** *26,* S10-S24.

78. P.A.Furman, J.A. Fyfe, M.H. St Clair, K. Weinhold, J.L. Rideout, G.A. Freeman, S.N. Lehrmann, D.P. Bolognesi, S. Broder, H. Mitsuya and D.W. Barry. *Proc. Natl. Acad. Sci. USA* **1986,** *83,* 8333-8337.

79. I. Lefebvre, C. Perigaud, A. Pompon, A-M. Aubertin, J-L. Girardet, A. Kirn, G. Gosselin and J-L. Imbach. *J. Med. Chem.* **1995,** *38,* 3941-3950.

80. H.B. Fung, E.A. Stone and F.J. Piacenti. *Clin Ther.* **2002,** *24*, 1515-1548.

81. R. Vig, C. Mao, T.K. Venkatachalam, L. Tuel-Ahlgren, E.A. Sudbeck and F.M. Uckan. *Bioorg. Med. Chem.* **1998,** *6,* 1789-1797.

82. E. De Clercq. *Med. Res. Rev.* **1996,** *16,* 125-157.

83. E. De Clercq. *Annu. Rev. Pharmacol. Toxicol.* **2011,** *51,* 1-24.

84. R. Pauwels, K. Andries, J. Desmyter, D. Schols, M.J. Kukla, H.J. Breslin, A. Raeymaeckers, J. Van Gelder, R. Woestenborghs, J. Heykants, K. Schellekens, M.A.C. Janssen, E. De Clercq and P.A.J. Janssen. *Nature* **1990,** *343,* 470-474.

85. B.L. De Corte. *J. Med. Chem.* **2005,** *48,* 1689-1696.

86. R. Pauwels, K. Andries, Z. Debyser, P. Van Daele, D. Schols, P. Stoffels, K. De Vreese, R. Woestenborghs, A.M. Vandamme, C. G. M. Janssen, J. Anne, G. Cauwenbergh, J. Desmyter, J. Heykants, M.A.C. Janssen, E. De Clercq and P.A.J. Janssen. *Proc. Natl. Acad. Sci. U.S.A.* **1993,** *90,* 1711-1715.

87. D.W. Ludovici, M.J. Kukla, P.G. Grous, S. Krishnan, K. Andries, M.P. de Bethune, H. Azijn, R. Pauwels, E. De Clercq, E. Arnold and P.A.J. Janssen. *Bioorg. Med. Chem. Lett.* **2001,** *11,* 2225-2228.

88. P.A.J. Janssen, P.J. Lewi, E. Arnold, F. Daeyaert, M. de Jonge, J. Heeres, L. Koymans, M. Vinkers, J. Guillemont, E. Pasquier, M. Kukla, D. Ludovici, K. Andries, M.-P. de Bethune, R. Pauwels, K. Das, A.D. Clark, Jr., Y.V. Frenkel, S.H. Hughes, B. Medaer, F. de Knaep, H. Bohets, F. de Clerck, A. Lampo, P. Williams and P. Stoffels. *J. Med. Chem.* **2005,** *48,* 1901-1909.

89. D. da Silva, L. Van Wesenbeeck, D. Breilh, S. Reigadas, G. Anies, K. Van Baelen, P. Morlat, D. Neau, M. Dupon, L. Wittkop, H. Fleury and B. Masquelier. *J Antimicrob. Chemother.* **2010,** *65,* 1262-1269.

90. D.J. Hazuda, P. Felock, M. Witmer, A. Wolfe, K. Stillmock, J.A. Grobler, A. Espeseth, L. Gabryelski, W. Schleif, C. Blau and M.D. Miller. *Science* **2000,** *287,* 646-650.

91. E. Serrao, S. Odde, K. Ramkumar and N. Neamati. *Retrovirology* **2009,** *6,* 25.

92. M.J. Rosemond, L. St John-Williams, T. Yamaguchi, T. Fujishita and J.S. Walsh. *Chem. Biol. Interact.* **2004,** *147*, 129-139.

93. L. Zhuang, J.S. Wai, M.W. Embrey, T.E. Fisher, M.S. Egbertson, L.S. Payne, J.P. Guare Jr., J.P. Vacca, D.J. Hazuda, P.J. Felock, A.L. Wolfe, K.A. Stillmock, W.V. Witmer, G. Moyer, W.A. Schleif, L.J. Gabryelski, Y.M. Leonard, J.J. Lynch Jr., S.R. Michelson and S.D. Young. *J. Med. Chem.* **2003,** *46,* 453-456.

94. V. Summa, A. Petrocchi, V.G. Matassa, C. Gardelli, E. Muraglia, M. Rowley, O.G. Paz, R. Laufer, E. Monteagudo and P. Pace. *J. Med. Chem.* **2006,** *49,* 6646-6649.

95. M. Iyer and A.J. Hopfinger. *J. Chem. Inf. Model.* **2007,** *47,* 1945-1960.

96. A. Brik and C.H. Wong. *Org. Bio. Chem.* **2003,** *1,* 5-14.

97. N.A. Roberts, J.A. Martin, D. Kinchington, A.V. Broadhurst, J.C. Craig, I.B. Duncan, S.A. Galpin, B.K. Handa, J. Kay, A. Krohn, R.W. Lambert, J.H. Merreit, J.S. Mills, K.E.B. Parkes, S. Redshaw, A.J. Ritchie, D.L. Taylor, G.J. Thomas and P.J. Machin. *Science* **1990,** *248,* 358-361.

98. S.H. Reich, M. Melnick, J.F. Davies, K. Appelt, K.K. Lewis, M.A. Fuhry, M.P. Pino, A.J. Trippe, D. Nguyen, H. Dawson, B. Wu, L. Musick, M. Kosa, D. Kahil, S. Webber, D.K. Gehlhaar, D. Andrada and B. Shetty. *Proc. Natl. Acad. Sci. USA* **1995,** *92,* 3298-3302.

99. S. Thaisrivongs, P.K. Tomich, K.D. Watenpaugh, K-T. Chong, J.W. Howe, C-P. Yang, J.W. Strohbach, S.R. Turner, J.P. McGrath, M.J. Bohanon, J.C. Lynn, A.M. Mulichak, P.A. Spinelli, R.R. Hinshaw, P.J. Pagano, J.B. Moon, M.J. Ruwart, K.F. Wilkinson, B.D. Rush, G.L. Zipp, R.J. Dalga, F.J. Schwende, G.M. Howard, G.E. Padbury, L.N. Toth, Z. Zhao, K.A. Koeplinger, T.J. Kakuk, S.L. Cole, R.M. Zaya, R.C. Piper and P. Jeffrey. *J. Med. Chem.* **1994,** *37,* 3200-3204.

100. R.A. Chrusciel and J.W. Strohbach. *Curr. Top. Med. Chem.* **2004,** *4,* 1097-1114.

101. P.Y.S. Lam, P.J. Jadhav, C.J. Eyermann, C.N. Hodge, Y. Ru, L.T. Bacheler, J.L. Meek, M.J. Otto, M.M. Rayner, Y.N. Wong, C-H.Chang, P.C. Weber, D.A. Jackson, T.R. Sharpe and S. Erickson-Viitanen. *Science* **1994,** *263,* 380-384.

102. Y.N. Wong, D.L. Burcham, P.L. Saxton, S. Erickson-Viitanen, M.F. Grubb, C.Y. Quon and S-M. Huang. *Biopharm. Drug Dispos.* **1994,** *15,* 535-544.

103. W. Han, J.C. Pelletier and C.N. Hodge. *Bioorg. Med. Chem. Lett.* **1998,** *8,* 3615-3620.

104. A. Hilgeroth, M. Wiese and A. Billich. *J. Med. Chem.* **1999,** *42,* 4729-4732.

105. S. Kurihara, T. Tsumuraya and I. Fujii. *Bioorg. Med. Chem. Lett.* **1999,** *9,* 1179-1184.

106. P.V. Murphy, J.L. O'Brien, L.J. Gorey-Feret and A.B. Smith, III. *Bioorg. Med. Chem. Lett.* **2002,** *12,* 1763-1766.

107. M. Chesney. *AIDS Patient Care and STDs.* **2003,** *17,* 169-177.

108. Z. Wang, E.M. Bennett, D.J. Wilson, C. Salomon and R. Vince. *J. Med. Chem.* **2007,** *50,* 3416- 3419.

109. R. Morphy and Z. Rankovic. *J. Med. Chem.* **2005,** *48,* 6523-6543.

110. D. Munoz-Torrero and P. Camps. *Curr. Med. Chem.* **2006,** *13,* 399-422.

111. M. Yamamoto, S. Ikeda, H. Kondo and S. Inoue. *Bioorg. Med. Chem. Lett.* **2002,** *12,* 375-378.

112. J. Didierjean, C. Isel, F. Querre, J-F. Mouscadet, A-M. Aubertin, J-Y. Valnot, S.R. Piettre and R. Marquet. *Antimicrob. Agents Chemother.* **2005,** *49,* 4884-4894.

113. W. Yang, W.A. Hendrickson, R.J. Crouch and Y. Satow. *Science* **1990,** *249,* 1398-1405.

114. J.F. Davies, II, Z. Hostomska, Z. Hostomsky, S.R. Jordan and D.A. Matthews. *Science* **1991,** *252,* 88-95.

115. G. Adrian, S. Mignonac and F. Lecoutteux. WO2000003999 2000.

116. Z. Wang and R. Vince. *Bioorg. Med. Chem.* **2008,** *16,* 3587-3595.

117. Y. Murakami, M. Tani, T. Ariyasu, C. Nishiyama, T. Watanabe and Y. Yokoyama. *Heterocycles* **1988,** *27,* 1855-1860.

118. Z. Wang and R. Vince. *Bioorg. Med. Chem. Lett.* **2008,** *18,* 1293-1296.

119. J. Tang, K. Maddali, C.D. Dreis, Y.Y. Sham, R. Vince, Y. Pommier and Z. Wang. *Bioorg. Med. Chem. Lett.* **2011,** *21,* 2400-2402.

120. J. Tang, K. Maddali, C.D. Dreis, Y.Y. Sham, R. Vince, Y. Pommier and Z. Wang. *ACS Med. Chem. Lett.* **2011,** *2,* 63-67.

121. Z. Wang, J. Tang, C.E. Salomon, C.D. Dreis and R. Vince. *Bioorg. Med. Chem.* **2010,** *18,* 4202-4211.

122. S. Budihas, I. Gorshkova, S. Gaidamakov, A. Wamiru, M. Bona, M. Parniak, R. Crouch, J. McMahon, J. Beutler and S. Le Grice. *Nucleic Acids Res.* **2005,** *33,* 1249-1256.

123. E.A. Semenova, A.A. Johnson, C. Marchand, D.A. Davis, R. Yarchoan and Y. Pommier. *Mol. Pharmacol.* **2006,** *69,* 1454-1460.

124. C. Marchand, J.A. Beutler, A. Wamiru, S. Budihas, U. Mollmann, L. Heinisch, J.W. Mellors, S.F. Le Grice and Y. Pommier. *Antimicrob. Agents Chemother.* **2008,** *52,* 361-364.

125. M. Billamboz, F. Bailly, M.L. Barreca, L. De Luca, J-F. Mouscadet, C. Calmels, M-L. Andreola, M. Witvrouw, F. Christ, Z. Debyser and P. Cotelle. *J. Med. Chem.* **2008,** *51,* 7717-7730.

126. D. Egan, R. O'Kennedy, E. Moran, D. Cox, E. Prosser and R.D. Thornes. *Drug Metab. Rev.* **1990,** *22,* 503-529.

127. A. Kar. In *Pharmacognosy and Pharmacobiotechnology;* New Age Intl. (P) Ltd.: New Delhi, 2003; pp 239-240.

128. A. Tosun and P. Tomek. Application of HPLC in Coumarin Analyses. In *High Performance Liquid Chromatography in Phytochemical Analysis;* M. Waksmundzka-Hajnos and J. Sherma., Ed.; CRC Press, 2011; pp 513-534.

129. A. Lacy and R. O'Kennedy. *Curr. Pharm. Des.* **2004,** *10,* 3797-3811.

130. S.R. Trenor, A.R. Shultz, B.J. Love and T.E. Long. *Chem. Rev.* **2004,** *104,* 3059-3077.

131. D.G. Illingworth. *Br. Med. J.* **1951,** *2*, 646-648.

132. Y. Fall, C. Teran, M. Taijeira, L. Santana and E. Uriarte. *Synthesis* **2000,** 643-645.

133. A. Maucher and E. von Angerer. *J. Cancer Res. Clin. Oncol.* **1994,** *120,* 502-504.

134. A.K. Rao, M.S. Raju and K.M. Raju. *J. Indian. Chem. Soc.* **1981,** *58,* 1021-1023.

135. G. Matthee, A.D. Wright and G.M. Konig. *Planta Med.* **1999,** *65,* 493-506.

136. Y. Takeuchi, L. Cosentino and K. Lee. *Bioorg. Med. Chem. Lett.* **1997,** *7,* 2573-2578.

137. W.H. Perkin. *J. Chem. Soc.* **1868,** *21,* 181-186.

138. H. von Pechmann and C. Duisberg. *Ber. Dtsch. Chem. Ges.* **1883,** *16,* 2119-2128.

139. E. Knoevenagel. *Chem. Ber.* **1894,** *27,* 2345-2346.

140. G.A. Kraus and J.O. Pezzanite. *J. Org. Chem.* **1979,** *44,* 2480-2482.

141. G. Wittig and W. Haag. *Chem. Ber.* **1955,** *88,* 1654-1666.

142. B.M. Trost and F.D. Toste. *J. Am. Chem. Soc.* **1996,** *118,* 6305-6306.

143. A.K. Chatterjee, F.D. Toste, S.D. Goldberg and R.H. Grubbs. *Pure Appl. Chem.* **2003,** *75,* 421-425.

144. J.R. Johnson. *Org. React.* **1942,** *1,* 210-265.

145. R. Bakhchinian, F. Terrier, S. Kirkiacharian, M. Resche-Rigon, F. Bouchoux, E. Cerede. *Il Farmaco* **2003,** *58,* 1201-1207.

146. A. Robertson, W.F. Sandrock and C.B. Hendry. *J. Chem. Soc.* **1931,** 2426-2432.

147. L.L. Woods and J. Sapp. *J. Org. Chem.* **1962,** *27,* 3703-3705.

148. D.S. Bose, A.P. Rudradas and M.H. Babu. *Tetrahedron Lett.* **2002,** *43,* 9195-9197.

149. S.M. Sethna, N.M. Shah and R.C. Shah. *J. Chem. Soc.* **1938,** 228-232.

150. P. Sun and Z. Hu. *Synth. Commun.* **2005,** *35,* 1875-1880.

151. A.J. Hoefnagel, E.A. Gunnewegh, R.S. Downing and H. van Bekkum. *J. Chem. Soc., Chem. Commun.* **1995,** *2,* 225-226.

152. V. Singh, S. Kaur, V. Sapehiyia, J. Singh and G.L. Kad. *Catal. Commun.* **2005,** *6,* 57-60.

153. A. de la Hoz, A. Moreno and E. Vazquez. *Synlett* **1999,** *5,* 608-610..

154. E.V.O. John and S.S. Israelstam. *J. Org. Chem.* **1961,** *26,* 240-242.

155. V. Singh, J. Singh, K.P. Kaur and G.L. Kad. *J. Chem. Res. (S)* **1996,** *1,* 58-59.

156. J.J. Li. *Name Reactions;* Springer: Berlin Heidelberg, 2006; pp 452-453.

157. J-P. Li, J-K. Qiu, H-J. Li and G-S. Zhang. *J. Chin. Chem. Soc.* **2011,** *58,* 268-271.

158. A.C. Cope. *J. Am. Chem. Soc.* **1937,** *59,* 2327-2330.

159. G. Jones. *Organic Synthesis;* John Wiley & Sons: New York, 1967; Vol. 15, pp 204-599.

160. A. Shaabani, R. Ghadari, A. Rahmati and A.H. Rezayan. *J. Iran. Chem. Soc.* **2009,** *6,* 710-714.

161. H.N. Harishkumar, K.M. Mahadevan, H.C. Kiran Kumar, N.D. Satyanarayan. *Org. Commun.* **2011,** *4,* 26-32.

162. G. Speranza, A.D. Meo, S. Zanzola, G. Fontanna and P. Manitto. *Synthesis* **1997,** *8,* 931-936.

163. I. Yavari, R. Hekmatt-Shoar and A. Zonouzi. *Tetrahedron Lett.* **1998,** *39,* 2391-2392.

164. J. Loffler and R. Schobert. *J. Chem. Soc., Perkin Trans.1* **1996,** 2799-2802.

165. R.S. Mali, V.J. Yadav and R.N. Zaware. *Indian J. Chem.* **1982,** *21B,* 759-760.

166. T. Harayama. *J. Pharm. Soc. Japan* **2006,** *126*, 543-564.

167. D. Astruc. *New J. Chem.* **2005,** *29,* 42-56.

168. J. Tijani, R. Suleiman and B. El Ali. *Appl. Organometal. Chem.* **2008,** *22,* 553-559.

169. N. Nenadis, L. Wang, M. Tsimidou and H.Y. Zhang. *J. Agric. Food Chem.* **2004,** *52,* 4669-4674.

170. C.K. Sharma, G.S. Chauhan and S.S. Kanwar. *J. Appl. Pol. Sci.* **2011,** *121,* 2674-2679.

171. G-S. Lee, A. Widjaja and Y-H. Ju. *Biotechnol. Lett.* **2006,** *28,* 581-585.

172. E.F. Healy, J. Sanders, P.J. King and W.E. Robinson Jr. *J. Mol. Graph. Model.* **2009,** *27,* 584-589.

173. L. Claisen. *Ber.* **1890,** *23,* 976-978.

174. C.S. Marvel and W.B. King. *Org. Synth. Coll.* **1941,** *1,* 252–254.

175. B-M. Lue, S. Karboune, F.K. Yeboah and S. Kermasha. *J. Chem. Technol. Biotechnol.* **2005,** *80,* 462-468.

176. R.F. Heck. *J. Amer. Chem. Soc.* **1969,** *91,* 6707-6714.

177. T.J. Speed, J.P. McIntyre and D.M. Thamattoor. *J. Chem. Educ.* **2004,** *81,* 1355-1356.

178. W.S. Wadsworth Jr. and W.D. Emmons. *J. Am. Chem. Soc.* **1961,** *83,* 1733-1738.

179. H.B. Patwardhan. *Indian J. Chem.* **1974,** *12,* 891-892.

180. E. Wenkert, N.F. Golob, R.P. Hatch and D. Wenkert. *Helv. Chim. Acta.* **1977,** *60,* 1-8.

181. K. Priya and A. Chadha. *Enzyme Microb. Technol.* **2003,** *32,* 485-490.

182. R.F. Heck and J.P. Nolley Jr. *J. Org. Chem.* **1972,** *37,* 2320-2322.

183. D. Zim and S.L. Buchwald. *Org. Lett.* **2003,** *5,* 2413-2415.

184. W. Cabri, I. Candiani, S. DeBernardinis, F. Francalanci, S. Penco and R. Santi. *J. Org. Chem.* **1991,** *56,* 5796-5800.

185. A. Ashimori, B. Bachand, M.A. Calter, S.P. Govek, L.E. Overman and D.J. Poon. *J. Am. Chem. Soc.* **1998,** *120,* 6488-6499.

186. G.V. Ambulgekar, B.M. Bhanage and S.D. Samant. *Tetrahedron lett.* **2005,** *46,* 2483-2485.

187. W.Cabri and I. Candiani. *Acc. Chem. Res.* **1995,** *28,* 2-7.

188. Z. Zhang, Z. Zha, C. Gan, C. Pan, Y. Zhou, Z. Wang and M. Zhou. *J. Org. Chem.* **2006,** *71,* 4339-4342.

189. G. Palmisano, W. Bonrath, L. Boffa, D. Garella, A. Barge and G. Cravotto. *Adv. Synth. Catal.* **2007,** *349,* 2338-2344.

190. D. Basavaiah, K.V. Rao and R.J. Reddy. *Chem. Soc. Rev.* **2007,** *36,* 1581-1588.

191. V. Singh and S. Batra. *Tetrahedron* **2008,** *64,* 4511-4574.

192. P.T. Kaye. *S. Afr. J. Sci.* **2004,** *100,* 545-548.

193. K. Morita, Z. Suzuki and H. Hirose. *Bull. Chem. Soc. Jpn.* **1968,** *41,* 2815.

194. S.E. Drewes and G.H.P. Roos. *Tetrahedron* **1988,** *44,* 4653-4670.

195. J. Auge, N. Lubin and A. Lubineau. *Tetrahedron Lett.* **1994,** *35,* 7947-7948.

196. D. Roy and R.B. Sunoj. *Org. Lett.* **2007,** *9,* 4873-4876.

197. D. Basavaiah, B.S. Reddy and S.S. Badsara. *Chem. Rev.* **2010,** *110,* 5447-5674.

198. M.L. Bode and P.T. Kaye. *J. Chem Soc., Perkin Trans. 1* **1990,** 2612-2613.

199. O.B. Familoni, P.T. Kaye and P.J. Klaas. *Chem. Commun.* **1998,** 2563-2564.

200. X.W. Nocanda and P.T. Kaye. *Synthesis* **2001,** 2389-2392.

201. P.T. Kaye and X.W. Nocanda. *J. Chem. Soc., Perkin.Trans. 1* **2002,** 1318-1323.

202. P.T. Kaye and X.W. Nocanda . *J. Chem. Soc., Perkin Trans 1* **2000,** 1331-1332.

203. M.L. Bode and P.T. Kaye. *Tetrahedron Lett.* **1991,** *32,* 5611-5614.

204. M.L. Bode and P.T. Kaye. *J. Chem. Soc. Perkin Trans. 1* **1993,** 1809-1813.

205. M.L. Bode, R.B. English and P.T. Kaye. *S. Afr. J. Chem.* **1992,** *45,* 25-27.

206. P.T. Kaye and R.S. Robinson. *Synth. Commun.* **1996,** *26,* 2085-2097.

207. J. Bacsa, P.T. Kaye and R.S. Robinson. *S. Afr. J. Chem.* **1998,** *51,* 47-54.

208. P.T. Kaye and M.A. Musa. *Synthesis* **2002,** 2701-2706.

209. P.T. Kaye, M.A. Musa, X.W. Nocanda and R.S. Robinson. *Org. Biomol. Chem.* **2003,** *1,* 1133-1138.

210. P.T. Kaye, M.A. Musa and X.W. Nocanda. *Synthesis* **2003,** 531-534.

211. P.T. Kaye and M.A. Musa. *Synth. Commun.* **2004,** *34,* 3409-3417.

212. T.J. Rashamuse, M.A. Musa, R. Klein and P.T. Kaye. *J. Chem. Res.* **2009,** 302-305.

213. T.J. Rashamuse, R. Klein and P.T. Kaye. *Synth. Commun.* **2010,** *40,* 3683-3690.

214. Y-C. Lee. MSc Thesis; Rhodes University, 2009.

215. C.O. Kappe and D. Dallinger. *Mol. Divers.* **2009,** *13,* 71-193.

216. M.K. Kundu, S.B. Mukherjee, N. Balu, R. Padmakumar and S.V. Bhat. *Synlett.* **1994,** *6,* 444.

217. M.B. Gawande, S.S. Deshpande, J.R. Satam and R.V. Jayaram. *Catal. Commun.* **2007,** *8,* 576-582.

218. T.O. Olomola, R. Klein, K.A. Lobb, Y. Sayed and P.T. Kaye. *Tetrahedron Lett.* **2010,** *51,* 6325-6328.

219. T.D.W. Claridge. In *High-Resolution NMR Techniques in Organic Chemistry,* 1st ed.; Elsevier: Oxford, 1999; pp 141-142.

220. H.C. Kolb, M.G. Finn and K.B. Sharpless. *Angew. Chem., Int. Ed.* **2001,** *40,* 2004-2021.

221. J.E. Moses and A.D. Moorhouse. *Chem. Soc. Rev.* **2007,** *36,* 1249-1262.

222. H.C. Kolb and K.B. Sharpless. *Drug Discov. Today* **2003,** *8,* 1128-1137.

223. R. Huisgen. *Proc. Chem. Soc.* **1961,** 357-369.

224. F. Himo, T. Lovell, R. Hilgraf, V.V. Rostovtsev, L. Noodleman, K.B. Sharpless and V.V. Fokin. *J. Am. Chem. Soc.* **2005,** *127,* 210-216.

225. L. Zhang, X. Chen, P. Xue, H.H.Y. Sun, I.D. Williams, K.B. Sharpless, V.V. Fokin and G. Jia. *J. Am. Chem. Soc.* **2005,** *127,* 15998-15999.

226. H. Sai, T. Ogikub and H. Ohmizu. *Tetrahedron* **2007,** *63,* 10345-10353.

227. B. Truscott. Honours Project; Rhodes University, 2007.

228. K.C. Idahosa, Y-C. Lee, D. Nyoni, P.T. Kaye and M.R. Caira. *Tetrahedron Lett.* **2011,** *52,* 2972-2976.

229. Gaussian 03, Revision E.01, M.J. Frisch, G.W. Trucks, H.B. Schlegel, G.E. Scuseria, M.A. Robb, J.R. Cheeseman, J.A. Montgomery, Jr., T. Vreven, K.N. Kudin, J.C. Burant, J.M. Millam, S.S. Iyengar, J. Tomasi, V. Barone, B. Mennucci, M. Cossi, G. Scalmani, N. Rega, G.A. Petersson, H. Nakasuji, M. Hada, M. Ehara, K. Toyota, R. Fukuda, J. Hasegawa, M. Ishida, T. Nakajima, Y. Honda, O. Kitao, H. Nakai, M. Klene, X. Li, J.E. Knox, H.P. Hratchian, J.B. Cross, C. Adamo, J. Jaramillo, R. Gomperts, R.E. Stratmann, O. Yazyev, A.J. Austin, R. Cammi, C. Pomelli, J.W. Ochterski, P.Y. Ayala, K. Morokuma, G.A. Voth, P. Salvador, J.J. Dannenberg, V.G. Zakrzewski, S. Dapprich, A.D. Daniels, M.C. Strain, O. Farkas, D.K. Malick, A.D. Rabuck, K. Raghavachari, J.B. Foresman, J.V. Ortiz, Q. Cui, A. G. Baboul, S. Clifford, J. Cioslowski, B.B. Stefanov, G. Liu, A. Liashenko, P.Piskorz, I.

Komaromi, D.J. Fox, T. Keith, M.A. Al-Laham, C.Y. Peng, A. Nanayakkara, M. Challacombe, P.M.W. Gill, B. Johnson, W. Chen, M.W. Wong, C. Gonzalez, J.A. Pople, Gaussian, Inc., Pittsburgh, PA, 2003.

230. S. Khene, K. Lobb, T. Nyokong. *Electrochimica Acta* **2010,** *56,* 706-716.

231. T.A. Halgren and W.N. Lipscomb. *Chem. Phys. Lett.* **1977,** *49,* 225-232.

232. G. Bartoli, M.C. Bellucci, M. Petrini, E. Marcantoni, L. Sambri and E. Torregiani. *Org. Lett.* **2000,** *2,* 1791-1793.

233. A. Shahrisa and Z. Ghasemi. *Chem. Heterocycl. Compd.* **2010,** *46,* 37-43.

234. P. Narender, U. Srinivas, M. Ravinder, B.A. Rao, C. Ramesh, K. Harakishore, B. Gangadasu, U.S.N. Murthy and V.J. Rao. *Bioorg. Med. Chem.* **2006,** *14,* 4600-4609.

235. H. Tanaka, M. Fukui, K. Haraguchi, M. Masaki and T. Miyasaka. *Tetrahedron Lett.* **1989,** *30,* 2567-2570.

236. D.H.R. Barton, S.D. Gero, B. Quiclet-Sire and M. Samadi. *Tetrahedron Lett.* **1989,** *30,* 4969-4972.

237. G.A. Freeman, J.L. Rideout, W.H. Miller and J.E. Reardon. *J. Med. Chem.* **1992,** *35,* 3192-3196.

238. Q. Xiao, Y. Ju and Y.F. Zhao. *Chin. Chem. Lett.* **2002,** *13,* 1057-1058.

239. B. Kaboudin and M.S. Balakrishna. *Synth. Commun.* **2001,** *31,* 2773-2776.

240. V. Thiel, T. Brinkhoff, J.S. Dickschat, S. Wickel, J. Grunenberg, I. Wagner-Dobler, M. Simon and S. Schulz. *Org. Biomol. Chem.* **2010,** *8,* 234-246.

241. P.T. Kaye, D.M. Molefe, A.T. Nchinda and L.V. Sabbagh. *J. Chem. Res.* **2004,** 303-306.

242. K. Kurosawa and H. Harada. *Bull. Chem. Soc. Jpn.* **1979,** *52,* 2386-2388.

243. T. Boehm, G. Schumann and H. Hansen. *Arch. Pharm.* **1933,** *271,* 490-513.

244. H.C. Schroeder and K.P. Link. *J. Am. Chem. Soc.* **1953,** *75,* 1886-1888.

245. K. Ito and K. Nakajima. *J. Heterocycl. Chem.* **1988,** *25,* 511-515.

246. T.O. Olomola, R. Klein and P.T. Kaye. *Synth. Commun.* **2012,** *42,* 251-257.

247. J.S. Yadav, E. Balanarsaiah, S. Raghavendra and M. Satyanarayana. *Tetrahedron Lett.* **2006,** *47,* 4921-4924.

248. N. Rose, MSc Thesis; Rhodes University, 2006.

249. J.S. Coates, Purification of tetrahydrofuran. US Patent 4257961, 1981.

250. C. Boisson, J.C. Berthet, M. Lance, M. Nierlich and M. Ephritikhine. *J. Chem. Soc., Chem. Commun.* **1996,** 2129-2130.

251. I.S. Akhrem, D.V. Avetisyan, S.V. Vitt and P.V. Petrovskii. *Mendeleev Commun.* **2005,** *15,* 185-187.

252. R.F. Moreira, E.Y. Tshuva and S.J. Lippard. *Inorg. Chem.* **2004,** *43,* 4427-4434.

253. P.T. Kaye and M.A. Musa. *Synth. Commun.* **2003,** *33,* 1755-1770.

254. G.H. Imanzadeh, A. Khalafi-Nezhad, A.Zare, A. Hasaninejad, A.R.M. Sare and A. Parhami. *Iran. Chem. Soc.* **2007,** *4,* 229-237.

255. J.K. MacLeod, B.R. Worth and R.J. Wells. *Aust. J. Chem.* **1978,** *31,* 1533-1544.

256. M.V. Veselovskaya, S.V. Shilin, M.M. Garaz and V.P. Khilya. *Chem. Nat. Compd.* **2003,** *39,* 177-181.

257. M.V. Veselovskaya, M.M. Garazd, V.I. Vinogradova and V.P Khilya. *Chem. Nat. Compd.* **2006,** *42,* 277-280.

258. M. Mayer and B. Meyer. *Angew. Chem. Int. Ed.* **1999,** *38,* 1784-1788.

259. B. Meyer and T. Peters. *Angew. Chem. Int. Ed.* **2003,** *42,* 864-890.

260. M. Mayer and B. Meyer. *J. Am. Chem. Soc.* **2001,** *123,* 6108-6117.

261. M. Mayer and T.L. James. *J. Am. Chem. Soc.* **2002,** *124,* 13376-13377.

262. C.A. David, T. Middleton, D. Montgomery, H.B. Lim, W. Kati, A. Molla, X. Xuei, U. Warrior, J.L. Kofron and D.J. Burns. *J. Biomol. Screen.* **2002,** *7,* 259-266.

263. B.Q. Wei, L.H. Weaver, A.M. Ferrari, B.W. Matthews and B.K. Shoichet. *J. Mol. Biol.* **2004,** *337,* 1161-1182.

264. H. Alonso, A.A. Bliznyuk and J.E. Gready. *Med. Res. Rev.* **2006,** *26,* 531-568.

265. D.J. Kempf, K.C. Marsh, J.F. Denissen, E. Mcdonald, S. Vasavanonda, C.A. Flentge, B.E. Green, L. Fino, C.H. Parks, X-P. Kong, N.E. Wideburg, A. Saldivar, L. Ruiz, W.M. Kati, H.L. Sham, T. Robins, K.D. Stewart, A. Hsu, J.J. Plattner, J.M. Leonard and D.W. Norbeck. *Proc. Natl. Acad. Sci. U.S.A.* **1995,** *92,* 2484-2488.

266. Discovery Visual Studio, Release 3.1, San Diego: Accelrys Software Inc., 2011.

267. G.M. Morris, D.S. Goodsell, R.S. Halliday, R. Huey, W.E. Hart, R.K. Belew and A.J. Olson. *J. Comput. Chem.* **1998,** *19,* 1639-1662.

268. J. Gasteiger and M. Marsili. *Tetrahedron* **1980,** *36,* 3219-3228.

269. J. Lindberg, S. Sigurdsson, S. Lowgren, H.O. Andersson, C. Sahlberg, R. Noreen, K. Fridborg, H. Zhang and T. Unge. *Eur. J. Biochem.* **2002,** *269,* 1670-1677.

270. Pedersen, O.S. Pedersen and E.B. *Antivir. Chem. Chemother.* **1999,** *10,* 285-314.

271. Y. Goldgur, R. Craigie, G.H. Cohen, T. Fujiwara, T. Yoshinaga, T. Fujishita, H. Sugimoto,T. Endo, H. Murai and D.R. Davies. *Proc. Natl. Acad. Sci. U.S.A.* **1999,** *96,* 13040-13043.

272. D.D. Perrin and W.L.F. Armarego. *Purification of Laboratory Chemicals,* 3rd ed.; Pergamon Press, Oxford, 1988.

273. T.J. Rashamuse. M.Sc Thesis; Rhodes University, 2008.

274. G.A. Cartwright and H. McNab. *J. Chem. Res. Synop.* **1997,** *8,* 296-297.

275. S.E. Drewes, O.L. Njamela, N.D. Emslie, N. Ramesar and J.S. Field. *Synth. Commun.* **1993,** *23,* 2807-2815.

276. S. Salisu, C. Kenyon and P.T. Kaye. *Synth. Commun.* **2011,** *41,* 2216-2225.

277. T.D. Harris and G.P. Roth. *J. Org. Chem.* **1979,** *44,* 2004-2007.

278. L. Chas, R. Ford and L.K. Tanzer. *J. Org. Chem.* **1941,** *6,* 722-731.

279. K.W. Merz and J. Fink. *Arch. Pharm.* **1956,** *289,* 347-358.

280. E. Profft. *J. Prakt. Chem.* **1957,** *5,* 175-181.

281. V.K. Rajwanshi, M. Prhavc, P. Fagan and J.L. Brooks, T. Hurd, P.D. Cook and G. Wang. *Nucleos. Nucleot. Nucl.* **2005,** *24,* 179-189.

282. L. Rene, A. Lefebvre and G. Auzou. *Synthesis* **1986,** 567-569.

283. T-S. Jin, M-J. Yu, L-B. Liu, Y. Zhao and T-S. Li. *Synth. Commun.* **2006,** *36,* 2339-2344.

284. Y-L. Shi and M. Shi. *Org. Lett.* **2005,** *7,* 3057-3060.

285. M-J. Qi and M. Shi. *Tetrahedron* **2007,** *63*, 10415-10424.

286. N.M. Shah and R.C. Shah. *Ber. Dtsch. Chem. Ges. [Abteilung] B: Abhandlungen* **1938,** *71B,* 2075-2081.

287. M.M. Garazd, Y.L. Garazd, A.S. Ogorodniichuk and V.P. Khilya. *Russian J. of Bioorg. Chem.* **2004,** *30,* 291-300.

288. A. Velazquez-Campoy, M.J. Todd, S. Vega and E. Freire. *Proc. Natl. Acad. Sci. U.S.A.* **2001,** *98,* 6062-6067.

289. Z. Ji, Z. Yao M. Liu. *Anal. Biochem.* **2009,** *385,* 380-382.

290. S-H. Ahn, H.N. Lim and K-J. Lee. *J. Hetero. Chem.* **2008,** *45,* 1701-1706.